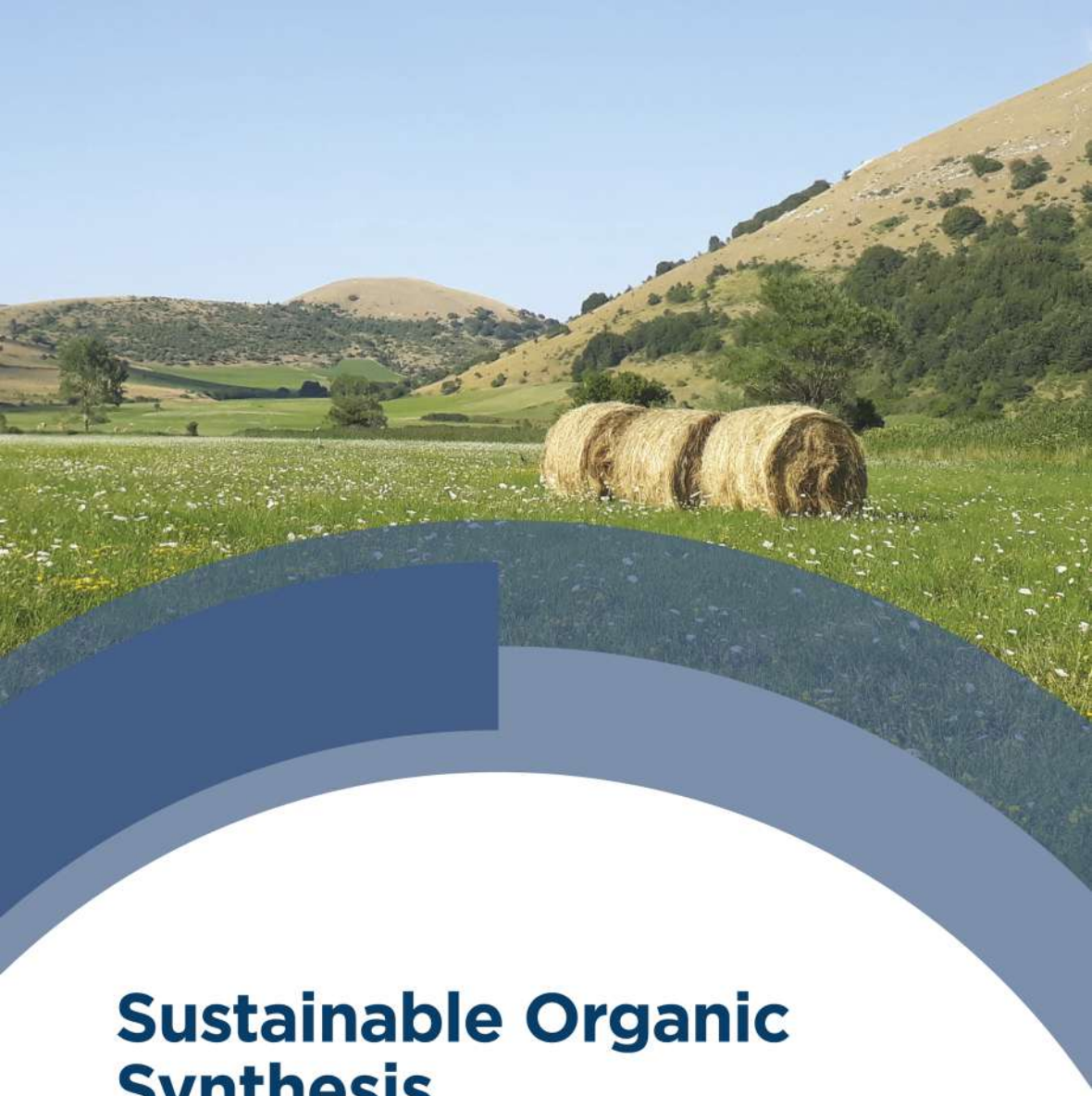

Sustainable Organic Synthesis

Tools and Strategies

Edited by Stefano Protti and Alessandro Palmieri

ROYAL SOCIETY OF CHEMISTRY

Sustainable Organic Synthesis
Tools and Strategies

Sustainable Organic Synthesis
Tools and Strategies

Edited by

Stefano Protti
University of Pavia, Italy
Email: stefano.protti@unipv.it

and

Alessandro Palmieri
University of Camerino, Italy
Email: alessandro.palmieri@unicam.it

Print ISBN: 978-1-83916-203-9
PDF ISBN: 978-1-83916-484-2
EPUB ISBN: 978-1-83916-485-9

A catalogue record for this book is available from the British Library

The Royal Society of Chemistry is a charity, registered in England and Wales, Number 207890, and a company incorporated in England by Royal Charter (Registered No. RC000524), registered office: Burlington House, Piccadilly, London W1J 0BA, UK, Telephone: +44 (0) 20 7437 8656.

Visit our website at www.rsc.org/books

Printed in the United Kingdom by CPI Group (UK) Ltd, Croydon, CR0 4YY, UK

Preface

Over the last sixty years, organic synthesis has reached a very high level of sophistication leading to the realization of innovative synthetic protocols for the construction of complex molecular architectures. Parallel to these achievements, new issues in today's world, dealing with the concepts of resilience (defined as *the capability and ability of an environmental system to return to a stable state after damage/disruption*),[1] sustainable development[2] and, in the case of chemical production, preventing pollution[3] have emerged.

Such issues have been levied by ordinary people to the Scientific Society, and institutions such as the International Union of Pure and Applied Chemistry (IUPAC) and the Organization for Economic Co-operation and Development (OECD) to assess the synthetic approaches in order to develop sustainable alternatives and to face this new challenge.

With the aim of spurring scientists and industries on the way to this new research philosophy, the U.S. Environmental Protection Agency, with the impregnable contribution of Paul Anastas and John Warner,[4] formalized in 1993 the concept of "Green Chemistry", as the design of chemical products and processes that reduce or eliminate the use and generation of hazardous substances. In this regard, both guidelines (denoted as twelve principles of green chemistry)[5] and green metrics, in order to assess and quantify the environmental impact of a chemical process,[6] have been introduced and are nowadays commonly used for assessing and optimizing synthetic protocols, as well as for comparing new and old synthetic processes. In the end, this new consciousness has led scientists to explore a variety of different tools to arrive at the common goal of more sustainable chemical production. In this regard, the realization of this handbook was undertaken with the aim of providing readers with an exhaustive overview on

Sustainable Organic Synthesis: Tools and Strategies
Edited by Stefano Protti and Alessandro Palmieri

Published by the Royal Society of Chemistry, www.rsc.org

Organic Green Synthesis, by covering all of the synthetic strategies that are currently adopted on the way to sustainability, corroborated also by the use of green/energy metrics.

With this purpose, the handbook is composed of three sections, namely *Activation of Chemical Substrates Under Sustainable Conditions*, *Benign Media for Organic Synthesis* and *Sustainable Approaches in Organic Synthesis*. Accordingly, the first section is focused on synthetic strategies that are well-established (including, among others, homogeneous and heterogeneous catalysis and biocatalysis), or have recently emerged (electrochemistry and visible-light photochemistry) in sustainable organic chemistry, while the second part of the handbook is devoted to bioderived and reusable solvents proposed in the literature as a sustainable alternative to VOCs as the reaction media. The aim of the third section is to describe synthetic philosophies that have recently emerged as a way of thinking to perform sustainable production. The last two chapters are finally focused to the contribution of Green Chemistry to Chemical Engineering and Industrial Chemistry. We believe that this contribution will play a key role in furnishing different practical examples to academic and industrial readers, as well as for introducing green chemistry topics to young researchers and as precious help for students.

We would like to thank the researchers that contributed to this handbook and the staff of the Royal Society of Chemistry (in particular Connor Sheppard and Helen Armes) that supported us in this project.

Alessandro Palmieri and Stefano Protti

References

1. R. Bhamra, S. Dani and K. Burnard, Resilience: the concept, a literature review and future directions, *Int. J. Prod. Res.*, 2011, **49**, 5375.
2. (a) World Commission on Environment and Development (WCED), *Our Common Future*, Oxford University Press, Oxford and New York, 1987; (b) B. R. Keeble, The Brundtland Report: 'Our Common Future', *Medicine and War*, 1988, vol. 4, p. 17.
3. F. J. Gomes da Silva and R. M. Gouveia, Cleaner Production Main Concept and History, in *Cleaner Production*, Springer Nature Switzerland AG, 2020.
4. P. Anastas and J. Warner, *Green Chemistry: Theory and Practice*, Oxford University Press Inc. 2000.
5. P. Anastas and N. Eghbali, *Chem. Soc. Rev.*, 2010, **39**, 301.
6. S. Protti and A. Albini, Green Metrics, an Abridged Glossary, in *Paradigms in Green Chemistry and Technology-SpringerBriefs in Green Chemistry for Sustainability*, Springer-UK, 2016.

Biographies

Stefano Protti obtained a Master's degree in 2003 (110/110 cum laude). In 2007, he completed his PhD in Pavia focusing on photochemical arylations *via* phenyl cations. Later he moved to the LASIR Laboratory (Lille, France), where he investigated the photoreactivity and the photophysics of flavonoids. He came back to Pavia and started working in the field of (photo)green synthetic chemistry. After a postdoctoral stay at the iBitTec-S laboratory (CEA Saclay, France) carrying out studies on photocatalyzed oxidation reactions for energy storage, he moved again to Pavia. Since 2018, he has been an Associate Professor at the University of Pavia, Italy. He is currently editor of the Specialist Periodical Reports in Photochemistry of the Royal Society of Chemistry, a member of the Early Career Board of ACS Sustainable Chemistry and Engineering and of the International Advisory Board of the European Journal of Organic Chemistry. The research activity of Stefano Protti has been mainly focused on the development of new synthetic methods for the light-driven formation of C–C and C-heteroatom bonds under metal free conditions.

Sustainable Organic Synthesis: Tools and Strategies
Edited by Stefano Protti and Alessandro Palmieri

Published by the Royal Society of Chemistry, www.rsc.org

Alessandro Palmieri obtained his Laurea degree *cum laude* in Chemistry in 2002 at the University of Camerino (Italy) where, five years later, he received a PhD degree in Chemical Sciences. Then, in the period 2007–2010 he held a post-doctoral fellowship and in 2008 he moved, as a visiting postdoctoral fellow, to the ITC laboratory at the University of Cambridge (Prof. Steven V. Ley). After experience as an assistant professor (2010–2013), in 2014 he was appointed associate professor in Organic Chemistry at the University of Camerino. Currently, his research interests involve (i) the chemistry of aliphatic nitro compounds, (ii) the realization of new one-pot protocols for generating and derivatizing heterocyclic systems, (iii) the preparation and use of solid supported reagents, and (iv) the development of new sustainable processes and (v) flow chemical protocols.

Contents

Sustainable Organic Synthesis: Tools and Strategies
Edited by Stefano Protti and Alessandro Palmieri

Published by the Royal Society of Chemistry, www.rsc.org

Section 1

Activation of Chemical Substrates under Sustainable Conditions

CHAPTER 1

Assessing the Sustainability of Syntheses of the Anti-tuberculosis Pharmaceutical Pretomanid by Green Metrics

JOHN ANDRAOS*

CareerChem, Research and Development, 504-1129 Don Mills Road, Toronto, ON M3B 2W4, Canada
*E-mail: johnandraos1964@gmail.com

1.1 Introduction

The sub-area of green metrics in the wider field of green chemistry is now a mature field of study, since the inaugural metric of atom economy was introduced in 1991.[1] Several books[2–6] and reviews[7–14] have been written on the subject, mainly focusing on the work of synthetic organic and process chemists in the pharmaceutical industry. The main purpose of introducing metrics is to provide some kind of measuring tool that can be used to gauge the reaction and synthesis efficiency with respect to input material utilization, waste production, and energy consumption of individual chemical reactions and entire synthesis plans for simple and complex target molecules. The most widely used metric among process chemists in industry that has been termed the "yardstick" by which material efficiencies of scaled-up synthesis plans are judged is process mass intensity (PMI), which is the mass ratio of

Sustainable Organic Synthesis: Tools and Strategies
Edited by Stefano Protti and Alessandro Palmieri

Published by the Royal Society of Chemistry, www.rsc.org

all input materials to final target product.[15] This metric has now superseded the long-standing overall yield metric, which is the multiplicative product of all reaction yields in a synthesis plan along the longest linear branch. For convenience to the reader, Table 1.1 summarizes a brief listing of traditional metrics and their definitions that have been used by synthetic organic and process chemists to gauge reaction and synthesis performance. Generally speaking, synthesis plans that are traditionally characterized as "efficient" are ones that have the lowest possible number of reaction steps, the highest possible overall yield, a higher proportion of construction steps compared to concession or sacrificial steps, and overall high throughput and reduced process time. When it comes to counting the number of reaction steps in a synthesis plan, process chemists count the number of isolations (*i.e.*, number of purifications) of intermediate products and the final product, rather than counting the total number of chemical transformations involved as is often done for reported academic syntheses. If the number of product isolations is less than the number of chemical transformations, then the synthesis plan contains telescoped or concatenated reactions, meaning that more than one chemical transformation has taken place sequentially in a reaction vessel. Often this is done using a solvent switching technique, where the reaction solvent of the first chemical transformation is evaporated leaving behind the first crude product and a second reaction solvent is added to carry out the following chemical transformation. The second intermediate product is isolated and purified, while the first one is not. Such a strategy clearly reduces solvent demand in work-up and purification phases, particularly recrystallization and chromatographic operations. However, the strategy only works if the by-products and other impurities from the former reaction, such as excess reagents, catalysts, and other additives, do not interfere with the performance of the following one. On the other hand, if the total number of chemical transformations is the same as the number of isolations in a synthesis plan, then this implies that each intermediate product along the way, including the final product, is isolated and purified.

Despite these advances in providing quantitative measures of reaction and synthesis efficiency, the often-discussed concept of sustainability has not yet reached the same level of quantitative rigor. In fact, a recent news report in 2019 revealed the fuzzy nature of the concept and various competing definitions of it by different stakeholders, which adds to the confusion in applying the idea in a scientifically sound manner.[16] The little literature that exists on quantifying what sustainability is has mainly gravitated to thermodynamic issues and energy consumption from fossil-fuel and renewable sources.[17–26] In 2020, we decided to tackle the problem of quantifying sustainability in the context of assessing the degree of sustainability of synthesis plans from the point of view of the provenance of the input materials and energy resources used and the fate of all output materials, including waste materials and the intended final product.[27] We reasoned that since scaled-up synthesis plan design represents the core effort made by process chemists and chemical engineers, a practical definition of sustainability would have to be demonstrated

Table 1.1 Summary of traditional metrics used by synthetic organic and process chemists.

Traditional metric	Performance application	Definition	Units
Biocatalysis yield	Reaction	Ratio of mass of product to mass of biocatalyst.	$g\ g^{-1}$
Carbon efficiency	Reaction	The number of carbon atoms appearing in the target product divided by the total number of carbon atoms appearing in the reactants of a balanced chemical equation.	%
Catalyst loading	Reaction	Ratio of moles of catalyst to moles of substrate (usually the limiting reagent).	Mol%
Conversion	Reaction	Fractional amount of starting material that gets transformed or converted to all products in a chemical reaction given by $(m_{final} - m_{initial})/m_{initial}$, where the m terms refer to the masses of starting material (usually the limiting reagent) at the beginning and end of a reaction.	%
Diastereomeric excess	Reaction	If a reaction produces two diastereomers A and B, and A is the dominant diastereomer, then the diastereomeric excess is defined as the ratio $(m_A - m_B)/(m_A + m_B)$, where the m parameters refer to the masses of the respective diastereomers.	%
Effective mass yield	Reaction	Ratio of mass of product to mass of all input materials excluding aqueous materials since they are considered to be benign.	%
Enantiomeric excess	Reaction	Same definition as diastereomeric excess but referring to enantiomeric products.	%
Ideality	synthesis	Number of construction reaction steps in a synthesis that are not concession or sacrificial steps divided by the total number of reaction steps.	%
Molar efficiency	Reaction	Ratio of moles of product to sum of moles of reactants, additives, and catalysts.	%
Number of reaction steps	synthesis	Total number of chemical transformations in a synthesis along the longest branch for academic syntheses. Total number of isolations of intermediate products and final product in a synthesis for process syntheses.	Dimensionless
Overall synthesis yield	synthesis	For a linear synthesis plan, the overall yield corresponds to the multiplicative product of the individual step reaction yields. For a convergent plan, the overall yield corresponds to the multiplicative product of the individual step reaction yields along the longest branch of the synthesis plan; that is, the branch having the most number of reaction steps.	%

(*continued*)

Table 1.1 (*continued*)

Traditional metric	Performance application	Definition	Units
Process time	synthesis	The length of time elapsed to carry out a chemical reaction from the point of adding all materials to the reaction vessel to isolating the purified target product. (a) In batch operations, process time = residence time (reaction time) + workup time + purification time. Process time does not depend on reaction scale. (b) In continuous flow operations using a single tube, process time = total reaction volume/flow rate. The reaction volume is composed of the volume of reactants and the volume of reaction solvents. Process time depends on reaction scale. (c) In continuous flow operations using multiple tubes in parallel, process time = (total reaction volume/flow rate) × (1/number of parallel tubes). This operation is called numbering up or scaling out.	hours (h)
Process solvent mass intensity	synthesis	Ratio of the total mass of solvent used (excluding water) to mass of target product.	kg kg^{-1}
Process water mass intensity	synthesis	Ratio of the total mass of water used to mass of target product. The mass of water used is the difference between freshwater usage and recycled water usage.	kg kg^{-1}
Selectivity	Reaction	For a reaction producing more than one product, such as regioisomers or stereoisomers, selectivity is the ratio of mass of the desired product to the total mass of products obtained in a reaction.	%
Solvent intensity	synthesis	Ratio of total mass of solvents used (including water) to mass of target product.	kg kg^{-1}
Space-time-yield	Reaction	Ratio of mass of product to multiplicative product of total process time times total volume of input materials. Sometimes the volume of the reactor is used instead of the total volume of input materials.	kg m^{-3} h^{-1} kg m^{-3} s^{-1} kg L^{-1} h^{-1} kg L^{-1} s^{-1}
Step reaction yield	Reaction	Ratio of moles of product to moles of limiting reagent times ratio of stoichiometric coefficient of limiting reagent to stoichiometric coefficient of product.	%
Throughput	Reaction or synthesis	For reactions, it is the ratio of mass of product to reaction time. For synthesis plans, it is the ratio of mass of final target product to entire synthesis process time.	kg h^{-1}
Turnover frequency	Reaction	Ratio of turnover number to reaction time.	h^{-1}
Turnover number	Reaction	Ratio of moles of product to moles of catalyst.	Dimensionless
Yield based on recovered starting material	Reaction	A calculation of reaction yield that includes both the intended target product and unreacted starting material in a chemical reaction as the desired products; this is usually reported in papers when the true reaction yield to the intended target compound is lower than 50%.	%

according to that activity. We were successfully able to illustrate the application of a quantitative definition of sustainability to the analysis of 22 academic and industrial synthesis plans of vanillin, which is the world's most manufactured flavor ingredient. In that work, we introduced a sustainability index (SI) parameter that could be used along with PMI, sacrificial reagent (SR) consumption, input enthalpic energy (IEE) consumption, and Rowan solvent greenness index (RSGI) to provide an overall picture of efficiency and sustainability for various synthesis plans for a given target molecule. Furthermore, the set of plans could be ranked according to these five attributes using both Borda count[28,29] and poset dominance[30] methodologies. These ideas further extend our efforts to formulate a standardized framework for evaluating and reporting synthesis plan greenness, particularly in the process industry.[31] In this chapter, we apply these quantitative techniques to the analysis of four syntheses of the novel anti-tuberculosis pharmaceutical pretomanid from the common starting material 4-nitroimidazole.[32–35] We chose this compound because its synthesis plans are well documented in the literature and they are sufficiently brief that they can serve the purpose of illustrating our methodologies with minimal difficulty (see Table 1.1 for an overview).

1.2 Syntheses of Pretomanid

Pretomanid (**1**, PA-824)[1] is a candidate anti-tuberculosis pharmaceutical[36–40] developed by Pathogenesis Corporation[32] and is currently undergoing Phase III clinical trials under the direction of TB Alliance. The structure of pretomanid possesses a unique [4.3.0] fused bicyclic ring system consisting of a [1,3]-oxazinane ring (ring A) and an imidazole ring (ring B) as shown in Figure 1.1.

The four synthesis plans for this pharmaceutical under consideration in this work are shown in Schemes 1.1–1.4 corresponding to Pathogenesis (Scheme 1.1),[32] Otera (Scheme 1.2),[33] Sorensen (Scheme 1.3),[34] and Liu (Scheme 1.4),[35] respectively.

In order to maintain a fair comparison among the routes, all plans were evaluated from the same common starting material, namely 4-nitroimidazole, and all metrics were calculated based on a basis production of 1 kg of pretomanid. Scheme 1.5 shows routes to two imidazole intermediates used in the four syntheses originating from 4-nitroimidazole.

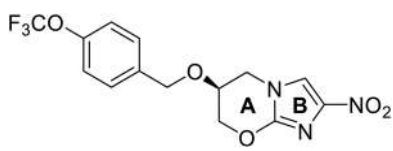

Figure 1.1 Chemical structure of pretomanid.

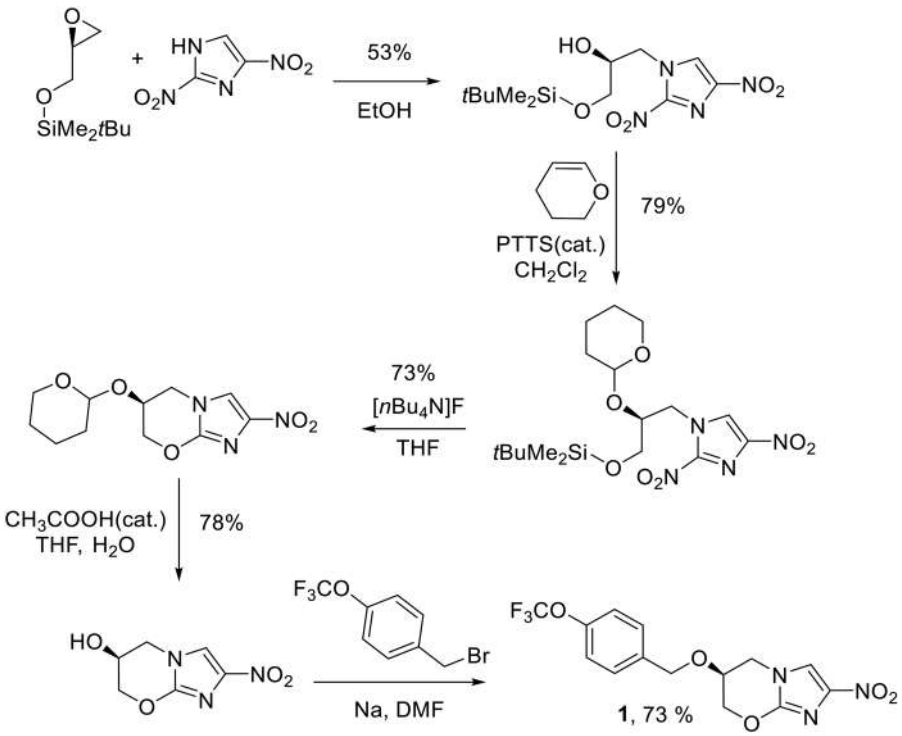

Scheme 1.1 Synthesis of pretomanid **1** by Pathogenesis (see ref. 32).

The originally discovered Pathogenesis route involves ring opening of an alcohol protected glycidol by 2,4-dinitroimidazole, followed by tetrahydropyran protection of an alcohol group, followed by ring closure and final *O*-alkylation to a bromobenzyl intermediate. The Otera route was advertised as adopting green chemistry principles, in which the authors stated that their synthesis had a reaction mass efficiency (RME) of 0.138 (or 13.8%) and consumed 258 L of reaction solvents and 46 300 L of total solvents in order to produce 1 kg of PA-824. The RME metric is the reciprocal of the PMI metric and can be expressed as a percentage, since its value is a fraction ranging between 0 and 1. These metric determinations may be directly compared with an RME of 4.1% and a consumption of 171 L of reaction solvents and 79 800 L of total solvents for the Pathogenesis route. The synthetic strategy used to build the molecule is identical to the Pathogenesis route; however, the key green attributes are that the first epoxide ring opening reaction was carried out without reaction solvent (solventless reaction) and that the synthesis was shortened by one step by telescoping two reactions so that the intermediate shown in square brackets in Scheme 1.2 was not isolated. Unlike the linear routes shown in Schemes 1.1 and 1.2,

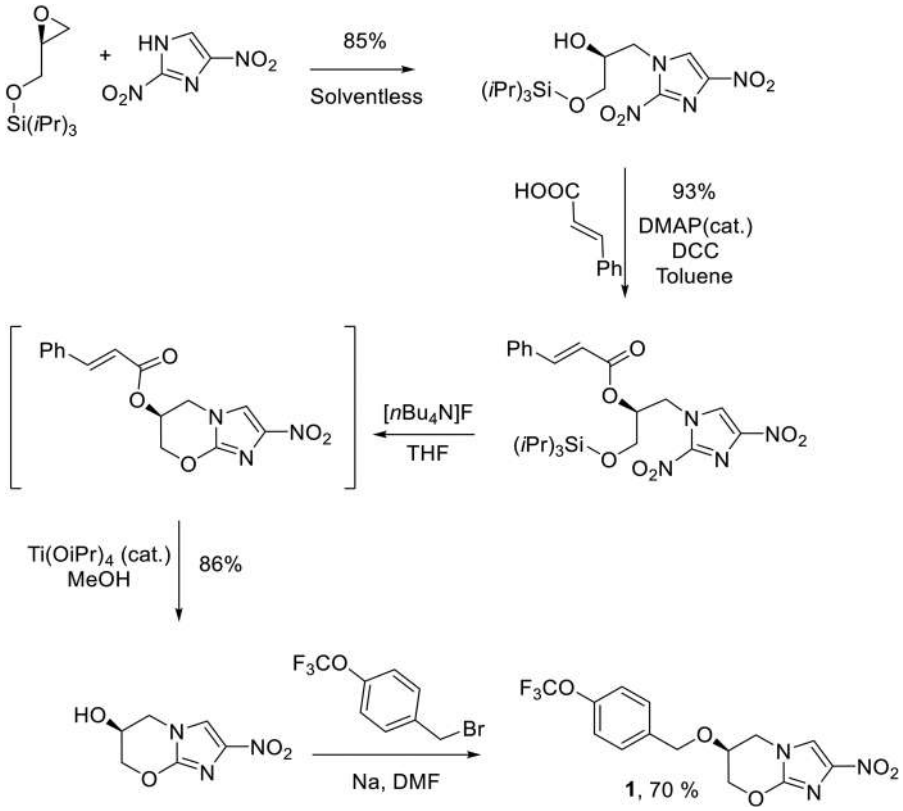

Scheme 1.2 Synthesis of pretomanid **1** by Otera and coworkers (see ref. 33).

Sorensen and coworkers at Princeton University employed a convergent strategy (see Scheme 1.3) using 2-chloro-4-nitroimidazole instead of 2,4-dinitroimidazole as the starting material. The main selling point of this synthesis is that the starting imidazole did not have the same explosive properties as the dinitro derivative, thus making it a safer reagent to handle. The syntheses of 2-chloro-4-nitroimidazole and 2,4-dinitroimidazole from 4-nitroimidazole are shown in Scheme 1.5. In the Sorensen plan, one branch involves the synthesis of a trichloroethanimidate intermediate labelled as **2**. The other branch involves first esterification to form a benzoate derivative, followed by *O*-alkylation using intermediate **2**, followed by *N*-alkylation with 2-chloro-4-nitroimidazole, followed by tandem ester saponification and ring closure. Finally, Liu and coworkers invented a 7-step linear route from 4-nitroimidazole that followed closely the Pathogenesis strategy with a slight modification in the choice of protecting group in the glycidol starting material from a silyl ether to an *n*-butyl ester.

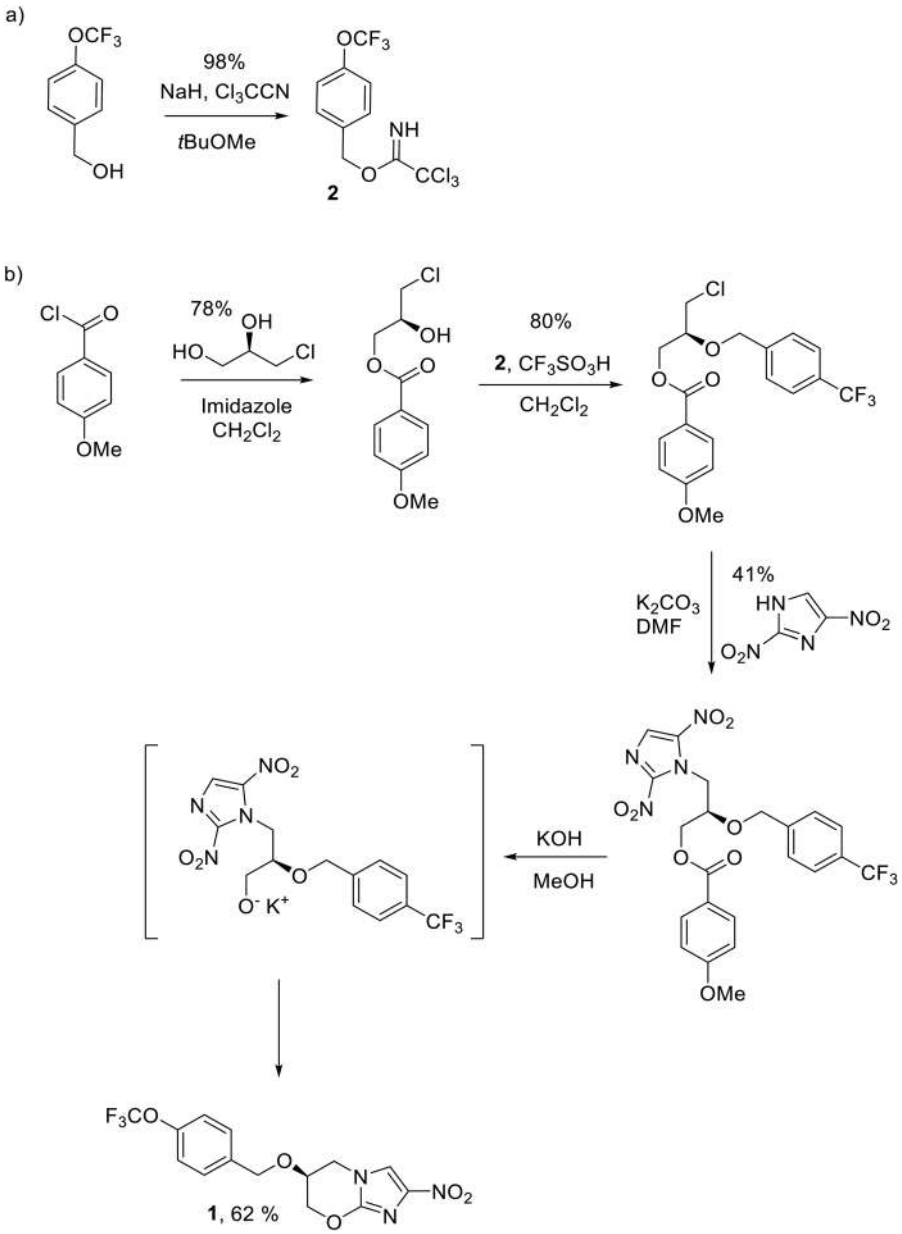

Scheme 1.3 Convergent synthesis of pretomanid **1** (parts a and b) by Sorensen and coworkers (see ref. 34).

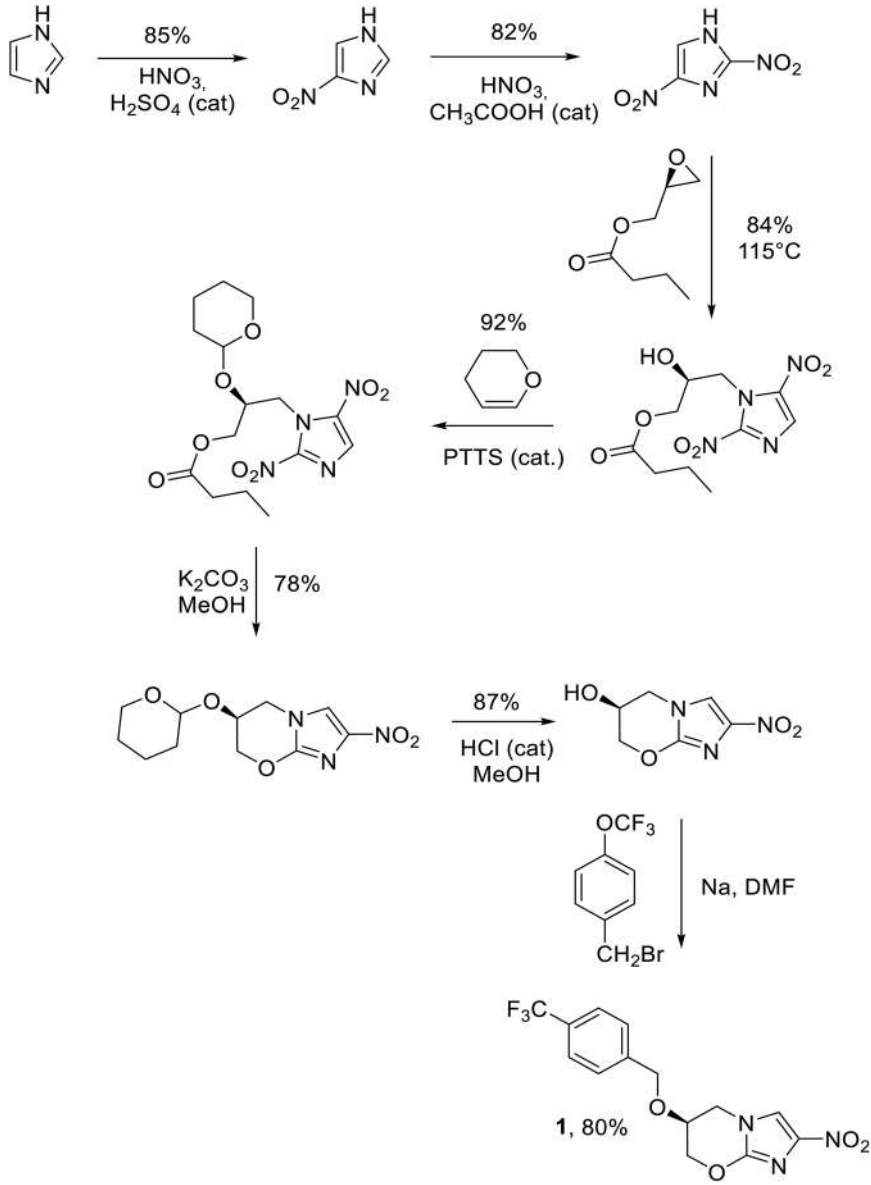

Scheme 1.4 Synthesis of pretomanid **1** by Liu and coworkers (see ref. 35).

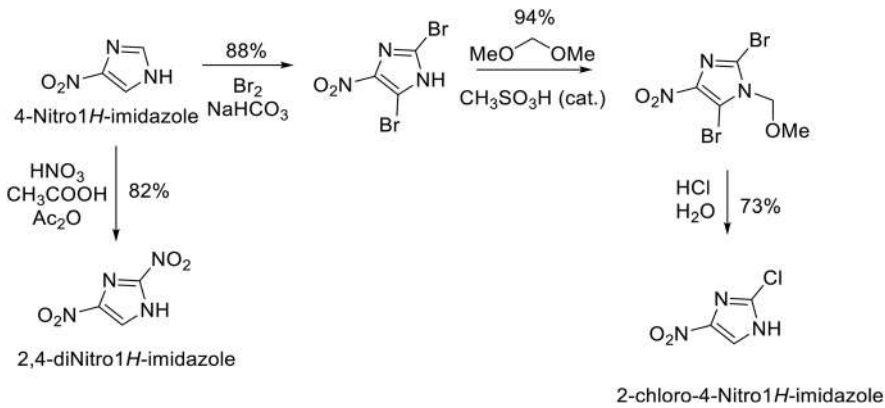

Scheme 1.5 Routes to various imidazole intermediates used in the four syntheses originating from 4-nitroimidazole (see ref. 40 and 41).

1.3 Sustainability Index

The sustainability index (SI)[27] for a synthesis plan is defined as the root-mean square of four fractional quantities according to eqn (1.1).

$$\mathrm{SI} = \frac{1}{2}\sqrt{\left(F_{\mathrm{VI}}\right)^2 + \left(F_{\mathrm{VO}}\right)^2 + \left(F_{\mathrm{VP}}\right)^2 + \left(F_{\mathrm{RE}}\right)^2} \tag{1.1}$$

where F_{VI}, F_{VO}, F_{VP}, and F_{RE} are the mass fraction of valorized inputs, mass fraction of valorized waste outputs, mass fraction of valorized target product, and input enthalpic energy fraction arising from renewable energy sources, respectively. Specifically, these four fractions are given by eqn (1.2)–(1.5).

$$F_{\mathrm{VI}} = \frac{M_{\mathrm{VI}}}{M_{\text{total inputs}}} = \frac{M_{\mathrm{VI}}}{M_{\mathrm{VI}} + M_{\mathrm{NVI}}} \tag{1.2}$$

$$F_{\mathrm{VO}} = \frac{W_{\mathrm{VO}}}{W_{\mathrm{VO}} + W_{\mathrm{NVO}}} \tag{1.3}$$

$$F_{\mathrm{VP}} = \frac{M_{\text{product}} - M^{*}_{\text{product}}}{M_{\text{product}}} \tag{1.4}$$

$$F_{\mathrm{RE}} = \frac{(\mathrm{IEE})_{\text{renewable}}}{(\mathrm{IEE})_{\text{total}}} \tag{1.5}$$

where M_{VI} is mass of valorized inputs, M_{NVI} is mass of non-valorized inputs, W_{VO} is waste mass of valorized outputs, W_{NVO} is waste mass of non-valorized outputs, M_{product} is mass of target product, M^{*}_{product} is mass of target product that is destined to be wasted, $(\mathrm{IEE})_{\text{renewable}}$ is the input enthalpy energy arising from renewable resources, and $(\mathrm{IEE})_{\text{total}}$ is the total input enthalpy energy obtained as a sum of all energy consumption as a result of heating and cooling over all input materials used in a synthesis plan above or below

a reference state representing the ambient temperature and pressure conditions of 298 K and 1 atm, respectively. A valorized input material is defined as one arising from renewable or recycled sources such as biomass, scrap metals, or retrieved by-products from other processes. A non-valorized input material is derived from non-renewable sources such as fossil fuels and virgin mineral ores. A valorized output material is defined as one destined to be recycled, reclaimed, or used in other processes. A non-valorized output material is defined as one that will end up as "dead waste" whether or not it undergoes treatment before release into the four main environmental compartments of air, water, soil, and sediment. The following energy sources are considered as renewable: hydroelectric, solar, wind, geothermal, and biofuels; and the following energy sources are considered as non-renewable: coal, other fossil-fuels such as petroleum and natural gas, and nuclear. According to the above mass quantities, the process mass intensity can be expressed as shown in eqn (1.6).

$$\text{PMI} = \frac{M_{\text{VI}} + M_{\text{NVI}}}{M_{\text{product}}} = \frac{M_{\text{total inputs}}}{M_{\text{product}}} \tag{1.6}$$

Based on this formalism, a given synthesis plan can therefore be said to be completely "sustainable" if the following conditions are satisfied: $F_{\text{VI}} = 1$, $F_{\text{VO}} = 1$, $F_{\text{VP}} = 1$, $F_{\text{RE}} = 1$, and SI = 1. Conversely, a given synthesis plan can be said to be completely "unsustainable" if the following conditions are satisfied: $F_{\text{VI}} = 0$, $F_{\text{VO}} = 0$, $F_{\text{VP}} = 0$, $F_{\text{RE}} = 0$, and SI = 0. Since each of the contributing fractions ranges between 0 and 1, then SI is also a fraction that can be expressed as a percentage. In the determination of SI, a number of limiting assumptions need to be made. If ethanol was used as an input material, then 10% of it was assumed to originate from renewable sources (*i.e.*, biomass) if the publication is dated after 1990, since that is the approximate time frame when biofuels were made widely available in the market. Water was considered a renewable input material due to the circulating global hydrological cycle. Mineral salts, metal-derived catalysts, and all non-aqueous and non-biologically derived materials from fossil fuels or ores were considered non-renewable inputs since their rate of renewal occurs on geological time scales that are several orders of magnitude longer than organism time scales. An arbitrary value of 0.9 was used for F_{VP} indicating that 90% of the manufactured pretomanid pharmaceutical is used as intended and 10% of it is wasted either by excretion from the human body or by shelf degradation in pharmacies. If a synthesis plan was published on or after the year 2000, $F_{\text{RE}} = 0.35$ following recent energy mix data,[43,44] and if it was published before 2000 then $F_{\text{RE}} = 0$. The cut-off year 2000 was chosen since it marked the beginning of the 21st century when ideas of sustainability began to take root in the general societal consciousness. In terms of degree of sustainability according to the definition of SI given in eqn (1.1), the Otera, Sorensen, and Liu plans are all tied at SI = 0.4823 and the Pathogenesis plan has SI = 0.4500. Table 1.2 summarizes the fractional breakdown of the contributing factors to SI for each plan. Overall, there is little differentiation between the plans based on

the two fractions F_{VP} = 0.9 (all plans), and F_{RE} = 0.35 (Liu, Otera, Sorensen) or F_{RE} = 0 (Pathogenesis) since these are set by the assumptions made. Generally, in SI analyses the greatest variation among synthesis plans arises from the F_{VI} and F_{VO} fractions. As observed in Table 1.2, the magnitudes of F_{VP} and F_{RE} significantly outweigh those of F_{VI} and F_{VO} and so their contribution to the magnitude of SI is larger. However, if reaction, work-up, and purification solvents are retrieved for re-use in the same syntheses or for entirely different syntheses, the value of F_{VO} (mass fraction of valorized outputs) dramatically increases for all plans according to the following: 0.0097 to 0.988 (Liu), 0.0010 to 0.989 (Otera), 0.0089 to 0.987 (Pathogenesis), and 0.0047 to 0.981 (Sorensen). This observation is not surprising since solvent consumption in all phases of carrying out reaction steps constitutes the bulk of materials used. In turn, the increase in F_{VO} has the effect of increasing the corresponding value of SI for each plan as shown in Table 1.3 where a 43 to 48% increase in value is calculated. The ranking of the four plans is also more spread out where the ranking order is Otera ~ Liu > Sorensen > Pathogenesis.

Table 1.4 summarizes the results of the metrics analysis based on the five attribute parameters PMI, SR, IEE, RSGI, and SI for each of the four

Table 1.2 Summary of contributing fractions for sustainability indexes determined for the four synthesis plans of pretomanid.

Plan	F_{VI}	F_{VO}	F_{VP}	F_{RE}	SI
Liu	0.0097	0.0097	0.9	0.35	0.4823
Otera	0.0023	0.0010	0.9	0.35	0.4823
Pathogenesis	0.0090	0.0089	0.9	0	0.4500
Sorensen	0.0054	0.0047	0.9	0.35	0.4823

Table 1.3 Ranking comparison of SI values upon retrieval or non-retrieval of reaction and/or chromatographic solvents.

Plan	SI (no solvent retrieval)	Rank	SI (solvent retrieval)	Rank	% Increase in SI value
Otera	0.4823	1	0.6908	1	43.2
Liu	0.4823	1	0.6904	2	43.1
Sorensen	0.4823	1	0.6880	3	42.6
Pathogenesis	0.4500	2	0.6678	4	48.4

Table 1.4 Summary of assessment parameters for an alphabetical list of the four synthesis plans for pretomanid beginning with 4-nitroimidazole.

Plan	PMI (kg kg^{-1})	SR (kg kg^{-1})	IEE (kJ kg^{-1})	RSGI (kg)	SI
Liu	15 766	24	7193	105 399	0.4823
Otera	45 276	5	18 833	313 748	0.4823
Pathogenesis	63 886	16	5730	462 158	0.4500
Sorensen	80 268	101	23 537	554 813	0.4823

pretomanid plans considered based on a production of 1 kg of the pharmaceutical from 4-nitroimidazole. PMI was determined according to eqn (1.6). The Liu plan has the lowest PMI value of 16 tonnes per kg and the Sorensen plan has the highest value of 80 tonnes per kg. In both cases, 97.5% of the PMI value arises from purification solvent consumption. The sacrificial reagent (SR) consumption parameter tracks the mass fraction of sacrificial reagents used in a synthesis plan compared to the total mass of reagents used, where sacrificial reagents are defined as those that do not contribute any atoms to the final product structure. Hence, SR is more probing than atom economy since it is directly linked with the final target bond map of the final product structure in a synthesis plan, which traces the origin of each atom back to the contributing reagent atoms and which target bonds were made in which reaction steps. Any reagents not included in this mapping are automatically classified as sacrificial. Eqn (1.7) shows the mathematical definition of SR.

$$\mathrm{SR} = \frac{\sum \text{mass sacrificial reagents}}{\sum \text{total mass reagents}} \tag{1.7}$$

Typically, sacrificial reagents are used in protecting and de-protecting group reaction steps, and oxidation and reduction reaction steps that do not contribute oxygen atoms or hydrogen atoms, respectively, toward the final target structure. Clearly, one key feature of a well-designed synthesis plan is that it maximizes its reagents consumption toward the building up of the target molecule, so that each reaction step is a target bond forming reaction. In the Pathogenesis plan (Scheme 1.1), the following sacrificial reagents were used: nitric acid (*for the synthesis of 2,4-dinitro-1H-imidazole*, see Scheme 1.5), 3,4-dihydro-2*H*-pyran (step 4), tetra-*n*-butylammonium fluoride (step 5), water (step 6), and sodium hydride (step 7). In the Otera plan (Scheme 1.2), the following sacrificial reagents were used: nitric acid (step 1), cinnamic acid and dicyclohexyldiimide (DCC) (step 4), tetra-*n*-butylammonium fluoride and methanol (step 5), and sodium hydride (step 6). In the Sorensen plan (Scheme 1.3), the following sacrificial reagents were used: bromine and sodium bicarbonate (step 1), methylal (step 2), sodium sulfite and water (step 3), *p*-methoxybenzoyl chloride and trichloroacetonitrile (step 3*), hydrochloric acid and water (step 4), potassium carbonate (step 5), and potassium hydroxide (step 6). In the Liu plan (Scheme 1.4), the following sacrificial reagents were used: dihydropyran (step 4), methanol and potassium carbonate (step 5), methanol (step 6), and sodium hydride (step 7). Among these four plans, the Otera plan utilizes the least sacrificial reagents at 5 kg per kg pretomanid and the Sorensen plan utilizes the most at 101 kg per kg pretomanid.

Based on the temperature and pressure reaction conditions for each reaction step, the input enthalpy energy (IEE) parameter tracks the enthalpic energy requirements from heating or cooling operations in the reaction, work-up, and purification phases. The largest contributor to IEE arises from heating or cooling reaction solvents since solvents constitute the bulk of the

input materials used in a synthesis plan. Among the four plans, the Pathogenesis plan utilizes the least input energy at 5700 kJ per kg pretomanid and the Sorensen plan utilizes the most at 24 000 kJ per kg pretomanid. In the Pathogenesis plan, steps 1 and 7 were carried out under cooling conditions at 0 °C and −60 °C, respectively, whereas, steps 2, 3, and 6 were carried out under heating conditions at 115 °C, 70 °C, and 45 °C, respectively. By contrast, in the Sorensen plan, steps 1, 3, 3*, 4*, and 6 were carried out under cooling conditions at 5 °C, 12 °C, 0 °C, 0 °C, and 0 °C, respectively, whereas, steps 1, 2, 4, and 5 were carried out under heating conditions at 65 °C, 40 °C, 95 °C, and 120 °C, respectively.

The Rowan solvent greenness index (RSGI)[45] quantifies the relative environmental, toxicological, and safety-hazard impacts of solvents used in reaction, work-up, and purification procedures for all reaction steps in a synthesis plan. It utilizes an overall solvent index (OSI) defined in eqn (1.8) that scales between 0 and 12 spanning the benign solvent water to the non-benign solvent benzene.

$$\mathrm{RSGI} = \sum_i m_i \left(\mathrm{OSI}_{12}\right)_i \tag{1.8}$$

where m_i is the mass of solvent i and OSI_{12} is defined as a normalized quantity over a set of solvents as shown in eqn (1.9).

$$\left(\mathrm{OSI}_{12}\right)_i = 12\left(\frac{\mathrm{OSI}_i - \mathrm{OSI}_{\min}}{\mathrm{OSI}_{\max} - \mathrm{OSI}_{\min}}\right) \tag{1.9}$$

where $\mathrm{OSI}_{\min}$ and $\mathrm{OSI}_{\max}$ are the minimum and maximum values of OSI for a set of solvents and OSI_i for a given solvent i is given by eqn (1.10).

$$\begin{aligned}\mathrm{OSI}_i = {} & 2\left(M_{\mathrm{OEL},i} + M_{\mathrm{LD50},i} + M_{\mathrm{LC50},i}\right) + M_{\mathrm{GWP},i} + M_{\mathrm{SFP},i} + M_{\mathrm{ODP},i} + M_{\mathrm{ABP},i} + M_{\mathrm{BCP},i} \\ & + M_{\mathrm{PER},i} + M_{\mathrm{soil},i} + M_{\mathrm{half\text{-}life},i} + M_{\mathrm{aqua},i} + M_{\mathrm{Q\text{-}phrase},i} + M_{\mathrm{SD},i} + M_{\mathrm{FP},i}\end{aligned} \tag{1.10}$$

where the metric parameters (M) cover occupational exposure limit (OEL, ppm), LD50 (ingestion toxicity, mg kg^{-1}), LC50 (inhalation toxicity, g m^{-3} for 4 h), global warming potential (GWP, unitless), smog formation potential (SFP, unitless), ozone depletion potential (ODP, unitless), acidity-basicity potential (ABP, unitless), bioconcentration potential (BCP, unitless), persistence potential (PER, unitless), soil sorption coefficient (soil, K_{oc}), half-life of the solvent in the environment (half-life, h), aquatic toxicity to fish (aqua, mg L^{-1} for 96 h), Q-phrase potential (Q-phrase, unitless), skin dose (SD, mg), and flash point (FP, degrees K). From eqn (1.8), it is observed that high values of RSGI can arise from high mass utilization of solvents, particularly in chromatographic purification steps (*i.e.*, high m values), as well as high impact solvents (*i.e.*, high OSI12 values). Synthesis plans that minimize solvent usage across the board and those that use benign solvents will have low overall RSGI values. Based on the RSGI metric, the Liu plan had the least solvent impact at 105 tonnes and the Sorensen plan had the most at 555 tonnes.

The most impactful solvents used in the Liu plan were chlorobenzene, acetic anhydride, dichloromethane, and dimethylformamide. In the Sorensen plan, they were hexane, dichloromethane, dimethylformamide, and methyl *t*-butyl ether. The high RSGI value in the Sorensen plan arises mainly from the large solvent consumption in the chromatographic purification operations in steps 3*, 4*, 5, and 6.

1.4 Ranking Analysis of the Pretomanid Synthesis Plans

In order to implement an unbiased ranking of synthesis plans according to various metrics, there are two well-documented methods for doing this, namely, the Borda count[28,29] method and the poset dominance[30] method. The Borda method is easy to implement and is also rapid in carrying out the computation. The poset dominance method involves a more tedious calculation but yields a more reliable result, since it considers all possible pairwise comparisons of attributes across all pairwise comparisons of synthesis plans. In the Borda count method, the plans are listed in ascending order of PMI, SR, IEE, and RSGI so that the plans having the lowest values for these attributes are ranked highest, and the plans are listed in descending order of SI so that the plans having the highest values are ranked highest. The highest score corresponds to the number of plans considered. In this case, since there are four pretomanid plans under consideration, the Borda scoring will have values of 1, 2, 3, or 4. Once these points are assigned for each attribute, the scores are tallied up and an overall Borda count is obtained for each plan. The plans are then ranked accordingly in descending order to obtain a final ranking order. Table 1.5 shows a summary of the Borda count rankings for the four pretomanid plans according to: Liu > Otera > Pathogenesis ≫ Sorensen. The Liu plan scored highest in three attributes: PMI, RSGI, and SI; whereas the Otera plan scored highest in two attributes: SR and SI. The Pathogenesis plan scored highest in only the IEE attribute, and the Sorensen plan ranked lowest in all attributes except SI.

In the poset dominance method, we first need to determine the number of pairwise attributes and the number of pairwise plan comparisons for each pairwise attribute in order to determine the overall size of the ranking exercise. Since there are five attributes, there are $5!/((5-2)!\,2!) = 10$

Table 1.5 Borda count ranking results of the four syntheses of pretomanid beginning with 4-nitroimidazole.

Plan	Borda score	Rank
Liu	17	1
Otera	16	2
Pathogenesis	14	3
Sorensen	8	4

pairwise attribute comparisons. The explicit list is as follows: PMI *versus* SR, PMI *versus* IEE, PMI *versus* RSGI, PMI *versus* SI, SR *versus* IEE, SR *versus* RSGI, SR *versus* SI, IEE *versus* RSGI, IEE *versus* SI, and RSGI *versus* SI. Since four synthesis plans are considered, there are $4!/((4-2)!\,2!) = 6$ pairwise plan comparisons that need to be made. Therefore, in total there are $10 \times 6 = 60$ pairwise comparisons that need to be made in the entire poset analysis for this illustrative example of pretomanid plans. For a given pairwise plan comparison, for a pair of attributes there are two possible outcomes: (a) a comparable pair in which plan A dominates plan B for both attributes X and Y; and (b) an incomparable pair in which plan A dominates plan B for attribute X and plan B dominates plan A for attribute Y. When a comparable pair for a given pairwise attribute comparison is found the dominant plan is identified. This sequence of steps is repeated for each pairwise attribute comparison and then the number of dominant occurrences for each plan is tallied up. As an example, if we consider the PMI *versus* SR comparison, we find that the ranking order for PMI is Liu > Otera > Pathogenesis > Sorensen and the ranking order for SR is Otera > Pathogenesis > Liu > Sorensen. The Liu *versus* Otera and Liu *versus* Pathogenesis comparisons result in incomparable pairs for both the PMI and SR attributes, *i.e.*, Liu dominates Otera for PMI but Otera dominates Liu for SR, and Liu dominates Pathogenesis for PMI but Pathogenesis dominates Liu for SR. However, the Liu *versus* Sorensen comparison results in a comparable pair since the Liu plan dominates the Sorensen plan in both PMI and SR attributes. Furthermore, the Otera plan dominates the Pathogenesis and Sorensen plans in both PMI and SR, and the Pathogenesis plan dominates the Sorensen plan in both PMI and SR. As a result of these pairwise comparisons, the Liu plan is assigned 1 dominance, the Otera plan is assigned 2 dominances, the Pathogenesis plan is assigned 1 dominance, and the Sorensen plan is assigned a 0 dominance. Table 1.6 summarizes the results of the 60-pair poset dominance analysis for the four pretomanid plans where the overall ranking order is as follows: Otera = Liu > Pathogenesis $\gg$ Sorensen. We observe that both ranking methods essentially give the same ranking result, since there is only a one-point difference between the Otera and Liu methods in the Borda count method compared to identical points in the poset method.

Table 1.6 Poset ranking results of the four syntheses of pretomanid beginning with 4-nitroimidazole.

Plan	Poset dominances	Rank
Otera	12	1
Liu	12	1
Pathogenesis	7	2
Sorensen	0	3

1.5 Conclusion

In this chapter, we have illustrated how process mass intensity (PMI), sacrificial reagent (SR) consumption, input enthalpic energy (IEE) consumption, Rowan solvent greenness index (RSGI), and sustainability index (SI) based on valorized input and output materials and fraction of renewable energy consumption can be used to evaluate overall synthesis plan greenness. Based on these five key attributes, it is possible to rank synthesis plans in an unbiased way by using Borda count or poset dominance analysis. In this illustrative example of four pretomanid syntheses beginning from the same starting material, we find that the Otera plan's claim to follow green chemistry principles is supported by the present quantitative analysis. We also have shown that the competing plan documented by Liu and coworkers is also highly ranked. Further improvements to the synthesis of this pharmaceutical are always possible and such plans can be evaluated by the same methodology described in this work, provided that full disclosure of their plan details is made. The sustainability index determined from input provenance and output fate is sensitive to various assumptions in the determination of the four contributing fractions and hence its reliability is strongly governed by the availability of detailed experimental procedures, and thermodynamic (temperature dependent heat capacity functions for substances and equation of state data), toxicological, and safety-hazard parameters for all materials involved. The most challenging contributing mass fraction to SI to determine is FVP, since there are no repository databases that keep track of each chemical commodity's fate once it is produced by any sector of the chemical industry. Nevertheless, the evaluation of SI is straight forward, and it is hoped that it will find use among process chemists to evaluate their plans according to green chemistry principles in a more rigorous, robust, and convincing way.

References

1. B. Trost, *Science*, 1991, **254**, 1471.
2. *Green Chemistry Metrics – Measuring and Monitoring Sustainable Processes*, ed. A. Lapkin, and D. Constable, Wiley, Chichester, 2008.
3. *Handbook of Green Chemistry – Green Metrics*, ed. D. J. C. Constable and C. Jiménez-González, Wiley-VCH, Weinheim, 2018, vol. 11.
4. A. P. Dicks and A. Hent, *Green Chemistry Metrics – A Guide to Determining and Evaluating Process Greenness*, Springer, Heidelberg, 2015.
5. J. Andraos, *Reaction Green Metrics: Problems, Exercises, and Solutions*, CRC Press-Taylor & Francis, Boca Raton, 2019.
6. J. Andraos, *Synthesis Green Metrics: Problems, Exercises, and Solutions*, CRC Press-Taylor & Francis, Boca Raton, 2019.
7. F. G. Calvo-Flores, *ChemSusChem*, 2009, **2**, 905.
8. M. Eissen and J. O. Metzger, *Chem. - Eur. J.*, 2002, **8**, 3580.
9. J. Andraos, *ACS Sustainable Chem. Eng.*, 2018, **6**, 3206.

10. J. Andraos, *ACS Sustainable Chem. Eng.*, 2016, **4**, 1917.
11. J. Andraos and A. Hent, *J. Chem. Educ.*, 2015, **92**, 1820.
12. J. Andraos and A. Hent, *J. Chem. Educ.*, 2015, **92**, 1831.
13. J. Andraos and M. Sayed, *J. Chem. Educ.*, 2007, **84**, 1004.
14. J. Andraos, *Org. Process Res. Dev.*, 2006, **10**, 212.
15. C. Jimenez-Gonzalez, C. S. Ponder, Q. B. Broxterman and J. B. Manley, *Org. Process Res. Dev.*, 2011, **15**, 912.
16. C. Hogue, *Chem. Eng. News*, 2019, **97**, 19.
17. P. Hinderink, H. J. van der Kooi and J. de Swaan Arons, *Green Chem.*, 1999, **1**, G176.
18. J. Dewulf, H. van Langenhove, J. Mulder, M. M. D. van den Berg, H. J. van der Kooi and J. de Swaan Arons, *Green Chem.*, 2000, **2**, 108.
19. S. Lems, H. J. van der Kooi and J. de Swaan Arons, *Green Chem.*, 2002, **3**, 308.
20. E. Csefalvay, G. R. Akien, L. Qi and I. T. Horvath, *Catal. Today*, 2015, **239**, 50.
21. I. T. Horvath, E. Csefalvay, L. T. Mika and M. Debreczeni, *ACS Sustainable Chem. Eng.*, 2017, **5**, 2734.
22. E. Csefalvay and I. T. Horvath, *ACS Sustainable Chem. Eng.*, 2018, **6**, 8868.
23. S. Sikdar, *AIChE J.*, 2003, **49**, 1928.
24. R. A. Sheldon and J. P. M. Sanders, *Catal. Today*, 2015, **239**, 3.
25. C. Fadel and K. Tarabieh, *Resources*, 2019, **8**, 115.
26. I. T. Horvath and E. Csefalvay, in *Green Synthetic Processes and Procedures*, ed. R. Ballini, Royal Society of Chemistry, London, 2019, ch. 1.
27. J. Andraos, *Beilstein J. Org. Chem.*, 2020, **16**, 2346.
28. J. C. de Borda, *Mémoire de l'Académie Royale. Histoire de l'Académie des Sciences*, 1781, 657. http://gerardgreco.free.fr/IMG/pdf/MA_c_moire-Borda-1781.pdf, accessed September 2019.
29. D. G. Saari, *The Optimal Ranking Method Is the Borda Count*, International Institute for Applied Systems Analysis, Laxenburg, Austria, 1985.
30. G. Restrepo and P. F. Stadler, *ACS Sustainable Chem. Eng.*, 2016, **4**, 2191.
31. J. Andraos, *Green Process. Synth.*, 2019, **8**, 787.
32. W. R. Baker, C. Shaopei and E. R. Keeler, *World Pat.*, WO9701562, Pathogenesis Corporation, 1997.
33. A. Orita, K. Miwa, G. Uehara and J. Otera, *Adv. Synth. Catal.*, 2007, **349**, 2136.
34. M. A. Marsini, P. J. Reider and E. J. Sorensen, *J. Org. Chem.*, 2010, **75**, 7475.
35. X. Liu, L. Wang, L. Mi and W. Chen, *Liu Pat.*, CN104177372, Fourth Military Medical University, 2014.
36. A. Lee, Y. L. Xie, C. E. Barry and R. Y. Chen, *Br. Med. J.*, 2020, **368**, m216.
37. P. Nahid, S. E. Dorman, N. Alipanah, P. M. Barry, J. L. Brozek, A. Cattmanchi, L. H. Chaisson, R. E. Chaisson, C. L. Daley, M. Grzemska, J. M. Higashi, C. S. Ho, P. C. Hopewell, S. A. Keshavjee, C. Lienhardt, R. Menzies, C. Merrifield, M. Narita, R. O'Brien, C. A. Peloquin, A. Raftery, J. Saukkonen, H. S. Schaaf, G. Sotgiu, J. R. Starke, G. B. Migliori and A. Vernon, *Clin. Infect. Dis.*, 2016, **63**, e147.

38. C. D. Mitnick, B. McGee and C. A. Peloquin, *Expert Opin. Pharmacother.*, 2009, **10**, 381.
39. A. Zumla, J. Chakaya, R. Centis, L. D'Ambrosio, P. Mwaba, M. Bates, N. Kapata, T. Nyirenda, D. Chanda, S. Mfinaga, M. Hoelscher, M. Mauerer and G. B. Migliori, *Lancet Respir. Med.*, 2015, **3**, 220.
40. *Treatment of Tuberculosis Guidelines*, World Health Organization, Geneva, 4th edn, 2010.
41. S. R. Pedada, V. S. Satam, P. J. Tambade, S. A. Kandadai, R. M. Hindupur, H. N. Pati, D. Launay and D. Martin, *Org. Process Res. Dev.*, 2013, **17**, 1149.
42. K. Shinhama, *US Pat.*, US20090082575, Otsuka Pharmaceutical Company Limited, 2009.
43. Ontario's System-wide Electricity Supply Mix, 2017 Data, https://www.oeb.ca/sites/default/files/2017-supply-mix-data.pdf, accessed September 2019.
44. Archived – 2017 Long-term Energy Plan: Discussion Guide, https://www.ontario.ca/document/2017-long-term-energy-plan-discussion-guide/ontarios-energy-mix-end-2015, accessed September 2019.
45. C. S. Slater and M. Savelski, *J. Environ. Sci. Health, Part A*, 2007, **42**, 1595.

CHAPTER 2

Homogeneous Catalysis

FELIPE DE LA CRUZ-MARTÍNEZ[a], MARC MARTÍNEZ DE SARASA BUCHACA[a], CARLOS ALONSO-MORENO[b], AGUSTIN LARA-SÁNCHEZ*[a] AND JOSÉ ANTONIO CASTRO-OSMA*[b]

[a]Universidad de Castilla-La Mancha, Departamento de Química Inorgánica, Orgánica y Bioquímica-Centro de Innovación en Química Avanzada (ORFEO–CINQA), Facultad de Ciencias y Tecnologías Químicas, 13071-Ciudad Real, Spain; [b]Universidad de Castilla-La Mancha, Departamento de Química Inorgánica, Orgánica y Bioquímica-Centro de Innovación en Química Avanzada (ORFEO–CINQA), Facultad de Farmacia, 02071-Albacete, Spain
*E-mail: Agustin.Lara@uclm.es, JoseAntonio.Castro@uclm.es

2.1 Introduction

The rapid growth of the human population has caused a high impact on the planet, resulting in the depletion of its resources and an increase in pollution. This fact is threatening the environment and causing health issues; therefore, more sustainable development is required. In 1987, the World Commission on Environment and Development stated that "*sustainable development should meet the needs of the present without compromising the ability of future generations to meet their own needs*".[1] Sustainable chemistry can be defined as one which: "*should use resources, including energy, at a rate at which they can be replaced naturally, and the generation of waste cannot be faster than the rate of their remediation*".[2] In this context, green chemistry emerged in the 1980s focusing on the elimination of the wastes generated by the industrial sector to minimise pollution of the environment.[3,4] Therefore, it is desired

Sustainable Organic Synthesis: Tools and Strategies
Edited by Stefano Protti and Alessandro Palmieri

Published by the Royal Society of Chemistry, www.rsc.org

that chemicals, reactions and processes are both sustainable and green at the same time when developing new synthetic methodologies.

Green chemistry is defined as the "*design of chemical products and processes that reduce or eliminate the use and generation of hazardous substances*".[5] Green chemistry aims at the efficient utilization of (preferably renewable) raw materials, and the elimination of waste, toxic and/or hazardous reagents and solvents in the manufacture and application of chemicals. This can be achieved by meeting the Twelve Principles of Green Chemistry in the development of new synthetic methodologies.[6]

1. It is better to prevent waste than to treat or clean up waste after it is formed.
2. Synthetic methods should be designed to maximise the incorporation of all materials used in the process into the final product.
3. Wherever practicable, synthetic methodologies should be designed to use and generate substances that possess little or no toxicity to human health and the environment.
4. Chemical products should be designed to preserve efficacy of function while reducing toxicity.
5. The use of auxiliary substances (*e.g.* solvents, separation agents *etc.*) should be made unnecessary wherever possible and innocuous when used.
6. Energy requirements should be recognized for their environmental and economic impact and should be minimized. Synthetic methods should be conducted at ambient temperature and pressure.
7. A raw material or feedstock should be renewable rather than depleting wherever technically and economically practicable.
8. Unnecessary derivatization (blocking group, protection/deprotection, temporary modification of physical/chemical processes) should be avoided whenever possible.
9. Catalytic reagents (as selective as possible) are superior to stoichiometric reagents.
10. Chemical products should be designed so that at the end of their function they do not persist in the environment and break down into innocuous degradation products.
11. Analytical methodologies need to be further developed to allow for real-time, in-process monitoring and control prior to the formation of hazardous substances.
12. Substances and the form of a substance used in a chemical process should be chosen so as to minimise the potential for chemical accidents, including releases, explosions and fires.

Green metrics provide important indicators to measure how green a process is. Although several metrics have been proposed, such as Reaction Mass Efficiency (RME) or Process Mass Intensity (PMI), the E-factor (environmental factor) and the Atom Economy (A. E.) are the most widely used.

The E-factor, defined as the mass of waste generated per mass of product (Eqn (2.1)),[7] is used to evaluate the amount of waste generated per kg of product synthesised in a chemical process.[8]

$$E = \frac{\text{Mass of waste (kg)}}{\text{Mass of final product (kg)}} \tag{2.1}$$

The table of E-factors for chemical industries (see Table 2.1) was published in 1992[9] and encourages fine chemical and pharmaceutical industries to reduce the quantity of waste generated in their processes. This is because the synthesis of fine chemicals and pharmaceuticals usually involves multi-step and stoichiometric syntheses rather than catalytic processes.

Another important factor to consider is the atom economy, which is calculated by dividing the molecular weight of the final desired product by the sum of the molecular weights of all chemical precursors, and expressed as a percentage (Eqn (2.2)).[10] Atom economy addresses the question of selectivity in organic chemistry and it is an important parameter in order to evaluate the amount of waste that can be generated.

$$\text{A. E.} = \frac{\text{Molecular weight of product}}{\text{Molecular weights of reagents}} \times 100 \tag{2.2}$$

It is expected that the E-factor and the A. E. are close to 0 and 100% respectively for a sustainable synthetic methodology. As can be seen in Scheme 2.1, the use of a catalyst has a huge impact on the E-factor and the A. E. in the oxidation reaction of 1-phenylethan-1-ol. The E-factor of *ca.* 0.1 and the A. E. close to 90% assures the development of more sustainable processes by the use of catalysis.

Table 2.1 E-Factors for chemical industries.

Industry sector	Tonnage	E-Factor (kg waste/kg product)
Oil refining	10^6–10^8	<0.1
Bulk chemicals	10^4–10^6	<1–5
Fine chemicals	10^2–10^4	5 to >50
Pharmaceuticals	10–10^3	25 to >100

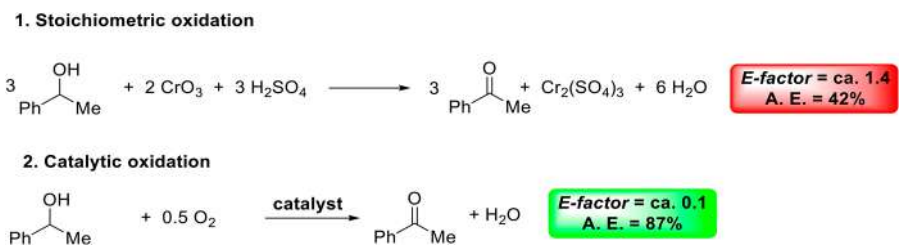

Scheme 2.1 Atom economies and E-factors for the stoichiometric and catalytic oxidation of 1-phenylethan-1-ol.

In recent decades, life cycle assessment (LCA) has emerged as a method for evaluating the environmental impact of a chemical product.[11–13] LCA not only analyses the extraction of the raw material and the production of the chemical product, which is known as cradle-to-gate analysis, but the whole life cycle of a product or process, from the extraction of raw materials to production, distribution, use and disposal or recycling of the product, which is known as cradle-to-grave analysis.

2.2 Catalysis

One of the major sources of waste generation is the use of stoichiometric reagents in organic synthesis, such as stoichiometric oxidations and reductions or the use of Lewis and Brønsted acids or bases in classical chemical syntheses. Therefore, it is required to shift from stoichiometric reactions with low atom economy and high E-factor to catalytic processes in which the amount of waste generated is minimised. A representative example could be the use of sustainable H_2, produced *via* water splitting using renewable electricity, in reduction reactions and in the presence of a catalyst instead of using stoichiometric amounts of $NaBH_4$ as a hydrogen source. In this scenario, no metal salts would be generated as by-products.

The term catalyst is defined by the IUPAC as "*a substance that increases the rate of a reaction without modifying the overall standard Gibbs energy change in the reaction; the process is called catalysis. The catalyst is both a reactant and product of the reaction*".[14] Two important parameters to evaluate the catalytic activity are the turnover number (TON) and turnover frequency (TOF) (Eqn (2.3) and (2.4)). The turnover number measures the number of turns of a catalytic cycle and is defined as the number of moles of products that a catalyst produces per mole of catalyst. On the other hand, the turnover frequency is the number of catalytic cycles in a specific time period.

$$\text{TON} = \frac{\text{mol product}}{\text{mol catalyst}} \tag{2.3}$$

$$\text{TOF} = \frac{\text{TON}}{\text{time (h)}} \tag{2.4}$$

A catalyst not only increases the reaction rate but can also direct the reaction to yield a certain product. Selectivity is one of the most important factors to control in catalysis since a subtle change in the catalyst may have a big influence on its selectivity. Different types of selectivity can be present in a chemical transformation (Scheme 2.2):[15]

1. Chemoselectivity, when one functional group reacts in the presence of other functional groups present within the same molecule.
2. Regioselectivity, when the reaction takes place at a specific atom in preference to the others within the same functional group.

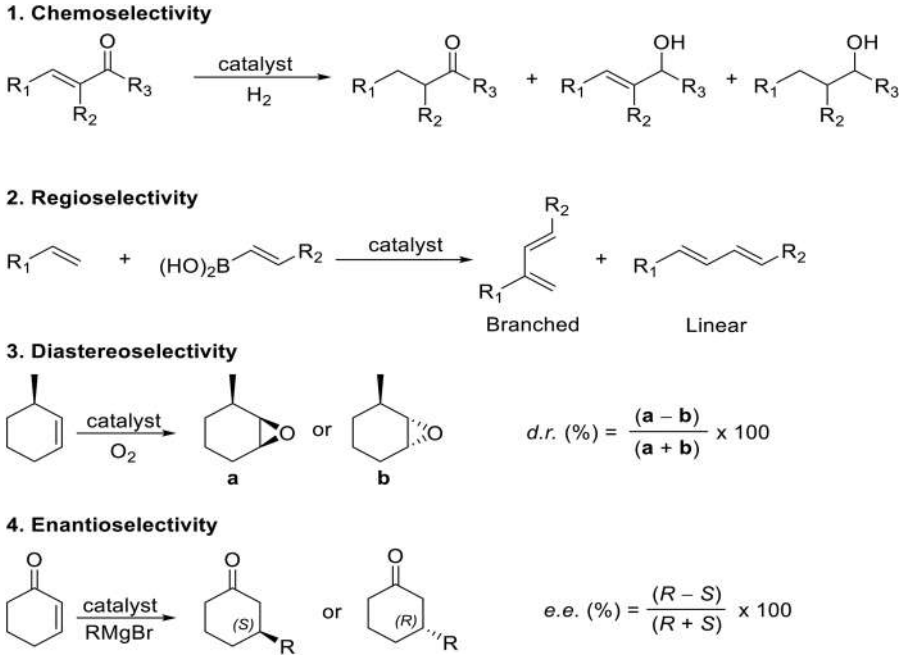

Scheme 2.2 Reaction selectivity in a chemical transformation.

3. Diastereoselectivity, when the reagent contains a stereogenic centre or diastereotopic faces and can direct the reaction to give two diastereoisomers in a different ratio (d.r., % represents the diastereoisomeric ratio of the possible diastereoisomers).
4. Enantioselectivity, when the substrate is achiral or contains enantiotopic faces and the use of an enantiopure catalyst produces one single enantiomer (e.e., % represents the enantiomeric ratio of the possible enantiomers).

To date, catalysis plays a fundamental role in the production of fuels, polymeric materials and chemical products in industry.[16–29] Even though heterogeneous catalysis is predominantly utilised in industry,[17,30,31] the use of homogeneous catalysts for the synthesis of fine chemicals has increased over the last few decades.[15,32–35] This can be explained by the fact that the mechanism of homogeneous-catalysed processes can be studied in detail easily by using modern techniques to detect reaction intermediates. In particular, great attention has been devoted to the use of metal catalysts to enable a range of chemical transformations such as hydrogenation, hydroformylation or C–heteroatom bond formation reactions (Scheme 2.3).[29,36–41]

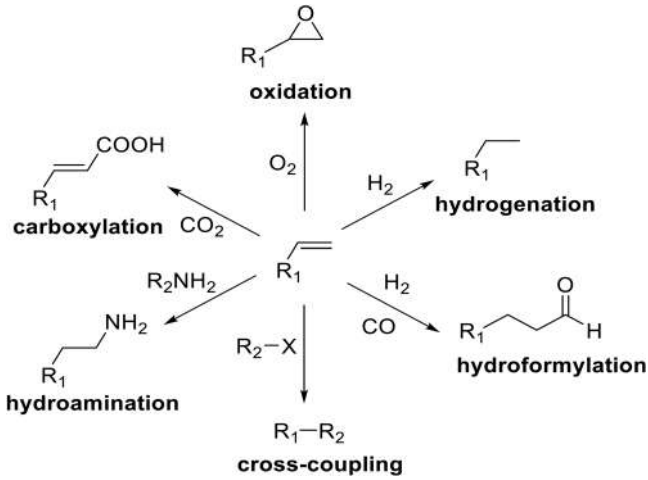

Scheme 2.3 Representative transformations of metal-catalysed processes.

2.3 Homogeneous Catalysis

Homogeneous catalysis refers to a catalytic process in which the catalyst and reagents are in the same phase, generally in solution. Even though a great variety of homogeneous catalysts, such as organocatalysts, enzymes, acids and bases or organometallic complexes, have been used for the synthesis of organic molecules and polymers,[42] this book chapter will be strictly focused on the use of metal complexes as homogenous catalysts for chemical transformations.

The most relevant industrial processes catalysed by homogeneous metal catalysts in industry are reflected in Figure 2.1. These processes are usually based on noble metal catalysts that are costly and whose abundance is very limited (Figure 2.2).[43] The choice of the metal centre is crucial to increase the activity and selectivity of a catalytic process, but it is desirable to pursue the use of Earth-abundant metal catalysts to maximise the sustainability of the process, due to their availability and low cost.[44] However, in many cases noble metal-based catalysts display activities and selectivities several orders of magnitude higher than Earth-abundant metal catalysts, such as the Cativa™ process and the Monsanto industrial synthesis of L-DOPA for which an iridium and rhodium catalyst are used, respectively. Iron complexes have shown high catalytic activity and selectivity for a range of organic transformations and are a potential alternative to noble-metal catalysts; however, the catalytic activity displayed by these complexes is usually lower than that observed when ruthenium catalysts are used.[45–47] Therefore, further improvements in the design of sustainable Earth-abundant metal catalysts are required to improve their catalytic activity and selectivity.

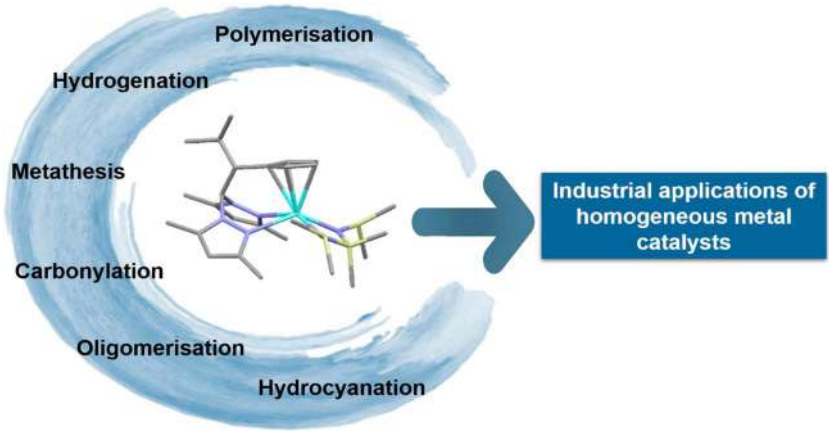

Figure 2.1 Industrial application of homogeneous catalysts to enable chemical transformations.

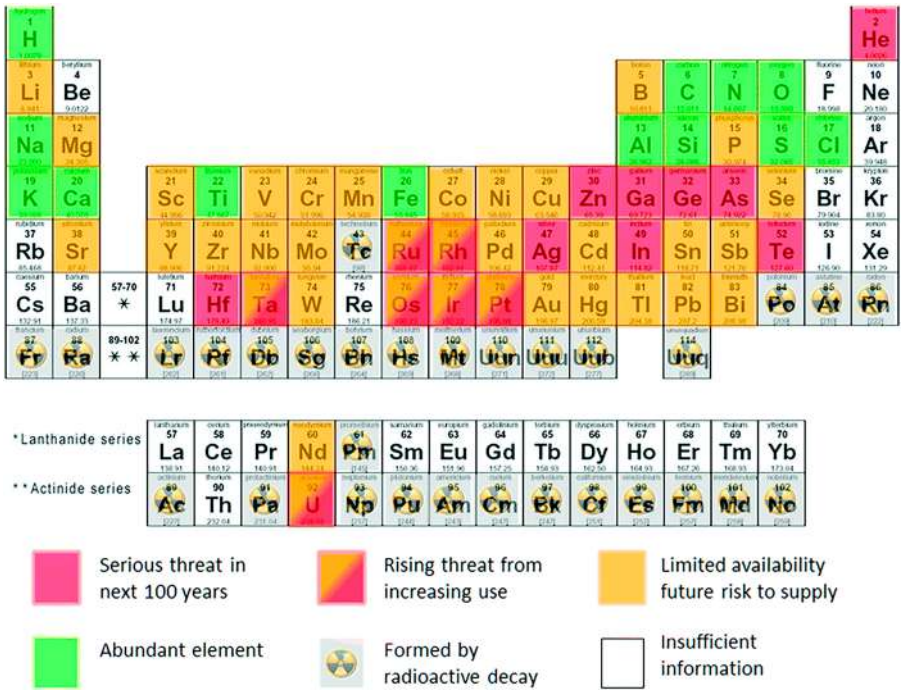

Figure 2.2 Representation of elemental sustainability. Reproduced from ref. 43 with permission from The Royal Society of Chemistry.

Ligand design is also key in homogeneous catalysis. Fine tuning the coordinated ligands may allow the formation of different organic products from the same reagents (see Scheme 2.4).[48] Besides, the catalytic activity can also be modulated for the auxiliary ligands surrounding the metal.[48] In fact, a great variety of metal complexes containing salen, P-based, pincer, porphyrin, scorpionate,

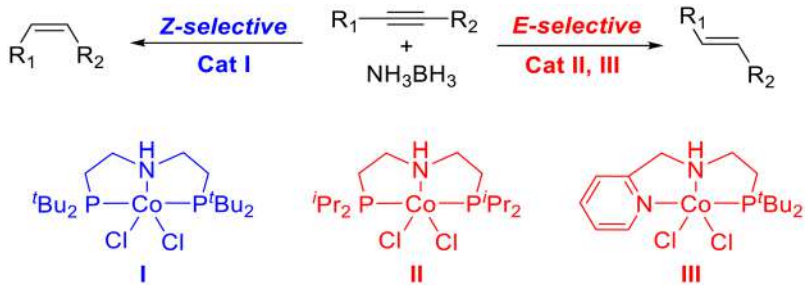

Scheme 2.4 Ligand-controlled hydrogenation of alkynes catalysed by cobalt complexes. Adapted from ref. 48 with permission from The American Chemical Society.

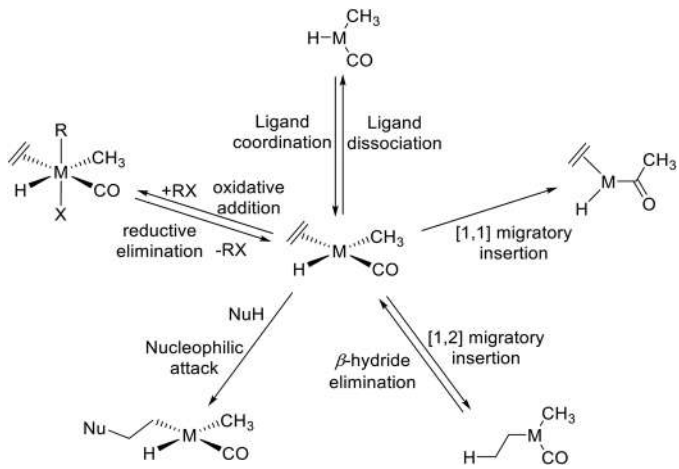

Scheme 2.5 Elementary steps in homogeneous catalysis. Adapted from ref. 42 with permission from Wiley.

and N-heterocyclic carbene ligands, among others, have been reported in the literature.[49–55] The ligand forces the metal centre to adopt a certain geometry and, therefore, improves the activity and selectivity of the catalyst.

Most homogeneous catalytic processes can be described as a combination of elementary reactions, such as ligand coordination and dissociation reactions, oxidative addition and reductive elimination reactions, migratory insertions and β-hydride elimination reactions (Scheme 2.5). Those interested in these elementary steps are recommended to read the following ref. 15 and 42.

2.4 Model Examples

In this section, some remarkable advances in the use of Earth-abundant metal complexes as homogeneous catalysts for hydrogenation processes, C–C and C–heteroatom bond forming reactions and polymerisation reactions for the sustainable synthesis of organic molecules and polymeric materials will be described.

2.4.1 Hydrogenation Reactions

Amongst the different catalytic reactions, the catalytic hydrogenation of unsaturated reagents is the most versatile process. It allows the selective synthesis of a broad range of chemical products in high yield under mild reaction conditions using metal complexes as catalysts. Solid-supported metal catalysts based on Pd, Pt, Rh, Ru and Ni have been used in industry for the chemoselective hydrogenation of organic compounds.[56,57] Since the development of Wilkinson's catalyst,[58] homogeneous catalysts based on Ru, Rh and Ir complexes supported by different enantiopure ligand scaffolds have allowed the stereoselective hydrogenation of unsaturated functional groups (Scheme 2.6).[59,60] In general, the hydrogenation catalyst systems comprise a noble-metal centre and one or more (enantiopure) ligands and anions, which can activate the H_2 molecule and add two hydrogen atoms to the unsaturated group. However, the development of non-precious metal-based complexes as hydrogenation catalysts has risen in recent years due to their lower cost, higher abundance and lower toxicity of the metal centre, in addition to their different reactivity compared to noble-metals.[46,60,61] Nevertheless, the use of precious-metal catalysts is still quite high due to their much higher catalytic activity and productivity, and the high recovery of the catalyst.

Outstanding achievements have been reported on the use of non-noble metal catalysts for hydrogenation processes. A chiral cobalt complex containing an electron-donating diphosphine ligand has been recently developed as a highly effective catalyst for the asymmetric hydrogenation of more than 30 α-substituted α,β-unsaturated acids with enantioselectivities up to >99% e.e. in isopropanol using Zn as an additive (Scheme 2.7).[62] The synthetic protocol has been successfully applied for the enantioselective synthesis of key intermediates in the synthesis of chiral drugs such as (*S*)-Equol, Rupintrivir, Sacubitril, Naproxen, Ibuprofen and Artemisinin. Control experiments and mechanistic studies suggested that the carboxylic acid group may interact with the metal centre to control the catalytic activity and the enantioselectivity of the process, since α,β-unsaturated esters did not react under standard conditions.

In recent years, many methods for CO_2 hydrogenation have been reported.[63,64] The most promising solution to the global energy problem is the hydrogenation of CO_2 to produce methanol, which is a valuable chemical

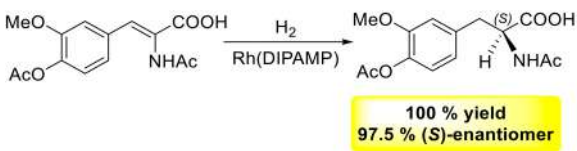

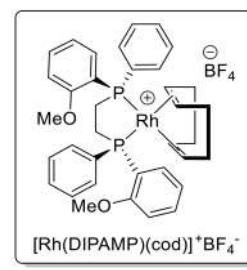

Scheme 2.6 Rhodium catalyst for the L-DOPA process.

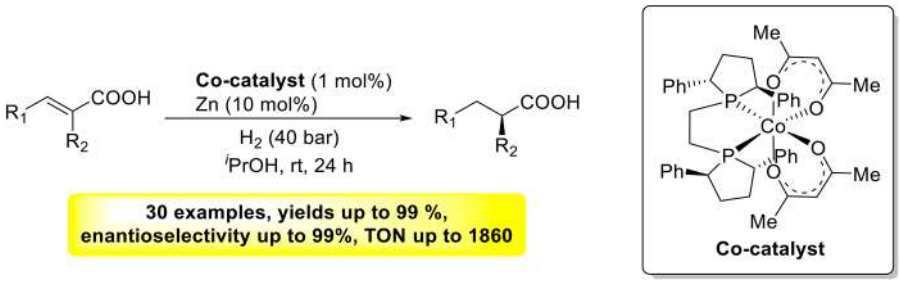

Scheme 2.7 Cobalt-catalysed enantioselective hydrogenation of α,β-unsaturated acids.

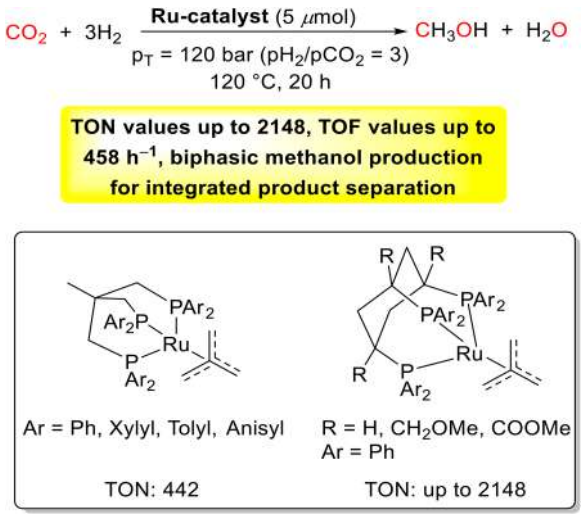

Scheme 2.8 Synthesis of methanol using ruthenium complexes containing tripodal P-based ligands.

intermediate for the synthesis of organic molecules and polymeric materials, as a sustainable alternative to the traditional synthesis from CO and H_2. Heterogeneous catalysts have been actively investigated with some success, but the conditions are still too harsh with the requirement of high temperature (>200 °C) and high pressure of CO_2 and H_2 (>50 bar).[63,64] On the other hand, the homogeneous direct hydrogenation of CO_2 to methanol has been less studied than heterogeneous catalysis and has been pursued especially with ruthenium catalysts. The formation of methanol, together with methane and CO, from CO_2 hydrogenation was achieved for the first time by using $Ru_3(CO)_{12}$ as a catalyst in the presence of alkaline iodides under harsh reaction conditions (240 °C, 80 bar).[65] In 2012, ruthenium complexes supported by Triphos ligands were reported as catalysts for the one-pot hydrogenation of CO_2 to methanol (Scheme 2.8).[66] In recent years, a range of tripodal P-based ligands

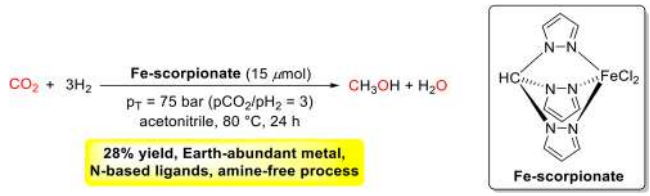

Scheme 2.9 Synthesis of methanol using an iron scorpionate complex.

have also been synthesised for application in the direct hydrogenation of CO_2, which has resulted in the development of homogeneous catalysts with unprecedented catalytic activity (Scheme 2.8), obtaining TON values up to 1100 for the direct hydrogenation of CO_2 or TON values up to more than 2100 when alcoholic solvents were used.[67–72]

There are only two homogeneous non-noble metal catalytic systems for the direct hydrogenation of CO_2 to methanol. The first Earth abundant metal-based catalyst system reported for this reaction comprised a combination of $Co(acac)_3$, a Triphos ligand and $HNTf_2$ as an acid additive, obtaining TON values up to 78 after 96 hours of reaction in a mixture of solvents THF : EtOH using 20 bar of CO_2 and 70 bar of H_2 pressure at 100 °C.[73]

The use of a scorpionate iron complex is a more sustainable alternative to the use of ruthenium and phosphorous-based ligands for the synthesis of methanol from CO_2 and H_2.[74] This process allows the conversion of carbon dioxide into methanol using an Earth-abundant metal catalyst containing nitrogen-based ligands. The iron compound catalysed the hydrogenation of CO_2 into methanol in acetonitrile using a low catalyst loading at 80 °C and 75 bar of total pressure (pH_2/pCO_2 = 3), obtaining methanol in 28% yield (Scheme 2.9). The use of pentaethylenehexamine (PEHA) was beneficial for the process and allowed an increase in the yield of methanol to 46%. However, even though the yield of methanol is higher when using PEHA, the sustainability of the process increases when the reaction is carried out under amine-free conditions.

2.4.2 C–C Bond Forming Reactions

Carbon–carbon bond forming reactions are fundamental transformations in organic synthesis. In this context, the development of highly efficient metal complexes as catalysts for C–C bond formation has received much attention.[75–77] Transition metal complexes have been traditionally used to promote C–C bond formation due to their high catalytic activity and functional group tolerance.[75,78–81] However, in recent years there has been a huge expansion in the use of homogeneous iron catalysts as an alternative to noble or expensive transition metal-based catalysts for cross-coupling reactions for the synthesis of pharmaceuticals and natural products.[82–87]

In 2018, the use of an iron(III) complex containing an NHC ligand as a catalyst was reported for the first time for the Suzuki biaryl cross-coupling reaction of organoborates and aryl chlorides at the *ortho* position containing

a π-coordinating directing group such as a pyrrole in the presence of $MgBr_2$ as an additive in THF at 60 °C for 3 hours (Scheme 2.10). Under the optimal reaction conditions, the catalyst system was able to couple a broad range of *N*-pyrrole amide-based aryl chlorides with substituted boronates affording the coupling products from moderate to good yields.[88]

A new class of chiral iron complexes containing two bidentate *N*-(2-pyridyl)-substituted NHC ligands have been recently developed as catalysts for the enantioselective Cannizzaro reaction of phenylglyoxal monohydrate and a broad range of alcohols to afford the corresponding mandelate ester product (Scheme 2.11a).[89] Under the optimised reaction conditions, the chiral-at-iron complexes catalysed the enantioselective formation of the mandelate esters in yields up to 96% and selectivities up to 88%, although

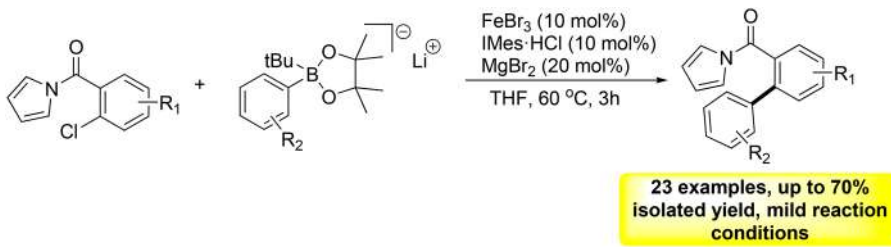

Scheme 2.10 Iron-catalysed Suzuki biaryl cross-coupling reactions.

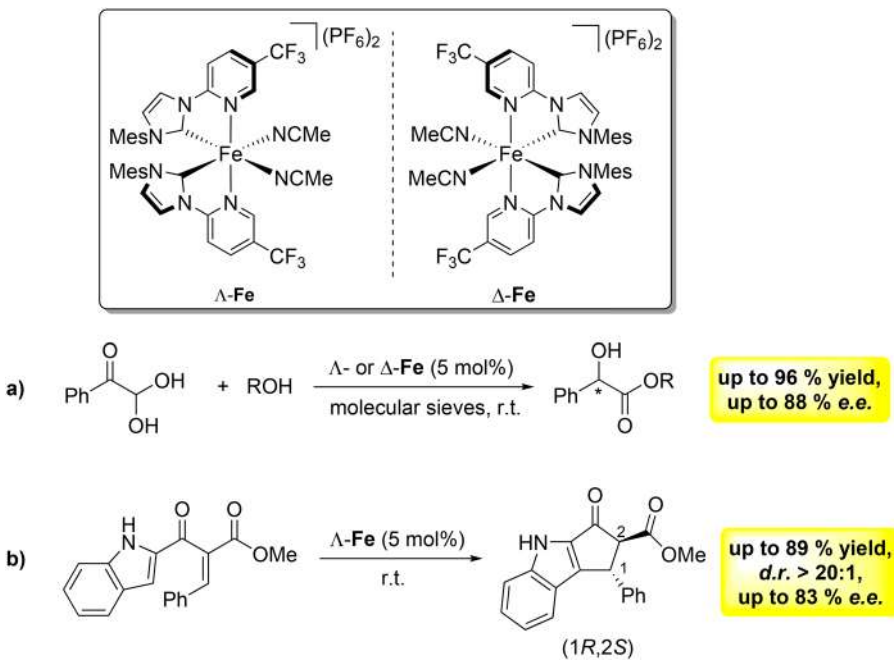

Scheme 2.11 Chiral iron complexes catalysing the (a) enantioselective Cannizzaro reaction and (b) asymmetric Nazarov reaction.

the enantioselectivity is highly dependent on the catalyst loading, the solvent and the alcohol used. This iron complex also catalysed the asymmetric Nazarov cyclisation to afford chiral cyclopentanones in 89% yield, with d.r. > 20:1 and 83% e.e. under the optimal reaction conditions (Scheme 2.11b).[89] The enantiomeric excess was highly dependent on the concentration and the solvent used. This new approach to develop chiral iron complexes containing achiral ligands constitutes a good example to enhance the sustainability of a chemical process, since it combines the use of an Earth-abundant metal centre and easily accessible ligand scaffolds for the development of a highly active and selective catalyst for C–C bond formation.

2.4.3 C–Heteroatom Bond Forming Reactions

The interest in Earth-abundant metal catalysed C–heteroatom bond forming reactions is increasing, since C–heteroatom bonds are present in a broad range of natural products and organic molecules used as building blocks, pharmaceuticals, agrochemicals and smart materials.[90] C–heteroatom bond formation has been traditionally catalysed by precious metal catalysts such as Ir, Rh, Au and Ag,[91–95] but in the last decade much attention has been devoted to the use of Earth-abundant metal-based complexes as catalysts for this transformation.[35,96–100] In this context, aluminium, iron and calcium are the three most abundant metals in the Earth's crust and their complexes have been used with success in a range of C–heteroatom bond formations, such as hydroelementation reactions, N-formylation of amines or the synthesis of cyclic carbonates from epoxides and CO_2.[35,96–100]

A hydride aluminium complex was used as a catalyst for the anti-Markovnikov hydroboration of terminal alkynes with pinacolborane at 30 °C for 12–32 h, obtaining the corresponding *trans*-vinylboronate esters in good to excellent yields (Scheme 2.12).[101] Theoretical investigations concluded that the mechanism proceeds through the formation of an acetylide aluminium complex, which is the rate-determining step.

A calcium scorpionate complex based on highly fluorinated 3-phenyl hydrotris(indazolyl)borate has been shown to be an efficient catalyst for the intramolecular hydroamination reaction of 1-amino-2,2-dimethyl-4-pentene

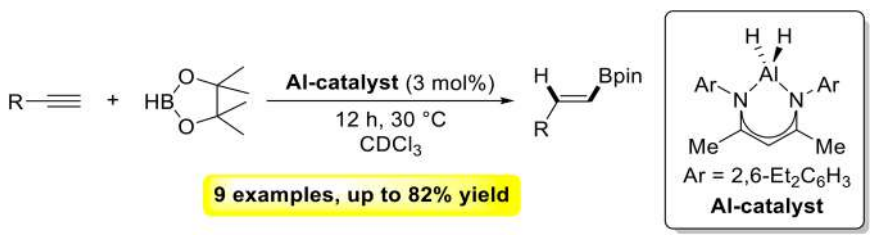

Scheme 2.12 Aluminium-catalysed anti-Markovnikov hydroboration of terminal alkynes.

at room temperature, obtaining the corresponding cyclic amine in good to excellent yields (57–99%) after only 6–27 minutes depending on the [substrate]:[Ca] ratio (Scheme 2.13).[102] The hydroamination reactions are first order with respect to the concentration of the substrate and the concentration of the catalyst. It is worth highlighting that this Ca complex constitutes one of the most active catalysts for the cyclohydroamination of 1-amino-2,2-dimethyl-4-pentene, obtaining TON and TOF values up to 342 and 19 min^{-1}, respectively.

A well-defined pincer iron complex has been recently developed as a highly efficient catalyst for the N-formylation of a broad range of amines through the hydrogenation of CO_2, obtaining the corresponding amide products in moderate to excellent yields using 0.02 mol% of catalyst loading (Scheme 2.14).[103] This pincer iron complex represents one of the most active catalysts for the N-formylation of amines, obtaining TON values higher than 4500 and high conversions after 4 hours.

Cyclic carbonate formation from epoxides and CO_2 is a 100% atom economic process that has been catalysed by a broad range of aluminium complexes.[43] In this context, bimetallic salen aluminium complexes have been shown to be excellent catalysts for this process even at room temperature and pressure, using tetrabutylammonium bromide (TBAB) as a cocatalyst.[104–110] Aminotriphenolate aluminium catalysts have also been developed as highly efficient catalysts for cyclic carbonate formation,[111–113] obtaining TOF values up to 906 h^{-1}. These complexes were shown to also be active for the synthesis of terpene-derived cyclic carbonates with high diastereoselectivity.[114]

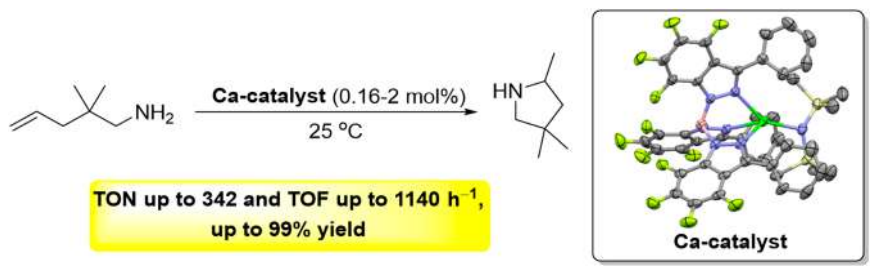

Scheme 2.13 Calcium-catalysed hydroamination of aminoalkenes.

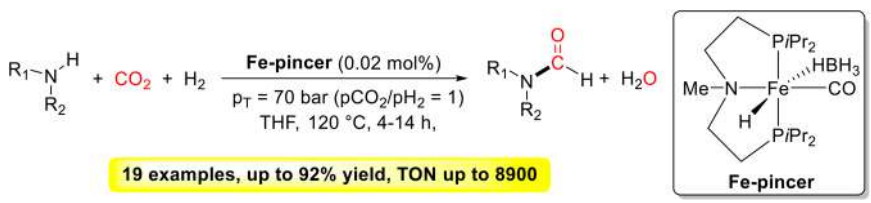

Scheme 2.14 Iron-catalysed N-formylation of amines *via* hydrogenation of CO_2.

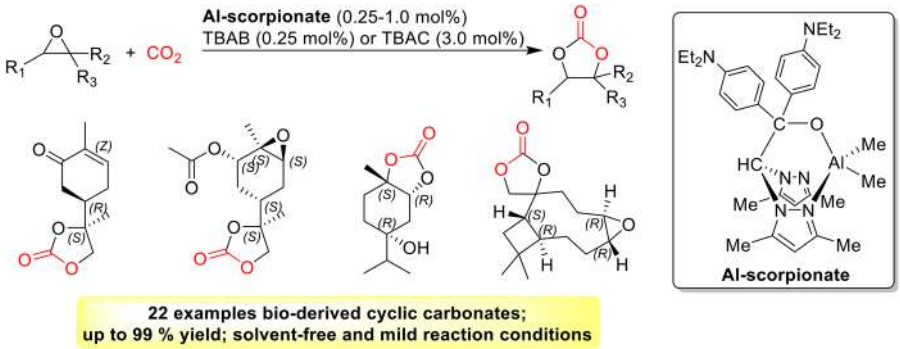

Scheme 2.15 Aluminium-catalysed synthesis of bioderived cyclic carbonates.

Scorpionate aluminium complexes have displayed good catalytic activity for the reaction of carbon dioxide and epoxides to afford a broad range of cyclic carbonates.[115–121] Amongst them, a scorpionate aluminium complex has recently been developed as a catalyst for the synthesis of a broad range of furan-, diacid- and terpene-derived cyclic carbonates from their corresponding bio-based epoxides and CO_2 under mild and solvent-free reaction conditions (Scheme 2.15).[122] It is worth highlighting that the synthesis of terpene-derived cyclic carbonates occurred with excellent diastereoselectivity, obtaining one single diastereoisomer in some cases. Moreover, some of the bis(cyclic carbonates) synthesised were used as bio-derived building blocks for the synthesis of non-isocyanate polyurethane materials *via* ring-opening reactions with 1,4-diaminobutane and 1,3-bis(aminomethyl)cyclohexane.

2.4.4 Polymerisation Reactions

The development of sustainable biodegradable polymeric materials to replace current petroleum-derived plastics is one of the biggest challenges for researchers in academia and industry. In this context, the use of appropriate metal-based catalysts for the catalytic transformation of renewable feedstocks into sustainable polymers is essential to accomplish such a challenge. The most relevant achievement in homogeneous catalysis by the use of Earth-abundant metals corresponds to the preparation of polyester and polycarbonate materials derived from bio-derived feedstocks *via* ring-opening copolymerisation (ROCOP) processes (Scheme 2.16a) as an alternative to the traditional synthesis of polyester and polycarbonate materials (Scheme 2.16b).

Homogeneous catalyst systems based on Al(III), Co(III), Cr(III), Fe(III) and Zn(II) supported by a broad range of ligands have been developed in recent decades and have displayed excellent catalytic activity and selectivity towards the ROCOP of (bioderived) epoxides and cyclic anhydrides or carbon dioxide to afford either polyester or polycarbonate materials (Scheme 2.17).[123–128]

The combination of an aminotriphenolate iron complex and PPNCl afforded the preparation of a broad range of bioderived polyesters from terpene oxides and aromatic anhydrides (Scheme 2.17a).[129] The polymerisation

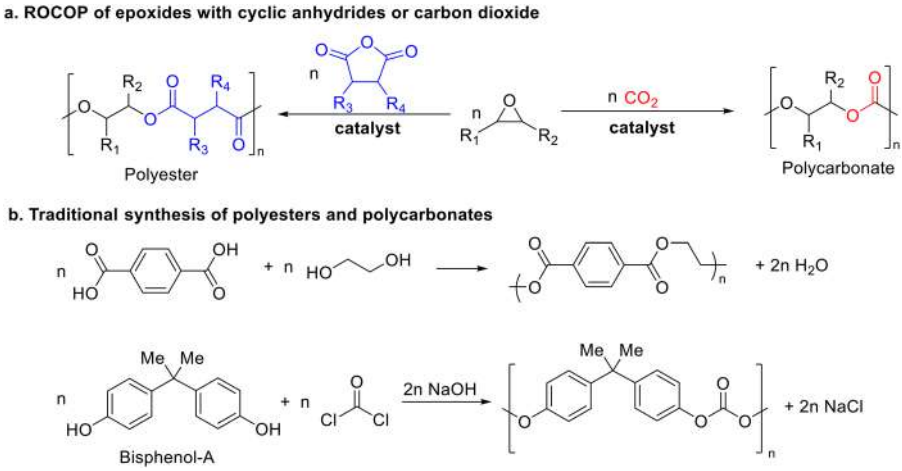

Scheme 2.16 (a) Ring-opening copolymerisation processes for the synthesis of polyesters or polycarbonates. (b) Traditional synthesis of polyesters and polycarbonates.

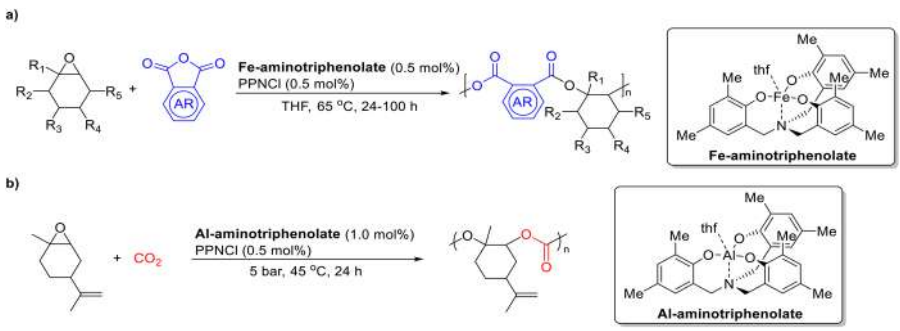

Scheme 2.17 (a) Iron-catalysed ROCOP of bioderived epoxides and aromatic cyclic anhydrides. (b) Aluminium-catalysed ROCOP of limonene oxide and carbon dioxide.

processes were carried out under mild reaction conditions using 0.5 mol% of catalyst loading in THF at 65 °C, obtaining the corresponding medium to high molecular weight polyester materials with a selectivity higher than 98%. It is worth highlighting that the thermal properties of the polyester materials prepared were highly dependent on the structure of the starting materials, obtaining glass transition temperatures (T_g) ranging from 53 to 243 °C. The same research group also employed an aminotriphenolate aluminium complex as the catalyst for the reaction of limonene oxide with carbon dioxide for the synthesis of stereoregular medium to high molecular weight polycarbonates with narrow polydispersities derived from renewable resources under mild and solvent-free reaction conditions (Scheme 2.17b). Although the catalyst system was able to convert both *cis*- and *trans*-LO, it showed preference for the ROCOP of carbon dioxide with *cis*-LO over *trans*-LO, obtaining the corresponding polycarbonate with around 70% *trans* units in its structure.[130]

The use of potentially renewable and fully renewable monomers for the synthesis of new bioderived and degradable block polyesters with high renewable content *via* ROCOP of limonene oxide (LO), ε-decalactone (DL) and tricyclic anhydrides (TCA) has been recently reported using a hetero-bimetallic complex as a catalyst in the presence of 1,4-benzene dimethanol as an initiating system at 140 °C (Scheme 2.18).[131] These block copolyester materials were investigated as pressure-sensitive adhesives, showing that for

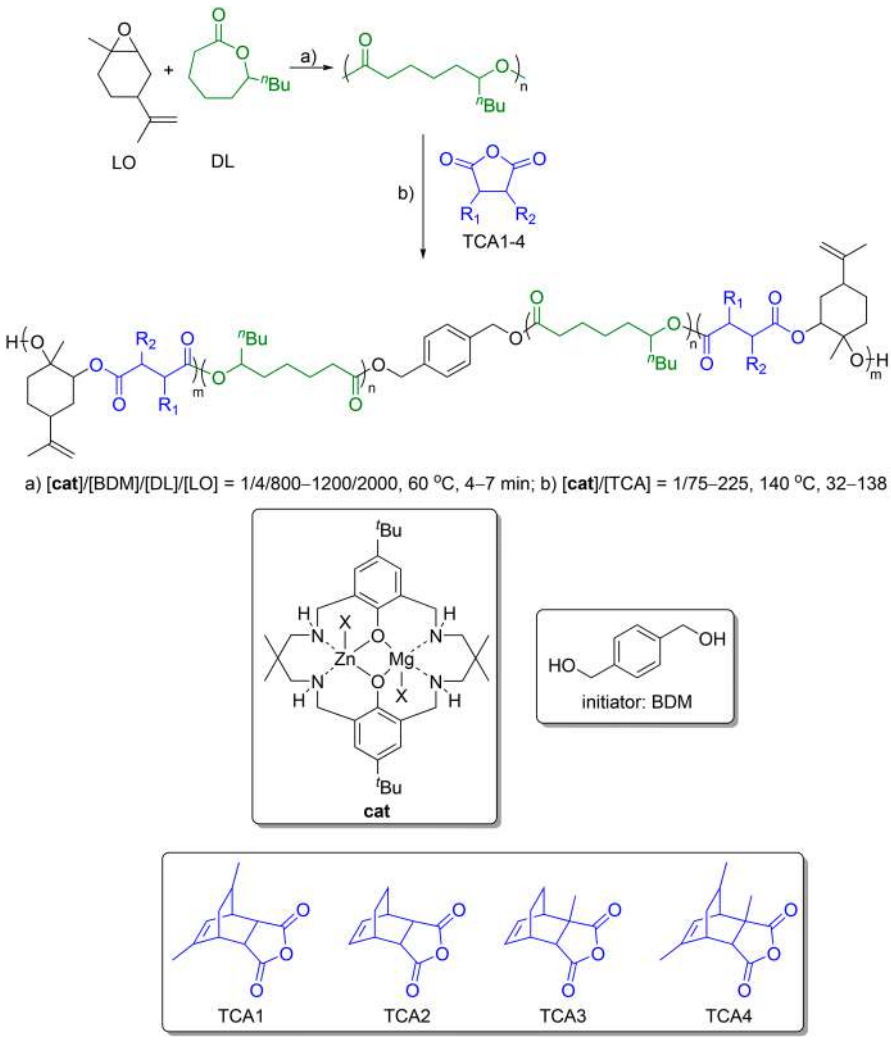

Scheme 2.18 Synthesis of bioderived block copolyesters *via* ROCOP of limonene oxide, ε-decalactone and tricyclic anhydrides catalysed by a hetero-bimetallic complex.

the same tricyclic anhydride, the peel adhesion increased when increasing the polyester content obtained *via* ROCOP of LO and TCA. Their mechanical and rheological properties are similar to commercial materials and constitute good examples of sustainable biodegradable polymeric materials to replace current commercial materials.

2.5 Conclusions

The use of Earth-abundant metal-based complexes as catalysts for a wide range of chemical transformations, such as hydrogenation, C–C and C–heteroatom bond formation and polymerisation reactions, is a sustainable alternative to the use of noble and precious metals. However, catalyst development is still required in order to match the catalytic activity obtained with precious-metal catalysts. Some outstanding results have been achieved using aluminium and iron catalysts amongst other Earth-abundant transition metal catalysts. These processes often occur *via* a different mechanism than when using noble-metal catalysts and have shown broad substrate scope and high catalytic activity under mild reaction conditions, obtaining the final products with excellent yields and/or selectivities. Despite the excellent results that Earth-abundant metal catalysts have shown, there are not many large-scale industrial applications for them. An alternative to increase the sustainability of the processes and implement them in industrial processes could be the development of supported homogeneous catalysts onto polymers or silica. This would improve catalyst separation and reusability.

On the other hand, the use of unsustainable solvents or reagents recently added to the "REACH" restricted chemical list should be avoided in order to develop greener chemical processes.[132] Further research is essential to (i) develop more active and selective homogeneous Earth-abundant metal catalysts, (ii) fully understand the mechanism of chemical processes catalysed by abundant-metal complexes, and (iii) translate the academic research into sustainable industrial processes.

References

1. World Commission on Environment and Development, *Our Common Future*, Oxford University Press, 1987.
2. I. T. Horváth, *Chem. Rev.*, 2018, **118**, 369.
3. P. T. Anastas, in *Advanced Green Chemistry: Part 1: Greener Organic Reactions and Processes*, World Scientific Publishing Co., 2017, pp. 1–17.
4. *Pollution Prevention Act of 1990*, Pollution Prevention (P2), US EPA, https://www.epa.gov/p2/pollution-prevention-act-1990, accessed 1 December 2020.
5. *Green Chemistry*, US EPA, https://www.epa.gov/greenchemistry, accessed 1 December 2020.
6. P. Anastas and N. Eghbali, *Chem. Soc. Rev.*, 2010, **39**, 301.

7. R. A. Sheldon, I. W. C. E. Arends and U. Hanefeld, in *Green Chemistry and Catalysis*, Wiley, 2007, pp. 1–47.
8. R. A. Sheldon, *Green Chem.*, 2017, **19**, 18.
9. R. A. Sheldon, *Chem. Ind.*, 1992, **23**, 903.
10. B. M. Trost, *Science*, 1991, **254**, 1471.
11. O. G. Griffiths, R. E. Owen, J. P. O'Byrne, D. Mattia, M. D. Jones and M. C. McManus, *RSC Adv.*, 2013, **3**, 12244.
12. M. L. Brusseau, in *Environmental and Pollution Science*, Elsevier, 2019, pp. 585–603.
13. D. Kralisch, D. Ott and D. Gericke, *Green Chem.*, 2015, **17**, 123.
14. IUPAC, *Compendium of Chemical Terminology*, IUPAC, 2009.
15. P. W. N. M. van Leeuwen, *Homogeneous Catalysis*, Springer Netherlands, 2004.
16. U. Hanefeld and L. Lefferts, *Catalysis: An Integrated Textbook for Students*, Wiley-VCH, Weinheim, Germany, 2018.
17. J. Hagen, *Industrial Catalysis*, Wiley-VCH Verlag GmbH & Co. KGaA, Weinheim, Germany, 2015.
18. X. Jiang, X. Nie, X. Guo, C. Song and J. G. Chen, *Chem. Rev.*, 2020, **120**, 7984.
19. L. Liu and A. Corma, *Chem. Rev.*, 2018, **118**, 4981.
20. A. Bavykina, N. Kolobov, I. S. Khan, J. A. Bau, A. Ramirez and J. Gascon, *Chem. Rev.*, 2020, **120**, 8468.
21. M. K. Samantaray, V. D'Elia, E. Pump, L. Falivene, M. Harb, S. Ould Chikh, L. Cavallo and J.-M. Basset, *Chem. Rev.*, 2020, **120**, 734.
22. N. Yan, C. Xiao and Y. Kou, *Coord. Chem. Rev.*, 2010, **254**, 1179.
23. M. K. Samantaray, E. Pump, A. Bendjeriou-Sedjerari, V. D'Elia, J. D. A. Pelletier, M. Guidotti, R. Psaro and J.-M. Basset, *Chem. Soc. Rev.*, 2018, **47**, 8403.
24. A. F. Lee, J. A. Bennett, J. C. Manayil and K. Wilson, *Chem. Soc. Rev.*, 2014, **43**, 7887.
25. C. Nájera, I. P. Beletskaya and M. Yus, *Chem. Soc. Rev.*, 2019, **48**, 4515.
26. D. Wang and D. Astruc, *Chem. Soc. Rev.*, 2017, **46**, 816.
27. C. Sambiagio, D. Schönbauer, R. Blieck, T. Dao-Huy, G. Pototschnig, P. Schaaf, T. Wiesinger, M. F. Zia, J. Wencel-Delord, T. Besset, B. U. W. Maes and M. Schnürch, *Chem. Soc. Rev.*, 2018, **47**, 6603.
28. W. Gao, S. Liang, R. Wang, Q. Jiang, Y. Zhang, Q. Zheng, B. Xie, C. Y. Toe, X. Zhu, J. Wang, L. Huang, Y. Gao, Z. Wang, C. Jo, Q. Wang, L. Wang, Y. Liu, B. Louis, J. Scott, A.-C. Roger, R. Amal, H. He and S.-E. Park, *Chem. Soc. Rev.*, 2020, **49**, 8584.
29. L. Alig, M. Fritz and S. Schneider, *Chem. Rev.*, 2019, **119**, 2681.
30. *Heterogeneous Catalysis for Energy Applications*, ed. T. R. Reina and J. A. Odriozola, Royal Society of Chemistry, Cambridge, 2020.
31. *Modern Heterogeneous Catalysis*, ed. R. A. van Santen, Wiley-VCH Verlag GmbH & Co. KGaA, Weinheim, Germany, 2017.
32. Z.-J. Shi, *Homogeneous Catalysis for Unreactive Bond Activation*, John Wiley & Sons, Inc., Hoboken, NJ, USA, 2014, vol. 9781118452233.

33. S. Bhaduri and D. Mukesh, *Homogeneous Catalysis*, John Wiley & Sons, Inc, Hoboken, NJ, 2014.
34. G. P. Chiusoli and P. M. Maitlis, *Metal-catalysis in Industrial Organic Processes*, Royal Society of Chemistry, Cambridge, 2007.
35. M. Manßen and L. L. Schafer, *Chem. Soc. Rev.*, 2020, **49**, 6947.
36. J. He, M. Wasa, K. S. L. Chan, Q. Shao and J.-Q. Yu, *Chem. Rev.*, 2017, **117**, 8754.
37. L. Ackermann, R. Vicente and A. R. Kapdi, *Angew. Chem., Int. Ed.*, 2009, **48**, 9792.
38. X. Chen, K. M. Engle, D.-H. Wang and J.-Q. Yu, *Angew. Chem., Int. Ed.*, 2009, **48**, 5094.
39. F. Meemken and A. Baiker, *Chem. Rev.*, 2017, **117**, 11522.
40. J. Song, Z.-F. Huang, L. Pan, K. Li, X. Zhang, L. Wang and J.-J. Zou, *Appl. Catal., B*, 2018, **227**, 386.
41. D. J. Scott, M. J. Fuchter and A. E. Ashley, *Chem. Soc. Rev.*, 2017, **46**, 5689.
42. R. A. Sheldon, I. W. C. E. Arends and U. Hanefeld, *Green Chemistry and Catalysis*, 2007.
43. J. W. Comerford, I. D. V. Ingram, M. North and X. Wu, *Green Chem.*, 2015, **17**, 1966.
44. A. J. Hunt and T. J. Farmer, in *Sustainable Catalysis: With Non-endangered Metals, Part 1*, ed. M. North, Royal Society of Chemistry, 2015, pp. 1–14.
45. R. Arevalo and P. J. Chirik, *J. Am. Chem. Soc.*, 2019, **141**, 9106.
46. D. Wei and C. Darcel, *Chem. Rev.*, 2019, **119**, 2550.
47. T. Zell and R. Langer, *ChemCatChem*, 2018, **10**, 1930.
48. S. Fu, N. Y. Chen, X. Liu, Z. Shao, S. P. Luo and Q. Liu, *J. Am. Chem. Soc.*, 2016, **138**, 8588.
49. T. Katsuki, *Chem. Soc. Rev.*, 2004, **33**, 437.
50. P. G. Cozzi, *Chem. Soc. Rev.*, 2004, **33**, 410.
51. D. Benito-Garagorri and K. Kirchner, *Acc. Chem. Res.*, 2008, **41**, 201.
52. P. C. J. Kamer and P. W. N. M. Van Leeuwen, *Phosphorus(III) Ligands in Homogeneous Catalysis: Design and Synthesis*, John Wiley & Sons, Ltd, Chichester, UK, 2012.
53. A. Otero, J. Fernández-Baeza, A. Lara-Sánchez and L. F. Sánchez-Barba, *Coord. Chem. Rev.*, 2013, **257**, 1806.
54. S. Díez-González and S. P. Nolan, *Coord. Chem. Rev.*, 2007, **251**, 874.
55. M. N. Hopkinson, C. Richter, M. Schedler and F. Glorius, *Nature*, 2014, **510**, 485.
56. Á. Molnár, G. A. Olah and G. K. S. Prakash, in *Hydrocarbon Chemistry, Two Volume Set*, Wiley, 2017, pp. 863–957.
57. P. Rylander, *Hydrogenation Methods*, Academic Press Inc., Orlando, 1985.
58. J. A. Osborn, F. H. Jardine, J. F. Young and G. Wilkinson, *J. Chem. Soc. A*, 1966, 1711.
59. H. U. Blaser, B. Pugin, F. Spindler and L. A. Saudan, in *Applied Homogeneous Catalysis with Organometallic Compounds*, Wiley, 2017, pp. 621–690.

60. *Homogeneous Hydrogenation with Non-precious Catalysts*, ed. J. F. Teichert, Wiley, 2019.
61. G. A. Filonenko, R. van Putten, E. J. M. Hensen and E. A. Pidko, *Chem. Soc. Rev.*, 2018, **47**, 1459.
62. X. Du, Y. Xiao, J.-M. Huang, Y. Zhang, Y.-N. Duan, H. Wang, C. Shi, G.-Q. Chen and X. Zhang, *Nat. Commun.*, 2020, **11**, 3239.
63. X. Nie, W. Li, X. Jiang, X. Guo and C. Song, in *Advances in Catalysis*, Academic Press Inc., 2019, vol. 65, pp. 121–233.
64. J. Zhong, X. Yang, Z. Wu, B. Liang, Y. Huang and T. Zhang, *Chem. Soc. Rev.*, 2020, **49**, 1385.
65. K. Tominaga, Y. Sasaki, T. Watanabe and M. Saito, *Bull. Chem. Soc. Jpn.*, 1995, **68**, 2837.
66. S. Wesselbaum, T. Vom Stein, J. Klankermayer and W. Leitner, *Angew. Chem., Int. Ed.*, 2012, **51**, 7499.
67. J. Klankermayer and W. Leitner, *Science*, 2015, **350**, 629.
68. J. Klankermayer, S. Wesselbaum, K. Beydoun and W. Leitner, *Angew. Chem., Int. Ed.*, 2016, **55**, 7296.
69. B. G. Schieweck, P. Jürling-Will and J. Klankermayer, *ACS Catal.*, 2020, **10**, 3890.
70. N. Westhues and J. Klankermayer, *ChemCatChem*, 2019, **11**, 3371.
71. M. Meuresch, S. Westhues, W. Leitner and J. Klankermayer, *Angew. Chem., Int. Ed.*, 2016, **55**, 1392.
72. S. Wesselbaum, V. Moha, M. Meuresch, S. Brosinski, K. M. Thenert, J. Kothe, T. Vom Stein, U. Englert, M. Hölscher, J. Klankermayer and W. Leitner, *Chem. Sci.*, 2015, **6**, 693.
73. J. Schneidewind, R. Adam, W. Baumann, R. Jackstell and M. Beller, *Angew. Chem., Int. Ed.*, 2017, **56**, 1890.
74. A. P. C. Ribeiro, L. M. D. R. S. Martins and A. J. L. Pombeiro, *Green Chem.*, 2017, **19**, 4811.
75. A. de Meijere, S. Bräse and M. Oestreich, *Metal-catalyzed Cross-coupling Reactions and More*, Wiley-VCH Verlag GmbH & Co. KGaA, Weinheim, Germany, 2014, vol. 3.
76. P. Nareddy, F. Jordan and M. Szostak, *ACS Catal.*, 2017, **7**, 5721.
77. L. Ackermann, *Acc. Chem. Res.*, 2014, **47**, 281.
78. R. Chinchilla and C. Nájera, *Chem. Soc. Rev.*, 2011, **40**, 5084.
79. A. H. Cherney, N. T. Kadunce and S. E. Reisman, *Chem. Rev.*, 2015, **115**, 9587.
80. F.-S. Han, *Chem. Soc. Rev.*, 2013, **42**, 5270.
81. K. Zhao, L. Shen, Z.-L. Shen and T.-P. Loh, *Chem. Soc. Rev.*, 2017, **46**, 586.
82. S. H. Kyne, G. Lefèvre, C. Ollivier, M. Petit, V.-A. Ramis Cladera and L. Fensterbank, *Chem. Soc. Rev.*, 2020, **49**, 8501.
83. Q. Liang and D. Song, *Chem. Soc. Rev.*, 2020, **49**, 1209.
84. A. Piontek, E. Bisz and M. Szostak, *Angew. Chem., Int. Ed.*, 2018, **57**, 11116.
85. J. R. Ludwig and C. S. Schindler, *Chem*, 2017, **2**, 313.
86. A. Fürstner, *Adv. Synth. Catal.*, 2016, **358**, 2362.

87. A. Fürstner, *ACS Cent. Sci.*, 2016, **2**, 778.
88. G. Rothenberg, in *Catalysis*, Wiley-VCH Verlag GmbH & Co. KGaA, 2008, pp. 39–75.
89. Y. Hong, L. Jarrige, K. Harms and E. Meggers, *J. Am. Chem. Soc.*, 2019, **141**, 4569.
90. A. Correa, O. G. Mancheño and C. Bolm, *Chem. Soc. Rev.*, 2008, **37**, 1108.
91. I. P. Beletskaya and V. P. Ananikov, *Chem. Rev.*, 2011, **111**, 1596.
92. J. Hartwig, *Organotransition Metal Chemistry: From Bonding to Catalysis*, 2010.
93. D. S. Surry and S. L. Buchwald, *Angew. Chem., Int. Ed.*, 2008, **47**, 6338.
94. *Metal-catalyzed Cross-coupling Reactions*, ed. A. de Meijere and F. Diederich, Wiley, 2004.
95. M. Beller, *Chem. Soc. Rev.*, 2011, **40**, 4891.
96. C. Darcel and J. B. Sortais, *Top. Organomet. Chem.*, 2015, **50**, 173.
97. L. C. Wilkins and R. L. Melen, *Coord. Chem. Rev.*, 2016, **324**, 123.
98. H. Hao and L. L. Schafer, *ACS Catal.*, 2020, **10**, 7100.
99. M. Fairley, L. Davin, A. Hernán-Gómez, J. García-Álvarez, C. T. O'Hara and E. Hevia, *Chem. Sci.*, 2019, **10**, 5821.
100. J. Schlüter, M. Blazejak and L. Hintermann, *ChemCatChem*, 2013, **5**, 3309.
101. Z. Yang, M. Zhong, X. Ma, K. Nijesh, S. De, P. Parameswaran and H. W. Roesky, *J. Am. Chem. Soc.*, 2016, **138**, 2548.
102. N. Romero, S.-C. Roşca, Y. Sarazin, J.-F. Carpentier, L. Vendier, S. Mallet-Ladeira, C. Dinoi and M. Etienne, *Chem. - Eur. J.*, 2015, **21**, 4115.
103. U. Jayarathne, N. Hazari and W. H. Bernskoetter, *ACS Catal.*, 2018, **8**, 1338.
104. X. Wu and M. North, *ChemSusChem*, 2017, **10**, 74.
105. J. A. Castro-Osma, M. North and X. Wu, *Chem. - Eur. J.*, 2016, **22**, 2100.
106. J. A. Castro-Osma, M. North, W. K. Offermans, W. Leitner and T. E. Müller, *ChemSusChem*, 2016, **9**, 791.
107. M. North, S. C. Z. Quek, N. E. Pridmore, A. C. Whitwood and X. Wu, *ACS Catal.*, 2015, **5**, 3398.
108. J. A. Castro-Osma, M. North and X. Wu, *Chem. - Eur. J.*, 2014, **20**, 15005.
109. J. Meléndez, M. North and R. Pasquale, *Eur. J. Inorg. Chem.*, 2007, 3323.
110. M. North and R. Pasquale, *Angew. Chem., Int. Ed.*, 2009, **48**, 2946.
111. C. J. Whiteoak, N. Kielland, V. Laserna, E. C. Escudero-Adán, E. Martin and A. W. Kleij, *J. Am. Chem. Soc.*, 2013, **135**, 1228.
112. V. Laserna, G. Fiorani, C. J. Whiteoak, E. Martin, E. Escudero-Adán and A. W. Kleij, *Angew. Chem., Int. Ed.*, 2014, **53**, 10416.
113. C. J. Whiteoak, N. Kielland, V. Laserna, F. Castro-Gómez, E. Martin, E. C. Escudero-Adán, C. Bo and A. W. Kleij, *Chem. - Eur. J.*, 2014, **20**, 2264.
114. G. Fiorani, M. Stuck, C. Martín, M. M. Belmonte, E. Martin, E. C. Escudero-Adán and A. W. Kleij, *ChemSusChem*, 2016, **9**, 1304.
115. M. A. Gaona, F. De La Cruz-Martínez, J. Fernández-Baeza, L. F. Sánchez-Barba, C. Alonso-Moreno, A. M. Rodríguez, A. Rodríguez-Diéguez, J. A. Castro-Osma, A. Otero and A. Lara-Sánchez, *Dalton Trans.*, 2019, **48**, 4218.

116. F. de la Cruz-Martínez, J. Martínez, M. A. Gaona, J. Fernández-Baeza, L. F. Sánchez-Barba, A. M. Rodríguez, J. A. Castro-Osma, A. Otero and A. Lara-Sánchez, *ACS Sustainable Chem. Eng.*, 2018, **6**, 5322.
117. J. Martínez, F. de la Cruz-Martínez, M. A. Gaona, E. Pinilla-Peñalver, J. Fernández-Baeza, A. M. Rodríguez, J. A. Castro-Osma, A. Otero and A. Lara-Sánchez, *Inorg. Chem.*, 2019, **58**, 3396.
118. J. Martínez, J. A. Castro-Osma, C. Alonso-Moreno, A. Rodríguez-Diéguez, M. North, A. Otero and A. Lara-Sánchez, *ChemSusChem*, 2017, **10**, 1175.
119. J. Martínez, J. A. Castro-Osma, A. Earlam, C. Alonso-Moreno, A. Otero, A. Lara-Sánchez, M. North and A. Rodríguez-Diéguez, *Chem. - Eur. J.*, 2015, **21**, 9850.
120. J. A. Castro-Osma, C. Alonso-Moreno, A. Lara-Sánchez, J. Martínez, M. North and A. Otero, *Catal. Sci. Technol.*, 2014, **4**, 1674.
121. J. A. Castro-Osma, A. Lara-Sánchez, M. North, A. Otero and P. Villuendas, *Catal. Sci. Technol.*, 2012, **2**, 1021.
122. F. De La Cruz-Martínez, M. Martínez De Sarasa Buchaca, J. Martínez, J. Fernández-Baeza, L. F. Sánchez-Barba, A. Rodríguez-Diéguez, J. A. Castro-Osma and A. Lara-Sánchez, *ACS Sustainable Chem. Eng.*, 2019, **7**, 20126.
123. S. Paul, Y. Zhu, C. Romain, R. Brooks, P. K. Saini and C. K. Williams, *Chem. Commun.*, 2015, **51**, 6459.
124. R. C. Jeske, A. M. DiCiccio and G. W. Coates, *J. Am. Chem. Soc.*, 2007, **129**, 11330.
125. C. M. Kozak, K. Ambrose and T. S. Anderson, *Coord. Chem. Rev.*, 2018, **376**, 565.
126. S. J. Poland and D. J. Darensbourg, *Green Chem.*, 2017, **19**, 4990.
127. B. Grignard, S. Gennen, C. Jérôme, A. W. Kleij and C. Detrembleur, *Chem. Soc. Rev.*, 2019, **48**, 4466.
128. A. J. Kamphuis, F. Picchioni and P. P. Pescarmona, *Green Chem.*, 2019, **21**, 406.
129. L. Peña Carrodeguas, C. Martín and A. W. Kleij, *Macromolecules*, 2017, **50**, 5337.
130. L. Peña Carrodeguas, J. González-Fabra, F. Castro-Gómez, C. Bo and A. W. Kleij, *Chem. - Eur. J.*, 2015, **21**, 6115.
131. T. T. D. Chen, L. P. Carrodeguas, G. S. Sulley, G. L. Gregory and C. K. Williams, *Angew. Chem., Int. Ed.*, 2020, **59**, 23450.
132. *Registry of restriction intentions until outcome*, ECHA, https://echa.europa.eu/registry-of-restriction-intentions, accessed 10 December 2020.

CHAPTER 3

Heterogeneous Catalysis

GIOVANNA BOSICA*

Laboratory of Green Synthetic Organic Chemistry, Department of Chemistry, University of Malta, Msida, MSD 2080 Malta
*E-mail: giovanna.bosica@um.edu.mt

3.1 Basic Concepts from a Historical Perspective

The use of the term "Heterogeneous Catalysis" within scientific journal titles in the chemical literature has been growing rapidly in the last 15–20 years, as the scientific data banks clearly reveal, while it is barely mentioned in the literature before the 1990s. The reason behind this can be found in the explosive growth of Green Chemistry.[1] The "Twelve Principles of Green Chemistry" identify catalysis as one of the fundamental pillars of green chemistry (Principle no. 9), and heterogeneous catalysis, in particular, addresses the goals of green chemistry by providing easy separation of the product and catalyst, thereby eliminating the need for separation through distillation or extraction. In addition, environmentally benign catalysts, such as clays and zeolites, may replace more hazardous catalysts currently in use (Principles no. 1, 5, 8 and 10).[2] Nevertheless, one must pay attention to the environmentally benign synthesis and degradation of heterogeneous catalysts at the end of their lifetime (Principle no. 10). A heterogeneous catalyst should be stable; no leaching of potentially toxic material should occur during the reactions and the best result would be no leaching of any material at all or negligible leaching of the active components.[3]

Catalysis as a scientific discipline originated in the early part of the last century. Catalysts were earlier recognized as substances that affect the reaction rate and selectivity, but are not consumed when added in small

Sustainable Organic Synthesis: Tools and Strategies
Edited by Stefano Protti and Alessandro Palmieri

Published by the Royal Society of Chemistry, www.rsc.org

quantities to a reaction. Then, Ostwald, one of the founding fathers of chemical thermodynamics, who won the Nobel prize in 1909, introduced thermodynamics into the physical chemical definition of a catalyst, specifying that it is a material that will leave the equilibrium of a reaction unchanged.[4]

Sabatier, who won the Nobel prize for catalytic hydrogenation in 1912, formulated the principle that the reaction intermediates formed at the surface of a catalytic material should have an intermediate stability. When too stable, they would not decompose, and when too unstable they would not be formed. This was the modern formulation of the molecular basis of catalytic action, not as a single reaction but as a cycle of reaction steps, in which intermediate complexes between a catalyst and a reagent are formed and then decay.[4]

Catalysis is often referred to as a foundation pillar of green chemistry.[2] Catalysis generally speeds up the reaction rates, by lowering the activation energy, and allows the formation of more complex chemo-, regio-, and stereoselective structures from less reactive or less functionalised starting materials.[5] This implies less energy, less feedstock consumption and less waste generated.[6] Catalysis also solves the problem of waste generation linked to the traditional use of stoichiometric inorganic reagents, the primary cause of waste in organic synthesis, particularly in fine chemicals and pharmaceutical manufacture.[7] Functional group protection and deprotection steps are normally eliminated and functional group activation is avoided. This results in step economy as well as reduction in waste, which makes the use of catalysts economically and environmentally attractive, since clean catalytic methodologies lower drastically the E-factor.[8,9]

Catalysis is of great importance and economical significance in industrial chemical processes. In fact, more than 80% of the reactions in the chemical, petrochemical and biochemical industries, as well as in polymer production and in environmental protection, use catalysts.[10] Moreover, catalytic technologies contribute to approximately 20% of the world's Gross National Product (GNP).[11]

Catalysts are classified into two areas according to their phase behaviour, the homogeneous and heterogeneous catalysts. In heterogeneous catalysis, the reagents and products are in a different phase from that of the catalyst, which is almost always in a solid phase, whereas homogeneous catalysis applies to those transformations where the catalyst, starting materials, and reaction products all reside in the same phase, almost always a liquid phase. A comparison of the two kinds of catalysis makes it evident that homogeneous catalysts are molecularly well-defined compounds in which the structure of the active centre can be determined even *in situ* with reasonable reliability by normal spectroscopic techniques. This allows an easier understanding of the reaction mechanism and the rational development of catalysts with improved performances. Homogeneous catalysis often takes place under much milder reaction conditions. On the other side, heterogeneous catalysts tend to be more stable and retain their activity for a longer

time even at high temperatures. Isolation of the products and recovery and recycling of the catalyst are more complicated in homogeneous than in heterogeneous catalysis.[12]

The inherent drawback of all homogeneous systems is the production of significant quantities of hazardous waste necessitated through washing and neutralization, and the difficulties in catalyst recovery. The use of water to quench the reaction leads to large amounts of gaseous and aqueous waste, as well as loss of the catalyst. The process therefore generally has a large E-factor. Heterogeneous catalysis offers a more environmentally benign approach, overcoming problems with catalyst recycling and generation of waste.[13] Moreover, novel reaction technologies, including alternative reaction media (like a solventless environment, ionic liquids, and supercritical CO_2) and ultrasound (US) or microwave (MW) irradiation, which also increase the reaction rate and reduce the energy consumption providing better yields and/or selectivity, can be easily combined with heterogeneous catalysis to further enhance its advantages.[14]

While homogeneous catalysts have dominated in organic synthesis and in the fine chemical industry, heterogeneous catalysis is by far the most used technology in large-scale petrochemical processes.[12] In recent years, catalysis has become a core tool for Green Chemistry and, almost undoubtedly, heterogeneous catalysis is the most significant contributor to sustainable development in the chemical industry.[15] In the drive to minimize waste in chemicals manufacturing, cleaner, catalytic alternatives are replacing classical organic chemistry processes of low atom utilization.[16] Since the 1990s, the challenge for chemists and chemical engineers has been to develop processes that not only yield the desired product but are also efficient and environmentally friendly; in this context, heterogeneous catalysis has been playing a major role as witnessed by the myriad of publications in the chemical literature in this field. Although in the past organic chemistry and catalysis evolved in two separate ways, catalysis being mainly applied in oil refining and bulk chemical manufacture, while fine chemicals manufacture with classical stoichiometric processes was the domain of synthetic organic chemists, nowadays, under the pressure of environmental legislation, the fine chemicals industry is being forced to focus more attention on waste minimisation and avoiding the use of hazardous and/or toxic reagents. Therefore, we are observing the widespread application of catalytic methodologies, and in particular of heterogeneous catalysis, following a synergy between organic synthesis, industry and the catalysis community.[16,17]

Despite the success of homogeneous catalysts in terms of activity and selectivity,[18] their application remains limited in industry due to catalyst instability, difficulty in catalyst separation, recovery and reuse, high cost in separation and catalyst losses, large amounts of waste produced, contamination of the product, corrosion and toxicity.[19,20] Hence, social and environmental pressure on the chemical industry has resulted in the substitution of homogeneous-catalysed reactions by more environmentally friendly solid heterogeneous technologies.[21]

In heterogeneous catalysis, kinetics provides the basis for the physical chemical description of catalytic reactivity. Reaction engineering is the discipline that connects reactor performance with the chemical reactivity of the catalyst. The link between chemical kinetics and molecular activation at the catalyst surface is through the mechanism of the catalytic reaction. This implies a physical organic chemistry type of understanding of the reaction paths involved when the reaction proceeds in its catalytic cycle.[4]

The Sabatier Principle states that a catalytic reaction has its maximum rate when there is an optimum interaction of the reactant or product molecules with the catalyst. This is because the catalytic reaction is a cycle of consecutive elementary reaction steps. The rate of the reaction has a maximum when the rate of reactant activation to give a surface reaction intermediate equals the rate of its removal. The intermediate complex of the reactant and surface should be stable enough that chemical bonds in the reactant molecule become activated, but have enough instability so that it can desorb.[22]

Any heterogeneous catalytic reaction involves at least two phases (fluid(s) and solid), with the reaction occurring on the surface of a solid catalyst. Therefore, the reacting molecules must be supplied from the bulk fluid to the fluid/solid interface, introducing complications in overall kinetics which are not present in homogeneous systems. Heterogeneous catalytic reactions involve, by their nature, a combination of reaction and transport processes.[23]

Heterogeneous catalysis relates catalytic performance to catalyst structure and composition searching indicators that determine the activity and selectivity of the overall reaction. However, it is the combination of surface coverage and a balance of rate-controlling elementary steps that determines the overall performance, which in turn strongly relates to the reaction conditions. Generally, there are three reactivity-determining catalyst parameters to consider: particle size and shape; catalyst composition; structure and composition of the surface during reaction.[24] Sabatier's principle was the formulation of the molecular basis of catalytic action and complemented Ostwald's physical chemical view. Currently, physical chemical instrumentation and computational and molecular chemistry provide the basis for the formulation of a molecular theory of catalysis. Transient and isotope-labelled kinetic studies, as well as *in situ* spectroscopic measurements, are the experimental tools, but they are limited to the investigation of a single elementary step of the overall catalytic reaction.[4]

Catalysts are used to tune both the path and the rate of chemical reactions. This is achieved by controlling the reaction barriers in such a way that the intended intermediates and products are formed. The two characteristic catalytic properties are activity and selectivity. The aim of catalyst development is to obtain a catalytically active material in such a way that it maximizes the reaction rate of the successive catalytic reaction steps up to the desired product. In addition, the catalysts have to remain chemically and mechanically stable and active under the reaction conditions for a long time to ensure an economic lifetime of the catalyst.[25]

The most important analytical tool in catalyst development is testing of catalytic activity, looking for the optimum combination of reactants, reaction conditions, and catalyst materials. Development may be mainly empiric, or supported by other techniques, like modelling, experimental design, and/or characterization of the catalyst material to achieve a more targeted approach and to establish a continuously growing knowledge pool for the specific catalytic reaction and process parameters.[25]

A central theme in the science of heterogeneous catalysis is the characterization of the catalytic material at the level of detail relevant to its performance. Due to the heterogeneous nature of a catalyst's particles, the molecular characterization of the catalyst surface is still not always completely possible, but for the model type catalysts a molecular description is becoming possible. Surface changes and surface chemistry are intimately coupled, and advanced spectroscopy in combination with computational approaches is getting to a stage where definitive study is becoming possible, therefore validating a now well-established discipline of computational catalysis. This has given rise to new generations of catalysts of increasing complexity, but also surfaces of increasingly better molecular definition.[4]

Whereas the early heterogeneous catalysts were simply metal powders, not much later they became materials with highly dispersed catalytically active components on high-surface supports. There are many examples of the sustained gradual improvement in catalyst performance that has occurred over many years. Catalyst preparation methods were based on increasing understanding of the chemistry of the often complex reaction mixtures, and zeolites, with their microscopic channel structure that is defined at the atomic level, can be considered to be an example of the ultimate molecular heterogeneous catalyst.[4]

Typical heterogeneous catalysts are inorganic solids such as metals, oxides, sulfides, and metal salts, but they may also be organic materials such as organic hydroperoxides, ion exchangers, and enzymes. The conditions under which catalytic processes occur on solid materials vary drastically.[26] It is plausible that it is extremely difficult, if not impossible, to describe the catalytic phenomenon by a general theory that covers the entire range of reaction conditions and observed site-time yields (that is reaction rates, site-time yields = number of product molecules formed per site and unit time). However, there are several general principles that are considered to be laws or rules of thumb that are useful in many situations.[10]

The Sabatier principle of an unstable surface intermediate requires chemical bonding of reactants to the catalyst surface, most likely between atoms or functional groups of reactant and surface atoms. This leads to the *principle of active sites*. When Langmuir formulated his model of chemisorption on metal surfaces,[27] he assumed an array of sites which were energetically identical and noninteracting, and which would adsorb just one molecule from the gas phase in a localized mode. The Langmuir adsorption isotherm results from this model. The sites involved can be considered to be active sites. Langmuir was already aware that the assumption of identical and noninteracting sites was an approximation which would not hold for real surfaces.[28]

The heterogeneity of active sites on solid catalyst surfaces and its consequences were emphasized by Taylor who recognized that "There will be all extremes between the case in which all atoms in the surface are active and that in which relatively few are so active".[29] In other words, exposed faces of a solid catalyst will contain terraces, ledges, kinks, and vacancies with sites having different coordination numbers. This would lead to a heterogeneity of the local environment of a surface atom and thus create non-equivalent sites. "The amount of surface which is catalytically active is determined by the reaction catalysed." In other words, the surface of a catalyst adapts itself to the reaction conditions for a particular reaction. The driving force for this reorganization of a catalyst surface is the minimization of the surface free energy, which may be achieved by *surface-reconstruction*.[30,31] As a consequence, a meaningful characterization of active sites requires experiments under working (*in situ*) conditions of the catalytic system. The principle of active sites is not limited to metals. Active sites include metal cations, anions, Lewis and Brønsted acids, acid–base pairs (acid and base acting simultaneously in chemisorption), organometallic compounds, and immobilized enzymes. Active sites may include more than one species (or atom) to form multiplets[32] or ensembles.[33] A mandatory requirement for these sites to be active is that they are accessible for chemisorption from the fluid phase. Hence, they must provide free coordination sites. Therefore, Burwell *et al.* coined the term coordinatively unsaturated sites in analogy with homogeneous organometallic catalysts.[34,35] Thus, active sites are to be considered as atoms or groups of atoms which are embedded in the surface of a matrix in which the neighboring atoms (or groups) act as ligands.[36] In supported catalysts, the active phase (metal, oxide, sulfide) undergoes active phase–support interactions.[37–39]

The catalytic cycle is the most fundamental principle of catalytic action. The cycle must be uninterrupted and repeated since otherwise the reaction is stoichiometric rather than catalytic. The number of turnovers, a measure of catalyst life, must be greater than unity, since the catalyst would otherwise be a reagent. The activity of the catalyst is defined by the number of cycles per unit time or turnovers, or turnover frequency (TOF; unit: s^{-1}). The life of the catalyst is defined by the number of cycles before it dies. The mechanism of a catalysed reaction can be described by the sequence of elementary reaction steps of the cycle, including adsorption, surface diffusion, chemical transformations of adsorbed species, and desorption, and it is the basis for deriving the kinetics of the reaction.[10]

It is a readily accepted fact that surface heterogeneity leads to a heterogeneous population of active sites on the surface of a catalyst. It is very often discussed but very seldom taken into account in practical cases, simply because there are very few tools with which to study the heterogeneity of active sites in catalysis. Most attempts to do so have been based upon the use of selective poisons. However, thanks to the improved sensitivity of calorimeters and to the development of refined data analysis techniques, adsorption calorimetry can make a significant contribution to the characterization

of a catalytic surface.[40] In particular, the surface properties of a solid can be conveniently investigated by studying the adsorption of suitably chosen probe molecules. The amount of heat evolved during the adsorption process is closely related to the adsorbate substrate bond strength. Furthermore, the differential heat of adsorption is often dependent on the surface coverage of the adsorbate, due to the lateral adsorbate–adsorbate interactions or due to the surface heterogeneity. So the role of the probe is one of the most decisive parameters in the determination of heats of adsorption. Moreover, many catalytic reactions are structure sensitive, and proceed at a rate that depends on the detailed geometric structure of the surface atoms of the catalyst. Norskov *et al.* demonstrated that the heat of adsorption of a species is directly related to the local structure of the catalyst, and that the more accessible sites are more active unless poisoned and bind the adsorbate more strongly.[36] Therefore, the determination of the energy profile, *i.e.* the energy of the adsorbed phase as a function of loading, is an essential component of the characterization of the surface-active sites of catalysts and/or supports of catalysts.[40]

3.1.1 Heterogeneous Catalysts

Heterogeneous catalysts are non-corrosive, safely handled, porous materials increasing the surface area, result in more effective encounter rates, are easily recovered from the reaction mixture without the need for reaction quenching, and can be recycled and reused.[20,41,42] Heterogeneous catalysts can be divided into two main families: the unsupported (bulk) catalysts and the supported catalysts.[11] These catalyse two main types of processes: redox reactions and acid-base reactions.

3.1.1.1 Bulk Inorganic Catalysts

Inorganic metal oxides are a large and important class of catalytically active materials due to their surface properties, chemical composition and structure. Amongst the most studied inorganic oxides is alumina, an amphoteric oxide containing three different surface species: O^{2-} basic sites, Al^{3+} Lewis acid sites and OH Brønsted acid sites.[10] In contrast, silica is a weak Brønsted acidic oxide due to silanol (SiOH) surface groups.[43] Silica gel (SiO_2) is among the inorganic adsorbents that are most employed as a support; this material possesses a structure consisting of tetrahedral units of SiO_4 connected by siloxane bridges Si–O–Si. Silica gel is a material of high superficial area, is resistant, porous and formed of irregular particles (amorphous), and can be purchased with diversified granulometry. The units that form this skeleton are resultants of a condensation of Si–O–Si silicic acid $Si(OH)_4$, which starts to form oligomers after hydrolysis. These oligomers are condensed to form particles of silica. The silica surface under normal conditions is recovered with reactive hydroxyl groups, SiOH, called silanol groups, while its interior is connected by siloxane groups (Si–O–Si). These silanol groups (Si–OH) determine the chemical behaviour of its surface, exercising an important

function in the adsorption processes. The silanol group is a weak acid, with pK_a of about 9. It strongly interacts with molecules of alcohol, acetone, and mainly water, forming hydrogen bridges.[44]

The role of complex multicomponent oxides as catalytic materials has increased over the years. The introduction of microporous solids, in particular zeolites, in the chemical industry has led to an economical and environmental revolution.[45]

Zeolites are crystalline aluminosilicates possessing a framework of corner-sharing SiO_4^{4-} and AlO_4^{5-} tetrahedra. They are microporous solids with a regular system of channels or cages.[10] They act as shape-selective catalysts, since the shape and size of a particular pore system exerts a steric effect on the reaction, controlling the access of reactants and exit of products.[46] Natural zeolites contain a mixture of cations, such as Na^+, K^+, Mg^{2+} and Ca^{2+}, which can be ion-exchanged. Both acidic and basic zeolites are widely used in organic reactions. Acidic zeolites possess both Lewis and Brønsted acid sites.[47–49] Weak basic zeolites are formed by ion-exchange with large alkali metal ions, such as Cs^+.[50] Zeolites and related materials have a crystalline structure and contain regular micropores, the diameters of which are determined by the structure of the materials. The pore sizes are well defined and have dimensions similar to those of small organic molecules. This permits shape-selective catalysis to occur.

Another type of inorganic solid catalyst that has been applied in organic synthesis is clays. Clays are easily available and are low-cost aluminosilicate minerals. They are layered structures with alkali metal cations occupying the interlamellar space. Examples of clays include commercially available montmorillonite K-10 and KSF, both of which contain acidic sites.[10,51]

Catalysis by heteropolyacids is a well-established area.[52] They comprise mixed oxygen-containing acids derived from a combination of inorganic amphoteric metal acids of Groups 5 or 6 (*e.g.* tungsten, molybdenum, vanadium) and a non-metal acid, such as phosphoric acid or silicic acid, which provides the central atom in the complex.[10] They are cluster compounds containing a central p-block atom (*e.g.* silicon, phosphorous) linked to metal–oxygen octahedra (oxometallate octahedra) linked together *via* oxygen atoms. The metal is in its highest oxidation state. Some oxygen atoms have acidic hydrogens attached to them, whose acidity is close to that of super acids in organic solutions.[53,54] Heteropolyacids have a mobile ionic structure with very strong Brønsted acid sites and oxidising properties. They operate efficiently under mild conditions due to the strong acidity, which is important since most heteropolyacids have a low thermal stability.

3.1.1.2 Bulk Organic Catalysts

The use of organocatalysis as a tool for organic synthesis has attracted much interest.[55] In this regard, ion exchange resins have been employed as a low energy catalytic route for organic reactions. Acidic organic polymers

are produced by suspension copolymerisation of styrene with divinylbenzene, followed by sulfonation of the cross-linked polymer matrix, resulting in polymer-bound analogues of organic Brønsted acids such as *p*-toluenesulfonic acid. The size of the pores produced during the copolymerisation reaction is inversely proportional to the amount of cross-linking.[10] One such polymeric resin is macroporous Amberlyst-15®, a polystyrene-based cation exchange resin with strongly acidic sulfonic groups, whereas acid strength is increased using persulfonated sulfonic resins such as Nafion®.[10] Anion exchange resins containing basic anions, such as OH^- or F^-, as well as neutral ion-exchange polymeric resins containing amine and phosphine groups, are typical polymer-supported basic catalysts.[55] One example is Amberlyst A-21, a tertiary amine-substituted macroreticular ion exchange polymeric resin, which has been applied in a number of organic reactions.[56]

3.1.1.3 Supported Catalysts

Supported catalysts have an important role in industrial chemical processes. Supports provide a high surface area and stabilise the dispersion of the active component. Active phase–support interactions, which are dictated by the surface chemistry of the support for a given active phase, are responsible for the dispersion and the chemical state of the latter. Whilst many supports are often inert, some supports may have an active functional role in the catalyst. This results in bifunctional catalysis. Ideal supports require a porous structure in order to have a high surface area and can stabilise the highly disperse active phase.[10] Supported catalysts are the most important class of catalysts in industry. In most cases, the active components comprise a metal (Ni, Co, Pt), metal oxide (Cr, V) or metal sulphide (Co, Mo) dispersed as nanoparticles on a high–surface-area support consisting of an oxide (Al_2O_3, SiO_2, or TiO_2) or carbon.

For more than a century, many methods for the preparation of supported catalysts have been developed and used in laboratories and industry. Broadly speaking, we can discern three fundamentally different routes for the preparation, which are selective removal, co-precipitation, and application of the active component on a separately produced support. The latter method may be performed in many ways, including grafting of organometallic precursors, deposition of colloidal particles, sol–gel techniques, and chemical vapour deposition, which are largely covered in the literature. In particular, the deposition of precursors of the active components from aqueous solutions, by ion absorption, impregnation and drying, is the most widely used in laboratories. Small metal oxide particles are the most used support materials and their surfaces are commonly terminated by hydroxyl groups. Depending on the metal cations, lattice structure, and detailed bonding of the OH groups, their nature may be considered as acidic, neutral, or basic in the context of aqueous acid-base chemistry.[57,58]

The catalytically active sites are located at the surface of a solid phase and in contact with the vapour or liquid phase reactants. Hence, the porosity of the solid phase is essential, as it provides a high surface area for catalysis and good accessibility to active sites. According to the IUPAC definition, pores can be classified as either micropores (<2.0 nm diameter), mesopores (2–50 nm diameter) or macropores (>50 nm diameter). Catalyst supports are typically mesoporous (such as Al_2O_3, SiO_2, or TiO_2), as this ensures a high specific area for anchoring the active material, while at the same time providing enough space for the active phase nanoparticles (typically 1–50 nm in diameter) and diffusion of the reactants and products (the choice of either a silica or an alumina support depends on the specific application. In general, alumina has a higher mechanical robustness as well higher thermal stability). Zeolites are microporous; however, this small pore size is also essential for size and shape-selective catalysis.[59]

Inorganic solid supports, especially mesoporous materials, are promising candidates as heterogeneous catalysts due to the possibility of controlling the morphology and local environment at the catalytic site depending upon the requirement of a particular reaction.[60] Such catalysts offer a high surface area, tunable pore size for a variety of functional groups to control product selectivity, good adsorption properties for easy diffusion of reactants and products, different types of surface functionalities to alter the textural property and tailoring of the surface polarity in order to influence the reaction yield. Moreover, they are more or less non-toxic, non-corrosive, non-air sensitive, highly reusable, completely pollution-free, and environmentally benign supports for catalytic transformations in the liquid phase. Typical mesoporous materials used for catalysis include silica and mesoporous alumina. Active transition metal oxides and metal atoms are normally supported on the mesoporous materials. Inorganic supports are also used to immobilise Brønsted or Lewis acids or bases to catalyse acid-base reactions. Mesoporous supported acids are widely used in industrial processes, such as silica-supported aluminium chloride, silica-supported sulfuric acid and silica-supported heteropolyacids.[49]

Clays also have a long history in organic reactions as inorganic supports.[61] Different transition metal chlorides, $InCl_3$, $GaCl_3$, $FeCl_3$, and $ZnCl_2$ amongst other Lewis acids, have been supported on montmorillonite K-10, as well as basic inorganic salts such as KF.

A second category for supported catalysis is the organic-inorganic hybrid system.[62] This involves the immobilisation of homogeneous organic moieties onto inorganic supports.[19] Hybrid catalysts combine homogeneous and heterogeneous catalytic transformations. The goal of the approach is to combine the positive aspects of homogeneous catalysts or enzymes in terms of activity, selectivity, and variability of steric and electronic properties by, *e.g.*, the appropriate choice of ligands (including chiral ligands), with the advantages of heterogeneous catalysts, such as ease of separation and recovery of the catalyst. This can be achieved by immobilization (heterogenization) of active metal complexes, organometallic compounds, or enzymes on a solid support.

Immobilisation of inorganic salts on organic supports is also found in the literature. Heterogenization of homogeneous metal salts on ion-exchange resins has been recently considered.[63] Completely organic-based catalysts offers several advantages compared to metal-supported catalysts since the problem of leaching toxic metals is avoided, and the reactions are more likely to be insensitive to oxygen and water.[64]

Heterogeneous catalysis is also an important application of metal–organic framework (MOF) materials.[65] MOFs are meso- and microporous crystalline solids made up of a 3-dimensional hybrid network of metal ions coordinated to multidentate organic molecules. They contain high surface areas and uniform, tunable pore and channel sizes, making them very reactive and selective catalysts.

The discovery, development and optimisation of solid catalysts is facing, and will continue to face, an enormous challenge this century.[66] Significant advances will be expected since the methods of preparing heterogeneous catalysts and the characterization of the surfaces have been developed, and heterogeneous catalysis plays a major role in the life of the general public, both in terms of the economy and also for the well-being of society.[67]

3.1.2 Heterogeneity Test

When operationally heterogeneous catalysts are exposed to reagents in solution, a question naturally arises: do they stay heterogeneous or is the active catalyst a soluble metal complex formed by reaction with the reactants?[68–70]

A formal distinction between homogeneous and heterogeneous catalysis was only made by Ostwald in 1901. This distinction, considered sharp, has since been blurred by work on clusters, metal nanoparticles (NPs), and nanomaterials. All of these intermediate forms between small molecules and extended solids have shown catalytic activity in a variety of cases.

As reported in a critical review by Crabtree,[68] *because the classical homogeneous/heterogeneous distinction is based on the phases involved, it stands or falls on the definition of a phase. When does a growing metal cluster* M_n *in solution become a new phase? No clear distinction can be drawn between homogeneous and heterogeneous catalysts in this intermediate size range, not just in practice but also in principle. We can still consider a catalyst as being operationally homogeneous or heterogeneous, perhaps depending on whether the catalytic activity resides in the filtrate or else is retained by the filter in a Maitlis hot filtration test*.[68,71]

In a supposedly heterogeneous catalyst, a fraction of the metal (or of the catalytically active component) may dissolve under the reaction conditions and the true catalyst may thus be homogeneous. The metal/active component can even redeposit on the catalyst support when the reaction is over, leaving no clue as to the true nature of the catalyst. Likewise, the possible heterogeneity of what were assumed to be homogeneous catalysts has been largely studied.[72]

The terms homogeneous and heterogeneous have been used to mean quite different things by different authors. One usage follows Ostwald's original vision, based on phases. In other papers, homogeneous and heterogeneous are considered as mechanistic categories, depending on whether the catalyst has a single molecular active site or is instead a collection of adjacent sites on a surface. Authors in general continue to use the terms in both senses,[73] although the distinction between homogeneous and heterogeneous catalysts is most often based on the phases involved.

The same problem arises for heterogenized homogeneous catalysts, where one of the precatalyst ligands is covalently grafted onto a support such as polystyrene. If that ligand decomposes or dissociates, leaching of the metal can occur.[74,75]

Conversely, workers in homogeneous catalysis may not always be fully alert to the possibility of artifacts, notably that heterotopic catalysts might be the true actors in particular systems under study. The converse is in principle possible, and heterogeneous catalysts could owe their activity to molecular compounds formed in solution under the catalytic conditions or to quasi-molecular specific sites on the surface.

No single criterion can be considered definitive; however, a series of tests/controls have been devised by different authors over the years. In the catalytic arena, the question becomes whether a soluble catalyst detaches from the solid-phase heterogeneous catalyst, say Pd/C, and contributes to the activity. One of these tests is Maitlis' hot filtration test, in which the reaction mixture is passed through a glass frit with a filter aid, ensuring that the appropriate reaction temperature is maintained during the procedure.[71] The catalytic activity of the filtrate is then assayed. The filter pad and any entrained particles are also tested with fresh substrate and reactants to check any resulting catalytic activity. In running the test on a nominally heterogeneous catalyst, any soluble material released from the catalyst should pass through the filter, in which case catalytic activity also appears in the filtrate. For reactants with low solubility, care must be taken to ensure that they have successfully passed through the filter. It is hard to maintain in operando conditions during the whole procedure, but the method is relatively easy to apply and needs no special instrumentation or apparatus. A simple related procedure, sometimes termed Sheldon's hot filtration test, involves filtration of a heterogeneous catalyst from the reaction mixture partway through a reaction, followed by continuation of the reaction in the absence of the solid catalyst. If the reaction comes to a halt, heterogeneous catalysis is considered to be confirmed.[76]

3.1.2.1 Recycling Test

Heterogeneous catalysts are compounds which remain ultimately chemically unaltered at the end of the reaction, exist in a different physical state from the reactants and hence can be easily separated from the reaction mixture by: (i) simple filtration – especially easy if the catalyst is in the form of beads;

(ii) magnetic extraction – in the case of magnetic catalysts. Consequently, heterogeneous catalysts can be reused after being washed with an appropriate solvent, dried and (in some cases) reactivated.[77]

The heterogenization of homogeneous catalysts presents both challenges and environmentally-related advantages. This is because, whilst heterogeneous catalysts are recoverable, they may become less selective or active, may result in more product adsorption, can induce side product formation *etc.* Not only that, but during the course of the reaction it is imperative to determine whether the heterogenized catalyst remains adsorbed to the support or if it gets leached out.[68,78]

A heterogeneous catalyst that simply releases its active species into the solution like Greek warriors from the Trojan horses is likely to have limited practical utility. The conventional practice of recycling a heterogeneous catalyst without observing any significant loss of activity is by no means proof of heterogeneity. One can envisage three different scenarios in the context of leaching:

(i) The metal/active component leaches, but is not an active homogeneous catalyst.
(ii) The metal/active component leaches to form an active homogeneous catalyst.
(iii) The metal/active component does not leach and the observed catalysis is truly heterogeneous in nature.

As previously explained, rigorous proof of heterogeneity can be obtained only by filtering the catalysts at the reaction temperature before completion of the reaction and testing the filtrate for activity. However, proof of heterogeneous catalysis is not necessarily proof that no leaching occurs.[79]

For a heterogeneous catalyst, it is important to examine its ease of separation, recoverability and reusability. For practical applications of heterogeneous catalysts, the level of reusability is a very important factor. The possibility that some operationally heterogeneous catalysts, including heterogenized catalysts, gradually lose metal to the solution over time, or lose activity while remaining bound to the support, raises issues about assessing recoverability of catalysts.[80]

In addition to recovered catalyst, three other quantities may be defined: (i) the amount of active catalyst that is leached during reaction or recycling (note that each species in the catalytic cycle is an independent candidate for leaching); (ii) the amount of decomposed inactive catalyst that is leached during reaction or recycling; (iii) the amount of decomposed inactive catalyst that is recycled. Depending upon the quantities and conditions, it may not be practical to measure all of these. Because a longer-lived catalyst is often more practically useful than a recyclable catalyst, it may be better in future to look more closely into ways of extending the catalyst lifetime, rather than concentrating on catalyst recycling.[81]

In a typical recycling test, the catalyst is recovered by a simple filtration technique after each experiment. The recovered catalyst is washed with the appropriate solvent, usually acetone, dried in a desiccator and reused directly with fresh reaction mixture and without further purification for the desired product synthesis up to a number of runs. The results then show that in each case, the catalyst remains active for several runs without significant loss of efficiency. The recovered catalyst is further investigated through available techniques (like N_2 adsorption–desorption, powder XRD studies or other analyses) to confirm that the characteristics of the catalyst are retained even after successive reactions and/or leaching tests should be performed for each recycling run.[82]

3.1.3 Examples of the Application of Heterogeneous Catalysis

Reactions forming new carbon–carbon bonds are central in synthetic organic chemistry, whereas one-pot organic reactions involving multiple catalytic events are important methods to achieve high synthetic efficiency. These transformations, known as tandem, domino, cascade or multicomponent reactions (MCRs), have become an important area of research in green organic chemistry since they improve the atom economy and lower the E factors, and energy and raw material consumption. In this context, MCRs in one-pot syntheses play a significant role in modern synthetic chemistry.[83,84]

MCRs, where three or more reactants are added together at the beginning of the reaction, are carried out under the same conditions and no additional reactants or catalysts are introduced during the process. Most components of the reactants end up in the structure of the product. They offer numerous advantages including: the creation of several bonds in a single operation, convergence, operational simplicity, facile automation, and reduction in the number of workup steps, such as extraction and purification processes, rendering the synthetic transformations more sustainable.[85–87]

Heterogeneous catalysts are promising candidates to perform multistep processes. The success of a given multistep sequential or multicomponent process requires a balance of equilibria and a suitable sequence of reversible and irreversible steps. MCRs involve more than two starting reagents that couple in an exclusive ordered mode under the same reaction conditions to form a single product that contains the essential parts of the starting materials.[83,85]

Selected examples of Mannich-type reactions in processes that combine the inherent green advantages of heterogeneous catalysis and the efficacy of one-pot MCRs are reported here.

Organic chemists have used various rational methods in order to develop new MCRs to build novel chemical libraries. Amongst such methods, the single reactant replacement (SRR) technique involves replacing one of the reactants with a related one, which can have a similar role in the overall mechanism of the reaction.[88] For example, whereas the Mannich reaction is classically a combination of an aldehyde, an amine and a carbonyl compound,

which acts as a nucleophile for the imine formed between the aldehyde and the amine, the carbonyl compound can be replaced by an alkyne in the A^3-coupling, by a nitro compound in the nitro-Mannich reaction, by an indole in the aza-Friedel-Crafts reaction or by a naphthol in the case of the Betti synthesis.[89–92]

In the following examples, with a clear aim towards the identification and use of a financially attractive, recyclable heterogeneous catalyst for each selected reaction and in order to accomplish the goal of achieving eco-friendly conditions, a set of criteria were identified: (a) a cheap, reusable catalyst which is easy to prepare and to handle; (b) no co-catalysts or other auxiliary substances; (c) solvent-free reaction conditions, and (d) high yields and compatibility with a variety of reagents.

The general approach was based on the preparation and screening of various catalysts with a model reaction, followed by the optimization trials with the identified promising catalyst to establish the ideal condition for each multicomponent reaction. Expanding the scope to different substrates was the final goal, together with the calculation of the main green metrics. As a general procedure for all the selected multicomponent reactions, the three starting materials were stirred in the presence of the corresponding catalyst under neat conditions at room temperature or heated in an oil bath. Upon completion, the reaction was stopped and allowed to cool down to room temperature, where heating was performed, and the catalyst was separated by filtration.

3.1.3.1 Lewis Acid-supported Catalysts: A^3/KA^2 Coupling and Nitro-Mannich Reactions

The three-component coupling of an aldehyde, amine and alkyne (A3-coupling) for the synthesis of propargylamine derivatives is one of the best examples of an MCR and has received much attention in recent years.[93]

Amberlyst A-21 supported CuI was found to be a suitable catalyst either for an environmentally benign, one-pot A^3-/KA^2-coupling reaction of various aldehydes/ketones, amines and terminal alkynes aiming at the synthesis of propargylamines under heterogeneous and solvent-free conditions (see Scheme 3.1),[89,94] or for the one-pot three-component nitro-Mannich reaction between aldehydes, amines and nitroalkanes.[90]

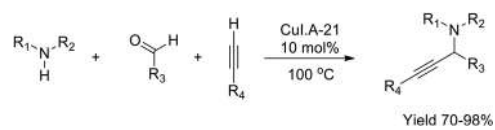

Scheme 3.1 Multicomponent reaction for the formation of propargylamines through A^3-coupling – the reaction between amines, aldehydes and alkynes. Adapted from ref. 89 with permission from the Royal Society of Chemistry.

The preparation of the supported catalyst is simple and involves the drying of Amberlyst A-21 followed by chelation of CuI on the polymeric support, with a clear colour change from white to greenish, assumed to be a result of successful fixation of the copper salt onto the polymer.[95,96] The developed A^3 protocol avoids the use of solvent and produces a variety of propargylamines in excellent yields within short reaction times.

The main advantage of the Amberlyst-based catalyst is the beaded nature of the resin. This makes the catalyst very easy to handle, especially during the filtration and recovery steps. Furthermore, the polymer support itself improves the green protocol of the reaction, as evidenced by data from a test carried out with unsupported copper(I) iodide (see Table 3.1). Although the GC yields were found to be identical, the advantage of the polymer support is evident, and gives an E-factor of just 0.34. Making use of the unsupported catalyst, on the other hand, gives a higher E-factor and also results in the loss of the catalyst, which diminishes the cost-effectiveness of the procedure.

The catalyst proved to be very stable and could easily be prepared from relatively cheap starting materials and subsequently stored for considerable periods of time. Recycling tests indicate that the catalyst can be used for five consecutive cycles without displaying a significant drop in activity (see Figure 3.1). Under the developed conditions, the reaction displays a very 'green' protocol with a high atom economy of roughly 95% and a low E-factor of around 0.3 in most cases and by totally excluding the need for toxic or dangerous solvents, while also having the added advantage of a recyclable heterogeneous catalyst, containing neither noble nor heavy or toxic metals.

Copper(I) iodide supported on Amberlyst A-21 was also employed successfully for propargylamine derivative synthesis through the KA^2-coupling reaction,[94] using the less reactive ketones. Its efficient catalytic activity, stability and recyclability were confirmed and the heterogeneity of the catalysis was proved by using a hot filtration test.[97]

Table 3.1 Comparison of the E-factors resulting from unsupported *versus* Amberlyst A-21-supported copper(I) iodide for the synthesis of a model reaction product.

	Unsupported CuI	CuI.A-21
Reagent Ratio[a]	1 (Aldehyde) : 1.2 (Amine) : 1.5 (Alkyne)	
Catalyst Quantity	20 mol%	
Yield[b]	85%	
Workup	Direct column loading	Catalyst filtration
Waste	0.2 mmol CuI catalyst 0.2 mmol amine excess 0.5 mmol alkyne excess 1 mmol H_20	0.2 mmol amine excess 0.5 mmol alkyne excess 1 mmol H_20
E-Factor	0.47 including loss of catalyst	0.34 with complete catalyst recovery

[a]Based on synthesis of the product model reaction using dibutylamine, 4-methylbenzaldehyde and phenylacetylene.
[b]GC Yield.

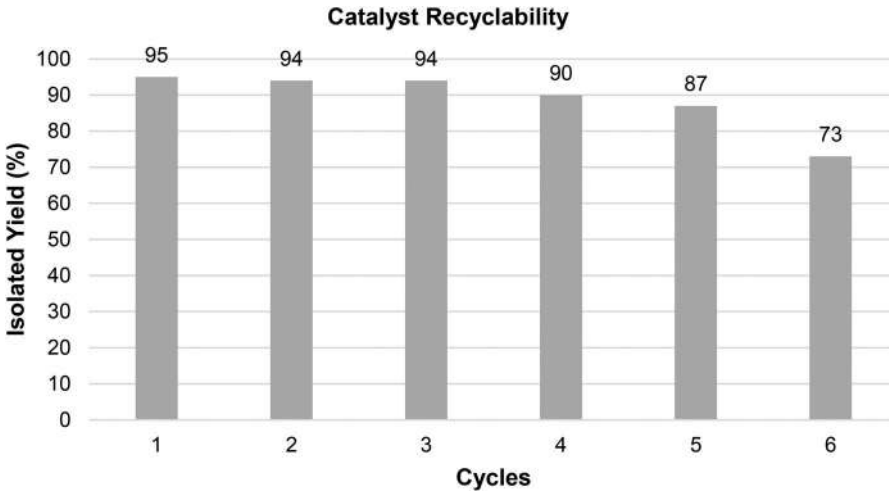

Figure 3.1 Recycling trials of the CuI.A-21 catalyst in an A^3-coupling reaction showing consistent performance over 5 cycles. Adapted from ref. 89 with permission from the Royal Society of Chemistry.

Under the same Amberlyst A-21 supported CuI catalysis, the one-pot three-component nitro-Mannich reaction exhibited a green protocol with a high atom economy of 93% and a low E-factor of 1.26 and afforded a wide scope of β-nitroamines, in moderate to excellent yields.[90]

The catalyst proved to be highly active due to its bifunctional Lewis acidic and Brønsted basic nature, and recycling tests indicated a consistent performance over eight cycles, in which a drop of 10% in yield was observed. A quantitative analysis of the stability of the heterogeneous catalyst was performed by atomic absorption spectroscopy (AAS), to determine the amount of copper that leached into the solution throughout each cycle. The stability of the catalyst was demonstrated, showing that only 1% Cu had leached into the solution after eight cycles.[90]

3.1.3.2 Heteropolyacid-supported Catalysts: Aza-Friedel-Crafts Reaction

As strong acid catalysts, heteropolyacids are able to catalyse at low temperatures a wide range of homogeneous catalytic processes.[85] Heteropolyacids can be heterogenized by either supporting them on a high surface area carrier, such as silica, or by forming their cesium or potassium salts, which are solids with micro and mesoporosity and are insoluble for organic reactions.[98,99]

Silicotungstic acid supported on Amberlyst 15 (WSi/A15) allowed a regioselective one-pot multicomponent aza-Friedel-Crafts (AFC) reaction for the synthesis of 3-substituted indoles *via* aldehyde, indole and primary/secondary

or tertiary anilines (see Scheme 3.2).[91] The aza-Friedel–Crafts reaction was performed under green, neat and heterogeneous conditions in the presence of 1.25 mmol% of 30% w/w silicotungstic acid supported on Amberlyst 15 beads. All three types of aromatic amines gave regioselective products having the same structure. All reactions proceeded *via* two separate C–C bond forming reactions rather than C–C and C–N bond forming steps, while previous studies have shown that the product from tertiary aromatic amines is different from secondary or primary ones.

The catalyst WSi/A15 (30% w/w) was easily prepared by stirring WSi with A15 in ethanol for 8 h before drying at 100 °C for 24 h. X-ray fluorescence (XRF) was performed on a sample of WSi/A15 catalyst in order to confirm the exact loading of WSi. Flame atomic absorption spectroscopy (FAAS) was performed on the crude reaction mixture for each separate recycling trial in order to calculate the amount of leaching of WSi from the catalyst WSi/A15 (see Table 3.2). No evidence for leaching or decomposition of the complex catalyst was observed during the catalytic reaction. A typical hot filtration

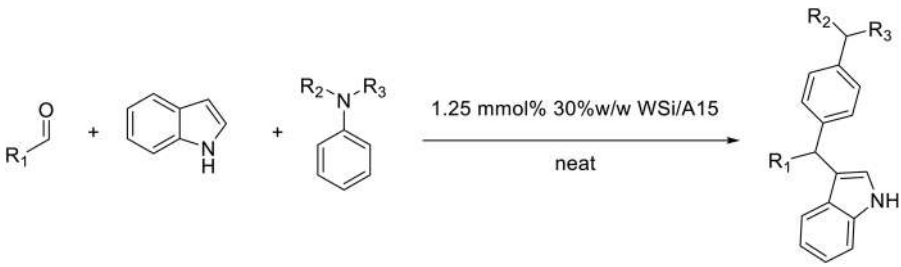

Scheme 3.2 Regioselective one-pot aza-Friedel-Crafts multicomponent reaction between aldehyde, indole and primary, secondary or tertiary anilines to form 3-substituted indoles. Adapted from ref. 91 with permission from the Royal Society of Chemistry.

Table 3.2 Leaching results for the WSi/A15 catalyst. Adapted from ref. 91 with permission from the Royal Society of Chemistry.

	Concentration of W in 40 mL samples (ppm)[a]	Amount of W in 40 mL samples (mg)[b]	Percentage leaching (%)[c]
Run 1	23.5	0.940	1.36
Run 2	59.6	2.38	3.46
Run 3	1.23	0.05	0.072
Run 4	180	7.20	10.4
Run 5	9.82	0.393	0.569
		Total	15.9

[a]Value obtained from an FAAS spectrometer.
[b]Total amount of W obtained after extraction from the crude reaction mixture using aqueous sodium hydroxide.
[c]This was calculated based on the fact that 0.3 g of 30% WSi/A15 was used with the mass percentage of W in WSi being 76.7%.

Table 3.3 E-factors for model reactions using separately WSi/A15, WSi and A15 as catalysts. Adapted from ref. 91 with permission from the Royal Society of Chemistry.

	Heterogeneous WSi/A15[a]	Homogeneous WSi[a]	Heterogeneous A15[a]
Yield[b]	92%	93%	74%
Total mass of starting materials	0.293 (indole) + 0.535 (amine) + 0.300 (aldehyde) + 0.300 (catalyst) = 1.428 g	0.293 (indole) + 0.535 (amine) + 0.300 (aldehyde) + 0.090 (catalyst) = 1.218 g	0.293 (indole) + 0.535 (amine) + 0.300 (aldehyde) + 0.300 (catalyst) = 1.428 g
Total mass of product + recovered catalyst (if any)	0.750 (product) + 0.300 (catalyst) = 1.050 g	0.756 g (product) [No recovered catalyst]	0.602 (product) + 0.300 (catalyst) = 0.902 g
Total mass of waste	1.428–1.050 = 0.378 g	1.218–0.756 = 0.462 g	1.428–0.902 = 0.526 g
E-factor (waste/product)	$\frac{0.378}{0.750} = 0.504$	$\frac{0.462}{0.756} = 0.611$	$\frac{0.526}{0.602} = 0.875$

[a]Reaction conditions: 2.5 mmol (4-methylbenzaldehyde), 2.5 mmol (indole), 5 mmol (*N*-methylaniline), RT, homogeneous/heterogeneous catalyst, neat.
[b]Pure isolated yield after column chromatography.

test was performed on the model reaction to investigate whether the reaction proceeded in a heterogeneous or a homogeneous fashion. In this case, no change in conversion was observed, which suggests that the catalyst is heterogeneous in nature, confirming that once the catalyst had been removed the reaction stopped proceeding.

A comparison of the green metrics calculated for the model reaction (see Table 3.3) showed that the reaction is significantly much more environmentally-benign, with a lowest *E-factor* value, than its homogeneous version or the one utilising A15 only.

3.2 Conclusions

The key to sustainability is catalysis and success will depend on an effective integration of catalysis in organic synthesis. Traditional barriers between catalysis and mainstream organic synthesis are gradually disappearing.

The use of heterogeneous catalysts not only enables catalyst immobilisation for easier handling, but also allows for the potential reuse, recycling or regeneration of the catalyst leading to far greener outcomes, as well as more economically viable reactions.

With several available strategies to design and prepare mesoporous catalysts, tune their pore structure and specific surface area and impregnate them with various active transition metal nanoparticles, or complex or organic functional groups at the pore surface, one can prepare a number

of new metal-doped and organically functionalized mesoporous materials and explore their potential in versatile catalytic transformations under heterogeneous reaction conditions. These green catalytic pathways are highly demanded for the development of industrial manufacturing processes.

References

1. P. T. Anastas and J. C. Warner, *Green Chemistry: Theory and Practice*, Oxford University Press, New York, 1998.
2. P. T. Anastas, M. M. Kirchhoff and T. C. Williamson, *Appl. Catal., A*, 2001, **221**, 3.
3. I. Pálinkó, in *Green Chemistry*, ed. B. Török and T. Dransfield, Elsevier, 2018, ch. 3.12, pp. 415–447.
4. R. van Santen, in *Catalysis: From Principles to Applications*, ed. M. Beller, A. Renken and R. van Santen, Wiley-VCH Verlag GmbH, Weinheim, 2012, ch. 1, pp. 3–19.
5. M. O. Simon and C. J. Li, *Chem. Soc. Rev.*, 2012, **41**, 1415.
6. P. Anastas and N. Eghbali, *Chem. Soc. Rev.*, 2010, **39**, 301.
7. R. A. Sheldon, *Chem. Soc. Rev.*, 2012, **41**, 1437.
8. R. A. Sheldon, *Green Chem.*, 2005, **7**, 267.
9. R. A. Sheldon, *Chem. Commun.*, 2008, 3352–3365.
10. O. Deutschmann, H. Knozinger, K. Kochloefi and T. Turek, in *Ullmann's Encyclopedia of Industrial Chemistry*, ed. B. Elvers, Wiley-VCH Verlag GmbH, Weinheim, 2009.
11. J. H. Clark, *Acc. Chem. Res.*, 2002, **35**, 791.
12. M. Belter, S. Gladioli, and D. Heller, in *Catalysis: From Principles to Applications,* ed. M. Beller, A. Renken and R. van Santen, Wiley-VCH Verlag GmbH, Weinheim, 2012, ch. 6, pp. 152–170.
13. R. Luque, J. H. Clark and D. J. Macquarrie, in *Experiments in Green and Sustainable Chemistry*, ed. H. von H. W. Roesky and D. K. Kennepohl, Wiley-VCH, Weinheim, 2009, ch. 1, pp. 3–6.
14. see for example: (a) B. Toukoniitty, J.-P. Mikkola, D. Yu. Murzin and T. Salmi, *Appl. Catal., A*, 2005, **279**, 1; (b) C. R. Strauss and R. S. Varma, *Top. Curr. Chem.*, 2006, **266**, 199.
15. M. Abid and B. Torok, in *Experiments in Green and Sustainable Chemistry*, ed. H. von H. W. Roesky and D. K. Kennepohl, Wiley-VCH, Weinheim, 2009, ch. 7, pp. 39–44.
16. (a) R. A. Sheldon, *Chemtech*, 1994, **24**, 38; (b) R. A. Sheldon, *Pure Appl. Chem.*, 2000, **72**(7), 1233.
17. R. A. Sheldon and H. van Bekkum, *Fine Chemicals through Heterogeneous Catalysis*, Wiley-VCH Verlag GmbH, Weinheim, 2001, ch. 1, pp.1–11.
18. Z. Wang, G. Chen and K. Ding, *Chem. Rev.*, 2009, **109**, 322.
19. P. Zhang, H. Li, G. M. Veith and S. Dai, *Adv. Mater.*, 2015, **27**, 234.
20. Y. Zhang and S. N. Riduan, *Chem. Soc. Rev.*, 2012, **41**, 2083.
21. Y. C. Sharma and B. Singh, *Biofuels, Bioprod. Biorefin.*, 2011, **5**, 69.

22. R. van Santen, in *Catalysis: From Principles to Applications,* ed. M. Beller, A. Renken and R. van Santen, Wiley-VCH Verlag GmbH, Weinheim, 2012, ch. 2, pp. 20–47.
23. R. van Santen, in *Catalysis: From Principles to Applications,* ed. M. Beller, A. Renken and R. van Santen, Wiley-VCH Verlag GmbH, Weinheim, 2012, ch. 4, pp. 67–109.
24. R. van Santen, in *Catalysis: From Principles to Applications,* ed. M. Beller, A. Renken and R. van Santen, Wiley-VCH Verlag GmbH, Weinheim, 2012, ch. 5, pp. 113–151.
25. K. Ruth and P. Albers, Materials for Solid Catalysts, in *Springer Handbook of Materials Data*, ed. H. Warlimont and W. Martienssen, Springer Handbooks. Springer, Cham. 2018.
26. M. Boudart, in *Handbook of Heterogeneous Catalysis*, ed. G. Ertl, H. Knözinger and J. Weitkamp, Wiley-VCH, Weinheim, 1997, p. 1.
27. I. Langmuir, *J. Am. Chem. Soc.*, 1915, **37**, 1139.
28. I. Langmuir, *Trans. Faraday Soc.*, 1922, **17**, 607.
29. H. S. Taylor, *Proc. R. Soc. A*, 1925, **108**, 105.
30. G. A. Somorjai, *Annu. Rev. Phys. Chem.*, 1994, **45**, 721.
31. G. Ertl, *Adv. Catal.*, 2000, **45**, 1.
32. A. Balandin, *Adv. Catal. Rel. Subj.*, 1969, **19**, 1.
33. V. Ponec and W. M. H. Sachtler, in *Proc. 5th Intern. Congr. Catal.*, ed. G. C. Bond, P. B. Wells and F. C. Tompkins, The Chemical Society, London, 1976, vol. 1, p. 645.
34. R. L. Burwell, G. L. Haller, K. C. Taylor and J. F. Read, *Adv. Catal.*, 1969, **20**, 1.
35. R. L. Burwell, in *Catalysis: Science and Technology*, ed. J. R. Anderson and M. Boudart, Springer, Heidelberg, 1991, vol. 9, p. 1.
36. B. Hammer and J. K. Nørskov, *Adv. Catal.*, 2000, **45**, 71.
37. S. A. Stevenson, J. A. Dumesic, R. T. K. Baker and E. Ruckenstein, *Metal Support Interactions in Catalysis, Sintering and Redispersion*, Van Nostrand Reinhold, New York, 1987, p. 141.
38. H. Knozinger and E. Taglauer, in *Handbook of Heterogeneous Catalysis*, ed. G. Ertl, H. Knozinger and J. Weitkamp, Wiley-VCH, Weinheim, 1997, vol. 1, p. 216.
39. G. C. Bond, in *Handbook of Heterogeneous Catalysis*, ed. G. Ertl, H. Knözingerand J. Weitkamp, Wiley-VCH, Weinheim, 1997, vol. 2, p. 752.
40. L. Damjanovic and A. Auroux, in *Handbook of Thermal Analysis and Calorimetry*, ed. M. E. Brown and P. K. Gallagher, Elsevier Science B.V., 2008, vol. 5, ch. 11, pp. 387–438.
41. H. Hittori, *Chem. Rev.*, 1995, **95**, 537.
42. G. W. Kabalka and R. M. Pagni, *Tetrahedron*, 1997, **53**, 7999.
43. S. Onitsuka, Y. Z. Jin, A. C. Shaikh, H. Furuno and J. Inanaga, *Molecules*, 2012, **17**, 11469.
44. N. L. D. Filho and D. R. do Carmo, in *Encyclopedia of Surface and Colloid Science -1*, Marcel Dekker, Inc., New York, 2004.
45. Y. Zhang and S. N. Riduan, *Chem. Soc. Rev.*, 2012, **41**, 2083.

46. P. Gupta and S. Paul, *Catal. Today*, 2014, **236**, 153.
47. H. Hartati, M. Santoso, S. Triwahyono and D. Prasetyoko, *Bull. Chem. React. Eng. Catal.*, 2013, **8**, 14.
48. E. G. Derouane, J. C. Védrine, R. R. Pinto, P. M. Borges, L. Costa, M. A. N. D. A. Lemos, F. Lemos and F. Ramôa Ribeiro, *Catal. Rev.*, 2013, **55**, 454.
49. R. A. Sheldon, I. Arends and U. Hannelfeld, *Green Chemistry and Catalysis*, Wiley-VCH Verlag GmbH & Co. KGaA, Weinheim, 2007.
50. Y. Ono and H. Hattori, *Solid Base Catalysis*, Springer-Verlag: Berlin Heidelberg and Tokyo Institute of Technology, Tokyo, 2011.
51. G. Nagendrappa, *Appl. Clay Sci.*, 2011, **53**, 106.
52. I. V. Kozhevnikov, *J. Mol. Catal. A: Chem.*, 2007, **262**, 86.
53. I. V. Kozhevnikov, *Catal. Rev.: Sci. Eng.*, 1995, **37**, 311.
54. K. M. Parida and S. Mallick, *J. Mol. Catal. A: Chem.*, 2007, **275**, 77.
55. F. Albericio and J. Tulla-Puche, *The Power of Functional Resins in Organic Synthesis,* Wiley-VCH Verlag GmbH & Co. KGaA, Weinheim, 2008.
56. M. Bihani, P. P. Bora, G. Bez and H. Askari, *ACS Sustainable Chem. Eng.*, 2013, **1**, 440.
57. R. van Santen, in *Catalysis: From Principles to Applications,* ed. M. Beller, A. Renken and R. van Santen, Wiley-VCH Verlag GmbH, Weinheim, 2012, ch. 20, pp. 420–430.
58. A. J. van Dillen, R. J. A. M. Terörde, D. J. Lensveld, J. W. Geus and K. P. de Jong, *J. Catal.*, 2003, **216**, 257.
59. R. van Santen, in *Catalysis: From Principles to Applications,* ed. M. Beller, A. Renken and R. van Santen, Wiley-VCH Verlag GmbH, Weinheim, 2012, ch. 21, pp. 431–444.
60. N. Pal and A. Bhaumik, *RSC Adv.*, 2015, **5**, 24363.
61. G. Nagendrappa, *Appl. Clay Sci.*, 2011, **53**, 106.
62. A. P. Wight and M. E. Davis, *Chem. Rev.*, 2002, **102**, 3589.
63. P. Barbaro and F. Liguori, *Chem. Rev.*, 2009, **109**, 515.
64. M. Benaglia, A. Puglisi and F. Cozzi, *Chem. Rev.*, 2003, **103**, 3401.
65. J. Y. Lee, O. K. Farha, J. Roberts, K. A. Scheidt, S. B. T. Nguyen and J. T. Hupp, *Chem. Soc. Rev.*, 2009, **38**, 1450.
66. E.-J. Ras and G. Rothenburg, *RSC Adv.*, 2014, **4**, 5963.
67. G. J. Hutchings, *J. Mater. Chem.*, 2009, **19**, 1222.
68. R. H. Crabtree, *Chem. Rev.*, 2012, **112**, 1536.
69. Q. Yin, J. M. Tan, C. Besson, Y. V. Geletii, D. G. Musaev, A. E. Kuznetsov, Z. Luo, K. I. Hardcastle and C. L. Hill, *Science*, 2010, **328**, 342.
70. J. J. Stracke and R. G. Finke, *J. Am. Chem. Soc.*, 2011, **133**, 14872.
71. J. E. Hamlin, K. Hirai, A. Millan and P. M. Maitlis, *J. Mol. Catal.*, 1980, **7**, 543.
72. See for example: (a) J. D. Aiken and R. G. Finke, *J. Mol. Catal. A: Chem.*, 1999, **145**, 1; (b) J. A. Widegren and R. G. Finke, *J. Mol. Catal. A: Chem.*, 2003, **198**, 317; (c) E. Bayram, J. C. Linehan, J. L. Fulton, J. A. S. Roberts, N. K. Szymczak, T. D. Smurthwaite, S. Özkar, M. Balasubramanian and R. G. Finke, *J. Am. Chem. Soc.*, 2011, **133**, 18889.
73. J. Schwartz, *Acc. Chem. Res.*, 1985, **18**, 302.

74. D. E. Bergbreiter, J. H. Tian and C. Hongfa, *Chem. Rev.*, 2009, **109**, 530.
75. N. E. Leadbeater and M. Marco, *Chem. Rev.*, 2002, **102**, 3217.
76. H. E. B. Lempers and R. A. Sheldon, *J. Catal.*, 1998, **175**, 62.
77. E. Farnetti, R. Di Monte and J. Kaspar, in *Inorganic and Bioinorganic Chemistry, Vol II*, ed. E. Bertin, *Encyclopedia of Life Support Systems*, UNESCO, EOLSS, Paris, 2007, pp. 50–86.
78. A. Choplin and F. Quignard, *Coord. Chem. Rev.*, 1998, **178–180**, 1679.
79. R. A. Sheldon, M. Wallau, I. W. C. E. Arends and U. Schuchardt, *Acc. Chem. Res.*, 1998, **31**, 485.
80. C. W. Jones, *Top. Catal.*, 2010, **53**, 942.
81. J. A. Gladysz, *Pure Appl. Chem.*, 2001, **73**, 1319.
82. B. Jyoti Borah, S. Jyoti Borah, L. Saikia and D. Kumar Dutta, *Catal. Sci. Technol.*, 2014, **4**, 1047.
83. M. J. Climent, A. Corma and S. Iborra, *Chem. Rev.*, 2011, **111**, 1072.
84. B. Ganem, *Acc. Chem. Res.*, 2009, **42**, 463.
85. M. J. Climent, A. Corma and S. Iborra, *RSC Adv.*, 2012, **2**, 16.
86. R. C. Cioc, E. Ruijter and R. V. A. Orru, *Green Chem.*, 2014, **16**, 2958.
87. J. Zhu, Q. Wang and M.-X. Wang, *Multicomponent Reactions in Organic Synthesis,* Wiley-VCh, Weinheim, 2015.
88. V. A. Chebanov and S. M. Desenko, *Diversity-Oriented Synth.*, 2014, **1**, 43.
89. G. Bosica and J. Gabarretta, *RSC Adv.*, 2015, **5**, 46074.
90. G. Bosica and R. Zammit, *PeerJ*, 2018, **6**, e506.
91. G. Bosica and R. Abdilla, *Green Chem.*, 2017, **19**, 5683.
92. G. Bosica, R. Abdilla and K. Demanuele, *Eur. J. Org. Chem.*, 2018, **44**, 6127.
93. N. Salam, S. K. Kundu, A. Singha Roy, P. Mondal, S. Roy, A. Bhaumik and Sk. Manirul Islam, *Catal. Sci. Technol.*, 2013, **3**, 3303.
94. G. Bosica and R. Abdilla, *J. Mol. Catal. A: Chem.*, 2017, **426**, 542.
95. C. Girard, E. Onen, M. Aufort, S. Beauvière, E. Samson and J. Herscovici, *Org. Lett.*, 2006, **8**, 1689.
96. M. Keshavarz, N. Iravani, A. Ghaedi, A. Z. Ahmady, M. Vafaei-Nezhad and S. Karimi, *SpringerPlus*, 2013, **2**, 1.
97. H. Gruber-Woelfler, P. F. Radaschitz, P. W. Feenstra, W. Haas and J. G. Khinast, *J. Catal.*, 2012, **286**, 30.
98. I. V. Kozhevnikov, *Catal. Rev. - Sci. Eng.*, 1995, **37**, 311.
99. Y. Izumi, M. Ogawa and K. Urabe, *Appl. Catal., A*, 1995, **132**, 127.

CHAPTER 4

Biocatalysis, an Introduction. Exploiting Enzymes as Green Catalysts in the Synthesis of Chemicals and Drugs

DOMIZIANA MASCI[a] AND DANIELE CASTAGNOLO*[a]

[a]School of Cancer and Pharmaceutical Sciences, King's College London, 150 Stamford Street, SE1 9NH, London, UK
*E-mail: daniele.castagnolo@kcl.ac.uk

4.1 Introduction

Catalysis is one of the 12 *Principles of Green Chemistry* and it can be described as the ability of a substance, known as a catalyst, to modify the rate of a chemical reaction when added to the reaction without being consumed during the process.[1] A catalyst can then be defined as "*a substance that changes the velocity of a reaction without itself being changed in the process*",[2] and, in principle, it can be used in small amounts (sub-stoichiometric) and, adopting appropriate strategies, it can be recycled indefinitely. This makes catalysis fit well with the principles of green chemistry, since the regeneration of a catalyst makes it possible to not produce any waste in chemical reactions, and most importantly, in industrial chemical processes. Catalysis can be classified into different categories, such as (a) heterogeneous and homogeneous catalysis, if the catalyst and the reactants are in the same or different phases, (b) organocatalysis, where

Sustainable Organic Synthesis: Tools and Strategies
Edited by Stefano Protti and Alessandro Palmieri

Published by the Royal Society of Chemistry, www.rsc.org

the catalyst is generally a small organic molecule, (c) photocatalysis, where a catalyst is used to accelerate a photoreaction, and finally (d) biocatalysis, which employs enzymes as catalysts. According to the principles of green chemistry and sustainable development, biocatalysis is considered both a green and sustainable technology.[3] Enzymes, often referred to as biocatalysts, can catalyse highly selective (chemo-, regio- and stereoselective) transformations allowing the synthesis of complex chiral molecules under mild reaction conditions. Biocatalysis offers many advantages over other classical chemical methods, such as the possibility to carry out chemical reactions at mild temperatures (4–60 °C), thus requiring a lower amount of energy, as well as in an aqueous medium, reducing the use and the disposal of petroleum-based solvents.[4]

Thanks to the enormous progress made in the fields of genome sequencing, molecular biology and protein engineering, enzymes can now be produced at large scale and limited costs and they can be immobilised on solid supports, remaining stable for long times. Today, biocatalysts are increasingly used in the pharmaceutical and chemical industries as well as in polymer sciences and food and flavour research.[5] As examples, nitrile hydratases are employed in chemical industries to convert acrylonitrile into acrylamide at multi-hundred thousand ton per annum scale,[6] while penicillin G amidase[7] is used by pharmaceutical companies for the industrial production of β-lactam antibiotics at ton scale. The use of enzymes in chemical synthesis and organic chemistry goes back to the beginning of the 20th century and microorganisms, such as yeasts, have been widely employed in the synthesis and production of various chemicals and pharmaceutical ingredients in the past.[8] However, it was only from the 1990s that biocatalysis research increased exponentially, mainly due to the progress made in the fields of protein engineering and enzyme evolution.[9] In 2012, Bornscheuer identified three waves of biocatalysis to describe the evolution of technological research and innovations that allowed biocatalysis to reach its current level and application in academia and industry.[10] In the first wave, which started a century ago, plant and animal tissue extracts and microbial strains containing enzymes with a specific activity were used to accomplish useful synthetic transformations, such as the production of (*R*)-mandelonitrile from benzaldehyde and hydrogen cyanide using a plant extract.[11] The second wave of biocatalysis emerged in the 1980s when scientists, taking advantage of gene technology and site-directed mutagenesis, become able to clone, express and improve the properties of the enzymes of interest. Finally, the third wave of biocatalysis began in the 1990s thanks to the development of advanced protein engineering technologies which, in combination with high-throughput screening methods, led to what is today commonly known as "*directed evolution*".[12] In 2017, Bornscheuer suggested that a fourth wave of biocatalysis is approaching where the design of enzymes for targeted and unnatural chemical transformations or the combination of enzymes in cascade reactions or *via* metabolic engineering will become established technologies and synthetic strategies.[13]

This book chapter aims to be an introduction for the reader to biocatalysis and enzyme-catalysed synthetic chemistry. Due to the high number of enzymes developed in the last few decades and the large amount of literature available in the field, it is out of the scope of this chapter to cover in depth all the biocatalytic transformations and the enzymatic synthetic methodologies described to date. Useful references will be provided in the chapter for those who want to have a more comprehensive overview of the topic. Rather, this chapter will mainly focus on a few selected enzymes, like hydrolytic lipases and nitrilases or oxidoreductive enzymes like monoamine oxidases, ketoreductases and monooxygenases, and it will provide examples on the use of such biocatalysts in the synthesis of chemicals and pharmaceutical ingredients and it will highlight the advantages of biocatalysis over classical chemical methodologies.

4.2 Lipases

Lipases are ubiquitous enzymes belonging to the group of serine hydrolases that in nature catalyse the hydrolysis of triglycerides to the corresponding fatty acids and glycerol. Due to their properties, such as a broad substrate specificity, no need of cofactors to work, capability to work at high substrate concentrations, high stereoselectivity (chemo-, regio-, enantio-) and the ability to operate both in aqueous and non-conventional media, lipases are the most used biocatalysts in industry and academia. Nowadays, lipases find broad applications in the detergent, food and pharmaceutical industries and, due to their low cost, are widely used in academia in many asymmetric syntheses.[14]

In 1990, the three-dimensional structures of *Mucor miehei* triglyceride lipase[15] and a pancreatic lipase (triacylglycerol acyl hydrolase) were first reported.[16] Later the structures of lipases from various sources (including *Geotrichum candidum*,[17] *Candida rugosa*[18] and *Chromobacterium viscosum*[19]) were described, while the crystal structure of lipase B from *Candida antarctica*, one of the most widely used lipase biocatalysts, was reported in 1994.[20] The main features present in all the lipase enzymes include an α/β-hydrolase fold and an active site characterised by a triad composed of Ser-His-Asp/Glu.

The active site is shielded by a helical oligopeptide unit and this so-called lid, upon interaction with a hydrophobic interface, undergoes sequential changes responsible for the exposition of the active site and the free access of the substrate (interfacial activation). Due to the similarity between the catalytic triad found in lipases and those observed in serine proteases, it is widely accepted that the mechanism of lipase catalysis is similar to the one of serine proteases.[21] The mechanism of lipase-mediated hydrolysis of esters, as shown in Scheme 4.1, involves initially a nucleophilic attack of the serine hydroxyl group on the ester group of a susceptible substrate, with the formation of an acyl-enzyme complex and the release of an alcohol molecule; then, the subsequent hydrolysis of the acyl-enzyme complex results in the release of the carboxylic acid product and the regenerated lipase enzyme.[22]

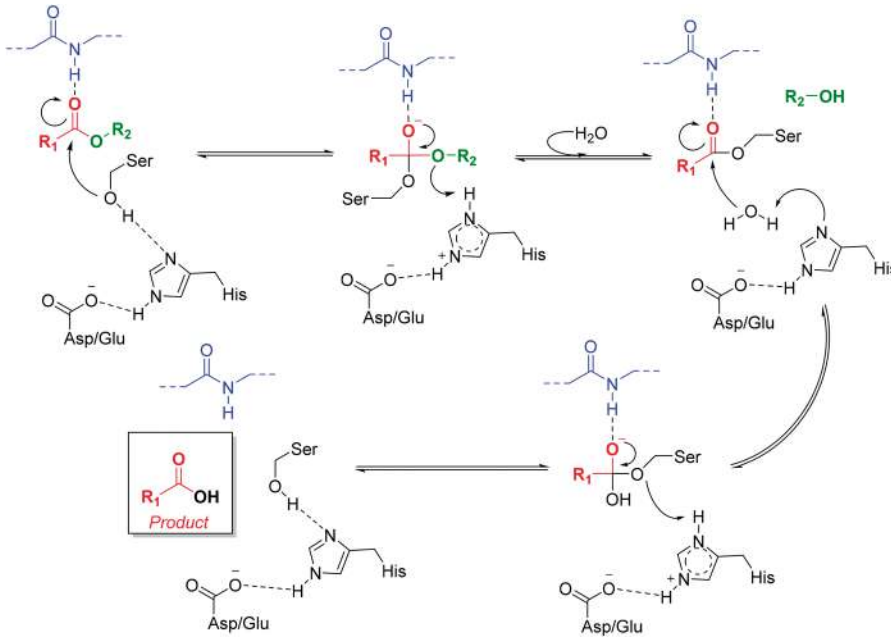

Scheme 4.1 General mechanism for the lipase-mediated hydrolysis of esters.

Over the past few years, lipases have received considerable attention as biocatalysts in organic chemistry and in various industrial applications, since they can catalyse a variety of chemical reactions other than simple hydrolysis of ester substrates; lipases have been in fact used also in esterification reactions, synthesis of amides and more recently in oxidation reactions, being able to catalyse the synthesis *in situ* of oxidative reactive intermediates (Scheme 4.2). Finally, the possibility of immobilizing lipases on various solid supports[23] allowed the use of such enzymes also in non-aqueous media, expanding broadly their use at an industrial level. This section will highlight some examples of lipase-catalysed reactions for the synthesis of pharmaceutical ingredients and chemical building blocks.

4.2.1 Lipase-catalysed Hydrolysis of Esters

A typical example of the use of lipases in the synthesis of active pharmaceutical ingredients (APIs) is the synthesis of (*S*)-naproxen from the racemic naproxen methyl ester **1** in the presence of lipase from *Candida rugosa* immobilized on Amberlite XAD7 (Scheme 4.3a). The activity of (*S*)-naproxen is 28-fold higher than that of the corresponding (*R*)-enantiomer. The two enantiomers can be separated through a lipase-catalysed enzymatic kinetic resolution (EKR) at 45 °C in a water/isooctane biphasic system. The lipase catalyses the selective hydrolysis of the (*S*)-enantiomer of **1** leading to the

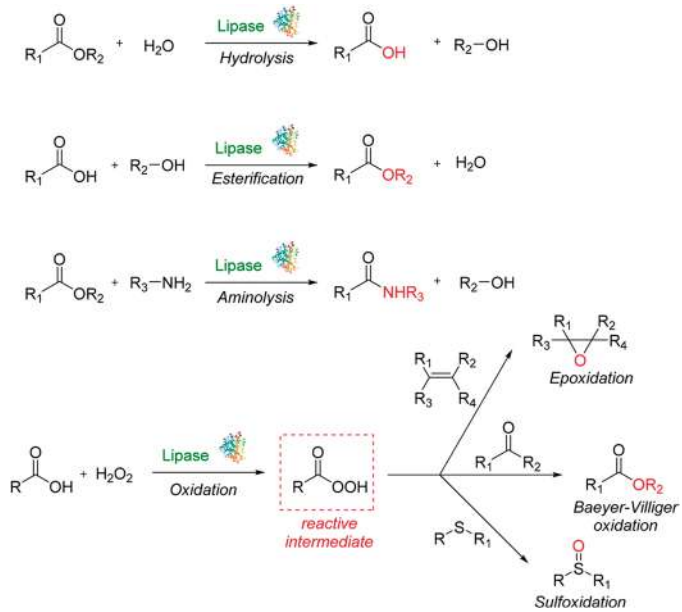

Scheme 4.2 Main examples of reactions catalysed by lipases, in particular CAL-B.

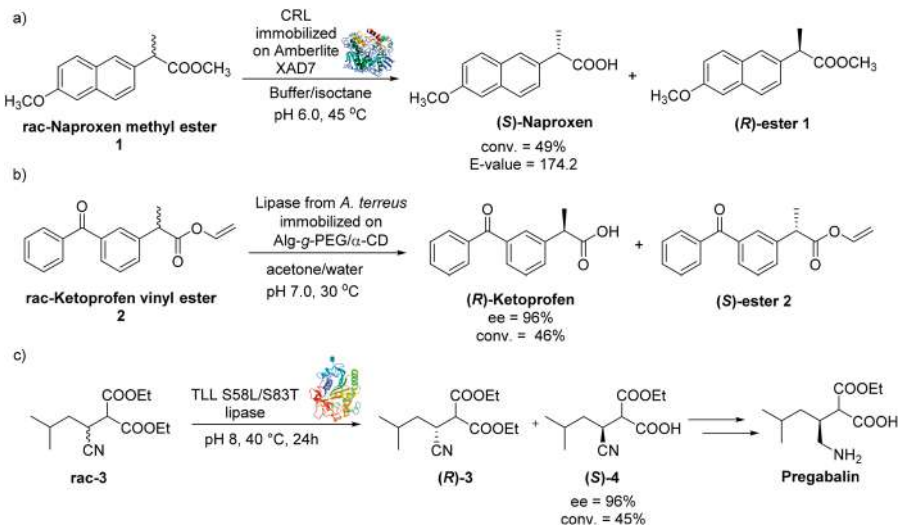

Scheme 4.3 Lipase catalysed synthesis of APIs (a. (*S*)-Naproxen, b. (*R*)-Ketoprofen, c. Pregabalin) through enzymatic kinetic resolution.

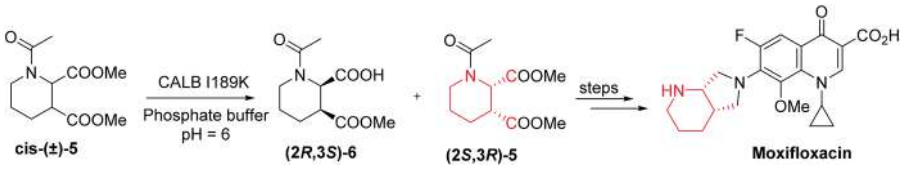

Scheme 4.4 Engineered CAL-B-catalysed synthesis of the moxifloxacin drug precursor **(2S, 3R)-5**.

formation of (*S*)-naproxen with good conversion (49%) and excellent E-value (174.2),[24] while the (*R*)-ester **1** is left unreacted. Similarly, the EKR of racemic ketoprofen was reported using lipase from *A. terreus* immobilised on Alg-g-PEG/a-CD (Scheme 4.3b).[25] The (*R*)-enantiomer of racemic ketoprofen ester **2** was selectively hydrolysed by the lipase leading to the separation of the two enantiomers, and the (*R*)-ketoprofen was isolated with 96% ee and 46% conversion. Later, other lipases were used in the EKR of rac-ketoprofen, namely the lipases from *Mucor javanicus*, *Rhizomucor miehei*, *Candida rugosa* and *Pseudomonas cepacia*. High enantioselectivity ($E > 200$) was observed when the immobilized *Mucor javanicus* lipase was employed, while *Rhizomucor miehei* lipase showed a moderate *E*-value (35) but high compatibility with various organic solvents including tert-butylmethyl ether (TBME), tetrahydrofuran (THF), 2-methyl-THF, 1,4-dioxane, acetone and acetonitrile.[26]

A team from Pfizer[27] developed an elegant process for the production of the drug pregabalin, through a lipase-catalysed resolution of the racemic substrate **rac-3** (Scheme 4c). *E. coli* whole cells expressing a mutated *Thermomyces lanuginosus* lipase (TLL S58L/S83T) were employed for the hydrolysis of the diester **rac-3** at 40 °C in 100 mM Tris-HCl buffer (pH 8.0) to give the mono-acid derivative **4**, a synthetic precursor of pregabalin, with 96% ee and 45% conversion. Lipase TLL S58L/S83T showed an improved (*S*)-enantioselectivity compared with the TLL wild type.

Recently, engineered *Candida antarctica* lipase B (CAL-B I189K) was used for the synthesis of the moxifloxacin chiral intermediate **(2*S*,3*R*)-5** through an efficient and cheap enzymatic resolution of racemic *cis*-(±)-dimethyl-1-acetylpiperidine-2,3-dicarboxylate **cis-(±)-5** (Scheme 4.4). Lipase CAL-B I189K displayed a 193-fold increase in catalytic efficiency compared to the wild-type enzyme without impacting on its enantioselectivity ($E > 2000$). As the catalytic activity increased, the mutated CAL-B I189K-mediated enzymatic resolution gave significantly higher productivity demonstrating its great potential for the industrial preparation of the chiral moxifloxacin precursor **(2*S*,3*R*)-5**.[28]

4.2.2 Lipase-catalysed Esterification Reactions

Lipases are enzymes able to catalyse both the hydrolysis of esters as well as the reverse reaction, namely the esterification of carboxylic acids, when used under appropriate conditions.[29] For instance, commercially available lipases

from C*andida rugosa* immobilized onto magnetic beads were used in the synthesis of enantiomerically pure ibuprofen *via* an esterification reaction (Scheme 4.5a). The *S*-enantiomer of the racemic ibuprofen was selectively esterified when treated with C*andida rugosa* lipase in the presence of *n*-PrOH. The (*S*)-ester **7** was obtained with an E-value of 19, 83% ee and conversion of 42%.[30]

Various lipases, such as Novozym 435, Lipozyme TL IM, Lipozyme RM IM, lipase Amano AS and lipase AYS Amano, have been investigated in the microwave-assisted synthesis of enantiopure ketorolac (Scheme 4.5b). Among them, Novozym 435 proved to be the most efficient biocatalyst leading to the selective esterification of the (*R*)-enantiomer of ketorolac with 50% conversion. Both the ester **8** and (*S*)-ketorolac were obtained with excellent ee (99%).[31]

Candida antarctica lipase B (CAL-B) has also been employed as a biocatalyst in flow-chemistry reactors for the enantioselective esterification of flurbiprofen racemate employing *n*-butanol as the nucleophilic reagent.[32] After 1 h the (*R*)-enantiomer was converted into the corresponding ester **(*R*)-9** allowing the recovery of the (*S*)-flurbiprofen with an enantiomeric excess ≥90% and a chemical purity >98% (Scheme 4.5c).

Lipases can also be used for the enzymatic resolution of racemic alcohol substrates through a transesterification process, as shown in Scheme 4.6. An ester, generally vinyl acetate or ethyl acetate, is employed as the lipase substrate, selectively transferring an acetyl group to the racemic alcohol. The mechanism of the reaction is similar to the hydrolysis reaction described in Scheme 4.1, with the alcohol in place of the water molecule. An example of

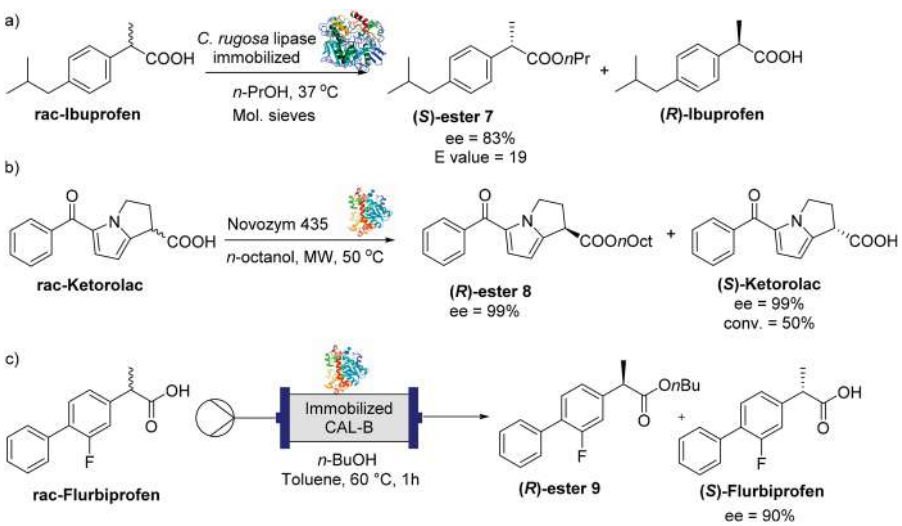

Scheme 4.5 Lipase-catalysed esterification of carboxylic acid substrates for the synthesis of enantiomerically pure drugs, such as: a) (*R*)-Ibuprofen; b) (*S*)-Ketorolac; c) (*S*)-Flurbiprofen.

enzymatic kinetic resolution of racemic alcohols with lipases is provided by the synthesis of enantiomerically pure 1-(2-furyl)ethanol **(*R*)-10**, a key building block in the manufacture of various natural products, antibiotics and carbohydrates. The lipase from *Candida antarctica* B (Novozym 435) catalyses the selective acetylation of the (*S*)-enantiomer of **rac-10**, leaving **(*R*)-10** unreacted with 89% ee and 47% conversion (Scheme 4.6a).[33]

The (*S*)-indanol was used as a building block in the synthesis of the anti-Parkinson drug rasagiline employing the lipase from *Thermomyces lanuginosus* (TLL) immobilized on immobead-150 as a biocatalyst. The lipase catalysed the selective acetylation of the (*R*)-enantiomer while the (*S*)-indanol was recovered unreacted with 99% ee. Further chemical transformations, including a Mitsunobu reaction with inversion of the configuration at the carbon stereocentre, allowed the conversion of (*S*)-indanol into the enantiopure rasagile (Scheme 4.6b).[34]

Another example reported in Scheme 4.6c shows the EKR of the racemic propargyl alcohol **13** with Amano lipase AK.[35] The enantiomerically enriched alcohol **(*S*)-13** was obtained with 97% ee and converted into the enantiopure allene **15**, in turn used for the synthesis of ene-1,5-diol substrates[35] as well as in the total synthesis of the antibiotic branimycin.[36]

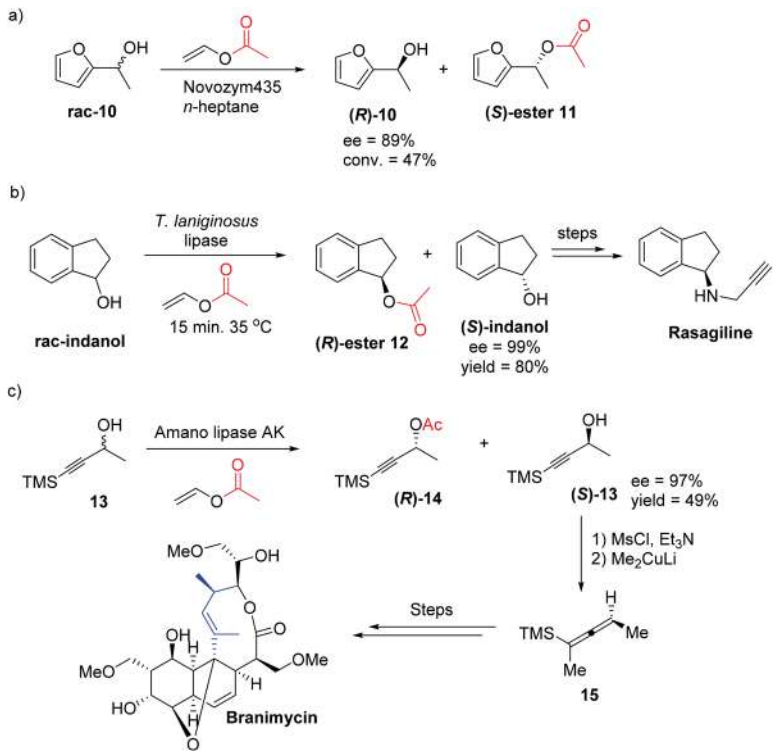

Scheme 4.6 Resolution of racemic alcohols with lipases.

4.2.3 Lipase-catalysed Aminolysis Reactions

Many examples of lipase-catalysed aminolysis of carboxylic esters or condensation of carboxylic acids and amines have been described over the years for the preparation of both chiral and non-chiral amines and amide building blocks.[37] In most cases, CAL-B has been employed as the biocatalyst,[38] since it can be used in non-aqueous media in its immobilised form. In fact, although water is the natural reaction medium of many enzymatic reactions, it cannot be used in lipase-catalysed aminolysis reactions as it may lead to the undesirable hydrolysis of the acyl donor substrate. Therefore, organic solvents together with immobilised CAL-B are commonly used in biocatalytic aminolysis reactions. Examples of CAL-B-catalysed aminolysis reactions are reported in Scheme 4.7.

The methyl (±)-3-hydroxypentanoate **rac-16** was reacted with ammonia or benzylamine in the presence of CAL-B by Gotor's group (Scheme 4.7a). The amides **17a-b** were produced selectively with E-values of 15 and 41.[39]

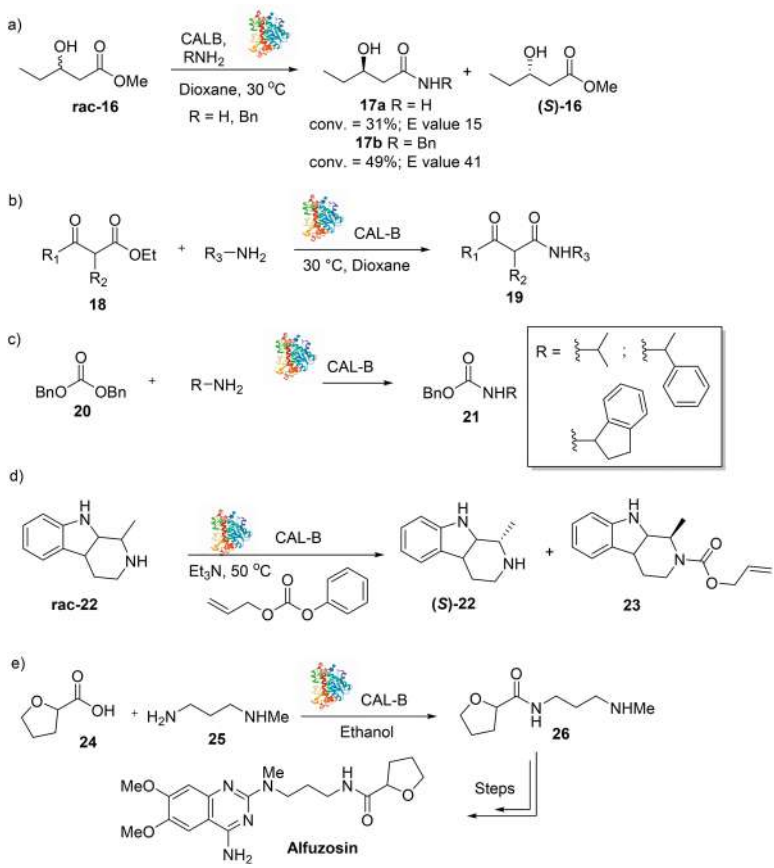

Scheme 4.7 Lipase-catalysed aminolysis reactions.

Similarly, the same authors also described the aminolysis of β-keto esters **18** with CAL-B (Scheme 4.7b).[39b]

Sheldon's group demonstrated the ability of CAL-B to catalyse the aminolysis of different symmetrical carbonates **20** (Scheme 4.7c). The reaction led to the formation of desired carbamates **21**, but, due to the known stability of the formed amide bond, the aminolysis did not proceed beyond the carbamate stage.[40] This strategy was used by Fülöp for the acylation of the secondary amine of β-carboline **rac-22** using allyl phenyl carbonate.[41] The carbamate **23** was produced with conversion of 50% and 98% ee (Scheme 4.7d).

Finally, Baldessari *et al.* described an interesting one pot CAL-B catalysed procedure for the preparation of *N*-substituted amides, such as **26**, from a variety of carboxylic acids *via* the formation of carboxylic acid ethyl esters and subsequent aminolysis (Scheme 4.7e). This enzymatic methodology was applied to the synthesis of the side chain of Alfuzosin, a quinazoline derivative able to reduce symptoms associated with benign prostatic hypertrophy.[42]

CAL-B can also be used for the resolution of racemic amines through stereoselective acylation. As an example, Botta's group reported the enzymatic kinetic resolution of racemic propargylamines **27** using CAL-B (Scheme 4.8a).[43]

A series of racemic 1-aryl-propargylamines was treated with CAL-B in diethyl ether using ethyl acetate as the acetyl group donor. The (*R*)-enantiomers **28** were selectively acylated leaving the (*S*)-amines **(*S*)-27** unreacted. Upon hydrolysis, the amides **28** were converted into enantiomerically pure **(*R*)-27** amines. Both enantiomers were obtained with excellent conversions and ee (up to 98%). This enzymatic methodology was later expanded to

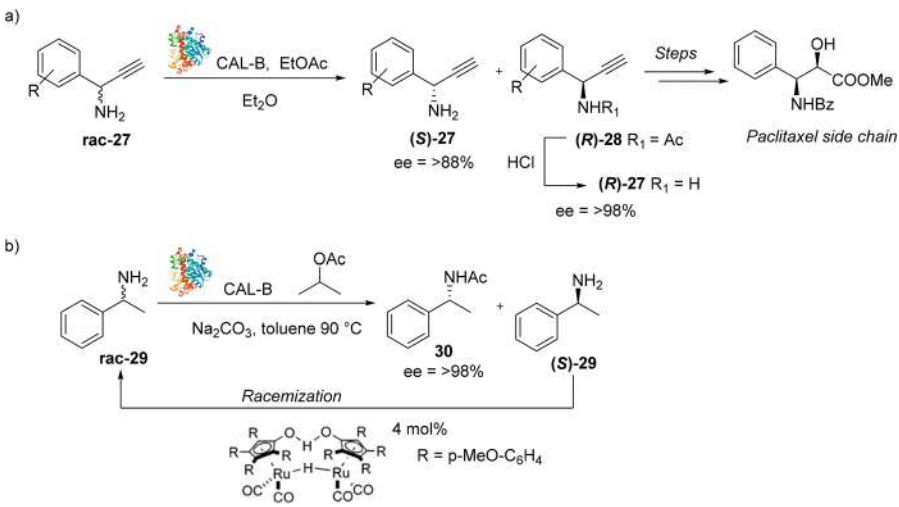

Scheme 4.8 a) Enzymatic kinetic resolution and b) enzymatic dynamic resolution of amines using CAL-B as a biocatalyst.

the synthesis of enantioenriched 1-aryl-allylamines and applied to the stereoselective synthesis of the Paclitaxel side chain.[44]

The main limitation of enzymatic kinetic resolution reactions is represented by the conversion, which can be max 50%, as only one enantiomer is processed by the enzyme. In 2005, Backvall's group developed an efficient chemoenzymatic one pot protocol that allowed the dynamic kinetic resolution (DKR) of several primary amines. Primary amine (*R*)-enantiomers were selectively acylated by CAL-B while the unreacted amine **(*S*)-29** was racemised *in situ* by Shvo's catalyst, leading to an overall DKR process.[45] The amide **30** was obtained with excellent ee values and yields up to 90% (Scheme 4.8b).

4.2.4 Lipase-catalysed Oxidation Reactions

The use of CAL-B as a biocatalyst in oxidative reactions such as epoxidations,[46] Baeyer–Villiger lactonizations/esterifications,[47] and amine[48] and sulfide[49] oxidations, has been investigated over the last few years. CAL-B is exploited to catalyse the synthesis *in situ* of peroxyacid reactive species from carboxylic acids or esters and hydrogen peroxide. Peroxyacids can then act as the oxidative species in a variety of oxidation reactions.

In 1992, Bjorkling *et al.* described the epoxidation of alkene substrates mediated by lipase enzymes, in particular CAL-B, which proved to be able to catalyse the synthesis *in situ* of peroxyacids in the presence of an acid precursor and aqueous hydrogen peroxide, as shown in Scheme 4.9a.[50] Several examples of CAL-B-catalysed epoxidation reactions followed this early work,[46] including the synthesis in high yield of 1,2-limonene oxide from the natural cyclic monoterpene (*R*)-(+)-limonene. Immobilised CAL-B (NS88011), octanoic acid and aqueous H_2O_2 were used at 50 °C to generate the oxidative intermediate octanoic peroxyacid.[51] In comparison to the use of hazardous commercial peroxyacids in stoichiometric quantity, such as *meta*-chloroperbenzoic acid (*m*CPBA), the lipase-catalysed process is milder and applicable at an industrial level in a more sustainable way.

The Baeyer–Villiger oxidation of cyclic ketones to lactones employing peroxide derivatives is a powerful methodology for oxygen insertion into a carbon–carbon bond breaking process.[52] CAL-B can be used in combination with H_2O_2 and an appropriate carboxylic acid for the biocatalytic synthesis of lactone derivatives from cyclic ketones.[47] In 2016, Drozdz *et al.* reported an interesting methodology for the asymmetric chemo-enzymatic Baeyer–Villiger oxidation of prochiral 4-methylcyclohexanone **33** to (*R*)-4-methylcaprolactone **(*R*)-35** in the presence of (±)-4-methyloctanoic acid, CAL-B as the biocatalyst and 30% aqueous hydrogen peroxide (Scheme 4.9b).[53] The reaction, carried out in toluene at 18 °C for 8 days, involves the CAL-B-catalysed conversion of the (*R*)-4-methyloctanoic acid enantiomer into the corresponding (*R*)-peroxyacid intermediate, which in turn oxidises **33** to the corresponding (*R*)-4-methylcaprolactone. Then, an additional CAL-B-catalysed kinetic resolution takes place allowing the final formation of the (*R*)-4-methylcaprolactone with a 97% yield and 96% ee.

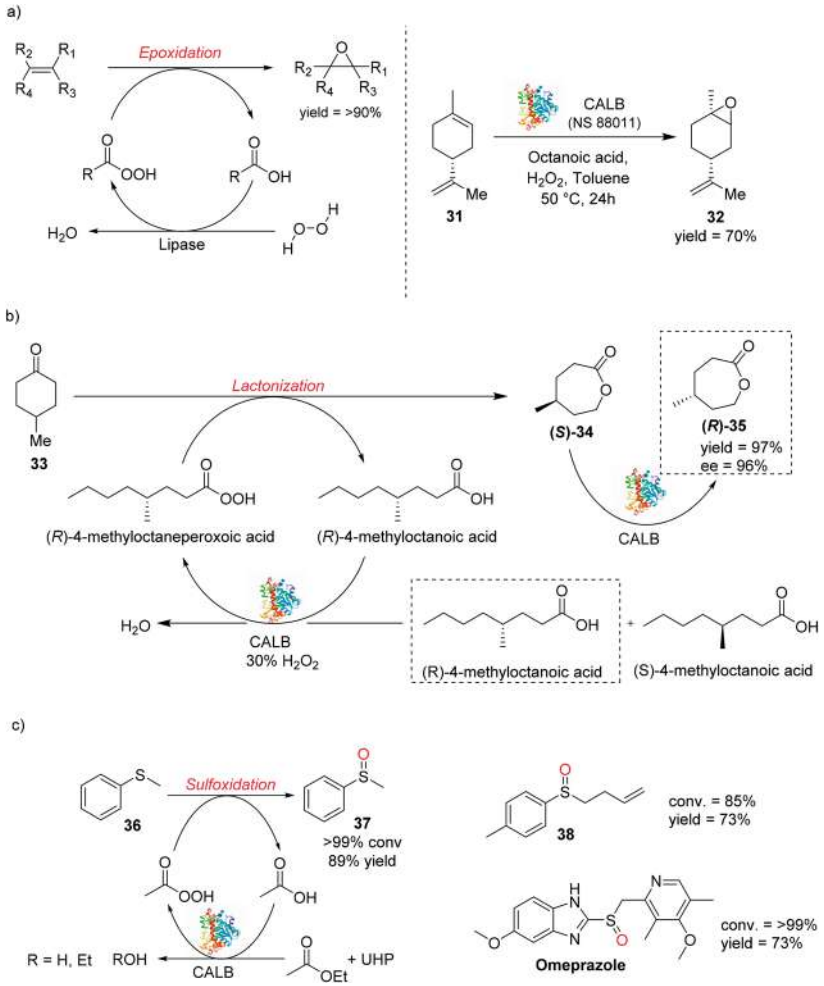

Scheme 4.9 Lipase-catalysed oxidation reactions, such as: a) epoxidation; b) lactonization; c) sulfoxidation.

Finally, in 2020, our group discovered a chemo-selective and scalable biocatalytic protocol for the synthesis of sulfoxide compounds employing CAL-B as a biocatalyst, ethyl acetate in the dual role of solvent and CAL-B co-substrate for the generation of the peroxyacid reactive intermediate, and urea hydrogen peroxide (UHP) as a more stable alternative to aqueous hydrogen peroxide solution.[49] The commercially available methyl phenyl sulfide was fully oxidised to the corresponding sulfoxide in a few hours with a conversion >99% and an 89% yield. Interestingly, the methodology proved to be highly chemoselective, since substrates bearing a double bond, such as **38**, were only oxidised at the sulfur atom, while no traces of epoxide by-products were detected. The protocol was finally applied to the synthesis of the drug

omeprazole and investigated at gram scale showing excellent yields and high conversion (Scheme 4.9c). Studies on the recyclability of CAL-B showed that the enzyme can be recycled up to four times without significant loss of oxidation activity.

4.3 Nitrilases

Nitrilases are an important class of enzymes able to catalyse the hydrolysis of nitrile substrates into the corresponding carboxylic acids with the consequent release of ammonia.[54] Nitrilases are widespread in nature and can be found in archaea, many types of bacteria, filamentous fungi and plants. Nitrilase enzymes belong to the nitrilase superfamily, which was firstly proposed by Pace and Brenner in 2001. Such superfamily comprises 13 different branches that share significant structural homology despite varying sequence conservation and differing substrate affinities.[55] According to their substrate specificity, nitrilases are differentiated into three categories: (a) aromatic nitrilases, which acts on aromatic or heterocyclic nitrile substrates; (b) aliphatic nitrilases, which acts on aliphatic nitrile substrates; and (c) arylacetonitrilases, which acts on arylacetonitrile substrates. It is worth clarifying that nitrile hydratases (NHase), namely metal-containing enzymes that convert a nitrile to the corresponding primary amide, are not members of this superfamily.[56]

The structure of the nitrilase protein is an α-β-β-α sandwich fold and all the superfamily members contain a conserved catalytic triad consisting of a cysteine, which acts as a nucleophile, a glutamate, which acts as a general base catalyst, and a lysine, which stabilizes the tetrahedral intermediate.[57] These three catalytic residues have been reported to be essential in the function of the nitrilase active site and enhance the performance of these enzymes. Although the nitrilase-catalysed hydrolysis mechanism is still unclear, the main accepted mode of action, as reported in Scheme 4.10, involves: (a) the

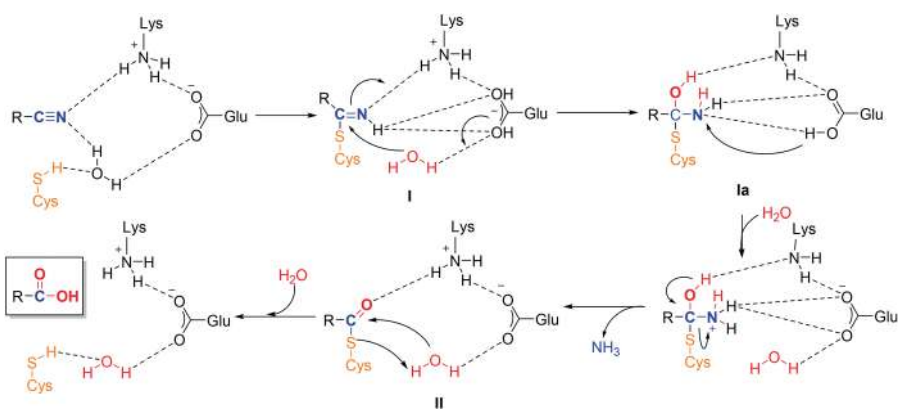

Scheme 4.10 Plausible catalytic mechanism for nitrilase-mediated nitrile hydrolysis.

nucleophilic attack of a sulfhydryl group from a conserved cysteine residue on the nitrile carbon atom to form an enzyme-linked tetrahedral thiomidate intermediate **I**; (b) the attack of a water molecule on the nitrile carbon and the protonation of the nitrogen atom, which is then eliminated as ammonia; (c) the hydrolysis of the acyl-enzyme intermediate **II** by the addition of a second water molecule to finally afford the corresponding carboxylic acid along with the regenerated enzyme. However, it has been suggested that in some cases the tetrahedral intermediate **Ia** can break down during the nitrile hydrolysis to produce amide products.

The first nitrile-metabolizing enzyme, isolated from the crude extract of barley leaves, was discovered by Thimann and Mahadevan in 1964. This enzyme was found to quantitatively convert 1*H*-indole-3-acetonitrile into the plant hormone 1*H*-indole-3-acetic acid (auxin) and was initially called indolacetonitrilase. After that, a substrate scope analysis on 26 nitrile derivatives showed that the enzyme had a broad substrate range, and indolacetonitrilase was renamed nitrilase to highlight its wider specificity.[58] Later, several bacterial and fungal nitrilases were isolated and found to be able to hydrolyse several natural and synthetic nitriles.

Over the past few decades, the use of nitrilases in biocatalysis has drawn considerable attention, since it provides a useful one step alternative to the conventional chemical hydrolysis approaches for the conversion of nitriles into carboxylic acids and for the degradation of nitrile compounds. These reactions often require the use of harsh reaction conditions such as high temperature or extreme pH-values, with the subsequent formation of significant quantities of toxic by-products such as HCN, that can be avoided instead with the use of nitrilase biocatalysts (Scheme 4.11). The biocatalytic hydrolysis of nitriles is attractive not only because of the advantages arising from the mild reaction conditions, lack of hazardous chemicals and sustainable development, but also for the possibility to carry out enantio- and regio-selective transformations that otherwise cannot be achieved through classical chemical hydrolysis.

Nowadays nitrilases are considered efficient and versatile biocatalysts to produce several pharmaceutically important compounds and chemicals.[59] In addition, by virtue of their ability to biodegrade the majority of the highly toxic, mutagenic and carcinogenic nitriles present in nature, these enzymes,

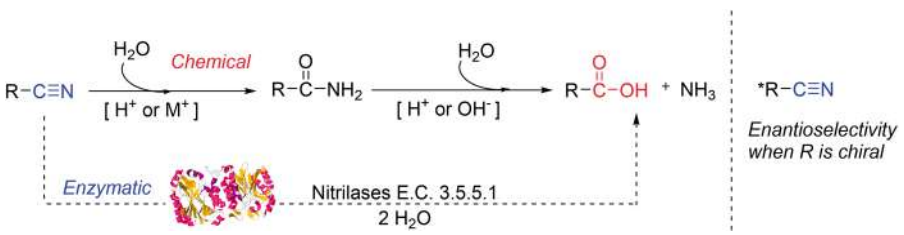

Scheme 4.11 Different pathways of nitrile hydrolysis.

along with other nitrile-converting enzymes, can also play an important role in environmental bioremediation.[60]

In 1980, the use of nitrilase biocatalysts in the synthesis of nicotinic acid was demonstrated as an efficient and alternative approach to the conventional chemical methods (Scheme 4.12a). Chemical approaches normally involve the oxidation of nicotine with potassium dichromate[61] or the hydrolysis of 3-cyanopyridine through the action of a strong base at high temperature (German patent 828246).[62] Nicotinic acid, also known as niacin or vitamin B3, has a strong demand among manufacturers of feedstuff additives and it is also used as a pharmaceutical intermediate for the synthesis of isoniazid and inositol hexanicotinate. In 1988, Mathew *et al.* firstly reported the use of *Rhodococcus rhodochrous* J1 cells, containing high benzonitrilase activity, to directly catalyse the hydrolysis of 3-cyanopyridine to nicotinic acid with a high yield and a quantitative conversion rate.[63] The *Rhodococcus rhodochrous* J1 strain was isolated by Yamada and Nagasawa and then immobilised in polyacrylamide for commercial use.[64] Later, Cowan *et al.* reported that a thermostable nitrilase biocatalyst, produced by the thermophilic bacterium *Bacillus pallidus* Dac521, was able to catalyse the direct hydrolysis of 3-cyanopyridine to nicotinic acid at 60 °C in a 0.1 M potassium phosphate buffer (pH 8.0) without detectable formation of nicotinamide as a by-product.[65]

(*R*)-(−)-Mandelic acid is an important chiral building block that is widely used for the production of pharmaceuticals such as semisynthetic penicillins, cephalosporins and antitumor agents. Mitsubishi Rayon (Japan) and

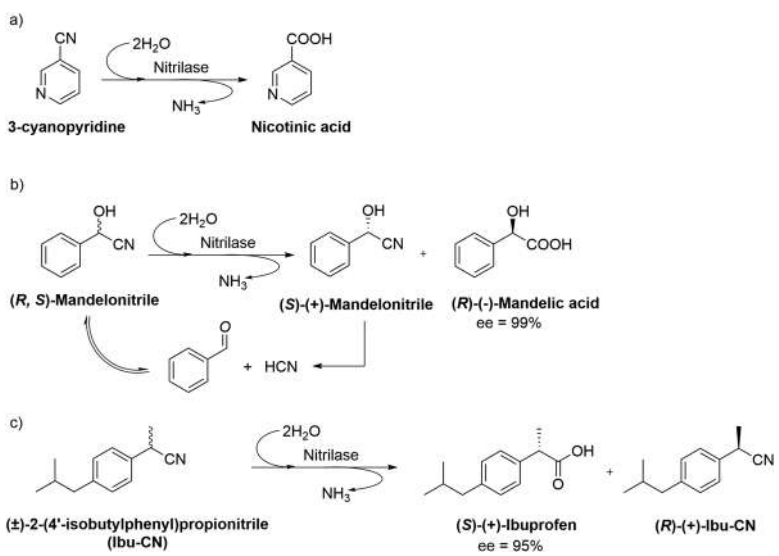

Scheme 4.12 Biocatalytic hydrolysis of nitrile-containing compounds using nitrilase biocatalysts for the production of: a) Nicotinic acid; b) (*R*)-Mandelic acid; c) optically pure (*S*)-(+)-Ibuprofen.

BASF (Germany) showed the great economic potential of nitrilase biocatalysts in the production of (*R*)-(−)-mandelic acid,[66,67] which was successfully obtained through a nitrilase-mediated enantioselective hydrolysis of the corresponding racemic mandelonitrile (Scheme 4.12b). This approach offers several advantages, such as a high degree of enantioselectivity, quantitative yields and the non-involvement of organic solvents or expensive biocatalyst cofactors. This biotransformation proceeds affording (*R*)-(−)-mandelic acid, while the (*S*)-(+)-mandelonitrile remains unreacted. The residual (*S*)-(+)-mandelonitrile spontaneously racemises and can then be re-used over again, leading to (*R*)-(−)-mandelic acid through a dynamic resolution process (Scheme 4.12b).[68] Over the years, many highly enantioselective nitrilases have been discovered from bacteria such as *A. faecalis* ATCC 8750, *Pseudomonas putida* MTCC 5110, and *Alcaligenes* sp. ECU0401 and have been characterized as excellent biocatalysts for the production of optically pure (*R*)-(−)-mandelic acid.[69] In 2010, Xue *et al.* isolated a new mutant strain of *A. faecalis* ZJUTB10 able to enantioselectively convert, at 35 °C and at a pH of 8.5, (*R,S*)-mandelonitrile into (*R*)-(−)-mandelic acid with high ee (99%) and high yield (93%).[68]

In the same year, Zhang *et al.* reported the overexpression of the nitrilase gene from *Alcaligenes* sp. ECU0401 in *E. coli* cells leading to a recombinant biocatalyst with high nitrilase activity, excellent enantioselectivity and strong substrate/product concentration tolerance, implying great potential for the large-scale production of optically pure (*R*)-(−)-mandelic acid.[70] More recently, Wang *et al.* reported the development of a continuous fed-batch process to hydrolyse mandelonitrile at concentrations as high as 2.9 M using an *E. coli* whole-cell system harbouring nitrilase BCJ2315 from *Burkholderia cenocepacia* J2315. This process allows (*R*)-(−)-mandelic acid to be obtained at the highest concentration (2.3 M) ever reported with a 97.4% ee.[71] Finally, in 1990, Yamamoto *et al.* demonstrated how nitrilase biocatalysts can be used in the synthesis of optically active drugs from racemic precursors.[72] An arylacetonitrilase, isolated from *Acinetobacter* sp. AK226 strain and suspended in a 0.1 M potassium phosphate buffer (pH 8.0), was employed as a biocatalyst for the synthesis of optically pure (*S*)-(+)-ibuprofen starting from racemic ibuprofen with 95% ee (Scheme 4.12c).

Another attractive feature of nitrilase enzymes is their ability to selectivity hydrolyse a single cyano group in a poly-nitrile substrate; such kind of reactions can be rarely accomplished in a single step using conventional chemical methods. Three examples of enzymatic regioselective hydrolysis of di-nitrile compounds are reported in Scheme 4.13. Whole cells of *Acidovorax facilis* (72W, ATCC 55746), having an aliphatic nitrilase activity, were suspended in a phosphate buffer (20 mM, pH 7.0) at 27 °C and were employed in the conversion of 2-methylglutaronitrile or 2-methyleneglutaronitrile into the corresponding 4-cyanopentanoic acid (>98% yield) or 4-cyano-4-pentenoic acid (100% yield, Scheme 4.13a).[73] The recombinant nitrilase from *Acidovorax facilis* 72W has been applied for the preparation of 1-cyanocyclohexaneacetic acid, a useful intermediate in the synthesis of gabapentin, a drug used in

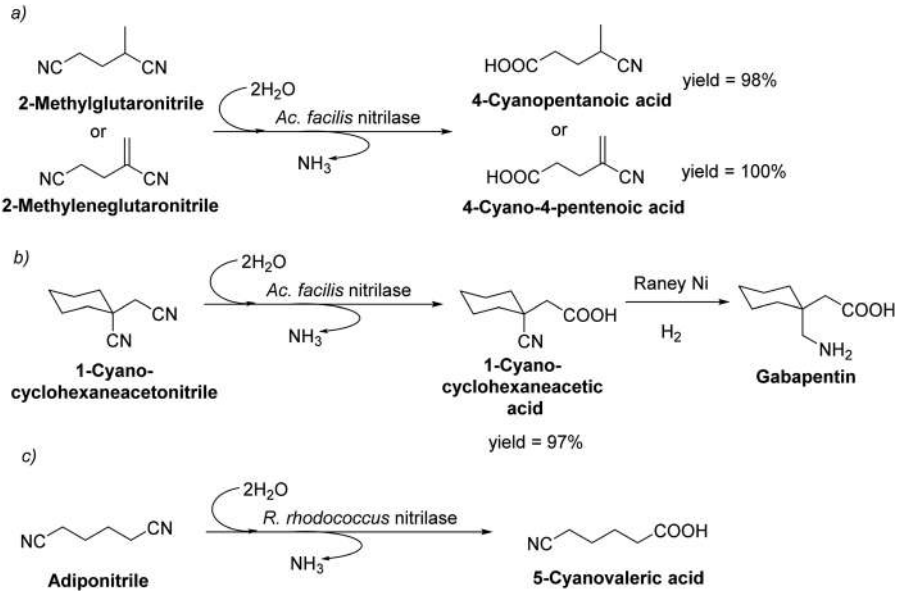

Scheme 4.13 Regioselective hydrolysis of aliphatic a,ω-dinitriles using nitrilase.

the treatment of different CNS disorders such as seizures and postherpetic neuralgia, with 97% yield (Scheme 4.13b).[74] The process utilised alginate-entrapped *E. coli* cells expressing *Ac. facilis* 72W nitrilase suspended in a 100 mM potassium phosphate buffer (pH = 7.0) and DMSO as a cosolvent to solubilise the nitrile substrate. Adiponitrile was converted to 5-cyanovaleric acid, a precursor of nylon-66, using *R. rhodococcus* K22 with a nitrilase activity (Scheme 4.13c).[75]

Finally, a nitrilase-catalysed approach for the synthesis of enantioenriched α-thiocarboxylic acids as synthetic drug precursors or analogues of flavouring agents has been reported by our group.[76] A panel of 35 nitrilase enzymes was screened on the α-thionitrile substrate **39**, exploiting a colourimetric assay[77] able to detect the NH_3 formed during the nitrile hydrolysis reaction by exploiting *o*-phthalaldehyde (OPA) (Scheme 4.14). The ammonia produced during the biocatalytic reaction reacts with OPA, leading, in the presence of trichloroacetic acid (TCA), to the formation of the chromophore **42**. The latter confers a characteristic blue colour to the reaction solution, thus indicating that the biocatalytic reaction is taking place. Nitrilases Nit27 and Nit34 emerged from the screening as the best biocatalysts for the hydrolysis of α-thionitrile substrates. Interestingly, even if both enzymes selectively hydrolyse only the (*S*)-enantiomer, the ammonia produced during the reaction promotes the racemization of the unreacted (*R*)-nitrile, leading in turn to a dynamic kinetic resolution of **39**. A series of α-thionitrile compounds was converted into the corresponding α-thiocarboxylic acids with high ee (up to 99%) and high conversions (up to 93%).

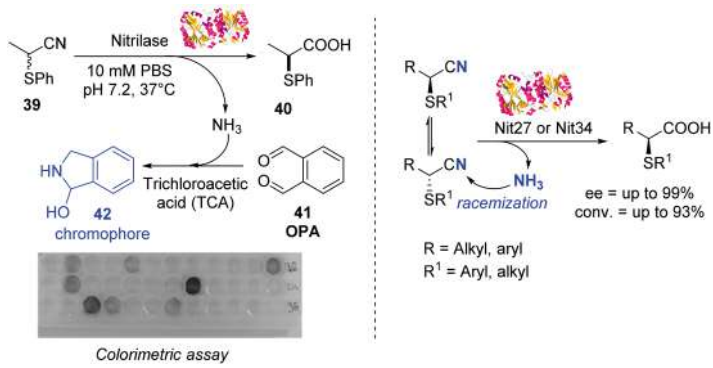

Scheme 4.14 Nitrilase-catalysed synthesis of a-thiocarboxylic acids.

4.4 Monoamine Oxidases (MAOs)

Monoamine oxidases (MAOs) are a family of enzymes involved, in humans, in the metabolism of biogenic and xenobiotic monoamines such as serotonin, norepinephrine, phenylethylamine and benzylamine. Two major isoforms (MAO-A and MAO-B) are present in humans, with MAO-A expressed in the central nervous system (CNS), liver, lungs and gastrointestinal tract, and MAO-B found almost exclusively in the CNS.[78] Despite a similar structure (~70% sequence identity), the two isoforms show great substrate specificity. Enzymes belonging to the MAO family can also be found in a broad range of organisms, from bacteria to mammals, where they are involved in the catalytic oxidation of biogenic primary amines. The MAOs belong to the family of flavin-containing amine oxidoreductases, and they contain the covalently bound cofactor FAD, which is involved in their oxidative catalytic mechanism. The typical reaction catalysed by MAO enzymes is the oxidative deamination of monoamines; an amine group is oxidised into an imine intermediate leading, after hydrolysis, to the corresponding aldehyde and ammonia.

The mechanism through which the MAO oxidation occurs is still not fully elucidated, as four distinct pathways are currently proposed.[79] The two main accepted mechanisms are reported in Scheme 4.15, and they involve (a) the nucleophilic attack of the monoamine to the FAD cofactor or (b) the abstraction of the hydride in the α-position to the nitrogen by the FAD. Even if recent studies suggest that the main mechanism is the hydride-extraction pathway, both mechanisms seem to occur depending on the nature of the enzymes and the substrates.[79c]

Since the early 1990s, monoamine oxidases from *Aspergillus niger*, from now on indicated as MAO-N, have been studied and fully characterised as possible enzymes for biocatalysis.[80] In 1991, Legge *et al.* reported the synthesis of norlaudanosoline from dopamine using *Aspergillus niger* as an *in situ* biotransformation system,[81] while a few years later Schilling and Lerch reported the isolation of MAO-N.[82] In 2002, Turner's group evolved MAO-N

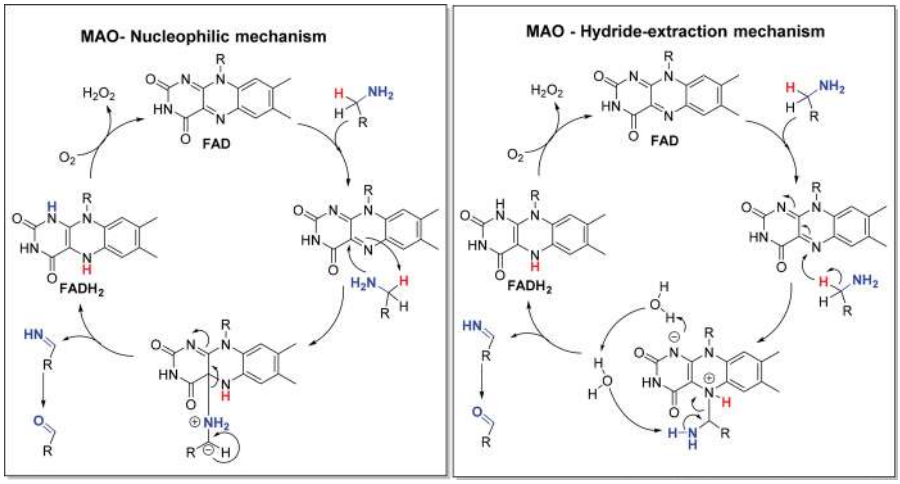

Scheme 4.15 Plausible MAO mechanisms.

into the first variant MAO-N D1, which, compared to the wild-type (WT) enzyme, showed increased activity on a variety of bulkier substrates.[83] Further evolution of MAO-N led to the variant MAO-N D3 with enhanced synthetic potential and increased catalytic activity.[84] Following these findings, MAO-N D5 was then developed to increase the catalytic activity on both secondary and tertiary amines,[85] followed by variants MAO-N D9 and MAO-N D11, with the latter able to oxidise bulky diaryl chiral amines.[86]

Today, MAO-N enzymes are robust biocatalysts that can be used for the synthesis of a wide variety of amine products. The substrate scope for such enzymes has been recently mapped by Turner's group and nowadays MAO-N enzymes are considered highly versatile and efficient biocatalysts for many synthetic applications.[87] In 2002, Turner's group ameliorated the synthetic applicability of MAO-N biocatalysts by developing a chemo-enzymatic cascade through which enantiomerically pure amines could be obtained in high yields and ee through repeated cycles of MAO-N catalysed oxidation followed by nonselective chemical reduction of the imine intermediate.[83]

As shown in Scheme 4.16, MAO-N D1 selectively oxidised the (*S*)-enantiomer of α-methylbenzylamine **rac-43** into the imine intermediate **44**, which was in turn reduced *in situ* by $NH_3{\cdot}BH_3$ to regenerate the racemic amine substrate. Repeated cycles of MAO-N oxidation and $NH_3{\cdot}BH_3$ reduction led finally to the amine **(*R*)-43** with 77% yield and 93% ee. Similarly, 2-phenylpyrrolidine was obtained with 80% yield and 98% ee using the MAO-N D3 variant, while MAO-N D5 was used for the deracemization of 2-propylpiperidine.

In 2013, Ghislieri *et al.* demonstrated that MAO-N biocatalysts can be used in the synthesis of pharmaceutical building blocks and alkaloid natural products (Scheme 4.17).[86] The anti-leishmania alkaloid harmicine, isolated from the Malaysian plant *Kopsia griffithii*, was synthesised through a

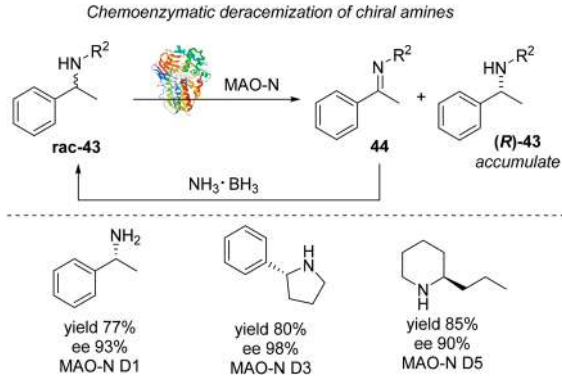

Scheme 4.16 MAO-N catalysed dynamic deracemization of racemic amine substrates.

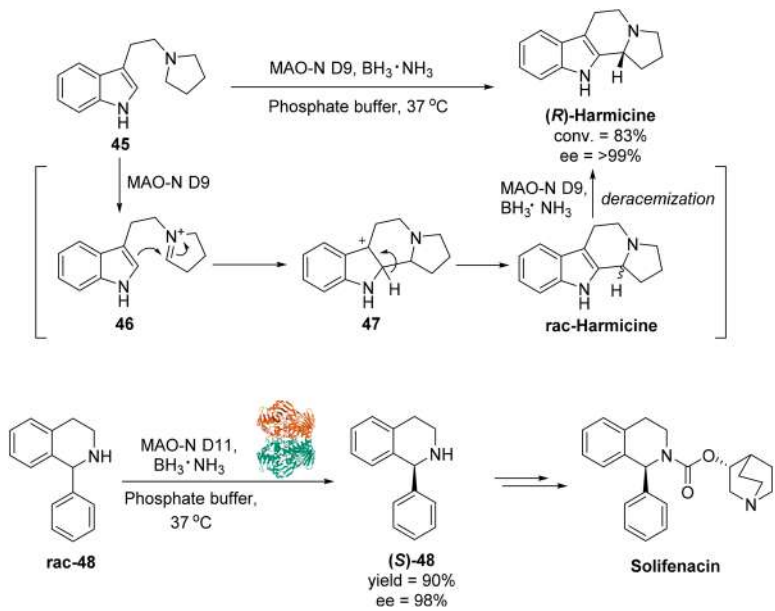

Scheme 4.17 MAO-N catalysed synthesis of natural products.

chemo-enzymatic cascade reaction involving a Pictet–Spengler-type cyclization. Biocatalyst MAO-N D9 promoted the oxidation of the pyrrolidine chain of the substrate **45** affording the iminium intermediate **46,** which underwent a spontaneous cyclization to form racemic harmicine. The (*S*)-enantiomer was then further oxidized into the corresponding iminium ion, which upon reduction with $BH_3{\cdot}NH_3$ and further rounds of oxidation/reduction, led to the desired (*R*)-harmicine with 83% conversion and >99% ee.

The biocatalyst MAO-N D11 was instead used in the synthesis of the (*S*)-1-phenyltetrahydroisoquinoline **(*S*)-48**, a precursor of solifenacin, a competitive muscarinic acetylcholine receptor antagonist used in the treatment of overactive bladder. The deracemization of **48** was carried out with MAO-N D11 variant in the presence of $BH_3{\cdot}NH_3$ and the (*S*)-enantiomer building block **(*S*)-48** was obtained with 90% yield and 98% ee.

MAO-N biocatalysts can also be combined with chemo-catalysts in chemo-enzymatic cascades to provide useful chemicals and pharmaceutical building blocks in one-pot reactions. In 2018, Turner and Greaney reported an elegant chemo-enzymatic cascade for the synthesis of alkynyl-tetrahydroisoquinoline compounds (Scheme 4.18a). The MAO-N D5 variant, as a whole cell biocatalyst, was combined in a single step reaction with the gold chemo-catalyst $HAuCl_4{\cdot}H_2O$. The MAO-N enzyme oxidised the tetrahydroisoquinoline substrate **49** into the corresponding iminium **51**, which in turn was attacked by the gold-activated terminal alkyne to afford the product **52** in good yields.[88]

Orru and co-workers employed MAO-N biocatalysts in Ugi-type 3-component reactions for the synthesis of substituted pyrrolidine derivatives (Scheme 4.18b).[89] The MAO-N D5 variant was first used in the desymmetrisation of the meso-pyrrolidine **53**, which was converted into the corresponding enantiopure imine **54**. The latter was then reacted with different carboxylic acids and isocyanides in a three-component Ugi reaction

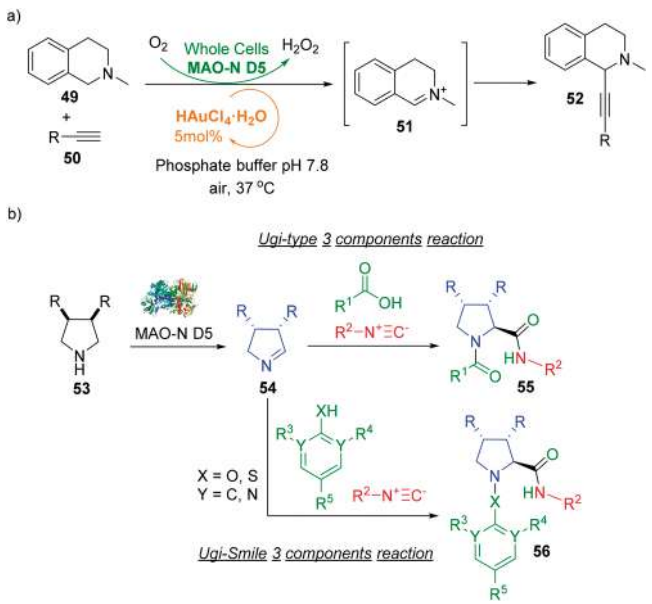

Scheme 4.18 Chemo-enzymatic cascade reactions using MAO-N biocatalysts for the synthesis of: a) alkynyl-tetrahydroisoquinoline compounds; b) substituted pyrrolidine derivatives.

affording proline derivatives **55**. The authors also reported a Ugi-Smile three component reaction to afford *N*-aryl-prolines **56** with excellent diastereomeric ratios and good yields by mixing the imine **54** with appropriate (thio) phenols and isocyanides.

In 2017, our group unveiled the aromatizing properties of monoamine oxidase biocatalysts for the synthesis of pyrrole compounds (Scheme 4.19).[90] Firstly, the aromatization of 3-pyrroline substrates was investigated using freeze-dried *E. coli* whole cells expressing the MAO-N D5, D9, and D11 variants. The biocatalysts were proved to oxidise/aromatise the pyrrolines **58** into pyrroles **59** with good to excellent conversions (up to 99%) in a buffer solution (pH 7.8) at 37 °C using the minimal amount of DMF as a cosolvent. The best conversions were obtained with the variant MAO-N D5, on both *N*-aryl and *N*-alkyl pyrrolines.

A one-pot chemo-enzymatic cascade to access the pyrroles **59** directly from allylamine precursors **57** was then investigated, by combining MAO-N biocatalysts and Grubbs' catalyst in the same reaction media. Grubbs' 2nd gen. catalyst promotes the ring-closing metathesis (RCM) of **57** into the pyrroline intermediate **58**. The latter can then be aromatised by the MAO-N into the desired pyrrole **59**. The optimal reaction conditions were identified using a biphasic 1 : 4 isooctane/buffer (pH 7.8) medium. The use of the biphasic

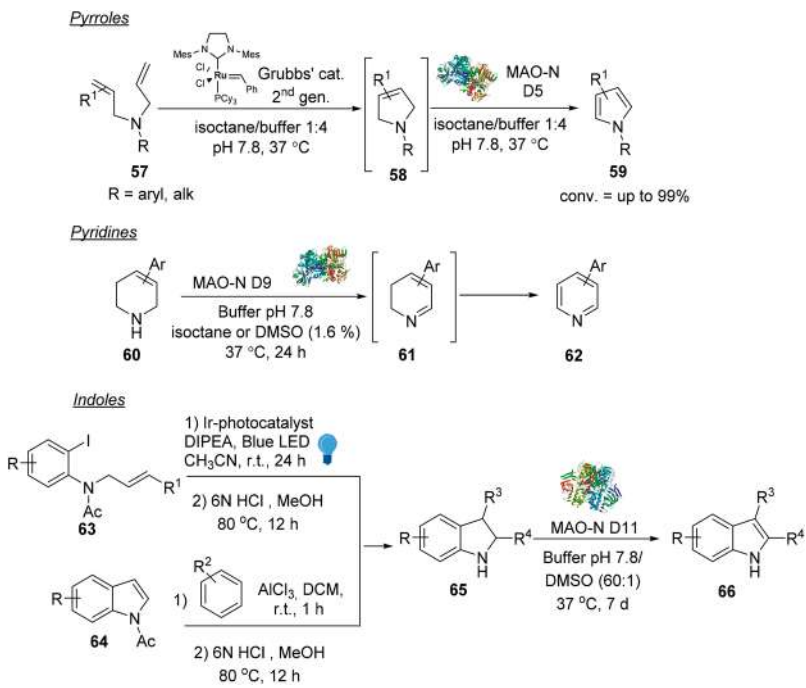

Scheme 4.19 MAO-N-catalysed synthesis of pyrroles, pyridines and indoles.

system proved to be crucial for the chemo-enzymatic cascade as it prevents the mutual inactivation of the chemo-catalyst (Grubbs' 2nd gen.) used in the RCM reaction with the MAO-N biocatalyst. A library of *N*-aryl/alkyl-pyrroles **59** was obtained with good to excellent conversions and yields. As a natural evolution of this work, MAO-N biocatalysts were then used for the synthesis of pyridine derivatives **62** from 1,2,5,6-tetrahydropyridine substrates **60** (Scheme 4.19).[91] The MAO-N D9 variant proved to be the best biocatalyst for this biotransformation. It was hypothesised that the aromatization proceeds through an initial C–N bond oxidation catalysed by MAO-N, which leads to the formation of intermediate **61**, followed by a second spontaneous oxidation by air. However, a second oxidation catalysed by MAO-N was not excluded. A set of blank experiments were also carried out with *E. coli* cells not harbouring MAO-N and in the presence of catalase enzyme, demonstrating that the aromatization is really catalysed by the enzyme rather than the H_2O_2 produced in the reaction media. Finally, the ability of MAO-N biocatalysts to catalyse the aromatization of indoline substrates **65** into indole **66** was reported.[92] The MAO-N D11 variant proved to be the best biocatalyst for this transformation and indole products were obtained in good to excellent conversions (up to 99%). The indoline substrates **65** were in turn synthesised *via* photocatalytic cyclization of *N*-allyl-2-iodo-anilines **63** in the presence of an Ir-based photocatalyst or *via* arylative functionalization/dearomatization of acetyl-indoles **64**. Computational studies were carried out to rationalize the biocatalytic mechanism of the reaction revealing that the aromatization of indolines into indoles is affected by the ability of the substrates to align to the FAD cofactor with the correct orientation in the catalytic site of the enzyme as well as by the electron distribution around the indoline nitrogen and the α-methylene group.

4.5 Ketoreductases (KRED)

Ketoreductases (KREDs) are a class of biocatalysts widely used at academic and industrial level to catalyse the reduction of ketones into the corresponding chiral alcohols. KREDs have a long history, since these enzymes are used by yeasts to reduce carbonyl compounds.[93] Baker's yeasts possess various ketoreductase enzymes and for this reason they have been employed for several decades as biocatalysts in the reduction of carbonyl compounds.[94] In 1964, it was demonstrated that Baker's yeasts could reduce a range of prochiral ketones with high selectivity of up to 90% ee.[95] The use of Baker's yeast in synthetic chemistry offered a number of advantages, such as availability, cheap cost and broad substrate scope. Nevertheless, Baker's yeast biocatalysts are disregarded in the current day on account of their low turnover numbers, low selectivity for some substrates due to competing enzymatic pathways, and tedious workups and product purifications. In the early 1990s, the first KRED enzymes were purified and since then they have become a robust and mature tool in the biocatalysis toolkit.[96] Today, a wide number of

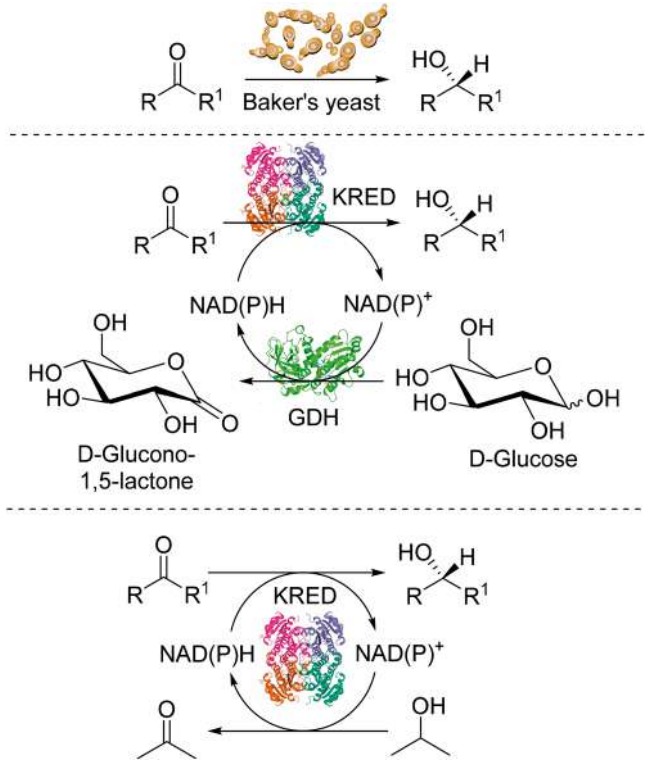

Scheme 4.20 Baker's yeast and KRED reduction of ketones.

highly enantioselective KRED biocatalysts are commercially available as pure enzymes or cell-free extracts together with a variety of biocatalyst screening kits. Compared to Baker's yeast, purified KREDs require the use of the expensive NAD(P)H cofactor to catalyse the reduction of carbonyls through hydride transfer and the subsequent formation of $NAD(P)^+$ as shown in Scheme 4.20. The specificity of KREDs for NADH or NADPH varies between different enzymes and can be assessed during the screening process. The high costs of the cofactors can be overcome by employing an appropriate cofactor recycling system which, using a sacrificial substrate (often isopropyl alcohol) or a second enzyme system (generally, GDH/glucose), allows the use of only catalytic amounts of NAD(P)H. The glucose dehydrogenase (GDH) enzyme coupled with D-glucose is a commonly used method for recycling NAD(P)H cofactors. Glucose is oxidised to D-glucono-1,5-lactone by the GDH and the NAD(P)H is regenerated. However, the GDH recycling option does suffer from some drawbacks, like the use of a secondary enzyme system whose optimal reaction conditions (pH, temperature) may not align with those of KREDs, or the presence of side reactions like the hydrolysis of D-glucono-1,5-lactone

into D-gluconic acid, which can lower the pH of the media affecting the activity of KREDs.

Another common method to recycle the NAD(P)H cofactor is to use a sacrificial alcohol co-substrate such as isopropanol (IPA), or EtOH. In the case of IPA, the hydroxyl group is oxidised by the KRED into a ketone forming acetone while reducing the oxidised $NAD(P)^+$ cofactor into NAD(P)H. The use of such co-substrates is an appealing option since they are readily and cheaply available and facilitate a single enzymatic system. Ideally, the choice of the recycling system should have minimal impact on the enzymatic reaction itself.

A possible enzymatic mechanism of action for the ketoreduction of a carbonyl was proposed by Kratzer in 2005.[97] In the example shown in Scheme 4.21, the substrate and the cofactor are held in place in the catalytic site of the enzyme by the amino acid tetrad of aspartic acid, tyrosine, lysine, and histidine. A hydride ion is transferred from the cofactor to the carbon of the carbonyl. To stabilise the charge, the oxygen then obtains a proton from tyrosine (Tyr-51). The loss of the hydride from the cofactor results in the formation of oxidised $NAD(P)^+$.

Several examples of KRED-catalysed reductions of carbonyls have been described in the literature and ketoreductases have also been used in the synthesis of drugs or drug precursors.[98] A team at Janssen Pharmaceuticals explored various routes to obtain alcohol **68**, as a precursor for the stereoselective construction of the antiviral agent simeprevir. The keto-group of **67** was reduced stereoselectively affording the desired product **68** in quantitative yield and 94% diastereomeric excess (Scheme 4.22a).[99]

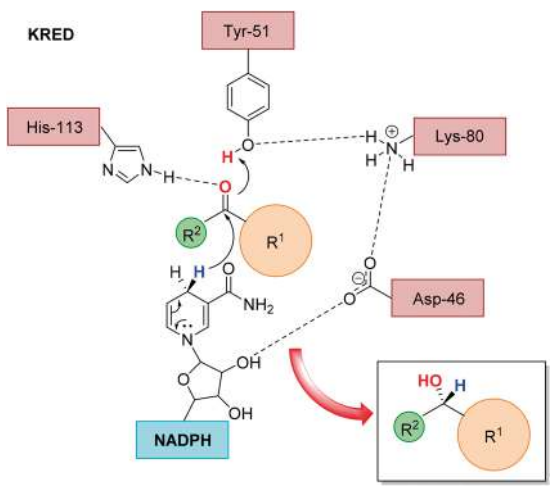

Scheme 4.21 Mechanism of KRED-catalysed reduction of ketone substrates.

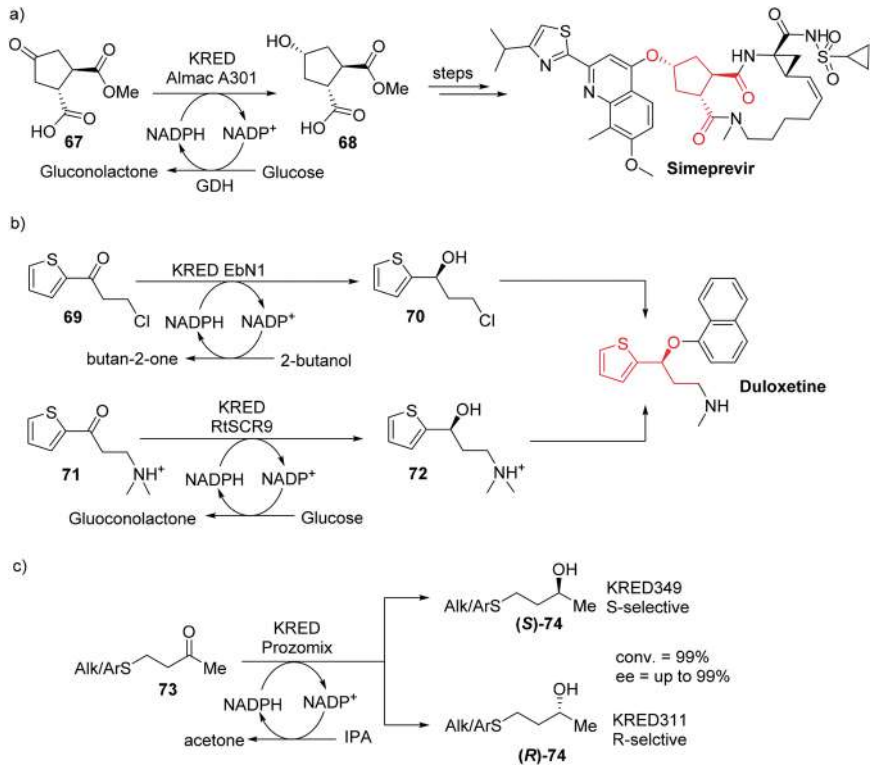

Scheme 4.22 KRED-catalysed reductions of ketone substrates.

The antidepressant duloxetine was also synthesised by researchers at BASF taking advantage of the KREDs LbADH from *Lactobacillus brevis* and EbN1 from *Aromatoleum aromaticum*.[100] Both enzymes were employed to reduce the chloro-ketone **69** into alcohol **70**, a precursor in the stereoselective synthesis of duloxetine. Racemic 2-butanol was used as a substrate for the recycling of the cofactor.

An alternative route was developed later using KRED RtSCR9 from *Rhodosporidium toruloides* and the ketone substrate **71** (Scheme 4.22b).[101]

More recently, our group exploited KRED biocatalysts for the synthesis of 1,3-mercaptoalkanols as analogues and precursors in the synthesis of volatile sulphur compounds. Two enzymes with opposite selectivity were identified from the Prozomix library. The biocatalyst KRED311 catalysed the reduction of ketone **73** into the alcohol **(*R*)-74**, while the alcohol **(*S*)-74** was obtained with KRED349. All the desired products were obtained in enantiomerically pure forms and excellent conversions. Isopropanol was used as a cosolvent and sacrificial substrate for the regeneration of the NAD(P)H cofactor.[102]

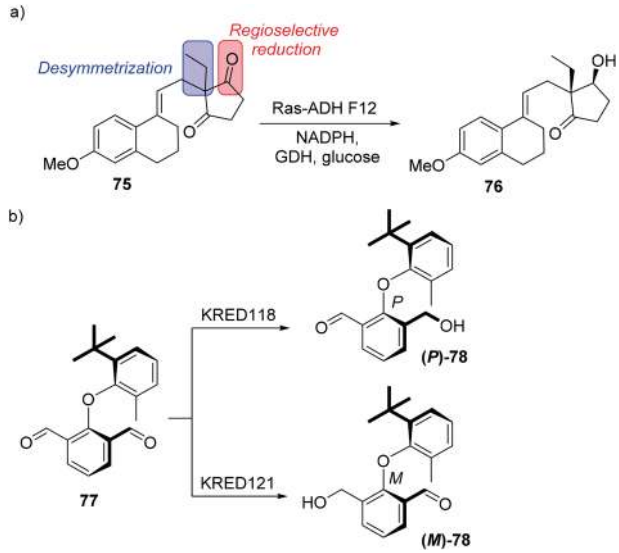

Scheme 4.23 KRED-catalysed desymmetrisation reactions.

KRED enzymes have also been applied in desymmetrisation reactions as shown in the synthesis of compound **76**, a key intermediate in the production of several steroidal drugs (Scheme 4.23a). The di-ketone **75** was regio- and stereoselectively reduced into alcohol **76** using the RasADH-F12 mutant of the reductase RasADH from *Ralstonia* sp. The mutant biocatalyst showed 183-fold activity compared to the wild-type enzyme and excellent selectivity.[103]

Clayden and Turner employed KRED enzymes for the enantioselective synthesis of atropisomers *via* desymmetrisation of appropriate achiral substrates containing a pair of enantiotopic functional groups. The symmetrical dialdehyde **77** was treated with two different KREDs with opposite selectivity. KRED118 afforded the enantiomerically enriched (***P***)**-78** isomer with 91% conversion and 71% ee, while the opposite isomer (***M***)**-78** was obtained with 84% conversion and 61% ee using KRED121.[104]

Finally, KREDs have been demonstrated to catalyse the dynamic kinetic resolution of ketone substrates. As an example, ketoesters **79** and **80** have been reduced into the cyclic amino acids 3-hydroxyprolines **81** and 3-hydroxypipecolic acids **82** using KRED enzymes. KREDs were reacted with racemic **79-80** in phosphate buffer at pH 6–7 at 30 °C. Under these reaction conditions, the α-stereocentre of the substrates underwent racemization, thus paving the way to a possible dynamic kinetic resolution. Several enzymes were screened showing in most cases high selectivity affording the desired proline and pipecolic acid derivatives in excellent yields and with excellent diastereomeric and enantiomeric purity. Both isopropanol and glucose/GDH were used as recycling systems as shown in Table 4.1.[105]

Table 4.1 Dynamic kinetic resolution of ketones **79** and **80**.

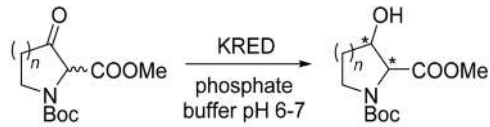

79 $n = 1$
80 $n = 2$

81 $n = 1$
82 $n = 2$

Diastereoisomer	KRED	Yield (%)	de (%)	ee (%)	Recycling system
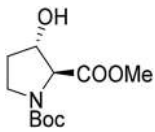	NADH-101	85	98	99	IPA
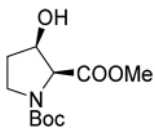	P1B2	93	99	99	IPA
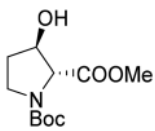	264	92	98	84	IPA
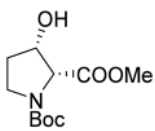	119	73	93	99	GDH glucose
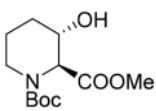	NADH-101	100	36	98	IPA
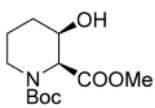	P1D3	92	99	98	IPA
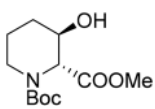	112	90	47	99	GDH glucose
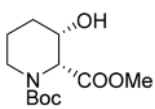	119	89	91	97	GDH glucose

4.6 Monooxygenases and Baeyer–Villiger Monooxygenases (BVMO)

Monooxygenases are oxidoreductase enzymes that catalyse the incorporation of a single oxygen atom into an organic substrate by activating molecular oxygen with the assistance of various (in)organic cofactors. There are numerous monooxygenase classes[106] that can be classified based on the type of cofactor they require; this section will focus exclusively on flavin-dependent monooxygenases, namely those enzymes using a flavin cofactor, and in particular on the use of Baeyer–Villiger Monooxygenases (BVMO) in biocatalysis. The two most common flavin cofactors present in flavin-dependent monooxygenases are flavin adenine dinucleotide (FAD) and flavin mononucleotide (FMN).[107]

A general mechanism for flavin monooxygenase is reported in Scheme 4.24.[108] Molecular oxygen binds the reduced flavin cofactor forming a 4a-hydroperoxyflavin (4a-HPF). This species is stabilized by $NADP^+$ in the catalytic site of the enzyme. A substrate is then oxidised through nucleophilic substitution at the distal O-atom of the prosthetic group. The hydroxyflavin formed then releases water to form the oxidised flavin cofactor, which is in turn reduced by NADPH.

Flavoprotein monooxygenases are capable of catalysing hydroxylation, epoxidation, sulfoxidation and Baeyer–Villiger oxidation reactions on a wide range of substrates.[109] The type of reaction catalysed by each monooxygenase relies upon the shape and chemical properties of the enzyme active site and therefore several subclasses of monooxygenases exist:[110] (a) the external flavoprotein monooxygenases which rely on reduced cofactors (NADPH or NADH) to equip and reduce their flavin cofactors through electron donation, (b) the internal flavoprotein monooxygenases which use a system whereby the substrates themselves reduce the flavins, and (c) a subclass of flavin-dependent enzymes that can catalyse hydroxylation reactions without

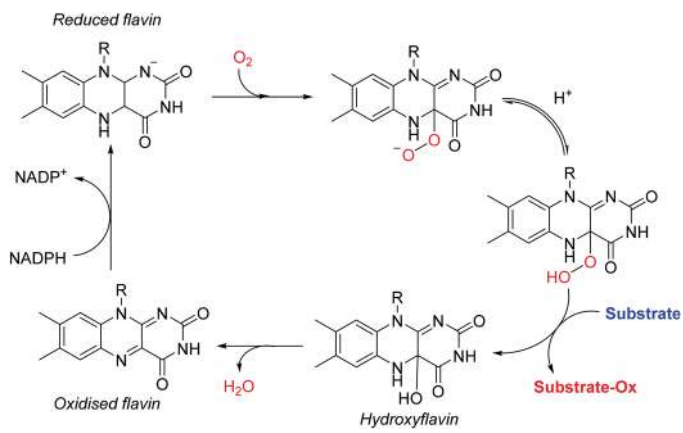

Scheme 4.24 General mechanism for flavin monooxygenase oxidation.

the direct involvement of the flavin cofactor in monooxygenation. A special class of external flavoprotein monooxygenases is represented by the Baeyer–Villiger monooxygenases (BVMOs), a class of enzymes able to catalyse the Baeyer–Villiger reaction, namely the oxidation of ketone substrates into esters.[111] Examples of Baeyer–Villiger oxidations catalysed by BVMO biocatalysts are reported in Scheme 4.25.[112]

A typical reaction catalysed by BVMO enzymes is the conversion of cyclohexanone into ε-caprolactone.[113] Recently, Bornscheuer reported a large scale process (200 mM scale) for the synthesis of ε-caprolactone using two stability-improved variants (QM and M15) of the Baeyer–Villiger monooxygenase CHMO (cyclohexanone monooxygenase).[114] Among the two variants the CHMO M15 showed higher oxidative stability and longer operational

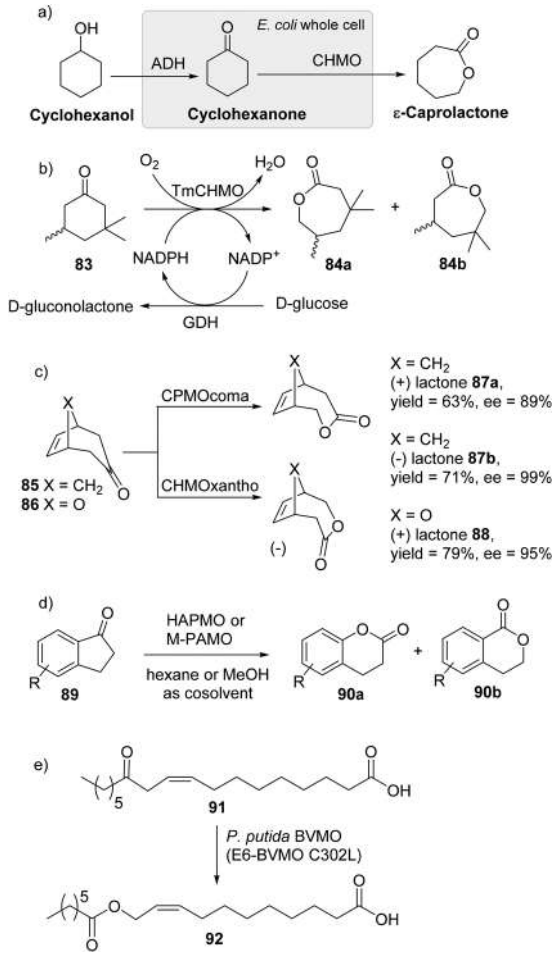

Scheme 4.25 Bayer-Villiger oxidations catalysed by BVMO enzymes.

stability (18 h) under process conditions than the QM variant. CHMO was combined with the alcohol dehydrogenase ADH from *Lactobacillus kefir* in an *E. coli* whole cell biocatalyst to allow the production of e-caprolactone directly from cylohexanol through an ADH-catalysed oxidation followed by a Baeyer–Villiger oxidation (Scheme 4.25a).

Similarly, the cyclohexanone monooxygenase from *Thermocrispum municipal* (TmCHMO) was used for the large scale production of the substituted ε-caprolactone **84a-b**. D-glucose and glucose dehydrogenases (GDH-105 and GDH-01) were used as a cofactor recycling system (Scheme 4.25b).[115]

The BVMO enzymes CHMO from *Xanthobacter* sp. ZL5 and CPMO from *Comamonas* sp. strain NCIMB 9872 have been employed for the synthesis of bicyclic lactones **87** and **88**, which were in turn used as building blocks for the production of kumausyne, goniofufurone, and C-nucleoside analogues. Interestingly, the appropriate choice of the BVMO biocatalyst allows the desymmetrisation and the synthesis of both enantiomers of the desired bicyclic lactones and it offers a shortened route compared to the classical chemical approaches (Scheme 4.25c).[116]

Gotor's group employed BVMO enzymes for the synthesis of benzo-fused lactones **90a-b**.[117] Two biocatalysts were used for this biotransformation, namely the 4-hydroxyacetophenone monooxygenase (HAPMO) from *Pseudomonas fluorescens* ACB and the M446G PAMO mutein (M-PAMO), a mutant of the phenylacetone monooxygenase (PAMO) from *Thermobifida fusca*. The activity of the two biocatalysts proved to be affected by the use of different co-solvents. When hydrophobic solvents were employed in the HAPMO-catalysed oxidation, an increase in the enzymatic activity was observed and the lactone **90a** was obtained with 44% conversion in the presence of 5% hexane. On the other hand, M-PAMO showed an opposite behaviour and the use of hydrophilic co-solvents such as 5% methanol led to the other isomer **90b** with high conversions (up to 79% at pH = 9.0, Scheme 4.25d).

Finally, the BVMO from *P. putida* KT2440 has been engineered and used for the production of (*Z*)-11-(heptanoyloxy)undec-9-enoic acid **92** from ricinoleic acid **91**[118] (Scheme 4.25e). The enzyme catalysed the Bayer-Villiger oxidation of the ketone moiety converting it into an ester group. The hydrolysis of the latter with an esterase allowed the synthesis of *n*-heptanoic acid and (*Z*)-11-hydroxyundec-9-enoic acid.

BVMOs have proved to be highly versatile enzymes able to catalyse also the oxidation of olefin, amine and sulfide substrates. As an example, the cyclohexanone monooxygenase (CHMO) from *Acinetobacter calcoaceticus* was used for the epoxidation[119] of diethyl vinyl phosphonate **93**. The desired epoxide **94**, an analogue of fosfomycin, was isolated with 40% yield and 98% ee (Scheme 4.26a). The cyclohexanone monooxygenase from *Acinetobacter calcoaceticus* (CYMO) was found to be able to catalyse the N-oxidation of (*S*)-(−)-nicotine into the N-oxide **95** with 99% diastereomeric excess (Scheme 4.26b).[120] Finally, a research team from Codexis developed an efficient biocatalytic method for the synthesis of the anti-ulcer drug esomeprazole through a BVMO-catalysed S-oxidation. A wild-type BVMO enzyme from *Acinetobacter*

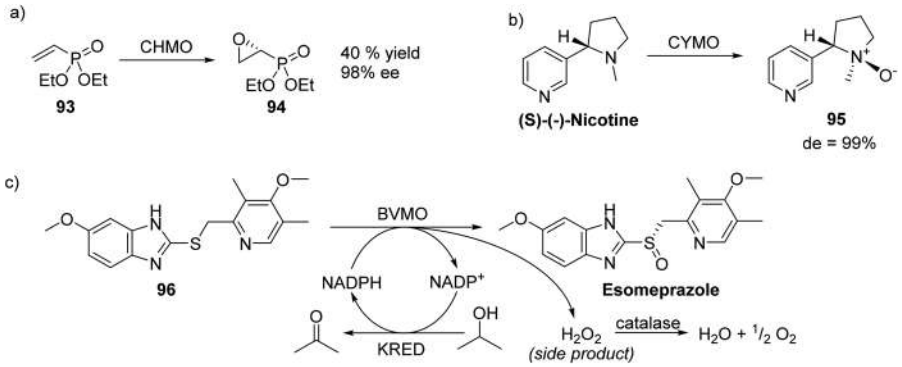

Scheme 4.26 BVMO-catalysed oxidations of a) olefins, b) amines and c) sulfides.

was engineered and the resulting evolved biocatalyst was able to catalyse the enantioselective oxidation of the sulfide **96** into esomeprazole with 87% yield and >99% ee. The NADPH cofactor was regenerated using isopropanol as a sacrificial co-substrate in the presence of a ketoreductase enzyme, while the H_2O_2 produced in the process as a side product was removed by adding catalase to the reaction system in order to avoid the overoxidation of esomeprazole to the corresponding sulfone.[121]

4.7 Transaminases

Transaminases (TA), or aminotransferases, are a class of pyridoxal-5′-phosphate (PLP)-dependent enzymes widely used in the synthesis of enantiomerically pure amines and chiral amino acids due to their capability to catalyse the reversible transfer of an amino group from an amino donor to a carbonyl acceptor. The history of transaminases can be traced back to 1930, when they were indirectly described by Needham *et al.* during the investigation of cell metabolism in the breast muscles of pigeons.[122] After several observations that muscle cells were able to perform transamination reactions, it was demonstrated that such transformations were catalysed by transaminase enzymes.[123]

Based on the structures of the amino donor substrate that is converted, and depending on the enzyme specificity towards various substrates, transaminases have been generally classified into two types, α-transaminases (α-TAs) and ω-transaminases (ω-TAs) (Scheme 4.27).[124] The α-TAs (which represent the majority of TAs) catalyse exclusively the conversion of α-amino acids into α-keto acids and *vice versa*, while the ω-TAs also catalyse the transfer of amino groups to carbonyls that are more distant from a carboxylic group (*i.e.* in the γ, δ or ε position). An interesting subgroup of ω-TAs is represented by the amine transaminases (ATAs), which find broad applications in the biocatalytic synthesis of chiral amines directly from the corresponding prochiral ketones.

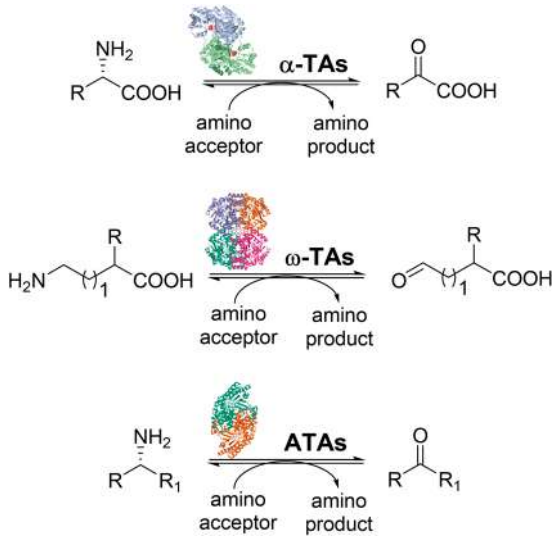

Scheme 4.27 Schematic nomenclature of transaminases based on the distance of the transferred amino group from the carboxylic function.

The main advantage of ATAs is that they allow the conversion of chiral amines independently from the presence of a carboxylic group in the substrate. Further classifications of transaminases into other subgroups or classes have been gradually introduced depending on their sequence and structure.[125]

The mechanism of the transamination reaction has been widely studied over the years, and it has been defined as a ping-pong bi–bi reaction mechanism involving the pyridoxal 5′-phosphate, covalently bound in the enzyme active sites, as a cofactor.[125b] The overall mechanism, depicted in Scheme 4.28, is composed of two half-reactions and involves: (a) the formation of an internal aldimine through an initial transaldimination step between the aldehyde group of the coenzyme PLP and the free ε-NH_2 group of a lysine residue; (b) the breakage of the bond in the internal Schiff base between the PLP and the ε-NH_2 group of the lysine residue that produces the detachment of the PLP and the formation of an equivalent Schiff base (external aldimine) with the amino donor substrate; (c) during the subsequent 1,3-prototropic shift, the free ε-NH_2 group acts as the catalyst yielding the formation of a ketimine through two separate steps, namely the deprotonation at the α-position by the ε-NH_2 group of the catalytic lysine residue that generates a planar quinonoid intermediate stabilized by resonance and the re-protonation of the Cα position on the opposite face performed by amino acid racemases and epimerases and the protonation of the C4′ of the PLP; (d) the ketimine is finally hydrolysed to obtain the keto acid and the pyridoxamine-5′-phosphate (PMP) completing the first half reaction in the transaminase mechanism; (e) the PMP will then form an external aldimine with the second substrate

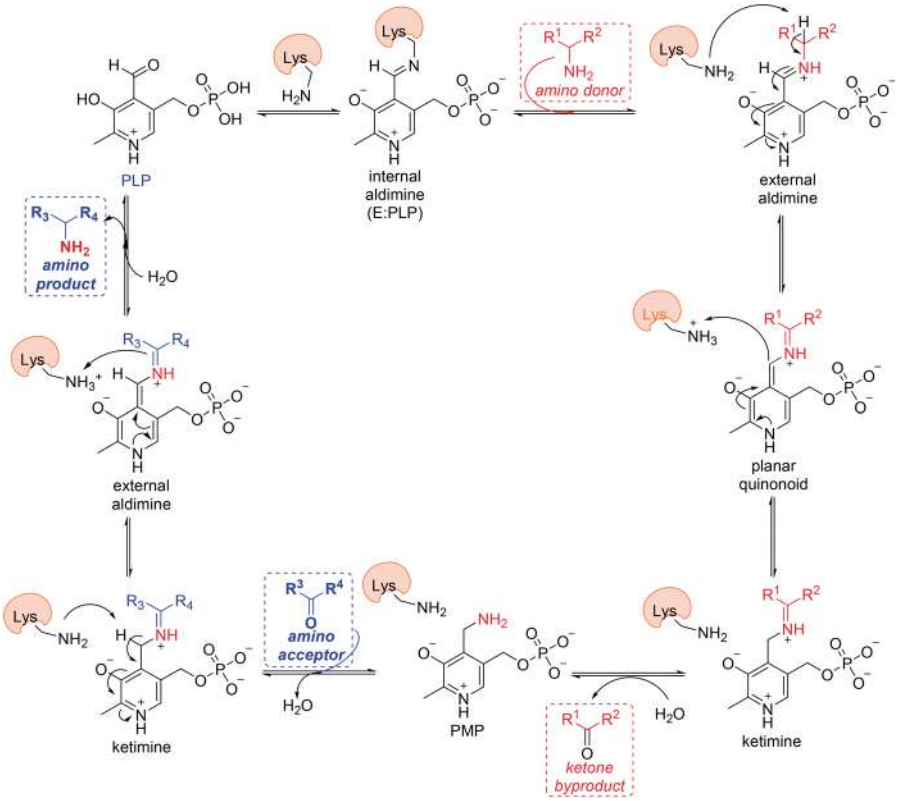

Scheme 4.28 General transaminase enzyme biocatalytic mechanism.

participant in the reaction (amino acceptor) and this adduct, following a mirrored sequence of events, will complete the second half reaction with the formation of the amino product and the regeneration of the PLP.[126]

Transaminases have shown rapid development over the past few decades, both in terms of enzyme discovery and industrial applications for the production of active pharmaceutical ingredients, agrochemicals and fine chemicals, thanks to their capability of catalysing both bond breaking and bond forming reactions in a single step with high selectivity and efficiency.[124] Recently, the development of transaminase-catalysed reactions in combination with a second biocatalyst, in the so-called "multi-enzyme system", has allowed some intrinsic limitations of transaminase biocatalysis to be overcome, such as substrate/product inhibition problems or equilibrium constraints.[127]

For instance, a simple method to avoid the recurring inhibitory effect caused by the ketone-by-product consists in its removal through a secondary enzymatic reaction (Scheme 4.29). This strategy also offers the advantage of shifting the equilibrium of the biocatalytic reaction towards the formation of the desired products. As an example, pyruvate, a by-product in transaminase-catalysed reactions and also a potent ω-TA inhibitor, can be removed from

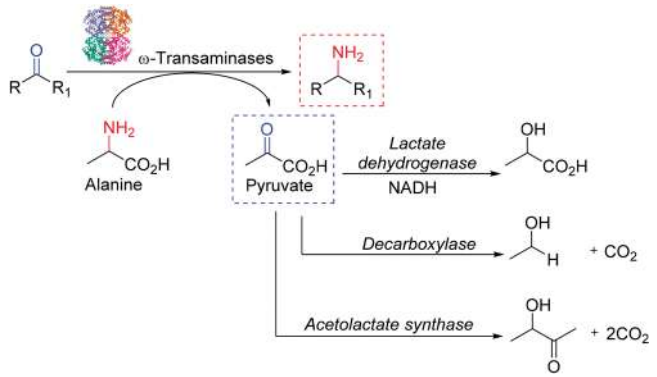

Scheme 4.29 Multi-enzyme strategy to remove the pyruvate by-product.

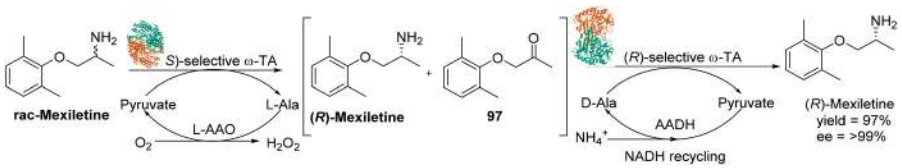

Scheme 4.30 Deracemization strategy for the synthesis of enantiopure (*R*)-mexiletine.

the reaction mixture by adding a second enzyme.[128] Pyruvate can be converted into lactic acid by lactate dehydrogenase,[129] or decarboxylated into ethanol by pyruvate decarboxylase,[130] or finally condensed into acetoin by acetolactate synthase.[131]

Transaminases have been widely used as viable biocatalysts to produce many pharmaceutically important compounds and chemicals. In 2009, Kroutil's group reported the deracemization of the anti-arrhythmic drug mexiletine into each single enantiomer using various ω-transaminases with opposite selectivity.[132] The deracemization protocol is based on a one-pot two-step sequence, that consists in a kinetic enzymatic resolution process followed by a stereoselective transaminase catalysed amination. For the synthesis of (*R*)-mexiletine, an (*S*)-selective ω-transaminase is first used to catalyse the selective conversion of the (*S*)-mexiletine into the ketone **97**, leaving the (*R*)-enantiomer unreacted. The ketone **97** is then converted selectively into (*R*)-mexiletine by a (*R*)-selective ω-transaminase, resulting in the production of the optically pure enantiomer with 97% yield and >99% ee (Scheme 4.30).

Changing the order of addition of the transaminases allowed the isolation of the other enantiomer (*S*)-mexiletine with 98% yield and 99% ee.

Another example of the use of ω-TA in the production of drugs was reported in 2010 by Faber's group, who disclosed a chemoenzymatic asymmetric total synthesis of (*S*)-rivastigmine, a drug used in the treatment of early stages of

Alzheimer's disease (Scheme 4.31).[133] The first step of this synthetic process involves an enzymatic asymmetric transamination reaction for the preparation of **(*S*)-99**, a key intermediate in the production of (*S*)-rivastigmine. The 3-methoxymethyl ether acetophenone **98** was treated with an (*S*)-selective ω-transaminase from *Vibrio fluvialis* previously suspended in a phosphate buffer (1 mM, pH 7) at 30 °C. In addition, a lactate dehydrogenase, combined with a glucose dehydrogenase/glucose recycling system, was chosen to shift the reaction equilibrium towards the amine product, through the removal of the pyruvate by-product. The desired key intermediate **(*S*)-99** was obtained with excellent conversion (99%) and enantioselectivity (>99%).

Recently, transaminases have been used also as biocatalysts in the production of unnatural amino acids, such as β- and γ-amino acids.[134] Various biocatalytic approaches for the synthesis of unnatural amino acids have been explored over the years due to the ever-growing attention on their use as chiral auxiliaries and ligands for asymmetric syntheses as well as building blocks for the production of chiral drugs.[135]

Finally, an interesting biocatalytic process for the conversion of natural L-threonine into L-homoalanine, a pharmaceutically valuable unnatural amino acid used as a key intermediate in the production of the drugs ethambutol and levetiracetam, has been developed through a cascade reaction involving the combination of a threonine deaminase from *E. coli* and an (*S*)-enantioselective ω-TA from *Paracoccus denitrificans* as a biocatalyst.[136] The biocatalytic cascade is a one-pot process and it requires an excess of threonine deaminase to catalyse the dehydration and deamination of L-threonine into 2-oxobutyrate, which is in turn converted into the corresponding optically pure L-homoalanine through an asymmetric transamination using benzylamine as an amino donor. L-Homoalanine was obtained with 91% conversion and 99% ee (Scheme 4.32).

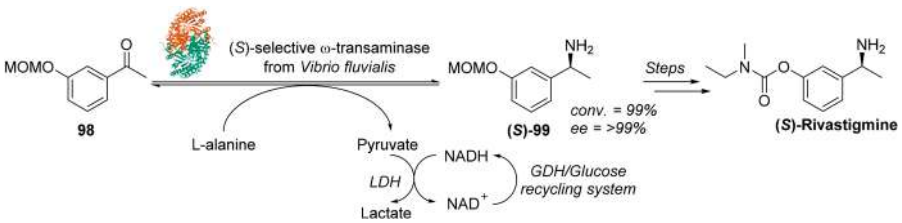

Scheme 4.31 Chemoenzymatic asymmetric synthesis of (*S*)-rivastigmine.

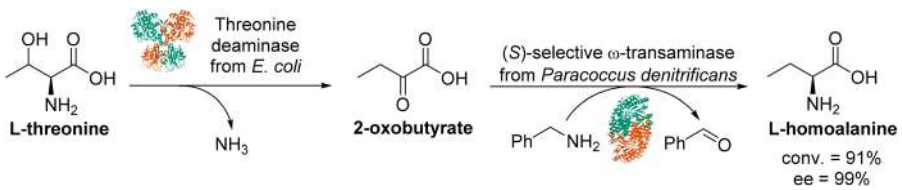

Scheme 4.32 Enzymatic cascade reaction for the synthesis of the unnatural amino acid L-homoalanine.

4.8 Other Enzymes and Perspectives

Enzymes are increasingly being used in academia and industry due to the advantages that biocatalysis offers in terms of green chemistry over classical chemical processes. In addition to the biocatalysts and biocatalytic transformations described above, a few other examples of old and newer enzymes employed in the synthesis of drugs and chemicals are presented in this section.[137]

Laccase enzymes are an attractive class of biocatalysts largely used both in academia and industry due to their ability to catalyse the oxidation of alcohols to aldehydes or ketones when used in combination with molecular oxygen or with the oxy-radical TEMPO.[138] Gotor's group used laccase enzymes in a one-pot reaction protocol to deracemise *rac*-2-phenyl-1-propanol **100** into the enantiomerically pure (*S*)- or (*R*)-2-phenyl-1-propanol **101**, key intermediates in the preparation of optically active profenol-like compounds. Laccase from *Trametes versicolor* was employed in combination with TEMPO to catalyse the non-stereoselective oxidation of the alcohol **100** into the corresponding aldehyde intermediate. The latter was then selectively reduced into **(*S*)-101** or **(*R*)-101** using two stereocomplementary alcohol dehydrogenases, HLADH (to achieve the (*S*)-enantiomer) and Evo-1.1.200 (to obtain the (*R*)-counterpart) in a kinetic dynamic resolution process (Scheme 4.33a).[139] Laccase is used to re-generate TEMPO, which is the real oxidant species in the reaction.

Our group exploited the laccase/TEMPO catalytic system for the aromatization of differently substituted 2,5-dihydrofurans **103** into the corresponding furans **104** with good to excellent conversions and good isolated yields (Scheme 4.33b).[140] In addition, a chemo-enzymatic cascade reaction for the synthesis of furan derivatives directly from the acyclic aliphatic precursors **102** was reported, involving the combination of Grubbs' catalyst and laccase/TEMPO in the same reaction medium (Scheme 4.33b). Grubbs' 2nd gen. catalyst catalysed the ring-closing metathesis of **102** into the 2,5-dihydrofurans **103**, which were in turn converted into the desired furan derivatives **104** by the laccase/TEMPO system.

Finally, laccases are also widely used in industry in the degradation of lignin and lignocellulosic biomass,[141] in the pre-treatment of agrofood wastes[142] as well as in other bioremediation processes of industrial waste.[143]

Another example of versatile biocatalysts that have been widely described in the literature is represented by cytochromes P450 (P450s or CYP).[144] The biocatalysts CYP505X from *Aspergillus fumigatus* and a variant harbouring five mutations, both expressed in *Pichia pastoris*, were employed to investigate the oxidation of more than 30 active pharmaceutical ingredients as substrates.[145] In particular, it was found that the anti-inflammatory drug ibuprofen was hydroxylated at the tertiary carbon atom (2-OH ibuprofen) and at the benzylic position on the lipophilic side chain (1-OH ibuprofen) by the CYP505X variant from *Komagataella phaffii* harbouring five mutations in the amino acid sequence (Scheme 4.33c).

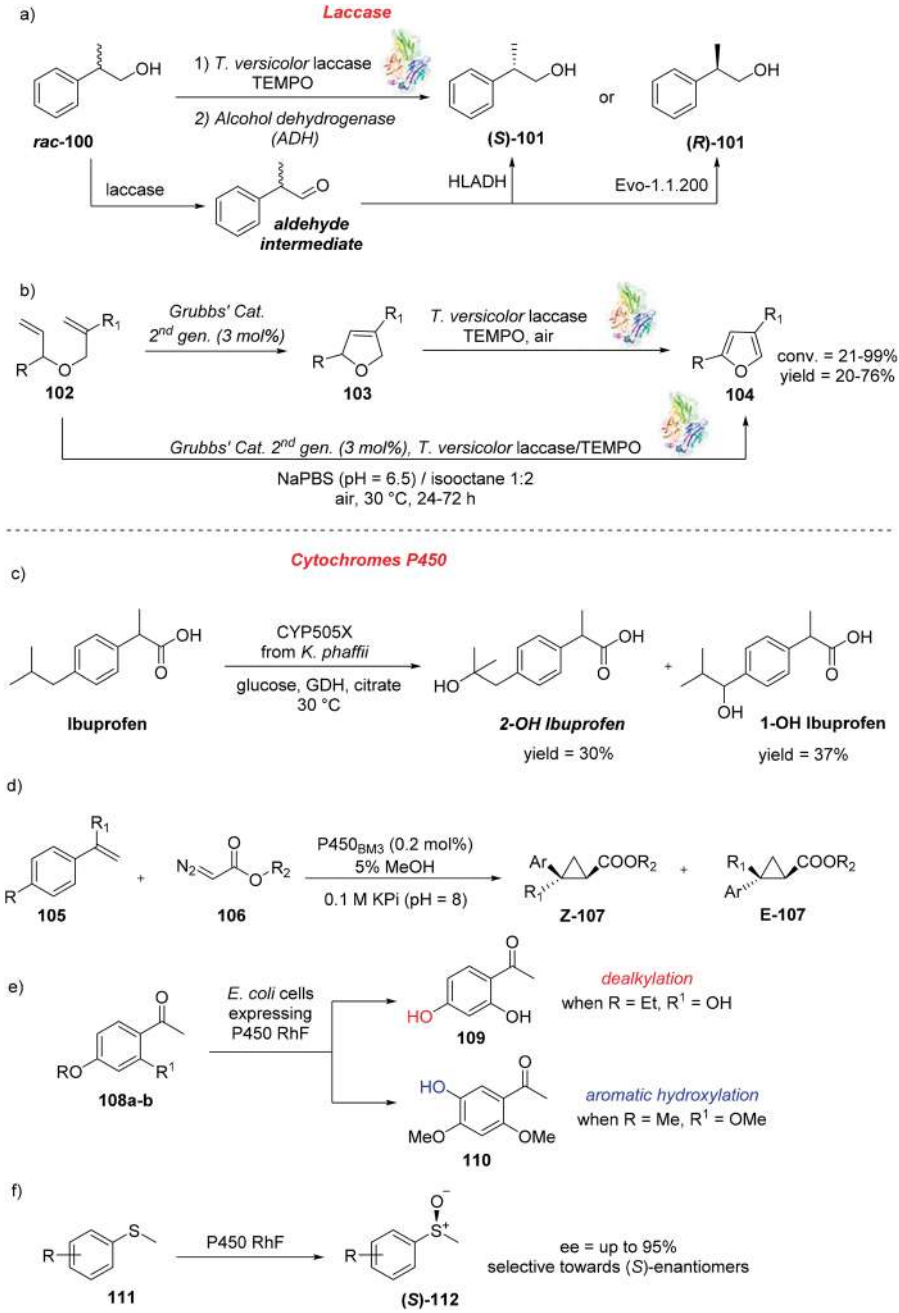

Scheme 4.33 Laccase (a) and cytochrome P450 (c–f) biocatalysed reactions.

Directed evolution of P450s has achieved remarkable success in the last few decades and it has allowed the generation of biocatalysts for the catalysis of non-natural reactions. In 2013, Arnold's group reported an engineered CYP102A1 (P450 BM3) biocatalyst able to catalyse the cyclopropanation of olefin substrates **105**. This highly diastereo- and enantioselective carbene-mediated biotransformation is outside the normal repertoire of P450-catalysed reactions and it represented a great innovation in the field (Scheme 4.33d).[146] A single mutation of the cytochrome residue Thr268 to alanine was sufficient to promote a carbene transfer reaction on an olefin substrate using the diazo-carbene **106**, leading in turn to the cyclopropane products **Z-107** and **E-107** with high enantioselectivity.

Turner's group described the high substrate promiscuity of the cytochrome P450 RhF biocatalyst.[147] Cytochrome P450RhF (RhF) (CYP116B2) from *Rhodococcus* sp. proved to be able to catalyse both O-dealkylation and aromatic hydroxylation reactions of the acetophenone substrates **108a-b** (Scheme 4.33e). The same biocatalyst was also used to catalyse the enantioselective sulfoxidation of sulfide precursors **111** (Scheme 4.33f).

Another interesting class of biocatalysts which have assumed an important role in the asymmetric synthesis of amines is represented by the imine reductases (IREDs).[148] In 2015, Turner and co-workers developed a protocol for the synthesis of different enantiopure cyclic amines **109** with excellent conversions and ee, through the asymmetric reduction of cyclic prochiral imine precursors **108**. An *R*-selective IRED from *Streptomyces* sp. GF3587 was overexpressed in *Escherichia coli* to generate a whole-cell biocatalyst with a broad substrate scope and activity (Scheme 4.34a).[149]

More recently, reductive aminase (RedAms) enzymes, a sub-group of IREDs, have emerged as powerful biocatalysts for the asymmetric synthesis of primary amines from ketone precursors.[150] Turner's group demonstrated the ability of two thermostable RedAms, namely NfRedAm from *Neosartorya fumigata* and NfisRedAm from *Neosartorya fischeri*, to catalyse the reductive amination of a range of ketones **110** using ammonia as the amine partner and affording a broad range of primary amine derivatives **111** with conversions up to >97% and excellent enantiomeric excess (Scheme 4.34b).[150a]

Alcohol dehydrogenases (ADH) are widely used biocatalysts which enable the selective oxidation of primary alcohols into aldehydes or carboxylic acids.[151] As an example, the alcohol dehydrogenases (pro-(+)-ADH and pro-(−)-ADH) from *C. pelliculosa* ZP22 have been used in the synthesis of both enantiomers of the lactone **118** from the meso diol precursor **117** (Scheme 4.34c).[152]

Finally, methyltransferase enzymes are an interesting class of biocatalysts that is receiving increasing attention. Such enzymes are ubiquitous in nature and typically catalyse the transfer of a methyl group from the S-adenosyl-L-methionine (SAM) cofactor to a large variety of acceptor substrates.[153] *N*-methyltransferases play a prominent role in the biosynthesis of many important alkaloids, such as benzylisoquinolines, which have been exploited also in the development of important therapeutic agents.

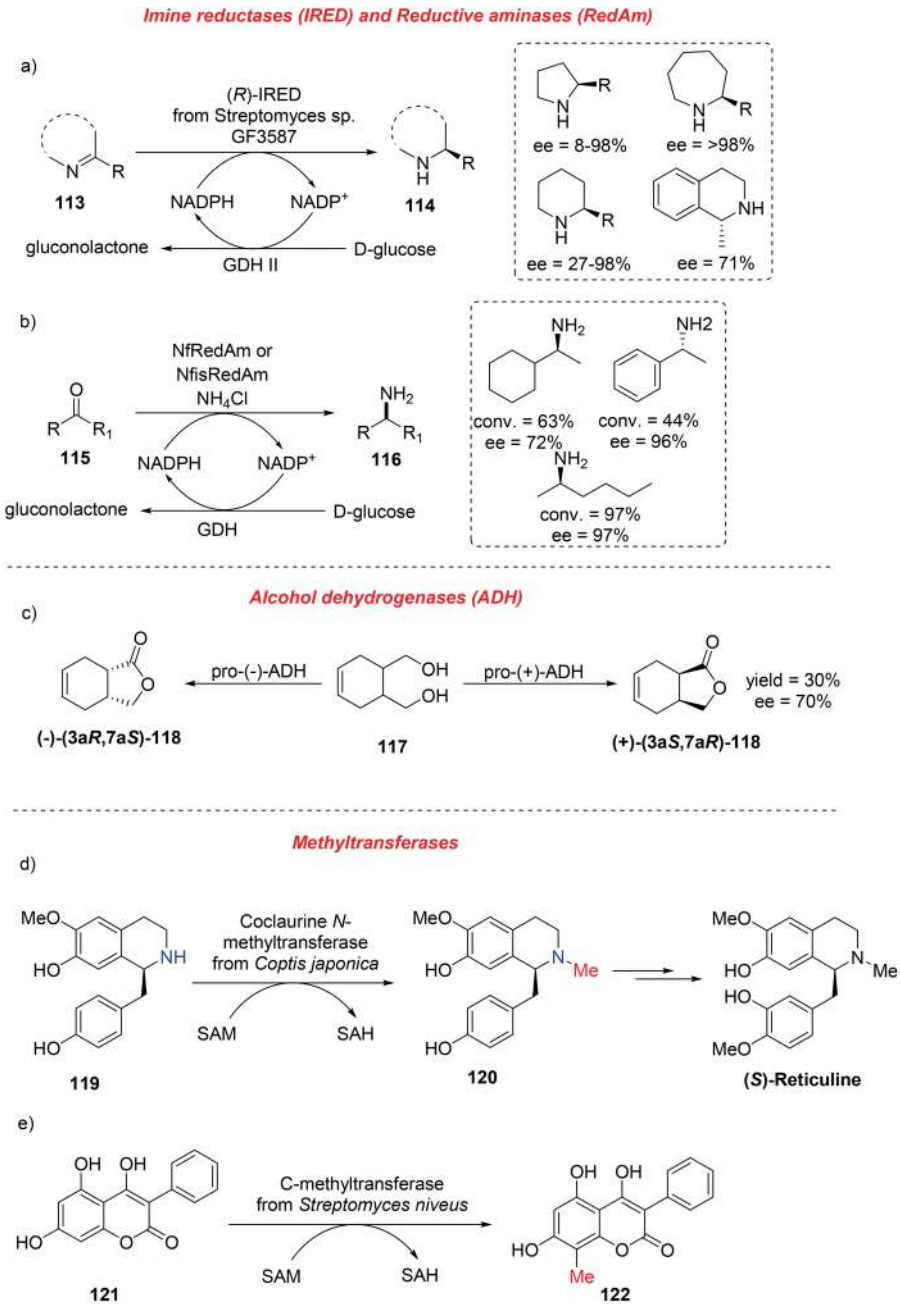

Scheme 4.34 Biocatalytic reactions catalysed by: a) IRED; b) RedAm; c) ADH; d) and e) methyltransferase enzymes.

Given the difficulties associated with the isolation of large quantities of these compounds from natural plants, in 2018 Micklefield's group reported the crystal structure of an engineered coclaurine *N*-methyltransferase from *Coptis japonica* (CNMT), an enzyme able to catalyse the synthesis of the (*S*)-reticuline precursor **120** from the substrate **119** through introduction of an *N*-methyl group (Scheme 4.34d).[154] In addition, further characterization of CNMT through active site mutagenesis and substrate screening was provided, paving the way for further biosynthetic and synthetic applications.

Recently, a SAM-dependent C-methyltransferase from *Streptomyces niveus* was used for the C-methylation of the hydroxy coumarin **121** into compound **122** (Scheme 4.34e).[155] This example clearly shows the potentiality of methyltransferase enzymes not only in the functionalization (methylation) of heteroatoms, but also in the construction of new C–C bonds.

In conclusion, enzymes and biocatalysis represent today a robust and valid strategy for the synthesis of many chemicals and drugs both at academic and industrial level. Enzymes constitute a green alternative to classical synthetic methods and, undoubtedly, the use of biocatalysis in synthetic chemistry will increase in the near future. Thanks to the advances made possible by genome sequencing, metagenomic, directed evolution and bioinformatic driven protein engineering, the toolbox of enzymes available for biocatalytic reactions will expand in the coming years and new enzymes, able also to catalyse non-natural reactions, will be discovered. Finally, the possibility to combine biocatalysis with other green catalytic techniques in one-pot synthetic processes or to use enzymes in flow-chemistry will represent valid strategies for a more sustainable and greener synthesis of chemicals and drugs.

List of Abbreviations

ADH	Alcohol dehydrogenase
API	Active pharmaceutical ingredient
ATAs	Amine transaminase
BVMO	Baeyer–Villiger monooxygenase
CALB	*Candida antarctica* lipase B
CHMO	Cyclohexanone monooxygenase
CNS	Central nervous system
DKR	Dynamic kinetic resolution
EKR	Enzymatic kinetic resolution
FAD	Flavin adenine dinucleotide
FMN	Flavin mononucleotide
GDH	Glucose dehydrogenase
HAPMO	4-Hydroxyacetophenone monooxygenase
IPA	Isopropaol
IRED	Imine reductase
KRED	Ketoreductase
MAO	Monoamine oxidase
MAO-N	Monoamine oxidases from *Aspergillus niger*

*m*CPBA	*meta*-Chloroperbenzoic acid
$NADP^+$	Nicotinamide adenine dinucleotide phosphate
OPA	*o*-Phthalaldehyde
P450 or CYP	Cytochrome P450
PLP	Pyridoxal-5′-phosphate
PMP	Pyridoxamine-5′-phosphate
RedAm	Reductive aminase
SAM	S-adenosyl-L-methionine.
TA	Transaminase
TCA	Trichloroacetic acid
UHP	Urea hydrogen peroxide
WT	Wild type
α-Tas	α-Transaminase
ω-Tas	ω-Transaminase

References

1. (a) A. R. Sheldon, *J. R. Soc., Interface*, 2016, DOI: 10.1098/rsif.2016.0087; (b) H. S. Taylor, *Catalysis*, Encyclopedia Britannica, 2018; (c) I. T. Horváth, *Chem. Rev.*, 2018, **118**, 369; (d) P. Anastas and N. Eghbali, *Chem. Soc. Rev.*, 2010, **39**, 301.
2. R. A. Sheldon, I. Arends and U. Hanefeld, *Green Chemistry and Catalysis*, Wiley-VCH, Weinheim, 2007, ISBN 978-3-527-30715-9.
3. (a) R. A. Sheldon and J. M. Woodley, *Chem. Rev.*, 2018, **118**(2), 801–838; (b) R. A. Sheldon, D. Brady and M. L. Bode, *Chem. Sci.*, 2020, **11**, 2587–2605; (c) G. Hughes and J. C. Lewis, *Chem. Rev.*, 2018, **118**, 1; (d) C. K. Winkler, J. H. Schrittwieser and W. Kroutil, *ACS Cent. Sci.*, 2021, **7**, 55.
4. E. M. M. Abdelraheem, H. Busch, U. Hanefeld and F. Tonin, *React. Chem. Eng.*, 2019, **4**, 1878.
5. (a) U. T. Bornscheuer and R. J. Kazlauskas, *Hydrolases in Organic Synthesis: Regio- and Stereoselective Biotransformations*, Wiley-VCH, Weinheim, Germany, 2nd edn, 2006; (b) M. Breuer, K. Ditrich, T. Habicher, B. Hauer, M. Keßeler, R. Stürmer and T. Zelinski, *Angew. Chem., Int. Ed.*, 2004, **43**, 788; (c) K. Buchholz, V. Kasche and U. T. Bornscheuer, *Biocatalysts and Enzyme Technology*, Wiley-VCH, NewYork, 2nd edn, 2012; (d) A. Liese, K. Seelbach and C. Wandrey, *Industrial Biotransformations*, Wiley-VCH, Weinheim, Germany, 2nd edn, 2006; (e) O. May, H. Gröger and K. Drauz, *Enzyme Catalysis in Organic Synthesis*, Wiley-VCH, Weinheim, Germany, 3rd edn, 2012; (f) K. Faber, *Biotransformations in Organic Chemistry*, Springer, Heidelberg, Germany, 6th edn, 2011.
6. H. Yamada and M. Kobayashi, *Biosci., Biotechnol., Biochem.*, 2014, **60**, 1391.
7. L. Cobos-Puc, R. Rodríguez-Herrera, J. C. Cano-Cabrera, H. Aguayo-Morales, S. Y. Silva-Belmares, A. C. F. Gallegos and J. L. M. Hernández, *Curr. Pharm. Biotechnol.*, 2020, **21**, 287–297.
8. G. Hughes and J. C. Lewis, *Chem. Rev.*, 2018, **118**, 1.

9. N. J. Turner, *Trends Biotechnol.*, 2003, **21**, 474.
10. U. T. Bornscheuer, G. W. Huisman, R. J. Kazlauskas, S. Lutz, J. C. Moore and K. Robins, *Nature*, 2012, **485**, 185.
11. L. Rosenthaler, *Biochem. Z.*, 1908, **14**, 238.
12. (a) M. S. Packer and D. R. Liu, *Nat. Rev. Genet.*, 2015, **16**, 379; (b) M. Wang, T. Sia and H. Zhao, *Bioresour. Technol.*, 2012, **115**, 117; (c) J. Sylvestre, H. Chautard, F. Cedrone and M. Delcourt, *Org. Process Res. Dev.*, 2006, **10**, 562.
13. U. T. Bornscheuer, *Philos. Trans. R. Soc.*, 2018, **376**, 20170063.
14. (a) M. T. Reetz, *Curr. Opin. Chem. Biol.*, 2002, **6**, 145; (b) P. Domínguez de María, G. de Gonzalo and A. R. Alcántara, *Catalysts*, 2019, **9**, 802; (c) A. Kumar, D. Dhar, S. S. Kanwar and P. K. Arora, *Biol. Proced. Online*, 2016, **18**, 2; (d) R. Kourist, F. Hollmann and G. S. Nguyen, *JSM Biotechnol. Bioeng.*, 2014, **2**, 1029.
15. L. Brady, A. M. Brzozowski, Z. S. Derewenda, E. Dodson, G. Dodson, S. Tolley, J. P. Turkenburg, L. Christiansen, B. Huge-Jensen, L. Norskov, L. Thim and U. Menge, *Nature*, 1990, **343**, 767.
16. F. K. Winkler, A. D'Arcy and W. Hunziker, *Nature*, 1990, **343**, 771.
17. J. D. Schrag and M. Cygler, *J. Mol. Biol.*, 1993, **230**, 575.
18. P. Grochulski, Y. Li, J. D. Schrag, F. Bouthillier, P. Smith, D. Harrison, B. Rubin and M. Cygler, *J. Biol. Chem.*, 1993, **268**, 12843.
19. D. Lang, B. Hoffman, L. Haalack, H.-J. Hecht, F. Spener, R. D. Schmid and D. Schomburg, *J. Mol. Biol.*, 1996, **259**, 704.
20. J. Uppenberg, S. Patkar, T. Bergfors and T. A. Jones, *J. Mol. Biol.*, 1994, **235**, 790.
21. K. E. Jaeger, B. W. Dijkstra and M. T. Reetz, *Annu. Rev. Microbiol.*, 1999, **53**, 315.
22. R. V. Almeida, PhD thesis, *Clonagem, expressao, caracterização e modelagem estrutural de uma esterase termoestavel de Pyrococcus furiosus*, University of Rio de Janeiro, 2005.
23. (a) R. C. Rodrigues, J. J. Virgen-Ortíz, J. C. S. dos Santos, Á. Berenguer-Murcia, A. R. Alcantara, O. Barbosa, C. Ortiz and R. Fernandez-Lafuente, *Biotechnol. Adv.*, 2019, **37**, 746; (b) B. R. Facin, M. S. Melchiors, A. Valério, J. V. Oliveira and D. de Oliveira, *Ind. Eng. Chem. Res.*, 2019, **58**, 5358.
24. (a) A. C. L. de Melo Carvalho, T. de Sousa Fonseca, M. C. de Mattos, M. C. de Oliveira, T. L. G. de Lemos, F. Molinari, D. Romano and I. Serra, *Int. J. Mol. Sci.*, 2015, **16**, 29682; (b) S. Takaç and M. Bakkal, *Process Biochem.*, 2007, **42**, 1021.
25. C. Hu, N. Wang, W. Zhang, S. Zhang, Y. Meng and X. Yu, *J. Biotechnol.*, 2015, **194**, 12.
26. W.-W. Zhang, J.-Q. Jia, N. Wang, C.-L. Hu, S.-Y. Yang and X.-Q. Yu, *Biotechnol. Rep.*, 2015, **7**, 1.
27. (a) C. A. Martinez, S. Hu, Y. Dumond, J. Tao, P. Kelleher and L. Tully, *Org. Process Res. Dev.*, 2008, **12**, 392; (b) R.-C. Zheng, L.-T. Ruan, H.-Y. Ma, X.-L. Tang and Y.-G. Zheng, *Biochem. Eng. J.*, 2016, **113**, 12.

28. J.-W. Shen, J.-M. Qi, X.-J. Zhang, Z.-Q. Liu and Y.-G. Zheng, *Catal. Sci. Technol.*, 2018, **8**, 4718.
29. A. Sikora, T. Siódmiak and M. P. Marszałł, *Chirality*, 2014, **26**, 663.
30. M. P. Marszałł and T. Siódmiak, *Catal. Commun.*, 2012, **24**, 80.
31. S. D. Shinde and G. D. Yadav, *Process Biochem.*, 2015, **50**, 230.
32. L. Tamborini, D. Romano, A. Pinto, A. Bertolani, F. Molinari and P. Conti, *J. Mol. Catal. B: Enzym.*, 2012, **84**, 78.
33. S. Devendran and G. D. Yadav, *Chirality*, 2014, **26**, 286.
34. (a) T. S. Fonseca, M. R. Silva, M. C. F. Oliveira, T. L. G. Lemos, R. A. Marques and M. C. Mattos, *Appl. Catal., A*, 2015, **492**, 76; (b) A. C. L. M. Carvalho, D. M. F. Araujo, L. R. B. Gonçalves, M. C. Mattos, M. R. Silva, M. C. F. Oliveira, R. A. Marques, T. L. G. Lemos, T. S. Fonseca and U. M. F. Oliveira, Desenvolvimento de um Processo Biocatalítico para a Produção do (*S*)-Indanol, Precursor do Fármaco Mesilato de Rasagilina, *Br Pat.*, BR102013024675–1A2, 2015.
35. A. B. Bahadoor, A. Flyer and G. C. J. Micalizio, *Am. Chem. Soc.*, 2005, **127**, 3694.
36. W. Felzmann, D. Castagnolo, D. Rosenbeiger and J. Mulzer, *J. Org. Chem.*, 2007, **72**, 2182.
37. (a) R. N. Lima, C. S. dos Anjos, E. V. M. Orozco and A. L. M. Porto, *Mol. Catal.*, 2019, **466**, 75; (b) M. R. Petchey and G. Grogan, *Adv. Synth. Catal.*, 2019, **361**, 3895; (c) M. J. J. Litjens, A. J. J. Straathof, J. A. Jongejan and J. J. Heijnen, *Chem. Commun.*, 1999, 1255.
38. F. van Rantwijk, M. A. P. J. Hacking and R. A. Sheldon, *Monatsh. Chem.*, 2000, **131**, 549.
39. (a) E. Garcia-Urdiales, N. Rios-Lombardia, J. Mangas-Sanchez, V. Gotor-Fernandez and V. Gotor, *ChemBioChem*, 2009, **10**, 1830; (b) M. J. García, F. Rebolledo and V. Gotor, *Tetrahedron Lett.*, 1993, **34**, 6141.
40. M. A. P. J. Hacking, F. van Rantwijk and R. A. Sheldon, *J. Mol. Catal. B: Enzym.*, 2000, **9**, 201.
41. B. Kovács, R. Megyesi, E. Forró and F. Fülöp, *Tetrahedron: Asymmetry*, 2017, **28**, 1829.
42. A. Baldessari and C. P. Mangone, *J. Mol. Catal. B: Enzym.*, 2001, **11**, 335.
43. F. Messina, M. Botta, F. Corelli, M. P. Schneider and F. Fazio, *J. Org. Chem.*, 1999, **64**, 3767.
44. D. Castagnolo, S. Armaroli, F. Corelli and M. Botta, *Tetrahedron: Asymmetry*, 2004, **15**, 941.
45. J. Paetzold and J. E. Bäckvall, *J. Am. Chem. Soc.*, 2005, **127**, 17620.
46. (a) P. Zhou, X. Wang, B. Yang, F. Hollmann and Y. Wang, *RSC Adv.*, 2017, **7**, 12518; (b) M. De Torres, G. Jiménez-Osés, J. A. Mayoral, E. Pires, R. M. Blanco and O. Fernández, *Catal. Today*, 2012, **195**, 76; (c) V. Skouridou, H. Stamatis and F. N. Kolisis, *J. Mol. Catal. B: Enzym.*, 2003, **21**, 67; (d) M. Rusch gen Klaas and S. Warwel, *J. Am. Oil Chem. Soc.*, 1996, **73**, 1453; (e) M. Steinhagen, A. Gräbner, J. Meyer, A. E. W. Horst, A. Drews, D. Holtmann and M. B. Ansorge-Schumacher, *J. Mol. Catal. B: Enzym.*, 2016, **133**, S179.

47. (a) G. Chávez, R. Hatti-Kaul, R. A. Sheldon and G. Mamo, *J. Mol. Catal. B: Enzym.*, 2013, **89**, 67; (b) D. González-Martínez, M. Rodríguez-Mata, D. Méndez-Sánchez, V. Gotor and V. Gotor-Fernández, *J. Mol. Catal. B: Enzym.*, 2015, **114**, 31; (c) A. Drożdż, K. Erfurt, R. Bielas and A. Chrobok, *New J. Chem.*, 2015, **39**, 1315.
48. D. Méndez-Sánchez, I. Lavandera, V. Gotor and V. Gotor-Fernández, *Org. Biomol. Chem.*, 2017, **15**, 3196.
49. S. Anselmi, S. Liu, S. H. Kim, S. M. Barry, T. S. Moody and D. Castagnolo, *Org. Biomol. Chem.*, 2021, **19**, 156.
50. F. Bjorkling, H. Frykman, S. E. Godtfredsen and O. Kirk, *Tetrahedron*, 1992, **48**, 4587.
51. M. S. Melchiors, T. Y. Vieira, L. P. S. Pereira, B. A. M. Carciofi, P. H. H. de Araújo, D. de Oliveira and C. Sayer, *Ind. Eng. Chem. Res.*, 2019, **58**, 13918.
52. M. Renz and B. Meunier, *Eur. J. Org. Chem.*, 1999, 737–750.
53. A. Drozdz and A. Chrobok, *Chem. Commun.*, 2016, **52**, 1230.
54. J.-S. Gong, Z.-M. Lu, H. Li, J.-S. Shi, Z.-M. Zhou and Z.-H. Xu, *Microb. Cell Fact.*, 2012, **11**, 142.
55. (a) H. Pace and C. Brenner, *Genome Biol.*, 2001, **2**, 1; (b) C. Brenner, *Curr. Opin. Struct. Biol.*, 2002, **12**, 775.
56. R. Singh, R. Sharma, N. Tewari, N. Geetanjali and D. S. Rawat, *Chem. Biodiversity*, 2006, **3**, 1279.
57. (a) H. C. Pace, S. C. Hodawadekar, A. Draganescu, J. Huang, P. Bieganowski, Y. Pekarsky, C. M. Croce and C. Brenner, *Curr. Biol.*, 2000, **10**, 907; (b) R. N. Thuku, D. Brady, M. J. Benedik and B. T. Sewell, *J. Appl. Microbiol.*, 2009, **106**, 703.
58. K. V. Thimann and S. Mahadevan, *Arch. Biochem. Biophys.*, 1964, **105**, 133.
59. J.-D. Shen, X. Cai, Z.-Q. Liu and Y.-G. Zheng, *Crit. Rev. Biotechnol.*, 2021, **41**, 72.
60. J. M. Park, B. T. Sewell and M. J. Benedik, *Appl. Microbiol. Biotechnol.*, 2017, **101**, 3029.
61. S. D. Van Arnum, *Niacin, Nicotinamide, and Nicotinic Acid, Kirk-Othmer Encyclopedia of Chemical Technology*, 2000.
62. H. Yamada and M. Kobayashi, *Biosci., Biotechnol., Biochem.*, 1996, **60**, 1391.
63. C. D. Mathew, T. Nagasawa, M. Kobayashi and H. Yamada, *Appl. Environ. Microbiol.*, 1988, **54**, 1030.
64. T. Nagasawa, C. D. Mathew, J. Mauger and H. Yamada, *Appl. Environ. Microbiol.*, 1988, **54**, 1766.
65. Q. A. Almatawah and D. A. Cowan, *Enzyme Microb. Technol.*, 1999, **25**, 718.
66. (a) A. Schmid, J. S. Dordick, B. Hauer, A. Kiener, M. Wubbolts and B. Witholt, *Nature*, 2001, **409**, 258–266; (b) J. Mills, K. K. Schmiegel and W. N. Shaw, *US Pat.*, 4391826, 1983; (c) M. Ress-Loschke, T. Friedrich, B. Hauer, R. Mattes and D. Engels, *DE Pat.*, DE198448129A1, BASF, 1998.
67. T. Endo and K. Tamura, *EP Pat.*, EP 0449648, 1991.
68. Y.-P. Xue, S.-Z. Xu, Z.-Q. Liu, Y.-G. Zheng and Y.-C. Shen, *J. Ind. Microbiol. Biotechnol.*, 2011, **38**, 337.

69. (a) Y. C. He, J. H. Xu, Y. Xu, L. M. Ouyang and J. Pan, *Chin. Chem. Lett.*, 2007, **18**, 677; (b) Z. Q. Liu, J. F. Zhang, Y. G. Zheng and Y. C. Shen, *J. Appl. Microbiol.*, 2008, **104**, 861; (c) K. Yamamoto, K. Oishi, I. Fujimatsu and K. I. Komatsu, *Appl. Environ. Microbiol.*, 1991, **57**, 3028.
70. Z.-J. Zhang, J.-H. Xu, Y.-C. He, L.-M. Ouyang, Y.-Y. Liu and T. Imanaka, *Process Biochem.*, 2010, **45**, 887.
71. H. Wang, H. Fan, H. Sun, L. Zhao and D. Wei, *Org. Process Res. Dev.*, 2015, **19**, 2012.
72. K. Yamamoto, Y. Ueno, K. Otsubo, K. Kawakami and K. Komatsu, *Appl. Environ. Microbiol.*, 1990, **56**, 3125.
73. J. E. Gavagan, S. K. Fager, R. D. Fallon, P. W. Folsom, F. E. Herkes, A. Eisenberg, E. C. Hann and R. DiCosimo, *J. Org. Chem.*, 1998, **63**, 4792.
74. M. P. Burns and J. W. Wong, *PCT Pat. Appl.*, WO/2004/111256, 2004.
75. M. Kobayashi, N. Yanaka, T. Nagasawa and H. Yamada, *Tetrahedron*, 1990, **46**, 5587.
76. K. Lauder, S. Anselmi, J. D. Finnigan, Y. Qi, S. J. Charnock and D. Castagnolo, *Chem. - Eur. J.*, 2020, **26**, 10422.
77. G. W. Black, N. L. Brown, J. J. B. Perry, P. D. Randall, G. Turnbull and M. Zhang, *Chem. Commun.*, 2015, **51**, 2660.
78. (a) T. A. Slotkin, *Brain Res. Bull.*, 1999, **50**, 373; (b) J. Finberg, M. Youdim, P. Riederer and K. Tipton, *MAO – The Mother of All Amine Oxidases*, Springer-Verlag GmbH: Wien, Austria, 1998.
79. (a) H. Gaweska and P. F. Fitzpatrick, *Biomol. Concepts*, 2011, **2**, 365; (b) S. Chajkowski-Scarry and J. M. Rimoldi, *Future Med. Chem.*, 2014, **6**, 697; (c) R. Orru, M. Aldeco and D. E. Edmondson, *J. Neural Transm.*, 2013, **120**, 847; (d) R. Vianello, M. Repič and J. Mavri, *Eur. J. Org. Chem.*, 2012, **2012**, 7057; (e) K. Cakir, S. S. Erdem and V. E. Atalay, *Org. Biomol. Chem.*, 2016, **14**, 9239.
80. V. F. Batista, J. L. Galman, D. C. G. A. Pinto, A. M. S. Silva and N. J. Turner, *ACS Catal.*, 2018, **8**, 11889.
81. L. K. Hoover, M. Moo-Young and R. L. Legge, *Biotechnol. Bioeng.*, 1991, **38**, 1029.
82. B. Schilling and K. Lerch, *Biochim. Biophys. Acta, Gen. Subj.*, 1995, **1243**, 529.
83. M. Alexeeva, A. Enright, M. J. Dawson, M. Mahmoudian and N. J. Turner, *Angew. Chem., Int. Ed.*, 2002, **41**, 3177.
84. R. Carr, M. Alexeeva, M. J. Dawson, V. Gotor-Fernández, C. E. Humphrey and N. J. Turner, *ChemBioChem*, 2005, **6**, 637.
85. (a) C. J. Dunsmore, R. Carr, T. Fleming and N. J. Turner, *J. Am. Chem. Soc.*, 2006, **128**, 2224; (b) I. Rowles, K. J. Malone, L. L. Etchells, S. C. Willies and N. J. Turner, *ChemCatChem*, 2012, **4**, 1259.
86. D. Ghislieri, A. P. Green, M. Pontini, S. C. Willies, I. Rowles, A. Frank, G. Grogan and N. J. Turner, *J. Am. Chem. Soc.*, 2013, **135**, 10863.
87. S. Herter, F. Medina, S. Wagschal, C. Benhaïm, F. Leipold and N. J. Turner, *Bioorg. Med. Chem.*, 2018, **26**, 1338.
88. M. Odachowski, M. F. Greaney and N. J. Turner, *ACS Catal.*, 2018, **8**, 10032.

89. (a) A. Znabet, S. Blanken, E. Janssen, F. J. J. de Kanter, M. Helliwell, N. J. Turner, E. Ruijter and R. V. A. Orru, *Org. Biomol. Chem.*, 2012, **10**, 941; (b) C. de Graaff, B. Oppelaar, O. Péruch, C. M. L. Vande Velde, B. Bechi, N. J. Turner, E. Ruijter and R. V. A. Orru, *Adv. Synth. Catal.*, 2016, **358**, 1555.
90. N. Scalacci, G. W. Black, G. Mattedi, N. L. Brown, N. J. Turner and D. Castagnolo, *ACS Catal.*, 2017, **7**, 1295.
91. A. Toscani, C. Risi, G. W. Black, N. L. Brown, A. Shaaban, N. J. Turner and D. Castagnolo, *ACS Catal.*, 2018, **8**, 8781.
92. F. Zhao, D. Masci, S. Ferla, C. Varricchio, A. Brancale, S. Colonna, G. W. Black, N. J. Turner and D. Castagnolo, *ACS Catal.*, 2020, **10**, 6414.
93. D. L. Hughes, *Org. Process Res. Dev.*, 2018, **22**, 1063.
94. (a) R. Csuk and B. I. Glaenzer, *Chem. Rev.*, 1991, **91**, 49; (b) C. J. Sih and C.-S. Chen, *Angew. Chem., Int. Ed. Engl.*, 1984, **23**, 570; (c) S. Servi, *Synthesis*, 1990, **1**, 1–25.
95. R. MacLeod, H. Pnxser, L. Fientscher, J. Lanyi and H. S. Mosher, *Biochemistry*, 1964, **3**, 838.
96. (a) G. de Gonzalo, I. Lavandera and V. Gotor, in *Catalytic Methods in Asymmetric Synthesis: Advanced Materials, Techniques*, ed. M. Gruttadauria and F. Giacalone, John Wiley and Sons: Hoboken, NJ, 2011, ch. 12, pp. 491–529; (b) G. W. Huisman, J. Liang and A. Krebber, *Curr. Opin. Chem. Biol.*, 2010, **14**, 122; (c) J. C. Moore, D. J. Pollard, B. Kosjek and P. N. Devine, *Acc. Chem. Res.*, 2007, **40**, 1412; (d) S. M. A. de Wildeman, T. Sonke, H. E. Schoemaker and O. May, *Acc. Chem. Res.*, 2007, **40**, 1260; (e) D. J. Pollard and J. M. Woodley, *Trends Biotechnol.*, 2007, **25**, 66; (f) T. S. Moody and J. D. Rozzell, in *Organic Syntheses Using Biocatalysis*, ed. A. Goswami and J. D. Stewart, Elsevier, Amsterdam, 2016, ch. 6, pp. 149–185; (g) G.-W. Zheng, Y. Ni and J.-H. Xu, in *Applied Biocatalysis: From Fundamental Science to Industrial Applications*, ed. L. Hilterhaus, A. Liese, U. Kettling and G. Antranikian, Wiley-VCH, Weinheim, Germany, 2016, pp. 219–250.
97. R. Kratzer and B. Nidetzky, *Biochem. J.*, 2005, **389**, 507.
98. (a) S. Wu, R. Snajdrova, J. C. Moore, K. Baldenius and U. T. Bornscheuer, *Angew. Chem., Int. Ed.*, 2021, **60**, 88; (b) Y.-G. Zheng, H.-H. Yin, D.-F. Yu, X. Chen, X.-L. Tang, X.-J. Zhang, Y.-P. Xue, Y.-J. Wang and Z.-Q. Liu, *Appl. Microbiol. Biotechnol.*, 2017, **101**, 987; (c) M. M. Musaa and R. S. Phillips, *Catal. Sci. Technol.*, 2011, **1**, 1311.
99. D. P. M. Depre´, D. J. Ormerod, A. Horvath, T. S. Moody, M. Brossat, O. Riant, N. Vriamont, S. F. E. Lemaire and S. N. J. Hermant, *US Pat.*, US20180093943A1, 2018.
100. (a) R. Stürmer, M. Kesseler, B. Hauer, T. Friedrich, M. Breuer and H. Schröder, *DE Pat.*, DE102005062662, BASF, 2007; (b) S. Leuchs and L. Greiner, *Chem. Biochem. Eng. Q.*, 2011, **25**, 267; (c) R. Stürmer, M. Kesseler, B. Hauer, T. Friedrich, M. Breuer and H. Schröder, *WO Pat.*, WO2005108590, BASF, 2005; (d) N. Schneider and W. Höffken, *WO Pat.*, WO2010079068, BASF, 2010.
101. X. Chen, Z.-Q. Liu, C.-P. Lin and Y.-G. Zheng, *Bioorg. Chem.*, 2016, **65**, 82.

102. K. Lauder, A. Toscani, Y. Qi, J. Lim, S. J. Charnock, K. Korah and D. Castagnolo, *Angew. Chem., Int. Ed.*, 2018, **57**, 5803.
103. X. Chen, H. Zhang, M. A. Maria-Solano, W. Liu, J. Li, J. Feng, X. Liu, S. Osuna, R.-T. Guo, Q. Wu, D. Zhu and Y. Ma, *Nat. Catal.*, 2019, **2**, 931.
104. B. Yuan, A. Page, C. P. Worrall, F. Escalettes, S. C. Willies, J. J. W. McDouall, N. J. Turner and J. Clayden, *Angew. Chem., Int. Ed.*, 2010, **49**, 7010.
105. C. K. Prier, M. M.-C. Lo, H. Li and N. Yasuda, *Adv. Synth. Catal.*, 2019, **361**, 5140.
106. D. E. Torres Pazmiño, M. Winkler, A. Glieder and M. W. Fraaije, *J. Biotechnol.*, 2010, **146**, 9.
107. M. L. Mascotti, M. Juri Ayub, N. Furnham, J. M. Thornton and R. A. Laskowski, *J. Mol. Biol.*, 2016, **428**, 3131.
108. W. J. H. van Berkel, N. M. Kamerbeek and M. W. Fraaije, *J. Biotechnol.*, 2006, **124**, 670.
109. P. Chaiyen, M. W. Fraaije and A. Mattevi, *Trends Biochem. Sci.*, 2012, **37**, 373.
110. R. D. Ceccoli, D. A. Bianchi and D. V. Rial, *Front. Microbiol.*, 2014, **5**, 25.
111. (a) J. L. J. Fürst, A. Gran-Scheuch, F. S. Aalbers and M. W. Fraaije, *ACS Catal.*, 2019, **9**, 11207; (b) N. M. Kamerbeek, D. B. Janssen, W. J. H. van Berkel and M. W. Fraaije, *Adv. Synth. Catal.*, 2003, **345**, 667.
112. S. Schmidta and U. T. Bornscheuerb, *Enzymes*, 2020, **47**, 231.
113. S. Schmidt, C. Scherkus, J. Muschiol, U. Menyes, T. Winkler, W. Hummel, H. Gröger, A. Liese, H.-G. Herz and U. T. Bornscheuer, *Angew. Chem., Int. Ed.*, 2015, **54**, 2784.
114. V. S. T. Srinivasamurthy, D. Böttcher, J. Engel, S. Kara and U. T. Bornscheuer, *Process Biochem.*, 2019, **88**, 22.
115. J. Solé, J. Brummund, G. Caminal, G. Álvaro, M. Schürmann and M. Guillén, *Org. Process Res. Dev.*, 2019, **23**, 2336.
116. (a) D. A. Bianchi, R. Moran-Ramallal, N. Iqbal, F. Rudroff and M. D. Mihovilovic, *Bioorg. Med. Chem. Lett.*, 2013, **23**, 2718; (b) F. Rudroff, D. A. Bianchi, R. Moran-Ramallal, N. Iqbal, D. Dreier and M. D. Mihovilovic, *Tetrahedron*, 2016, **72**, 7212.
117. A. Rioz-Martínez, G. de Gonzalo, D. E. Torres Pazmiño, M. W. Fraaije and V. Gotor, *Eur. J. Org. Chem.*, 2009, **15**, 2526.
118. J.-H. Seo, H.-H. Kim, E.-Y. Jeon, Y.-H. Song, C.-S. Shin and J.-B. Park, *Sci. Rep.*, 2016, **6**, 28223.
119. S. Colonna, N. Gaggero, G. Carrea, G. Ottolina, P. Pasta and F. Zambianchi, *Tetrahedron Lett.*, 2002, **43**, 1797.
120. G. Ottolina, S. Bianchi, B. Belloni, G. Carrea and B. Danieli, *Tetrahedron Lett.*, 1999, **40**, 8483.
121. Y. K. Bong, S. Song, J. Nazor, M. Vogel, M. Widegren, D. Smith, S. J. Collier, R. Wilson, S. M. Palanivel, K. Narayanaswamy, B. Mijts, M. D. Clay, R. Fong, J. Colbeck, A. Appaswami, S. Muley, J. Zhu, X. Zhang, J. Liang and D. Entwistle, *J. Org. Chem.*, 2018, **83**, 7453.
122. D. M. Needham, *Biochem. J.*, 1930, **24**, 208.

123. (a) A. E. Braunstein, *Nature*, 1939, **143**, 609; (b) P. Cohen, *J. Biol. Chem.*, 1940, **136**, 565; (c) M. G. Kritzmann, *Nature*, 1939, **143**, 603.
124. F. Steffen-Munsberg, C. Vickers, H. Kohls, H. Land, H. Mallin, A. Nobili, L. Skalden, T. van den Bergh, H.-J. Joosten, P. Berglund, M. Höhne and U. T. Bornscheuer, *Biotechnol. Adv.*, 2015, **33**, 566.
125. (a) P. K. Mehta, T. I. Hale and P. Christen, *Eur. J. Biochem.*, 1993, **214**, 549; (b) K. Szmejda, T. Florczak, I. Jodlowska and M. Turkiewicz, *Biotechnol. Food Sci.*, 2017, **81**, 23.
126. D. F. A. R. Dourado, S. Pohle, A. T. P. Carvalho, D. S. Dheeman, J. M. Caswell, T. Skvortsov, I. Miskelly, R. T. Brown, D. J. Quinn, C. C. R. Allen, L. Kulakov, M. Huang and T. S. Moody, *ACS Catal.*, 2016, **6**, 7749.
127. I. Sánchez-Moreno, I. Oroz-Guinea, L. Iturrate and E. García-Junceda, *Comprehensive Chirality*, Elsevier, 2012, ch. 7.20, pp. 430–453.
128. M. D. Patil, G. Grogan, A. Bommarius and H. Yun, *Catalysts*, 2018, **8**, 254.
129. J. S. Shin and B. G. Kim, *Biotechnol. Bioeng.*, 1999, **65**, 206.
130. M. Hohne, S. Kuhl, K. Robins and U. T. Bornscheuer, *ChemBioChem*, 2008, **9**, 363.
131. H. Yun and B.-G. Kim, *Biosci., Biotechnol., Biochem.*, 2008, **72**, 3030.
132. D. Koszelewski, D. Pressnitz, D. Clay and W. Kroutil, *Org. Lett.*, 2009, **11**, 4810.
133. M. Fuchs, D. Koszelewski, K. Tauber, W. Kroutil and K. Faber, *Chem. Commun.*, 2010, **46**, 5500.
134. F. Guo and P. Berglund, *Green Chem.*, 2017, **19**, 333.
135. B. Seisser, R. Zinkl, K. Gruber, F. Kaufmann, A. Hafner and W. Kroutil, *Adv. Synth. Catal.*, 2010, **352**, 731.
136. E. Park, M. Kim and J.-S. Shin, *Adv. Synth. Catal.*, 2010, **352**, 3391–3398.
137. (a) A. Fryszkowska and P. N. Devine, *Curr. Opin. Chem. Biol.*, 2020, **55**, 151–160; (b) P. N. Devine, R. M. Howard, R. Kumar, M. P. Thompson, M. D. Truppo and N. J. Turner, *Nat. Rev. Chem.*, 2018, **2**, 409–421; (c) S. Jenny, R. Katrin, S. Radka, K. Matthias and L. Stephan, *CHIMIA Int. J. Chem.*, 2020, **74**, 368–377; (d) D. J. Pollard and J. M. Woodley, *Trends Biotechnol.*, 2007, **25**, 66–73; (d) D. L. Hughes, *Org. Process Res. Dev.*, 2018, **22**, 1063–1080.
138. (a) D. M. Mate and M. Alcalde, *Microbiol. Biotechnol.*, 2017, **10**, 1457–1467; (b) W. Zhou, W. Zhang and Y. Cai, *Chem. Eng. J.*, 2021, **403**, 126272; (c) N. A. Daronch, M. Kelbert, C. S. Pereira, P. H. Hermes de Araujo and D. De Oliveira, *Chem. Eng. J.*, 2020, **397**, 125506; (d) M. Bilal, T. Rasheed, F. Nabeel, H. M. N. Iqbal and Y. Zhao, *J. Environ. Manage.*, 2019, **234**, 253–264.
139. A. Diaz-Rodriguez, N. Rios-Lombardia, J. H. Sattler, I. Lavandera, V. Gotor-Fernandez, W. Kroutil and V. Gotor, *Catal. Sci. Technol.*, 2015, **5**, 1443–1446.
140. C. Risi, F. Zhao and D. Castagnolo, *ACS Catal.*, 2019, **9**, 7264–7269.

141. (a) L. P. Christopher, Y. Bin and J. Yun, *Front. Energy Res.*, 2014, **2**, 12; (b) A. K. Sitarz, J. D. Mikkelsen and A. S. Meyer, *Crit. Rev. Biotechnol.*, 2016, **36**, 70–86.
142. (a) S. Giacobbe, C. Pezzella, V. Lettera, G. Sannia and A. Piscitelli, *Bioresour. Technol.*, 2018, **265**, 59–65; (b) K. Mayolo-Deloisa, M. González-González and M. Rito-Palomares, *Front. Bioeng. Biotechnol.*, 2020, **8**, 222.
143. R. Chandra and P. Chowdhary, *Environ. Sci.: Processes Impacts*, 2015, **17**, 326–342.
144. (a) A. K. Migglautsch, M. Willim, B. Schweda, A. Glieder, R. Breinbauer and M. Winkler, *Tetrahedron*, 2018, **74**, 6199–6204; (b) Y. Wei, E. L. Ang and H. Zhao, *Curr. Opin. Chem. Biol.*, 2018, **43**, 1–7; (c) V. B. Urlacher and S. Eiben, *Trends Biotechnol.*, 2006, **24**, 324–330; (d) J. B. Y. H. Behrendorff, W. Huang and E. M. J. Gillam, *Biochem. J.*, 2015, **467**, 1–15; (e) V. B. Urlacher and M. Girhard, *Trends Biotechnol.*, 2019, **37**, 882–897; (f) E. O'Reilly, V. Köhler, S. L. Flitsch and N. J. Turner, *Chem. Commun.*, 2011, **47**, 2490–2501.
145. C. Rinnofner, B. Kerschbaumer, H. Weber, A. Glieder and M. Winkler, *Biocatal. Agric. Biotechnol.*, 2019, **17**, 525–528.
146. P. S. Coelho, E. M. Brustad, A. Kannan and F. H. Arnold, *Science*, 2013, **339**, 307–310.
147. E. O'Reilly, M. Corbett, S. Hussain, P. P. Kelly, D. Richardson, S. L. Flitsch and N. J. Turner, *Catal. Sci. Technol.*, 2013, **3**, 1490.
148. (a) J. Mangas-Sanchez, S. P. France, S. L. Montgomery, G. A. Aleku, H. Man, M. Sharma, J. I. Ramsden, G. Grogan and N. J. Turner, *Curr. Opin. Chem. Biol.*, 2017, **37**, 19–25; (b) F. Leipold, S. Hussain, D. Ghislieri and N. J. Turner, *ChemCatChem*, 2015, **12**, 3505–3508; (c) G.-D. Roiban, M. Kern, Z. Liu, J. Hyslop, P. L. Tey, M. S. Levine, L. S. Jordan, K. K. Brown, T. Hadi, L. A. F. Ihnken and M. J. B. Brown, *ChemCatChem*, 2017, **9**, 4475; (d) M. Lenz, N. Borlinghaus, L. Weinmann and B. M. Nestl, *World J. Microbiol. Biotechnol.*, 2017, **33**, 199; (e) P. N. Scheller, M. Lenz, S. C. Hammer, B. Hauer and B. M. Nestl, *ChemCatChem*, 2015, **7**, 3239; (f) M. Lenz, J. Meisner, L. Quertinmont, S. Lutz, J. Kästner and B. M. Nestl, *ChemBioChem*, 2017, **18**, 253; (g) K. Mitsukura, M. Suzuki, S. Shinoda, T. Kuramoto, T. Yoshida and T. Nagasawa, *Biosci., Biotechnol., Biochem.*, 2011, **75**, 1778–1782.
149. S. Hussain, F. Leipold, H. Man, E. Wells, S. P. France, K. R. Mulholland, G. Grogan and N. J. Turner, *ChemCatChem*, 2015, **7**, 579–583.
150. (a) J. Mangas-Sanchez, M. Sharma, S. C. Cosgrove, J. I. Ramsden, J. R. Marshall, T. W. Thorpe, R. B. Palmer, G. Grogan and N. J. Turner, *Chem. Sci.*, 2020, **11**, 5052–5057; (b) K. Chen and F. H. Arnold, *Nat. Catal.*, 2020, **3**, 203–221.
151. (a) W. Kroutil, H. Mang, K. Edegger and K. Faber, *Curr. Opin. Chem. Biol.*, 2004, **8**, 120–126; (b) W. Kroutil, H. Mang, K. Edegger and K. Faber, *Adv. Synth. Catal.*, 2004, **346**, 125–142.

152. F. Boratyński, A. Janik-Polanowicz, E. Szczepańska and T. Olejniczak, *Sci. Rep.*, 2018, **8**, 468.
153. (a) M. R. Bennett, S. A. Shepherd, V. A. Cronin and J. Micklefield, *Curr. Opin. Chem. Biol.*, 2017, **37**, 97–106; (b) A.-W. Struck, M. L. Thompson, L. S. Wong and J. Micklefield, *ChemBioChem*, 2012, **13**, 2642–2655; (c) M. R. Bennett, S. A. Shepherd, V. A. Cronin and J. Micklefield, *Curr. Opin. Chem. Biol.*, 2017, **37**, 97–106; (d) L. E. Zetzsche and A. R. H. Narayan, *Nat. Rev. Chem.*, 2020, **4**, 334–346.
154. M. R. Bennett, M. L. Thompson, S. A. Shepherd, M. S. Dunstan, A. J. Herbert, D. R. M. Smith, V. A. Cronin, B. R. K. Menon, C. Levy and J. Micklefield, *Angew. Chem., Int. Ed.*, 2018, **57**, 10600.
155. A. Gutmann, M. Schiller, M. Gruber-Khadjawi and B. Nidetzky, *Org. Biomol. Chem.*, 2017, **15**, 7917–7924.

CHAPTER 5

Activation of Chemical Substrates Under Sustainable Conditions: Electrochemistry and Electrocatalysis

LUCA MARIUS GROßMANN[a] AND TILL OPATZ*[a]

[a]Department of Chemistry, University of Mainz, Duesbergweg 10-14, D-55128 Mainz, Germany
*E-mail: opatz@uni-mainz.de

5.1 Introduction

Over the past few decades, increasing public awareness about environmental pollution and sustainability has led to a global discussion about climate change and the need for immediate solutions. Restrictions in greenhouse gas emissions as well as the limitations of fossil resources motivate researchers to implement alternative and more sustainable synthesis techniques into their workflow.[1] In response to these external stimuli, already well known technologies like photochemistry[2,3] and electrochemistry[4–9] have re-emerged, providing chemists with novel tools to substitute conventional, stoichiometric oxidizing or reducing agents by the use of electric current as a sustainable and inherently safe pseudo-reagent.[4] Since Kolbe's pioneering work on the use of electrical current as a reagent, more than 170 years have passed with preparative electrolysis nowadays enabling many of the largest

Sustainable Organic Synthesis: Tools and Strategies
Edited by Stefano Protti and Alessandro Palmieri

Published by the Royal Society of Chemistry, www.rsc.org

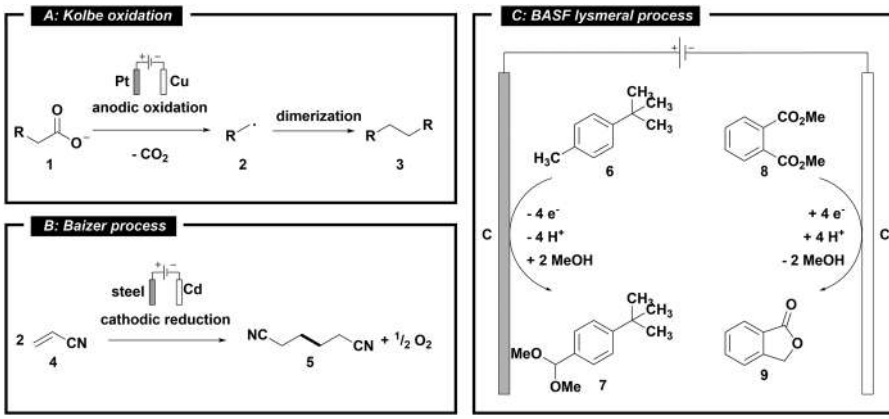

Scheme 5.1 Examples of currently used technical scale electro-syntheses: (a) Kolbe oxidation; (b) Baizer process operated by Monsanto; (c) paired electrolysis utilized by BASF in the production of lysmeral.

scale industrial processes (Scheme 5.1a).[10] Classic examples include the chloralkali process, in which chlorine gas and sodium hydroxide are produced by the electrolysis of aqueous sodium chloride, as well as the Hall-Héroult process providing elemental aluminium by electroreduction of Al_2O_3.[11] Accounting for over 90% of the electricity used in industrial-scale electrolysis, both processes are still operating to date, producing millions of metric tons of these chemicals.[4]

A prominent example of technical-scale electroorganic synthesis is the Baizer process operated by Monsanto. The cathodic hydrodimerization of acrylonitrile (**4**) to adiponitrile (**5**) (see Scheme 5.1b) gives access to the central precursor for the synthesis of polyamides, such as Nylon-6.6, which reached a total capacity of 180.000 tons per year in the late 1970s. The reaction was initially conducted using a cadmium cathode and a steel anode in an aqueous phosphate buffer using an undivided bipolar cell design with molecular oxygen being the only co-product. Interestingly, the reduction of acrylonitrile occurs at a very negative potential without the evolution of hydrogen taking place as a competitive process. This could be attributed to the use of cadmium as a cathode material, since it has a high overpotential for the hydrogen evolution reaction, which causes the hydrogen evolution to only take place at an even more negative potential. In addition, the quaternary ammonium salts used as electrolyte helped to further suppress the evolution of hydrogen by adsorbing to the cathode surface instead of the protons. Due to the environmental concerns coming from the use of cadmium as a cathode material, BASF switched to a less-hazardous copper-lead alloy when they took over the process. Owning to high energy requirements, most of the plants were shut down at the end of the 20th century.[11–13]

A major contributor to organic electrochemistry on a technical scale is BASF. Their currently largest process that utilizes electric current as a reagent is the anodic dimethoxylation of 4-*tert*-butyltoluene (**6**) to the

corresponding 4-*tert*-butylbenzaldehyde dimethyl acetal (**7**). By further condensation of the latter with propanal and subsequent hydrogenation, the fragrance lysmeral (lilial) introduced by the Givaudan company was readily accessible. This electrochemical technique provides substituted benzaldehydes on the scale of several tens of thousands of tons per year by BASF and others.[13] In order to maximize the energy efficiency, BASF combined this process with the cathodic reduction of dimethyl phthalate (**8**) to phthalide (**9**) to reach 100% atom efficiency and about 180% current efficiency, since the involved electrons[14,15] are utilized in both the anodic and cathodic process to form valuable products (see Scheme 5.1c).[14,15] This paired electrolysis is an example on how the sustainability of an electrochemical reaction can be further increased.

The following chapter will provide the reader with the basic concepts of synthetic organic electrochemistry.

5.2 Principles of Synthetic Organic Electrochemistry

5.2.1 General Setup

In order to carry out an electrochemical reaction, only a few crucial parts are required. A basic electrochemical setup consists of a reaction vessel, an external power supply connected to two electrodes (anode and cathode) and a liquid reaction medium. The latter is composed of a solvent, the substrate(s) and, in case the conductivity is insufficient, a supporting electrolyte.

In electrochemistry, the process of substrate activation occurs through single electron transfer (SET) from or to the electrode, resulting in reactive radical or ionic intermediates, which eventually form the desired product. In order to favour electron transfer, an external energy source is mandatory to raise the energy level of the electrons inside the cathode material, while simultaneously lowering the electrons of the anode material in their energy. This resembles the substrate activation in photochemistry by exciting a ground state electron to a higher energy level *via* irradiation.[16] If the applied potential difference exceeds the redox potential of the substrate, two separate electrochemical reactions will occur, one of which is the desired electron transfer between one of the electrodes and the substrate molecules, generating reactive intermediates. If the reaction of interest takes place at the anode, the substrate molecule releases electrons to the electrode and is therefore being oxidized, while at the cathode, the electron transfer occurs from the electrode to the substrate. Depending on which process is desired, the corresponding electrode is called the working electrode, while the other electrode is called the counter electrode.

Since both oxidation and reduction are coupled, one will not happen without the other. Electrons removed at the anode are returned to the solution *via* the cathode by reduction of solvent molecules, protons or other species, resulting in a net redox-neutral system. When conducting an electrochemical reaction, it is thus important to pay attention to the reaction at the counter

electrode as this could be the rate-limiting factor. For anodic processes, the most common counter reaction is solvent degradation or proton reduction leading to dihydrogen evolution.[17–19] The latter could be further enhanced by addition of acids or other proton sources in combination with electrode materials, which possess a low overpotential for the hydrogen evolution reaction (*vide infra*).

For cathodic reductions, solvent degradation, as well as the oxidation of a sacrificial metal anode (Mg, Al, *etc.*) or other sacrificial additives like amines are often utilized as a typical counter reaction.[6,18,20] The latter is analogous to the use of tertiary amines as sacrificial quenchers in photochemistry.[2]

5.2.2 Potential *vs.* Current

The two main parameters in electrochemistry are the electric current (I) and the potential, or voltage (U). The current describes the movement of electric charge carriers (electrons), which determines how many electrons are transferred into and extracted from the reaction medium. Therefore, the current, or more commonly used, the current density (current divided by the surface area of the electrode) relates to the reaction rate. The total quantity of electrons passed into the reaction solution is described by the charge (Q), which is the integrated current over time and corresponds to the stoichiometry of a traditional oxidant or reductant. The potential describes the energy by which the electrons are moved into the reaction medium. For an electron transfer to occur, the potential of the working electrode needs to be adjusted to match the redox potential of the desired process. If the potential is not high enough, the electron transfer is likely not to take place. On the other hand, if the applied potential exceeds the redox potential of the reaction drastically, a loss of selectivity might occur. Typical potentials at which synthetically useful electron transfer reactions occur range up to 2 V.

The relation between current and potential is given by Ohm's law (Eqn (5.1)), which states, that the potential is directly proportional to the current flowing through a conductor and its resistance (R). In an electrochemical reaction, the latter is comprised of different parameters, such as the electrode material, but most importantly the reaction solution.

$$U = R \cdot I \tag{5.1}$$

U: potential in volt [V], R: resistance in ohm [Ω], I: current in ampere [A]

Since these three parameters are related through Ohm's law, it is not possible to change one parameter without altering the others. Hence, two mayor modes of operation have been shown to be practical for conducting an electrochemical transformation. Reactions can be run either under galvanostatic conditions by applying a constant current or under potentiostatic conditions by maintaining a constant electrode potential. Both modes have their individual advantages and disadvantages, which will be discussed in the following sections.

5.2.2.1 Potentiostatic Conditions

Classical chemical reactions often do not proceed at a satisfactory rate under the initially chosen conditions due to a too high activation barrier, which is defined as the minimum energy necessary to permit two molecules to react with each other. Therefore, elevated reaction temperatures or the use of catalysts are required to overcome this activation barrier and to achieve acceptable reaction kinetics. Electrochemical reactions often run under milder conditions with respect to temperature and pressure as an additional parameter is available: the electrode potential. By alteration of the electrode potential, it is possible to vary the electron transfer rate by several orders of magnitude to a degree at which the reaction occurs at room temperature with sufficient velocity.

When an electrode is immersed in an electrolyte solution, a reversible electrochemical reaction will proceed spontaneously until a dynamic equilibrium is reached. The latter is achieved if cathodic reduction and anodic oxidation are proceeding at the same reaction rate without an externally detectable current flow. The internal current is called the exchange current density. This phenomenon leaves each electrode charged to a characteristic equilibrium potential E_{cat} and E_{an} for the cathode and anode, respectively. The difference between these two potentials is called the *open-circuit-potential* (*OCV* in volts), which corresponds to the energy required to perform this particular reaction.[21]

To compensate for the charge at the electrode surface and the charge imbalance across the reaction medium, a reorganization of solvated charged particles in close proximity to the electrode surface will occur, forming the electrochemical double layer (Figure 5.1).[22] The interaction between the

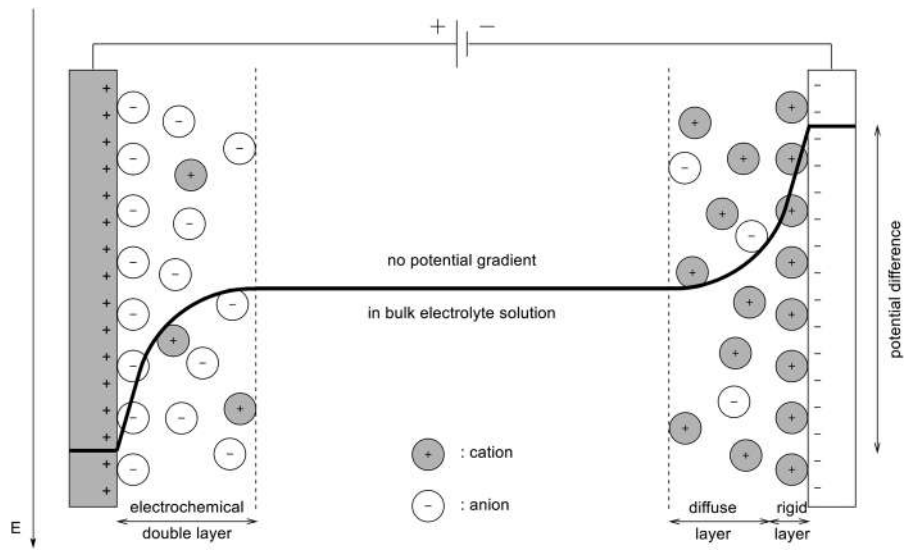

Figure 5.1 Schematic model of the electrochemical double layer and the potential distribution across the double layer. Adapted from ref. 22 with permission from John Wiley and Sons, Copyright 2014.

charged particles in solution and the electrode surface is strongest for the first layer of ions, which is why this layer is referred to as the *compact layer* or *Helmholtz layer*. Since the compact layer partly compensates the electrical field, the charge density of the following layers as well as the interaction between the ions and the electrode surface decreases, making the next layer less rigid than the first one. Hence, this layer is called the diffuse layer. Both the compact and the diffuse layer form an electrochemical double layer, which is described by the *Stern model*.[23]

Across the double layer, the electrode potential decays and a potential gradient is formed, which eventually fades into the bulk solution potential. Since the double layer has a thickness of only a few Ångstrøms, a potential difference of one volt or more between the electrode surface and bulk electrolyte results in an extremely steep potential gradient across the electrochemical double layer, generating an electrical field of considerable strength. The potential-gradient is the strongest in the compact layer and thus close to the electrode surface and almost absent in the bulk electrolyte. This is the reason why electrochemical processes exclusively occur at the electrode surface. Therefore, a potential increase at the electrode results in an increase of the potential gradient in proximity to the surface, eventually leading to an electron transfer reaction of the most oxidizable or reducible species at the anode or cathode, respectively.

Since all electrochemical transformations of interest happen at the surface of the working electrode, precise control of the respective electrode potential is crucial. However, it is not possible to determine or manipulate this potential without introducing a third electrode into the solution, which is called the *reference electrode*. This specific electrode utilizes a well-defined chemical process with a known redox potential, making it possible to precisely determine the potential of the working electrode. With this additional electrode, the function of the counter electrode is split between the reference and counter electrode, since the potential difference between the working and reference electrode is controlled, while the current passes through the counter electrode ensuring a constant value for the potential difference between the working and reference electrode. Hence, the three electrode setup allows for the exact control of the electrode potential and therefore enables the possibility to selectively oxidize or reduce a substrate at the anode or cathode, respectively.

Why this is of utmost importance can be shown by considering a simple redox reaction occurring at the anode surface (eqn (5.2)):

$$\text{Red} \rightleftharpoons \text{Ox} + e^- \tag{5.2}$$

where Red and Ox resemble the reduced and oxidized form of a given substrate. To illustrate what happens when the electrode potential is changed, it is necessary to focus on the energy levels of the electrons in the substrate and the electrode. While the electrons in the substrate occupy well-defined energy levels (the molecular orbitals) with the HOMO being the highest occupied molecular orbital, the electrons in the electrode material, however, are located in a continuum of energy states. The Fermi-level (E_F) in a conducting

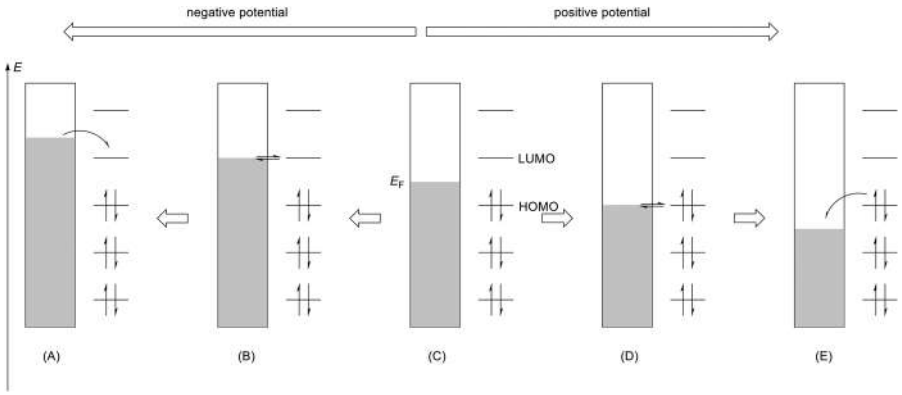

Figure 5.2 Change of Fermi-level depending on the applied potential along with the HOMO and LUMO energy of the substrate. (A) Fermi level exceeding the LUMO, enabling electron transfer from the electrode. (B) Fermi level matching the LUMO energy of the substrate. (C) Fermi level lying between the HOMO and LUMO without an external potential applied. (D) Fermi level matching the HOMO energy of the substrate. (E) Fermi level below the HOMO energy enabling electron transfer to the electrode.

material corresponds to the HOMO in a discrete molecule giving the highest occupied energy level. The Fermi-level is not at a fixed value but can be altered by applying a positive or negative potential to the conducting material.[22] As shown in Figure 5.2, the application of a positive potential results in a shift of the Fermi-level to lower energy, while a negative potential causes the opposite. Depending on the relative position of the Fermi-level to the HOMO or LUMO of a substrate, an electron transfer reaction may occur. The critical potential at which the reduction (Figure 5.2B) or the oxidation (Figure 5.2D) will take place indicates the standard potential of the corresponding redox couple.

Potentials for the desired redox reaction can be estimated or obtained from tables with standard potentials or by performing cyclic voltammetry (CV) experiments (*vide infra*). Tables with standard reduction potentials can be found in the literature.[24,25] Typical potential ranges for common functional groups or substance classes are shown in Figure 5.3. However, the applied potential often has to exceed the value of the standard potential for the reaction to take place, since electrochemical reactions are typically not performed under standard conditions (25 °C, 1 mol L^{-1}, 1 atm). A specific potential excess is typically needed to overcome kinetic hindrance, which is called the overpotential.

It is important to note that the potential of a redox reaction is dependent on the concentration of the oxidized and reduced form of the substrate. For a reversible redox reaction, this relationship is described by the Nernst equation.

$$\mathrm{Ox} + z\,e^- \rightleftharpoons \mathrm{Red} \tag{5.3}$$

$$E = E^\circ + \frac{RT}{zF} \ln \frac{c_{\mathrm{ox}}}{c_{\mathrm{Red}}} \tag{5.4}$$

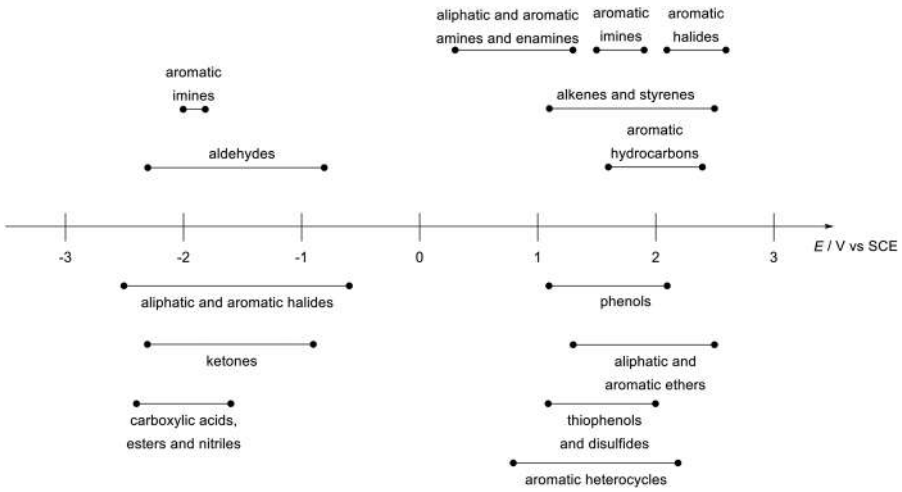

Figure 5.3 Redox potential ranges for common functional groups in organic chemistry.

R: gas constant, *T*: absolute temperature in Kelvin, *z*: number of transferred electrons, *F*: Faraday constant, c_{ox}: concentration of oxidized species, c_{red}: concentration of reduced species.

Since the quotient of c_{ox} and c_{red} changes as the reaction progresses, the potential necessary to keep the reaction going will change as well. Thus, if the reaction proceeds to 99% conversion and assuming that the reaction proceeds at room temperature, the total potential can be calculated as:

$$E = E^\circ + \frac{0.059\,\mathrm{V}}{z} \lg \frac{0.01}{0.99} = E^\circ - 0.12\,\mathrm{V} \tag{5.5}$$

When setting the electrode potential, an increase of 0.12 V being necessary to keep the reaction running at a desirable rate should therefore be considered.

As mentioned above, cyclic voltammetry is an analytical tool to determine the redox potentials for electrochemical transformation of given substrates. The typical setup for cyclic voltammetry comprises a working electrode, usually gold, platinum or glassy carbon, a counter electrode and a reference electrode, similar to a potentiostatic electrolysis setup. During a CV experiment, the current is measured, while the potential of the working electrode is scanned using a triangular waveform (see Figure 5.4a). If there is no increase in the current observed while the potential gradually increases to more positive potentials, then there is no reaction occurring on the working electrode. The presence of a species that is oxidizable or reducible at the applied potential will lead to an increase of the current, until the species is depleted at the electrode surface. This will cause the current to decrease again, resulting in

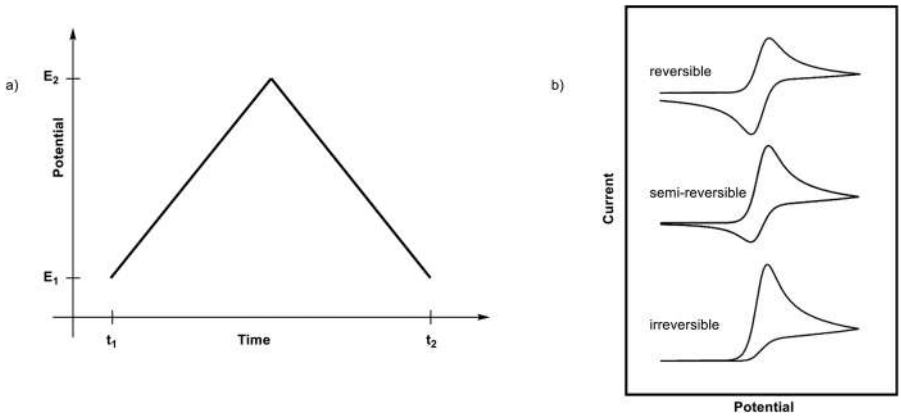

Figure 5.4 (a) Potential profile for cyclic voltammetry. (b) Cyclic voltammograms for reversible, semi-reversible and irreversible mechanisms.

an anodic peak potential E_{pa}. On the backward scan, the potential is reduced again, leading to a reversal of the formerly observed electron transfer, resulting in a cathodic peak potential E_{pc}. Depending on the potential window scanned, it may also occur that the solvent is oxidized or reduced. This can be recognized by a strong increase in current.

For reversible electrochemical processes, the average value of the anodic and cathodic peak potentials corresponds to the reduction potential $E°$ of the observed electron transfer process. At this potential, the concentrations of oxidized and reduced species at the electrode surface are equal, which, following Nernst's equation, gives $E°$. For a chemically and electrochemically reversible process, the difference between the anodic and cathodic peak potentials (ΔE_p) is 57 mV at 25 °C.[22] If ΔE_p exceeds this value, the process is called semi-reversible, corresponding to a slow electron transfer rate. On the other hand, when the electron transfer step is followed by an irreversible chemical reaction that is fast compared to the electron transfer, the size of the back scan peak will decrease or it will even vanish completely (see Figure 5.4b). The process is then denoted as irreversible and only the position of the peak potential is reported in this case. However, it should be mentioned that the scan rate might have a significant influence on the result of the cyclic voltammetry experiment, as a higher scan rate may restore a reversible electron transfer step, owing to the fact that the subsequent chemical step is just too slow compared to the electron transfer.[26,27]

Therefore, cyclic voltammetry is a powerful analytical tool to not only determine thermodynamic parameters such as the redox potential or electron transfer rate, but also to elucidate the mechanism of an electrochemical reaction. For a more comprehensive guide to cyclic voltammetry, we refer to the work of Dempsey and co-workers, who focus particularly on synthetic organic chemistry.[26]

For the above-mentioned reasons, operating an electrolysis under potentiostatic conditions ensures the best selectivity and should be employed if the desired transformation requires precise control of the redox potential. Reasons for this could be numerous undesired side reactions, like overoxidation, or a lack of selectivity. Additionally, if the substrate possesses more than one redox active group, knowledge of the redox potentials and the possibility to address the transformation of a specific group by controlling the electrode potential give access to a selectivity that could hardly be achieved by classic molecular redox chemistry. However, the use of potentiostatic reaction conditions is accompanied by some drawbacks, including the more sophisticated setup required. Additional disadvantages arise during execution of a potentiostatic electrolysis. In the beginning, the concentration of the starting material is sufficiently high to ensure a constant mass transport to the electrode surface and therefore a constant current. As the reaction progresses, the substrate concentration decreases and mass transport becomes the limiting factor and thus the current flow will decrease as well and it might eventually stop. Therefore, incomplete conversion can be an issue with potentiostatic electrolyses. Calculation of the electron equivalents passed through the medium is also difficult since the current is not constant over the reaction time, which renders the use of an ammeter to record the current over time essential.

5.2.2.2 Galvanostatic Conditions

Operation of an electrolysis cell in galvanostatic mode is straightforward and uses a simple and inexpensive reaction setup, since only the working and the counter electrode are required. Due to the constant current maintained over the entire electrolysis time, the exact stoichiometry of electrons transferred into the reaction medium can be calculated using Faraday's law. This term is often used to describe the combination of the first and second laws of electrolysis, which describe the direct proportionality of electrolyzed mass m to the charge Q and molar mass M, respectively. By the combination of these two laws, it is possible to calculate the charge needed to oxidize or reduce a certain amount of substrate with a given valency z (see eqn (5.6)).[28–30] The charge passed through an electrochemical reaction could also be calculated as the current (I) over time (t) (eqn (5.7)).

$$m = \frac{Q \cdot M}{F \cdot z} \Leftrightarrow Q = z \cdot n \cdot F \tag{5.6}$$

$$Q = I \cdot t \tag{5.7}$$

$$t = \frac{z \cdot n \cdot F}{I} \tag{5.8}$$

n: number of moles [mol], Q: charge in Coulomb [C = A s], z: number of electrons per substrate, F: Faraday constant [96 485 C mol^{-1}], t: time [s].

By combination of eqn (5.6) and (5.7), it is possible to calculate the time necessary for the charge to pass through the reaction at a given constant current (eqn (5.8)). In synthetic organic electrochemistry, the valency z can be referred to as the electron equivalents since it gives the number of electrons required per substrate molecule to achieve the desired bond formation or bond breaking reaction. The electron equivalent is denoted as 1 F or 1 F mol^{-1}, which corresponds to one electron per substrate molecule. Similar to traditional redox reagents, it can be beneficial to exceed the electron equivalent above the stoichiometric value by a certain factor to account for a less efficient electron transfer. For example, the application of 2.2 F in a two electron oxidation process means using a 10% excess of additional electrons.

A useful metric to evaluate and compare electrochemical reactions is the Faradaic efficiency η or current efficiency. This describes the fraction of the electrons transferred into the reaction medium, that end up forming the product. The Faradaic efficiency is calculated by dividing the theoretical charge Q_{theo} by the experimental charge Q_{exp}. The theoretical charge describes the quantity of electrons necessary to obtain the amount of observed product, while the experimental charge describes how many electrons were transferred into the reaction medium. Since the current efficiency includes the yield and the electron equivalents, it is a useful metric to compare reactions or reaction conditions with different electron equivalents.[17]

$$\eta = \frac{Q_{theo}}{Q_{exp}} = \frac{z_P \cdot n_P \cdot F}{z_{exp} \cdot n \cdot F} \tag{5.9}$$

η: Faradaic efficiency [%], Q_{theo}: theoretical charge [C], Q_{exp}: experimental charge [C], z_P: number of electrons per product, z_{exp}: experimental number of electrons per substrate, n_P: number of moles of product.

Under galvanostatic conditions, the electrode potential adapts automatically and is not externally controlled. Since it is coupled to the current and the resistance by Ohm's law, the cell voltage depends on the overall resistance of the system. Due to a change in chemical composition, the resistance will change over the course of the electrolysis and hence the potential will vary to maintain a constant current. A high cell voltage is usually related to a high resistance between the two electrodes, which can be reduced by adding more supporting electrolyte, by decreasing the distance between the anode and cathode or by increasing the electrode surface.

It is most common in synthetic organic electrochemistry to use the term current density as a synonym for current since it gives the current relative to the surface area of the electrode, allowing for better comparison between different experimental setups. It also facilitates the direct scale-up of a process from a small screening cell to a preparative and further to an industrial-scale setup, since the current can simply be adjusted to fit the employed electrode surface area. Lowering the current density corresponds to milder reaction conditions, as electrons are transferred into the reaction medium at a lower rate. A higher current density also

Table 5.1 Advantages and disadvantages of potentiostatic and galvanostatic reaction conditions.

	Potentiostatic electrolysis		Galvanostatic electrolysis
+	High selectivity due to potential control	−	Selectivity might be lower due to over-oxidation or side reactions
−	More sophisticated setup since a reference electrode is required	+	Simple setup
−	Full conversion might not be achieved	+	Full conversion can be achieved more easily
−	No direct possibility to determine amount of charge passed through medium	+	Amount of charge can be controlled directly

results in a higher potential, possibly favouring undesired side reactions and lowering the overall selectivity. Additionally, higher current densities might lead to ohmic heating and therefore to a non-negligible increase in reaction temperature, rendering external cooling inevitable. Despite the possible disadvantages that result from a higher current density, a trade-off between milder conditions/selectivity and reaction time can often be found (Table 5.1).

5.2.3 Reaction Setup

5.2.3.1 Power Supply

The power supply is probably the most crucial part of an electrolysis setup as it provides the necessary electricity to the system and moves electrons from the anode to the cathode. In the simplest case, a battery with suitable voltage to overcome the cell resistance can supply the electricity to drive the electrochemical transformation.[31] However, the current and voltage output of the battery cannot be controlled without additional equipment.

A more elaborate setup usually consists of a simple bench-top power supply or a modern potentiostat, so that either the current or potential can be adjusted to fit the desired reaction conditions. Generally, potentiostats can provide both a constant current and a constant potential, since they allow for the use of a reference electrode to precisely control the electrode potential. For electrochemical reactions at a constant current, the use of a simple and affordable bench-top power supply is usually sufficient. The functionality of the power supply can be further extended by multichannel power output or by software control.

To facilitate the start into organic electrochemistry, there are pre-configured setups provided by *IKA* like the *ElectraSyn 2.0* system co-developed by the Baran lab or the screening setup from the Waldvogel group that both include a potentiostat as the power supply.

5.2.3.2 Reaction Vessels

Choosing the right reaction vessel, often referred to as an electrochemical cell, suitable for the desired reaction is not as difficult as it may seem at first glance. In the simplest case, the reaction is conducted in an undivided cell, meaning that both electrodes are fitted in the same compartment and immersed into the same reaction mixture. This setup is suitable for reactions where the resulting product is stable against back-reaction or decomposition at the counter electrode and stable against the product of the counter reaction. Different kinds of vessels like simple beakers or round bottom flasks have been employed successfully.[32,33] However, this results in changes of the electrode arrangement each time a new setup is being constructed, which may have an influence on the reaction outcome. To overcome this, setups with fixed electrode positions as well as systems for screening have been constructed to ensure a higher reproducibility.[31,34–36] Despite the variety of standardized reaction setups reported in the literature, there is a lack of commercially available reaction cells, since most of them are produced by in-house workshops.

For transformations in which the reaction at the counter electrode interferes with the desired reaction at the working electrode, or in cases where the reaction product is prone to further reactions at the counter electrode, the use of a divided cell is recommended. In this case, the electrochemical cell is divided into the anodic and cathodic compartment separated by a diaphragm (sintered glass frit or ion-exchange membrane) to prevent the anodic and cathodic solutions from mixing. The use of a diaphragm results in an increase in cell resistance and consequently the cell voltage will increase under galvanostatic conditions or the current will decrease under potentiostatic conditions. To minimize this effect, the electrodes should be placed as close as possible from each other.

In addition to batch electrolysis, electrochemical reactions could also be performed in continuous flow, for which different types of flow cells have been developed, allowing for an easily scalable and mild process.[37,38] The cell usually consists of two electrodes separated by a thin spacer, which has the flow channels cut into it. This leads to a high electrode surface area compared to the volume of the reaction solution, which has several advantages over the batch process, one of which is the enhanced energy transfer from the electrode to the solution, as well as mass transfer to the electrode. The small electrode gap also minimizes the cell resistance and hence allows for the use of less or no supporting electrolyte at all, which reduces waste and facilitates the further purification process.

5.2.3.3 Electrodes

When optimizing an electrochemical reaction, the choice of electrode material is one of the most critical factors for the success of the reaction, since it is not only the surface at which the electron transfer occurs, but also may

interact differently with the substrate. Whilst electrodes can generally be made from any conductive material, there are numerous general and specific material properties to be considered. Ideally, an electrode should consist of a readily available and inexpensive material that is non-toxic and stable towards a variety of solvents, supporting electrolytes, temperatures and pressures. Also, the material should be able to come in different forms and sizes, likes plates, rods, wires, foams or meshes.

The electrode should be chemically and mechanically inert under the chosen reaction conditions, as it would otherwise change during the electrolytic process and hence disturb the desired process, potentially rendering it irreproducible. In addition, the electrode should also be electrochemically stable. If the electrode can be oxidized or reduced, this will lead to electrode degradation and, if it is the working electrode, to low current efficiency due to the competing reaction. However, this phenomenon can also be useful, when employed as a counter electrode. Therefore, the degradation of a sacrificial anode acts as a suitable counter reaction to cathodic reductions, facilitating electron transfer. In these cases, non-precious metals such as Mg, Al, Zn or Cu are employed as the anode material. Suitable anode materials for oxidation reactions are platinum and carbon-based materials, such as graphite, glassy carbon (GC), reticulated vitreous carbon (RVC) or Boron Doped Diamond (BDD). While platinum electrodes generally tend to form radical intermediates exclusively, carbon electrodes usually facilitate a subsequent oxidation to generate cationic intermediates. This is attributed to the presence of paramagnetic centers in carbon-based materials, which causes anodically generated radicals to adhere to the anode surface and undergo a second oxidation.[22,39]

Boron-doped diamond electrodes were recently the subject of increased interest due to their outstanding electrochemical performance, which includes a large potential window in protic solvents (up to 5 V in hexafluoroisopropanol, HFIP), high overpotentials for the evolution of hydrogen (HER) and oxygen (OER) in aqueous media (−1.1 V for HER, 2.3 V for OER) and the direct conversion of alcohols to the corresponding alkoxy radicals.[40–45]

In contrast to their use as an anode, most materials are sufficiently stable for use as a cathode. The selection of the right cathode material largely depends on a material specific property, the overpotential for the hydrogen evolution reaction. As discussed in Section 5.2.2.1, the overpotential for a reaction is the potential difference between the theoretical redox potential needed and the electrode potential applied to overcome the activation barrier. Therefore, choosing a cathode material with a high overpotential for the HER is crucial in order to prevent the liberation of molecular hydrogen as a competing electrode process that would otherwise decrease the overall current efficiency or even produce hydrogenated side products. However, when it comes to choosing the right cathode material as a counter electrode, a cathode material with low HER overpotential is a good choice for acidic conditions or in protic solvents as it promotes the counter reaction.

Table 5.2 Overpotentials for the hydrogen and oxygen evolution reaction of selected electrode materials.

Electrode material	H_2 Evolution η_{HER}[a]/V	O_2 Evolution η_{OER}[e]/V
Al	−0.58 [47]	
Cd	−0.99 [47]	0.80 [48]
Cu	−0.60 [47]	0.58 [48]
Hg	−1.04 [47]	
Pb	−0.67 [47]	0.80 [48]
Pt	−0.09 [47]	1.11 [48]
Stainless steel mesh	−0.42[b] [49]	0.28 [49]
Graphite	−0.47 [47]	0.50 [48]
GC	−1.18[c] [50]	
BDD	−1.10[d] [51]	2.30 [51]

[a]HER overpotential recorded with 1 M HCl in H_2O, 1 mA cm^{-2}, 25 °C if not otherwise stated.
[b]1 M KOH in H_2O, 10 mA cm^{-2}, 25 °C.
[c]Aqueous phosphate buffer at pH 3.4, 0.1 M NaCl, 25 °C.
[d]0.2 M H_2SO_4 in H_2O.
[e]OER overpotential recorded at 1 M KOH in H_2O, 1 mA cm^{-2}, 25 °C.

In Table 5.2, properties of some typically used electrode materials are listed. For a more comprehensive review on different electrode materials and their influence on reactions, we refer to the review article of Lennox and co-workers.[46]

If potentiostatic conditions are applied, a reference electrode is necessary in addition to the working and the counter electrode to accurately determine the applied potential at the working electrode. The reference electrode uses a well-defined redox process with a stable potential, which is utilized to precisely measure the working electrode's potential, without participating in the reaction. Commonly used reference electrodes in synthetic electrochemistry are the saturated calomel electrode (SCE) or the Ag/AgCl electrode, since their reference potential remains constant, as long as the concentrations of Hg^{2+} or Ag^{+} cations do not change. There are several other reference electrode types being employed and their potentials can be interconverted using literature known values; however, care should be taken since the potentials can be affected by the solvent or the supporting electrolyte.[52] Therefore it is recommended to use the same reference electrode, against which the redox potential of the substrate has been reported.

5.2.3.4 Solvents

As in classical chemistry, the selected solvent may have a significant influence on the outcome of the electrochemical reaction. Traditional factors, such as substrate solubility, as well as stabilization of intermediates, also apply for electrochemical reactions and are expanded by conductivity, promotion of the counter reaction and the potential window (see below). Electrochemical reactions are usually conducted in polar organic solvents in

which the supporting electrolyte can dissociate into solvent separated ions to ensure sufficient conductivity. Acetonitrile is one of the most frequently used solvents in electrochemistry due to its high stability against oxidation and reduction, it has a large potential window to work with and thus can be used for both anodic oxidation, as well as cathodic reduction. Other commonly used solvents in electrochemistry are the polar aprotic solvents THF, DCM, DMF, DMA and DMSO, as well as the protic solvents MeOH, EtOH, trifluoroethanol (TFE) and hexafluoroisopropanol (HFIP). The latter is also known for its outstanding performance in electrochemistry due to its large potential window in combination with the ability to stabilize generated radicals, increasing their half-lives by a factor of up to 100 compared to the same radical generated in trifluoroacetic acid.[53–56]

The potential window of a solvent is determined by the potentials at which it is decomposed by either anodic oxidation or cathodic reduction. It is largely dependent on the electrode material, supporting electrolyte species and concentration.[17] When selecting the solvent, these limits have to be considered as otherwise solvent degradation will become the main reaction. However, when performing an oxidation reaction, only the oxidation potential of the solvent is relevant. The reductive degradation of the solvent might even be useful as a suitable counter reaction. Depending on the desired reaction, the use of a dry and degassed solvent has to be considered if water or the evolution of oxygen might interfere with the desired reaction.

5.2.3.5 Supporting Electrolytes

In order to decrease the overall resistance and hence to ensure sufficient conductivity of an electrolytic system, the addition of a supporting electrolyte is essential. This electrolyte could either be a salt, an acid or a base. By how much the resistance is lowered by the added electrolyte depends mainly on its concentration, but also on its nature and ability to dissociate into separated ions. The latter requires a good solubility in the employed solvent. In addition, similar to the reaction solvent, the electrolyte has to be stable against oxidation or reduction under the applied electrochemical conditions and provide a large potential window, and it should also not interfere with the electrode reaction.

For organic solvents, tetraalkylammonium salts are most frequently employed as the supporting electrolyte due to their good solubility. Most commonly, the tetraethylammonium ion (TEA^+, Et_4N^+) or tetrabutylammonium ion (TBA^+, Bu_4N^+) will be found as the cationic part of the electrolyte, while perchlorate (ClO_4^-), tosylate (TsO^-), tetrafluoroborate (BF_4^-) and hexafluorophosphate (PF_6^-) represent the frequently used counter anions. It is worth mentioning that the use of perchlorates is strongly discouraged since organic perchlorates could precipitate, which are often highly explosive. Apart from organic salts, inorganic salts like alkali metal salts have also been employed, particularly in aqueous solutions. The use of halides (X^-) can be problematic since oxidation to halonium ions (X^+) is also possible

and might interfere with the desired reaction. However, this oxidation has been exploited as a simple counter reaction or in electrochemical halogenation reactions.[57–59] In batch operation, typically stoichiometric amounts of supporting electrolytes are required rendering further purification more challenging. When switching from batch to continuous flow operation, the required amount of electrolyte can be reduced to a minimum, if needed at all.

5.2.3.6 Modes of Electron Transfer

Electro-organic conversions are usually achieved by direct electron transfer between an organic substrate and the electrode surface to generate a reactive intermediate, which will undergo a subsequent chemical transformation or engage in a second electron transfer (see Figure 5.5a). While this represents the most atom-efficient approach to electrochemical reactions, non-productive processes like overoxidation/-reduction or electrode passivation might arise and hinder the reaction. In these cases, indirect electrolysis can be a useful method, as it shifts the electron transfer from a heterogeneous to a homogeneous process by using a redox mediator. Ideally, this mediator undergoes a reversible redox reaction at the electrode and promotes a subsequent homogeneous electron transfer between the mediator and the substrate molecule (see Figure 5.5b). The use of a redox mediator allows for a more selective transformation and often eliminates the kinetic hindrance associated with direct electron transfer between electrode and substrate.[60,61]

Common mediators are *N*-oxyl radicals like (2,2,6,6-Tetramethylpiperidin-1-yl)oxyl (TEMPO) or ferrocene, but also transition metal salts have been employed.[62] A third interesting but under-represented approach is the use of sub-stoichiometric amounts of charge to catalyse an overall redox-neutral reaction (electrocatalysis). This process involves an initial electrochemical generation of a radical or radical ionic species, which after subsequent chemical steps engages in either a backward electron transfer or initiates a chain mechanism to generate the desired product (see Figure 5.5c).[63–66] As this chapter focuses on direct electrolytic processes, we would like to refer the reader to comprehensive reviews about indirect electrolyses[60–62] and electrocatalysed processes.[67]

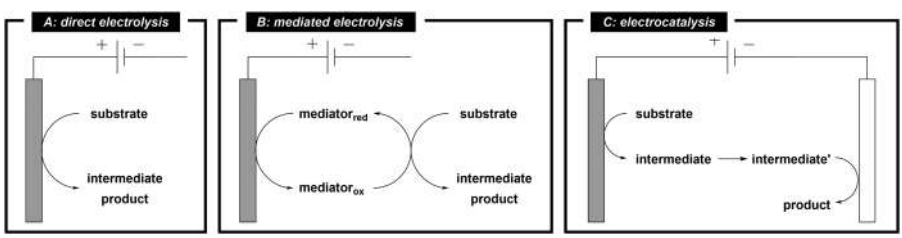

Figure 5.5 Modes of electron transfer in organic electrochemistry: (a) direct electron transfer, (b) mediated electron transfer and (c) electrocatalysis.

5.3 Application of Electrochemical Procedures for Sustainable Activation of Substrates

In the following section, the reader is provided with some prominent case studies, which have successfully integrated electrochemical transformations to access a sustainable substrate activation by either anodic oxidation or cathodic reduction.

5.3.1 Shono Oxidation

Essential structural motifs in natural products are nitrogen heterocycles. Functionalisation in the α-position to the nitrogen is an important way to construct natural products from simple cyclic or acyclic amines. In 1975, Shono and co-workers developed an electrochemical method for the oxidation of alkoxycarbonyl-protected amines **10** to furnish *N*-alkoxycarbonyl iminium ions **11**.[68–70] The initial oxidation step occurs at the nitrogen atom to form a nitrogen-centered radical cation, which undergoes subsequent deprotonation and further oxidation to the iminium ion intermediate **11**. The latter is typically trapped by an alcoholic solvent molecule like methanol to furnish stable α-methoxylated products **12**, which are well established stable precursors to *N*-acyl iminium ions (see Scheme 5.2).[71–79] Substrates that contain alcohol moieties can undergo intramolecular trapping of the intermediate iminium ion to produce oxazoline derivatives, such as **12c** (see Scheme 5.2b). This method represents a clean and operationally simple way to produce stable iminium precursors, which upon treatment with Brønsted- or Lewis acids liberate the acyl iminium for further trapping by a nucleophile, which would otherwise decompose under the electrochemical conditions. A variety of nucleophiles like cyanide,[80–82] furans,[83] isocyanides,[84] allyl silanes,[85–87] silyl enol ethers[88] and trialkyl phosphites[89] have been employed to produce α-functionalised amides or carbamates.

The Shono oxidation represents one of the first examples to demonstrate how electrochemistry, more specifically anodic oxidations, can be employed as a sustainable tool for substrate activation, rather than using stoichiometric amounts of toxic and costly inorganic oxidants. Since only methanol and a small amount of supporting electrolyte are required, the atom economy of the Shono oxidation is extremely high. However, Bornemann and

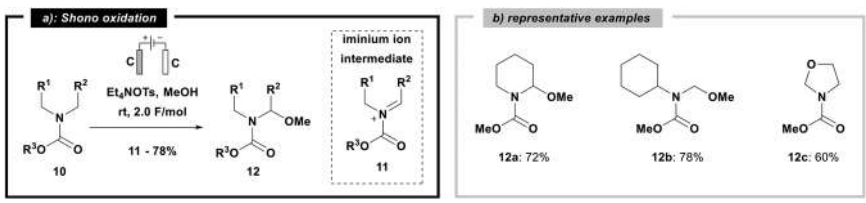

Scheme 5.2 (a) General procedure for the formation of α-methoxylated or alkoxycarbonyl-protected amines *via* Shono oxidation. (b) Selected representative examples.

Handy demonstrated, that the atom economy of this reaction can be further increased by the use of room temperature ionic liquids (RTIL) like tributyldecylammonium tosylate ($Bu_3DecNOTs$), tributyldecylammonium triflimide ($Bu_3DecNNTf_2$) or 1-methyl-3-ethylimidazolium triflimide ($EMIMNTf_2$), which are a promising substance class since they can serve as both a supporting electrolyte and solvent for electrochemical reactions.[90,91] Thus, by employing RTILs, the authors were able to reduce the required amount of methanol to 25 vol-% giving the desired products in 81–95% yield. To further improve the sustainability of this reaction, the ionic liquids could be easily reused after evaporation of methanol, extraction of the product with diethyl ether and drying *in vacuo* overnight, without a noticeable decrease in yield or degradation of the ionic liquids. This renders the Shono oxidation even more eco-friendly, addressing the fifth principle of green chemistry to avoid auxiliary substances where possible.[92]

Despite being a sustainable method for the generation of acyl iminium ion precursors, the subsequent reaction with various nucleophiles still requires the use of equimolar amounts of Lewis- or Brønsted acids to regenerate the iminium ion. Hence, a direct method for reacting carbon nucleophiles with oxidatively generated iminium ions is desirable. Pioneering work of Yoshida and co-workers lead to the development of the "cation pool" method, which involves the generation and accumulation of cations by anodic oxidation at −78 °C. The low temperatures prevent the decomposition of the generated cations and allow for a subsequent addition of the nucleophile under non-oxidative conditions. Yoshida and co-workers applied this methodology to various carbon-based nucleophiles, like allyl silanes, enol silyl ethers and enol acetates, as well as aromatic and 1,3-dicarbonyl compounds (see Scheme 5.3).[93] Later, they extended the library of suitable nucleophiles to organometallic compounds like alkyl stannanes, Grignard reagents and organoaluminium[94–96] (see Scheme 5.3). With the development of the "cation pool" method, trapping and releasing of the generated acyliminium cation is

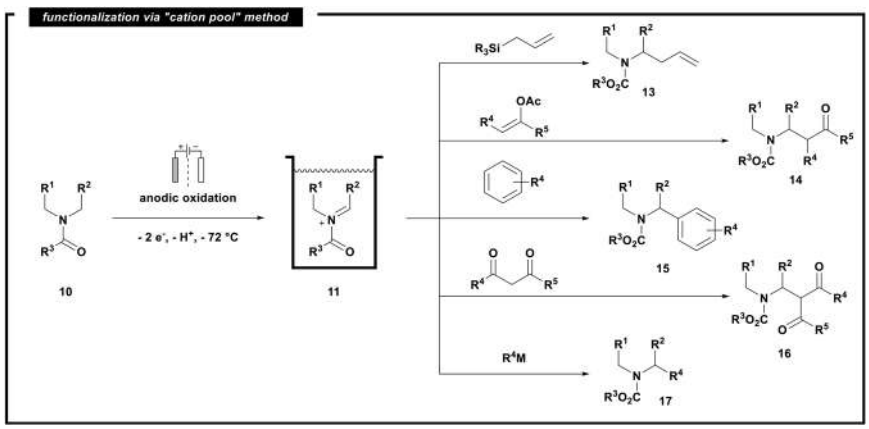

Scheme 5.3 α-Functionalisation of carbamates with different nucleophiles *via* the "cation pool" method.

not necessary anymore. This gives access to an even better atom economy for the entire reaction sequence at the cost of a slightly higher energy consumption due to the low temperatures required for stabilizing the intermediate cation. The versatility of the "cation pool" concept, meaning generation and accumulation of cations by anodic oxidation, is illustrated by its extension to a variety of different carbo cations as well as heteroatom-centered cations like pyridinium, phosphonium and sulfonium ions.[97]

5.3.2 Dehydrogenative Aryl–Aryl Coupling

The significance of the biaryl motif as an import structural element is demonstrated by its presence in various pharmaceuticals,[98] agrochemicals[99] and ligand systems.[100–106] The main synthetic route to this biaryl structure relies on well-established transition metal-catalysed cross-coupling reaction as a rapid and selective method to construct the C–C bond. However, these systems suffer from the use of expensive noble metal catalysts as well as from the requirement of pre-functionalisation of the building blocks adding additional synthetic steps prior to the desired coupling reaction.

This leads to the generation of stoichiometric amounts of chemical waste. Therefore, the direct coupling of two C–H fragments appears as a highly appealing concept in synthetic chemistry. The group of Waldvogel published pioneering work in the field of direct anodic oxidation of phenols and demonstrated that the oxidation of 2,4-dimethylphenol furnished the desired 2,2′-biphenol, albeit in low yield and with several by-products of different coupling motifs (Scheme 5.4a).[107] By employing boron-doped diamond

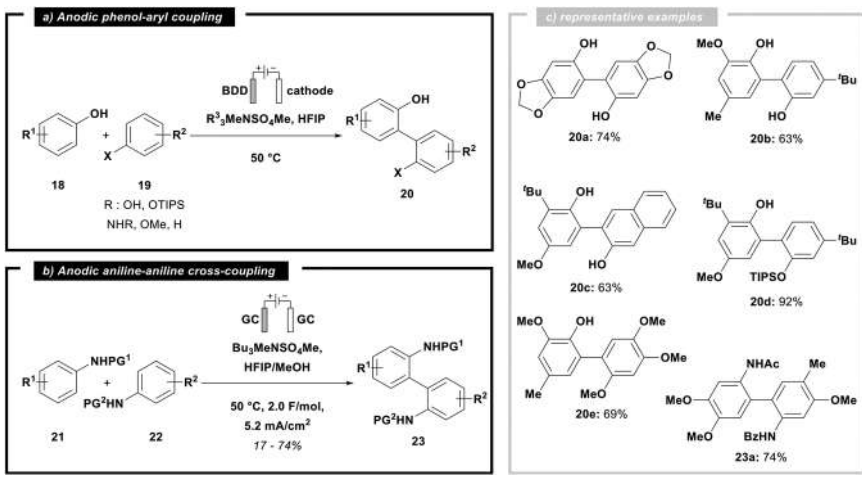

Scheme 5.4 (a) General procedure for anodic (cross)-coupling reaction of various aromatic compounds with phenols. (b) General procedure for anodic cross-coupling of protected aniline derivatives. (c) Selected, representative examples for the various biaryl moieties accessed by oxidative cross-coupling.

electrodes, the authors were able to circumvent the lack of selectivity to produce the *ortho–ortho* coupled biphenol almost exclusively. They attributed this observation to the outstanding performance of BDD electrodes with respect to anodic alkoxyl radical generation. Furthermore, switching to fluorinated alcohols/mediators such as hexafluoroisopropanol (HFIP) resulted in a significantly increased yield as well as an enlarged scope for the anodic aryl–aryl coupling of different phenols[108] and even guaiacol derivatives.[109] These results led to the development of successful protocols for the anodic cross-coupling of phenols with different protected and unprotected phenols,[110,111] naphthols[112] and electron rich arenes[113,114] as well as cross-coupling reactions between aniline derivatives[115–117] (see Scheme 5.4b). Further development even gave access to symmetric as well as non-symmetric *meta*-terphenyl-2,2″-diols **26**[118,119] (see Scheme 5.5), 2,5-bis(2-hydroxyphenyl)thiophenes[120] and phenol-benzofuran cross-coupling products[121] by a similar anodic oxidation protocol (Scheme 5.4c).

With their extensive research, the Waldvogel lab has developed a general, robust and scalable protocol to give direct access to a large library of symmetrical and non-symmetrical biarylic compounds from simple substrates without prefunctionalization. With the direct anodic aryl–aryl coupling of the various aryl moieties needing nothing more than HFIP (+18 vol% MeOH), a supporting electrolyte and carbon-based electrodes, Waldvogel and coworkers also addressed the eighth principle of green chemistry by reducing derivatization.[92]

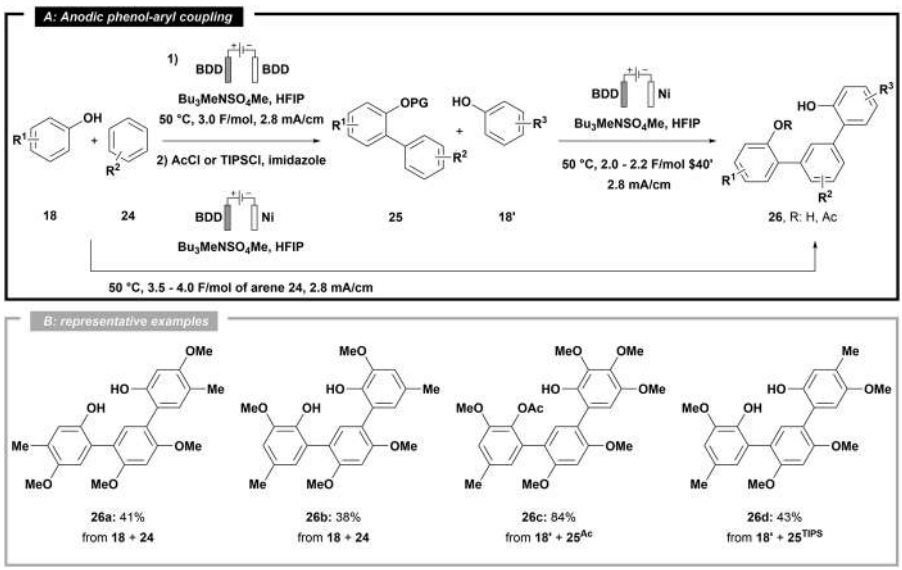

Scheme 5.5 (a) General procedure for the preparation of symmetric and non-symmetric *meta*-terphenyl-2,2″-diols by a one-step (symmetrical) or a two-step (unsymmetrical) process. (b) Selected, representative examples.

Although fluorinated solvents resemble a major drawback regarding the "greenness" of a chemical reaction, the authors demonstrated that, due to its relatively low boiling point, hexafluoroisopropanol can almost be quantitatively redistilled in order to reuse it and minimize the liberation of fluorinated solvents into the environment.[44]

5.3.3 Electroreductive Difunctionalisation of Alkenes

The functionalisation of alkenes is among the most widely investigated transformations in organic chemistry, since it enables simple and direct access to structural diversity and complexity from readily available feedstocks.[122–124] In this context, electrochemistry has proven to be a versatile and sustainable tool for the functionalisation of olefins.[4,97,125] The group of Lin has achieved ground-breaking developments in the field of electrochemical difunctionalisation of simple alkenes to introduce various functionalities, like (di-)azido,[126–128] (di-)chloro,[127,129,130] trifluoromethyl[127,131] and phosphinoyl[130] groups. All these methodologies rely on the activation of a nucleophile to generate the corresponding radical intermediate by either direct oxidation or transition metal-catalysed oxidation. In contrast to this approach, electroreductive protocols remain scarce. Current electrochemical methods predominantly focus on the formation of carbon-heteroatom bonds. Protocols to access C–C bond formation reactions are rare and rely mainly on the oxidative activation of prefunctionalised substrates like CF_3SO_2Na, CF_3CO_2H or 1,3-dicarbonyl compounds.

The lack of reductive methods for carbon radical generation prompted the Lin lab to develop an electroreductive carbofunctionalisation of alkenes with readily available alkyl halides *via* a radical-polar crossover mechanism. They envisioned the reaction to proceed through initial radical generation by cathodic reduction of an alkyl bromide (**28**), which upon addition to the alkene substrate (**27**) affords a new C-centered radical (**int-2**). The latter then undergoes subsequent cathodic reduction to form an intermediate carbanion (**int-3**), which can be trapped with another nucleophile.

Through initial experiments, the authors found that the carboformylation of 4-*tert*-butylstyrene (**27a**) with isopropyl bromide (^{i}PrBr, **28a**) was feasible in LiOTf-containing DMF with Mg as a sacrificial anode and graphite as a cathode material. DMF served as both the solvent and formylating agent. Alongside the desired product (**29a**, 72%), small amounts of hydroalkylated (**30a**, 7%) and dialkylated product (6%) could be observed. By further optimization studies, Lin and co-workers identified that doubling the concentration by halving the solvent volume and amount of supporting electrolyte had the most significant impact on the reaction, as the yield could be increased to 89% (86% isolated yield). Switching to a more reactive alkyl iodide did not improve the yield of the carboformylated product, but instead lead to an increased amount of dialkylated product. With this operationally simple method, Lin and co-workers were able to convert a large library of substituted styrenes, heteroaromatic styrene derivatives and various different

cyclic and acyclic secondary and tertiary alkyl bromides to the corresponding carboformylated products in moderate to high yields (see Scheme 5.6). However, strong electron-withdrawing substituents (*e.g.* *p*-CN or *p*-CF_3) as well as 1,2-disubstituted styrenes and primary alkyl bromides showed poor reactivity under these conditions.

The authors attributed the outstanding chemoselectivity to different reasons (see Scheme 5.6c). The initial reduction of the alkyl bromide **28** to the alkyl radical **int-1** occurs preferentially, since its standard reduction potential (around 2.0 V *vs.* SCE) is less negative than that of the subsequent reduction to the anion (**int-4**, about 2.3 V) or the reduction of **27** to the corresponding anion **int-5** (about 2.6 V). Upon radical addition to the styrene, a benzylic radical intermediate **int-2** is formed, which is further reduced to the corresponding anion **int-3** (at 1.6 V), rather than adding to another styrene molecule (**int-6**), due to polarity mismatching. Final trapping of the anion by another alkyl bromide is sterically hindered, giving the formylated product **29** almost exclusively.

The Lin group extended the scope of this methodology to hydroalkylated products (**30**) by simply changing the solvent to acetonitrile and additional diethylamine under otherwise identical conditions. This gave access to an *anti*-Markovnikov-type $C(sp^3)$–$C(sp^3)$ coupling of alkyl bromide to different

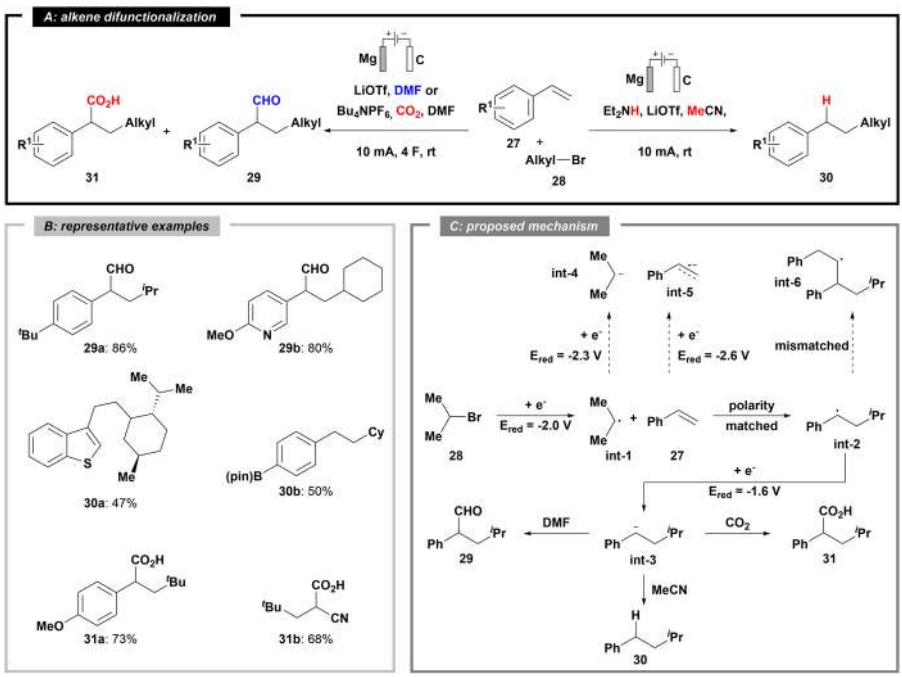

Scheme 5.6 (a) Alkene difunctionalisation by cathodic generation of alkyl radicals. (b) Selected, representative examples. (c) Proposed mechanism with possible, but not-observed side reactions.

styrenes and heteroaromatic alkenes in moderate to good yields. Phenylacetic acids (**31**) could be obtained by slight modifications of the original procedure. The solution was saturated with CO_2 and $LiClO_4$ was substituted with $TBAPF_6$, furnishing carbocarboxylated products in moderate to high yields with similar limitations, like the carboformylation. Additionally, this method was applicable to non-styrenoid alkenes like aryl vinyl sulphides or common Michael acceptors like acrylates, acrylamide and acrylonitrile (see Scheme 5.6).

With their developed protocol, Lin and co-workers proved that cathodic reduction of simple alkyl halides gives easy access to alkyl radicals, an activation pathway that was traditionally achieved by employing tin- or silicon-based initiators.[132–135] Despite recent advances which utilize transition metal (Ni,[136] Pd[137]) or photoredox[2,138] catalysis to activate alkyl halides, they still call for additional activating reagents as opposed to the demonstrated cathodic approach, which solely relies on the use of electrons as a sustainable pseudo-reagent. In addition, the authors utilized the electrochemically generated alkyl radicals in a rather complex multi component reaction with a high intrinsic atom economy, increasing the sustainability of the reported method.

5.3.4 Electrochemical Birch Reduction

Realizing strongly reductive reaction conditions is typically achieved by using alkali metals as a reagent. The most prominent example of this type is the Birch reduction to afford sp^3-rich structures from simple arenes.[139–142] However, this methodology relies on the potentially hazardous condensation of ammonia at cryogenic temperatures as the solvent and the use of pyrophoric alkali metals. While these conditions are manageable on a laboratory scale, scaling this reaction up to an industrial scale raises safety and environmental concerns combined with the significant engineering effort necessary to handle and recycle the liquid ammonia. One of the few applications of the Birch reduction on an industrial scale is the kilogram-scale synthesis of the possible anti-Parkinson drug sumanirole (**35**), which requires 2200 L of liquid ammonia and 6.2 kg of lithium metal for a typical production run.

Quenching of the excess lithium after full conversion liberates an additional 2300 L of hydrogen gas, rendering the reaction cumbersome and hazardous.[143,144] Inspired by the outstanding utility of the Birch reduction and motivated by its drawbacks, the Baran lab established a robust, general, sustainable and scalable electrochemical approach to Birch reductions.

They chose Li-based electrolytes and THF for initial screening reactions due to their good stability towards reductive conditions. Evaluation of the anodic stability of the resulting 1,4-diene products (**33**) revealed an easy rearomatization by reoxidation; hence, non-precious metals like Mg and Al were identified as sacrificial anode materials to suppress re-oxidation, combined with a Zn-based cathode material. Yet these combinations gave no desired Birch product, but instead a thick solid layer on the cathode, which was identified to be metallic lithium. Motivated by advances in Li-ion battery technology, a screening of

additives revealed tris(pyrrolidino)phosphoramide (TPPA) to be exceptionally powerful in controlling the thickness of the solid electrolyte interface (SEI) and promoting product formation. Upon further optimization, LiBr as the supporting electrolyte, dimethylurea (DMU) as the proton source and galvanized steel wire as the cathode material were identified as optimal reaction parameters at room temperature to compete with classical Birch reactions. A variety of different substrates including heterocycles and complex natural product derivatives were tested giving selectively the expected Birch products in moderate to high yields, some of which even exceed the yields obtained under classical Birch conditions. Applying this reaction in a 10 g-scale batch reaction and on a 100 g-scale flow electrolysis was also achieved in comparable yield without major changes in the protocol.[144]

The developed electroreduction protocol was ultimately applied to non-Birch reductive transformations that require liquid ammonia and alkali metals. Reactions like ether debenzylation, deoxygenation of fluorenone and ring opening of epoxides proceeded smoothly without undesired side reactions occurring. Even a tandem aziridine opening and debenzylation by the Pfizer company to yield sumanirole (**35**) was achieved at room temperature in 67% yield (Scheme 5.7).[144]

With their electrochemical approach to the Birch reaction, Baran and co-workers demonstrated how the use of electrons as a "green" reductant can significantly enhance the ecological footprint of a classical chemical reduction reaction. They not only eliminated the use of hazardous and toxic reagents, but also reduced the energy consumption of this process by a lot. Since the electrolysis is feasible at room temperature, excessive cooling is not required anymore.

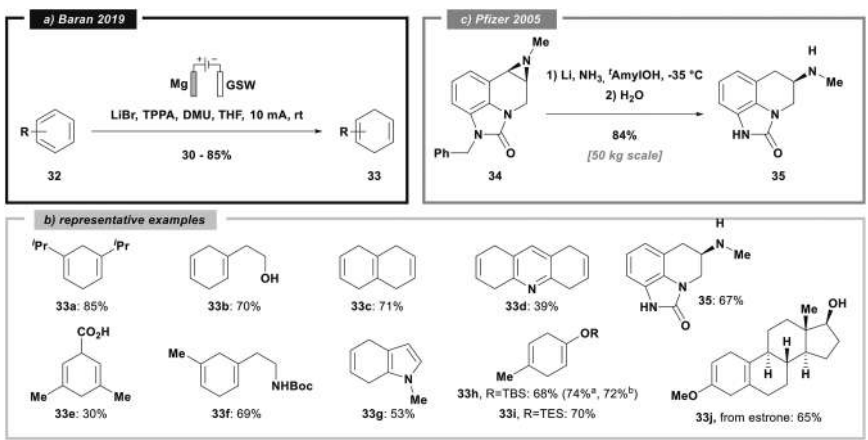

Scheme 5.7 (a) Lithium-ion based electroreduction of different arenes. (b) Representative examples of electrochemical reduction. [a]10 g scale in batch operation. [b]100 g scale in flow operation. (c) Industrial-scale Birch reduction implemented by Pfizer.

5.4 Conclusion

In this chapter, we intended to provide the reader with a brief introduction into the field of synthetic organic electrochemistry to overcome the barriers that hinder a widespread adoption of this synthetically useful technique. It covers the fundamental principles behind electrochemical transformations and explains the basic requirements beginners need in order to construct a suitable electrolysis setup. The given examples demonstrate that electrochemistry is a generally sustainable and safe method to selectively activate various substrates and achieve structural complexity in a green and atom efficient way, since only electrons are employed as a pseudo-reagent.

The synthetic organic chemist is encouraged to try out the unique opportunities that electrochemical methods offer. Adoption of already well-established electro-organic methods to substitute conventional, wasteful and potentially hazardous processes as well as future developments in this active field will ultimately lead to an eco-friendlier and more sustainable era of synthetic organic chemistry.

References

1. R. Cernansky, *Nature*, 2015, **519**, 379.
2. C. K. Prier, D. A. Rankic and D. W. C. MacMillan, *Chem. Rev.*, 2013, **113**, 5322.
3. N. A. Romero and D. A. Nicewicz, *Chem. Rev.*, 2016, **116**, 10075.
4. E. J. Horn, B. R. Rosen and P. S. Baran, *ACS Cent. Sci.*, 2016, **2**, 302.
5. S. R. Waldvogel, S. Lips, M. Selt, B. Riehl and C. J. Kampf, *Chem. Rev.*, 2018, **118**, 6706.
6. M. Yan, Y. Kawamata and P. S. Baran, *Chem. Rev.*, 2017, **117**, 13230.
7. J.-I. Yoshida, K. Kataoka, R. Horcajada and A. Nagaki, *Chem. Rev.*, 2008, **108**, 2265.
8. L. Geske, E. Sato and T. Opatz, *Synthesis*, 2020, **52**, 2781.
9. K. D. Moeller, *Tetrahedron*, 2000, **56**, 9527.
10. H. Kolbe, *Justus Liebigs Ann. Chem.*, 1849, **69**, 257.
11. C. A. C. Sequeira and D. M. F. Santos, *J. Braz. Chem. Soc.*, 2009, **20**, 387.
12. D. E. Danly, *J. Electrochem. Soc.*, 1984, **131**, 435C.
13. S. Möhle, M. Zirbes, E. Rodrigo, T. Gieshoff, A. Wiebe and S. R. Waldvogel, *Angew. Chem., Int. Ed.*, 2018, **57**, 6018.
14. H. Putter and H. Hannebaum, Preparation of phthalides, *US Pat.*, 6063256A, 2000.
15. R. Matthessen, J. Fransaer, K. Binnemans and D. E. De Vos, *Beilstein J. Org. Chem.*, 2014, **10**, 2484.
16. R. H. Verschueren and W. M. De Borggraeve, *Molecules*, 2019, **24**, 2122.
17. C. Schotten, T. P. Nicholls, R. A. Bourne, N. Kapur, B. N. Nguyen and C. E. Willans, *Green Chem.*, 2020, **22**, 3358.
18. H. Wang, X. Gao, Z. Lv, T. Abdelilah and A. Lei, *Chem. Rev.*, 2019, **119**, 6769.

19. S. Tang, Y. Liu and A. Lei, *Chem*, 2018, **4**, 27.
20. C. Gütz, M. Selt, M. Bänziger, C. Bucher, C. Römelt, N. Hecken, F. Gallou, T. R. Galvão and S. R. Waldvogel, *Chem. - Eur. J.*, 2015, **21**, 13878.
21. O. Hammerich and B. Speiser, *Organic Electrochemistry: Revised and Expanded*, CRC Press, 2015.
22. T. Fuchigami, M. Atobe and S. Inagi, *Fundamentals and Applications of Organic Electrochemistry: Synthesis, Materials, Devices*, John Wiley & Sons, 2014.
23. O. Stern and Z. Elektrochem, *Angew. Phys. Chem.*, 1924, **30**, 508.
24. W. M. Haynes, *CRC Handbook of Chemistry and Physics*, CRC press, 2014.
25. H. G. Roth, N. A. Romero and D. A. Nicewicz, *Synlett*, 2016, **27**, 714.
26. N. Elgrishi, K. J. Rountree, B. D. McCarthy, E. S. Rountree, T. T. Eisenhart and J. L. Dempsey, *J. Chem. Educ.*, 2018, **95**, 197.
27. C. Sandford, M. A. Edwards, K. J. Klunder, D. P. Hickey, M. Li, K. Barman, M. S. Sigman, H. S. White and S. D. Minteer, *Chem. Sci.*, 2019, **10**, 6404.
28. M. Faraday, *Philos. Trans. R. Soc. London*, 1834, **124**, 77.
29. F. C. Strong, *J. Chem. Educ.*, 1961, **38**, 98.
30. W. B. Jensen, *J. Chem. Educ.*, 2012, **89**, 1208.
31. E. J. Horn, B. R. Rosen, Y. Chen, J. Tang, K. Chen, M. D. Eastgate and P. S. Baran, *Nature*, 2016, **533**, 77.
32. E. E. Finney, K. A. Ogawa and A. J. Boydston, *J. Am. Chem. Soc.*, 2012, **134**, 12374.
33. B. R. M. Lake, E. K. Bullough, T. J. Williams, A. C. Whitwood, M. A. Little and C. E. Willans, *Chem. Commun.*, 2012, **48**, 4887.
34. C. Gütz, B. Klöckner and S. R. Waldvogel, *Org. Process Res. Dev.*, 2016, **20**, 26.
35. T. Gieshoff, A. Kehl, D. Schollmeyer, K. D. Moeller and S. R. Waldvogel, *Chem. Commun.*, 2017, **53**, 2974.
36. G. Laudadio, E. Barmpoutsis, C. Schotten, L. Struik, S. Govaerts, D. L. Browne and T. Noël, *J. Am. Chem. Soc.*, 2019, **141**, 5664.
37. M. Atobe, H. Tateno and Y. Matsumura, *Chem. Rev.*, 2018, **118**, 4541.
38. D. Pletcher, R. A. Green and R. C. D. Brown, *Chem. Rev.*, 2018, **118**, 4573.
39. M. P. J. Brennan and R. Brettle, *J. Chem. Soc., Perkin Trans. 1*, 1973, 257.
40. P. Cañizares, J. Lobato, R. Paz, M. A. Rodrigo and C. Sáez, *Water Res.*, 2005, **39**, 2687.
41. S. R. Waldvogel, S. Mentizi and A. Kirste, in *Radicals in Synthesis III*, ed. M. Heinrich and A. Gansäuer, Springer Berlin Heidelberg, Berlin, Heidelberg, 2012, pp. 1–31.
42. T. A. Ivandini and Y. Einaga, *Chem. Commun.*, 2017, **53**, 1338.
43. S. J. Cobb, Z. J. Ayres and J. V. Macpherson, *Annu. Rev. Anal. Chem.*, 2018, **11**, 463.
44. B. Gleede, T. Yamamoto, K. Nakahara, A. Botz, T. Graßl, R. Neuber, T. Matthée, Y. Einaga, W. Schuhmann and S. R. Waldvogel, *ChemElectroChem*, 2019, **6**, 2771.
45. S. Lips and S. R. Waldvogel, *ChemElectroChem*, 2019, **6**, 1649.

46. D. M. Heard and A. J. J. Lennox, *Angew. Chem., Int. Ed.*, 2020, **59**, 18866.
47. A. Hickling and F. W. Salt, *Trans. Faraday Soc.*, 1940, **36**, 1226.
48. A. Hickling and S. Hill, *Discuss. Faraday Soc.*, 1947, **1**, 236.
49. X. Hu, X. Tian, Y.-W. Lin and Z. Wang, *RSC Adv.*, 2019, **9**, 31563.
50. A. Koca, *Int. J. Hydrogen Energy*, 2009, **34**, 2107.
51. A. Kraft, *Int. J. Electrochem. Sci.*, 2007, **2**, 355.
52. V. V. Pavlishchuk and A. W. Addison, *Inorg. Chim. Acta*, 2000, **298**, 97.
53. L. Eberson, M. P. Hartshorn and O. Persson, *J. Chem. Soc., Chem. Commun.*, 1995, 1131.
54. L. Eberson, M. P. Hartshorn and O. Persson, *J. Chem. Soc., Perkin Trans. 2*, 1995, 1735.
55. L. Eberson, O. Persson and M. P. Hartshorn, *Angew. Chem., Int. Ed.*, 1995, **34**, 2268.
56. R. Francke, D. Cericola, R. Kötz, D. Weingarth and S. R. Waldvogel, *Electrochim. Acta*, 2012, **62**, 372.
57. T. Raju, K. Kulangiappar, M. A. Kulandainathan and A. Muthukumaran, *Tetrahedron Lett.*, 2005, **46**, 7047.
58. T. Raju, K. Kulangiappar, M. Anbu Kulandainathan, U. Uma, R. Malini and A. Muthukumaran, *Tetrahedron Lett.*, 2006, **47**, 4581.
59. L. Sun, X. Zhang, Z. Li, J. Ma, Z. Zeng and H. Jiang, *Eur. J. Org. Chem.*, 2018, **2018**, 4949.
60. E. Steckhan, *Angew. Chem., Int. Ed. Engl.*, 1986, **25**, 683.
61. E. Steckhan, in *Electrochemistry I*, ed. E. Steckhan, Springer, Berlin, Heidelberg, 1987, pp. 1–69.
62. R. Francke and R. D. Little, *Chem. Soc. Rev.*, 2014, **43**, 2492.
63. K. Chiba, T. Miura, S. Kim, Y. Kitano and M. Tada, *J. Am. Chem. Soc.*, 2001, **123**, 11314.
64. Y. S. Park and R. D. Little, *J. Org. Chem.*, 2008, **73**, 6807.
65. Y. Okada, Y. Yamaguchi, A. Ozaki and K. Chiba, *Chem. Sci.*, 2016, **7**, 6387.
66. T. Broese, A. F. Roesel, A. Prudlik and R. Francke, *Org. Lett.*, 2018, **20**, 7483.
67. R. Francke and R. D. Little, *ChemElectroChem*, 2019, **6**, 4373.
68. T. Shono, H. Hamaguchi and Y. Matsumura, *J. Am. Chem. Soc.*, 1975, **97**, 4264.
69. T. Shono, Y. Matsumura, K. Tsubata, Y. Sugihara, S. Yamane, T. Kanazawa and T. Aoki, *J. Am. Chem. Soc.*, 1982, **104**, 6697.
70. T. Shono, *Synthesis of Alkaloidal Compounds Using an Electrochemical Reaction as a Key Step*, Springer Berlin Heidelberg, Berlin, Heidelberg, 1988.
71. T. Shono, Y. Matsumura and K. Inoue, *J. Org. Chem.*, 1983, **48**, 1388.
72. P. D. Palasz, J. H. P. Utley and J. D. Hardstone, *J. Chem. Soc., Perkin Trans. 2*, 1984, 807.
73. T. Shono, Y. Matsumura, K. Uchida and H. Kobayashi, *J. Org. Chem.*, 1985, **50**, 3243.
74. K. D. Moeller, P. W. Wang, S. Tarazi, M. R. Marzabadi and P. L. Wong, *J. Org. Chem.*, 1991, **56**, 1058.

75. G. Butora, J. W. Reed, T. Hudlicky, L. E. Brammer, P. I. Higgs, D. P. Simmons and N. E. Heard, *J. Am. Chem. Soc.*, 1997, **119**, 7694.
76. M. K. S. Vink, C. A. Schortinghuis, J. Luten, J. H. van Maarseveen, H. E. Schoemaker, H. Hiemstra and F. P. J. T. Rutjes, *J. Org. Chem.*, 2002, **67**, 7869.
77. T. Shono, Y. Matsumura and K. Tsubata, *Org. Synth.*, 2003, **63**, 206.
78. M. R. Faust, G. Höfner, J. Pabel and K. T. Wanner, *Eur. J. Med. Chem.*, 2010, **45**, 2453.
79. T. Golub and J. Y. Becker, *Electrochim. Acta*, 2015, **173**, 408.
80. S. S. Libendi, Y. Demizu, Y. Matsumura and O. Onomura, *Tetrahedron*, 2008, **64**, 3935.
81. S. S. Libendi, Y. Demizu and O. Onomura, *Org. Biomol. Chem.*, 2009, **7**, 351.
82. A. D. Tereshchenko, J. S. Myronchuk, L. D. Leitchenko, I. V. Knysh, G. O. Tokmakova, O. O. Litsis, A. Tolmachev, K. Liubchak and P. Mykhailiuk, *Tetrahedron*, 2017, **73**, 750.
83. S. Tatsuya, M. Yoshihiro, T. Kenji and T. Jiro, *Chem. Lett.*, 1981, **10**, 1121.
84. T. Shono, Y. Matsumura and K. Tsubata, *Tetrahedron Lett.*, 1981, **22**, 2411.
85. T. Shono, Y. Matsumura, O. Onomura and M. Sato, *J. Org. Chem.*, 1988, **53**, 4118.
86. Y. Demizu, H. Shiigi, H. Mori, K. Matsumoto and O. Onomura, *Tetrahedron: Asymm.*, 2008, **19**, 2659.
87. X. Wang, J. Li, R. A. Saporito and N. Toyooka, *Tetrahedron*, 2013, **69**, 10311.
88. T. Shono, Y. Matsumura and K. Tsubata, *J. Am. Chem. Soc.*, 1981, **103**, 1172.
89. T. Shono, Y. Matsumura and K. Tsubata, *Tetrahedron Lett.*, 1981, **22**, 3249.
90. S. Bornemann and S. T. Handy, *Molecules*, 2011, **16**, 5963.
91. B. A. Frontana-Uribe, R. D. Little, J. G. Ibanez, A. Palma and R. Vasquez-Medrano, *Green Chem.*, 2010, **12**, 2099.
92. P. T. Anastas and J. C. Warner, *Green Chemistry: Theory and Practice*, Oxford University Press, 1998.
93. J.-i. Yoshida, S. Suga, S. Suzuki, N. Kinomura, A. Yamamoto and K. Fujiwara, *J. Am. Chem. Soc.*, 1999, **121**, 9546.
94. S. Suga, M. Okajima and J.-i. Yoshida, *Tetrahedron Lett.*, 2001, **42**, 2173.
95. S. Suga, T. Nishida, D. Yamada, A. Nagaki and J.-i. Yoshida, *J. Am. Chem. Soc.*, 2004, **126**, 14338.
96. T. Maruyama, Y. Mizuno, I. Shimizu, S. Suga and J.-i. Yoshida, *J. Am. Chem. Soc.*, 2007, **129**, 1902.
97. J.-i. Yoshida, A. Shimizu and R. Hayashi, *Chem. Rev.*, 2018, **118**, 4702.
98. A. Markham and K. L. Goa, *Drugs*, 1997, **54**, 299.
99. M. E. Matheron and M. Porchas, *Plant Dis.*, 2004, **88**, 665.
100. A. Alexakis, D. Polet, C. Benhaim and S. Rosset, *Tetrahedron: Asymmetry*, 2004, **15**, 2199.

101. A. Alexakis, D. Polet, S. Rosset and S. March, *J. Org. Chem.*, 2004, **69**, 5660.
102. G. A. Cortez, R. R. Schrock and A. H. Hoveyda, *Angew. Chem., Int. Ed.*, 2007, **46**, 4534.
103. L. Palais, I. S. Mikhel, C. Bournaud, L. Micouin, C. A. Falciola, M. Vuagnoux-d'Augustin, S. Rosset, G. Bernardinelli and A. Alexakis, *Angew. Chem., Int. Ed.*, 2007, **46**, 7462.
104. R. Singh, C. Czekelius, R. R. Schrock, P. Müller and A. H. Hoveyda, *Organometallics*, 2007, **26**, 2528.
105. M. Vuagnoux-d'Augustin, S. Kehrli and A. Alexakis, *Synlett*, 2007, **2007**, 2057.
106. C. Hawner, K. Li, V. Cirriez and A. Alexakis, *Angew. Chem., Int. Ed.*, 2008, **47**, 8211.
107. I. M. Malkowsky, C. E. Rommel, K. Wedeking, R. Fröhlich, K. Bergander, M. Nieger, C. Quaiser, U. Griesbach, H. Pütter and S. R. Waldvogel, *Eur. J. Org. Chem.*, 2006, **2006**, 241.
108. A. Kirste, M. Nieger, I. M. Malkowsky, F. Stecker, A. Fischer and S. R. Waldvogel, *Chem. - Eur. J.*, 2009, **15**, 2273.
109. A. Kirste, G. Schnakenburg and S. R. Waldvogel, *Org. Lett.*, 2011, **13**, 3126.
110. B. Elsler, D. Schollmeyer, K. M. Dyballa, R. Franke and S. R. Waldvogel, *Angew. Chem., Int. Ed.*, 2014, **53**, 5210.
111. A. Wiebe, D. Schollmeyer, K. M. Dyballa, R. Franke and S. R. Waldvogel, *Angew. Chem., Int. Ed.*, 2016, **55**, 11801.
112. B. Riehl, K. M. Dyballa, R. Franke and S. R. Waldvogel, *Synthesis*, 2017, **49**, 252.
113. A. Kirste, G. Schnakenburg, F. Stecker, A. Fischer and S. R. Waldvogel, *Angew. Chem., Int. Ed.*, 2010, **49**, 971.
114. B. Elsler, A. Wiebe, D. Schollmeyer, K. M. Dyballa, R. Franke and S. R. Waldvogel, *Chem. - Eur. J.*, 2015, **21**, 12321.
115. L. Schulz, M. Enders, B. Elsler, D. Schollmeyer, K. M. Dyballa, R. Franke and S. R. Waldvogel, *Angew. Chem., Int. Ed.*, 2017, **56**, 4877.
116. B. Dahms, R. Franke and S. R. Waldvogel, *ChemElectroChem*, 2018, **5**, 1249.
117. L. Schulz, R. Franke and S. R. Waldvogel, *ChemElectroChem*, 2018, **5**, 2069.
118. S. Lips, A. Wiebe, B. Elsler, D. Schollmeyer, K. M. Dyballa, R. Franke and S. R. Waldvogel, *Angew. Chem., Int. Ed.*, 2016, **55**, 10872.
119. A. Wiebe, B. Riehl, S. Lips, R. Franke and S. R. Waldvogel, *Sci. Adv.*, 2017, **3**, eaao3920.
120. A. Wiebe, S. Lips, D. Schollmeyer, R. Franke and S. R. Waldvogel, *Angew. Chem., Int. Ed.*, 2017, **56**, 14727.
121. S. Lips, B. A. Frontana-Uribe, M. Dörr, D. Schollmeyer, R. Franke and S. R. Waldvogel, *Chem. - Eur. J.*, 2018, **24**, 6057.
122. R. I. McDonald, G. Liu and S. S. Stahl, *Chem. Rev.*, 2011, **111**, 2981.
123. R. M. Romero, T. H. Wöste and K. Muñiz, *Chem. - Asian J.*, 2014, **9**, 972.

124. J. C. Siu, N. Fu and S. Lin, *Acc. Chem. Res.*, 2020, **53**, 547.
125. D. Pollok and S. R. Waldvogel, *Chem. Sci.*, 2020, **11**, 12386.
126. N. Fu, G. S. Sauer, A. Saha, A. Loo and S. Lin, *Science*, 2017, **357**, 575.
127. G. S. Sauer and S. Lin, *ACS Catal.*, 2018, **8**, 5175.
128. J. C. Siu, G. S. Sauer, A. Saha, R. L. Macey, N. Fu, T. Chauviré, K. M. Lancaster and S. Lin, *J. Am. Chem. Soc.*, 2018, **140**, 12511.
129. N. Fu, G. S. Sauer and S. Lin, *J. Am. Chem. Soc.*, 2017, **139**, 15548.
130. L. Lu, N. Fu and S. Lin, *Synlett*, 2019, **30**, 1199.
131. K.-Y. Ye, Z. Song, G. S. Sauer, J. H. Harenberg, N. Fu and S. Lin, *Chem. - Eur. J.*, 2018, **24**, 12274.
132. W. P. Neumann, *Synthesis*, 1987, **1987**, 665.
133. C. Chatgilialoglu, C. Ferreri, Y. Landais and V. I. Timokhin, *Chem. Rev.*, 2018, **118**, 6516.
134. G. H. Lovett, S. Chen, X.-S. Xue, K. N. Houk and D. W. C. MacMillan, *J. Am. Chem. Soc.*, 2019, **141**, 20031.
135. T. Constantin, M. Zanini, A. Regni, N. S. Sheikh, F. Juliá and D. Leonori, *Science*, 2020, **367**, 1021.
136. D. J. Weix, *Acc. Chem. Res.*, 2015, **48**, 1767.
137. P. Chuentragool, D. Kurandina and V. Gevorgyan, *Angew. Chem., Int. Ed.*, 2019, **58**, 11586.
138. M. Giedyk, R. Narobe, S. Weiß, D. Touraud, W. Kunz and B. König, *Nat. Catal.*, 2020, **3**, 40.
139. A. Paptchikhine, K. Itto and P. G. Andersson, *Chem. Commun.*, 2011, **47**, 3989.
140. B. K. Peters, J. Liu, C. Margarita, W. Rabten, S. Kerdphon, A. Orebom, T. Morsch and P. G. Andersson, *J. Am. Chem. Soc.*, 2016, **138**, 11930.
141. J. Liu, S. Krajangsri, T. Singh, G. De Seriis, N. Chumnanvej, H. Wu and P. G. Andersson, *J. Am. Chem. Soc.*, 2017, **139**, 14470.
142. W. Rabten, C. Margarita, L. Eriksson and P. G. Andersson, *Chem. - Eur. J.*, 2018, **24**, 1681.
143. D. K. Joshi, J. W. Sutton, S. Carver and J. P. Blanchard, *Org. Process Res. Dev.*, 2005, **9**, 997.
144. B. K. Peters, K. X. Rodriguez, S. H. Reisberg, S. B. Beil, D. P. Hickey, Y. Kawamata, M. Collins, J. Starr, L. Chen, S. Udyavara, K. Klunder, T. J. Gorey, S. L. Anderson, M. Neurock, S. D. Minteer and P. S. Baran, *Science*, 2019, **363**, 838.

CHAPTER 6

Colored Compounds for Eco-sustainable Visible-light Promoted Syntheses

MAURIZIO FAGNONI*

PhotoGreen Lab, Department of Chemistry, University of Pavia, Pavia, Italy
*E-mail: fagnoni@unipv.it

6.1 Introduction

In recent years photochemistry has acquired a predominant role in organic synthesis and in the production of bioactive molecules thanks to the mild conditions required.[1–5] In fact, as is widely recognized, there is a strict connection between photochemistry and green chemistry, since a traceless reagent (the photon) is able to induce a chemical transformation or the generation of a chemical intermediate with no need for a catalyst/additive that would need to be removed during the work-up procedures.[6–11] However, the wide applicability of the photochemical method is hampered by the adoption of dedicated equipment and the design of a photochemical reactor functioning with UV light.[12] In favorable cases, the UV content of solar light is sufficient to induce the desired transformations.[13–19]

The ideal case, however, is having a photoreactive colored organic compound able to undergo a valuable chemical transformation upon excitation by visible light photons. In the latter case, even beginners may design new photochemical reactions due to the wide availability of visible light sources, including inexpensive Compact Fluorescent Lamps, LEDs and obviously

Sustainable Organic Synthesis: Tools and Strategies
Edited by Stefano Protti and Alessandro Palmieri

Published by the Royal Society of Chemistry, www.rsc.org

costless sunlight.[20] Finding colored organic molecules seems easy, since in nature a lot of organic compounds are colored belonging to different classes. In some cases, they contain a chromophore that imparts a sort of photoactivity.[21] Figure 6.1 collects some classes of natural compounds that may behave as photosensitizers in a biological environment.[21] Nonetheless, the direct photochemistry of natural compounds has no practical significance for synthetic practitioners.

A way to overcome this hurdle is adding into the reaction mixture a compound that has the role of absorbing visible light and promoting the photochemical reaction, and is regenerated at the end of the reaction. This approach is nowadays known as photoredox catalysis, where a colored photocatalyst (PC) upon visible light irradiation may engage in an electron transfer, hydrogen atom transfer or energy transfer reaction (even causing the generation of singlet oxygen) with the desired reaction partner. In the last 10 years, we have observed a steep growth in the use and application of this strategy, it now being the main approach used in photochemical synthesis.[22–27] As a matter of fact, this strategy allows the easy photochemical conversion of colorless compounds making use of visible photons (Scheme 6.1a). A question however remains: are there any valuable reactions occurring by using visible photons under photocatalyst-free conditions?

Interestingly, there are several strategies that have been devised to form a colored species in solution, such as chromophore activation mainly induced by a complexing agent (CA, including a proton, Scheme 6.1b)[28] or the *in situ* generation of a colored Electron Donor Acceptor (EDA) complex by interaction with another reaction partner (R′, Scheme 6.1c).[29–31] In rare instances, the colored species is formed *in situ* by a chemical reaction with an organic catalyst.[32] The ideal case, however, is the conversion of a colored compound into a valuable product by using visible photons as the real green promoting agents (Scheme 6.1d).

The aim of this chapter is to collect the reactions involving organic compounds that have chromophores able to impart them with a color, making them able to undergo promising photochemical transformations with no need for any interaction with other additives and/or photocatalysts.

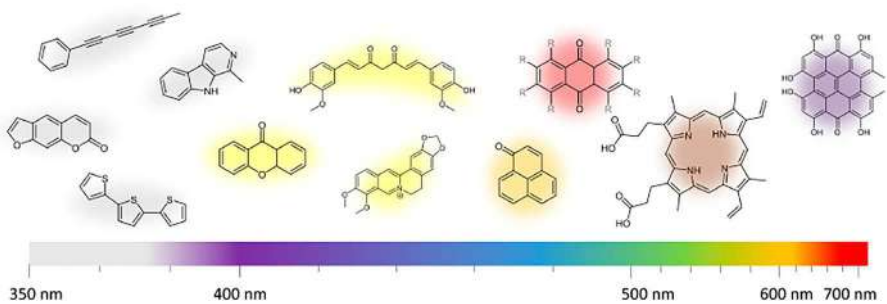

Figure 6.1 Reproduced from ref. 21 with permission from Elsevier, Copyright 2019.

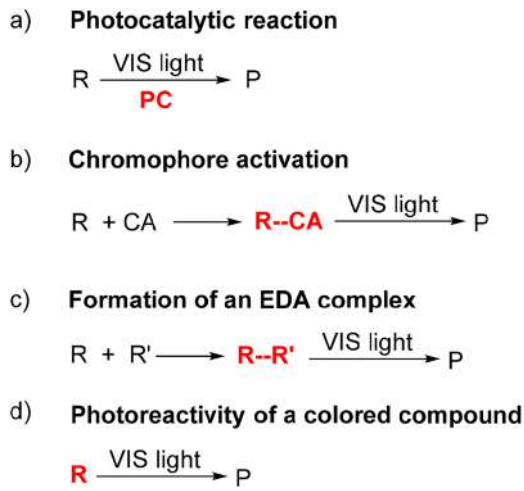

Scheme 6.1 Strategies for the use of visible photons to promote a chemical transformation Reagent (R) → Product (P) *via* activation of colorless organic molecules by (a) a photocatalytic process, (b) a chromophore activation and (c) the *in situ* formation of an EDA complex. The ideal case is (d), the direct photolysis of a colored compound. In red are the species that absorb the visible light.

This work does not include examples where the colored compound is formed *in situ* or when the light source emits UV photons along with visible light photons to promote the process.

The reactions are organized by collecting the reactions derived from the same classes of colored compounds or with different classes of organic molecules used as the photochemical precursors of the same ground state intermediate (*e.g.* radicals, carbenes *etc.*).

6.2 Classes of Colored Compounds Applied in Photochemical Syntheses

6.2.1 Thioketones

Thioketones are rarely used in photochemical reactions in comparison with the corresponding oxygenated derivatives due to their lower photoreactivity.[33] The color in the 500–600 nm region is due to a dipole-forbidden n → π* transition. Excited thiones promote a hydrogen transfer reaction either intermolecularly[33] or intramolecularly as in the case depicted in Scheme 6.2 regarding the photochemistry of β-substituted arylalkyl thione **2-1**. Visible light irradiation of a benzene solution of **2-1** induced a Norrish-Type II reaction to form the unusual 1,3-biradical **2-2** that upon radical recombination afforded the cyclopropyl thiol **2-3** in a very good yield.[34,35]

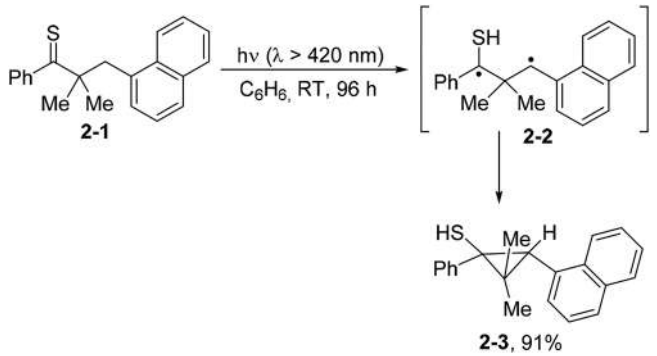

Scheme 6.2 Intramolecular hydrogen transfer in thioketones.

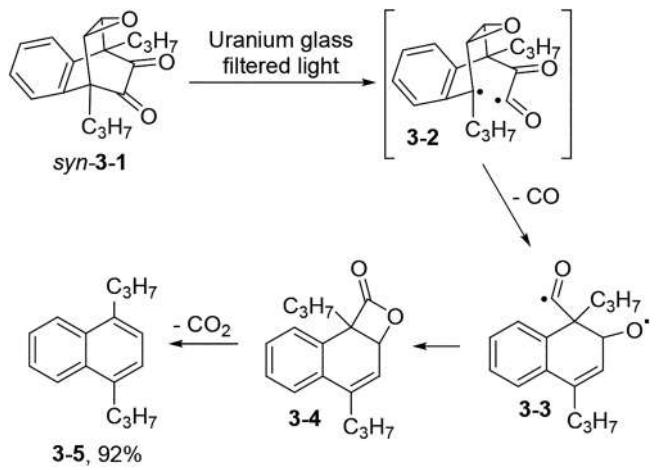

Scheme 6.3 Norrish type I cleavage in α-diketones.

6.2.2 α-Diketones

Simple ketones do not absorb in the visible region, except in the case of some photoorganocatalysts[26] such as thioxanthone,[36] 9-fluorenone[36] and 5,7,12,14-pentacenetetrone.[37] However, α-diketones are slightly colored and may undergo the typical reactions of the carbonyl group (*via* an nπ* state) but under visible light irradiation.[38,39] α-Diketones may be engaged in several reactions. As an example, irradiation of *syn*-9,10-epoxy-1,4-dihydro-1,4-dipropyl-1,4-ethanonaphthalene-2,3-dione (*syn*-**3-1**) led to 1,4-di-*n*-propylnaphthalene (**3-5**) in a high yield (Scheme 6.3). A tentative mechanism was proposed and involved an initial Norrish type I cleavage (to give **3-2**), followed by the ring opening of the epoxide ring and the subsequent extrusion of CO to yield diradical **3-3**. Radical recombination gave lactone **3-4** and **3-5** from it by a rapid carbon dioxide loss.[40] Irradiation of *anti*-**3-1** under the same conditions curiously gave a mixture of products.

One of the carbonyl groups can be engaged in a Paternò–Büchi reaction. Thus, visible light absorption of 1-acetylisatin (**4-1**) in the presence of vinyl ether (**4-2**) smoothly formed the spiro(3*H*-indole-3,2′-oxetane) **4-3** with high regio- (only one C=O bond is engaged in the reaction) and diastereoselectivity (the *syn* isomer was largely preferred, Scheme 6.4).[41] The reaction proceeded from the nπ* triplet state of **4-1** and the stability of the conformers of the resulting 1,4-diradical intermediate was invoked to explain both the preference for the formation of head-to-tail products and the obtainment of thermodynamically less stable *syn*-spirooxetanes.[41]

The versatility of the photochemistry of the carbonyl group in 1,2-diketones is witnessed by their use in intramolecular hydrogen abstraction, such as the Norrish Type II reaction. In fact, irradiation of compound **5-1** (obtained from the corresponding non-2-ynitol) promoted the hydrogen atom abstraction from one of the two carbonyls to the hydrogens placed adjacent to the oxygen atom of the tetrahydro-2*H*-pyran ring (Scheme 6.5). A 1,4-biradical (**5-2**) was formed and fragmented to release the rather stable *Z* photoenol **5-3**, which upon heating underwent an intramolecular aldol reaction to give **5-4**.[42,43] This is considered as a surprisingly diastereoselective simple route to densely functionalized cyclopentitols starting from pyranoses.

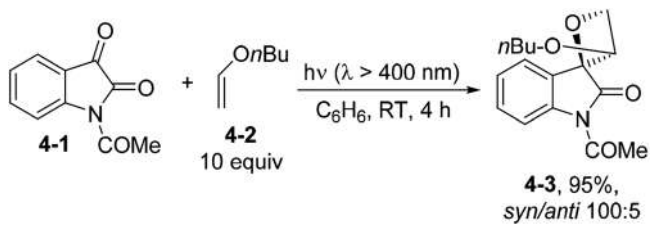

Scheme 6.4 Paternò–Büchi reaction on 1,2-diketones.

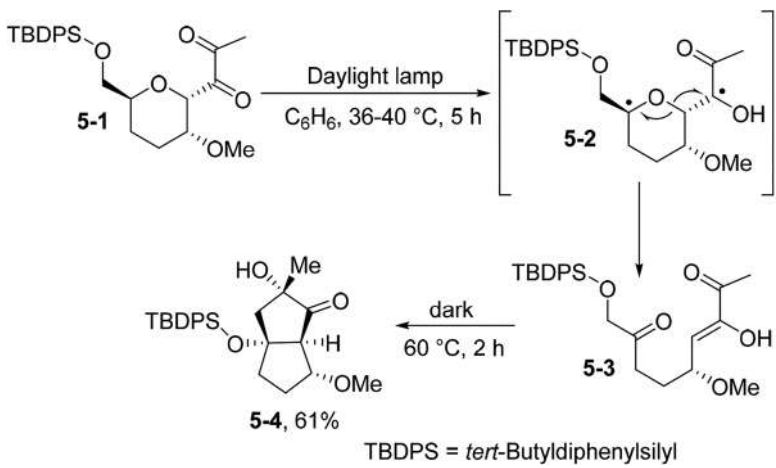

Scheme 6.5 Synthesis of functionalized cyclopentitols.

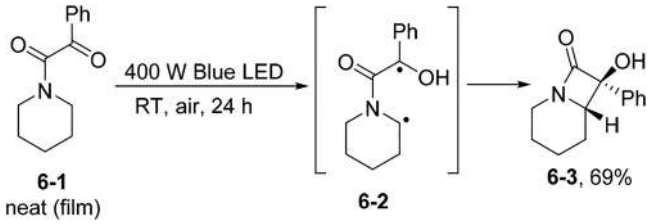

Scheme 6.6 Norrish–Yang Type II reaction of α-ketoamides.

When the starting carbohydrate structure containing a 1,2-diketone moiety was slightly modified to 1-glycosyl-2,3-butanodiones, the biradicals formed by the initial Norrish-Type II process led to chiral 1-hydroxy-1-meth yl-5-oxaspiro[3.5]nonan-2-ones (having the 1-hydroxy-1-methyl-2-cyclobutan one moiety) by a Yang cyclization.[44] A key intermediate for the preparation of (+)-lactacystin (a potent inhibitor of the 20S proteasome) has been again obtained by a Norrish-Yang cyclization on a tetrahydro-3*H*,5*H*-pyrrolo[1,2-*c*] oxazol-5-one.[45] The photocyclization of 1,2-ketones for the preparation of a variety of functionalized 2-hydroxycyclobutanones was achieved under blue LED irradiation under flow conditions.[46]

A related reaction may also be applied to other derivatives having two adjacent carbonyl groups such as α-ketoamides (see the case of 1-phenyl-2-(piperidin-1-yl)ethane-1,2-dione **6-1**, Scheme 6.6). This C–H functionalization of azacycles was induced again by a Norrish–Yang Type II reaction giving access to the α-hydroxy-β-lactam **6-3**.[47] Noteworthily, the reaction was carried out under solvent free conditions where a film of compound **6-1** on the glass walls of a 20 mL vial was photolyzed.

6.2.3 Barton Esters

An interesting class of colored compounds designed for the tin-free generation of radicals is that of Barton esters.[48] These derivatives may be easily obtained from the corresponding carboxylic acids by esterification with *N*-hydroxythiopyridone. The thus formed N–O bond in Barton esters is very labile either under heating or by visible light exposure. The photocleavage of the N–O bond followed by CO_2 loss is a smooth way to release a carbon-based radical.[48,49] A dated example is that of the Minisci reaction[50] depicted in Scheme 6.7. The irradiation of ester **7-1** with a tungsten lamp caused a decarboxylative addition of an adamantyl radical onto lepidinium camphorsulphonate **7-2** (a heteroaromatic protonated base) to afford the 2-substituted lepidine **7-3** as the sole product in an almost quantitative yield.[51]

The Barton ester derived from oleic acid **8-1** was used for the visible light reaction with methanesulfonyl cyanide **8-2** to afford the corresponding nitrile **8-3** in a high yield (Scheme 6.8).[52] In a similar fashion, a smooth way to form thiocyanates involved the photolysis of Barton ester in the presence of methanesulfonyl (or *p*-toluenesulfonyl) isothiocyanate.[53]

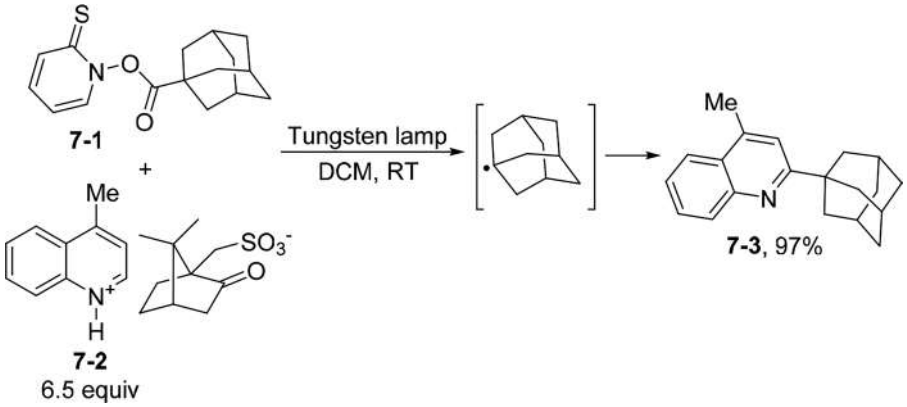

Scheme 6.7 Barton esters for the functionalization of lepidine.

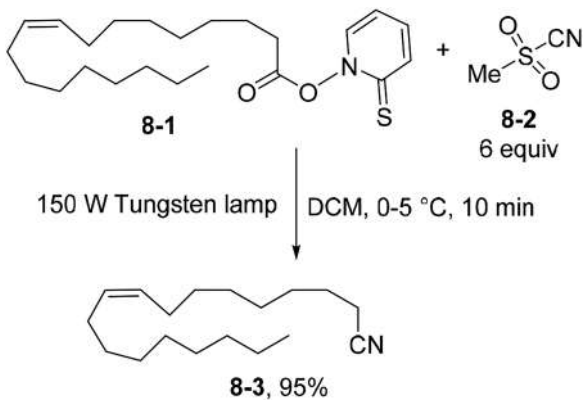

Scheme 6.8 Visible light-promoted synthesis of nitriles.

The radicals obtained from a Barton ester may be used even for the forging of valuable C-heteroatom bonds. As for the C–N bond formation, it is worth mentioning the photoinduced reaction between these esters and thionitrites to give *trans* nitroso dimers[54] and the synthesis of alkyl azides by reaction with a sulfonyl azide.[55] An approach for the construction of C–P bonds was the trapping of the alkyl radical with white phosphorous (P_4) in the presence of water. This unusual route allowed potentially biologically active phosphonic acids to be prepared starting from the corresponding carboxylic acids.[56]

The conversion of carboxylic acids into alcohols may be achieved by using a modified version of Barton esters, namely *N*-hydroxy-4-methyl-2-thiazolinethiones (*e.g.* **9-1**, Scheme 6.9). Thus, the photocleavage of the N–O bond in compound **9-1**, followed by decarboxylation, gave an alkyl radical that upon reaction with oxygen and a mercaptane gave a hydroperoxide readily converted to the corresponding alcohol **9-2** by reaction with PPh_3.[57]

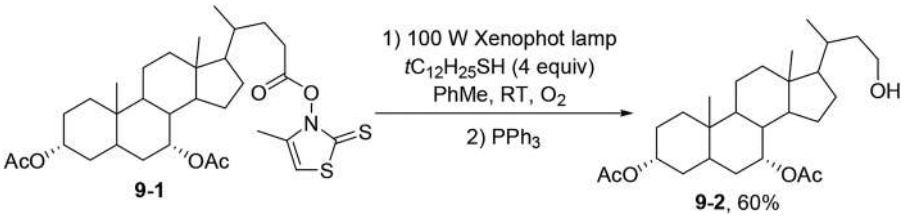

Scheme 6.9 Decarboxylative hydroxylation *via* modified Barton esters.

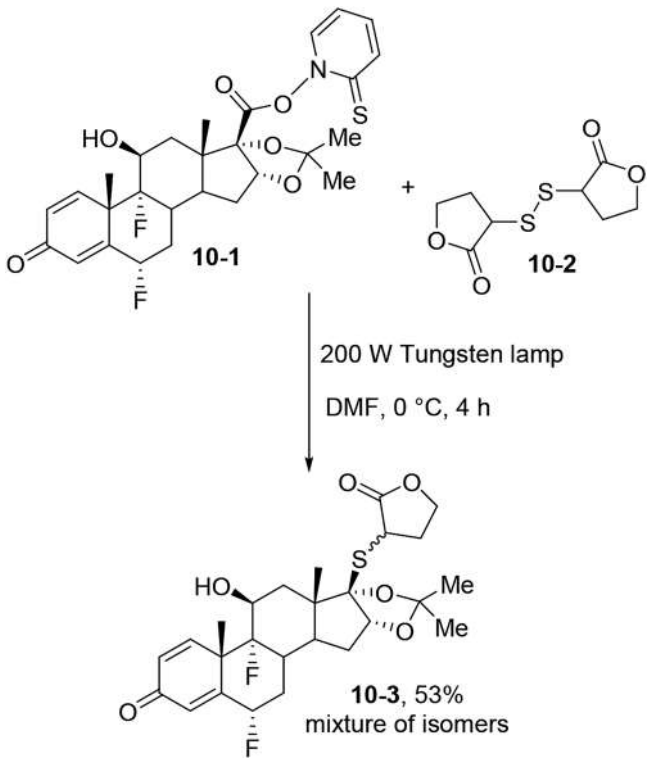

Scheme 6.10 Synthesis of an androstane-17β-(γ-lactone) sulfide.

On the contrary, C–S bonds may be easily formed by trapping of the photogenerated alkyl radical by liquid SO_2 (used as a cosolvent of the reaction in combination with DCM) to form the corresponding thiosulfonates of formulae RSO_2SPy (Py = pyridine).[58] The latter compounds, however, were easily converted into sulfones and sulfonamides. The release of an alkyl radical was effective even on a solid phase and this approach has been used for the synthesis of peptides containing modified amino acids.[59] An interesting application in this frame was the synthesis of compound **10-3** (as a mixture of isomers, Scheme 6.10) belonging to the class of 17β-glucocorticoid

butyrolactones incorporating the 16α,17α-isopropylidene group. Here, the γ-lactone group has been introduced by reaction of Barton ester **10-1** and disulfide **10-2** upon tungsten lamp irradiation. The *R* and *S* isomers of androstane-17β-(γ-lactone) sulfides **10-3** were separated and tested showing some modest antiinflammatory activity in the rat ear edema *in vivo* model.[60] The C-heteroatom bond can be formed even in an intramolecular fashion as in the conversion of the 5-(benzylseleno)pentanoic acid derived Barton ester into tetrahydroselenophene.[61]

The versatility of the *N*-hydroxy-2-thiopyridone esters is apparent in Scheme 6.11 where the photocleavage induced in *O*-carboxymethyl oxime **11-1** generated an α-oxy radical **11-2.** At this stage, two competitive processes may operate, *viz* coupling with another molecule of **11-1** to give pyridine derivative **11-3** or formaldehyde loss to give an iminyl radical **11-4.** Radical cyclization and further reaction with **11-1** yielded pyrrolenine **11-6.** The **11-6**/**11-3** ratio strictly depended on the concentration of **11-1** in solution reaching *ca.* 11 under diluted conditions ([**11-1**] = 0.04 M).[62,63]

The photogenerated iminyl radical may undergo an intramolecular attack onto the Se atom present in $ArSeCH_2Ph$, thus inducing the release of the benzyl radical with the concomitant formation of a 1,2-benzoselenazole.[64] Even the amidyl radical **12-2** may be obtained by visible light irradiation of carbamate

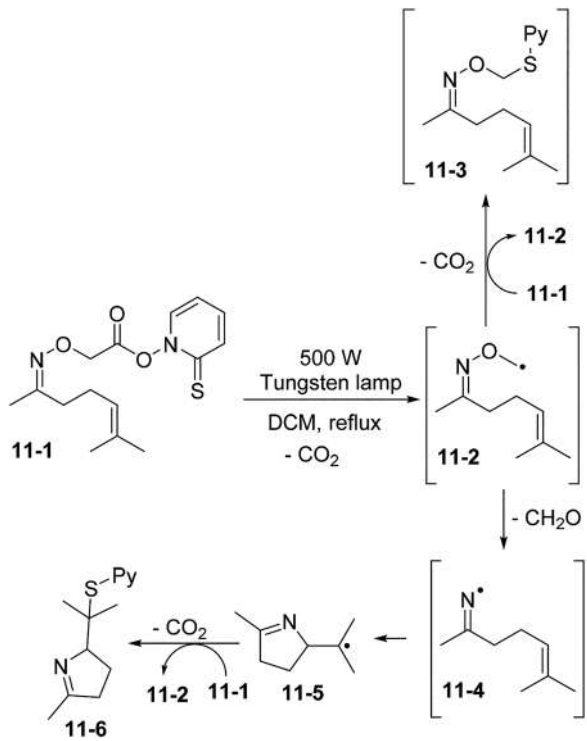

Scheme 6.11 Photochemical preparation of pyrrolenines.

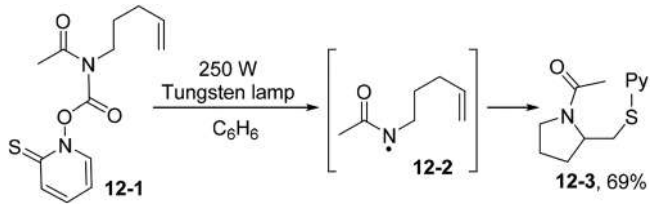

Scheme 6.12 Synthesis of *N*-acyl pyrrolidines *via* amidyl radicals.

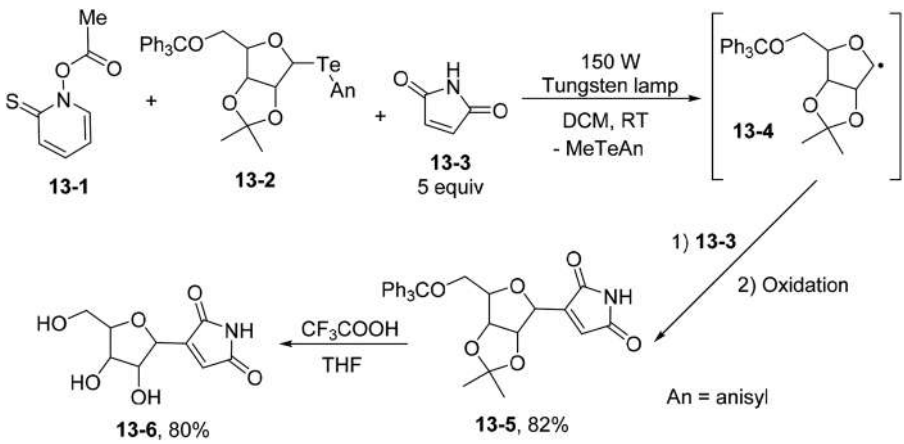

Scheme 6.13 Photoinduced synthesis of showdomycin.

12-1 (Scheme 6.12). Radical cyclization followed by incorporation of the -SPy group allowed the isolation of *N*-acyl pyrrolidine **12-3** in 69% yield.[65]

In rare instances, the radical formed from the decomposition of a Barton ester induced the generation of a further reactive radical by a radical substitution reaction. The latter strategy has been adopted for the synthesis of showdomycin **13-6** (a nucleoside antibiotic, Scheme 6.13). The photocleavage of the Barton ester **13-1** led to the liberation of the methyl radical that engaged a substitution reaction with compound **13-2** causing the cleavage of the labile C–Te bond along with the formation of radical **13-4**. Addition of this radical onto **13-3** afforded maleimide **13-5** in a quite good yield. Deprotection of the alcoholic groups released the desired **13-6**.[66]

6.2.4 Cyanoarenes

Cyanoarenes are important compounds that have opened the way for valuable electron transfer processes due to their high reduction potential in the excited state.[67] Some of them, such as 9,10-dicyanoanthracene (DCA) and 2,6,9,10-tetracyanoanthracene (TCA), are colored. Their typical reactions are

with electron donors[68] causing a photoaddition/photosubstitution onto the aromatic ring under visible light irradiation (Scheme 6.14).[69] As an example, a reaction was promoted by an initial electron transfer reaction between excited **14-1** and the α-silyl amine **14-2**. A trimethylsilyl cation was eliminated from the resulting radical ion couple and dinitrile **14-3** has been formed by radical–radical anion recombination. In other cases, this recombination led to an ipso-substitution reaction with cyanide loss.[70]

6.2.5 Azoderivatives of Formulae R–N=N–R

The azo group (N=N) is responsible for the visible light absorption in several classes of compounds. When the azo group is tethered to two aromatic rings, the resulting substituted (heteroaryl)azo derivatives, in the most stable *trans* configuration (**15-1**, Scheme 6.15), may undergo *E*/*Z* isomerization to the corresponding *cis* isomers **15-2**. The reaction is induced by the initial absorption of the weak band in the visible region due to the forbidden nπ* transition. The reaction may be reversed ($Z \rightarrow E$) simply by heating or by visible light absorption. Although this process has been used in several applications, it has limited synthetic importance.[71]

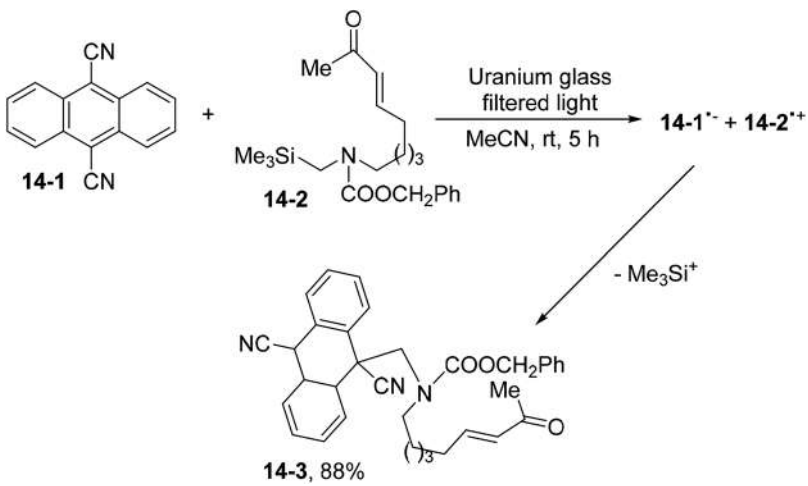

Scheme 6.14 Visible light functionalization of cyanoarenes.

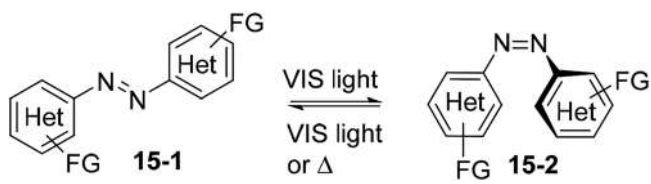

Scheme 6.15 $E \rightarrow Z$ isomerization in (heteroaryl)azo derivatives.

However, when at least one substituent of the diazo group is different from a (hetero)aromatic ring, a photocleavage liberating a dinitrogen molecule may take place finally leading to a photoextrusion reaction. In other instances, the N=N bond may be used for [4+2] photocycloadditions to promote a chemical dearomatization in nonactivated arenes.[72] A dated example is reported in Scheme 6.16, where the *N*-methyltriazolinedione **16-1** gave the photoadduct **16-2** at a low temperature upon white light exposure.[73] The reaction was effective also on naphthalene and phenanthrene as the aromatic partners.[73,74]

Compound **16-1** or related compounds have been used as N–N-arenophiles for the photoinduced dearomative dihydroxylation and diaminodihydroxylation of simple arenes. The reaction led to derivatized cyclohexenes and cyclohexadienes in turn used for the synthesis of biologically active compounds such as Conduramine A.[75]

Another important class of photolabile colored compounds (yellow to orange) incorporating the N=N bond moiety attracting increasing attention for application in synthesis is that of arylazo sulfones **17-1** (Scheme 6.17). These crystalline compounds may be considered as the shelf stable form of the corresponding aryl diazonium salts. Converting colorless diazonium salts into arylazo sulfones allows the incorporation of a dyedauxiliary group able to impart both color and photolability to the starting material.[76] Accordingly, under visible light irradiation a homolytic N–S cleavage occurred to form a diazenyl radical **17-2** and the sulfonyl radical **17-3**. An aryl radical **17-4** was then liberated upon nitrogen loss. Compounds **17-1** are very versatile[77] since both aryl radicals and sulfonyl radicals may be used for synthetic purposes.

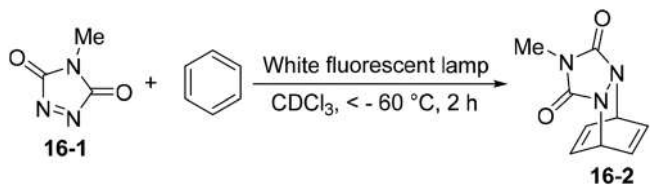

Scheme 6.16 Photochemical dearomatization *via* [4+2] photocycloadditions in nonactivated arenes.

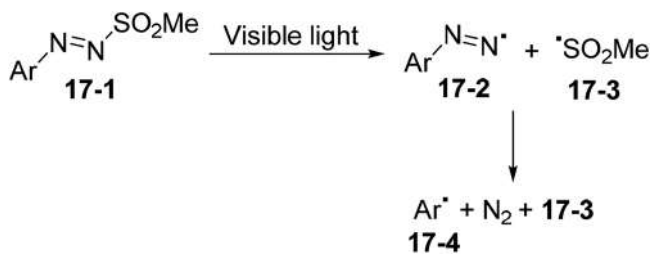

Scheme 6.17 Photocleavage in arylazo sulfones.

A collection of the processes feasible to forge Ar–C bonds is shown in Scheme 6.18 by using cyanoderivative **18-1** as the model. In all cases, a blue LED light (λ = 410–456 nm) was adopted to promote the reaction. Thus, aryl radicals may be trapped by five-membered ring heteroaromatics, including *N*-protected pyrrole **18-2**. The reaction was regioselective since only the 2-substituted derivative **18-3** was formed, albeit a large excess of **18-2** was required (Scheme 6.18, path *a*).[78] The reaction may be efficiently applied also to substituted furans and thiophenes.[78]

If the arylation took place on aryl boronic acids (*e.g.* **18-4**) under gold catalyzed conditions, an ipso-substitution resulted, directed by the presence of the $B(OH)_2$ group. The yields are, however, modest due to the competitive formation of homocoupling products (Scheme 6.18, path *b*).[79] A particular case was the trapping of the radical by isonitriles. Thus, compound **18-6** was able to trap the photogenerated aryl radical and oxidation of the resulting iminyl radical along with water addition facilitated the synthesis of amide **18-7** in a good yield (Scheme 6.18, path *c*). This carboamidation of aryl radicals was applied to the synthesis of the antidepressant moclobemide.[80]

In other instances, the dyedauxiliary group can be easily removed leaving a hydrogen (or a deuterium) atom instead. This hydro/deutero deamination was simply promoted in the absence of any additives since the reaction media (*i*PrOH/H_2O 9 : 1 or isopropanol-d^8/H_2O 9 : 1) functioned as a hydrogen donor in the process.[81]

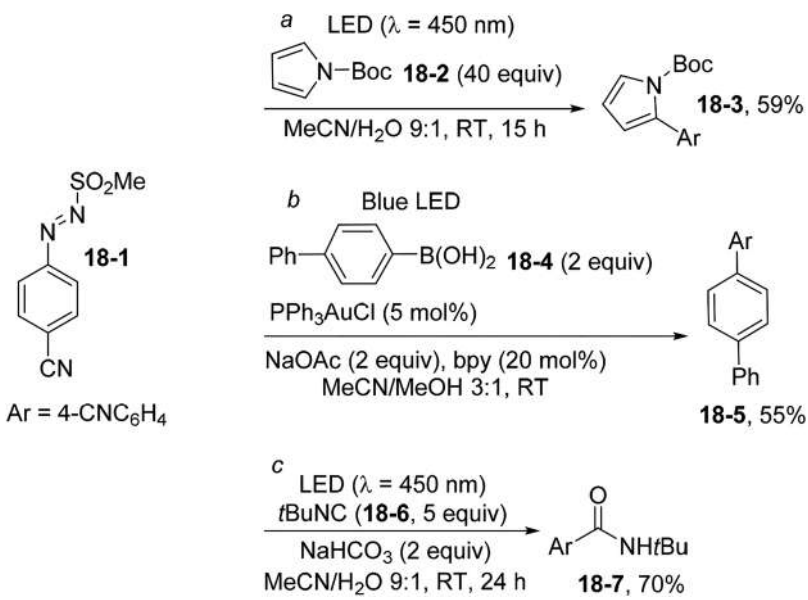

Scheme 6.18 Forging of C–C bonds *via* photogenerated aryl radicals.

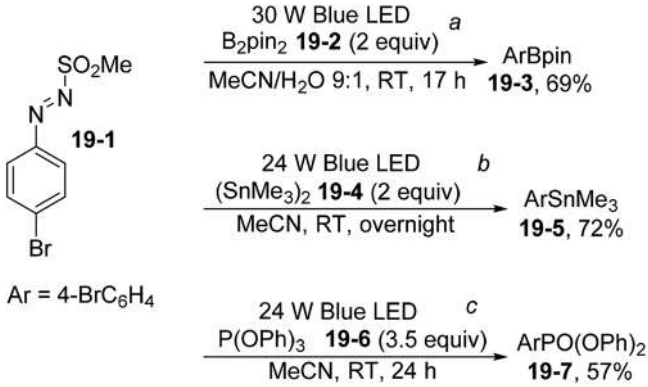

Scheme 6.19 Construction of C–X bonds *via* photogenerated aryl radicals.

When using suitable radical traps, it is possible to divert the usual C–C bond formation into the construction of a C–X bond, as exemplified in Scheme 6.19 Thus, blue LED irradiation of the brominated arylazo sulfone **19-1** in the presence of bis(pinacolato)diboron (**19-2**, B_2pin_2) gave the hoped for arylboronate **19-3** in a discrete yield (Scheme 6.19, path *a*).[82] Interestingly, the reaction repeated by using bisboronic acid followed by treatment with KHF_2 gave further access for the formation of a C–B bond, forming the corresponding aryl trifluoroborate salts.[82] Visible light was again used to promote the forging of an Ar–Sn bond in (hetero)aryl stannanes. The strategy was based on the reaction of the aryl radical generated from sulfone **19-1** with hexaalkyldistannane **19-4** that smoothly gave compound **19-5** in a good yield (Scheme 6.19, path *b*).[83] Similarly, a photoinduced Arbuzov-like process was devised by trapping of the aryl radical with a triaryl phosphite (**19-6**) to give an aryl phosphonate (**19-7**). The reaction showed a broad substrate scope and in selected cases the (hetero)aryl phosphonate can be prepared in up to gram scale (Scheme 6.19, path *c*).[84]

However, the release of the sulfonyl radical in the photolysis of arylazo sulfones may be used for the oxysulfonylation of alkenes. As an example, photolysis of **20-1** caused the liberation of radical **20-3** and addition onto styrene **20-2** followed by reaction with the oxygen of the resulting benzyl radical gave access to β-oxo sulfone **20-4** (Scheme 6.20).[85] β-Keto sulfones may be also formed by reaction of photogenerated **20-3** with phenyl alkynes under aerated conditions.[86] Moreover, when the sulfonyl radical attacked a cinnamic acid, a decarboxylative sulfonylation occurred to yield (*E*)-vinyl sulfones.[87]

6.2.6 4-Substituted-1,4-dihydropyridines

Although 1,4-dihydropyridine derivatives are well-known colored compounds, their use in synthesis is quite recent. The 4-aryl derivatives are, in some cases, known drugs such as Nifedipine (4-(2-nitrophenyl)-1,4-dihydropyridine).

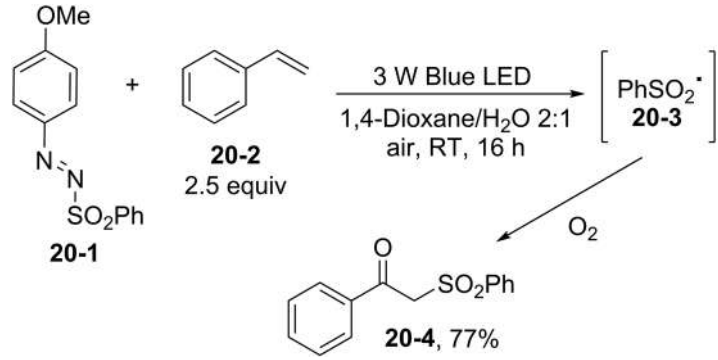

Scheme 6.20 Visible light-induced synthesis of β-keto sulfones.

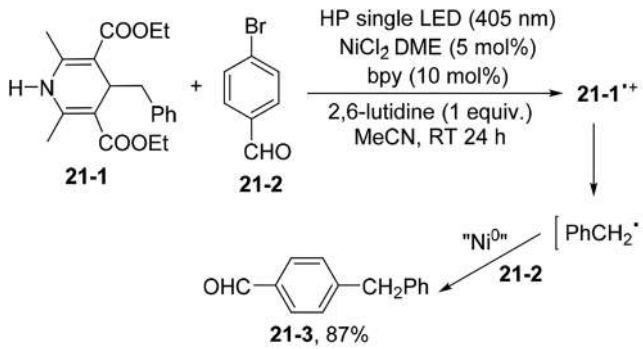

Scheme 6.21 Direct photocleavage of the C–C bond in 4-substituted 1,4-dihydropyridines.

This calcium-channel blocking drug is photoreactive *in vitro* and *in vivo* where the nitro group is converted to the corresponding nitroso group by exposure to visible light.[88,89] A particular class of 4-alkyl-1,4-dihydropyridines, however, known as Hantzsch esters (*e.g.* **21-1**, Scheme 6.21), has found application as electron donors,[90] proton sources[90] and alkyl radical precursors[49] in photoredox-catalyzed processes. Although in the latter applications these esters did not absorb the light directly, a recent example shown in Scheme 6.21 demonstrated that the photochemistry of these compounds may have a role when combined with a Ni-based catalyst. Thus, upon visible light excitation, compound **21-1** engaged in an electron transfer reaction with the metal catalyst to reduce the Ni^{II} precatalyst to the active Ni^{0} species. This species intercepted the benzyl radical (released by the fragmentation of **21-1**$^{\bullet+}$) and

an oxidative addition of aryl bromide **21-2** ensued to promote a $C(sp^2)$–$C(sp^3)$ cross-coupling process.[91]

As so far shown, visible light is an important tool for the easy generation of intermediates starting from selected classes of colored compounds. However, different classes of visible light absorbing derivatives may be adopted for the generation of a certain intermediate. Exemplary cases are when the compounds acted as the precursors of carbon or heteroatom-based radicals, carbenes and nitrenes.

6.2.7 Other Radical Precursors

In addition to the classes of compounds quoted so far, there are other derivatives that have sufficient absorption in the visible region to be able to release radicals by direct irradiation upon cleavage of a labile bond. An example is explained in Scheme 6.22. Ethyl difluoroiodoacetate **22-1** has a weak absorption in the 400–500 nm region, enough to cause the hydrodifluoroalkylation of alkyne **22-2.** The initial photocleavage of the C–I bond in compound **22-1** generated the difluoroalkyl radical that upon addition onto the triple bond formed a vinyl radical prone to abstract a hydrogen atom from the reaction medium to release the final styrene **22-3** in a good yield, but with a poor stereoselectivity.[92]

A carbon-centered radical may be formed in an indirect fashion. In fact, visible light induced (by a 100 W tungsten lamp) cleavage of the N–Br bond in certain bromoamides caused the liberation of a reactive nitrogen-based radical that abstracted a hydrogen atom from cycloalkanes leading to the preparation of the corresponding bromoalkanes in a modest yield.[93]

Another class of colored compounds that can be used for the formation of heteroatom-based radicals is that of diselenides. In fact, diphenyldiselenide has an absorption tail in the visible region related to the n → σ* transition.[94] The lability of the Se–Se bond has been used in various synthetic applications, such as the selenofunctionalization of alkenes (Scheme 6.23). Irradiation of diselenide **23-1** in the presence of cyclohexene derivative **23-2** and of CBr_4 caused the formation of **23-3** in an 85% yield. Compound **23-3** was further derivatized to form the Amaryllidaceae alkaloid (±)-γ-lycorane **23-4.**[95]

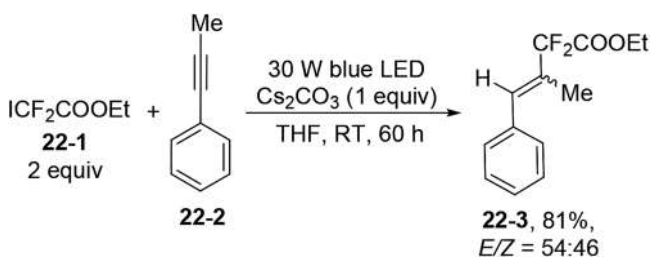

Scheme 6.22 Photocleavage of the C–I bond for the hydrodifluoroalkylation of alkynes.

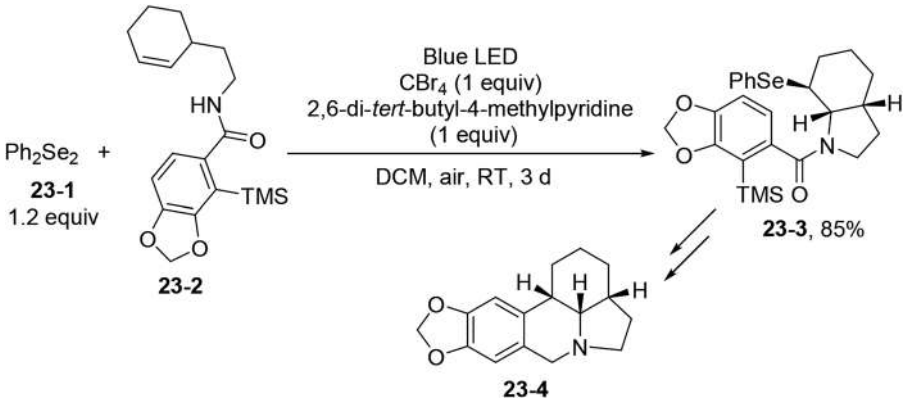

Scheme 6.23 Synthesis of the alkaloid (±)-γ-lycorane.

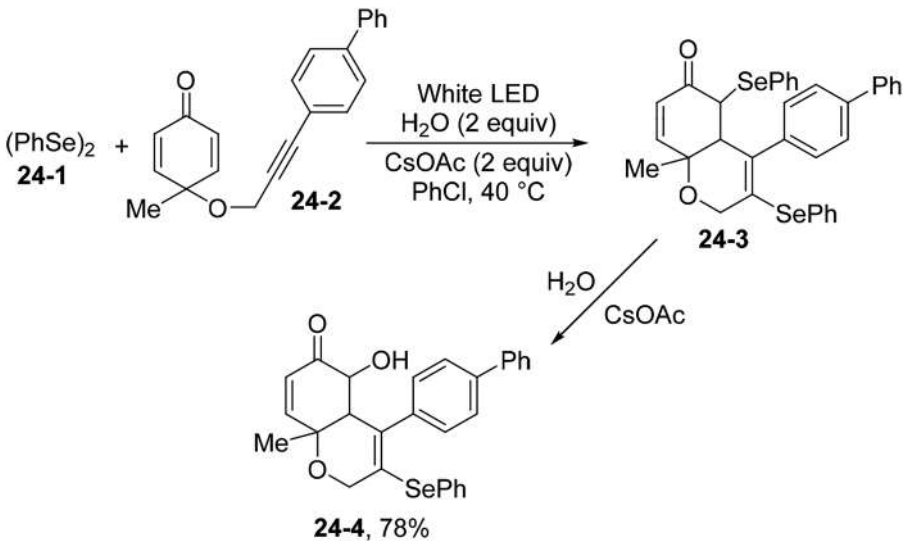

Scheme 6.24 Photogenerated phenylselenyl radicals for the preparation of chromen-6(5*H*)-ones.

The mechanism of the reaction is not clear but seems to involve the initial formation of the phenylselenyl radical prone to abstract a bromine atom from CBr_4 to yield PhSeBr.[95]

The addition of the phenylselenyl radical may take place on a triple C–C bond as shown in Scheme 6.24. This radical generated from the irradiation of **24-1** added to the C–C triple bond of **24-2** in a regioselective fashion to give an alkenyl radical that was engaged in an intramolecular addition onto the cyclohexadienone scaffold. The resulting α-keto radical captured another phenylselenyl radical to give compound **24-3**. Nucleophilic addition of water

promoted by the acetate base released the 5-hydroxy-3-selenyl-4*a*,8*a*-dihyd ro-2*H*-chromen-6(5*H*)-one **24-4**.[96] Noteworthily, compound **24-4** showed a potent cytotoxic activity against the HepG-2 cell line.[96]

Ynones **25-2a,b** were the elective substrates for the synthesis of 3-selenospiroindolenines (**25-4a,b**, a class of promising derivatives having an anticancer activity) in moderate to good yields (Scheme 6.25). The reaction involved the formation of the adduct radicals **25-3a,b**, followed by oxidation and removal of the hydrogen atom of the NH group by a base.[97]

In a related case, an aromatic homologated-ynone underwent the attack of a phenylselenyl radical under oxygenated conditions, thus inducing a dearomative selenylative carbo-spirocyclization to give spiro-cyclohexadienones.[98] If the reaction mixture comprised a phenyl acetylene, a diselenide and sulfur dioxide, a three-component reaction occurred to give β-sulfonylvinylselanes *via* the construction of multiple C–Se and C–S bonds.[99]

The selenium centered radical may likewise add to (hetero)aromatics as in the case of indole **26-2** (Scheme 6.26). Thus, blue light photolysis of diorganyl diselenides **26-1a–c** in the presence of **26-2** gave 3-selenylindoles **26-3a–c** in variable yields. The protocol was applied also for the functionalization of electron-rich arenes under mild conditions in a benign solvent (EtOH).[100]

An intriguing reaction was that involving the contemporary presence of two dichalcogenides. When a mixture of $(PhS)_2$ and $(PhSe)_2$ was irradiated in the presence of aromatic isocyanides (ArNC), thioselenated products were formed by the incorporation of both thio and seleno groups.[94]

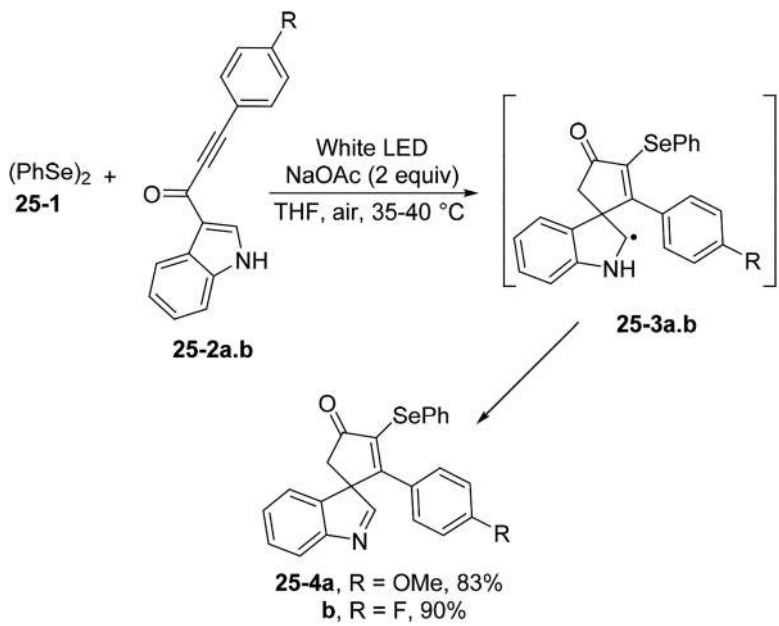

Scheme 6.25 Synthesis of 3-selenospiroindolenines.

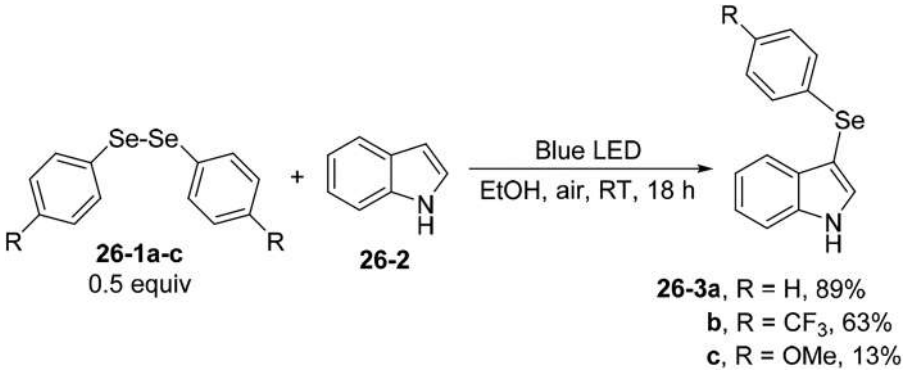

Scheme 6.26 Derivatization of indoles *via* irradiation of diorganyl diselenides.

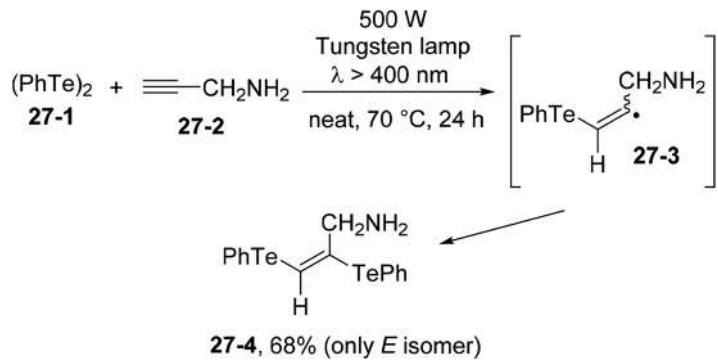

Scheme 6.27 Visible light induced forging of C–Te bonds.

Tellurium-based substituents may be easily introduced in organic compounds having recourse to photogenerated tellurium-based radicals (mainly from diaryltellurides **27-1**). These compounds absorb roughly in the 400–550 nm region,[101] thus causing the cleavage of the Te–Te bond. If the reaction was performed in the presence of acetylenes, bis(phenyltelluro)alkenes were formed *via* the construction of two C–Te bonds.[101] An example is shown in Scheme 6.27, where compound **27-2** underwent a photochemical ditelluration to give alkene **27-4** in a modest yield but in a complete *E* selectivity.[102]

Moreover, a regioselective thiotelluration took place making use of a $(PhS)_2$–$(PhTe)_2$ binary system that allowed the functionalization of norbornene **28-3** to prepare compound **28-4** in a good yield again by starting from a photogenerated PhTe$^{\bullet}$ (Scheme 6.28).[103]

An analogous thiotelluration was applied to the functionalization of isonitrile **29-3** where the nitroaromatic **29-4** was easily obtained (Scheme 6.29). Changing **29-3** with substituted 2-vinylphenyl isocyanides (or 2-allylphenyl isocyanides) the same protocol led to an intramolecular radical reaction, allowing the construction of the indole (or quinoline) nucleus.[104]

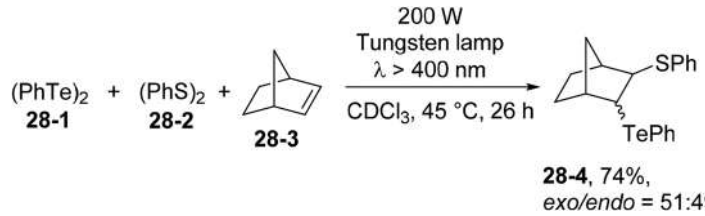

Scheme 6.28 Photoinduced three-component thiotelluration of norbornene.

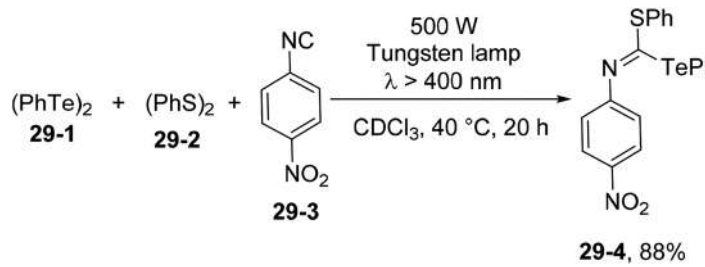

Scheme 6.29 Functionalization of aryl isocyanides *via* photocleavage of the C–Te bond.

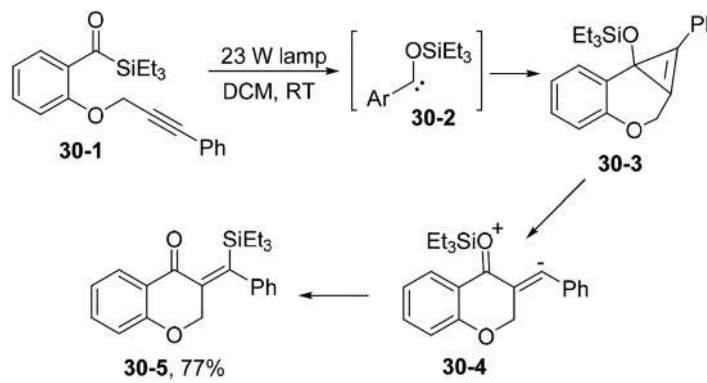

Scheme 6.30 Silylacylations *via* siloxycarbenes.

6.2.8 Carbene Precursors

Carbenes are useful intermediates that are emerging in synthetic planning thanks to their easy generation under visible light irradiation.[105–108] A class of carbene precursors is that of acyl silanes to be used in photochemical silylacylations. These compounds (*e.g.* **30-1**) underwent a photoinduced Brook rearrangement to form the nucleophilic siloxycarbene **30-2** prone to add intramolecularly to a triple C–C bond (Scheme 6.30). The resulting

cyclopropene adduct **30-3** underwent a retro-Brook rearrangement forming silylated chromone derivative **30-5**.[109]

The reaction likewise worked in an intermolecular fashion providing that an electrophilic alkyne was used as the coupling partner to furnish functionalized enonyl silanes in a good yield.[110] The photogenerated siloxycarbenes were likewise able to give insertion reactions within the B–H bond in HBpin allowing the easy preparation of α-alkoxyorganoboronate esters in almost quantitative yields. Mechanistic investigations demonstrated that the insertion occurred in a concerted manner arising from the T_1 state of the acylsilane.[111]

However, the most promising class of colored precursors of carbenes is that of diazo compounds (α-diazo ketones or α-diazo esters).[105,106] α-Diazo ketones are known to undergo Wolff rearrangement to form α-ketocarbenes and electrophilic ketenes. An asymmetric Wolff rearrangement has been used for the conversion of α-diazoketone **31-1** into α,α-disubstituted carboxylic ester **31-5** that was easily transformed into (*R*)-ibuprofen **31-6** (Scheme 6.31). Irradiation of **31-1** induced the formation of ketene **31-4** and thanks to the reaction with phenol **31-2** mediated by the interaction with the nucleophilic benzotetramisole-type catalyst (*S*)- **31-3**, the aryl ester **31-5** was formed. Elaboration of **31-5** led to the desired drug **31-6** in an excellent enantiomeric ratio.[112]

The ketene formed in the Wolff rearrangement can be intercepted also by a chiral isothiourea to catalyze a [4+2] annulation reaction with an aurone derived α,β-unsaturated imine for the synthesis of substituted 3,4-dihydrobenzofuro[3,2-*b*]pyridin-2(1*H*)-ones.[113] The photolysis of α-diazo ketones when carried out in the presence of a 3-alkylenyloxindole under *N*-heterocyclic carbene catalysis led to the stereoselective synthesis of tetrahydropyrano[2,3-*b*]indoles obtained in good yields with excellent diastereo- and enantioselectivities.[114] The photogenerated ketene may be engaged in a Pd-catalyzed [3+2] cycloaddition with vinyl cyclopropanes to give

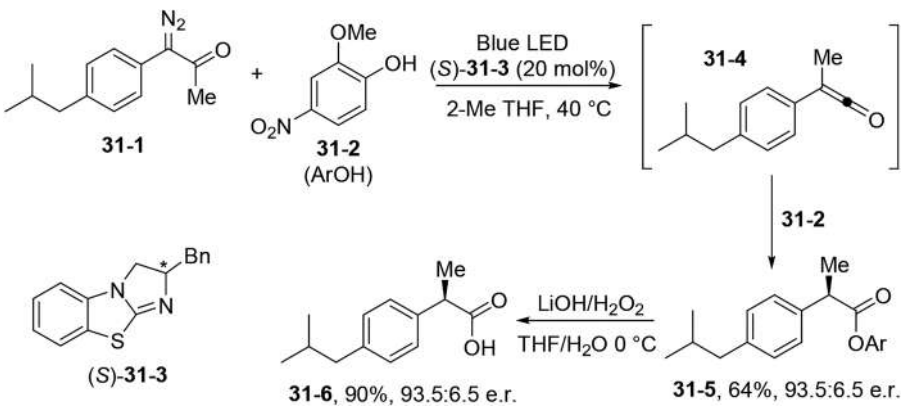

Scheme 6.31 Photochemical synthesis of (*R*)-ibuprofen.

highly functionalized tetrahydrofurans *via* a tandem C–C/C–O bond formation.[115] In a related process, an enantioselective [8+2] cycloaddition took place between the ketene (in the role of dipolarophile) and a Pd-containing 1,8-dipole (formed from a vinyl carbamate) to release a nitrogen containing 10-membered heterocycle bearing chiral quaternary stereocenters.[116]

When the diazoderivative bears an electron-withdrawing group different from a COAlk group, the resulting carbene did not undergo rearrangement and gave the typical carbene reactions. One typical case is the addition onto a double or a triple C–C bond leading to a cyclopropane or a cyclopropene, respectively. An example is shown in Scheme 6.32a where a cyclopropenation of phenyl acetylene **32-2** led to ester **32-4** in almost quantitative yield. Here, the use of blue light caused the dediazoniation of diazoderivative **32-1** to form carbene **32-3** as the reaction intermediate.[117] The reaction worked as well starting again from the same diazoderivative but in the presence of propargylic alcohols.[118]

In a related fashion, a cyclopropane has been formed by the photoinduced reaction of aryl(diazo)acetates with the double bond of a heteroaromatic ring to give cyclopropane-fused indolines. This metal-free mild approach was very straightforward and allowed the cyclopropanated derivative to be prepared in moderate to excellent yields and high diastereoselectivities.[119] The same reaction was carried out in an intramolecular fashion by reacting a diazoacetate obtained from a tryptamine. This intramolecular cyclopropanation promoted the synthesis of azepino[4,5-*b*]indoles in a satisfying yield.[120]

The addition of the photogenerated carbene can be regioselective as in the cyclopropanation of polyunsaturated carbocycles such as cyclooctatetraene, where only one C=C bond was functionalized to give a cyclic triene.[121] The formation of a cyclopropane may take place even on unreactive substrates, as exemplified in Scheme 6.32b. The aryl(diazo)acetate **32-1** upon visible light irradiation in neat benzene formed the norcaradiene **32-5** in a discrete yield in a highly regio- and stereoselective fashion.[122]

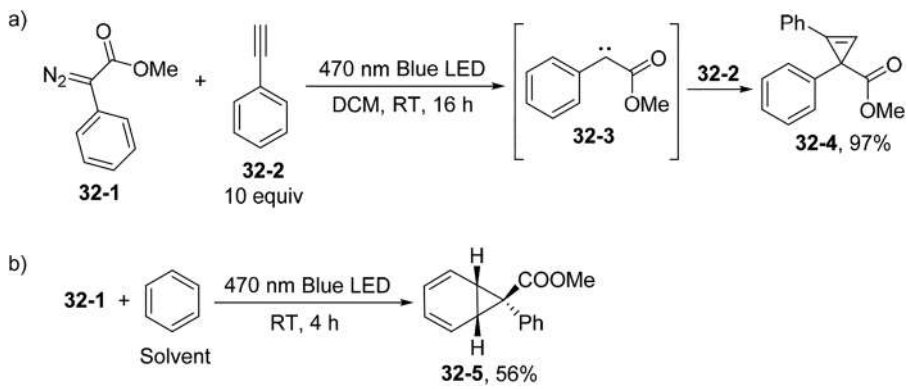

Scheme 6.32 Photogenerated carbenes for the synthesis of (a) cyclopropenes and of (b) norcaradienes.

A carbene may add to the n-type electrons of heteroatoms. The addition of carbenes to the sulfur or a nitrogen atom of allyl sulfides or allyl amines induced a formal [2,3]-sigmatropic shift mimicking in the former case the Doyle–Kirmse reaction. Visible light irradiation of diazoesters **33-1a–c** led to the generation of the corresponding carbenes in the singlet state that are easily trapped by the sulfur atom of allyl sulfide **33-2** forming the 3,3-difluoroallylated sulfonium ylides **33-3a–c** (Scheme 6.33a). The sigmatropic shift occurring on **33-3a–c** formed the highly functionalized *gem*-difluoroallyl esters **33-4a-c**.[123] When using propargylic sulfides in place of **33-2**, functionalized allenes were formed.[124] However, when using a *N*-sulfenyl phthalimide as the source of nucleophilic sulfur, a S–N insertion product was obtained by a [1,2] sigmatropic rearrangement taking place on the ylide intermediate.[125] The sulfur atom may be attacked by a carbene even when it is part of a C=S bond. The carbene obtained by irradiation of an α-diazo 1,3-diketone initially added to a β-ketothioamide to induce an *S*-alkylation and the *N*-cyclization occurring in the resulting *N*,*S*-acetal led to the thiazoline synthesis even on a gram scale.[126]

Interestingly, photolysis of α-diazoarylester **33-1a** in the presence of amine **33-5** furnished valuable α,α-disubstituted amino esters (*e.g.* **33-6**) by a [2,3]-sigmatropic shift *via* a free ammonium ylide (Scheme 6.33b).[127]

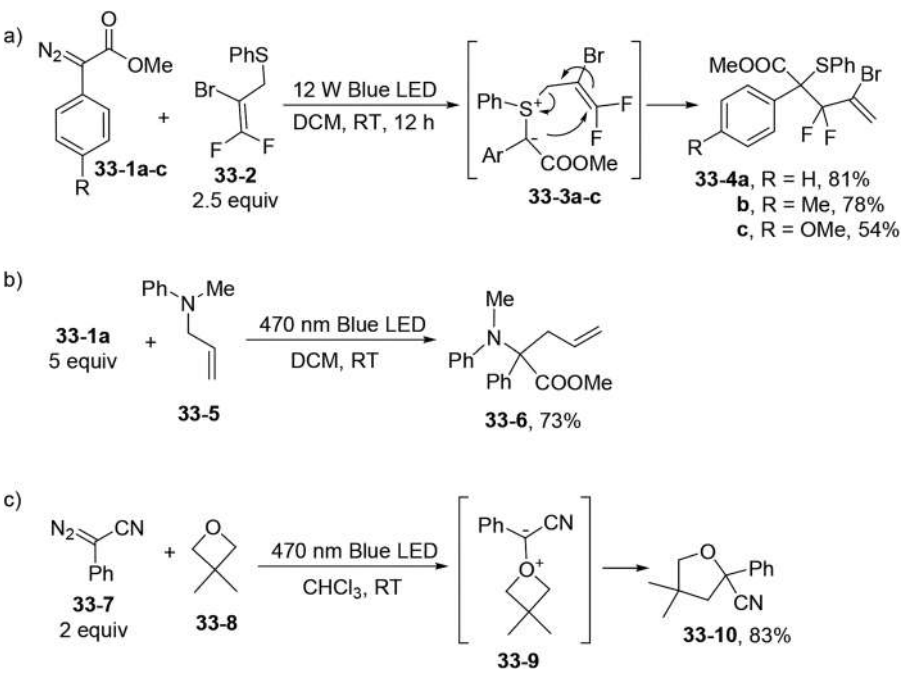

Scheme 6.33 Formation of ylides by the addition of a photogenerated carbene onto (a) allyl sulfides, (b) allyl amines and (c) oxetanes.

The addition of the carbene onto the oxygen atom (sulfur atom) in oxetanes (thietanes) caused a ring expansion process leading to substituted tetrahydrofurans (thiolanes). Scheme 6.33c shows a representative case where oxetane **33-8** is converted in tetrahydrofuran **33-10** *via* ylide **33-9**.[128] A related process again involving the formation of an oxonium ylide intermediate was reported in the attack of the carbene (formed from an α-aryldiazo ester) onto THF. The ylide then reacted with a carbamate anion formed *in situ* by the reaction of carbon dioxide and an amine to release a functionalized carbamate *via* a three-component process.[129] In one case, the oxonium ylide (generated by nucleophilic addition of 1,4-dioxane onto the carbene) may be intercepted by *N*-fluorobenzenesulfonimide (NFSI) to form the desired fluoroamino etherification product. This strategy has been applied for the development of novel opioid drugs.[130]

In rare instances, the carbene was trapped by a boron-containing compound. Thus, addition of an α-carboxymethyl carbene to a boronic acid formed in the usual way an ylide that upon 1,2-sigmatropic shift led to a substituted boronic acid that upon protodeboronation afforded a substituted ester. Some reactivity has been found even in the dark. This approach was applied to the preparation of bioactive Adiphenine, Benactyzine and Aprophen.[131]

Another typical reaction of carbenes is that of insertion into a X–H bond. Although this reaction may always happen when a carbene is generated, only in selected cases does this process have synthetic significance. A C–C bond has been smoothly forged by the C–H insertion of a carbene (derived from **34-1**) and cycloalkanes **34-2a–c** (Scheme 6.34a). Cycloalkyl adducts **34-3a–c**

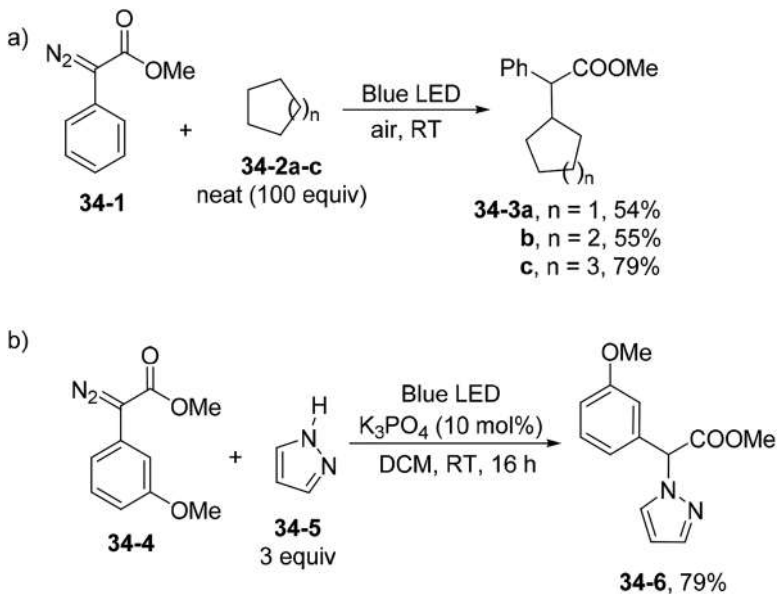

Scheme 6.34 Photoinduced insertion reactions on (a) a C–H bond and (b) a N–H bond.

were then formed at room temperature in modest to good yields.[132] Another valuable process was the N–H insertion into *N*-heterocycles. The reaction was effective when applied to carbazole and azepine heterocycles[133] as well as pyrazole **34-5** (Scheme 6.34b). In the latter case, the photochemical reaction between aryldiazoacetate **34-4** and **34-5** led to the N–H inserted product **34-6**.[134] The reaction met some success even when using 1,2,3-triazoles.[134] The visible light-induced insertion of carbenes into the Si–H bond of silanes was another application that led to α-trialkylsilyl esters.[135]

In particular cases, a mixture of two diazoesters may be selectively irradiated causing the photogeneration of a single carbene that reacted with the other diazoester to form a trisubstituted alkene (*E* configuration) *via* nitrogen loss.[136]

6.2.9 Nitrene Precursors

Nitrenes are other reactive nitrogen-based intermediates that are available under visible light irradiation. Vinyl azides are the preferred nitrene precursors. Thus, compound **35-1** produced nitrene **35-3** by a photodenitrogenative process that underwent an intramolecular attack on the double bond to form 2*H*-azirine **35-4** (Scheme 6.35). The three membered ring was opened by reaction with a cyanamide anion, finally leading to 2-aminoimidazole **35-6** (a useful key scaffold in medicinal chemistry) in a satisfying yield.[137]

If the photodecomposition took place of 3-(2-aminoaryl)-2-azido-1-arylpro p-2-en-1-ones, (*E*)-stilbenes were formed promoted by a 1,2-acyl migration in the reaction course.[138] α-Keto vinyl azides are the substrates that have been used in the preparation of substituted pyrroles. The approach was again based on the initial formation of a 2*H*-azirine.[139] To ameliorate the nitrene insertion into a C–H bond, another class of less hazardous nitrene precursors has been devised, namely aryl sulfilimines (**36-1**, Scheme 6.36).

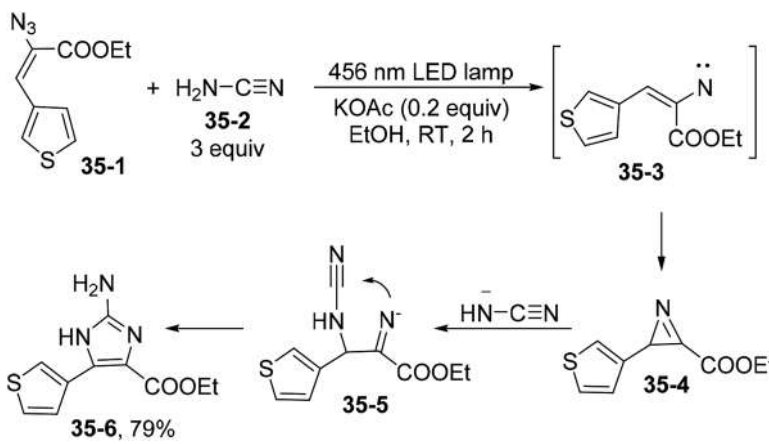

Scheme 6.35 Preparation of 2-aminoimidazoles *via* photogenerated nitrenes.

Scheme 6.36 Aryl sulfilimines as precursors of aryl nitrenes.

Thus, photolysis of **36-1** generated the corresponding nitrene, which upon intramolecular C–H insertion delivered the natural compound Clausine C (**36-2**) in a very good yield.[140]

6.3 Conclusions

As apparent from this work, despite the majority of organic compounds found in a laboratory being colorless, there are several classes of organic compounds that are photoreactive under visible light irradiation that can be used for synthetic purposes. In most cases, the color is due to a particular electronic transition (mainly n → π* or n → σ*) related to a given chromophore (*e.g.* a C=S, N=N, Se–Se or 1,2 diketone moiety). In other instances, a dyedauxiliary group[76] is purposely tethered to the compound in order to make it colored and photolabile (see the case of Barton esters and arylazo sulfones). This fact allows for the development of visible photon induced synthetic procedures that can be employed at an industrial level due to their low operational cost and, in favorable cases, may open a route to the extensive use of costless solar light widely available throughout the scientific world.

References

1. N. Hoffmann, *Chem. Rev.*, 2008, **108**, 1052.
2. T. Bach and J. P. Hehn, *Angew. Chem., Int. Ed.*, 2011, **50**, 1000.
3. M. D. Kärkäs, J. A. Porco Jr and C. R. J. Stephenson, *Chem. Rev.*, 2016, **116**, 9683.
4. M. Di Filippo, C. Bracken and M. Baumann, *Molecules*, 2020, **25**, 356.
5. S. Protti, M. Fagnoni and A. Albini, *Green Techniques for Organic Synthesis and Medicinal Chemistry*, ed. W. Zhang and B. W. Cue, John Wiley & Sons, Chichester, 2nd edn, 2018, pp. 373–406.
6. A. Albini and M. Fagnoni, *Green Chem.*, 2004, **6**, 1.
7. A. Albini and M. Fagnoni, *ChemSusChem*, 2008, **1**, 63.
8. A. Albini and M. Fagnoni, *New Methodologies and Techniques for a Sustainable Organic Chemistry*, ed. A. Mordini and F. Faigl, Springer Science + Business Media B.V., 2008, pp. 279–293.

9. A. Albini and M. Fagnoni, *Green Chemical Reactions*, ed. P. Tundo and V. Esposito, Springer Science + Business Media B.V., 2008, pp. 173–189.
10. A. Albini and M. Fagnoni, *ChemSusChem*, 2008, **1**, 63.
11. S. Protti, S. Manzini, M. Fagnoni and A. Albini, *Eco-friendly Synthesis of Fine Chemicals*, ed. R. Ballini, *RSC Green Chemistry Book Series*, Royal Society of Chemistry, 2009, pp. 80–111.
12. A. Albini and L. Germani, *Handbook of Synthetic Photochemistry*, ed. A. Albini and M. Fagnoni, Wiley-VCH Verlag, Weinheim, 2010, pp. 1–24.
13. G. Ciamician, *Science*, 1912, **36**, 385.
14. P. Esser, B. Pohlmann and H. D. Scharf, *Angew. Chem., Int. Ed. Engl.*, 1994, **33**, 2009.
15. M. Oelgemoeller, C. Jung and J. Mattay, *Pure Appl. Chem.*, 2007, **79**, 1939.
16. V. Balzani, A. Credi and M. Venturi, *ChemSusChem*, 2008, **1**, 26.
17. S. Protti and M. Fagnoni, *Photochem. Photobiol. Sci.*, 2009, **8**, 1499.
18. D. M. Schultz and T. P. Yoon, *Science*, 2014, **343**, 985.
19. D. Ravelli, S. Protti and M. Fagnoni, *Applied Photochemistry: When Light Meets Molecules*, ed. G. Bergamini and S. Silvi, Springer International Publishing, Switzerland, 2016, pp. 281–342.
20. *Photochemically-generated Intermediates in Synthesis*, ed. A. Albini and M. Fagnoni, John Wiley & Sons, Hoboken, 2013, pp. 1–40.
21. B. Siewert and H. Stuppner, *Phytomedicine*, 2019, **60**, 152985.
22. D. Ravelli, D. Dondi, M. Fagnoni and A. Albini, *Chem. Soc. Rev.*, 2009, **38**, 1999.
23. T. P. Yoon, M. A. Ischay and J. Du, *Nat. Chem.*, 2010, **2**, 527.
24. *Chemical Photocatalysis*, ed. B. Koenig, De Gruyter, Berlin, Germany, 2013.
25. *Visible Light Photocatalysis in Organic Chemistry*, ed. C. R. J. Stephenson, T. P. Yoon and D. W. C. MacMillan, Wiley-VCH, Weinheim, Germany, 2018.
26. *Photoorganocatalysis in Organic Synthesis*, ed. M. Fagnoni, P. Protti and D. Ravelli, World Scientific Publishing Europe, Ltd, Singapore, 2019.
27. *Green Photocatalysts. Environmental Chemistry for a Sustainable World*, ed. M. Naushad, S. Rajendran and E. Lichtfouse, Springer Nature Switzerland AG, 2020, vol. 34.
28. C. Brenninger, J. D. Jolliffe and T. Bach, *Angew. Chem., Int. Ed.*, 2018, **57**, 14338.
29. C. G. S. Lima, T. de M. Lima, M. Duarte, I. D. Jurberg and M. W. Paixão, *ACS Catal.*, 2016, **6**, 1389.
30. G. E. M. Crisenza, D. Mazzarella and P. Melchiorre, *J. Am. Chem. Soc.*, 2020, **142**, 5461.
31. Y.-Q. Yuan, S. Majumder, M.-H. Yang and S.-R. Guo, *Tetrahedron Lett.*, 2020, **61**, 151506.
32. B. Schweitzer-Chaput, M. A. Horwitz, E. de Pedro Beato and P. Melchiorre, *Nat. Chem.*, 2019, **11**, 129.
33. J. D. Coyle, *Tetrahedron*, 1985, **41**, 5393.
34. A. Couture, J. Gdmez and P. de Mayo, *J. Org. Chem.*, 1981, **46**, 2010.

35. A. Couture, M. Hoshino and P. de Mayo, *J. Chem. Soc., Chem. Commun.*, 1976, 131.
36. C. Raviola and D. Ravelli, *Synlett*, 2019, **30**, 803.
37. S. Kamijo, K. Kamijo, K. Maruoka and T. Murafuji, *Org. Lett.*, 2016, **18**, 6516.
38. M. B. Rubin, Recent photochemistry of α-diketones, in *Photochemistry and Organic Synthesis*, *Topics in Current Chemistry*, Springer, Berlin, Heidelberg, 1985, vol. 129.
39. C. Huang, M. Zheng, J. Xu and Y. Zhang, *Molecules*, 2013, **18**, 2942.
40. C. C. Liao and H. S. Lin, *J. Am. Chem. Soc.*, 1982, **104**, 292.
41. Y. Zhang, J. Xue, Y. Gao, H.-K. Fun and J.-H. Xu, *J. Chem. Soc., Perkin Trans. 1*, 2002, 345.
42. D. Alvarez-Dorta, E. León, A. R. Kennedy, C. Riesco-Fagundo and E. Suárez, *Angew. Chem., Int. Ed.*, 2008, **47**, 8917.
43. D. Alvarez-Dorta, E. Leòn, A. R. Kennedy, A. Martìn, I. Pèrez-Martìn, C. Riesco-Fagundo and E. Suàrez, *Chem. - Eur. J.*, 2014, **20**, 2663.
44. A. J. Herrera, M. Rondón and E. Suárez, *J. Org. Chem.*, 2008, **73**, 3384.
45. S. Yoshioka, M. Nagatomo and M. Inoue, *Org. Lett.*, 2015, **17**, 90.
46. F. Secci, S. Porcu, A. Luridiana, A. Frongia and P. C. Ricci, *Org. Biomol. Chem.*, 2020, **18**, 3684.
47. J. S. Ham, B. Park, M. Son, J. B. Roque, J. Jurczyk, C. S. Yeung, M.-H. Baik and R. Sarpong, *J. Am. Chem. Soc.*, 2020, **142**, 13041.
48. M. F. Saraiva, M. R. C. Couri, M. Le Hyaric and M. V. de Almeida, *Tetrahedron*, 2009, **65**, 3563.
49. S. Crespi and M. Fagnoni, *Chem. Rev.*, 2020, **120**, 9790.
50. R. S. J. Proctor and R. J. Phipps, *Angew. Chem., Int. Ed.*, 2019, **58**, 13666.
51. D. H. R. Barton, B. Garcia, H. Togo and S. Z. Zard, *Tetrahedron Lett.*, 1986, **27**, 1327.
52. D. H. R. Barton, J. Cs. Jaszberenyi and E. A. Theodorakis, *Tetrahedron Lett.*, 1991, **32**, 3321.
53. D. H. R. Barton, J. Cs. Jaszberenyi and E. A. Theodorakis, *Tetrahedron*, 1992, **48**, 2613.
54. P. Girard, N. Guillot, W. B. Motherwell, R. S. Hay-Motherwell and P. Potier, *Tetrahedron*, 1999, **55**, 3573.
55. D. S. Masterson and N. A. Porter, *Org. Lett.*, 2002, **4**, 4253.
56. D. H. R. Barton and J. Zhu, *J. Am. Chem. Soc.*, 1993, **115**, 2071.
57. D. H. R. Barton, S. D. Géro, P. Holliday, B. Quielet-Sire and S. Z. Zard, *Tetrahedron*, 1998, **54**, 6751.
58. D. H. R. Barton, B. Lather, B. Misterkiewicz and S. Z. Zard, *Tetrahedron*, 1988, **44**, 1153.
59. M. E. Attardi and M. Taddei, *Tetrahedron Lett.*, 2001, **42**, 3519.
60. P. A. Procopiou, K. Biggadike, A. F. English, R. M. Farrell, G. N. Hagger, A. P. Hancock, M. V. Haase, W. R. Irving, M. Sareen, M. A. Snowden, Y. E. Solanke, C. J. Tralau-Stewart, S. E. Walton and J. A. Wood, *J. Med. Chem.*, 2001, **44**, 602.
61. C. H. Schiesser and K. Sutej, *J. Chem. Soc., Chem. Commun.*, 1992, 57.

62. J. Boivin, E. Fouquet and S. Z. Zard, *Tetrahedron Lett.*, 1991, **32**, 4299.
63. J. Boivin, E. Fouquet, A.-M. Schiano and S. Z. Zard, *Tetrahedron*, 1994, **50**, 1769.
64. M. C. Fong and C. H. Schiesser, *Tetrahedron Lett.*, 1993, **34**, 4347.
65. J. L. Esker and M. Newcomb, *J. Org. Chem.*, 1994, **59**, 2779.
66. D. H. R. Barton and M. Ramesh, *J. Am. Chem. Soc.*, 1990, **112**, 891.
67. M. Mella, M. Fagnoni, M. Freccero, E. Fasani and A. Albini, *Chem. Soc. Rev.*, 1998, **27**, 81.
68. I. R. Gould, D. Ege, J. E. Moser and S. Farid, *J. Am. Chem. Soc.*, 1990, **112**, 4290.
69. Y. T. Jeon, C.-P. Lee and P. S. Mariano, *J. Am. Chem. Soc.*, 1991, **113**, 8847.
70. E. Hasegawa, M. A. Brumfield, P. S. Mariano and U.-C. Yoon, *J. Org. Chem.*, 1988, **53**, 5435.
71. H. M. D. Bandarab and S. C. Burdette, *Chem. Soc. Rev.*, 2012, **41**, 1809.
72. W. C. Wertjes, E. H. Southgate and D. Sarlah, *Chem. Soc. Rev.*, 2018, **47**, 7996.
73. S. J. Hamrock and R. S. Sheridan, *J. Am. Chem. Soc.*, 1989, **111**, 9247.
74. D. P. Kjell and R. S. Sheridan, *J. Am. Chem. Soc.*, 1984, **106**, 5368.
75. E. H. Southgate, J. Pospech, J. Fu, D. R. Holycross and D. Sarlah, *Nat. Chem.*, 2016, **8**, 922.
76. D. Qiu, C. Lian, J. Mao, M. Fagnoni and S. Protti, *J. Org. Chem.*, 2020, **85**, 12813.
77. N. Kamigata and M. Kobayashi, *Sulfur Rep.*, 1982, **2**, 87.
78. S. Crespi, S. Protti and M. Fagnoni, *J. Org. Chem.*, 2016, **81**, 9612.
79. C. Sauer, Y. Liu, A. De Nisi, S. Protti, M. Fagnoni and M. Bandini, *ChemCatChem*, 2017, **9**, 4456.
80. M. Malacarne, S. Protti and M. Fagnoni, *Adv. Synth. Catal.*, 2017, **359**, 3826.
81. H. I. M. Amin, C. Raviola, A. A. Amin, B. Mannucci, S. Protti and M. Fagnoni, *Molecules*, 2019, **24**, 2164.
82. Y. Xu, X. Yang and H. Fang, *J. Org. Chem.*, 2018, **83**, 12831.
83. C. Lian, G. Yue, J. Mao, D. Liu, Y. Ding, Z. Liu, D. Qiu, X. Zhao, K. Lu, M. Fagnoni and S. Protti, *Org. Lett.*, 2019, **21**, 5187.
84. D. Qiu, C. Lian, J. Mao, Y. Ding, Z. Liu, L. Wei, M. Fagnoni and S. Protti, *Adv. Synth. Catal.*, 2019, **361**, 5239.
85. Q. Liu, F. Liu, H. Yue, X. Zhao, J. Li and W. Wei, *Adv. Synth. Catal.*, 2019, **361**, 5277.
86. Y. Lv, Q. Liu, F. Liu, H. Yue, J. Li and W. Wei, *Tetrahedron Lett.*, 2020, **61**, 151335.
87. R. Chawla, S. Jaiswal, P. K. Dutta and L. D. S. Yadav, *Tetrahedron Lett.*, 2020, **61**, 151898.
88. H. de Vries and G. M. J. Beijersbergen van Henegouwen, *J. Photochem. Photobiol., B*, 1998, **43**, 217.
89. E. Fasani, D. Dondi, A. Ricci and A. Albini, *Photochem. Photobiol.*, 2006, **82**, 225.
90. P.-Z. Wang, J.-R. Chen and W.-J. Xiao, *Org. Biomol. Chem.*, 2019, **17**, 6936.

91. L. Buzzetti, A. Prieto, S. R. Roy and P. Melchiorre, *Angew. Chem., Int. Ed.*, 2017, **56**, 15039.
92. K. Li, X. Zhang, J. Chen, Y. Gao, C. Yang, K. Zhang, Y. Zhou and B. Fan, *Org. Lett.*, 2019, **21**, 9914.
93. V. A. Schmidt, R. K. Quinn, A. T. Brusoe and E. J. Alexanian, *J. Am. Chem. Soc.*, 2014, **136**, 14389.
94. K. Tsuchii, Y. Tsuboi, S.-i. Kawaguchi, J. Takahashi, N. Sonoda, A. Nomoto and A. Ogawa, *J. Org. Chem.*, 2007, **72**, 415.
95. E. S. Conner, K. E. Crocker, R. G. Fernando, F. R. Fronczek, G. G. Stanley and J. R. Ragains, *Org. Lett.*, 2013, **15**, 5558.
96. X.-L. Ma, Q. Wang, X.-Y. Feng, Z.-Y. Mo, Y.-M. Pan, Y.-Y. Chen, M. Xin and Y.-L. Xu, *Green Chem.*, 2019, **21**, 3547.
97. X. J. Zhou, H.-Y. Liu, Z.-Y. Mo, X.-L. Ma, Y.-Y. Chen, H.-T. Tang, Y.-M. Pan and Y.-L. Xu, *Chem. - Asian J.*, 2020, **15**, 1536.
98. S. R. Sahoo, B. Das, D. Sarkar, F. Henkel and H. Reuter, *Eur. J. Org. Chem.*, 2020, 891.
99. H. Chen, R. Ding, H. Tang, Y. Pan, Y. Xu and Y. Chen, *Chem. - Asian J.*, 2019, **14**, 3264.
100. I. D. Lemir, W. D. Castro-Godoy, A. A. Heredia, L. C. Schmidt and J. E. Argüello, *RSC Adv.*, 2019, **9**, 22685.
101. A. Ogawa, K. Yokoyama, H. Yokoyama, R. Obayashi, N. Kambe and N. Sonoda, *J. Chem. Soc., Chem. Commun.*, 1991, 1748.
102. A. Ogawa, K. Yokoyama, R. Obayashi, L.-B. Han, N. Kambe and N. Sonoda, *Tetrahedron*, 1993, **49**, 1177.
103. A. Ogawa, I. Ogawa, R. Obayashi, K. Umezu, M. Doi and T. Hirao, *J. Org. Chem.*, 1999, **64**, 86.
104. T. Mitamura, Y. Tsuboi, K. Iwata, K. Tsuchii, A. Nomoto, M. Sonoda and A. Ogawa, *Tetrahedron Lett.*, 2007, **48**, 5953.
105. N. R. Candeias and C. A. M. Afonso, *Curr. Org. Chem.*, 2009, **13**, 763.
106. Ł. W. Ciszewski, K. Rybicka-Jasińska and D. Gryko, *Org. Biomol. Chem.*, 2019, **17**, 432.
107. C. Empel and R. M. Koenigs, *Synlett*, 2019, **30**, 1929.
108. D. L. Priebbenow, *Adv. Synth. Catal.*, 2020, **362**, 1927.
109. H.-J. Zhang, P. Becker, H. Huang, R. Pirwerdjan, F.-F. Pan and C. Bolm, *Adv. Synth. Catal.*, 2012, **354**, 2157–2161.
110. P. Becker, D. L. Priebbenow, H.-J. Zhang, R. Pirwerdjan and C. Bolm, *J. Org. Chem.*, 2014, **79**, 814.
111. J.-H. Ye, L. Quach, T. Paulisch and F. Glorius, *J. Am. Chem. Soc.*, 2019, **141**, 16227.
112. J. Meng, W.-W. Ding and Z.-Y. Han, *Org. Lett.*, 2019, **21**, 9801.
113. T. Fan, Z.-J. Zhang, Y.-C. Zhang and J. Song, *Org. Lett.*, 2019, **21**, 7897.
114. C. Wang, Z. Wang, J. Yang, S.-H. Shi and X.-P. Hui, *Org. Lett.*, 2020, **22**, 4440.
115. J. Liu, M.-M. Li, B.-L. Qu, L.-Q. Lu and W.-J. Xiao, *Chem. Commun.*, 2019, **55**, 2031.

116. Q.-L. Zhang, Q. Xiong, M.-M. Li, W. Xiong, B. Shi, Y. Lan, L.-Q. Lu and W.-J. Xiao, *Angew. Chem., Int. Ed.*, 2020, **59**, 14096.
117. R. Hommelsheim, Y. Guo, Z. Yang, C. Empel and R. M. Koenigs, *Angew. Chem., Int. Ed.*, 2019, **58**, 1203.
118. F. He and R. M. Koenigs, *Chem. Commun.*, 2019, **55**, 4881.
119. X. Zhang, C. Du, H. Zhang, X.-C. Li, Y.-L. Wang, J.-L. Niu and M.-P. Song, *Synthesis*, 2019, **51**, 889.
120. J. Chauhan, M. K. Ravva, L. Gremaud and S. Sen, *Org. Lett.*, 2020, **22**, 4537.
121. Y. Guo, C. Empel, C. Pei, I. Atodiresei, T. Fallon and R. M. Koenigs, *Org. Lett.*, 2020, **22**, 5126.
122. Y. Guo, T. V. Nguyen and R. M. Koenigs, *Org. Lett.*, 2019, **21**, 8814.
123. J. Yang, J. Wang, H. Huang, G. Qin, Y. Jiang and T. Xiao, *Org. Lett.*, 2019, **21**, 2654.
124. K. Orłowska, K. Rybicka-Jasińska, P. Krajewski and D. Gryko, *Org. Lett.*, 2020, **22**, 1018.
125. Z. Yang, Y. Guo and R. M. Koenigs, *Chem. - Eur. J.*, 2019, **25**, 6703.
126. M. Arbaz Ansari, D. Yadav and M. S. Singh, *Chem. - Eur. J.*, 2020, **26**, 8083.
127. F. Li, F. He and R. M. Koenigs, *Synthesis*, 2019, **51**, 4348.
128. S. Jana, Z. Yang, C. Pei, X. Xu and R. M. Koenigs, *Chem. Sci.*, 2019, **10**, 10129.
129. R. Cheng, C. Qi, L. Wang, W. Xiong, H. Liu and H. Jiang, *Green Chem.*, 2020, **22**, 4890.
130. F. He, C. Pei and R. M. Koenigs, *Chem. Commun.*, 2020, **56**, 599.
131. A. F. da Silva, M. A. S. Afonso, R. A. Cormanich and I. D. Jurberg, *Chem. - Eur. J.*, 2020, **26**, 5648.
132. I. Jurberg and H. M. L. Davies, *Chem. Sci.*, 2018, **9**, 5112.
133. C. Empel, F. W. Patureau and R. M. Koenigs, *J. Org. Chem.*, 2019, **84**, 11316.
134. M. L. Stivanin, A. A. G. Fernandes, A. F. da Silva, C. Y. Okada Jr and I. D. Jurberg, *Adv. Synth. Catal.*, 2020, **362**, 1106.
135. F. He, F. Li and R. M. Koenigs, *J. Org. Chem.*, 2020, **85**, 1240.
136. T. Xiao, M. Mei, Y. He and L. Zhou, *Chem. Commun.*, 2018, **54**, 8865.
137. L. Man, R. C. B. Copley and A. L. Handlon, *Org. Biomol. Chem.*, 2019, **17**, 6566.
138. S. Borra, L. Borkotoky, U. D. Newar, A. Kalwar, B. Das and R. A. Maurya, *Org. Biomol. Chem.*, 2019, **17**, 5971.
139. S. Borra, L. Borkotoky, U. D. Newar, B. Das and R. A. Maurya, *Adv. Synth. Catal.*, 2020, **362**, 3364.
140. X. Tian, L. Song and A. S. K. Hashmi, *Angew. Chem., Int. Ed.*, 2020, **59**, 12342.

CHAPTER 7

Activation of Chemical Substrates Under Sustainable Conditions: Mechanochemistry

VJEKOSLAV ŠTRUKIL*[a] AND DAVOR MARGETIĆ[a]

[a]Ruđer Bošković Institute, Bijenička cesta 54, 10000 Zagreb, Croatia
*E-mail: vstrukil@irb.hr

7.1 Introduction

With growing concerns about the negative impact of industry on the environment, the last few decades have witnessed enormous efforts in the chemistry community to come up with new concepts that would enable clean and sustainable production of chemicals. This search for efficient processes, producing less waste and consuming less energy, gave birth to green chemistry – a subdiscipline of modern chemical science devoted to the design and development of environmentally friendly methodologies following the Twelve Principles of Green Chemistry.[1] In this respect, mechanochemical grinding and milling have been recognised to fully comply with the requirements of green chemistry. Emerging at the interface of materials chemistry, organic synthesis, catalysis and pharmaceutical science, mechanochemistry is expected to play an important role in relieving the stress on the environment and reducing the pollution from chemical sources in the years to come. The importance and potential of mechanochemistry was ultimately recognized by the International Union for Pure and Applied Chemistry (IUPAC) in 2019 when it was ranked on the list of ten chemical innovations that would change the world.[2]

Sustainable Organic Synthesis: Tools and Strategies
Edited by Stefano Protti and Alessandro Palmieri

Published by the Royal Society of Chemistry, www.rsc.org

For a long time, mechanochemical phenomena have been unrighteously neglected in preparative chemistry. Although mechanical processing of substrates dates back to prehistoric times, it was only in the 19th century that the first systematic observations of chemical reactions induced by external force began. An American scientist, Matthew Carey Lea, known in the literature as "*the father of mechanochemistry*", made notes on the effect of weak shearing forces on decomposition of silver and mercury halides during manual grinding.[3] He realised that those effects were different from the ones induced by heat in thermochemical reactions, paving the way to the establishment of mechanochemistry as an independent discipline within physical chemistry. It would take another century for chemists to rediscover and fully exploit mechanochemical reactivity as a tool to make organic molecules, or even go beyond into the realm of supramolecular chemistry and crystal engineering.

The popularity of mechanochemistry has been increasing over the last two decades. This is not surprising since performing reactions in the solid state by means of manual grinding or automated ball milling offers many advantages over conventional stirring and/or heating in solution. Due to the inherent solid-state character of mechanochemical reactions, toxic and harmful solvents are eliminated, or their amount reduced to only catalytic quantities, while reagent solubility (and possibly reactivity in solvents) poses no additional issues. An additional benefit in this respect is the broad choice of potential reactants. Next, the ability to control the reaction environment and milling parameters affords high efficiency (often quantitative), selectivity and product purity, making purification simple or even unnecessary. Such reactions typically take place at room temperature (or slightly above), but are fast enough to allow for a high-throughput screening operation mode. All this has made solid-state grinding and milling an attractive area of research, which is particularly visible in the field of organic synthesis where thousands of examples have been described and already reviewed in several excellent contributions.[4–6] Although mechanochemistry has found applications across different areas of research, this chapter will primarily focus on its use in organic synthesis and is intended to provide readers with background information on how to set up, run and analyze mechanochemical reactions, including several recent examples.

7.2 Methodology in Mechanochemistry

7.2.1 Laboratory Instrumentation

The most essential piece of equipment in mechanochemistry research is a reactor where an external oscillating physical force is exerted on the reaction mixture. Such energy conversion from mechanical into chemical is traditionally performed by manual grinding using a mortar and pestle. This simple grinding tool that has been in use for thousands of years in various forms, has become a trademark of mechanochemistry and is available in almost every chemical laboratory. Despite numerous examples of successful solid-state

transformations carried out by manual grinding, this approach becomes inadequate when moisture- and/or air-sensitive, volatile and toxic reagents are used, especially if prolonged manual agitation is required. Moreover, the control over parameters such as the intensity and homogeneity of mixing is hard to achieve and may lead to inconsistent results which are difficult to reproduce.

Nowadays, mortar and pestle grinders have been superseded by electrical automated ball mills as they offer multiple advantages over manual grinding. Precise control of parameters such as milling time and frequency, number, size and material of milling balls and jars, filling degree, ball-to-powder ratio *etc.* allows for systematic investigations of mechanochemical reactions. Furthermore, reaction vessels are tightly sealed during milling, and hence the whole process can be conducted in a controlled atmosphere, even with gaseous reactants.[7] This also eliminates safety issues of working with hazardous chemicals. In addition, their relatively low cost, dimensions, robustness and easy maintenance make this equipment perfectly suited for modern laboratory research, but also for teaching purposes in schools and universities. The most popular ball milling instruments are mixer (or shaker) mills and planetary mills (see Figure 7.1). Although they differ in construction, the basic physical mechanisms are the same and rely on exerting friction and shearing forces, along with high-energy impacts.

In the case of a mixer ball mill, the principal mode of action is by impact. A sample is placed in a jar containing milling balls, securely attached to a jar holder and shaken at a high speed horizontally. The balls move rapidly inside the jar (speed of several m s^{-1}) producing primarily high-energy impacts, compression and shearing, as well as sliding along the jar walls while describing the figure of eight. Such motion exerts friction forces on the sample and is usually referred to as the friction mode. As a result, the milled material undergoes particle size reduction, compaction, aggregation, surface defect formation and amorphization. A typical laboratory mixer mill

Figure 7.1 Equipment for mechanochemistry research.

operates at a maximum vibration frequency of 25–30 Hz (depending on the model and manufacturer) and can be set to run for 99 minutes continuously. If even higher energy input is required, milling devices that combine impact with high friction and go up to 35 Hz are also available on the market. Mixer mills can be adjusted for milling at low temperatures (so-called cryomilling), in which case liquid nitrogen is used to cool down the apparatus,[8] or high temperatures with the use of heating jackets or specially designed milling jars.[9,10]

In a planetary ball mill, reaction vessels are vertically aligned and securely clamped on the main rotating disk, also called the sun wheel. During operation, the sun wheel rotates at a speed of 30–650 rpm, while the grinding jars simultaneously rotate in the opposite direction. This type of ball milling deserved its name because of obvious similarity to planetary motion around the Sun. Like in mixer mills, the maximum reaction time for continuous milling can be adjusted to 99 minutes, with an option to introduce breaks and reverse the direction of milling (the interval operation). Such a design of planetary mills is optimized for achieving maximum shear and friction forces acting on a sample. Less pronounced are high-energy impacts that also take place since the centrifugal forces vary in intensity. Due to very strong centrifugal forces (the so-called Coriolis forces) that provide high pulverization energy to the milled material and ensure the highest degree of fineness, planetary mills are especially useful in applications such as mechanical alloying and colloidal mixing.

The rapid expansion of mechanochemistry is also reflected in the growing need for more customized milling equipment. For example, Komatsu and Murata have made important contributions to mechanochemistry of fullerenes by designing a custom-made high-speed ball mill capable of reaching frequencies up to 60 Hz.[11] Recently, Casati *et al.* have developed a milling device suitable for real-time *in situ* monitoring of mechanochemical reactions by powder diffraction of synchrotron radiation, which enabled the collection of diffraction data with sharper Bragg reflections and significantly reduced background.[12] Besides mixer and planetary mills, other types of ball milling instruments such as drum and rod mills, attritors and even kitchen grinders[13] have been used to perform solid-state mechanochemical reactions.[14]

Since laboratory ball mills usually have 2–4 milling stations, only a limited number of reactions can be performed simultaneously. This becomes a serious obstacle in the cases of reaction screening and optimization studies. Such a low throughput of commercial ball mills was elegantly addressed by Cravotto and Colacino with their design of a special, multiposition jar adapter that can replace standard jars in planetary ball mills (see Figure 7.2a).[15] These adapters can hold up to 12 vials at the same time, depending on their size: 4 × 100 mL vials, 8 × 20 mL vials or 12 × 2 mL vials. In other words, a planetary ball mill with 4 milling stations can easily be converted into a mechanochemical screening device capable of running up to 48 reactions simultaneously. In this way, more than 60 reactions/week can be

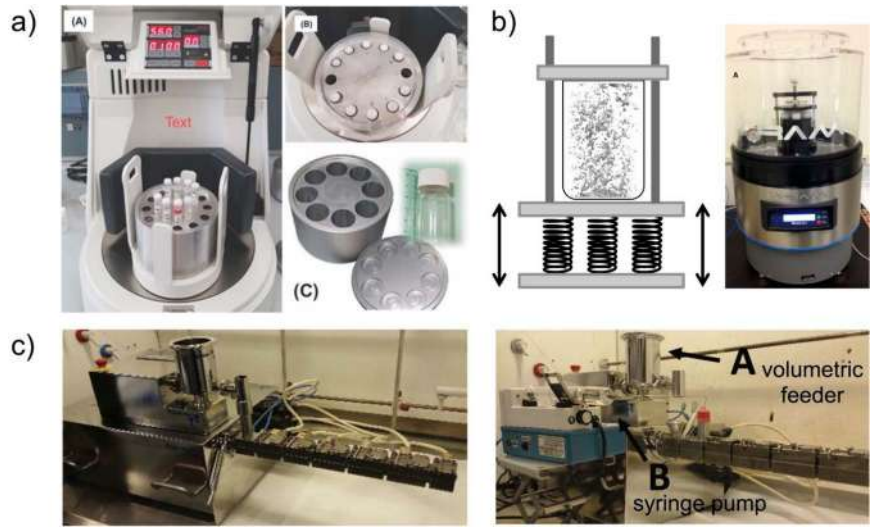

Figure 7.2 (a) Multiposition jar adapter developed by Cravotto and Colacino, (b) working principle of RAM and a laboratory RAM device and (c) a twin screw extruder. Panels (a) and (c) reproduced/adapted from ref. 15 and 23 with permission from The Royal Society of Chemistry, Copyright 2017 and 2018. Panel (b) reprinted with permission from *Org. Proc. Res. Dev.*, 2014, **18**, 331–341, Copyright 2014 American Chemical Society.

carried out directly in glass vials using small stainless steel balls (1 mm diameter) or glass beads (3 mm diameter), as shown by the authors in the synthesis of a library of 3,4-dihydro-2*H*-benzo[*e*][1,3] oxazines. Another feature of such a design is slightly different motion experienced by the vials – the *lunar motion* which arises from a superposition of rotations about the sun wheel, jar/adapter and vial axes.

Another emerging methodology that is gaining popularity in mechanochemistry research is resonant acoustic mixing (RAM).[16] In contrast to classical ball milling where the mechanical energy is conveyed onto the substrates by impact, friction and shearing caused by rapid movement of milling balls at high frequency, RAM is specific in that it does not require any grinding media. Hence, it is often referred to as "ball-free mechanochemistry".[17] While the number, size, mass and material of milling balls are important parameters in ball milling, the efficiency of RAM reactions depends on factors such as acceleration, expressed in *g* units ("G-force") and reaction time. In a typical RAM instrument, the mechanical (vibration) energy is transferred through a system of springs onto a plate holding the sample container (see Figure 7.2b). The acceleration, *i.e.* the intensity of mixing of the sample components, is adjusted by changing the amplitude of vibration, whereas its resonance frequency is usually kept at a fixed value (*e.g.* autoresonance mode at 60 Hz). Such design generates local zones of very intense mixing in the sample, but without significant temperature rise and physical damage

to sample particles as often encountered in ball milling (*e.g.* aggregation, compaction, snow-balling and amorphization). As a softer technique than ball milling, RAM has been employed in the screening and preparation of cocrystals of active pharmaceutical ingredients (API),[18,19] as well as energetic materials.[20] These examples illustrate the potential of RAM to aid in the assembly of crystalline materials *via* non-covalent interactions. In a recent report by Friščić, RAM has been used for the first time to construct coordination bonds in archetypal metal-organic frameworks (MOFs), such as zinc imidazolate frameworks ZIF-8 and ZIF-L, or the well-known copper(II) polymer HKUST-1.[21]

With the growing interest in mechanochemical synthesis, the question of scalability has imposed itself. Laboratory-sized planetary ball mills, and mixer mills in particular, have a limited processing capacity and can only deliver products on scales up to several hundred grams. Any potential industrial application of mechanochemistry would require much higher loadings, as well as the possibility to conduct the process continuously. A methodology that fulfils these criteria is twin-screw extrusion (TSE). Moreover, TSE processes can run at higher temperatures, a feature that is normally not encountered in ball milling. The basic operating principle of TSE relies on the synchronous action of a pair of co- or counter-rotating screws that convey the powdered reactants, fed at a certain rate, through the extruder barrel with mixing and kneading elements (see Figure 7.2c). The mechanical activation in the form of shearing and compression forces is exerted on the fed material, which undergoes a mechanochemical transformation into products collected at the exit side of the TSE instrument. Several examples of large-scale solid-state syntheses by TSE have been published by Crawford *et al.*[22] In their 2017 seminal paper, the authors described how TSE under optimized conditions (feed rate, screw speed, temp. and screw configuration) could be applied for the continuous and high-yielding scale-up of organic transformations such as the Knoevenagel reaction, imine (Schiff base) formation, Michael addition and aldol condensation. Space time yields (STY, as indicators of process efficiency) as high as >250 000 kg m^{-3} day^{-1} for the Knoevenagel reaction, 14 900 kg m^{-3} day^{-1} for Schiff base synthesis, 35 000 kg m^{-3} day^{-1} for Michael addition and 32 000 kg m^{-3} day^{-1} for the aldol condensation reaction were calculated.[23] Recently, the same group reported the use of TSE for the large-scale synthesis of commercially important perylenediimide-based dyes,[24] as well as hydrazone-based active pharmaceutical ingredients nitrofurantoin and dantrolene.[25]

7.2.2 Sample Preparation

Setting up experiments in mechanochemistry is often easy and straightforward. If a solvent-free (neat) mechanochemical reaction is to be done by manual grinding, reactants are weighed out and thoroughly mixed in a mortar using a pestle. At the end, the product or the crude reaction mixture is collected with a spatula and purified further if necessary. In the case of ball

milling, specially designed reaction vessels called grinding (or milling) jars are charged with pre-weighed reactants, followed by one or more grinding balls. Typical volumes of grinding jars range from 1.5–50 mL for mixer mills, to 12–500 mL for planetary mills, which are a better option if a large-scale reaction is planned. The balls can differ in size (diameters of 2, 3, 5, 7, 10, 12 and 15 mm are common, although larger balls of 20 or 25 mm are also used) and can be made of different materials. For organic synthesis purposes, the milling media is usually stainless steel (SS), tungsten carbide (WC), zirconia (ZrO_2), Teflon (PTFE) or polymethyl methacrylate (PMMA) plastic, the choice of which depends on the reactivity of the starting materials and product(s) and the energy input necessary for the reaction (see Figure 7.1). As a rule of thumb, more dense materials provide more energy – if harsh milling conditions are needed, WC medium is a good choice. On the contrary, PTFE or PMMA medium is preferred for soft grinding. Recently, Germann *et al.* demonstrated by *in situ* measurements how milling media could have a profound effect on the outcome of mechanochemical cocrystallization. More efficient transfer of mechanical energy in stainless steel media (high Young module) enabled the synthesis of a metastable polymorph, while cocrystallization in PMMA (characterized by low Young module) resulted in the thermodynamically more stable polymorph.[26]

Besides reactants, inert grinding auxiliaries such as silica, celite, sand or different inorganic salts are sometimes added in before milling. Their role is to adsorb liquid reactants or facilitate ball milling, since in some cases reaction mixtures turn into a paste or glue-like mass, or even adhere to the ball surface ("snow-balling" effect), where efficient mixing and mass transfer are severely compromised.[27] Some recent kinetic observations of sigmoidal behaviour of an organic model system under milling conditions suggest that such cohesive states and change in rheology play a critical role in the progression of mechanochemical reactions.[28]

The physical state of reactants in mechanochemical reactions is often assumed to be exclusively solid; however, liquids and gases are also routinely employed.[7] In fact, the presence of a liquid phase in sub-stoichiometric quantity (added deliberately or already present in the form of solvates or inadvertent moisture from air) can have a dramatic effect on the course of a mechanochemical reaction.[29] Another benefit of conducting chemical reactions by ball milling is the possibility to avoid using glovebox and Schlenk line techniques. In a nice demonstration by Kubota *et al.*, the Buchwald-Hartwig amination, typically run in solution under inert atmosphere, is readily carried out in air by ball milling in the presence of an air-stable phosphine ligand and $Pd(OAc)_2$ catalyst.[30] Still, working with organometallic compounds is always challenging and would normally require an inert atmosphere. In these cases, grinding jars should be loaded and sealed in a glovebox, thus excluding air and moisture during milling. Notable examples were described by Hanusa's group who successfully synthesized by this technique the elusive unsolvated tris[1,3-bis(trimethylsilyl)allyl]aluminium complex and its scandium analogue,[31] followed by preparation of tris(allyl)

stannate and tetra(allyl)tin species.[32] Upon completion of the reaction, the jar is opened in air (or under inert gas for sensitive compounds) and the solid products are simply scraped off the jar walls or solubilized with an appropriate solvent and purified accordingly.

7.2.3 Control of Solid-State Reactivity

The outcome of solvent-free or neat grinding/milling experiments can be further improved by employing different strategies aimed at controlling the reactivity in the solid state. Over the years, several techniques have been discovered that alter the kinetics of mechanochemical reactions[33] and allow for higher conversions, better yields and greater purity of final products.

7.2.3.1 Liquid-Assisted Grinding (LAG)

One such strategy is called liquid-assisted grinding or LAG.[34] Developed from the initial observations that a few drops of a solvent dramatically enhanced the kinetics of cocrystallization of 1,3,5-cyclohexane tricarboxylic acid with 4,4′-bipyridine and 4,7-phenanthroline during manual grinding (also known as solvent-drop grinding),[35] LAG has evolved from a chemical curiosity into an established mechanochemical technique for improving the solid-state reactivity. By introducing the η parameter, defined as the ratio of the liquid phase volume (μL) to the total reactant mass (mg), the amount of added liquid could be precisely quantified and its effects measured and compared across various reaction conditions.[36] The η is 0 for solvent-free (neat) milling, and LAG is characterized by $0 < \eta < 1–2$ in a concentration regime independent of solubility, whereas in slurries (η = 2–12 μL mg^{-1}) and homogenous solutions ($\eta > 12$ μL mg^{-1}) solubility starts to play a major role in determining the final products. LAG is also a practical method to control the polymorphism[37] and the composition (stoichiometry) of hydrogen- and halogen-bonded cocrystals.[38] In addition, LAG products are highly crystalline solids, while neat grinding often leads to partial amorphization.[39] For setting up a LAG reaction, the selected grinding liquid is measured out with a pipette into a jar charged with reactants and ball(s), the jar is tightly sealed and milling started.

Although the mechanisms of LAG are not fully understood, several examples demonstrate interesting effects through which the added liquid controls the outcome of mechanochemical reactions. In one of the earliest attempts to systematically investigate the role of the liquid phase in LAG mechanosynthesis, Friščić *et al.* showed how water steered the reactivity during the assembly of a zinc fumarate coordination polymer starting from zinc oxide and fumaric acid.[40]

Our group reported on a gas–solid mechanochemical amination of thiocarbamoyl benzotriazoles as masked synthetic equivalents of isothiocyanates. It was found that increasing the mole fraction of water above 0.8 in binary acetonitrile : water or ethanol : water mixtures, used as grinding liquids, gradually led to a complete shutdown of reactivity, presumably due to differences in hydrogen bond basicities of acetonitrile and ethanol (see Figure 7.3a).[41]

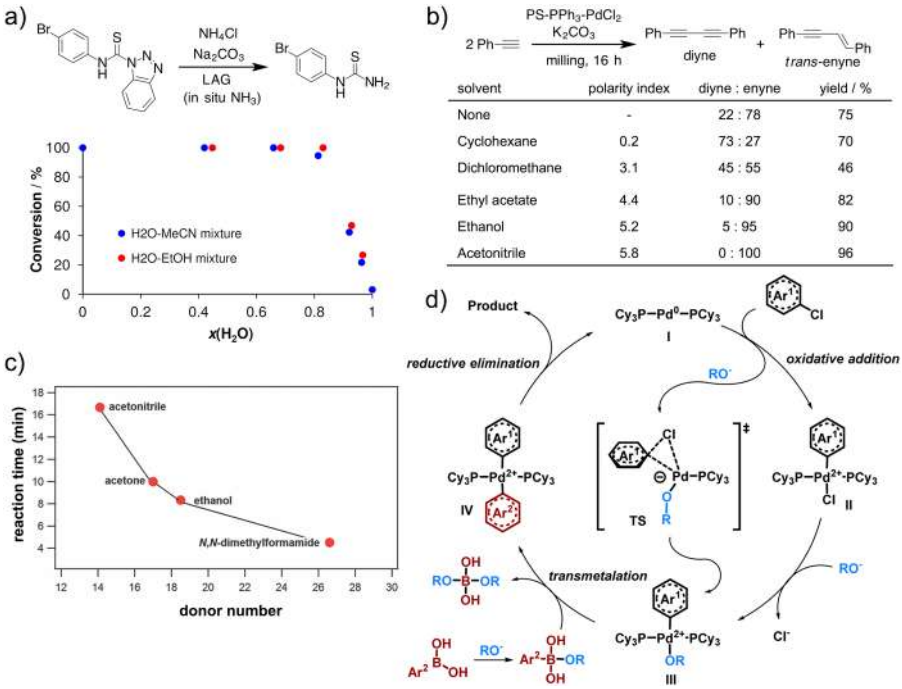

solvent	polarity index	diyne : enyne	yield / %
None	-	22 : 78	75
Cyclohexane	0.2	73 : 27	70
Dichloromethane	3.1	45 : 55	46
Ethyl acetate	4.4	10 : 90	82
Ethanol	5.2	5 : 95	90
Acetonitrile	5.8	0 : 100	96

Figure 7.3 The effect of LAG in mechanochemical organic synthesis: (a) Gas–solid amination of thiocarbamoyl benzotriazoles, (b) homocoupling of terminal alkynes, (c) nucleophilic substitution on an acyl derivative and (d) LAG with alcohols as ligands in the Suzuki–Miyaura reaction. Panels (a) and (c) reproduced/adapted from ref. 41 and 44 with permission from The Royal Society of Chemistry, Copyright 2015 and 2016. Panels (b) and (d) reprinted with permission from *ACS Catal.*, 2016, **6**, 868–872, and *J. Org. Chem.*, 2016, **81**, 10049–10055, Copyright 2016 American Chemical Society.

The Mack's group investigated the effect of changing the grinding liquid polarity in the mechanochemical homocoupling of terminal alkynes. The authors found that a nonpolar environment during LAG (*e.g.* cyclohexane) with a polymer-supported bis(triphenylphosphine)palladium(II) dichloride catalyst and potassium carbonate as the base favoured the formation of the diyne product. Increasing the polarity by using ethanol or acetonitrile in LAG resulted in a reverse selectivity as the *trans*-enyne became the major product (see Figure 7.3b).[42] The same group reported that the diastereoselectivity in a mechanochemical Wittig reaction can also be controlled by the liquid phase polarity.[43] That the grinding liquid basicity could also play an important role in liquid-assisted mechanochemical organic transformations was corroborated in a study by Halasz *et al.* The nucleophilic substitution of an acyl azide with an aromatic amine, monitored by *in situ* Raman spectroscopy, proceeded at an increasing rate under LAG conditions in the order: acetonitrile < acetone < ethanol < DMF. In this case, the correlation of the reaction rate and polarity could not be established, however using the Gutmann's donor numbers revealed a connection to the solvent basicity (see Figure 7.3c).[44]

With reactive electrophiles such as aromatic isocyanates, a potential reaction with the grinding liquid in LAG must also be taken into consideration. As illustrated by the reaction of phenyl iso(thio)cyanates with aromatic amines, the sulfur analogues were compatible with both neat and LAG conditions using methanol, however more reactive isocyanates must be milled exclusively neat, since methanol could react as a nucleophile diminishing the yield and purity of the (thio)urea product.[45] The chemical reactivity of the grinding liquid in LAG was explored in the Suzuki–Miyaura reaction of challenging aryl chlorides by Su *et al.*[46] Screening for the optimal grinding liquid in LAG revealed alcohols as the best performing solvents with near-quantitative yields. The unexpected positive effect exerted by alcohols in the $Pd(OAc)_2$/PCy_3 catalytic system was traced down to the ability of LAG to engage solvent molecules as ligands in transition metal-catalyzed reactions. Under mechanochemical milling conditions, the carbonate base can deprotonate alcohol molecules and generate alkoxide anions, which typically participate in steps of ligand exchange and boronic acid activation (see Figure 7.3d).

7.2.3.2 Ion- and Liquid-Assisted Grinding (ILAG)

Since its introduction, LAG has been demonstrated as an approach superior to neat grinding. However, there are cases where LAG performance is insufficient to drive the solid-state reaction to completion, or even fails completely to affect the reactivity. This was noted by Friščić *et al.* in their attempt to mechanochemically prepare a pillared $[Zn_2(BDC)_2(DABCO)]$ MOF (BDC = 1,4-terephthalate, DABCO = 1,4-diazabicyclo[2.2.2]octane). While LAG using DMF led to a partial reaction and low yields, addition of a catalytic quantity of a nitrate salt, alongside DMF as the grinding liquid, resulted in quantitative conversion of reactants. This new technique was termed ion- and liquid-assisted grinding or ILAG.[47] Ever since, the ILAG approach has been extensively used in MOF synthesis, particularly for zinc imidazolate frameworks (ZIFs).[48] In the same paper where the basicity of liquids in LAG was discussed, ILAG provided an additional support in favour of the proposed effect of solvent basicity on the rate of nucleophilic substitution on a carbonyl group.[44]

7.2.3.3 Polymer-Assisted Grinding (POLAG)

Since LAG can in some cases lead to unintentional solvate formation during mechanochemical cocrystallization, Jones *et al.* introduced a technique that relied on the use of polyethylene glycol (PEG) polymers as catalysts. The new approach was named polymer-assisted grinding or POLAG. By studying the formation of a caffeine-citric acid cocrystal as a model reaction, it was found that liquid and solid PEG additives of different molecular weight (200–10.000) accelerated the rate of cocrystallization.[49] In a follow-up paper, the authors showed that POLAG was also effective in controlling the polymorphic

outcome of the caffeine cocrystallization with glutaric acid.[50] More recently, an *in situ* mechanistic study on the same system confirmed earlier findings and revealed that POLAG enhanced the rate of cocrystallization with a characteristic induction time of 3–4 minutes, placing it in between neat grinding (*ca.* 7 minutes) and LAG (0–2 minutes).[51]

PEGs were also employed as reaction media in mechanochemical organic reactions. Lamaty's group published in 2012 a mechanochemical palladium-catalyzed Mizoroki–Heck reaction involving iodobenzene and *tert*-butyl acrylate as the olefin component. Optimization of the reaction parameters led to quantitative conversion of iodobenzene to a cinammate ester after one hour of milling at 30 Hz when PEG-2000-OH was used as an additive, potassium carbonate as the base (3 eq.), and 5 mol% of $Pd(OAc)_2$ as the source of palladium catalyst. Whereas the scope of the reaction was limited to only *tert*-butyl acrylate as the olefin partner, different substituents on the aryl iodide component were tolerated. As an additional benefit, a phosphine ligand was not required since OH groups present in PEG stabilized the Pd(0) species.[52] The same group later utilized a MeO-PEG-2000-OMe additive in the mechanosynthesis of 3,5-disubstituted hydantoins in a planetary ball mill.[53]

7.2.3.4 Ionic Liquid-Assisted Grinding (IL-AG)

Except organic solvents, other liquid phases can be employed to alter the reactivity of substrates and kinetics of mechanochemical solid-state reactions. One such example was reported by Myerson who used imidazolium-based ionic liquids (ILs) as additives to prepare caffeine cocrystals with citric and glutaric acids, and also to control their polymorphism by manual grinding with a mortar and pestle. The authors named this approach "ionic liquid-assisted grinding" (IL-AG), to differentiate it from ILAG.[54] A series of ILs differing in hydrophobicity and polarity were screened as potential additives. Whereas this study identified ILs as an alternative liquid additive for solid-state reactions, they could be also synthesized by manual grinding despite their liquid state, as described by Branco and Duarte who prepared several ILs derived from pharmaceutically-relevant molecules gabapentin (neuroleptic drug) and L-glutamic acid.[55]

7.2.3.5 Liquid-Assisted Resonant Acoustic Mixing (LA-RAM)

Similarly to LAG in ball milling, the addition of a small amount of liquid phase during RAM synthesis has been found to accelerate the formation of cocrystals and MOFs, and was conveniently termed "liquid-assisted resonant acoustic mixing" or LA-RAM. For example, mixing carbamazepine (**cbz**) and nicotinamide (**na**) without any solvent did not lead to product formation, nor did solvent-free attempts to prepare zinc or copper MOFs turned out to be successful. However, the presence of water in the 1:1 mixture of **cbz** and

na produced *ca.* 40% of carbamazepine dihydrate (**cbz**)($\mathbf{H_2O}$)$_2$ and only about 10% of a cocrystal (**cbz**)(**na**) at lower 50*g* intensity. At 100*g* acceleration, the reaction profile dramatically changed as cocrystallization readily took place, yielding *ca.* 70% of (**cbz**)(**na**). The results indicated that LA-RAM at higher accelerations allowed for more intimate mixing of reactants through mechanisms of aggregate dissociation, particle comminution and disintegration of reactant particles coated with the dihydrate and cocrystal products, which all led to exposure of fresh reactive surfaces and an increase of the cocrystallization rate.[17]

In the case of Cu-MOF synthesis by LA-RAM, copper(II) acetate monohydrate and trimesic acid were mixed in a stoichiometric 3 : 2 ratio with different amounts of liquid additives (*e.g.* alcohols, acetonitrile and DMF) to afford the desired HKUST-1 framework at 95*g* acceleration. While the purity of HKUST-1 was slightly compromised when organic liquids were used, LA-RAM in the presence of water gave the pure phase in excellent yield after one hour, which also exhibited porosity comparable to the same material obtained *via* other synthetic routes. The optimized LA-RAM procedure was also applied to the synthesis of ZIF-8, mixed ligand ZIFs, and also ZIF-L forms of zinc and cobalt analogues.[21]

7.3 Analysis of Mechanochemical Reactions

In order to understand the reactivity and reaction mechanisms operating under mechanochemical conditions, which is a prerequisite for the rational design of novel solid-state synthetic routes and the development of the mechanochemistry field in general, a suitable set of analytical tools is necessary. Since mechanochemical processes predominantly take place in the solid state, analytical methods such as powder X-ray diffraction (PXRD), infrared (IR) and Raman spectroscopy, solid-state nuclear magnetic resonance spectroscopy (SSNMR), thermogravimetric analysis (TGA) and differential scanning calorimetry (DSC), or scanning/tunnelling electron microscopy (SEM/TEM) are often used. Assuming that the studied reaction does not proceed in the absence or after interruption of milling, sample preparation and analyses can also be performed in a solution environment (*e.g.* NMR, thin-layer, liquid or gas chromatography *etc.*). Initially, *ex situ* measurements, where the milling process had to be interrupted for sampling, were performed to reveal the composition of the reaction mixtures and provide hints on possible mechanisms of product formation. However, this approach proved to be unreliable, since many mechanochemical reactions continue even after the ball milling is suspended. Moreover, the reaction mixtures have to be deliberately exposed to air or moisture during sampling, which can trigger further changes in the composition or alter the reactivity. Nevertheless, *ex situ* analysis is still widely used, providing useful information on the extent of milling reactions (*e.g.* conversion rates), the presence of desired products, intermediates, impurities *etc.*

On the other hand, an *in situ* approach would eliminate the need to open the jars and physically remove a sample of the reaction mixture for analysis. Instead, mechanochemical reactions could be analyzed directly in real time, allowing simultaneous ball milling and probing, with time-resolved data collected as the reaction took place. In this way, valuable information on the mechanisms and kinetics of ball milling reactions could be obtained, and in combination with theoretical modelling help unravel the secrets of mechanochemical processes on a microscopic level.[56]

7.3.1 Powder X-Ray Diffraction

The first analytical method that was successfully coupled with ball milling into a real-time *in situ* technique for monitoring the progress of mechanochemical reactions was powder X-ray diffraction (PXRD).[57] As a classical analytical tool in solid-state chemistry, PXRD is particularly suitable for analysis of crystalline materials involved in ball milling. To ensure high-quality diffraction data, intense X-rays produced in a synchrotron facility were passed through a low-absorbing PMMA plastic jar containing the mixture oscillating at 30 Hz on a modified mixer mill. The diffracted beams were then collected on a 2-D detector, providing the first glimpse into an ongoing mechanochemical process with temporal resolution measured in seconds. Since this pioneering work, *in situ* PXRD analysis has been used to study the course of many mechanochemical reactions, especially MOF synthesis.[58,59]

Emmerling's group utilized *in situ* PXRD to monitor the progress of the uncatalyzed Knoevenagel reaction between 4-nitrobenzaldehyde and malononitrile, conducted for 60 minutes with two 10 mm balls at 50 Hz. After *ca.* 35–45 minutes, the reflections of the product phase were identified with concomitant decrease of the intensity of aldehyde reflections. Malononitrile reflections could not be seen, probably due to melting.[60] Further studies on the same reaction type using 4-fluorobenzaldehyde as the electrophile and piperidine as the catalyst, showed the unexpected formation of an unstable monoclinic polymorph of the product (4-fluorobenzilidene)malononitrile, followed by its transformation to the more stable triclinic phase. At higher catalyst loadings, the reaction proceeded directly to yield the triclinic polymorph. Depending on the milling frequency, the initial period of the reaction was characterized by the complete absence of diffraction patterns, indicating the presence of liquid or molten states.[61]

7.3.2 Raman Spectroscopy

The two main disadvantages of *in situ* PXRD measurements, which limit their routine use in the scientific community, are (1) access to a synchrotron source and (2) the inability to see changes in systems undergoing amorphization or involving liquid/molten phases (as seen in the above example). Organic compounds, often considered as soft materials, are susceptible to amorphization

under harsh ball milling, whereas molten eutectic phases or intermediates could form due to their relatively low melting points (compared to inorganic materials). In the context of mechanochemical organic synthesis, the information on the localized molecular-level changes can be readily obtained by molecular spectroscopic techniques such as infrared or Raman spectroscopy. In the case of Raman spectroscopy, the setup is simple and easy to implement in routine laboratory work. Similarly to PXRD measurements, PMMA jars transparent to laser light from the Raman probe are used, while the probe itself is placed below the oscillating jar on a precision positioner to allow fine laser focusing, typically 1–2 mm inside the jar (see Figure 7.4a). First developed for a real-time *in situ* monitoring of mechanochemical formation of cadmium coordination polymers with cyanoguanidine ligand,[62] time-resolved Raman spectroscopy rapidly found application in the mechanistic studies of several reactions.[63–65] Our group adopted this technique to follow the progress of aromatic thiourea mechanosynthesis under LAG conditions using bis(benzotriazolyl) methanethione as the thioacylating reagent and substituted anilines in a 1 : 2 molar ratio. The *in situ* Raman spectroscopy revealed the presence of an intermediate with characteristic absorption

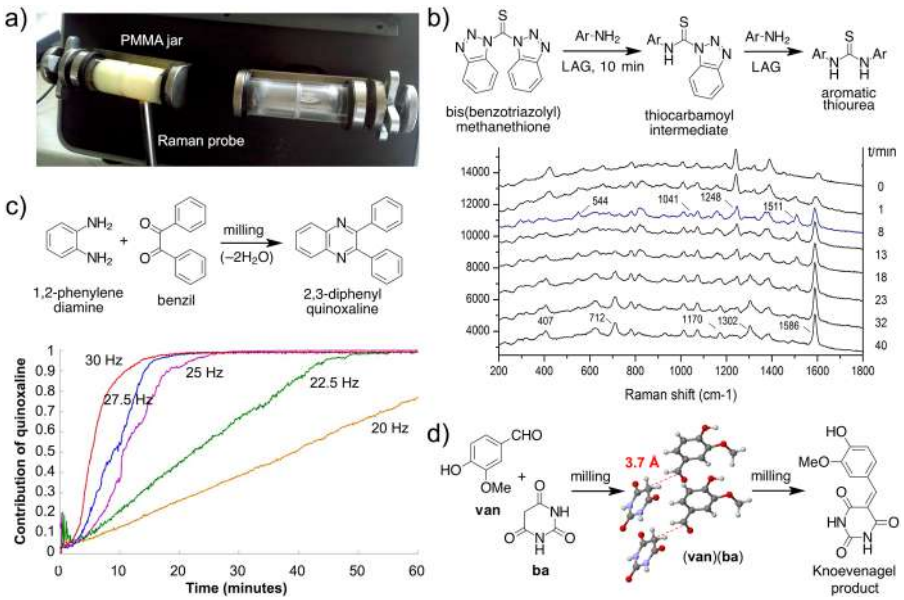

Figure 7.4 (a) Set up for *in situ* Raman spectroscopy monitoring of a mechanochemical reaction. (b) Solid-state synthesis of thioureas by thioacylation of anilines proceeds through a thiocarbamoyl benzotriazole intermediate detected by *in situ* Raman spectroscopy. (c) The effect of milling frequency on the mechanochemical synthesis of 2,3-diphenylquinoxaline studied by *in situ* Raman monitoring. (d) A vaniline : barbituric acid cocrystal intermediate detected during the *in situ* Raman monitoring of the Knoevenagel reaction. Panel (c) reproduced from ref. 67 with permission from Beilstein-Institut, Copyright 2017.

bands that were visible in the initial stages of the reaction. As the thiourea product started to form, the intensity of these absorption bands gradually decreased and completely vanished upon completion of the reaction (see Figure 7.4b). Thiocarbamoyl benzotriazole intermediates were subsequently isolated and fully characterized by IR, $^{13}C/^{15}N$ SSNMR and TG, while their molecular and crystal structures were successfully determined from PXRD data. In stark contrast to solution synthesis, solid-state mechanochemistry enabled an efficient synthesis of elusive reactive intermediates, while *in situ* Raman spectroscopy was established as a powerful method for monitoring organic reaction mechanisms in the solid state.[66]

Friščić *et al.* investigated the effect of milling frequency on the kinetics of the solid-state reaction between benzil and 1,2-phenylenediamine to form 2,3-diphenylquinoxaline by time-resolved Raman spectroscopy.[67] The reaction profiles at 20, 22.5, 25, 27.5 and 30 Hz suggested a switch from a linear regime at lower frequencies to a sigmoidal behaviour at higher values (see Figure 7.4c). *In situ* Raman spectroscopy was also central to the detection and isolation of the first example of a cocrystal intermediate preceding the formation of covalent bonds during a mechanochemical organic reaction. As reported by Halasz *et al.*, the cocrystal was composed of reactant molecules, vaniline (**van**) and barbituric acid (**ba**) in a 1 : 1 stoichiometric ratio, and emerged as a transient phase on the way to the Knoevenagel product (see Figure 7.4d).[68] The intermediate cocrystal (**van**)(**ba**) was isolated by stopping the reaction after > 70 minutes of solvent-free milling with two 7 mm balls at 30 Hz, while its structure was determined from the diffraction data collected on a laboratory X-ray diffractometer. In the cocrystal, **van** and **ba** molecules are arranged in such a way to facilitate the nucleophilic attack of the **ba** methylene group to the carbonyl group in **va**, separated by *ca.* 3.7 Å. As complementary analytical methods, *in situ* PXRD and Raman spectroscopy have been coupled into a tandem technique to allow investigations of mechanochemical milling reactions in unprecedented detail and accuracy.[69]

7.3.3 TRIS-XANES and Solid-State NMR

The two most recent additions to analytical techniques used in monitoring mechanochemical reactions are time-resolved *in situ* X-ray absorption near edge spectroscopy (TRIS-XANES) and solid-state nuclear magnetic resonance. de Oliveira *et al.* developed an approach where PXRD and X-ray absorption spectroscopy, both as synchrotron-based methods, were coupled into a tandem technique to obtain complementary information during the mechanosynthesis of gold micro- and nanoparticles.[70] The main advantage of using TRIS-XANES in this combination stems from the fact that PXRD only provides the data on the long-range ordered structure, while X-ray absorption is sensitive to the local environment of the absorbing element on a much smaller scale.

Due to its specific construction, high magnetic fields, sample preparation and manipulation, real-time *in situ* solid-state NMR (SSNMR) measurements of mechanochemical reactions have remained virtually unexplored.[71] In 2020, Wüllen *et al.* published a paper describing the first attempt to study a true ball milling reaction by the *in situ* SS-NMR technique. For this purpose, a home-made NMR probe with a miniature vibrational ball mill integrated into the measuring coil was designed, thus enabling static SSNMR measurements. The milling vessel, manufactured from polyoxymethylene plastic, contained a small sample chamber which was kept inside the coil during the spectra acquisition. The chamber was charged with 12–100 zirconia balls of 1 mm diameter, along with zinc acetate dihydrate and phenylphosphonic acid as reactants in the model reaction of zinc phosphonate salt formation, and shaken at vibration frequencies from 15–35 Hz. This work demonstrated that SSNMR, following further modifications in the probe design, holds promise for the *in situ* analysis of ball milling reactions, particularly in combination with already established real-time monitoring techniques.[72]

7.3.4 Temperature Measurement during Milling

Although some vendors offer sophisticated milling equipment for planetary ball mills with integrated temperature and pressure sensors, the task of measuring and controlling the temperature in a mechanochemical reaction is not trivial to perform. The easiest method to estimate the temperature rise, resulting from high-energy impacts and friction during ball milling, is to use a thermocouple embedded in the jar walls.[73–75] A technically more advanced approach was described by Emmerling who employed tandem PXRD and Raman spectroscopy, in combination with an IR thermal camera, to monitor the progress of the Knoevenagel reaction between *p*-nitrobenzaldehyde and malononitrile.[76] More precise temperature measurements would ideally require a direct heat transfer from the milled sample to the probe, which was successfully demonstrated by Užarević *et al.*[77] A resistance temperature detector, that was in contact with a piece of aluminium plug, was inserted into a custom-made PMMA jar for *in situ* experiments. The aluminium plug was placed on the inner walls of the jar, allowing a direct thermal contact with the milled reaction mixture, whilst avoiding destructive ball impacts on the temperature sensor. This setup provided an unprecedented insight into the thermal effects related to mechanochemical reactions, and revealed that unexpected temperature profiles observed during MOF mechanosynthesis originated from frictional heating rather than from reaction enthalpy contributions, which were found to be very small or even negligible. The same group constructed an in-house mechanochemical reactor for thermally-assisted milling reactions, which allows prolonged milling at a desired and precisely controlled temperature.[9] Thermally-assisted milling was shown to accelerate solid-state organic reactions, as well as influence their mechanisms and product selectivities.

7.4 Organic Synthesis Under Mechanochemical Conditions

Substrate activation modes traditionally linked with solution chemistry, *e.g.* metal-, organo-, photo- and enzyme catalysis, have been successfully transferred into the solid state. Their mechanochemical counterparts perform equally well, or in many cases even better, despite the absence of solvent molecules. Likewise, classical organic reactions, run with the use of a mortar and pestle or ball mills, also proceed with excellent yields and selectivities, enabling in some cases reactivity previously not observed in solution.

The number of organic reactions performed by manual grinding or ball milling has grown rapidly over the last 15 years, but even more so in the last 5 years when mechanochemistry has become widely recognized as a highly efficient, yet environmentally-friendly synthetic method. In the area of small organic molecule synthesis, including marketed drugs, organocatalysts and anion sensors, a diverse set of reactions such as aldol condensations,[78] amidations,[79–81] fluorinations,[82] desymmetrizations,[45] (thio)carbamoylations[83,84] and guanylations,[85,86] oxidations of alcohols to carboxylic acids,[87] and ester reductions,[88] hydrogenations,[89,90] aldehyde-alkyne-amine couplings,[91] to name only a few, have been addressed so far. Famous name reactions such as the Wittig reaction[92] or Diels–Alder reaction,[93] or molecular rearrangements, *e.g.* Hofmann,[94] Lossen[95] and benzilic,[96] are also on the list of successful milling protocols. Finally, mechanochemistry has found its place in the synthesis of large molecules like fullerenes[97] and complex supramolecular architectures such as cavitands, rotaxanes and molecular cages.[98] A more comprehensive overview of many interesting mechanochemical organic reactions can be found in several review papers,[4–6] chapters and books.[99,100] In a typical case study example shown below, a recent mechanochemical approach to amide bond synthesis, as one of the most important organic reactions and a structural fragment found in things from living systems to advanced materials, is highlighted.

The amidation of N- and C- protected amino acids and pharmaceutically relevant amine substrates, carried out by Kananovich and Aav, showcases the advantageous use of mechanochemistry for the construction of a ubiquitous –CONH– amide bond (see Figure 7.5).[101] The procedure deals with more difficult amino substrates with reduced nucleophilicity (reactivity) and sterically hindered carboxylic acids to provide amides in high yields. Of importance for satisfactory conversion was the finding that LAG using ethyl acetate in combination with dipotassium phosphate (K_2HPO_4) significantly improved the conversion. In addition, environmentally-friendly uronium-type amide coupling reagents COMU and TCFH were found to be more efficient than traditionally used HATU and EDC. The amidation protocol was completed by a simple workup consisting of water wash and filtration.

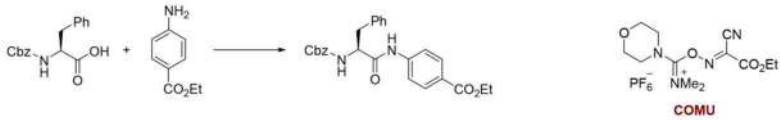

Metrics	Mechanochemistry		Solution[a]
	COMU / K_2HPO_4	TCFH / K_2HPO_4	COMU / DIPEA in DMF
Yield (%)[b]	96	92	70
Atom economy (%)[c]	50	60	50
RME (%)	46	53	35
PMI (total), including:	196.3	203.7	1464.7
PMI (reactants)	3.4	3.1	3.7
PMI (solvent)	0.6	0.6	18.9
PMI (work-up)	192.3	200	1442.2[d]
Solvent choice	EtOAc, water	EtOAc, water	DMF
Work-up, isolation	filtration	filtration	chromatography
Health and safety			
Main hazard statements[e]	H302, H312	H360	H226, 312, 332, 360

Figure 7.5 Green metrics for the model amidation reaction between Cbz-protected L-phenylalanine and ethyl 4-aminobenzoate under mechanochemical conditions and in DMF solution. Reprinted with permission from *ACS Sustainable Chem. Eng.*, 2020, **8**, 15703–15715, Copyright 2020 American Chemical Society.

Optimized reaction conditions were applied to the synthesis of a biotin[6]uril hexaamide derivative. The challenging six-fold amide coupling reaction with phenylalanine in the solid state circumvented the problems of low solubility of the biotin[6]uril compound in common organic solvents. For this transformation, *N*-methylimidazole was used as a base, resulting in an excellent 80% isolated yield and outstanding 98% purity. Synthetic and environmental improvements and shortcomings of the developed mechanochemical method for amidation are illustrated for the reaction of CBz-protected L-phenylalanine with ethyl 4-aminobenzoate. Atom economy (AE), reaction mass efficiency (RME) and process mass intensity (PMI) parameters were used for comparison with solution conditions. Here, RME relates to atom economy and product yield and it is lower for classical solution conditions, whereas PMI relates to amount of waste production. A reaction carried out in solution had 84% of PMI, while the mechanochemical reaction had only 15% PMI (LAG), without taking into account the mass-extensive workups. Sustainable solvents (water and ethyl acetate) were advantageous in contrast to toxic DMF. Safety health risks and toxicity and hazards were also diminished in the ball milling procedure.

7.4.1 Metal Catalysis

The activation of substrates through metal catalysis can readily be achieved in the solid state by means of ball milling. In one of the earliest reports on mechanochemical metal-catalyzed reactions in 2000, Peters *et al.* investigated

solvent-free Suzuki coupling,[102] followed by Leadbeater *et al.* who optimized the reaction under ligand-free conditions in 2003.[103] Frejd described in the period 2004–2006 the Pd-catalyzed Mizoroki–Heck couplings between aryl iodides and 2-*tert*-butoxycarbonylaminoacrylic acid methyl ester as the olefin partner.[104,105] Ever since, this field of mechanochemistry has expanded enormously, with authors reporting on mechanochemical protocols for Suzuki–Miyaura, Negishi, Sonogashira and Heck couplings, Friedel–Crafts acylations and alkylations, olefin metathesis, Buchwald-Hartwig amination, C–H activations *etc.*[106] Since mechanochemical reactions are normally run in metal media, it seemed natural to explore the possibility of metal catalysis using grinding jars and balls as the source of metal catalyst.[107] In a report by Mack *et al.*, the Sonogashira coupling of aryl iodides and bromides with trimethylsilylacetylene, in the presence of a $Pd(PPh_3)_4$ catalyst, was carried out in a copper vial with copper balls, producing the coupling products in excellent yields compared to reactions run in stainless steel media without the copper co-catalyst (see Figure 7.6a). This approach was next applied in the Huisgen [3 + 2] cycloaddition (the famous "click-reaction") between an alkyne and an azide (used directly or formed *in situ*), affording triazoles in high isolated yields.[108] Palladium balls were employed as catalysts for Suzuki cross-coupling polymerization of 4-bromo- or 4-iodophenylboronic acid to

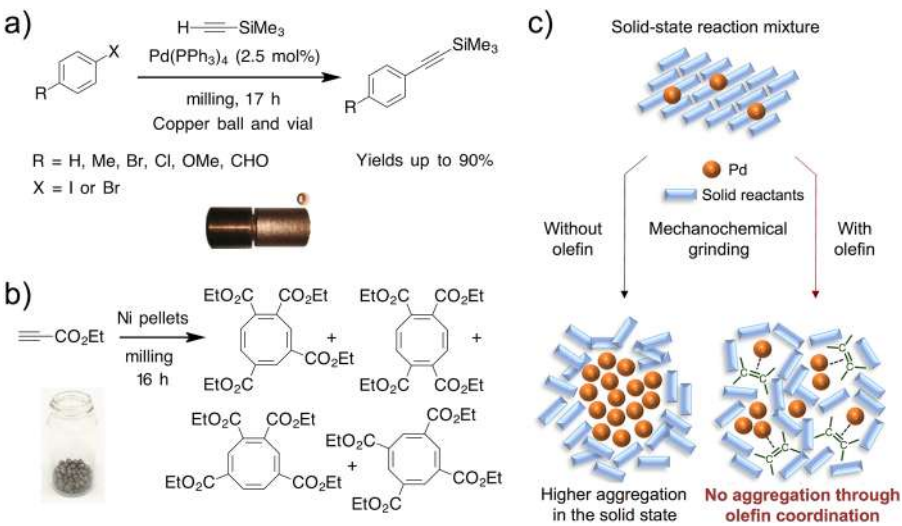

Figure 7.6 Examples of metal-catalyzed mechanochemical reactions: (a) The Sonogashira reaction in copper media and (b) nickel pellet-catalyzed [2 + 2 + 2 + 2] cycloaddition of terminal alkynes by Mack *et al.* (c) Olefins as molecular dispersants in the solid-state Buchwald–Hartwig amination developed by Kubota and Ito. Panels (a) and (b) reproduced from ref. 107 with permission from the Royal Society of Chemistry, Copyright 2017. Panel (c) reproduced from ref. 122 with permission from Springer Nature, Copyright 2019.

poly(*para*-phenylene), resulting in one of the highest degrees of polymerization for this type of reaction.[109] Mack's group also endeavored to achieve the synthesis of cyclopropane derivatives by reacting alkenes with diazoacetates in an intermolecular [2 + 1] cyclopropanation reaction using silver foil-lined stainless steel jars.[110] Another interesting contribution from the same group is the use of nickel pellets as catalysts and grinding media in the [2 + 2 + 2 + 2] cycloaddition of terminal alkynes to selectively afford cyclooctatetraene products (see Figure 7.6b).[111] While substituted benzenes are the major products in solution synthesis, this example highlights the potential of mechanochemistry to induce different reactivity and reaction paths in metal-catalysis. This was also reported by the Friščić group, who found that the carbon-nitrogen coupling reactions between sulfonylamines and carbodiimides, as well as amides and isocyanates, efficiently proceeded only under mechanochemical conditions in the presence of a copper catalyst, with no or traces of products during solution synthesis.[112,113]

Oxidation of alcohols with the $Cu(MeCN)_4(OTf)$/TEMPO/bipy/*N*-methylimidazole system under Stahl's conditions was exploited by Porcheddu to synthesize a range of aldehydes and ketones.[114] Olefin metathesis, an industrially important ruthenium-catalyzed transformation, was also successfully carried out by mechanochemical ball milling, as shown by Friščić *et al.*[115] Bolm *et al.* demonstrated that ball milling is a viable alternative to solution chemistry in the case of metal-catalyzed asymmetric alkylation of indoles with arylidene malonates.[116] Mechanochemical copper-catalyzed asymmetric cross-dehydrogenative coupling reactions of unreactive 2-aryl-3-arylmethylindoles with 1,3-dicarbonyl substrates were also scrutinized by Su *et al.*[117] In the context of metal-catalyzed coupling reactions, the same group has published several important papers, focusing on the C–H activation,[118] Heck,[119] Suzuki[46] and Buchwald-Hartwig couplings carried out in air.[120] The latter reaction, also known as Buchwald-Hartwig amination, was the subject of investigation by Browne's group, who reported Pd-catalyzed reaction of aryl chlorides and bromides with secondary amines. The ball milling conditions were compatible with liquid and solid substrates, and without the need to work in an air- and moisture-free atmosphere.[121] Kubota and Ito have recently made significant contributions to the application of mechanochemistry for solid-state carbon–carbon and carbon–nitrogen couplings by employing glovebox- and Schlenk-line-free protocols.[30] In particular, the solid-state Buchwald-Hartwig amination required the addition of an olefin component to enable efficient dispersion of the palladium catalyst, preventing its aggregation and low performance (see Figure 7.6c). Using a $Pd(OAc)_2$ catalyst, tri-*tert*-butylphosphine ligand and sodium *tert*-butoxide as the base, only 33% yield in the model reaction was achieved. LAG with toluene and THF increased the yields up to 55%, however the presence of olefin additives such as cyclohexene, cyclooctene and especially 1,5-cyclooctadiene (1,5-COD) led to almost quantitative yields. TEM analysis of palladium particles in crude reaction mixtures revealed the critical role of 1,5-COD as a molecular dispersant.[122] Also, mechanochemical iridium-catalyzed C–H borylation of indoles, pyrroles and furans was recently reported by the same

group, providing access to arylboronates as substrates for the Suzuki coupling reaction.[123]

While these are only representative examples with many remaining out of reach of this short overview, mechanochemically-promoted metal-catalyzed reactions have recently been extensively reviewed by Porcheddu.[106] Here, as an illustrative example, the formation of $C(sp^3)$–$C(sp^3)$ bonds by Reformatsky reaction described by Browne was selected.[124] In the reaction, 2 equivalents of zinc and a slight excess of nucleophile (1.2 equivalent) are required for the full conversion and formation of hydroxyesters. One-step, one-pot preparation and use of organozinc species provided hydroxyesters in high yields (up to 87%) starting from various aldehydes and ketones as carbonyl electrophiles and different nucleophiles (see Figure 7.7).

Under these conditions, a reductive aldehyde coupling (pinacol reaction) side-reaction was not observed for halogen-containing substrates. Ball milling was found to be advantageous for the *in situ* generation of organozinc species without the need for dry solvents and the inert atmosphere that must be secured in a classical solution reaction. Important improvements of the green metrics of this reaction could be illustrated by reaction of benzaldehyde and ethyl 2-bromoacetate. Mechanochemical milling provides yields 53–87%, without any solvent, inert gas or additives, whereas a reaction in THF under a nitrogen atmosphere led to mere 7% and 4% yields, when flake 325 mesh and granular zinc were applied. The main benefit of performing the Reformatsky reaction by means of ball milling was that it avoided the preparation of fresh organozinc reagents and the associated, often tedious,

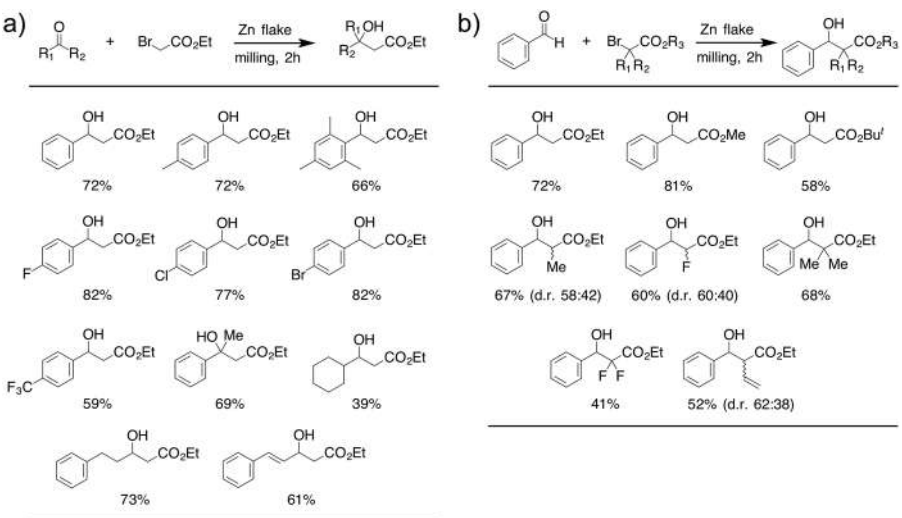

Figure 7.7 The scope of mechanochemical Reformatsky reaction by Browne *et al.* (a) A range of aldehydes and ketones as electrophiles and (b) latent nucleophiles are well tolerated under milling conditions with zinc flakes as the source of metal for *in situ* generation of organozinc intermediates. Reproduced from ref. 124 with permission from John Wiley and Sons, Copyright 2019.

activation of zinc powder. Detailed study of the influence of the various forms of zinc led to the conclusion that the Reformatsky reaction carried out in a ball mill was successful, regardless of the form of zinc reagent. In general, zinc forms with higher surface area to volume ratio showed better results. This study clearly indicated that mechanical energy applied by milling was sufficient to break down oxide layers on the metal surface and activate zinc, in addition to decreasing the particle size.

7.4.2 Organocatalysis

The benefits of conducting asymmetric organic reactions under ball milling conditions were first recognized by Bolm *et al.*, who studied (*S*)-proline-catalyzed aldol condensations of aromatic aldehydes with ketones,[125] and asymmetric meso-anhydride opening with cinchona-derived quinidine.[126] Juaristi and coworkers made notable contributions to mechanochemical organocatalysis by describing several examples of enantioselective transformations of both aldehydes and ketones as electrophiles, using chiral dipeptides as organocatalysts.[127] In all these cases, ball milling reactions were considerably faster than solution ones with magnetic stirring, the products were isolated in high yields, the amount of solvent in the work-up steps was significantly reduced and finally, they gave comparable or even better enantioselectivities. These were remarkable achievements, especially given the fact that bulk solvents can have a profound effect on the stereochemical outcome of such reactions.

Browne *et al.* recently reported an organocatalytic aza-Morita-Baylis–Hillman reaction, catalyzed by tertiary amines such as DABCO or quinuclidine derivatives.[128] The Šebesta group investigated the asymmetric Michael addition between aldehyde substrates and nitroalkenes, catalyzed by diphenyl-2-pyrrolidinemethanol trimethylsilyl ether,[129] as well as the enantioselective carbon-nitrogen coupling of azodicarboxylates with propionaldehydes. Excellent stereoselectivity and good isolated yields were achieved with a proline-derived catalyst.[130] The full potential of mechanochemical organocatalysis is still to be explored since the number of publications in this field lags behind other areas mentioned in previous sections.[131,132]

In this chapter, another example from the Šebesta group, a mechanochemical one-pot two-step asymmetric synthesis of fluorinated oxindole pyrazolone adducts by a domino Mannich reaction/fluorination, is outlined below .[133] The first step was the Mannich addition of pyrazolones to mono-Boc-protected iminoindolinones effected by the quinine-derived squaramide catalysts (see Figure 7.8a). The second step was the diastereoselective fluorination using *N*-fluorobenznesulfonimide (NFSI) reagent added to the same reaction jar after completion of the Mannich step. Enantioselectivity by ball milling was much improved by the addition of a small amount of dichloromethane (LAG, 50 μL), whereas other solvents like diethyl ether, toluene, ethyl acetate, acetonitrile or water gave lower yields and modest enantioselectivities. The use of the LAG protocol greatly shortened the reaction time from hours in classical solution conditions to only 5 minutes for the Mannich reaction and 20–24 minutes for the fluorination step. At the same

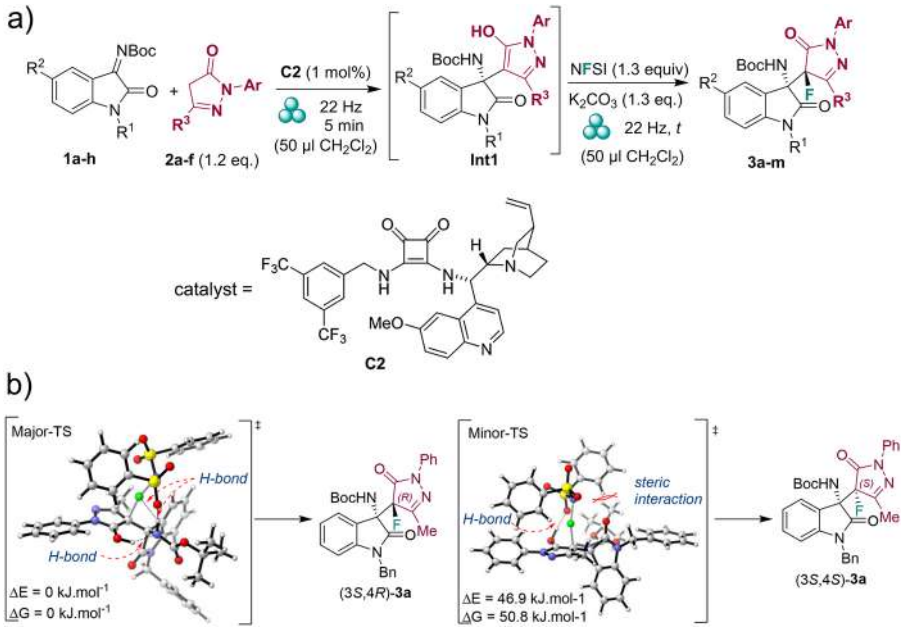

Figure 7.8 (a) A mechanochemical diastereoselective domino Mannich reaction/fluorination of oxindole pyrazolones studied by Šebesta *et al.* (b) Hydrogen bonding and steric hindrance in transition structures govern the diastereoselectivity of the fluorination reaction. Reprinted with permission from *ACS Sustainable Chem. Eng.*, 2020, **8**(38), 14417–14424, Copyright 2020 American Chemical Society.

time, the consumption of undesirable chlorinated solvents was significantly reduced, which is of high importance from an environmental standpoint.

The optimized reaction conditions led to high yields (up to 98%) and enantioselectivities of fluorinated products (up to 99:1). A range of substituted Boc-protected iminoindolinones successfully reacted with *N*-arylpyrazolones to afford Mannich intermediates, which were then stereoselectively fluorinated using NFSI. The same domino sequence with isoxazolones as substrates was less efficient with lower yields and enantioselectivities.

This simple synthetic protocol exemplifies the fact that weak interactions in the transition state, which govern asymmetric catalytic reactions in the solution phase, also operate under mechanochemical conditions and are presumably equally important. DFT calculations on the diastereoselective fluorination of the Mannich intermediate revealed the importance of hydrogen bonding in the transition structure leading to the isolated product with (3*S*,4*R*)-configuration, which was favoured by *ca.* 50 kJ mol^{-1} over the (3*S*,4*S*)-diastereomer. Additionally, steric repulsions in the (3*S*,4*S*)-transition structure between NFSI and *tert*-butyl in the Boc-protection group destabilized this reaction path (see Figure 7.8b). The higher efficiency of the ball milling conditions was estimated by the calculation of the mass intensity (MI – the total mass used in the process relative to the mass of product).

The yield, stoichiometry of the reagents, amounts of reagents and solvent are accounted for here. MI for ball milling synthesis of 3a is calculated to be 10 times more efficient than solution conditions (4.1 mg mg^{-1} *vs.* 42.2 mg mg^{-1}) and this efficiency is mainly due to great reduction of solvent use.

In the context of asymmetric organic reactions, enzyme catalysis *via* ball milling is becoming an attractive alternative to small molecule organocatalysts. Bolm and Hernandez described kinetic resolution of racemic secondary alcohols using *Candida antarctica* lipase B (CALB) enzyme immobilized on acrylic resin and isoprenyl acetate as the acylation reagent. After ball milling for 3 hours in zirconia media, (*R*)-enantiomers were acylated while (*S*)-alcohols were separated in high enantioselectivities and yields.[134] Pérez-Venegas and Juaristi adopted the same approach to resolve racemic mixtures of primary amines by converting the (*R*)-enantiomers into amides. The enantiomeric purity of (*R*)-amides was in many cases >99% with conversions ranging from 20–48% (50% max.), thus affecting the enantiomeric excess of the free (*S*)-amine.[135] Mechanochemical esterifications and hydrolyses of amino esters catalyzed by immobilized CALB followed next, while the scope of mechanoenzymatic transformations was further expanded through the use of proteases like papain to enable preparation of dipeptides and oligopeptides.[136] Mechanoenzymatic reactions have recently been in the focus of the Friščić and Auclair groups, who developed a new strategy termed "reactive aging (RAging)". This approach combines the power of enzymes to catalyze ball milling-induced reactions with high efficiency provided by the aging process in a humid/wet environment. The authors demonstrated how biopolymers such as cellulose, hemicellulose, chitin, cellobiose and lignocellulosic biomass could be successfully hydrolysed by alternating cycles of brief five-minute ball milling and aging in a humid atmosphere at slightly elevated temperatures for several hours.[137]

7.4.3 Photocatalysis

One field of organic synthesis that has not been much considered in the new era of mechanochemical research is photochemistry. This is most likely due to the fact that typical ball milling instrumentation and milling media are not designed or intended for photochemical activation of substrates. A way to circumvent these technical issues is to conduct a mechanochemical reaction inside a laboratory photochemical reactor using vials transparent to the UV-Vis spectral range. This approach was pursued by MacGillivray's group who performed milling in a vortex device under UV-irradiation during a photochemical [2 + 2] cycloaddition to afford cyclobutane products.[138] Another interesting practical solution came from König's group. Solvent-free alcohol oxidations and aryl halide coupling reactions with pyrroles and phosphites were carried out using riboflavin tetraacetate or rhodamine 6G photocatalysts in a rod mill-like apparatus[139] or a rotating glass vial,[140] while the reaction mixture, in the form of a thin liquid film, was irradiated under visible light.

Our group developed a different and unique approach based on ball milling in a commercially available mixer mill, coupled with simultaneous visible light irradiation. This new method, termed "mechanochemically-assisted solid-state photocatalysis" or MASSPC, relied on the use of visible light-transparent custom-made glass jars in combination with a specially designed photochemical LED reactor that permitted high-speed vibrational milling and irradiation of the milled sample at the same time (see Figure 7.9).[141] Ordinary LED strips were not robust enough to withstand prolonged high-speed milling without breaking. An aerobic, photocatalytic oxidation of an alkyne, promoted by 4-chlorothiophenol (2 eq.), was chosen as the model reaction. The best photocatalyst for the conversion of diphenylacetylene to the diketone benzil was found to be eosin Y (2 mol%), in a reaction that proceeded through the formation of a vinyl sulfide photoactive species, determined by GC analysis. At low light intensity (input power 5 W), the reaction progress was slow. Increasing the power to 14.5 W led to significant rate enhancement, however, the yield slowly deteriorated if too intense light (32 W) was applied. Since tetraphenylporphyrin, among other tested photocatalysts, also induced the formation of the product (albeit with lower conversion), this suggested that a mechanism involving singlet oxygen generation was underway. Based on these observations and detection and isolation of by-products such as a diaryldisulfide, benzothioate and benzoic acid, a plausible reaction mechanism was proposed. The vinyl sulfide underwent a [2 + 2] cycloaddition reaction with the *in situ* formed singlet oxygen $^1O_2$, to afford

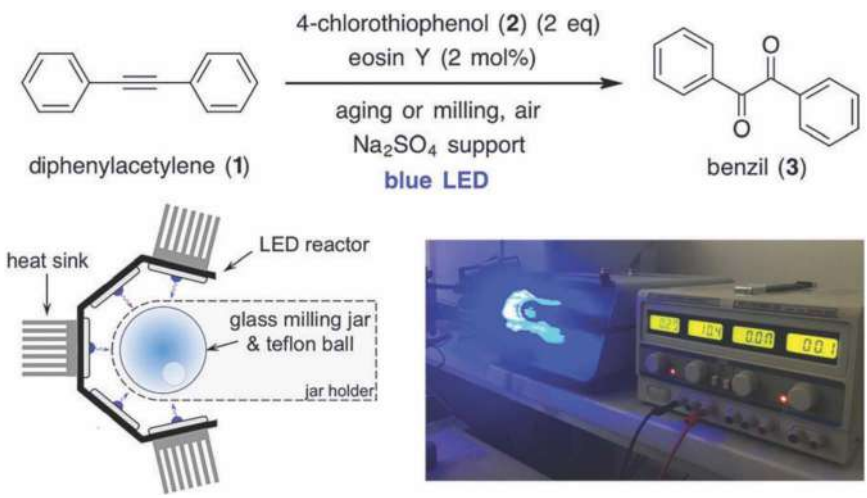

Figure 7.9 Mechanochemically-assisted solid-state photocatalysis (MASSPC): A model solid-state aerobic photocatalytic oxidation of diphenylacetylene and the LED reactor design (left) in operation with simultaneous ball milling (right). Reproduced from ref. 141 with permission from the Royal Society of Chemistry, Copyright 2017.

an unstable cyclic intermediate, which decomposed further and gave benzil diketone in a modest 40% yield. The presence of $^1O_2$ was confirmed in a separate experiment by reacting anthracene and eosin Y, and trapping the *endo*-peroxide product under MASSPC conditions.

Next, LED strips and plastic PMMA jars were used by Hernández in the green-light promoted mechanochemical borylation of aromatic diazonium salts with eosin Y photocatalyst.[142] The MASSPC technique has also recently been successfully adopted by Vilela and Lloyd to generate anthracene-9,10-*endo*-peroxide from anthracene and *N*-(7-iodobenzo[*c*][1,2,5]thiadiazol-4-yl)benzamide (also synthesized by milling) as the singlet oxygen phtosensitizer.[143]

References

1. P. T. Anastas and J. C. Warner, *Green Chemistry: Theory and Practice*, Oxford University Press, Oxford, 1998.
2. F. Gomollón-Bel, *Chem., Int.*, 2019, **41**, 12.
3. L. Takacs, *J. Mater. Sci.*, 2018, **53**, 13324.
4. D. Tan and T. Friščić, *Eur. J. Org. Chem.*, 2018, **2018**, 18.
5. T. Friščić, C. Mottillo and H. M. Titi, *Angew. Chem., Int. Ed.*, 2020, **59**, 1018.
6. J. Andersen and J. Mack, *Green Chem.*, 2018, **20**, 1435.
7. C. Bolm and J. G. Hernández, *Angew. Chem., Int. Ed.*, 2019, **58**, 3285.
8. H. Junghare, M. Hamjade, C. K. Patil, S. B. Girase and M. M. Lele, *Int. J. Curr. Eng. Technol.*, 2017, 420.
9. N. Cindro, M. Tireli, B. Karadeniz, T. Mrla and K. Užarević, *ACS Sustainable Chem. Eng.*, 2019, **7**, 16301.
10. G. Kaupp, *CrystEngComm*, 2003, **5**, 117.
11. Y. Murata, N. Kato, K. Fujiwara and K. Komatsu, *J. Org. Chem.*, 1999, **64**, 3483.
12. V. Ban, Y. Sadikin, M. Lange, N. Tumanov, Y. Filinchuk, R. Černy and N. Casati, *Anal. Chem.*, 2017, **89**, 13176.
13. M. Samal, J. Panda, B. P. Biswal and R. Sahu, *CrystEngComm*, 2018, **20**, 2486.
14. P. Baláž, M. Achimovičevá, M. Baláž, P. Billik, Z. Cherkezova-Zheleva, J. M. Criado, F. Delogu, E. Dutková, E. Gaffet, F. J. Gotor, R. Kumar, I. Mitov, T. Rojac, M. Senna, A. Streletskii and K. Wieczorek-Ciurowa, *Chem. Soc. Rev.*, 2013, **42**, 7571.
15. K. Martina, L. Rotolo, A. Porcheddu, F. Delogu, S. R. Bysouth, G. Cravotto and E. Colacino, *Chem. Commun.*, 2018, **54**, 551.
16. J. G. Osorio and F. J. Muzzio, *Powder Technol.*, 2015, **278**, 46.
17. A. A. L. Michalchuk, K. S. Hope, S. R. Kennedy, M. V. Blanco, E. V. Boldyreva and C. R. Pulham, *Chem. Commun.*, 2018, **54**, 4033.
18. K. Nagapudi, E. Yanez Umanzor and C. Masui, *Int. J. Pharm.*, 2017, **521**, 337.
19. D. J. am Ende, S. R. Anderson and J. S. Salan, *Org. Process Res. Dev.*, 2014, **18**, 331.

20. S. R. Anderson, D. J. am Ende, J. S. Salan and P. Samuels, *Propellants, Explos., Pyrotech.*, 2014, **39**, 637.
21. H. M. Titi, J.-L. Do, A. J. Howarth, K. Nagapudi and T. Friščić, *Chem. Sci.*, 2020, **11**, 7578.
22. D. E. Crawford, L. A. Wright, S. L. James and A. P. Abbott, *Chem. Commun.*, 2016, **52**, 4215.
23. D. E. Crawford, C. K. G. Miskimmin, A. B. Albadarin, G. Walker and S. L. James, *Green Chem.*, 2017, **19**, 1507.
24. Q. Cao, D. E. Crawford, C. Shi and S. L. James, *Angew. Chem., Int. Ed.*, 2020, **59**, 4478.
25. D. E. Crawford, A. Porcheddu, A. S. McCalmont, F. Delogu, S. L. James and E. Colacino, *ACS Sustainable Chem. Eng.*, 2020, **8**, 12230.
26. L. S. Germann, M. Arhangelskis, M. Etter, R. E. Dinnebier and T. Friščić, *Chem. Sci.*, 2020, **11**, 10092.
27. M. Carta, S. L. James and F. Delogu, *Molecules*, 2019, **24**, 3600.
28. B. P. Hutchings, D. E. Crawford, L. Gao, P. Hu and S. L. James, *Angew. Chem., Int. Ed.*, 2017, **56**, 15252.
29. I. A. Tumanov, A. A. L. Michalchuk, A. A. Politov, E. V. Boldyreva and V. V. Boldyrev, *CrystEngComm*, 2017, **19**, 2830.
30. K. Kubota, R. Takahashi, M. Uesugi and H. Ito, *ACS Sustainable Chem. Eng.*, 2020, **8**, 16577.
31. N. R. Rightmire, T. P. Hanusa and A. L. Rheingold, *Organometallics*, 2014, **33**, 5952.
32. R. F. Koby, T. P. Hanusa and N. D. Schley, *J. Am. Chem. Soc.*, 2018, **140**, 15934.
33. J. L. Howard, M. C. Brand and D. L. Browne, *Angew. Chem., Int. Ed.*, 2018, **57**, 16104.
34. T. Friščić, A. V. Trask, W. Jones and W. D. S. Motherwell, *Angew. Chem., Int. Ed.*, 2006, **45**, 7546.
35. N. Shan, F. Toda and W. Jones, *Chem. Commun.*, 2002, **38**, 2372.
36. T. Friščić, S. L. Childs, S. A. A. Rizvi and W. Jones, *CrystEngComm*, 2009, **11**, 418.
37. A. V. Trask, W. D. S. Motherwell and W. Jones, *Chem. Commun.*, 2004, **40**, 890.
38. D. Cinčić, T. Friščić and W. Jones, *J. Am. Chem. Soc.*, 2008, **130**, 7524.
39. K. L. Nguyen, T. Friščić, G. M. Day, L. F. Gladden and W. Jones, *Nat. Mater.*, 2007, **6**, 206.
40. F. C. Strobridge, N. Judaš and T. Friščić, *CrystEngComm*, 2010, **12**, 2409.
41. M. Đud, O. V. Magdysyuk, D. Margetić and V. Štrukil, *Green Chem.*, 2016, **18**, 2666.
42. L. Chen, M. Regan and J. Mack, *ACS Catal.*, 2016, **6**, 868.
43. K. Leahy Denlinger, L. Ortiz-Trankina, P. Carr, K. Benson, D. C. Waddell and J. Mack, *Beilstein J. Org. Chem.*, 2018, **14**, 688.
44. M. Tireli, M. Juribašić Kulcsar, N. Cindro, D. Gracin, N. Biliškov, M. Borovina, M. Ćurić, I. Halasz and K. Užarević, *Chem. Commun.*, 2015, **51**, 8058.

45. V. Štrukil, D. Margetić, M. D. Igrc, M. Eckert-Maksić and T. Friščić, *Chem. Commun.*, 2012, **48**, 9705.
46. Z.-J. Jiang, Z.-H. Li, J.-B. Yu and W.-K. Su, *J. Org. Chem.*, 2016, **81**, 10049.
47. T. Friščić, D. G. Reid, I. Halasz, R. S. Stein, R. E. Dinnebier and M. J. Duer, *Angew. Chem., Int. Ed.*, 2010, **49**, 712.
48. P. J. Beldon, L. Fábián, R. S. Stein, A. Thirumurugan, A. K. Cheetham and T. Friščić, *Angew. Chem., Int. Ed.*, 2010, **49**, 9640.
49. D. Hasa, G. Schneider Rauber, D. Voinovich and W. Jones, *Angew. Chem., Int. Ed.*, 2015, **54**, 7371.
50. D. Hasa, E. Carlino and W. Jones, *Cryst. Growth Des.*, 2016, **16**, 1772.
51. L. S. Germann, S. T. Emmerling, M. Wilke, R. E. Dinnebier, M. Moneghini and D. Hasa, *Chem. Commun.*, 2020, **56**, 8743.
52. V. Declerck, E. Colacino, X. Bantreil, J. Martinez and F. Lamaty, *Chem. Commun.*, 2012, **48**, 11778.
53. L. Konnert, M. Dimassi, L. Gonnet, F. Lamaty, J. Martinez and E. Colacino, *RSC Adv.*, 2016, **6**, 36978.
54. A. Mukherjee, R. D. Rogers and A. S. Myerson, *CrystEngComm*, 2018, **20**, 3817.
55. I. C. B. Martins, M. Conceição Oliveira, H. P. Diogo, L. C. Branco and M. T. Duarte, *ChemSusChem*, 2017, **10**, 1360.
56. E. Colacino, M. Carta, G. Pia, A. Porcheddu, P. C. Ricci and F. Delogu, *ACS Omega*, 2018, **3**, 9196.
57. T. Friščić, I. Halasz, P. J. Beldon, A. M. Belenguer, F. Adams, S. A. J. Kimber, V. Honkimäki and R. E. Dinnebier, *Nat. Chem.*, 2013, **5**, 66.
58. M. Wilke and N. Casati, *Chem. - Eur. J.*, 2018, **24**, 17701.
59. T. Stolar, L. Batzdorf, S. Lukin, D. Žilić, C. Mottillo, T. Friščić, F. Emmerling, I. Halasz and K. Užarević, *Inorg. Chem.*, 2017, **56**, 6599.
60. S. Haferkamp, F. Fischer, W. Kraus and F. Emmerling, *Beilstein J. Org. Chem.*, 2017, **13**, 2010.
61. S. Haferkamp, A. Paul, A. A. L. Michalchuk and F. Emmerling, *Beilstein J. Org. Chem.*, 2019, **15**, 1141.
62. D. Gracin, V. Štrukil, T. Friščić, I. Halasz and K. Užarević, *Angew. Chem., Int. Ed.*, 2014, **53**, 6193.
63. A. Bjelopetrović, M. Robić, I. Halasz, D. Babić, M. Juribašić Kulcsar and M. Ćurić, *Organometallics*, 2019, **38**, 4479.
64. I. Sović, S. Lukin, E. Meštrović, I. Halasz, A. Porcheddu, F. Delogu, P. C. Ricci, F. Caron, T. Perilli, A. Dogan and E. Colacino, *ACS Omega*, 2020, **5**, 28663.
65. C. Fiore, I. Sović, S. Lukin, I. Halasz, K. Martina, F. Delogu, P. C. Ricci, A. Porcheddu, O. Shemchuk, D. Braga, J.-L. Pirat, D. Virieux and E. Colacino, *ACS Sustainable Chem. Eng.*, 2020, **8**, 18889.
66. V. Štrukil, D. Gracin, O. Magdysyuk, R. E. Dinnebier and T. Friščić, *Angew. Chem., Int. Ed.*, 2015, **54**, 8440.
67. P. A. Julien, I. Malvestiti and T. Friščić, *Beilstein J. Org. Chem.*, 2017, **13**, 2160.

68. S. Lukin, M. Tireli, I. Lončarić, D. Barišić, P. Šket, D. Vrsaljko, M. di Michiel, J. Plavec, K. Užarević and I. Halasz, *Chem. Commun.*, 2018, **54**, 13216.
69. K. Užarević, I. Halasz and T. Friščić, *J. Phys. Chem. Lett.*, 2015, **6**, 4129.
70. P. F. M. de Oliveira, A. A. L. Michalchuk, A. Guilherme Buzanich, R. Bienert, R. M. Torresi, P. H. C. Camargo and F. Emmerling, *Chem. Commun.*, 2020, **56**, 10329.
71. Y. Xu, L. Champion, B. Gabidullin and D. L. Bryce, *Chem. Commun.*, 2017, **53**, 9930.
72. J. Gerrit Schiffmann, F. Emmerling, I. C. B. Martins and L. Van Wüllen, *Solid State Nucl. Magn. Reson.*, 2020, **109**, 101687.
73. L. Takacs, *Prog. Mater. Sci.*, 2002, **47**, 355.
74. V. Štrukil, L. Fábián, D. G. Reid, M. J. Duer, G. J. Jackson, M. Eckert-Maksić and T. Friščić, *Chem. Commun.*, 2010, **46**, 9191.
75. K. Užarević, V. Štrukil, C. Mottillo, P. A. Julien, A. Puškarić, T. Friščić and I. Halasz, *Cryst. Growth Des.*, 2016, **16**, 2342.
76. H. Kulla, M. Wilke, F. Fischer, M. Röllig, C. Maierhofer and F. Emmerling, *Chem. Commun.*, 2017, **53**, 1664.
77. K. Užarević, N. Ferdelji, T. Mrla, P. A. Julien, B. Halasz, T. Friščić and I. Halasz, *Chem. Sci.*, 2018, **9**, 2525.
78. B. Rodriguez, A. Bruckmann and C. Bolm, *Chem. - Eur. J.*, 2007, **13**, 4710.
79. V. Štrukil, B. Bartolec, T. Portada, I. Đilović, I. Halasz and D. Margetić, *Chem. Commun.*, 2012, **48**, 12100.
80. I. Dokli and M. Gredičak, *Eur. J. Org. Chem.*, 2015, **2015**, 2727.
81. T.-X. Métro, J. Martinez and F. Lamaty, *ACS Sustainable Chem. Eng.*, 2017, **5**, 9599.
82. J. L. Howard, Y. Sagatov and D. L. Browne, *Tetrahedron*, 2018, **74**, 3118.
83. V. Štrukil, M. D. Igrc, M. Eckert-Maksić and T. Friščić, *Chem. - Eur. J.*, 2012, **18**, 8464.
84. V. Štrukil, M. D. Igrc, L. Fábián, M. Eckert-Maksić, S. L. Childs, D. G. Reid, M. J. Duer, I. Halasz, C. Mottillo and T. Friščić, *Green Chem.*, 2012, **14**, 2462.
85. M. Đud, Z. Glasovac and D. Margetić, *Tetrahedron*, 2019, **75**, 109.
86. V. Štrukil, *Beilstein J. Org. Chem.*, 2017, **13**, 1828.
87. K. Leahy Denlinger, P. Carr, D. C. Waddell and J. Mack, *Molecules*, 2020, **25**, 364.
88. J. Mack, D. Fulmer, S. Stofel and N. Santos, *Green Chem.*, 2007, **9**, 1041.
89. T. Portada, D. Margetić and V. Štrukil, *Molecules*, 2018, **23**, 3163.
90. A. Y. Li, A. Segalla, C.-J. Li and A. Moores, *ACS Sustainable Chem. Eng.*, 2017, **5**, 11752.
91. Z. Li, Z. Jiang and W. Su, *Green Chem.*, 2015, **17**, 2330.
92. V. P. Balema, J. W. Wiench, M. Pruski and V. K. Pecharsky, *J. Am. Chem. Soc.*, 2002, **124**, 6244.
93. Z. Zhang, Z.-W. Peng, M.-F. Hao and J.-G. Gao, *Synlett*, 2010, **19**, 2895.
94. R. Mocci, S. Murgia, L. De Luca, E. Colacino, F. Delogu and A. Porcheddu, *Org. Chem. Front.*, 2018, **5**, 531.

95. A. Porcheddu, F. Delogu, L. De Luca and E. Colacino, *ACS Sustainable Chem. Eng.*, 2019, **7**, 12044.
96. K. J. Ardila-Fierro, S. Lukin, M. Etter, K. Užarević, I. Halasz, C. Bolm and J. G. Hernández, *Angew. Chem., Int. Ed.*, 2020, **59**, 13458.
97. S.-E. Zhu, F. Li and G.-W. Wang, *Chem. Soc. Rev.*, 2013, **42**, 7535.
98. T. Friščić, *Chem. Soc. Rev.*, 2012, **41**, 3493.
99. B. Ranu and A. Stolle, *Ball Milling towards Green Synthesis: Applications, Projects, Challenges*, Royal Society of Chemistry, Cambridge, 2015.
100. D. Margetić and V. Štrukil, *Mechanochemical Organic Synthesis*, Elsevier, Amsterdam, 2016.
101. T. Dalidovich, K. A. Mishra, T. Shalima, M. Kudrjašova, D. G. Kananovich and R. Aav, *ACS Sustainable Chem. Eng.*, 2020, **8**, 15703.
102. S. F. Nielsen, D. Peters and O. Axelsson, *Synth. Commun.*, 2000, **30**, 3501.
103. L. M. Klingensmith and N. E. Leadbeater, *Tetrahedron Lett.*, 2003, **44**, 765.
104. E. Tullberg, D. Peters and T. Frejd, *J. Organomet. Chem.*, 2004, **689**, 3778.
105. E. Tullberg, F. Schacher, D. Peters and T. Frejd, *Synthesis*, 2006, 1183.
106. A. Porcheddu, E. Colacino, L. De Luca and F. Delogu, *ACS Catal.*, 2020, **10**, 8344.
107. R. A. Haley, J. Mack and H. Guan, *Inorg. Chem. Front.*, 2017, **4**, 52.
108. T. L. Cook, J. A. Walker and J. Mack, *Green Chem.*, 2013, **15**, 617.
109. W. Pickhardt, S. Grätz and L. Borchardt, *Chem. - Eur. J.*, 2020, **26**, 12903.
110. L. Chen, M. O. Bovee, B. E. Lemma, K. S. M. Keithley, S. L. Pilson, M. G. Coleman and J. Mack, *Angew. Chem., Int. Ed.*, 2015, **54**, 11084.
111. R. A. Haley, A. R. Zellner, J. A. Krause, H. Guan and J. Mack, *ACS Sustainable Chem. Eng.*, 2016, **4**, 2464.
112. D. Tan, C. Mottillo, A. D. Katsenis, V. Štrukil and T. Friščić, *Angew. Chem., Int. Ed.*, 2014, **53**, 9321.
113. G. Dayaker, D. Tan, N. Biggins, A. Shelam, J.-L. Do, A. D. Katsenis and T. Friščić, *ChemSusChem*, 2020, **13**, 2966.
114. A. Porcheddu, E. Colacino, G. Cravotto, F. Delogu and L. De Luca, *Beilstein J. Org. Chem.*, 2017, **13**, 2049.
115. J.-L. Do, C. Mottillo, D. Tan, V. Štrukil and T. Friščić, *J. Am. Chem. Soc.*, 2015, **137**, 2476.
116. P. Staleva, J. G. Hernández and C. Bolm, *Chem. - Eur. J.*, 2019, **25**, 9202.
117. J. Yu, P. Ying, H. Wang, K. Xiang and W. Su, *Adv. Synth. Catal.*, 2020, **362**, 893.
118. J. Yu, C. Zhang, X. Yang and W. Su, *Org. Biomol. Chem.*, 2019, **17**, 4446.
119. W. Shi, J. Yu, Z. Jiang, Q. Shao and W. Su, *Beilstein J. Org. Chem.*, 2017, **13**, 1661.
120. Q.-L. Shao, Z.-J. Jiang and W.-K. Su, *Tetrahedron Lett.*, 2018, **59**, 2277.
121. Q. Cao, W. I. Nicholson, A. C. Jones and D. L. Browne, *Org. Biomol. Chem.*, 2019, **17**, 1722.
122. K. Kubota, T. Seo, K. Koide, Y. Hasegawa and H. Ito, *Nat. Commun.*, 2019, **10**, 111.
123. Y. Pang, T. Ishiyama, K. Kubota and H. Ito, *Chem. - Eur. J.*, 2019, **25**, 4654.

124. Q. Cao, R. T. Stark, I. A. Fallis and D. L. Browne, *ChemSusChem*, 2019, **12**, 2554.
125. B. Rodriguez, T. Rantanen and C. Bolm, *Angew. Chem., Int. Ed.*, 2006, **45**, 6924.
126. T. Rantanen, I. Schiffers and C. Bolm, *Org. Process Res. Dev.*, 2007, **11**, 592.
127. J. G. Hernández, V. García-López and E. Juaristi, *Tetrahedron*, 2012, **68**, 92.
128. M. T. J. Williams, L. C. Morrill and D. L. Browne, *ACS Sustainable Chem. Eng.*, 2020, **8**, 17876.
129. E. Veverková, V. Poláčková, L. Liptáková, E. Kázmerová, M. Mečiarová, Š. Toma and R. Šebesta, *ChemCatChem*, 2012, **4**, 1013.
130. E. Veverková, V. Modrocká and R. Šebesta, *Eur. J. Org. Chem.*, 2017, **2017**, 1191.
131. I. N. Egorov, S. Santra, D. S. Kopchuk, I. S. Kovalev, G. V. Zyryanov, A. Majee, B. C. Ranu, V. L. Rusinov and O. N. Chupakhin, *Green Chem.*, 2020, **22**, 302.
132. C. G. Avila-Ortiz and E. Juaristi, *Molecules*, 2020, **25**, 3579.
133. D. Krištofíková, M. Mečiarová, E. Rakovsky and R. Šebesta, *ACS Sustainable Chem. Eng.*, 2020, **8**, 14417.
134. J. G. Hernández, M. Frings and C. Bolm, *ChemCatChem*, 2016, **8**, 1769.
135. M. Pérez-Venegas and E. Juaristi, *Tetrahedron*, 2018, **74**, 6453.
136. K. J. Ardila-Fierro, D. E. Crawford, A. Körner, S. L. James, C. Bolm and J. G. Hernández, *Green Chem.*, 2018, **20**, 1262.
137. S. Kaabel, T. Friščić and K. Auclair, *ChemBioChem*, 2020, **21**, 742.
138. J. Stojaković, B. S. Farris and L. R. MacGillivray, *Chem. Commun.*, 2012, **48**, 7958.
139. M. Obst and B. König, *Beilstein J. Org. Chem.*, 2016, **12**, 2358.
140. M. Obst, R. S. Shaikh and B. König, *React. Chem. Eng.*, 2017, **2**, 472.
141. V. Štrukil and I. Sajko, *Chem. Commun.*, 2017, **53**, 9101.
142. J. G. Hernández, *Beilstein J. Org. Chem.*, 2017, **13**, 1463.
143. E. Broumidis, M. C. Jones, F. Vilela and G. O. Lloyd, *ChemPlusChem*, 2020, **85**, 1754.

CHAPTER 8

Sustainable Activation of Chemical Substrates Under Sonochemical Conditions

MICHELINE DRAYE[a], MARION CHEVALLIER[a], VANILLE QUINTY[a], CLAIRE BESNARD[a], ALEXANDRE VANDEPONSEELE[a] AND GREGORY CHATEL*[a]

[a]Univ. Savoie Mont Blanc, CNRS, EDYTEM, 73000 Chambéry, France
*E-mail: gregory.chatel@univ-smb.fr

8.1 Introduction

Sonochemistry is the use of power ultrasound for chemical reactions. Some chemists reported the first reaction involving ultrasound in 1927,[1,2] although the term "sonochemistry" has only been used since 1980.[3] Ultrasound is often viewed, and particularly in organic chemistry, as a simple and efficient mixing tool in the lab. However, control of the sonochemical parameters and experimental conditions has made it possible to demonstrate, in many cases, significant improvements in terms of reaction yields and/or reaction speed, thanks to the use of ultrasound. In some cases, unexpected reactivities and selectivities have also been observed under ultrasound, making it possible to imagine new perspectives and applications of sonochemistry in organic chemistry. After having introduced sonochemistry by presenting its basic theoretical and practical aspects, some case studies from recent literature are summarized to show the major advantages of using ultrasound in an organic reaction. Finally, this chapter aims to highlight the current and future challenges of organic sonochemistry.

Sustainable Organic Synthesis: Tools and Strategies
Edited by Stefano Protti and Alessandro Palmieri

Published by the Royal Society of Chemistry, www.rsc.org

8.2 Sonochemistry, a Chemistry based on Power Ultrasound

8.2.1 Acoustic Cavitation and Associated Effects

Acoustic cavitation in liquid media is the phenomenon of formation, growth and violent collapse induced by sound waves that generate fluctuation of pressure. Liquid media usually contain free gas bubbles or gas molecules trapped in solid impurities, which can act as nuclei for cavitation.[4] Once the cavitation bubble is formed, its diameter increases throughout the expansion and compression phases to achieve a critical size at which it violently collapses. Indeed, expansion phases being isotherm and compression phases adiabatic, a large amount of acoustic energy is accumulated inside the bubble. At the moment of bubble implosion, temperatures of about 5000 K and pressures close to 1000 bar are then reached within the bubble (see Figure 8.1). These extreme conditions lead to different local effects such as radical formation, shock waves, acoustic micro-currents and violent liquid microjets, which are at the origin of the application of sonochemistry.[5,6]

8.2.2 Ultrasonic Parameters and Experimental Factors Affecting Cavitation

The ambient conditions of a reaction system can strongly influence the acoustic cavitation threshold and its intensity, which then directly affects the kinetics and/or the yield of the chemical reaction. The acoustic cavitation

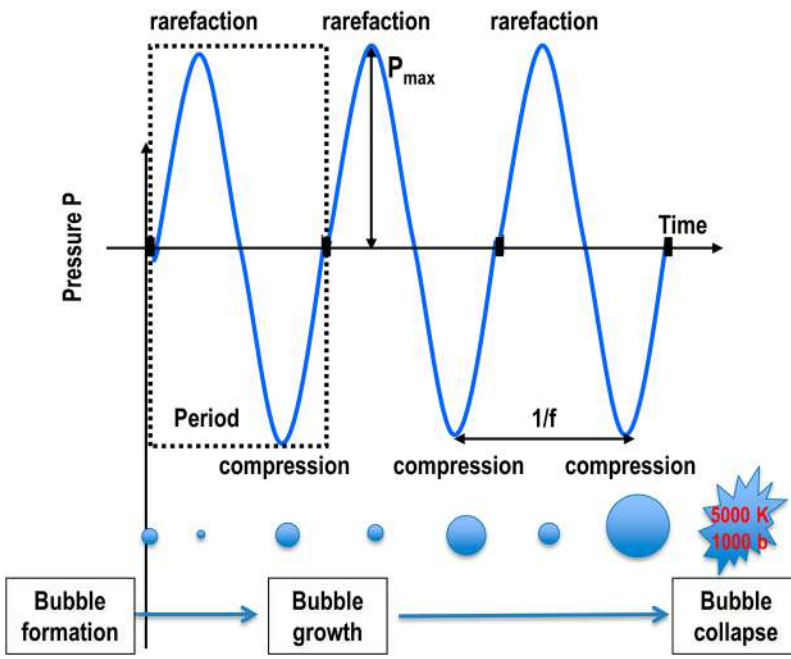

Figure 8.1 Schematic representation of bubble formation, growth and collapse.

in the liquid may be affected by several parameters, such as the frequency and power of the ultrasound, the hydrostatic and external pressures, the temperature, the nature of the solvent and dissolved gas.

8.2.2.1 Ultrasonic Frequency

Ultrasound is a sound wave with a frequency (f, Eqn (8.1)) greater than the upper limit of human hearing, which is generally over 20 kHz and below 10 MHz. When it propagates in an elastic medium, it presents all the general properties of periodic progressive waves such as propagation, attenuation and reflection.[7]

$$f = \frac{c}{\lambda} \tag{8.1}$$

where f is the frequency (Hz), c is the celerity of sound (m s^{-1}) and λ is the wavelength (m).

In water, low frequencies, ranging between 20 and 80 kHz, lead to relatively few and large transient cavitation bubbles; physical effects such as micromixing, erosion, *etc.* predominate over chemical effects. High frequencies, ranging between 150 and 2000 kHz, produce many small transient cavitation bubbles; chemical effects such as production of hydroxyl radicals in water predominate over physical effects. It is noteworthy that, when the frequency increases, the depth of penetration of the ultrasonic wave decreases, decreasing the maximum pressure reached during implosion. It is therefore necessary to increase the sound power to obtain the same effects as at low frequency.[7,8]

8.2.2.2 Dissipated Ultrasonic Power

A piezoelectric transducer converts electrical energy into mechanical energy that is thus transmitted to the liquid, which is irradiated.[9] No transducer is 100% efficient in converting electrical to mechanical power. To determine the power output (P_{out}) for a given power input (P_{in}), it is necessary to know the transducer efficiency (h), according to eqn (8.2).

$$P_{out} = h \times P_{in} \tag{8.2}$$

The mechanical energy is then converted into acoustical energy generating acoustic cavitation if the minimum power required is reached, *i.e.*, at the Blake threshold, which is 0.5 W cm^{-2} at 20 kHz in pure water and at atmospheric pressure.[7] It is easy to measure the electrical energy delivered by a transducer, but this value in no way reflects the acoustic energy absorbed by the medium, which is the only that can be active. Different methods are proposed for the determination of ultrasonic power (P_{acous}), such as thermoacoustic sensors,[10] acousto-optic interaction,[11] piezoelectric hydrophones,[12] sonoluminescence, and chemical dosimetry.[8] Nevertheless,

one of the most useful methods has been found to be the calorimetric one.[8,13] Therefore, the absorbed acoustic power P_{acous} in W mL^{-1} transmitted to the solution can be measured using a conventional thermal probe method.[14,15] Using this method, all energy delivered to the system is considered as dissipated as heat (Eqn (8.3)).

$$P_{acous} = m \times c_p \times \left(\frac{dT}{dt}\right)_0 \tag{8.3}$$

where P_{acous} is the absorbed acoustical power in W (or reported relative to the volume in W mL^{-1}), m is the mass in kg of liquid in the sonoreactor, c_p is the specific heat capacity in J kg^{-1} K^{-1}, and $\left(\frac{dT}{dt}\right)_0$ is the initial slope of the increase of the temperature of the solution *versus* time of ultrasonic irradiation.

8.2.2.3 Hydrostatic Pressure

Hydrostatic pressure is a crucial parameter as the conditions within a collapsing cavitation bubble become more extreme as it increases.[16] Thus, it has been shown that the cavitation threshold in ultrapure water increases linearly with the hydrostatic pressure, as well as the intensity of bubble collapse.[8] Thereby, an optimal hydrostatic pressure is required to increase the efficiency of ultrasound when used in sonochemical processes.[17]

8.2.2.4 Temperature

When increasing the temperature of a liquid, the solubility of gases it contains decreases, whereas its vapor pressure increases decreasing the cavitation efficiency.[18] The influence of temperature on cavitation threshold is especially noticeable at elevated hydrostatic pressures and for fluids with large amounts of dissolved gases.[19]

8.2.2.5 Nature of the Solvent

Properties such as (1) solvent viscosity, (2) its vapor pressure, and (3) its surface tension can impact ultrasound intensity. For pure solvents, the most determining parameter is the vapor pressure, which when high, decreases cavitation effects.[8] Thus, combination of a high surface tension with a low viscosity and a low vapor pressure favors cavitation.[18]

8.2.2.6 Dissolved Gas

After a few acoustic cycles, transient bubbles violently collapse into smaller tiny bubbles that act as nuclei of new bubbles and create a hot spot with temperatures of up to 10 000 K.[19] This adiabatic collapse of the bubbles is

assumed to allow the calculation of the temperature and the pressure inside the bubbles according to eqn (8.4) and (8.5).[20] Meanwhile, eqn (8.6) allows the calculation of the pressure inside the bubble at the moment of collapse.

$$P_{max} = P\left[\frac{P_m(\gamma-1)}{P}\right]^{\frac{\gamma}{\gamma-1}} \tag{8.4}$$

$$T_{max} = T_0\left[P_m\frac{(\gamma-1)}{P}\right] \tag{8.5}$$

$$P_m = P_a + P_n \tag{8.6}$$

where P_{max} and T_{max} are the maximum pressure and temperature at collapse, P is the pressure inside the bubble at its maximum size, which is usually equal to the vapor pressure P_v, P_m is the pressure inside the liquid at the moment of collapse, T_0 is the ambient temperature, P_a is the acoustic pressure applied, and P_h is the pressure within the fluid. It is usually taken to be ambient or atmospheric pressure. The polytropic factor γ is the ratio of the specific heat capacities of the gas or the gas vapor mixture.

Thus, according to eqn (8.4) and (8.5) a monatomic gas leads to higher maximum temperatures and pressures and thereby to more violent collapse of the bubble than a polyatomic gas because its γ value is greater. Thermal effects consecutive to the collapse of the bubble mainly depend on the gas phase thermal properties, such as heat capacity and thermal conduction.

In the presence of a gas with high thermal conduction, the temperature reached at the time of implosion is lower than in the presence of a gas with low thermal conduction, thus decreasing T_{max}. In addition, increasing the gas content, *i.e.* the number of gas nuclei of a liquid, leads to lowering of both the cavitational threshold and the intensity of the shock wave released on the collapse of the bubble.

8.2.2.7 External Pressure

An increase of P_h leads to an increase of P_m, which is the pressure of the medium (Eqn (8.6)). In eqn (8.4) and (8.5), when P_m increases, T_m and P_m increase, leading to an increase in the cavitation threshold and the intensity of cavity collapse.

8.2.2.8 Ultrasonic Intensity

The ultrasonic intensity, I_{max}, can be expressed as eqn (8.7):[7]

$$I_{max} = \frac{P_A^2}{2\rho c} \tag{8.7}$$

where P_A is the acoustic amplitude, ρ is the density of the medium, and c is the velocity of the sound in the medium.

If considering ρ and c constant in the medium where the sound propagates, then I_{max} is proportional to the square of the acoustic amplitude P_A. Thus, an increase in P_A leads to an increase of the ultrasonic intensity, which increases the sonochemical effects up to an optimal value. Indeed, an increase of P_A leads to a decrease of the time available for the collapse of the too large bubble formed that may become thus insufficient.

Likewise, during their propagation through a medium, the intensity of ultrasound waves decreases when their distance from the emitting source increases (Eqn (8.8)). Indeed, sound is attenuated in a liquid medium due to reflection, refraction, diffraction and/or scattering of the waves, or the conversion of some of their mechanical energy into heat.

$$I_{max} = I_0 e^{-2\alpha d} \tag{8.8}$$

where I_0 is the initial sound intensity, α is the absorption coefficient of the medium and I_{max} is the ultrasonic intensity at the distance d.

In addition, if too many bubbles are produced at the transducer/liquid interface, the ultrasonic energy entering the system is attenuated, decreasing the efficiency by decoupling of the system.

8.2.3 Mode of Irradiation and Sonoreactors

8.2.3.1 Modes of Irradiation

Two physics phenomena are widely used to generate ultrasonic waves from ultrasonic devices: magnetostriction and piezoelectricity. The phenomenon of magnetostriction takes place when ferromagnetic materials transform an oscillating magnetic field into mechanical vibration.[7] The piezoelectric effect is the ability of certain crystalline materials when subjected to an electric field to convert electrical energy into mechanical energy. The strain is then proportional to the applied field and the mechanical vibrations may lead to ultrasonic sound.[21] This phenomenon is the most widely used in ultrasound devices.

The main materials used are barium titanate ($BaTiO_3$), synthetic crystals of lithium niobate ($LiNbO_4$) and lead zirconate titanate ($PbTiZrO_3$). These materials are separated from the reactor by metal or glass and ultrasound waves irradiate directly or indirectly the reaction medium (see Figure 8.2). An immerged titanium probe is often used as a waveguide.

8.2.3.2 Equipment

Three major sonoreactors are used in the lab: ultrasonic bath, cup horn and probe (Figures 8.2 and 8.3).[22–24]

An ultrasonic bath, which represents the most common source of ultrasound in laboratories, is widely used due to its low cost. With a frequency of 20 to 60 kHz and acoustic intensities of 1 to 5 W cm^{-2}, this device is not well adapted to organic reactions due to the non-homogeneous

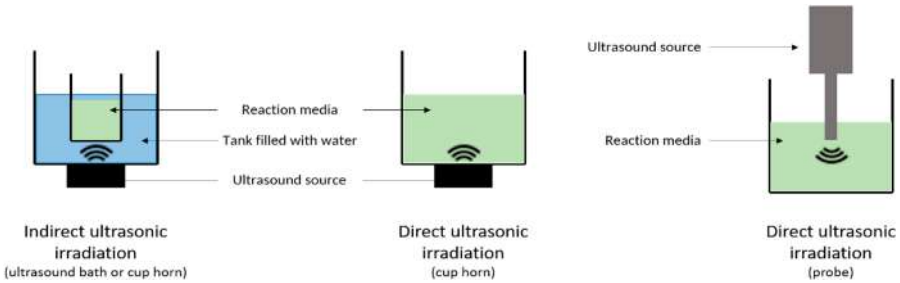

Figure 8.2 Schematic representation of the mode of irradiation depending on the main device used in laboratories. Adapted from ref. 6 with permission from World Scientific, Copyright 2017.

Figure 8.3 Cup horn system (left) and ultrasonic probe (right) in the lab.

dissipation of ultrasound energy and the associated lack of reproducibility of the experiments.[25]

Cup-horn reactors present high intensity, which is generally 50 times more intense than in US baths, and directly irradiate the liquid medium.[26] Their geometry allows a good distribution of the ultrasonic field. This device is able to produce low and high frequencies depending on the piezoelectric ceramic chosen and positioned at the bottom of the reactor for upward irradiation.

Ultrasonic probes provide intense ultrasonic energy, which is concentrated at their tip and approximately 100 times higher compared to ultrasonic baths; they allow a direct irradiation of the medium.

In both cases, the use of a jacketed reactor is recommended to control the temperature of the medium during the study of organic reactions in the lab.[6]

In addition, a study of the shape of the reactor may be relevant to avoid dead zones or to optimize certain physical, thermal and/or chemical effects. Thus, tubular reactors, providing radial irradiations, make it possible to focus the high-intensity ultrasonic field in the heart of the tube and to develop continuous processes.[27]

8.2.3.3 Characterization of the Ultrasonic Parameters

A rigorous characterization of sonochemical parameters is crucial to facilitate the comparison between each study reported in the literature and to understand the involved mechanisms.[6] Indeed, the used frequency, electric and acoustic powers, ultrasonic intensity, radical production, shape and geometry of the reactor and other experimental conditions (temperature, pressure, gas atmosphere, nature and volume of solvent, *etc.*) have to be rigorously reported in the experimental part of scientific publications.

The frequency, inherent to the equipment used, is the first parameter to report to identify which range is used between low frequency (20–80 kHz) and high frequency (200–2000 kHz). The electric power, also called "nominal electric power" or "electric power input", is the energy delivered by the device, measured by a wattmeter (in W). The absorbed acoustical power (P_{acous}, expressed in W or W mL^{-1}) can be estimated through a calorimetric method using eqn (8.3). Acoustic intensity (I_{acous}) is defined as the acoustic power per unit area of the probe (eqn (8.9), W cm^{-2}).

$$I_{max} = I_0 e^{-2\alpha d} \tag{8.9}$$

As previously mentioned, the extreme conditions during the collapse of the bubbles lead to radical production. For example, the sonolysis of water (Scheme 8.1) and the recombination of radical species into hydrogen peroxide (Scheme 8.2) are observed under ultrasonic conditions.

The radical species production can be experimentally estimated or measured by dosimetry methods,[28,29] Electron Paramagnetic Resonance (EPR),[30] spin-trapping and/or sonochemiluminescence experiments.[31–33] Chemical dosimetry is the most convenient and employed method. For example, KI dosimetry involves the oxidation of iodide ions into iodine by hydroxyl radicals formed under ultrasound, through the reaction shown in Scheme 8.3. The concentration of I_3^- can be easily measured using UV-Visible spectrophotometry at a wavelength of 355 nm (ε_λ = 26 303 L mol^{-1} cm^{-1}) to deduce the concentration of HO$^\bullet$ radicals.

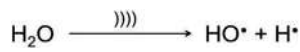

Scheme 8.1

Scheme 8.2

Scheme 8.3

Other methods are used such as Fricke dosimetry (oxidation of Fe^{2+} to Fe^{3+}), terephthalate dosimetry (use of terephthalic acid in alkaline solution) or nitrite and nitrate dosimetry.[6] The Sonochemical Efficiency (SE) can be defined combining electric/acoustic power and rate of radical formation determined by dosimetry (Eqn (8.10)). It constitutes an efficient assessment method to compare different ultrasonic conditions/reactors.

$$I_{\text{acous}} = \frac{P_{\text{acous}}}{S_{\text{probe}}} \tag{8.10}$$

where I_{acous} is the acoustic intensity (W cm^{-2}), P_{acous} is the acoustic power (W) and S_{probe} is the surface of the irradiating probe.

In EPR spin-trapping experiments, diamagnetic nitroso or nitrone compounds are used as spin traps for the conversion of short-lived radicals into relatively longer lived nitroxyl radicals that are observable by EPR spectroscopy.[30,34] This accurate characterization method is limited by the non-availability of the equipment in the lab.

The sonoluminescence is the emission of photons during the collapse of bubbles. The activity of radical or excited species formed in the gas phase of the bubbles during this collapse can be explored using specific detectors by observing the UV-Visible spectra of the sonoluminescence.[35,36] The use of a luminol solution (3-aminophtalhydrazide) oxidized by $HO^{\bullet}$ radicals formed in water under sonochemical activation leads to the formation of 3-aminophthalic acid with electrons in an excited state. The visible blue light emission (λ = 430 nm) due to the de-energization of these electrons allows the mapping of effective zones in a sonoreactor, through this chemiluminescence method.[36]

8.3 Organic Sonochemistry: beneficial Effects and New Reactivities

8.3.1 Green Organic Sonochemistry

The effects of ultrasound during organic reactions have led to serious improvements in terms of reactivity and performance, often under mild conditions, in accordance with a green chemistry approach.[37] Sonochemical reactions in water or biphasic aqueous systems constitute great potential for further developments.

Sonocatalysis often allows the use of environmentally friendly conditions, and makes it possible to decrease reaction times and reach higher yields. In addition, the cavitation phenomenon leads to physical and chemical effects, the consequences of which are interesting for catalyst surface cleaning and free reactive radical production.[38,39] In the most general cases, the combination of ultrasound activation and a catalyst can lead to synergistic effects, mainly observed through the physical effects of US on solid catalysts. Indeed, the physical effects generated by the cavitation

bubble collapse leads to improved mass transfer that contributes to permanent cleaning of the catalyst's surface and increases the probability for compounds to meet and react. Shear forces induced by shock waves and microstreaming provoke the de-agglomeration of the catalyst, and the reduction of the particle size, which implies an increase in surface area.[40] For these reasons, poisoning of the catalyst can be avoided, the active surface of the catalyst is increased, which leads to higher reaction rates, improved yields and lower chemicals consumption; this makes sonocatalysis an effective tool for green chemistry.[41–45] As an example, the *S*-alkylation of hetaryl thiols was performed at room temperature six times faster and led to an increased yield under US (74% in 30 min) compared to silent conditions (66% in 3 h).[42] Another synergistic aspect relies in the microbubbles present in the crevices of the solid catalysts. They constitute nuclei for the cavitational bubble, increasing the number of collapsing events.[46] When a bubble collapses near a solid surface, such as a solid catalyst particle or vessel, the inrush of liquid generates an "asymmetrical collapse" disaggregation of the catalyst but also the fragmentation of the bubble into smaller bubbles that constitute new nuclei for more cavitation bubbles and collapsing events.[47,48]

In the case of a semiconductor catalyst such as TiO_2, electron/hole pairs can be generated at its surface through the absorption of energy: (UV-)light in the case of sonoluminescence from cavitation bubbles, or by heat from the extreme temperature resulting from the collapse of bubbles.[41,49] These charges (electron and hole) operate in redox reactions with the solvent to form radical species or directly with organic compounds of the medium. In a sonicated reaction medium, the generation of radical species will favor the reaction mechanism implying electron transfer rather than an ionic path.[23] For example, the heterocyclization of 1,2-propanediol with fullerene to form a fullerene-fused dioxane adduct was enabled by the improved mixing of the non-miscible liquid phases, provided by US and also possibly by secondary radical reaction in the reaction bulk that would react with the C60 fullerene structure.[50] A change in mechanism and selectivity was describe by Ando where benzyl bromide reacted with potassium cyanide and alumina in toluene with a Friedel–Crafts mechanism to afford *o*- and *p*-benzyltoluene when stirred mechanically at 50 °C. Under 45 kHz US irradiation, the mechanism switched to a nucleophilic substitution and lead to the production of benzyl cyanide in 71% yield.[51] Bubbles generated by acoustic waves in the reaction medium are influenced by the presence of solid catalyst particles and *vice versa*, justifying the beneficial effect of their combination, called synergy.

Another meaning of sonocatalysis is the activation of a reaction by US, through physical and chemical effects generated by cavitation activity.[23] In that case, the origins for the effects observed are separated into two categories: true and false sonocatalysis, "true" being linked to chemical effects such as the generation of radicals, and false referring to mechanical effects of US.[52]

8.3.2 Cases Studies in Organic Sonochemistry

8.3.2.1 Examples of Oxidation Reactions

Many oxidation reactions such as aldehyde[53] or alcohol[54] oxidations have been studied under ultrasonic irradiation, because their mechanisms pass through a radical route.

The aerobic oxidation of D-glucose into D-glucuronic acid was investigated under high frequency ultrasound (550 kHz, P_{acous} = 0.36 W mL^{-1}) (see Scheme 8.4).[55] In the absence of oxygen, D-glucose was oxidized into D-gluconic acid as the main product (40% yield), while D-glucose under oxygen bubbling was oxidized into D-glucuronic acid with excellent yield and selectivity (94% and 98%, respectively). The presence of oxygen bubbling into the reaction media allows the production rate of HO$^{\bullet}$ radicals to be increased. In this case, mechanisms involving HO$^{\bullet}$ and HOO$^{\bullet}$ were suspected.

In a very recent study, the H_2O_2-mediated epoxidation of *cis*-cyclooctene performed under high frequency ultrasonic irradiation (800 kHz, P_{acous} = 0.58 W mL^{-1}) led to improved results compared to silent conditions and revealed important mechanistic insights of the studied reaction (see Scheme 8.5).[56] Indeed, while a maximum yield of 89% and a selectivity of 91% were observed under silent conditions, better results were obtained (96% yield and 98% selectivity) in 30 min under high frequency ultrasound induced by a good thermoregulation and mild mixing brought by the sonoreactor. In addition, the non-radical nature of the *cis*-cyclooctene epoxidation mechanism has been demonstrated.

Finally, the oxidative cleavage of the double bond of olefins has been studied under ultrasonic irradiation (see Scheme 8.6).[56] Simultaneous use of ultrasound and Aliquat 336® as a phase transfer catalyst was essential to perform the oxidative cleavage of olefins without organic solvent and in less

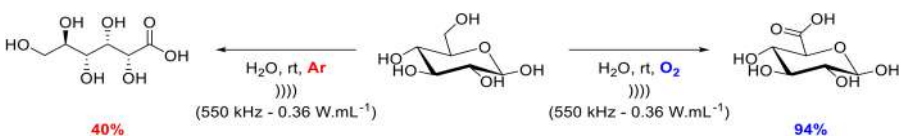

Scheme 8.4

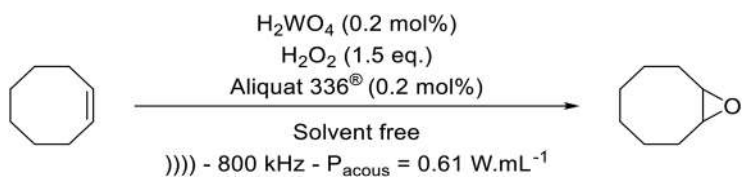

Scheme 8.5

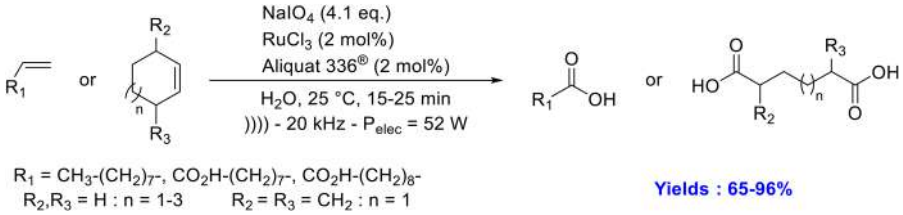

Scheme 8.6

than 1 h. At room temperature and thanks to a 20 kHz ultrasound probe, mono- and diacids derived from linear and cyclic olefins are obtained with good to excellent yields, from 65% to 96%.

8.3.2.2 Examples of Reduction Reactions

Amines are important molecules that are involved in the synthesis of amino acids[57] or vitamins[58] and many of them exhibit interesting biological activities. Therefore, they are used as antihistaminics, analgesics, antiglycemics,[59] anesthesics,[60] decongestants,[61] pyschostimulants[62] or antidepressants.[63] Classical preparation of amine derivatives relies on the reduction of nitro precursors using different methods. Among them, hydrogenation catalyzed by metals is still the most used in the petrochemical and pharmaceutical industries.[64] However, these methods are often associated with a lack of chemoselectivity in the presence of other reducible functions. In addition, the reaction is exothermic, and involves pressurized hydrogen and flammable solvents, requiring thus particular precautions in terms of safety.[65] The research of more selective, safe and environmentally friendly methods of reduction is thus an important issue. It is well known that low frequency ultrasonic irradiation (20 kHz < f < 80 kHz) may enhance the catalyst activity and chemical reactions' kinetics and selectivity.[66] Thus, in 2000, Basu *et al.* described the reduction of nitroaromatic compounds to the corresponding amines using a Sm/NH_4Cl reducing agent under 10 to 25 min of ultrasonic irradiation (see Table 8.1).[67]

In Table 8.1, 86% of 6-aminochrysene was obtained from 6-nitrochrysene (Table 8.1, compound **2**) after 10 min of sonication using a Sm/NH_4Cl reducing agent in methanol, whereas no reaction was observed under silent conditions. 2-Nitro-9*H*-fluorene (Table 8.1, compound **3**) was reduced to 2-aminofluorene in 10 min under ultrasonic irradiation, whereas no transformation was observed when the reducing agent was changed for In/NH_4Cl or for Fe powder/NH_4Cl. Under silent conditions, 10 h under methanol reflux were required to reduce 2-nitro-9H-fluorene (Table 8.1, compound **3**) to the corresponding amine. In addition, the reaction was shown to be selective towards sensitive functional groups such as bromo (Table 8.1, compound **4**), cyano (Table 8.1, compound **5**), ester (Table 8.1, compound **6**), unsaturated bonds (Table 8.1, compound **7**) and heterocycles (Table 8.1, compound **8**). Unfortunately, ultrasonic frequency and power are not given, making it impossible to reproduce the experiments under identical conditions.

Table 8.1 Reduction of aromatic nitro compounds by Sm/NH_4Cl under ultrasonic irradiation (ultrasonic bath, frequency not indicated, room temperature).[67]

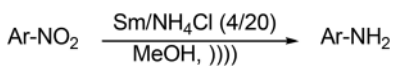

$Ar\text{-}NO_2$	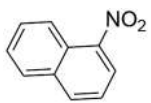	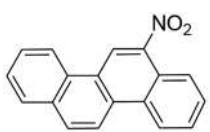	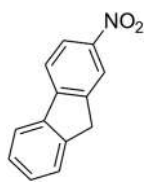	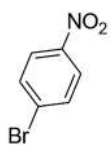	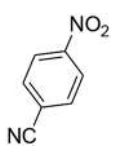	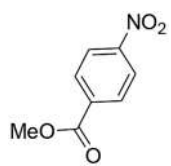	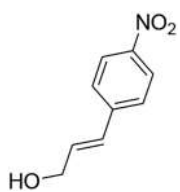	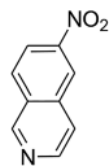
Time, min	10	10	10	10	10	10	10	25
Yield, %	88	86	92	88	87	74	90	56

Hypophosphorous acid and its salts are mild, cheap and powerful reducing agents commonly used for electrochemical applications.[68] Furthermore, sodium hypophosphite was registered as a non-hazardous substance for Man and for the Environment in 2010 by REACH.[69] In this context, with sodium hypophosphite/hypophosphorous acid as a reducing system and Pd/C as a catalyst, Letort *et al.* studied the reduction of nitro compounds to the corresponding amines in H_2O/2-MeTHF at 60 °C.[70] The authors studied the reaction in terms of solvent effect, NaH_2PO_2/H_3PO_2 ratio, temperature, and Pd/C catalyst loading, with 2-nitroethylbenzene as a model substrate. The methodology scope was then extended to other aliphatic nitro compounds (see Table 8.2) and the results obtained were compared to those obtained under ultrasonic irradiation.

Under the same conditions and even with 1.25 mol% of Pd/C the reduction of β-nitrostyrene did not lead to the corresponding unsaturated amines nor to the saturated one, but to a mixture of 44% of (*Z*)- and 38% of (*E*)-2-phenylacetaldehyde oximes.[70] The reaction was found to be faster under ultrasonic irradiation and especially in the mixture H_2O/Me-THF (2 : 1). Thus, a maximum yield of 92% of 2-phenylethan-1-amine was obtained at 60 °C in only 15 min under ultrasonic irradiation, compared to 90 min required under silent conditions. In water as a solvent, 90 min were required to obtain 35% of amine under silent conditions, whereas almost double the amount was obtained under ultrasonic irradiation. In water and under ultrasonic irradiation, a maximal yield of 90% was obtained in 15 min when the temperature was increased to 70 °C. The use of a vibromixer allowed the authors to attribute the effects of ultrasound to the formation of an intense microemulsion and classified the reaction as a type II reaction termed as "false sonochemistry".

Table 8.2 Reduction of aliphatic nitro compounds under silent and ultrasonic conditions (ultrasonic microtip, 20 kHz, P_{acous} = 3.94 W, 3 mL).[70]

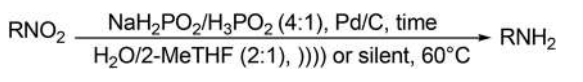

R =

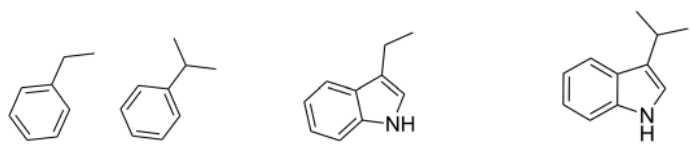

Activation method	Silent	))))	Silent	))))	Silent	))))	))))	))))	))))	Silent	))))	))))	))))	))))
Time, min	90	15	90	15	90	10	20	30	30	90	15	20	30	30
Catalyst loading, mol%	0.6	0.6	0.6	0.6	0.6	0.6	0.6	0.6	1.25	0.6	0.6	0.6	0.6	1.25
Yield, %	90	90	84	84	98	61	78	84	98	80	78	80	85	85

8.3.2.3 Examples of Fused Heterocycles

N-containing heterocycles are essential building blocks for the synthesis of many biologically active compounds.[71,72] In this context, Nongrum *et al.* described the synthesis of fused benzo *N,N*-containing heterocycles under ultrasonic activation and using 1-désoxy-1-(methylamino)-D-glucitol, *i.e.*, meglumine, as an organocatalyst.[73] The authors used meglumine, an environmental water-soluble amino sugar, to catalyze the reaction in association with ultrasound as an alternative activation technique with a mixture of ethanol–water as the solvent. The reaction was optimized in terms of catalyst loading, solvent and activation technique with 1,2-phenyldiamine, dimedone and tolualdehyde as substrates. The scope of the reaction was then extended to aromatic aldehydes bearing electron-withdrawing and -donating substituents, leading to excellent yields under 20 to 30 min of ultrasonic irradiation (see Table 8.3).[73] Two hypotheses have been formulated to explain the role of meglumine, which is suggested to act *via* electrophilic or nucleophilic activation of dimedone. Under the same conditions, 85 to 90% of quinoxaline derivatives were synthesized under 25 to 35 min of ultrasonic irradiation at 50 °C.

Table 8.3 Synthesis of 1*H*-dibenzo[*b*,*e*][1,4]diazepin-1-one derivatives with 5 mol% of meglumine as a catalyst under silent and ultrasonic conditions (ultrasonic bath).[73]

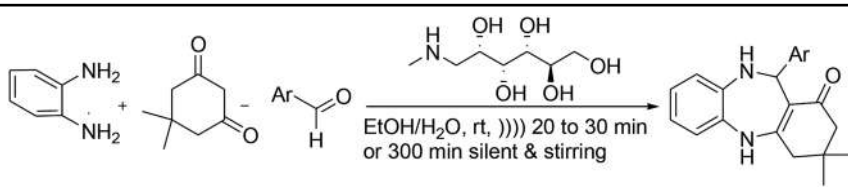

	))))		Silent, 300 min
Ar	Times, min	Yield, %	Yield, %
C_6H_5	20	92	65
4-$CH_3C_6H_4$	20	92	68
4-$OCH_3C_6H_4$	20	88	65
4-ClC_6H_4	25	90	60
4-BrC_6H_4	25	92	68
4-$NO_2C_6H_4$	30	85	58
4-OHC_6H_4	25	88	60
4-$N(CH_3)_2C_6H_4$	30	88	64
2-ClC_6H_4	25	82	62
2-$NO_2C_6H_4$	30	85	55
1-Naphthyl	25	88	55
Furfuryl	30	88	64
$C_6H_5CH{=}CH$	30	82	60
4-(OH) and 3-$(OCH_3)C_6H_3$	25	90	65
3,4-$(OCH_3)_2C_6H_3$	20	90	60

Table 8.4 Synthesis of various benzodiazepines with 0.5 mmol of ionic liquid as a catalyst under silent and ultrasonic conditions (ultrasonic bath, 45 kHz, P_{in} = 305 W).[74]

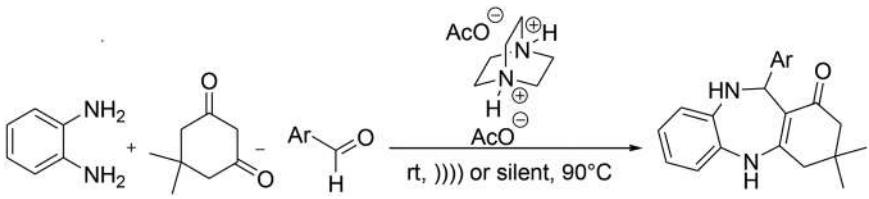

	))))		Silent, 90 °C	
Ar	Time, min	Yield, %	Time, min	Yield, %
C_6H_5	10	95	75	82
4-ClC_6H_4	8	97	60	84
4-$OCH_3C_6H_4$	8	96	60	85
4-$NO_2C_6H_4$	8	98	60	89
3-$NO_2C_6H_4$	10	95	75	88
3-ClC_6H_4	10	96	75	89
4-$N(CH_3)_2C_6H_4$	12	93	90	85
2,4-diClC_6H_4	15	94	90	83
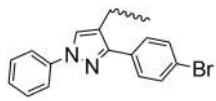	6	95	60	82
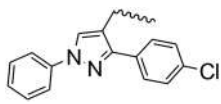	17	94	90	81

Using an acidic ionic liquid, 1,4-diazabicyclo[2,2,2]octanium diacetate, *i.e.*, DABCO diacetate, Fekri *et al.* synthesized 93 to 97% of various benzodiazepines under 8 to 17 min of ultrasonic irradiation (see Table 8.4).[74] The reaction under silent conditions and at 90 °C afforded the products in higher reaction times and lower yields. A mechanism involving the ionic liquid for increasing the electrophilicity of the carbonyl substrates was then proposed.

8.3.2.4 Examples of Organometallic Reactions

Sonochemistry is a green alternative method to classical methods to promote the synthesis of organic compounds, offering then versatile and easy pathways for a wide variety of transformations such as Reformatsky, Barbier-Grignard or Michael reactions.[75]

The Reformatsky reaction, which converts aldehydes and ketones to β-hydroxyesters, was one of the first organometallic reactions with problems of metal activation under silent conditions that was studied under ultrasound. In 1982, it was shown that the addition of ultrasound resulted in

better reaction yields in less time compared to silent conditions.[76] In fact, for a reaction time of 12 h, the yield was 58% while with ultrasound (ultrasonic bath, frequency not indicated), it rose to 98% in only 30 min. Several studies were carried out in order to understand the role of ultrasound in this reaction.[77–79] The authors reported successful syntheses with quantitative yields of β-hydroxyester by reacting phenylketones, α-bromoesters, zinc dust and a catalytic amount of iodine under high intensity ultrasonic irradiation.[80] But, the role of iodine was not fully understood. Reformatsky reactions could then be carried out using non-traditional electrophiles such as glyoxylic oximes.[81]

In the Barbier-Grignard type reaction, the organometallic reagent, which intervenes, serves as a nucleophile for the formation of a carbon–carbon bond.[82] The zinc mediated Barbier reaction was carried out in a biphasic CO_2/H_2O system allowing a preferential partitioning of the desired homoallyl alcoholic product.[83] Here, pulsed ultrasound is efficient for dispersing and mixing the two phases, thus creating an emulsion while ensuring kinetic control.

The Michael reaction is often a first choice organic transformation because there are a large number of Michael acceptors and nucleophiles. Indeed, almost all activated alkenes, such as α,β-unsaturated ketones, can act as acceptors. It is also possible in a single step to form stereogenic centers.[84] Numerous studies have demonstrated the need for basic or acidic catalysts in the reaction of addition of nucleophiles 1,4-conjugated to unsaturated carbonyl compounds.[85] However, these conditions gave way to side reactions. The effects of ultrasound then allowed a more efficient approach when adding the conjugate.[86] In a recent study, researchers studied the chemical behavior of 3-diethyl phosphonocoumarin in an ultrasound-assisted Michael-type reaction.[87] Several organometallic compounds have been selected to react with this coumarin as hard nucleophile isomers (see Scheme 8.7). This approach allowed the use of a simpler experimental set-up and milder reaction conditions. Excellent reproducibility of the yield is reported as well as high diastereoselective activity of the isolated *trans* isomers.[87]

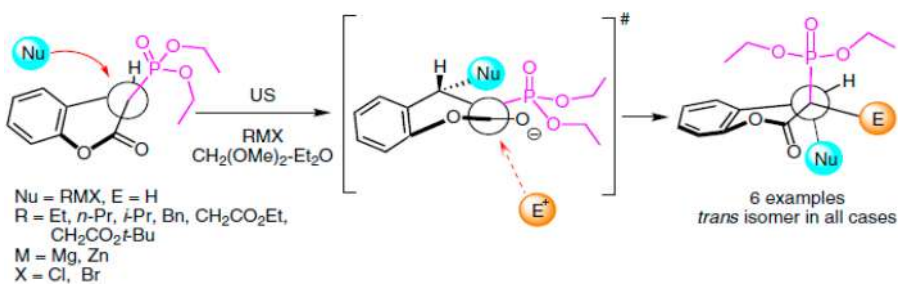

Scheme 8.7

8.3.3 Scale-up and Industrial Applications

In organic sonochemistry, a series of macroscopic characteristics, namely the use of less toxic/hazardous chemicals, eco-friendly solvents, and alternative or renewable raw materials, the development of reaction conditions to increase the selectivity of the product or even the minimization of the energy consumption during transformations reinforce the aspects sought in green chemistry and encourage the use of ultrasound on a larger scale.[6,88]

As presented previously, lab scale experiments in organic chemistry are very promising to create green processes in industry.[23,89] However, to our knowledge, no industrial scale sonoreactor has been successfully employed for organic synthesis. Large scale transfers require adjustments concerning various parameters and a scale-up methodology is lacking.[90]

The efficiency of sonochemical reactions relies on hydrodynamics, mixing and mass transfer. Two types of parameters need to be studied when scaling up a lab-scale experiment for industrial purposes: (i) the operating parameters such as the frequency, the intensity and the initial radius of bubble nuclei and (ii) the geometric parameters such as the size and location of transducers, and the shape and dimensions of the reactor. Both types of parameters will impact the mixing and hydrodynamic characteristics that define the cavitation field. The main problems in intensifying organic reactions relate to the fact that the yield and selectivity of the chemical reaction are non-linearly based on operating parameters and geometry; a proportional amplification of the dimensions of the reactor is therefore not sufficient to reproduce the same experimental conditions. Fine predictions of many parameters such as pressure, temperature, and cavitational activity distribution are required to achieve chemical reaction effectiveness. Another problem frequently encountered is that cavitation events happen mainly near the irradiating surfaces. The adjustment of the lab-scale reaction at large-scale requires higher energy input to counterbalance energy dissipation in the wider bulk media leading to fast erosion of the sonication surfaces.[90] Large-scale reactors contain larger volumes, which brings the issue of US attenuation, due to reflection, refraction or absorption of the incident sound wave, and leads to spatial variation of the cavitational activity, creating active and passive zones in the reactor. This needs to be avoided to perform chemical reactions at an industrial scale.[91]

To anticipate the problematics related to large scale sonoreactors, experimental measurements and theoretical techniques exist to predict the cavitational activity distribution. The mapping of a sonoreactor can contribute to upscale chemical reactions. It consists in the characterization of the cavitational phenomena and implies the quantification of primary effects (generated at the same time as the bubble collapse) and secondary effects (generated after bubble collapse). Parameters like pressure can be quantified using a hydrophone, while changes in local temperature can be measured with a thermocouple,[92] and give information on the local cavitation activity and are used to quantify the efficacy of the sonochemical reactor in

terms of energy transfer. The quantification of secondary parameters, such as radical production, can be assessed through dosimetry. Chemical reaction implying hydroxyl radicals enable an indirect measure of their concentration and they can have large measurement errors.[93] The modelling of cavitational parameters such as pressure and temperature, but also the bubble radius and the chemical species formed, can be predicted through modelling.[94,95] Large scale reactors imply specific studies as for example, the pressure of the reaction medium is a function of depth and impacts the conditions of cavitation bubble collapse, like pressure and temperature, and thus the physical and chemical effects on chemical reactions.[96,97] Concerning sonochemical efficiency assessment, most studies are conducted on the single bubble model,[98,99] which does not take into account the neighbor bubbles behavior mutually influencing the other bubble behavior.[100,101]

The scaling-up of organic reaction under US would enable great energy and chemical savings. The main difficulty to design large scale reactors is to ensure a uniform distribution of cavitational activity. Empirical methods and theoretical modelling can be used to work on this aspect and contribute to the industrialization of US for organic synthesis.

8.4 Conclusions: from the Challenges to New Perspectives of Organic Sonochemistry

Since the evaluation of the eco-compatibility of a process cannot be done subjectively, there are a certain number of calculations of green chemistry, such as the economy of atoms, the mass reaction efficiency, the intensity mass, the effective mass yield, the carbon efficiency, the E-factor, the Eco-Scale or other green metrics.[102,103] These tools are still little exploited by sonochemists and the systematization of their use is recommended. Systematic comparisons between silent and ultrasonic conditions are necessary, under the same conditions, to highlight the improvements brought by ultrasound in terms of efficiency and eco-compatibility. For example, the energy consumption should be also measured. At lab scale, *in situ* data monitoring can be collected to extrapolate the ultrasound conditions at a higher scale.[104]

In terms of equipment, the combined efforts of chemists, physicists and equipment manufacturers will be needed for the chemical process industry to exploit cavitation as a more viable option for chemical transformations.

As a perspective, the combination of ultrasound with other physical and chemical methods of activation seems promising. For example, the use of subcritical H_2O (hydrothermal, 200 °C) under ultrasonic irradiation (20 kHz) shows stable cavitation with nonlinear bubble oscillations. On the other hand, in the formation of hydrogen peroxide (H_2O_2), thermal instability is not observed.[105] Sonohydrothermal synthesis is described for the synthesis of inorganic nanomaterials,[106] but not yet for organic synthesis. Indeed, the combination of ultrasound with supercritical CO_2 has not been used in organic chemistry due to the high pressure and lack of phase boundaries

observed in the supercritical state.[107] Hence, for biomass valorization, a positive influence of ultrasound in supercritical CO_2 is observed thanks to mechanical effects (micro- and macro-mixing, cell damage) that could be useful in organic synthesis.[108]

In organic synthesis, the use of US and microwaves in tandem or simultaneously at laboratory scale improves the selectivity and yield, and lowers the reaction times,[109,110] satisfying some principles of green chemistry criteria. The synergistic effects observed are commonly attributed to the improved heat transfer provided by microwaves and the intense mass transfer resulting from US. Each irradiation technology compensates the weakness of the other, which justifies the added value of their simultaneous use, especially in heterogeneous systems.[110,111]

Despite the many advantages of microreactors, one major drawback is the potential clogging of their channels[112] In that context, the synergy of ultrasound and microfluidics has shown its potential. Thus, Sedelmeier *et al.*[113] used an ultrasonic bath to avoid the fouling of the microreactor due to the deposition of manganese dioxide used for the oxidation of nitralkanes into their corresponding carboxylic acids. Recently, Delacour *et al.*[114] developed a scaled-up ultrasonic reactor to prevent clogging in particle forming reactions. The millireactor was used for the synthesis of barium sulphate. The results showed that only 0.48 W mL^{-1} was required to prevent channel clogging and to increase the productivity by two orders of magnitude compared to a microreactor.

Sonophotocatalysis, which is the combination of sonochemistry and photocatalysis, has mainly been used as an advanced oxidation process for the removal of pollutants. Its recent use in organic synthesis showed promising results as a synergistic effect of both activation methods afforded an alkyl carbon chain elongation from 3C (malonic acid) to 4C (succinic acid). The carbon chain elongation was observed only when US and UV irradiations were combined.[115]

Finally, the physicochemical properties of some ionic liquids (ILs), such as their large thermal stability, their wide liquid domain or even their low vapor pressure make them very interesting reaction media for green chemistry. The combination of ultrasound with the appropriate ionic liquid is a powerful tool for performing various organic transformations.[116] The rates of reaction, selectivity and yields are often improved. Their combination with US then makes it possible to obtain the desired products without using inorganic of organic catalysts, even at room temperature.[117] The possible degradation phenomena (few ppm) of ILs under US conditions nevertheless need to be considered.[118] Deep eutectic solvents are also very promising as a green alternative in synergy with ultrasound in organic syntheses.[119]

When combining processes, technologies, tools or reagents, an interesting way to assess the efficiency of the coupling is to calculate its synergy. Synergy corresponds to a beneficial effect from a coupling that is positive if the results obtained with the coupling of processes is superior to the sum of the results obtained with each independent process.[109] Several indicators of synergy can

be found in the literature, but their definition and the equations that are used should always be detailed to avoid confusion. Among indicators for synergy, the following can be found: synergy, synergy effect, synergistic effect, %synergy or synergy index.[120–122] For example, the equation for percentage of synergy (Eqn (8.11)) and the synergy index (Eqn (8.12)) for n processes leading to chemical reactions with k as the rate constant, are detailed below.

$$\%\text{synergy} = 100\frac{k_{\text{combined processes}} - \sum_{i=1}^{n} k_{\text{process}\,i}}{k_{\text{combined processes}}} \tag{8.11}$$

$$\text{synergy index} = \frac{k_{\text{combined processes}}}{\sum_{i=1}^{n} k_{\text{process}\,i}} \tag{8.12}$$

The calculation of the %synergy and synergy index is recommended when ultrasound is combined in an organic reaction with another physical or chemical activation method in order to prove the advantages of the used combination.

List of Abbreviations

c	Celerity of sound
c_p	Specific heat capacity
DABCO	1,4-Diazabicyclo[2.2.2]octane
$E_{elec/acous}$	Electrical or acoustic power
EPR	Electron Paramagnetic Resonance
f	Frequency
I_0	Initial sound intensity
I_{acous}	Acoustic intensity
I_{max}	Ultrasonic intensity
ILs	Ionic Liquids
m	Mass of liquid in the sonoreactor
P	Pressure inside the bubble at its maximum size
P_a	Acoustic pressure applied
P_A	Acoustic amplitude
P_{acous}	Acoustical power
P_h	Pressure within the fluid
P_{in}	Power input
P_m	Pressure inside the liquid at the moment of the collapse
P_{max}	Maximum pressure at the collapse
P_{out}	Power output
P_v	Vapor pressure at the moment of the collapse
REACH	Registration, Evaluation and Authorisation of Chemicals
SE	Sonochemical Efficiency
S_{probe}	Surface of the irradiating probe

T_0	Ambient temperature
T_{max}	Temperature at the collapse
US	Ultrasound
UV	Ultraviolet
λ	Wavelength
$\left(\frac{dT}{dt}\right)_0$	Initial slope of the increase of the temperature of the solution *versus* time of ultrasonic irradiation
α	Absorption coefficient of the medium
γ	Polytropic factor
ρ	Density of the medium

References

1. R. Woods and A. Loomis, *Philos. Mag.*, 1927, **4**, 414.
2. T. Richards and A. Loomis, *J. Am. Chem. Soc.*, 1927, **49**, 3086.
3. E. Neppiras, *Phys. Rep.*, 1980, **61**, 159.
4. S. K. Bhangu and M. Ashokkumar, *Top. Curr. Chem.*, 2016, **374**, 1.
5. T. Lepoint and F. Lepoint-Mullie, Theoretical Bases, in *Synthetic Organic Sonochemistry*, Plenum Press, 1998, pp. 1–49.
6. G. Chatel, *Sonochemistry: New Opportunities for Green Chemistry*, World Scientific, 2017.
7. M. Draye, J. Estager and N. Kardos, in *Activation Methods: Sonochemistry and High Pressure*, ed. J.-P. Goddard, M. Malacria and C. Ollivier, Willey, 2019, p. 26.
8. B. G. Pollet, *Electrocatal*, 2014, **5**, 330.
9. N. Ghasemi, F. Zare, P. Davari, P. Weber, C. Lagton and A. Gosh, *Proceedings of the 7th IEEE Conference on Industrial Electronics and Applications*, ICIEA, 2012, p. 647.
10. B. Fay and M. Rinker, *Ultrason*, 1996, **34**, 563.
11. L. He, F. Zhu, Y. Chen, K. Duan, X. Lin, Y. Pan and J. Tao, *Rev. Sci. Instrum.*, 2016, **87**, 054903.
12. G. Harris, *Ultrasound Med. Biol.*, 1985, **11**, 803.
13. T. Uchida, T. Kikuchi, M. Yoshioka, Y. Matsuda and R. Horiuchi, *Acoust. Sci. Technol.*, 2015, **36**, 445.
14. N. Navarro, T. Chave, P. Pochon, I. Bisel and S. Nikitenko, *J. Phys. Chem. B*, 2011, **115**, 2024.
15. I. Margulis and M. Margulis, *Acoust. Phys.*, 2005, **51**, 695.
16. C. C. Church, D. F. Gaitan, Y. A. Pishchalnikov and T. J. Matula, *J. Acoust. Soc. Am.*, 2011, **129**, 2620.
17. H. Delmas, N. Tuan Le, L. Barthe and C. Julcour-Lebigue, *Ultrason. Sonochem.*, 2015, **25**, 51.
18. Y. T. Shah, A. B. Pandit and V. S. Moholkar, in *Cavitation Reaction Engineering*, ed. D. Luss, The Plenum Chemical Engineering Series, Springer Science, 1999, p. 79.
19. J. Rooz, E. V. Rebrov, J. C. Schouten and J. T. F. Keurentjes, *Ultrason. Sonochem.*, 2013, **20**, 1.

20. B. E. Noltingk and E. A. Neppiras, *Proc. Phys. Soc. B*, 1950, **63**, 674.
21. L. H. Thompson and L. K. Doraiswamy, *Ind. Eng. Chem. Res.*, 1999, **38**, 1215.
22. T. J. Mason and J. P. Lorimer, *Applied Sonochemistry: The Uses of Power Ultrasound in Chemistry and Processing*, 2002.
23. G. Cravotto and P. Cintas, *Chem. Soc. Rev.*, 2006, **35**, 180.
24. P. R. Gogate and P. N. Patil, Sonochemical reactors, in *Sonochemistry*, Springer, 2017, p. 255.
25. V. S. Moholkar, S. P. Sable and A. B. Pandit, *AIChE J.*, 2000, **46**, 684.
26. J.-P. Bazureau and M. Draye, *Ultrasound and Microwaves: Recent Advances in Organic Chemistry*, Transworld Research Network, Kerala, 2011, p. 241.
27. G. Chatel, M. Draye, R. Duwald, C. Piot and P. Fanget, *FR Pat.*, FR 20 06171, 2020.
28. Y. Iida, K. Yasui, T. Tuziuti and M. Sivakumar, *Microchem. J.*, 2005, **80**, 159.
29. Y. Asakura, M. Maebayashi, T. Matsuoka and S. Koda, *Electron. Commun. Jpn.*, 2007, **90**, 1.
30. K. Makino, M. M. Mossoba and P. Riesz, *J. Am. Chem. Soc.*, 1982, **104**, 3537.
31. E. N. Harvey, *J. Am. Chem. Soc.*, 1939, **61**, 2392.
32. Y. Hu, Z. Zhang and C. Yang, *Ultrason. Sonochem.*, 2008, **15**, 665.
33. R. J. Wood, J. Lee and M. J. Bussemaker, *Ultrason. Sonochem.*, 2019, **58**, 104645.
34. Q.-A. Zhang, Y. Shen, X.-H. Fan, J. F. Garcia Martin, X. Wang and Y. Song, *Ultrason. Sonochem.*, 2015, **27**, 96.
35. W. B. McNamara, Y. Didenko and K. S. Suslick, *Nature*, 1999, **401**, 772.
36. K. Yasuda, T. Torii, K. Yasui, Y. Iiad, T. Tuziuti, M. Nakamura and Y. Asakura, *Ultrason. Sonochem.*, 2007, **14**, 699.
37. G. Chatel, *Ultrason. Sonochem.*, 2018, **40**, 117.
38. G. Cravotto, E. Borretto, M. Oliverio, A. Procopio and A. Penoni, *Catal. Commun.*, 2015, **63**, 2.
39. A. Tuulmets, S. Salmar and J. Järv, *Sonochemistry in Water Organic Solutions*, Novinka Books, 2010.
40. T. Lepoint and F. Lepoint-Mullie, in *Synthetic Organic Sonochemistry*, ed. J.-L. Luche, Springer, Boston, MA, 1998.
41. G. H. Mahdavinia, S. Rostamizadeh, A. M. Amani and Z. Emdadi, *Ultrason. Sonochem.*, 2009, **16**, 7.
42. T. Deligeorgiev, S. Kaloyanova, N. Lesev and J. J. Vaquero, *Ultrason. Sonochem.*, 2010, **17**, 783.
43. A. Maleki, *Ultrason. Sonochem.*, 2018, **40**, 460.
44. I. Mohammadpoor-Baltork, M. Moghadam, S. Tangestaninejad, V. Mirkhani and Z. Eskandari, *Ultrason. Sonochem.*, 2010, **17**, 857.
45. R. S. Disselkamp, Y.-H. Chin and C. H. F. Peden, *J. Catal.*, 2004, **227**, 552.
46. P. Qiu, B. Park, J. Choi, B. Thokchom, A. B. Pandit and J. Khim, *Ultrason. Sonochem.*, 2018, **45**, 29.

47. N. Bremond, M. Arora, S. M. Dammer and D. Lohse, *Phys. Fluids*, 2006, **18**, 121505.
48. D. E. Yount, E. W. Gillary and D. C. Hoffman, *J. Acoust. Soc. Am.*, 1984, **76**, 1511.
49. P. Gholami, A. Khataee, R. D. C. Soltani and A. Bhatnagar, *Ultrason. Sonochem.*, 2019, **58**, 104681.
50. Z. S. Kinzyabaeva and G. L. Sharipov, *Ultrason. Sonochem.*, 2018, **42**, 119.
51. T. Ando, S. Sumi, T. Kawate, J. Ichihara and T. Hanafusa, *J. Chem. Soc., Chem. Commun.*, 1984, 439.
52. J.-L. Luche, *Ultrason. Sonochem.*, 1996, **3**, S215.
53. U. Neuenschwander, J. Neuenschwander and I. Hermans, *Ultrason. Sonochem.*, 2012, **19**, 1011.
54. R. Naik, A. Nizam, A. Siddekha and M. A. Pasha, *Ultrason. Sonochem.*, 2011, **18**, 1124.
55. P. N. Amaniampong, A. Karam, Q. T. Trinh, K. Xu, H. Hirao, F. Jérôme and G. Chatel, *Sci. Rep.*, 2017, **7**, 40650.
56. T. Cousin, G. Chatel, N. Kardos, B. Andrioletti and M. Draye, *Ultrason. Sonochem.*, 2019, **53**, 120.
57. P. Hu, Y. Ben-David and D. Milstein, *J. Am. Chem. Soc.*, 2016, **138**, 6143.
58. P. Contant, L. Forzy, U. Hengartner and G. Moine, *Helv. Chim. Acta*, 1990, **73**, 1300.
59. W. Lijinsky, *Cancer Res.*, 1974, **34**, 255.
60. D. Lambert, Local Anesthetic Pharmacology, in *Anesthesiology and Pain Management*, ed. Stanley T. H. and Ashburn M. A., Developments in Critical Care Medicine and Anesthesiology, Springer, 1994, vol. 29, p. 35.
61. S. Perrin, D. Montani, C. O'Connell, S. Günther, B. Girerd, L. Savale, C. Guignabert, O. Sitbon, G. Simonneau, M. Humbert and M.-C. Chaumais, *Eur. Respir. J.*, 2015, **46**, 1211.
62. R. Rothman and M. Baumann, *Eur. J. Pharmacol.*, 2003, **479**, 23.
63. L. Antkiewicz-Michaluk, I. Romanska, A. Wąsik and J. Michaluk, *Neurotoxic. Res.*, 2017, **32**, 94.
64. T. Kahl, K.-W. Schröder, F. Lawrence, W. Marshall, H. Höke and R. Jäckh, Aniline, in *Ullmann's Encyclopedia of Industrial Chemistry*, Wiley-VCH, 2012.
65. S. M. Kelly and B. H. Lipshutz, *Org. Lett.*, 2014, **16**, 98.
66. M. Draye, G. Chatel and R. Duwald, *Pharmaceuticals*, 2020, **13**, 1.
67. M. K. Basu, F. F. Becker and B. K. Banik, *Tetrahedron Lett.*, 2000, **41**, 5603.
68. O. ECdu, M. Ojewumi, Y. D. Yeboah and E. E. Kalu, *Int. J. Electrochem. Sci.*, 2015, **10**, 10792.
69. ECHA, Sodium phosphinate, online: https://echa.europa.eu/fr/substance-information/-/substanceinfo/100.028.791, accessed December 2020.
70. S. Letort, M. Lejeune, N. Kardos, E. Métay, F. Popowycz, M. Lemaire and M. Draye, *Green Chem.*, 2017, **19**, 4583.

71. G. Chen, Z. Liu, Y. Zhang, X. Shan, L. Jiang, Y. Zhao, W. He, Z. Feng, S. Yang and G. Liang, *ACS Med. Chem. Lett.*, 2013, **4**, 69.
72. M. Gaba, S. Singh and C. Mohan, *Eur. J. Med. Chem.*, 2014, **76**, 494.
73. N. Nongrum, G. K. Kharmawlong, J. W. S. Rani, N. Rahman, A. Dutta and R. Nongkhlaw, *J. Heterocycl. Chem.*, 2019, **56**, 2873.
74. S. Sarhandi, L. Zare Fekri and E. Vessally, *Acta Chim. Slov.*, 2018, **65**, 246.
75. M. Mohamed, *J. Pharm. Sci.*, 2016, **53**, 108.
76. B. H. Han and P. Boudjouk, *J. Org. Chem.*, 1982, **47**, 5030.
77. P. Boudjouk, D. P. Thompson, W. H. Ohrbom and B. Han, *Organometallics*, 1986, **5**, 1257.
78. K. S. Suslick and S. J. Doktycz, *J. Am. Chem. Soc.*, 1989, **111**, 2342.
79. N. A. Ross and R. A. Bartsch, *J. Heterocycl. Chem.*, 2001, **38**, 1255.
80. N. A. Ross and R. A. Bartsch, *J. Org. Chem.*, 2003, **68**, 360.
81. R. G. Soengas and A. M. Estévez, *Ultrason. Sonochem.*, 2012, **19**, 916.
82. C.-J. Li, *Tetrahedron*, 1996, **52**, 5643.
83. S. M. Cenci, L. R. Cox and G. A. Leeke, *ACS Sustainable Chem. Eng.*, 2014, **2**, 1280.
84. B. D. Mather, K. Viswanathan, K. M. Miller and T. E. Long, *Prog. Polym. Sci.*, 2006, **31**, 487.
85. J. Christoffers, *Eur. J. Org. Chem.*, 1998, **1998**, 1259.
86. Y.-L. Song, Y.-F. Dong, F. Wu, T. Yang and G.-L. Yang, *Ultrason. Sonochem.*, 2015, **22**, 119.
87. A. Koleva, N. Petkova and R. Nikolova, *Synlett*, 2016, **27**, 2676.
88. B. Banerjee, *Ultrason. Sonochem.*, 2017, **35**, 1.
89. M. Draye and N. Kardos, *Top. Curr. Chem.*, 2016, **374**, 74.
90. P. R. Gogate, V. S. Sutkar and A. B. Pandit, *Chem. Eng. J.*, 2011, **166**, 1066.
91. V. S. Sutkar and P. R. Gogate, *Chem. Eng. J.*, 2009, **155**, 26.
92. J. W. K. Kambiz Farahmand, *Exp. Heat Transfer*, 2001, **14**, 107.
93. Y. Iida, K. Yasui, T. Tuziuti and M. Sivakumar, *Microchem. J.*, 2005, **80**, 159.
94. S. Merouani, O. Hamdaoui, Y. Rezgui and M. Guemini, *Res. Chem. Intermed.*, 2015, **41**, 881.
95. K. Yasui, T. Kozuka, T. Tuziuti, A. Towata, Y. Iida, J. King and P. Macey, *Ultrason. Sonochem.*, 2007, **14**, 605.
96. N. Kerabchi, S. Merouani and O. Hamdaoui, *Ultrason. Sonochem.*, 2018, **48**, 136.
97. N. Kerabchi, S. Merouani and O. Hamdaoui, *Sep. Purif. Technol.*, 2018, **206**, 118.
98. Y. T. Didenko and K. S. Suslick, *Nature*, 2002, **418**, 394.
99. S. Koda, K. Tanaka, H. Sakamoto, T. Matsuoka and H. Nomura, *J. Phys. Chem.*, 2004, **108**, 11609.
100. A. A. Doinikov and S. T. Zavtrak, *Phys. Fluids*, 1995, **7**, 1923.
101. T. Tuziuti, K. Yasui, Y. Iida, M. Sivakumar and S. Koda, *J. Phys. Chem.*, 2004, **108**, 9011.
102. R. A. Sheldon, *Green Chem.*, 2007, **9**, 1273.
103. R. A. Sheldon, *ACS Sustainable Chem. Eng.*, 2018, **6**, 32.

104. P. Tierce, *Fr. Pat.*, FR2768948B1, 1998.
105. S. I. Nikitenko, M. Brau and R. Pflieger, *Ultrason. Sonochem.*, 2020, **67**, 105189.
106. C. Cau, Y. Guari, T. Chave, J. Larionova, P. Pochon and S. I. Nikitenko, *J. Phys. Chem.*, 2013, **117**, 22827.
107. S. Balachandran, S. E. Kentish, R. Mawson and M. Ashokkumar, *Ultrason. Sonochem.*, 2006, **13**, 471.
108. E. S. Dassoff and Y. O. Li, *Trends Food Sci. Technol.*, 2019, **86**, 492.
109. G. Cravotto and P. Cintas, *Chem. - Eur. J.*, 2007, **13**, 1902.
110. V. G. Gude, *Resour.-Effic. Technol.*, 2015, **1**, 116.
111. Y. Peng and G. Song, *Green Chem.*, 2003, **5**, 704.
112. D. Fernandez Rivas and S. Kuhn, *Top. Curr. Chem.*, 2016, **374**, 70.
113. J. Sedelmeier, S. V. Ley, I. R. Baxendale and M. Baumann, *Org. Lett.*, 2010, **12**, 3618.
114. C. Delacour, D. Stephens, C. Lutz, R. Mettin and S. Kuhn, *Org. Process Res. Dev.*, 2020, **24**, 2085.
115. Y. Naruke, H. Tanaka and H. Harada, *Electrochemistry*, 2011, **79**, 826.
116. G. Chatel and D. R. MacFarlane, *Chem. Soc. Rev.*, 2014, **43**, 8132.
117. G. Kaur, A. Sharma and B. Banerjee, *ChemistrySelect*, 2018, **3**, 5283.
118. G. Chatel, R. Pflieger, E. Naffrechoux, S. I. Nikitenko, J. Suptil, C. Goux-Henry, N. Kardos, B. Andrioletti and M. Draye, *ACS Sustainable Chem. Eng.*, 2013, **1**, 137.
119. N. D. Oktaviyanti, Kartinin and A. Mun'im, *Heliyon*, 2019, **5**, e02950.
120. D. Panda and S. Manickam, *Ultrason. Sonochem.*, 2017, **36**, 481.
121. Y. Son, M. Lim, J. Khim and M. Ashokkumar, *Ind. Eng. Chem. Res.*, 2012, **51**, 232.
122. R. Abazari, A. R. Mahjoub, S. Sanati, Z. Rezvani, Z. Hou and H. Dai, *Inorg. Chem.*, 2019, **58**, 1834.

Section 2

Benign Media for Organic Synthesis

CHAPTER 9

Biomass-derived Solvents

MARGHERITA MIELE[a], LAURA IELO[a,b], VERONICA PILLARI[a], MARÍA FERNÁNDEZ[c], ANDRÉS. R. ALCÁNTARA*[c] AND VITTORIO PACE*[b]

[a]Department of Pharmaceutical Chemistry, University of Vienna, Althanstrasse 14, 1090, Vienna, Austria; [b]Department of Chemistry, University of Torino, Via P. Giuria 7, 10125 Torino, Italy; [c]Department of Chemistry in Pharmaceutical Sciences, Complutense University, Plaza de Ramón y Cajal, 28040, Madrid, Spain
*E-mail: vittorio.pace@unito.it, andalcan@ucm.es

9.1 Introduction

A well-known paradigm inside Green Chemistry states that "the best solvent is no solvent".[1,2] Nevertheless, most of the known organic transformations do require the use of solvents, as they are crucial not only for running a reaction, but also for the subsequent work-up (separation and/or purification of the final products). Consequently, it has been assessed that solvents (annual industrial-scale production higher than 20 million metric tons[3]) typically constitute around 80% of all materials required for the effective completion of an archetypal synthetic procedure,[3,4] this value approaching 90% when the synthesis of active pharmaceutical ingredients (APIs) is intended.[1,5] This not very sustainable scenario turns even worse bearing in mind that most commonly used organic solvents, usually displaying high toxicities, are generally derived from non-renewable fossil resources; accordingly, this fact causes severe environmental and economic concerns when facing large-scale chemical processes.[6,7]

Sustainable Organic Synthesis: Tools and Strategies
Edited by Stefano Protti and Alessandro Palmieri

Published by the Royal Society of Chemistry, www.rsc.org

Therefore, modern green chemistry is focussed on the smart replacement of these solvents by more sustainable alternatives.[7] In this sense, a "green solvent" must fulfil some physicochemical characteristics,[2,8–11] such as low vapour pressure, high boiling point and high biodegradability under environmental conditions. Additionally, it must be odourless, easily recyclable and possess an almost universal capability for dissolving as many chemicals as possible; finally, yet importantly, it must be reasonably priced and should derive from renewable resources.

Inside the denomination of "green solvents", we can include a great variety of chemical structures; obviously, water has been traditionally considered as the greenest possible solvent, due to its cost, ready availability and non-toxic, non-polluting, and non-flammable behaviour.[12] However, as most organic compounds are not soluble in water, it has not commonly been used for synthetic purposes, due to the commonly accepted axiom (*corpora non agunt nisi soluta*) that substances should be dissolved "in water" to react; nevertheless, organic reactions involving water-insoluble compounds can be efficiently conducted "on water", that is, at the water interface.[13] This concept has fostered the use of water for organic reactions. Additionally, other commonly cited green solvents are ionic liquids (ILs),[14–18] supercritical fluids[19,20] (mainly supercritical CO_2[21,22]), deep-eutectic solvents (DES)[23–34] and, last but not least, biomass-derived solvents, usually abbreviated as "biosolvents".[35] These solvents, which share similar properties to those derived from fossil resources, satisfy several of the criteria required for being catalogued as a green solvent, such as accessibility, biodegradability, little toxicity and affordable prices.[36] For this reason, their use is increasingly being considered as a valuable and sustainable alternative compared to petrol-derived counterparts.[11,36,37]

Biosolvents are some of the compounds that could be obtained in a biorefinery, that is, a refinery that converts biomass to bioenergy (biofuels, power and/or heat) and other beneficial bio-based products (food, feed, chemicals, materials and solvents).[38,39] Most of the biorefineries actually working (or planned to start working)[40–42] are based on lignocellulosic material,[43] consisting of high recalcitrance phenolic lignin and polymeric carbohydrates such as cellulose and hemicelluloses. From these, different carbohydrate molecules possessing 5 (xylose, arabinose) or 6 carbon atoms (glucose, mannose, galactose and rhamnose) can be obtained, serving as starting materials for the generation (*via* biological or chemical conversions) of different building blocks classified into different platforms,[43] which in turn can subsequently be converted into valuable chemicals, materials and solvents, as presented in Scheme 9.1.

As can be seen, most of the main biosolvents used in organic synthesis today are covered in Scheme 9.1. The most obvious choice is bioethanol,[44–47] which is the starting building block for the production of acetaldehyde diethyl acetal (1,1-diethoxyethane), an attractive bisolvent.[48] Some other biosolvents are glycerol, its ether, acetals, carbonates and esters;[49–55] several low-melting mixtures of carbohydrates;[56,57] esters of lactic acid[58,59] and gluconic acid;[60–63]

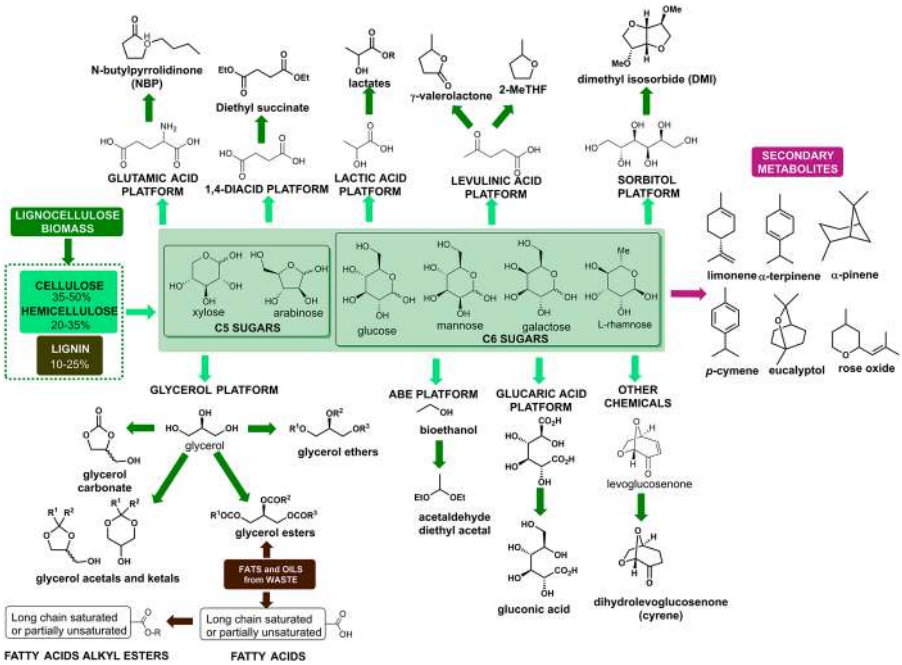

Scheme 9.1 A resume of the most common biosolvents and their precedence.

2-methyltetrahydrofuran (2MeTHF),[64–66] dihydrolevoglucosenone (commercial name Cyrene[67,68]), or γ-valerolactone (GVL[69–76]). More recently, some other biomass-derived chemicals have been proposed as green solvents, such as isosorbide dimethyl ether (Me_2Isos or DMI)[77–80] and diethyl succinate (Et_2Suc),[81–84] both derived from cellulose, or *N*-butylpyrrolidinone (NBP), a dipolar aprotic solvent[85–91] that can be obtained from glutamic acid.[92] Finally, we cannot forget to mention that a very common solvent, namely ethyl acetate (EtOAc), is readily available from biomass[93,94] and is often disregarded in the context of biosolvents.

Another important family of biosolvents comes from secondary metabolites of plants, accessible through biorefineries derived from lignocellulose waste.[95] In this sense, the most commonly used terpenes acting as biosolvents are limonene[96–102] or *p*-cymene;[3,103–105] some new alternatives, such as γ-terpinene,[48,106,107] α-pinene,[48] eucalyptol[48,108–110] or (+)-rose oxide[48] (4-methyl-2-(2-methylprop-1-en-1-yl)tetrahydro-2*H*-pyran) have been recently reported.

Additionally, from waste fats and oils, apart from glycerol also available from C5–C6 sugars, it is possible to obtain fatty acids that, upon esterification, would furnish fatty acid alkyl esters. These methyl esters (FAMEs), known as biodiesel, although mainly used as biofuels, can be also used as biosolvents,[111–114] methyl soyate being one of the most reported.[115,116]

Thus, to illustrate the use of these green biosolvents, different examples will be presented hereinafter, considering their applicability in classical organic chemistry, as well as in biocatalyzed procedures.

9.2 Methyltetrahydrofuran (2-MeTHF)

Although originally considered as a biofuel,[4] 2-methyltetrahydrofuran (2-MeTHF) is a renewable alternative to THF and other organic solvents,[65,66,117] as it can be synthesized from xylose or glucose, through furfural and levulinic acid valorization[118] (see Scheme 9.1). Remarkably, following the furfural route, a reduction of 97% solvent emissions compared to non-renewable THF production has been reported;[119] furthermore, applying acidic pathways starting from levulinic acid (*via* γ-valerolactone (GVL) intermediate), it is possible to generate a dual high value stream of 2-MeTHF and GVL.[66] A detailed Life Cycle Assessment (LCA, a tool to assess the environmental impacts and resources used throughout a product's life cycle, *i.e.*, from raw material acquisition, *via* production and use phases, to waste management[120]) for the production of 2-MeTHF from three biomass sources (corn stover, sugar cane bagasse, and rice straw) has been described,[121] showing that the energy demand and environmental damage caused by crop production far prevailed over that of biomass processing, reporting an energy consumption of around 0.2 MJ kg^{-1}.

Regarding its chemical–physical properties, 2-MeTHF shows a lower water miscibility, higher stability, and lower volatility compared to THF (2-MeTHF has melting and boiling points of −136 °C and 80.2 °C respectively, whereas the values for THF are −108.4 °C and 66 °C, respectively). Likewise, it has been reported that 2-MeTHF displays low toxicity, possessing neither mutagenicity nor genotoxicity characteristics,[122,123] and the human Permitted Daily Exposure (PDE) limit (below which there would be negligible safety concerns for patients exposed to 2-MeTHF) is 6.2 mg per day.[124] Very recently, a No Observed Adverse Effect Level (NOAEL) of 250 mg kg^{-1} day^{-1} has been reported, therefore supporting the safe use of 2-MeTHF in the pharmaceutical industry.[125] Although 2-MeTHF is generally considered to be readily degradable,[66,126] literature focusing on the degradation pathways is still scarce. Anyhow, regardless of its biogenic origin, the CHEM21 selection guide still ranks 2-MeTHF as problematic due to its high flammability,[127] even considering that its flash point (−11 °C) is higher than that of hexane (−30 °C).[118]

9.2.1 2-MeTHF as a Solvent in Organic Chemistry Reactions

For all these reasons already mentioned, in the last few years, many researchers have started to use 2-MeTHF as an alternative reaction solvent; in this sense, different reviews have been published covering different examples,[65,66,117,128] so we will only comment here on some recent ones. Fairley and coworkers, for instance, reported the amidation and transamidation

reactions of ethyl esters and *N*-Boc-substituted benzamides using lithium amides as metal precursors[129] (Scheme 9.2).

The reaction takes place in just 20 seconds under air at room temperature using 2-MeTHF as a solvent, which seems to play a key role in these reactions, warranting full solubilization of the lithium reagent and favouring the formation of small kinetically activated aggregates that react quickly with the organic substrate avoiding the decomposition reactions due to the air. In another example, Mulks *et al.*[130] described a straightforward alkali-metal-mediated procedure for alkylation of styrenes using 2-MeTHF as a solvent under air (Scheme 9.3a). Surprisingly, despite the well-known incompatibility of organolithium reagents with air and moisture, they reported that the presence of moisture is the main point for promoting the formation of the desired phenethylamines over competing olefin polymerisation products. This procedure is also valid for hydroamination with sodium amides, showing excellent product yields (Scheme 9.3b).

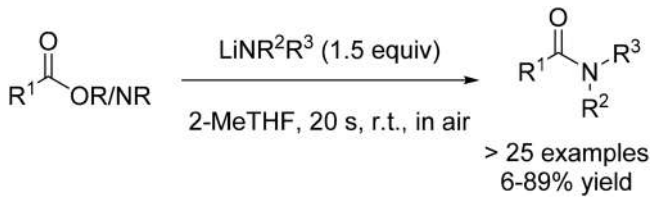

Scheme 9.2 Amidation and transamidation of ethyl esters and *N*-Boc-substituted benzamides in 2-MeTHF.

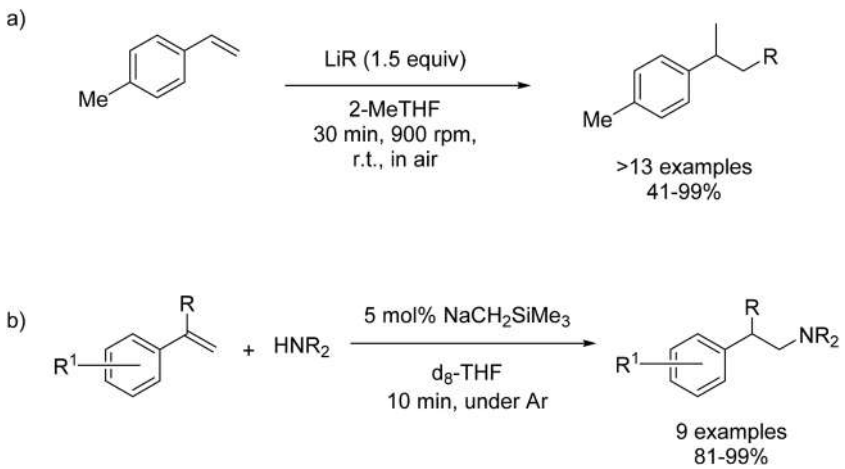

Scheme 9.3 Alkali-metal-mediated procedure for alkylation (a) and hydroamination (b) of styrenes in 2-MeTHF.

Szostak and coworkers[131] reported the iron-catalyzed cross-coupling of aryl chlorides and tosylates with challenging organometallics possessing β-hydrogens using 2-MeTHF as a solvent. The authors hypothesized that, despite the increased steric hindrance at the 2-position, the high basicity of 2-MeTHF (compared to THF) should aid its coordination to iron and favour the generation of catalytically active, solvent-coordinated iron(II) species.[132] The reaction proceeds in very good yield and under very mild conditions and different functional groups were tolerated. Moreover, large-scale cross-coupling, cross-coupling of heteroaromatic substrates, and cross-coupling of challenging aryl tosylates and carbamates mediated by Fe–NHC catalytic systems were described (Scheme 9.4). Subsequently, this methodology was employed for the synthesis of fibrinolysis inhibitors.

Luisi and coworkers[133] described a CBS-asymmetric reduction of aryl and heteroaryl ketones by using microreactor technology (Scheme 9.5). One of the main problems in CBS-asymmetric reductions is the employment of hazardous borane compounds, difficult to cope with at a large scale. These authors demonstrated that it is possible to safely handle the borane solution using microreactors and that the reaction proceeds well using 2-MeTHF as a greener alternative to traditional solvents. Furthermore, the employment of flow technology enabled a reduction of the amount of the chiral catalyst, avoiding the use of an additive such as DEAN (*N*,*N*-diethylaniline), and also the in-line monitoring and work up procedures helped to optimize the process.

The palladium-NHC-catalyzed (NHC = *N*-heterocyclic carbene) Suzuki–Miyaura cross-coupling of amides and esters *via* highly chemoselective N–C(O) and O–C(O) cleavage with aryl boronic acids using 2-MeTHF was

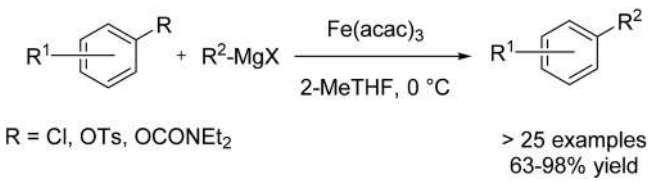

Scheme 9.4 Iron-catalyzed cross-coupling of aryl chlorides and tosylates in 2-MeTHF.

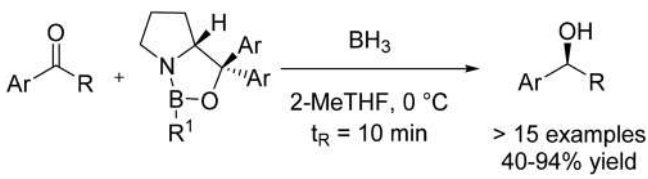

Scheme 9.5 CBS-asymmetric reduction of aryl and heteroaryl ketones in 2-MeTHF *via* microreactor technology.

recently reported by Szostak *et al.*[134] This methodology employs commercially-available, air- and moisture-stable Pd(II)–NHC precatalysts, and works with a wide range of amides and boronic acids (Scheme 9.6). The potential of this reaction has been proved in large-scale synthesis, one-pot activation/cross-coupling and the synthesis of a bioactive ketone intermediate.

Furthermore, Szostak and coworkers[135] described the first example of Ru-catalyzed C–H arylation directed by sulfur-containing groups and a rare example of C–H arylation directed by the versatile thiobenzamide moiety (Scheme 9.7). In particular, they reported the ruthenium(II)-catalyzed ortho-C–H arylation of *N*,*N*-dialkylthiobenzamides with boronic acids *via* $[RuCl_2(p\text{-cym})]_2$ in the presence of $Cu(OTf)_2$ and Ag_2O oxidant using 2-MeTHF as a solvent.

Rajkiewicz and coworkers[136] have reported a ring-closing metathesis/isomerization procedure by using 2-MeTHF as a solvent. This reaction can be considered as an effective synthesis method of the vinylic ethers and amides (Scheme 9.8).

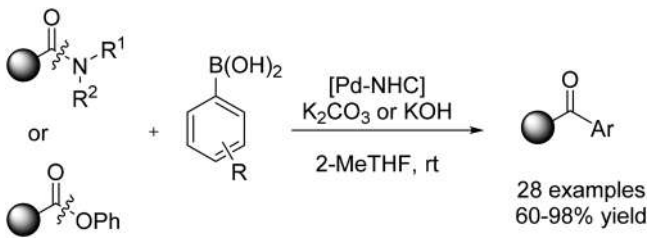

Scheme 9.6 Palladium-NHC-catalyzed Suzuki–Miyaura cross-coupling of amides and esters in 2-MeTHF.

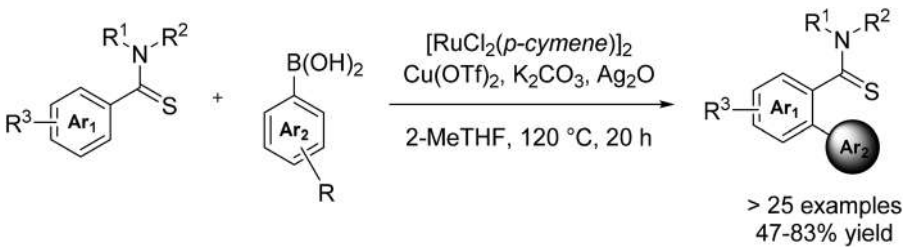

Scheme 9.7 Ruthenium(II)-catalyzed ortho-C–H arylation of *N*,*N*-dialkylthiobenzamides with boronic acids in 2-MeTHF.

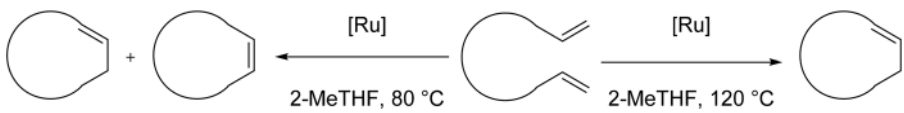

Scheme 9.8 Ring-closing metathesis/isomerization procedure in 2-MeTHF.

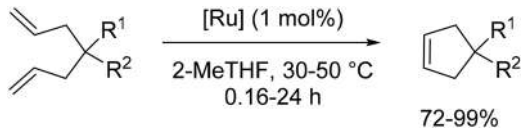

Scheme 9.9 Olefin metathesis in 2-MeTHF *via* ruthenium complexes.

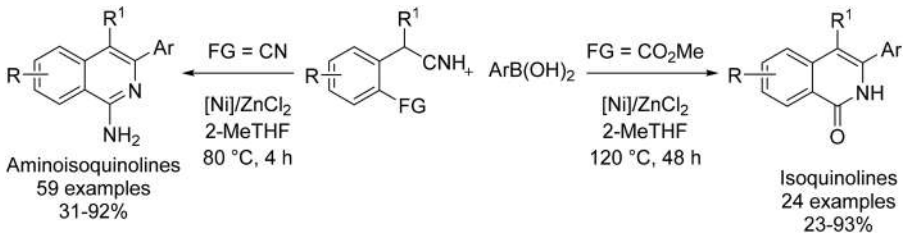

Scheme 9.10 Nickel-catalyzed addition/cyclization of 2-(cyanomethyl)benzonitriles with arylboronic acids in 2-MeTHF.

On the other hand, Smoleń and coworkers[137,138] have described olefin metathesis using as a selective catalyst ruthenium complexes bearing thiophene-based unsymmetrical *N*-heterocyclic carbene ligands, using 2-MeTHF as solvent (Scheme 9.9).

Finally, Zhen *et al.*[139] have reported the first example of the nickel-catalyzed tandem addition/cyclization of 2-(cyanomethyl)benzonitriles with arylboronic acids using 2-MeTHF as a solvent. This procedure allowed the synthesis of aminoisoquinolines possessing different functional groups under mild conditions. By using this methodology, the synthesis of isoquinolones was also possible by reacting methyl 2-(cyanomethyl)benzoates with arylboronic acids (Scheme 9.10).

9.2.2 2-MeTHF as a Solvent in Biotransformations

2-MeTHF has been briefly benchmarked to other solvents in some previous publications;[140,141] nevertheless, the work conducted by Simeó *et al.*,[142] describing the regioselective acylation of several nucleosides catalysed by lipase B from *Candida antarctica*, to render either 3′or 5′-esters depending on the substrate, can be considered as the real starting point for the modern use of 2-MeTHF as an alternative for biotransformations. Subsequently, many other examples have been reviewed elsewhere by Alcántara and coworkers,[64,66] so we will only comment here on examples published afterwards. For instance, in a very recent paper, Peris *et al.*[143] reported the combination of multiple and consecutive multicatalytic steps in a single cascade combining organocatalytic supported ionic-liquid like phases (SILLPs) with Novozym 435 for the preparation of optically pure chiral cyanohydrins (Scheme 9.11).

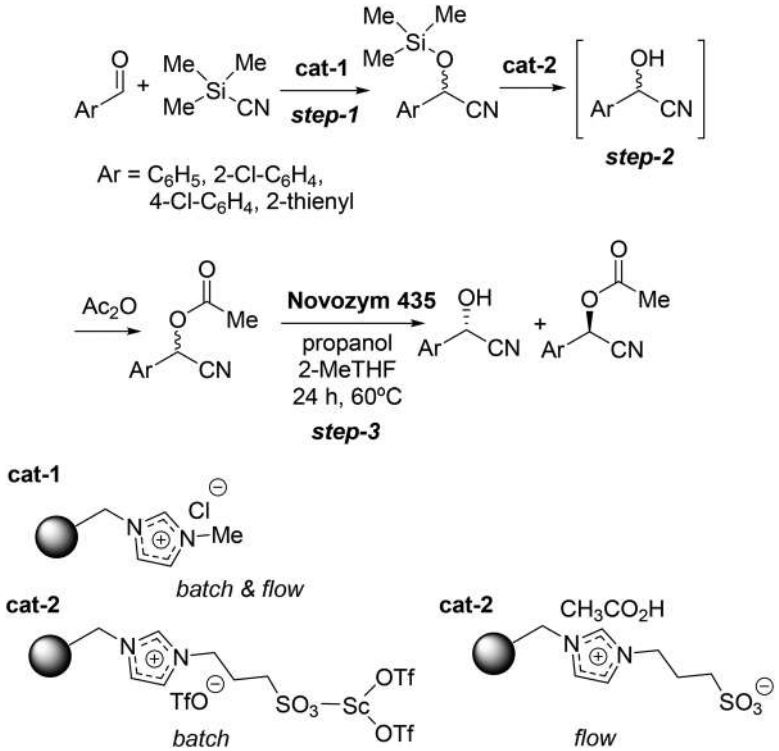

Scheme 9.11 Chemoenzymatic cascade for the preparation of optically pure cyanohydrins in 2-MeTHF.

These cyanohydrins are very useful building blocks for the ulterior synthesis of a plethora of pharmaceuticals and agrochemicals.[144,145] The process depicted in Scheme 9.11 implies three consecutive steps and four catalytic reactions: an organocatalytic cyanosylilation of different aromatic aldehydes to furnish racemic *O*-sylilated α-aromatic acetonitriles (**step-1**), its transformation into the corresponding esters *via* two consecutive reactions (hydrolysis of the cyanosylil ether and subsequent acetylation, **step-2**) and, finally, enzymatic kinetic resolution of the racemic cyanohydrin ester by transesterification with propanol (**step-3**). The authors reported the optimization of each individual step under batch conditions, using SILLP catalysts 1 and 2 shown in Scheme 9.11 for the initial steps (yields ranging from 95% to 99%); the enzymatic kinetic resolution was carried out using Novozym 435 and 2-MeTHF (yields from 52–57%, ee higher than 99% in all cases). The authors reported that the best SILLP catalyst for the second step was different from that used in the batch process; with this modification, they were able to obtain an excellent continuous process, leading to a noticeable space-time yield (STY) of 124 g g^{-1} cat h^{-1} L^{-1}, comparable to that obtained with hydroxynitrile lyases and HCN[146] (a highly hazardous reagent), in a much greener manner.

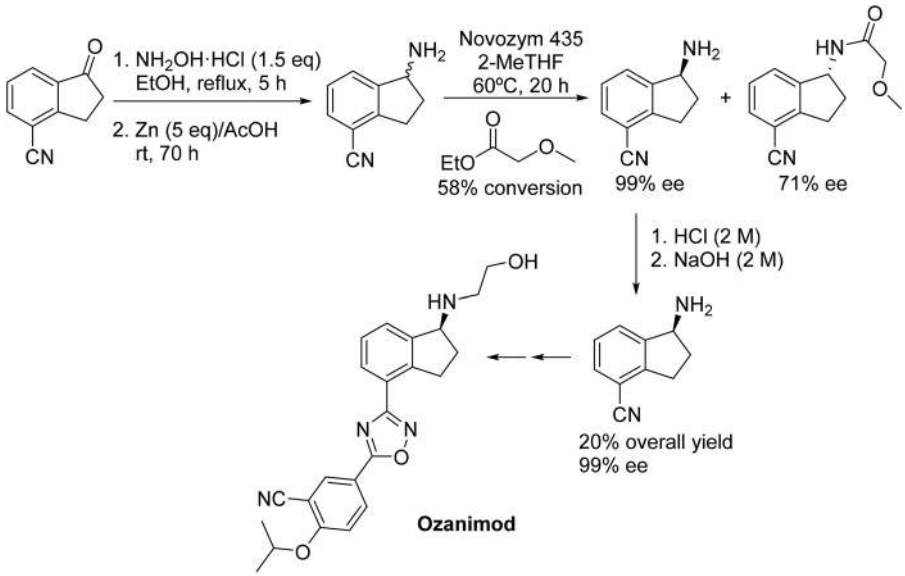

Scheme 9.12 Chemoenzymatic synthesis, using 2-MeTHF in the biocatalytic step, of an enantiopure precursor of Ozanimod, a drug for the treatment of relapsing multiple sclerosis.

Another recent example of lipase-catalyzed kinetic resolution using 2-MeTHF has been reported in a recent patent,[147] depicted in Scheme 9.12, for the preparation of an enantiopure precursor of Ozanimod (Zeposia®), a sphingosine-1-phosphate (S1P) receptor agonist acting as an immunomodulatory drug for the treatment of relapsing multiple sclerosis.[148]

In this sense, the kinetic resolution of racemic 1-amino-2,3-dihydro-1*H*-indene-4-carbonitrile was the key step for introducing the desired chirality. This was carried out by *N*-acylation with ethyl 2-methoxyacetate in 2-MeTHF, once again using commercial Novozym 435 as the catalyst, obtaining pure (*S*)-amine in an overall 20% yield in the reductive amination starting from the corresponding carbonylic compound.

Very recently, 2-MeTHF has become very useful in polymerizations to furnish polyesters. Thus, lipase-catalyzed preparation of adipate- and furan-2,5-dicarboxylate-based polyesters, using several 2-MeTHF and other neoteric solvents (2,2,5,5-tetramethyloxolane, 2,5-dimethyltetrahydrofuran and pinacolone) as substitutes for traditional solvents such as PhMe or THF, has been reported.[149] These polymers were prepared by enzymatic esterification of both diacids with 1,4-butanediol (BDO) or 1,8-octanediol (ODO), as shown in Scheme 9.13.

Solvent selection was based on their capability for dissolving both the monomers and the resulting polymer, while retaining enzymatic activity. Additionally, the solvents should ideally be relatively volatile (70–139 °C

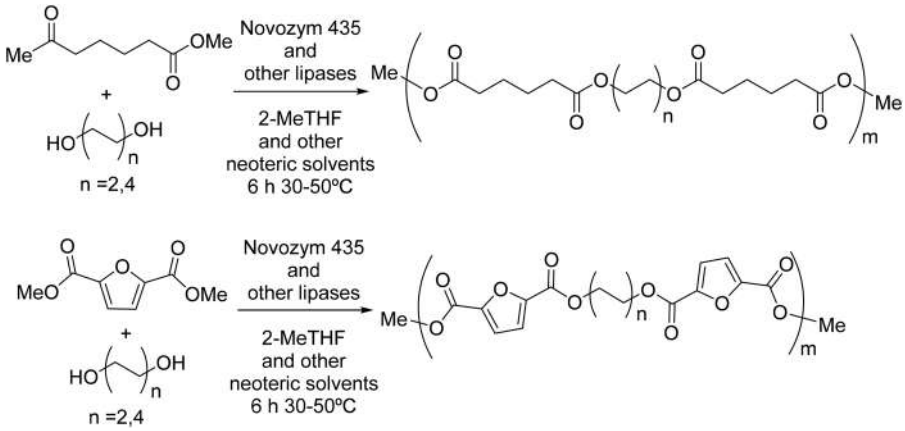

Scheme 9.13 Enzymatic synthesis of polyesters in 2-MeTHF.

range, as set by the CHEM21 solvent selection guide[127]), therefore allowing their easy removal from reaction media. In fact, solvents with higher boiling points would make distillation more energy-demanding. No significant differences were observed between the new solvents in the reaction of dimethyl adipate and diols catalysed by Novozym 435 (best of the lipases tested) at reaction temperatures of 30 and 50 °C, in all cases being comparable or even better than conventional THF or PhMe, in terms of monomer conversions and molecular mass of the polymers. Synthesis of furan-derived polymers generally gave lower monomer conversions, although all the neoteric solvents allowed better conversions than THF of PhMe, with 2-MeTHF being one of the best alternatives.

In another example, Englezou *et al.*[150] have assessed the use of 2-MeTHF for ring opening polymerizations (ROPs), comparing the lipase-catalysed opening of ε-caprolactone (oxepan-2-one) with methyl-polyethylene glycol (mPEG) *versus* the ROP of lactide (lactone cyclic di-ester derived from lactic acid) with DBU (1,8-diazabicyclo[5.4.0]undec-7-ene), as shown in Scheme 9.14.

These linear amphiphilic block copolymers (polylactides or polycaprolactones) have been used for different biomedical applications,[151] after nanoprecipitation to generate nanoparticles, as they are biocompatible, mechanically strong and can be obtained starting from natural feedstocks. The use of 2-MeTHF as a solvent reduced the carbon footprint in the polymerization, leading to excellent results compared to classical solvents such as DBM or THF.

2,5-bis-(hydroxymethyl)furan (BHMF, Scheme 9.15) is an extremely attractive building block, easily obtainable by reduction of 5-(hydroxymethyl) furfural (HMF), an important and versatile bioderived platform chemical obtainable from renewable C5–C6 carbohydrate feedstocks[152] (see Scheme 9.1). In fact, BHMF is used as a building block for polymers, foams and crown

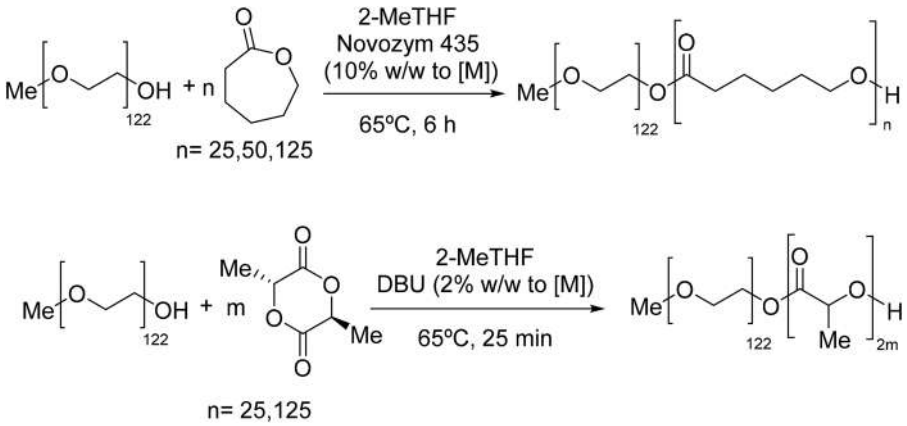

Scheme 9.14 Enzymatic *versus* chemical synthesis of amphiphilic copolymers using 2-MeTHF as a biosolvent.

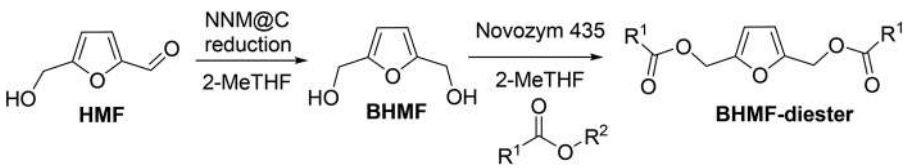

Scheme 9.15 Chemoenzymatic synthesis of BHMF diesters in 2-MeTHF.

ethers, and as an intermediate in the preparation of different pharmaceuticals.[153] The reduction of HMF to BHMF can be performed using different procedures; the use of stoichiometric amounts of metal hydride salts such as $LiAlH_4$ had been the archetypical methodology,[154] although the generation of great amounts of waste and the high cost of metal hydrides prevents this methodology for being used at industrial scale. Thus, a great variety of catalytic pathways (conventional hydrogenation, hydrogen transfer procedures, photocatalytic and electrocatalytic reductions) have been proposed;[155–157] additionally, also biocatalytic reductions,[158] mainly using whole cells,[159–161] have been reported for the transformation of HMF into BHMF. Very recently, Arias *et al.*[162] have described a chemoenzymatic protocol for the preparation of BHMF-derived diesters, through a first catalytic reduction using non-noble metal nanoparticles (NNM@C) and a subsequent esterification of the diol using Novozym 435 (Scheme 9.15).

BHMF-diesters are biobased plasticizers that can act as an alternative to petroleum-derived phthalates;[158] the use of 2-MeTHF as a solvent allowed the implementation of the cascade reaction depicted in Scheme 9.15, as it acts as an effective solvent both for the chemical and the enzymatic steps. In a batch mode reactor, using hexanoic acid as an acyl donor and Novozym 435, esterification of BHMF led to 99% yield after 11 h reaction time. In the overall process

starting from HMF, the chemical reduction using a Co@C catalyst was carried out in 2-MeTHF at 110 °C for 10 h; after that time, the catalyst was removed with a magnet, and subsequently hexanoic acid, Novozym 435 and molecular sieves (to eliminate the water molecules produced upon esterification) were added, lowering the reactor temperature down to 35 °C. Excellent results were reported (total yield 91%, total selectivity 96%) and similar performance was observed using butyric or octanoic acid, while acetic acid turned out not to be adequate for the esterification, due to its lower pK_a. When conducting repetitive batches, a deactivation of both catalysts was observed, so that the reaction time had to be increased; additionally, changing form esterification with carboxylic acids to transesterification with vinyl hexanoate led to much better results, as long as excellent yield (97%) and selectivity to BHMF dihexanoate (100%) were obtained in only 0.5 h, affording an overall diester yield of 89%. In a further step, the process was implemented in a continuous-flow reactor by coupling two fixed-bed reactors, one containing Co@C and the other the immobilized lipase, which afforded an overall yield of the desired diester of close to 90% and remained stable for 60 h of operation.

In any case, the enzymatic esterification of BHMF with fatty acids (10:0, 12:0, 14:0, 16:0 or 18:0) in 2-MeTHF had been previously reported by Lăcătuş *et al.*[163] These authors pointed out that Novozym 435 was the best catalyst, by comparing its performance with that from five other immobilized enzyme preparations commonly used for biofuel productions, also observing that the small water amount present in the enzymatic preparations was enough to allow the hydrolysis of diesters when incubated in dry 2-MeTHF. These authors optimized the reaction variables, such as molar ratio, temperature, reaction time, fatty acid alkane length or amount of catalyst, to finally scale up to a preparative scale using capric, lauric, myristic, palmitic or stearic acid. This same group have recently reported the double esterification of BHMF with a fatty acid mixture (FAM) resulting from the hydrolysis of commercial sunflower oil.[164] Novozym 435 and 2-MeTHF were again selected for this esterification, although finally it was observed that conducting the reaction under solvent-free conditions (solid BHMF is scarcely soluble in FAM, although as the reaction progressed the gradually formed diesters were acting as solvents) and removing the water under reduced pressure allowed the complete conversion of BHMF into esters at 60 °C.

9.3 Gamma-Valerolactone (GVL)

γ-Valerolactone (GVL, see Scheme 9.1), a naturally occurring chemical found in fruits and generally used as a food additive, can be considered an archetypical sustainable liquid,[165] as it can be obtained from renewable sources,[69] and displays very useful properties: low melting (−31 °C) and high boiling (207 °C) and flash (96 °C) points, a definitive but acceptable smell for easy recognition of leaks and spills, nontoxicity, and high water-solubility, therefore favouring its biodegradation; furthermore, its vapour pressure is 0.65 kPa at 25 °C, and it only increases to 3.5 kPa at 80 °C. On the other hand, it does not suffer

hydrolysis under neutral conditions and can be considered as safe, as it did not form any measurable amount of peroxides in a glass flask kept under air for several weeks. Additionally, its extraction from reaction mixtures is very easy, as its high solubility in water allows the use of a certain amount of water for solubilising and removing it; afterwards, a simple distillation would separate GVL from water, allowing its reuse in another reaction cycle.[165]

9.3.1 GVL as a Solvent in Organic Chemistry Reactions

In fact, GVL is an excellent replacement choice for non-eco-friendly dipolar aprotic solvents,[127,166] generally used in metal-catalysed processes, commented on in this section. Regarding the use of palladium catalysts, the Mizoroki–Heck coupling of iodoarenes and styrenes (or acrylates) in GVL catalysed by commercially available Pd/C (0.1% mol) was reported by Strappaveccia *et al.*,[167] leading to 80–90% yields in a short reaction time (Scheme 9.16a).

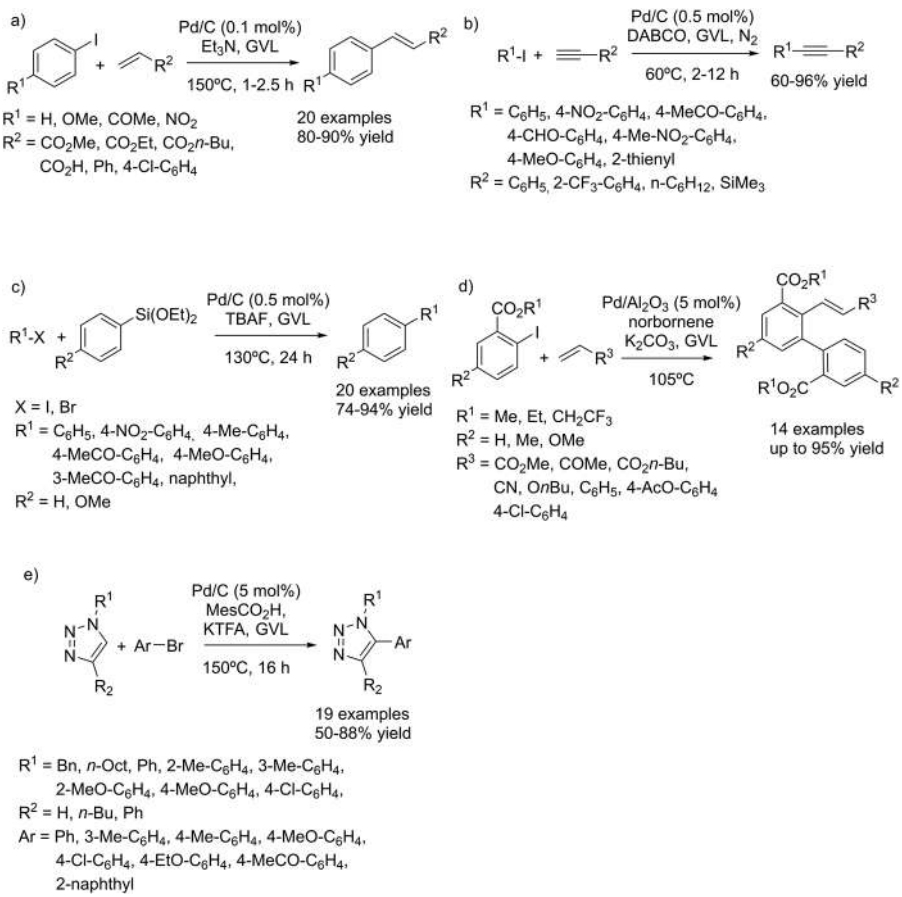

Scheme 9.16 Several Pd-catalysed coupling reactions performed in GVL. a) Mizoroki-Heck coupling; b) Sonogashira-Hagihara cross-coupling; c) Hiyama reaction; d) Catellani reaction; e) C–H arylation of 1,2,3-triazoles.

Notably, the working up was really straightforward, as only by removing the catalyst by filtering and adding small amounts of water, it was possible to precipitate the final products; this methodology implies a substantial reduction of waste compared to typical procedures requiring a tedious aqueous work-up. The authors compared this procedure using GVL with those carried out using other common reaction media (DMF, NMP, DMSO, MeCN, H_2O or H_2O/DMF 4 : 1), reporting the excellent behaviour of GVL, which led to similar yields compared to DMF or NMP, but with a considerable reduction in the amount of metal released (down to 6 ppm *versus* 660 ppm in NMP for the synthesis of poly (2,5-dihexylphenylenedivinylene-*alt*-1,4-phenylenevynilene), a model semiconductor) from the heterogeneous catalyst to the reaction medium. In a similar way, these authors assessed the use of GVL in Pd/C catalysed Sonogashira–Hagihara cross-coupling (Scheme 9.16b).[168] The chemical efficiency of GVL as a medium was again excellent and the best results were obtained using DABCO as the base, allowing the isolation of products in 60–96% yields. For this coupling, the use of conventional solvents such as DMF, DMSO, NMP or MeCN required shorter reaction times (5–30 min) compared to GVL, although once again the use of GVL resulted in a sensible diminution of the metal contamination. Other Pd-catalysed reactions in which GVL has proven to be an excellent biosolvent are the Hiyama reaction in the presence of tetrabutylammonium fluoride (Scheme 9.16c), leading to excellent yields of the *para*-disubstituted benzene products,[169] or the Catellani reaction (Scheme 9.16d), using heterogenous Pd/Al_2O_3, allowing not only good yields with a very small metal release (2.2 ppm), but also the possible reuse of the Pd catalyst for at least four consecutive reaction runs, without noticeable loss of its catalytic efficiency.[170] Similarly, Tian *et al.*[171] reported the C–H arylation of 1,2,3-triazoles catalysed by Pd/C in GVL (Scheme 9.16e). Once again, the use of the biomass-based GVL led to moderate-to-good yields with the possibility of re-using the Pd catalyst for at least three reaction cycles, with only small amounts of metal detected in the final products. In subsequent studies, Ferlin *et al.*[172] described the C–H functionalization of 1,2,3-triazoles in a continuous flow regime using the same heterogeneous catalyst (Pd/C), a soluble organic base (TBAAc), and GVL as the green reaction medium. By using this continuous-flow protocol, it was possible to ensure the high durability of the solid catalyst, also achieving very low associated E-factor values as a result of the efficient recovery and reuse of the reaction medium.

On the other hand, the use of microwave irradiation for the C–H arylation of thiophenes by arylbromides in GVL using $Pd(OAc)_2$ has also been reported[173] (Scheme 9.17).

As shown, the reactions proceeded regioselectively at the free Cα position, leading to 82% yield starting with 2-methylthiophene or 72% yield using benzo[*b*]thiophene. Furthermore, the synthesis of poly(3-hexyl) thiophene (P3HT) through the C–H (hetero)arylation polymerization of 2-bromo-3-hexylthiophene was also reported. By using computing studies, these authors pointed towards a dual role played by GVL, acting both as a

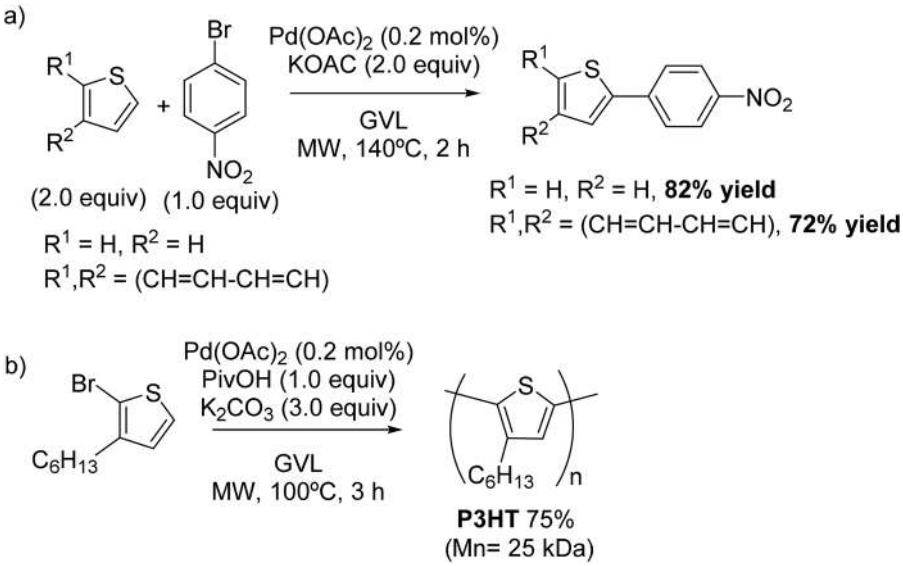

Scheme 9.17 Pd-catalysed reactions in GVL promoted by microwave irradiation. a) Arylation at C-alpha of several thiophenes; b) synthesis of poly(3-hexyl)thiophene (P3HT).

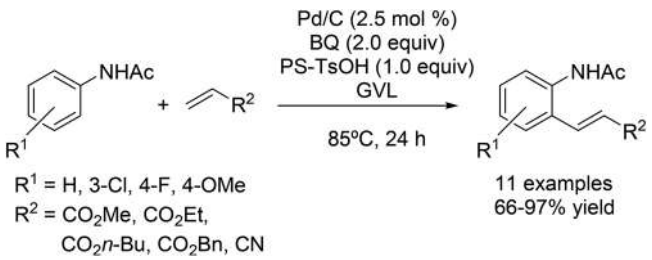

Scheme 9.18 Fujiwara–Moritani alkenylation in GVL.

solvent and as a feasible weakly coordinating ligand to generate the key palladium species. Interestingly, palladium-catalysed C–H activation in GVL is not limited to C–H arylations; for instance, Ferlin *et al.* reported Fujiwara–Moritani alkenylation in GVL using the commercially available heterogeneous palladium catalyst Pd/C (Scheme 9.18);[174] to this aim, 1,4-benzoquinone (BQ) was identified as the optimal oxidant in combination with polystyrene-bounded *p*-toluenesulfonic acid (PS-TsOH) as an acid additive, in order to allow an easier recovery of both the catalyst as well as the additive.

Using this protocol, diversely substituted anilides were efficiently alkenylated with a series of electron-deficient alkenes; interestingly, it was possible to reuse the catalytic system of Pd/C and PS-TsOH for at least five consecutive runs without major loss of product yield and negligible metal

leaching, compared to other commonly used polar aprotic solvents, such as DMF or DMA (*ca.* 4 ppm *vs.* 80 and 31 ppm, respectively). Additionally, these authors also reported the straightforward scale up of the process in a custom-built continuous flow reactor, leading to improved isolated yields.

The versatility of GVL is shown by the fact that not only can Pd catalysts be used for C–H activation, but also ruthenium or cobalt are compatible with this biosolvent. Thus, the Ackermann group has reported[175] the synthesis of phthalides starting from aryl carboxylic acids and electron-deficient alkenes (containing different functional groups such as ketones, esters, bromides, iodides or amines), using ruthenium(II) catalysis and molecular oxygen as the only oxidant (H_2O the only byproduct), as shown in Scheme 9.19a.

Likewise, this same group pinpointed GVL as a valuable solvent for the alkenylation of arylacetamide substrates (Scheme 9.19b),[176] as this biosolvent seemed to expedite the formation of the challenging six-membered ruthenacycle required for the catalytic mechanism *via* weakly coordinating amide assistance. Very recently, the Rh(III)-catalyzed synthesis of isoquinoline derivatives starting from *N*-hydroxyoximes and alkynes *via* C–H activation/annulation in GVL has been reported[177] (Scheme 9.19c). The reaction conditions were mild, allowing the use of a series of functional groups to furnish the final products in good to excellent yields.

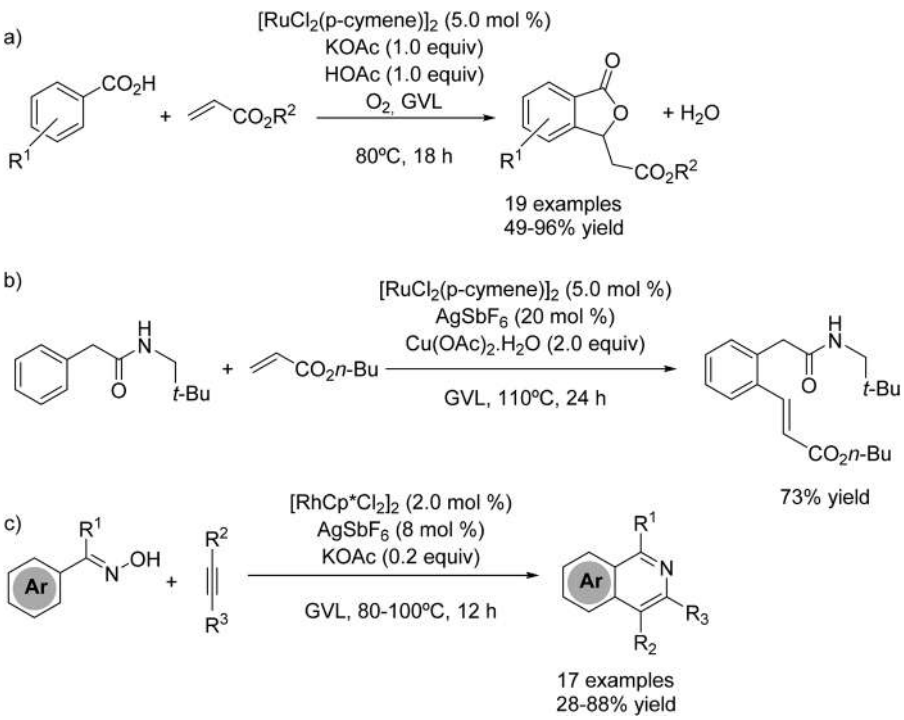

Scheme 9.19 Several Ru-catalysed coupling reactions performed in GVL. a) Synthesis of phthalides; b) alkenylation of arylacetamides; c) synthesis of isoquinoline derivatives.

Moving from precious late transition 4d metals to more abundant 3d transition metals enhances the global sustainability of the process;[178] in this sense, GVL is also suited as a substitute for polar aprotic solvents in cobalt-catalysed C–H activation.[179] Thus, an interesting electrochemical cross-dehydrogenative cobalt-catalysed C–H/N–H functionalization amination in GVL has been reported, as depicted in Scheme 9.20.[180]

This electrochemical C–H amination was carried out under mild reaction conditions at 40 °C, and was operative under ambient air in GVL, which bested all of the conventional organic solvents tested. Remarkably, headspace analysis by gas chromatography unambiguously confirmed the formation of H_2 as the only by-product, proving the advantages of the electrochemical procedure.[181] In another example, this cobalt-catalysed C–H activation in GVL has been reported in the Hiyama-type C–H arylation of *N*-(quinolin-8-yl)benzamides with arylsiloxanes, as shown in Scheme 9.20;[182] interestingly, GVL proved particularly beneficial for the C–H arylation of challenging C(sp^3)–H bonds, as depicted in Scheme 9.20c starting from *N*-(quinolin-8-yl) pivalamide.

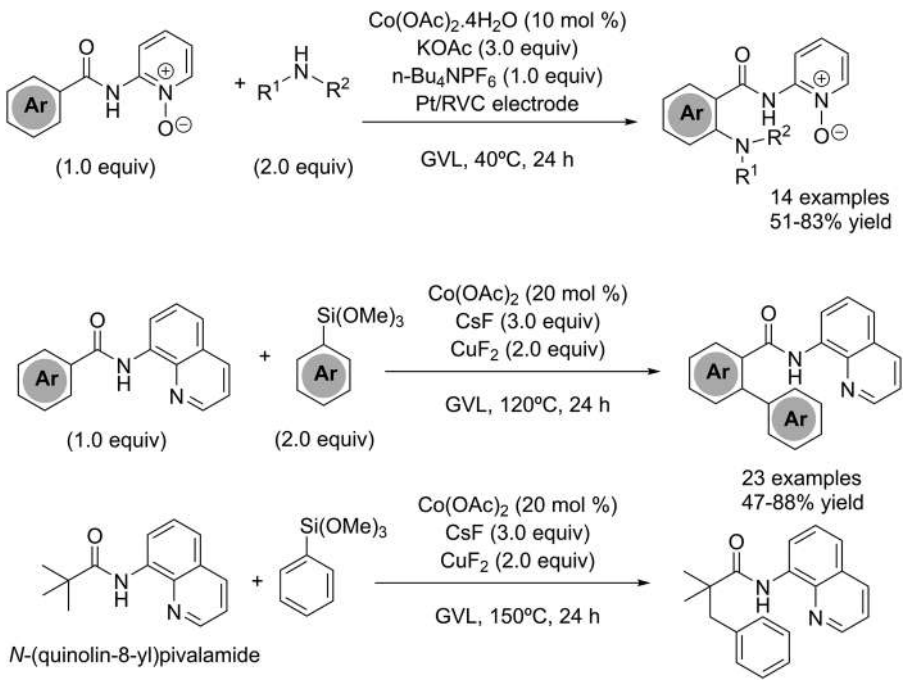

Scheme 9.20 Several Co-catalysed coupling reactions performed in GVL.

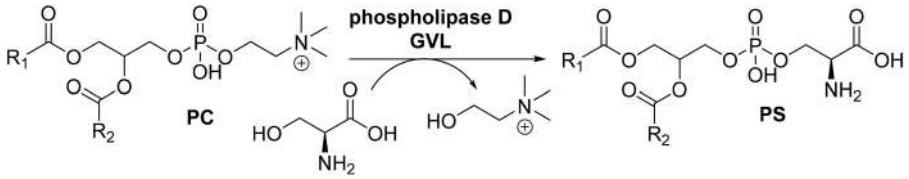

Scheme 9.21 Phospholipase-mediated transphosphatidylation of phosphatidylcoline (PC) with L-serine in GVL.

9.3.2 GVL as a Solvent in Biotransformations

The use of GVL as a solvent for biotransformations is relatively scarce. Indeed, in different examples, GVL has been incorporated into the group of bio-based and green solvents tested for a particular biocatalyzed process, although its performance has not been the best. In this way, Zhu *et al.*[183] reported the use of recombinant *E. coli* cells harbouring nitrile hydratase activity for transforming 2-amino-2, 3-dimethylbutyronitrile (ADBN) into 2-amino-2,3-dimethylbutyramide (ADBA) in various green solvent/aqueous reaction systems, including GVL, but the best results were obtained with the methoxyperfluorobutane/H_2O (v/v, 10%) biphasic system. Iemhoff *et al.*[184] included GVL in their assessment of the performance of Novozyme 435 in the esterification of racemic 2-phenylpropionic acid with EtOH in different bio-based solvents, although they selected *p*-cymene as the best option. Similarly, Paggiola *et al.* have recently investigated different bio-based solvents for the biocatalysed amidation reactions of various ester-amine combinations by *Pseudomonas stutzeri* lipase;[101] once again GVL was tested, although terpene-based solvents (terpinolene, *p*-cymene, D-limonene) were demonstrated to perform better.

Anyhow, there is an interesting reported example in which GVL was used for a biocatalytic process, more concretely for the phospholipase-mediated transphosphatidylation of phosphatidylcoline (PC) with L-serine (shown in Scheme 9.21) to furnish phosphatidylserine (PS).[185] Among the phospholipases tested, the best results were obtained using the enzyme from *Streptomyces chromofuscus*, which allowed the preparation of PS, a compound with many applications in functional food and pharma industries, with 95% yield at 40 °C.

9.4 Dihydrolevoglucosenone

6,8-Dioxabicyclo[3.2.1]octanone, also known as dihydrolevoglucosenone (or Cyrene™, name registered by Merck) has been synthesized from a number of different biomass starting materials under a variety of conditions, but most of these processes start from levoglucosenone

(LGO, (1*S*,5*R*)-6,8-dioxabicyclo[3.2.1]oct-2-en-4-one), which in turn is obtained from cellulose (see Scheme 9.1).[186] Recently, Circa and coworkers[187] developed a thermal methodology for processing wood pulp under acid conditions affording LGO in up to 40% yield, which was afterwards scaled up to 50 tons per year production levels.[188] The conversion of LGO into dihydrolevoglucosenone is carried out by hydrogenation in order to achieve the reduction process.[186] Dihydrolevoglucosenone is only poorly ecotoxic (OECD No. 201, 202 and 209) and has no mutagenicity (OECD No. 471 and 487) with a LD_{50} > 2000 mg kg^{-1} (OECD No. 423, acute toxicity method).[189] Anyway, it has a hazard warning as an eye irritant (E319), but it received ECHA level 7 certification.[190] Comparing the Kamlet–Abboud–Taft and Hansen solubility parameters, Kudo *et al.* found that dihydrolevoglucosenone owns: (a) dispersion parameters closest to DMSO (18.8 *vs.* 18.4 MPa), (b) polarity closest to DMAc (10.6 *vs.* 11.5 MPa) and (c) hydrogen-bonding like interactions that were most similar to NMP (6.9 *vs.* 7.2 MPa).[191] One of the key features of dihydrolevoglucosenone is its high miscibility with water, as it is in equilibrium with its ketal hydrate,[192,193] in contrast to other ketones; additionally, the derivatization of dihydrolevoglucosenone with 1,2-diols allows the formation of novel solvent types (the so-called Cygnets solvent family[194,195]).

9.4.1 Dihydrolevoglucosenone as a Solvent in Organic Chemistry Reactions

Dihydrolevoglucosenone has been used in many organic reactions, as recently reviewed,[186] and shows also great potential for liquid–liquid extractions.[196] In fact, since its launch as a bio-available solvent in 2014 by Clark *et al.*, Cyrene™ has been employed for different applications.[197] Five metal–organic frameworks (MOFs) were synthesized in Cyrene™ and their BET surface areas were compared to MOFs synthesized in DMF realizing that the major part of MOFs synthesized in DMF had higher surface areas.[189] Recently, two different groups[198,199] reported the processing of graphene by using Cyrene™ which acts as an exfoliant and dispersion agent resulting in an order of magnitude increase in graphene dispersion compared to DMF. Cyrene™ is also able to raise some resins, such as NovalGel and ChemMatrix, that are used in solid-phase peptide synthesis.[200] From the synthetic point of view, Cyrene™ was also employed by different research groups. An S_N2 reaction starting from 1,2-dimethylimidazole and 1-bromodecane forming the imidazolium ionic liquid was developed by Clark and coworkers.[197] The rate of this Menschutkin reaction in Cyrene™ was better in comparison with standard dipolar aprotic solvents. However, the fluorination of 2-chloro-5-nitropyridine with potassium fluoride advanced at a reasonable rate to form 2-fluoro-5-nitropyridine (Scheme 9.22).

Cyrene™ has been employed also in a metal-catalyzed process by Watson and co-workers.[201] It is an effective reaction medium for the Sonogashira reaction involving terminal alkynes and sp^2-hybridized halogens.

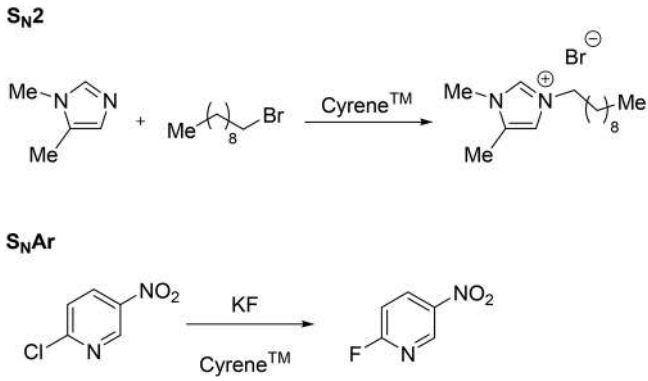

Scheme 9.22 S_N2 and S_NAr reactions using Cyrene™ as a solvent.

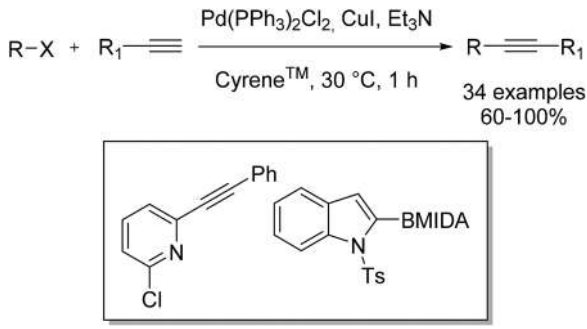

Scheme 9.23 Sonogashira and Cacchi-type annulation reactions by using Cyrene™ as a solvent.

In addition, a Cacchi-type annulation using 2-iodophenols and 2-iodoanilines with terminal alkynes was carried out in Cyrene™ to obtain benzofurans and indoles (Scheme 9.23).

Moreover, the stability of Cyrene™ with different bases was assessed. In the presence of the majority of the common bases, Cyrene™ reacts with itself leading to the formation of the aldol adduct or the aldol condensation product (Scheme 9.24). Conversely, in the presence of amine bases, triethyl amine (TEA) and *N*,*N*-diisopropylethylamine (DIPEA), Cyrene™ was demonstrated to be stable up to 50 °C.[186]

Cyrene™, like the others dipolar aprotic solvents, promotes acyl substitution reactions. Camp *et al.*[202] reported the synthesis of a urea derivative starting from aryl isocyanate and secondary amines. The yield of the reaction was excellent and comparable with DMF and DCM. Furthermore, the treatment of the crude product of the reaction with water led to the precipitation of the

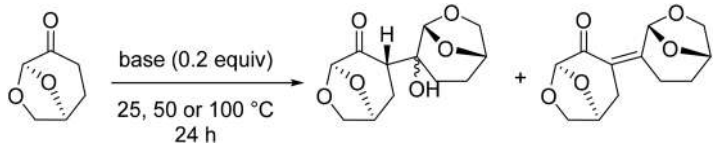

Scheme 9.24 Reactivity of dihydrolevoglucosenone in the presence of bases.

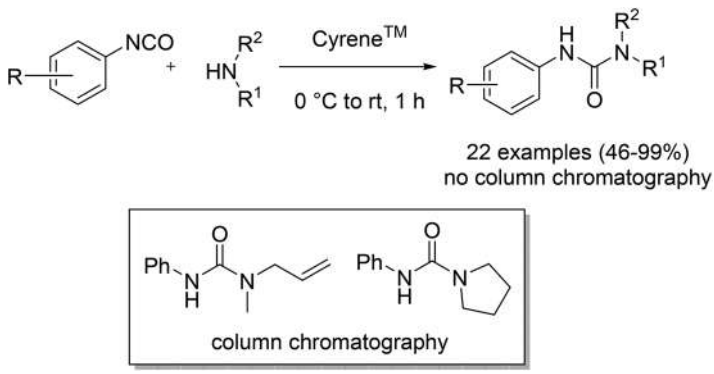

Scheme 9.25 Acyl substitution reactions using Cyrene™ as a solvent.

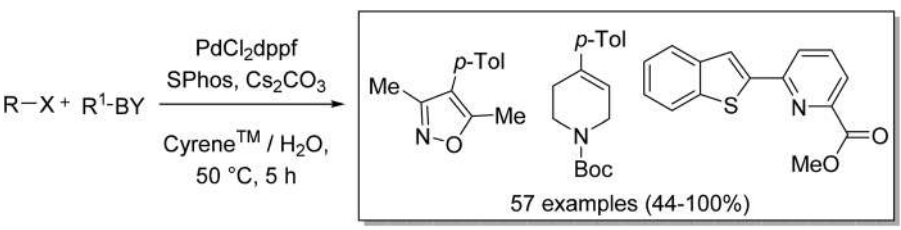

Scheme 9.26 Suzuki–Miyaura cross coupling reaction using Cyrene™ as a solvent.

pure product avoiding any further workup and solving the key problem of the high boiling solvents regarding their removal from the products. When primary amines were used instead, column chromatography was necessary to obtain the pure compound (Scheme 9.25).

The Suzuki–Miyaura cross coupling procedure is also possible using Cyrene™ as a solvent. Watson *et al.*[203] reported the reaction of aryl-, heteroaryl- and vinylhalides with different organoboranes (*e.g.* boronic acids, BPin esters, BMIDA and BF3K). The reaction was demonstrated to be scalable at 22.8 mmol. The key point of this reaction was the use of an active catalyst allowing the process to run at 50 °C (Scheme 9.26).

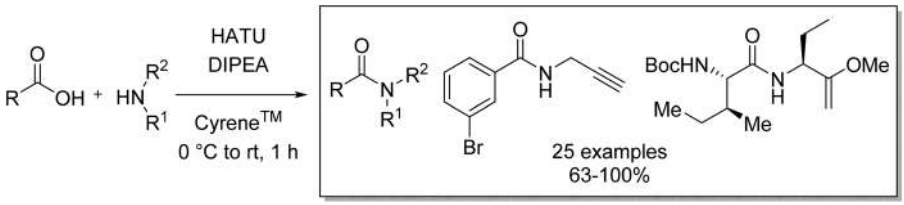

Scheme 9.27 Synthesis of amides using Cyrene™ as a biobased solvent.

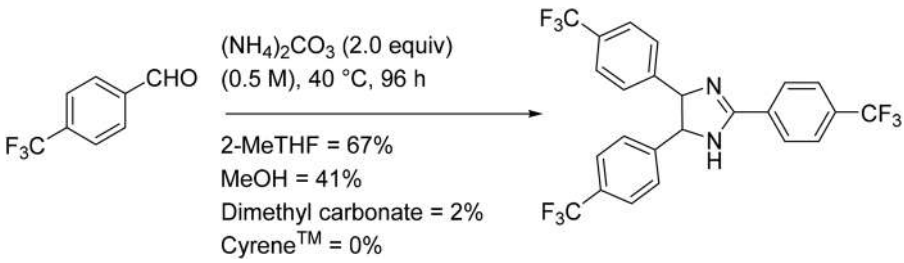

Scheme 9.28 Comparative synthesis of 2,4,5-trisubstituted-2-imidazolines in different solvents.

Watson and coworkers[204] described also the synthesis of amides using Cyrene™ as a biobased solvent, starting from carboxylic acids and amines, in the presence of HATU (a peptide-coupling agent) and excess DIPEA (Scheme 9.27). The process was scalable to 4.3 mmol preserving the enantiomeric excess. The obtainment of the pure compounds was possible after an aqueous wash, followed by a trituration method, allowing the complete elimination of Cyrene™.

Anyway, the employment of Cyrene™ as a solvent was not always effective. Indeed, Hunt *et al.* demonstrated that the synthesis of β-sitosterol *via* the bio-catalyzed reaction of β-sitosterol and fatty acids was not possible.[205] Cyrene™ was also not a good solvent for the synthesis of 2,4,5-trisubstituted-2-imidazolines starting from an aldehyde, such as 4-(trifluoromethyl) benzaldehyde and ammonium carbonate (Scheme 9.28).[206] A complex reaction mixture was obtained, probably due to the reaction of the solvent with the substrates.

9.4.2 Dihydrolevoglucosenone in Biotransformations

Regarding its use in biotransformations, it was included in some studies, such as the esterification of racemic 2-phenylpropionic acid with EtOH catalyzed by Novozyme 435[184] or the synthesis of β-sitosterol esters through the reaction of β-sitosterol and fatty acids using lipase from *Candida rugosa*,[207] but the results were not satisfactory. Nevertheless, very recently Guajardo

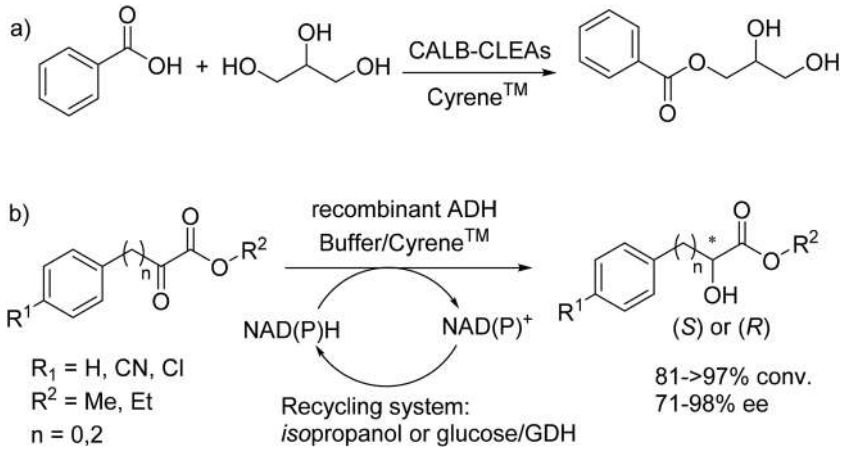

Scheme 9.29 Recently reported biotransformations using Cyrene™ as a biosolvent. a) Lipase-catalyzed glycerol benzoylation; b) bioreduction of alpha oxoesters.

and Domínguez de María[67] have assessed its potential as a solvent in the regioselective esterification of glycerol with benzoic acid catalyzed by cross-linked aggregates of CALB (Scheme 9.29a). The selection of alcohol and acid was based on their unpaired solubilities, leading to moderate-to-high conversions using conventional solvents; by adding a small amount of buffer (up to 2% v/v), full conversion in the production of α-monobenzoate glycerol (α-MBG) was reported.

On the other hand, de Gonzalo has just published[208] the use of Cyrene™ as a co-solvent in the bioreduction of α-ketoesters, using different commercial recombinant alcohol dehydrogenases (ADHs) from Codexis, using either substrate- (*iso*propanol) or enzyme-coupled (glucose and glucose dehydrogenase, GDH) methodologies for cofactor recycling. When this solvent was employed in 2.5% v/v, it was feasible to furnish both the (*S*)- and the (*R*)-hydroxyesters (depending on the ADH used) with complete conversion. Interestingly, bioreductions catalysed by the *iso*propanol-tolerant alcohol dehydrogenase KRED P2-D03 could be carried out using up to 30% v/v of Cyrene™ with only a small loss in the biocatalyst properties, whereas the substrate concentration can be increased up to 1.0 M, obtaining a higher conversion in the presence of this cosolvent compared to that reported in its absence. These promising results pave the way to an increased use of this biosolvent in the near future.

9.5 Glycerol and Glycerol-based Solvents (GBs)

Glycerol has undoubtedly become a broadly-available biogenic product, as the production of biodiesel starting from raw materials is increasingly growing[209,210] and the uses of glycerol are expanding,[211,212] in the food industry (sweetener, thickener and ingredient), in the pharma and cosmetic industries

(additive, for skin and hair care, and more) or as a building block for the preparation of other active compounds. In fact, the crude glycerol price has diminished hugely, as its production, only in the EU, has increased from 1.16 to 2 Mtons from 2015 to 2017, and it is foreseen to reach >5 Mtons by 2026.[211] Thus, the availability and low-cost of glycerol make it a good green candidate for use as a biosolvent, although some issues must be taken into account, derived from its high viscosity; therefore, either glycerol is usually fluidified with a co-solvent or the reactions must be carried out at temperatures higher than 60 °C in order to decrease the glycerol viscosity.

9.5.1 Glycerol and Glycerol-based Solvents (GBs) in Organic Chemistry Reactions

Regarding glycerol, different revisions have covered its utility as a solvent in different organic chemistry processes,[51,213–216] so only some recent examples will be commented on here. Thumula has recently reported[217] the one-pot three-component synthesis of 2-(3*H*-imidazo[4,5-*b*]pyridin-2-yl)-*N*-phenylbenzamide derivatives from diethylphthalate, anilines and pyridine-2,3-diamine in glycerol/phosphoric acid, requiring short reaction time, leading to excellent yields following an easy workup (Scheme 9.30a). Similarly, this same author reported the preparation of 2-(1*H*-benzo[*d*]thiazole-2-yl)-*N*-arylbenzamides, starting from diethyl phthalate, anilines and 2-amino-benzenethiol in similar conditions[218] (Scheme 9.30b)

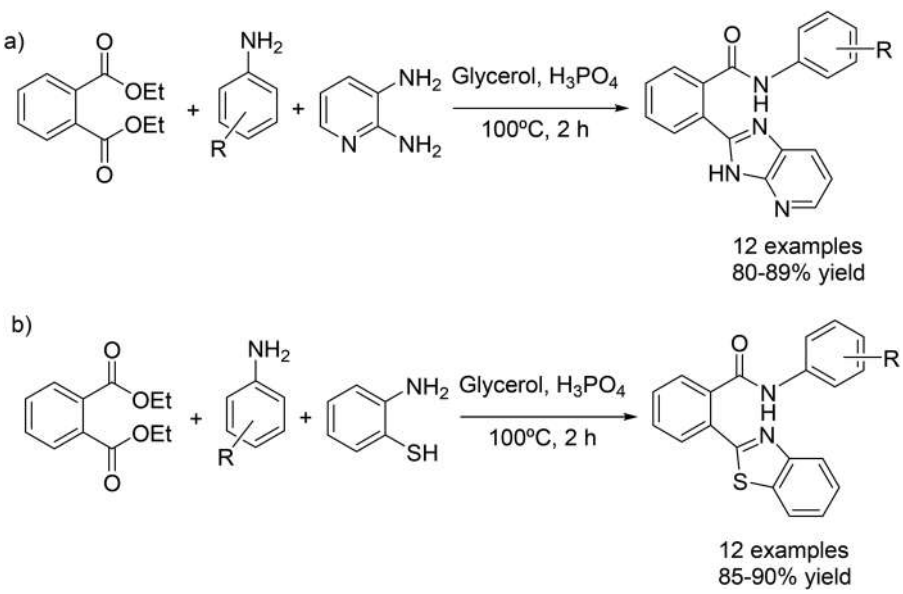

Scheme 9.30 One-pot three-component synthesis of *N*-substituted 2-aryl benzamides using glycerol as a solvent. a) Synthesis of 2-(3*H*-imidazo [4,5-*b*]pyridin-2-yl)-*N*-phenylbenzamide derivatives; b) preparation of 2-(1*H*-benzo[*d*]thiazole-2-yl)-*N*-arylbenzamides.

The *N*-arylbenzamides synthesized proved to have significant cytotoxic potential against various cancer cells, *viz.*, A549 (lung cancer), HeLa (cervical cancer) and MCF-7 (breast cancer) using the MTT assay. In another recent example, 2-amino-benzenethiol has been also used, in combination with chalcone, for the one-pot synthesis of benzothiazepines in glycerol (Scheme 9.31),[219] with moderate to excellent yields.

Finally, in another example of catalyst-free reactions in glycerol, a series of 4-(1*H*-pyrazol-4-yl)-polyhydroquinolines were synthesized through one-pot four-component Hantzsch condensation of 1,3-diphenyl-1*H*-pyrazole-4-carbaldehydes, ammonium acetate, dimedone, and alkyl acetoacetate, as shown in Scheme 9.32.[220]

The so-prepared compounds were screened for their antimicrobial activity against *Mycobacterium tuberculosis* H37RV strain, showing excellent antitubercular activity based on minimum inhibitory concentration. Furthermore, as recently illustrated, glycerol is also adequate for being used in reactions promoted by irradiation with ultrasound[221] or microwaves,[222–224] as well as for metal-catalysed processes. In this context, Serrano-Maldonado *et al.*[225] have described the Rh-catalysed hydroaminomethylation of terminal alkenes in glycerol, which proceeded efficiently under mild conditions to furnish the corresponding amines in relatively high selectivity towards linear amines, and moderate to excellent yields, by using a low catalyst loading (1 mol%[Rh], 2 mol% phosphine) and relatively low pressure (H_2/CO, 1:1, total pressure 10 bar) (Scheme 9.33)

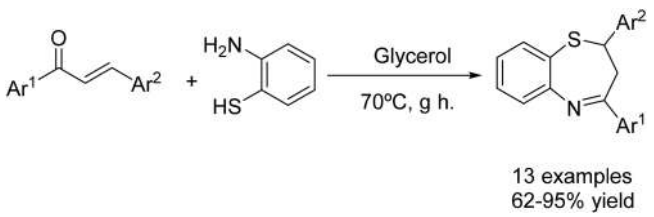

Scheme 9.31 One-pot synthesis of benzothiazepines in glycerol.

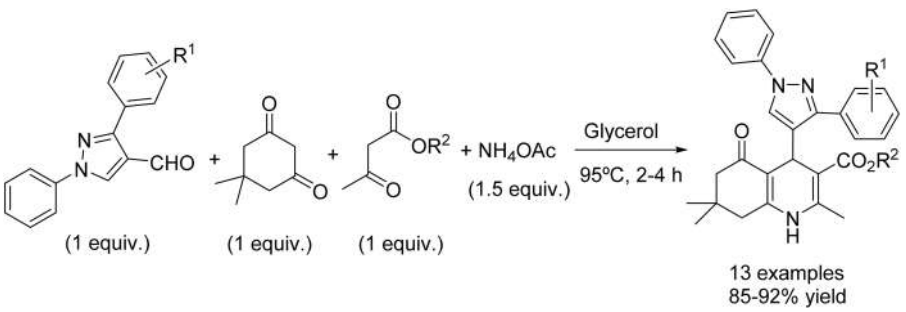

Scheme 9.32 One-pot four-component Hantzsch condensation in glycerol.

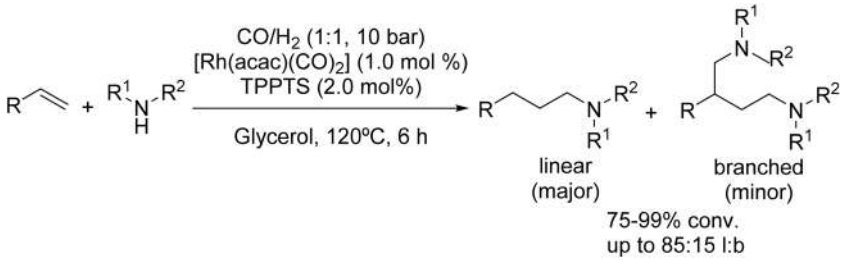

Scheme 9.33 Rh-catalysed hydroaminomethylation of terminal alkenes in glycerol.

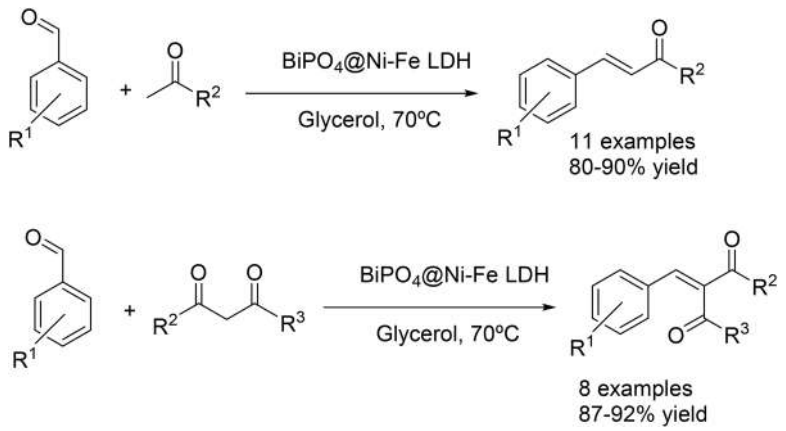

Scheme 9.34 Aldol condensations catalysed by BiPO4@Ni–Fe LDH using glycerol as the biogenic solvent.

Compared to other solvents tested, glycerol provided the best results in terms of chemo- and regioselectivity for linear amines, outperforming both non-protic and other protic solvents in terms of deleterious olefin isomerization/hydrogenation side-reactions. In another recent example, a $BiPO_4$ decorated with Ni–Fe layered double hydroxide ($BiPO_4$@Ni–Fe LDH) catalyst has been successfully designed and tested in the aldol condensation of different substituted benzaldehydes with acetophenone, ethyl acetoacetate or diethyl malonate, using glycerol as the biogenic solvent[226] (Scheme 9.34)

In any case, precautions have to be taken to ensure that glycerol is acting only as a solvent and is not involved in any undesired side-reaction, as the presence of 3 hydroxyl groups, acting as acidic sites, may interfere with the main reaction. To ensure the inertness of the solvent, different glycerol-based solvents (GBs), such as carbonates, ketals, esters, and ethers derived from glycerol have been proposed as green biosolvents, due to their chemical

stability, moderate reactivity, low acute ecotoxicity and tunable physicochemical properties, easily modified simply by changing the number, size, substitution, and nature of their substituents.[53,55,227,228] Once again, different articles[53,55,214] and book chapters[229–232] have covered this topic.

9.5.2 Glycerol and Glycerol-based Solvents (GBs) in Biotransformations

Glycerol has been used as a solvent in biocatalyzed redox whole-cells, to solve the problem caused by the low solubility of generally bulky prochiral ketones in aqueous reaction media, leading to low yields. Wolfson and coworkers reported the reduction of prochiral β-keto esters and ketones by adding yeast powder or immobilized yeast to a pure glycerol medium to give a high yield and high enantiomeric excess (e.e.) value.[213,233] Glycerol is generally used as a co-solvent in aqueous media for bioreductions catalyzed by whole cells[234] or by isolated enzymes.[235–237] Interestingly, glycerol can be used as a biogenic component of Natural Deep Eutectic Solvents (NDES), formed by a eutectic mixture of Lewis (or Brønsted) acids and bases. In this sense, the use of choline chloride/glycerol (ChCl/Gly) in biotransformations has increased in the last few years; in particular, the mixture ChCl/Gly at 1/2 (mol mol^{-1}), also known as glyceline, has been frequently used.[238]

As commented on before, glycerol can be easily derivatized to furnish glycerol-based solvents (GBSs), which have received attention in the last few years.[53,55] These solvents have been frequently used mixed with aqueous buffers; thus, a remarkable improvement in the synthesis of carbohydrates through glycosidase-catalysed processes was reported by Perez *et al.*,[239] showing how the presence of GBSs (ethereal type) compared to buffered media considerably decreased the hydrolytic activity of the β-galactosidase from *E. coli* in the synthesis of *N*-acetyl-D-allolactosamine *via* transglycosylation of *p*-nitrophenyl β-D-galactopyranoside as a donor and *N*-acetylglucosamine as an acceptor. Similar results were observed in the synthesis of *N*-acetyl-D-lactosamine by a β-galactosidase from *T. thermophilus*;[240] in fact, using GBSs as cosolvents, it was possible to reduce the amount of undesired self-condensation product derived from the donor [Gal-β(1 → 3)-Gal-β-pNP], leading to an increase in the synthesis of the target disaccharide. This fact was attributed to an alteration of the secondary and tertiary structure of the enzyme, causing a modification in the protein flexibility, which enabled the proper interaction of the substrate in the active site of the enzyme.[240] Analogously, Perez-Sanchez *et al.*[241,242] reported the effect of these GBSs in the activity of β-galactosidase from *B. circullans*, leading to *N*-acetyl-D-allolactosamine as the main product (quantitative conversion) *versus N*-acetyl-D-lactosamine, the major product when the same reaction is performed in buffered media. Some other examples of the use of ether-type GBSs as cosolvents for enzymatic reactions have been reported so far.[243–245]

References

1. R. A. Sheldon, *Green Chem.*, 2005, **7**, 267–278.
2. K. Hackl and W. Kunz, *C. R. Chim.*, 2018, **21**, 572–580.
3. J. H. Clark, T. J. Farmer, A. J. Hunt and J. Sherwood, *Int. J. Mol. Sci.*, 2015, **16**, 17101–17159.
4. C. J. Clarke, W. C. Tu, O. Levers, A. Brohl and J. P. Hallett, *Chem. Rev.*, 2018, **118**, 747–800.
5. D. J. C. Constable, C. Jimenez-Gonzalez and R. K. Henderson, *Org. Process Res. Dev.*, 2007, **11**, 133–137.
6. R. Ratti, *SN Appl. Sci.*, 2020, **2**, 7.
7. R. A. Sheldon, *Curr. Opin. Green Sustain. Chem.*, 2019, **18**, 13–19.
8. C. Capello, U. Fischer and K. Hungerbuhler, *Green Chem.*, 2007, **9**, 927–934.
9. P. G. Jessop, *Green Chem.*, 2011, **13**, 1391–1398.
10. M. Cvjetko Bubalo, S. Vidović, I. Radojčić Redovniković and S. Jokić, *J. Chem. Technol. Biotechnol.*, 2015, **90**, 1631–1639.
11. F. G. Calvo-Flores, M. J. Monteagudo-Arrebola, J. A. Dobado and J. Isac-Garcia, *Top. Curr. Chem.*, 2018, **376**, 40.
12. F. Zhou, Z. Hearne and C. J. Li, *Curr. Opin. Green Sustain. Chem.*, 2019, **18**, 118–123.
13. R. N. Butler and A. G. Coyne, *Org. Biomol. Chem.*, 2016, **14**, 9945–9960.
14. J. P. Hallett and T. Welton, *Chem. Rev.*, 2011, **111**, 3508–3576.
15. J. Hulsbosch, D. E. De Vos, K. Binnemans and R. Ameloot, *ACS Sustainable Chem. Eng.*, 2016, **4**, 2917–2931.
16. Z. G. Lei, B. H. Chen, Y. M. Koo and D. R. MacFarlane, *Chem. Rev.*, 2017, **117**, 6633–6635.
17. N. Nasirpour, M. Mohammadpourfard and S. Z. Heris, *Chem. Eng. Res. Des.*, 2020, **160**, 264–300.
18. S. K. Singh and A. W. Savoy, *J. Mol. Liq.*, 2020, **297**, 23.
19. Z. Knez, *J. Supercrit. Fluids*, 2018, **134**, 133–140.
20. Z. Knez, E. Markocic, M. Leitgeb, M. Primozic, M. K. Hrncic and M. Skerget, *Energy*, 2014, **77**, 235–243.
21. T. Matsuda, *J. Biosci. Bioeng.*, 2013, **115**, 233–241.
22. J. Peach and J. Eastoe, *Beilstein J. Org. Chem.*, 2014, **10**, 1878–1895.
23. P. Domínguez de María, N. Guajardo and S. Kara, in *Deep Eutectic Solvents*, ed. D. J. Ramón and G. Guillena, Wiley-VCH Verlag GmbH & Co. KGaA., Weinheim, Germany, 2019, pp. 257–271.
24. D. A. Alonso, A. Baeza, R. Chinchilla, G. Guillena, I. M. Pastor and D. J. Ramon, *Eur. J. Org. Chem.*, 2016, 612–632.
25. N. Guajardo, C. R. Muller, R. Schrebler, C. Carlesi and P. D. de Maria, *ChemCatChem*, 2016, **8**, 1020–1027.
26. I. Juneidi, M. Hayyan and M. A. Hashim, *Process Biochem.*, 2018, **66**, 33–60.
27. A. Paiva, A. A. Matias and A. R. C. Duarte, *Curr. Opin. Green Sustain. Chem.*, 2018, **11**, 81–85.

28. L. I. N. Tomé, V. Baião, W. da Silva and C. M. A. Brett, *Appl. Mater. Today*, 2018, **10**, 30–50.
29. C. Florindo, F. Lima, B. D. Ribeiro and I. M. Marrucho, *Curr. Opin. Green Sustain. Chem.*, 2019, **18**, 31–36.
30. Y. Marcus, *Deep Eutectic Solvents*, Springer Nature Switzerland AG, Cham, Switzerland, 2019.
31. M. Patzold, S. Siebenhaller, S. Kara, A. Liese, C. Syldatk and D. Holtmann, *Trends Biotechnol.*, 2019, **37**, 943–959.
32. M. Panic, M. C. Bubalo and I. R. Redovnikovic, *J. Chem. Technol. Biotechnol.*, 2020, 17.
33. J. Płotka-Wasylka, M. de la Guardia, V. Andruch and M. Vilková, *Microchem. J.*, 2020, **159**, 105506.
34. J. N. Tan and Y. Q. Dou, *Appl. Microbiol. Biotechnol.*, 2020, **104**, 1481–1496.
35. F. Jerome and R. Luque, *Bio-based Solvents*, John Wiley & Sons, Inc, Hoboken, NJ, 2017.
36. Y. L. Gu and F. Jerome, *Chem. Soc. Rev.*, 2013, **42**, 9550–9570.
37. L. Lomba, E. Zuriaga and B. Giner, *Curr. Opin. Green Sustain. Chem.*, 2019, **18**, 51–56.
38. E. de Jong and G. Jungmeier, in *Industrial Biorefineries and White Biotechnology*, Elsevier, 2015, pp. 3–33.
39. F. Cherubini, *Energy Convers. Manage.*, 2010, **51**, 1412–1421.
40. H. P. Vu, L. N. Nguyen, M. T. Vu, M. A. H. Johir, R. McLaughlan and L. D. Nghiem, *Sci. Total Environ.*, 2020, **743**, 140630.
41. V. K. Garlapati, A. K. Chandel, S. P. J. Kumar, S. Sharma, S. Sevda, A. P. Ingle and D. Pant, *Renewable Sustainable Energy Rev.*, 2020, **130**, 13.
42. S. S. Hassan, G. A. Williams and A. K. Jaiswal, *Renewable Sustainable Energy Rev.*, 2019, **101**, 590–599.
43. F. H. Isikgor and C. R. Becer, *Polym. Chem.*, 2015, **6**, 4497–4559.
44. M. Gavahian, P. E. S. Munekata, I. Eş, J. M. Lorenzo, A. Mousavi Khaneghah and F. J. Barba, *Green Chem.*, 2019, **21**, 1171–1185.
45. S. Niphadkar, P. Bagade and S. Ahmed, *Biofuels*, 2018, **9**, 229–238.
46. A. Bušić, N. Mardetko, S. Kundas, G. Morzak, H. Belskaya, M. I. Šantek, D. Komes, S. Novak and B. Šantek, *Food Technol. Biotechnol.*, 2018, **56**, 289–311.
47. M. Vohra, J. Manwar, R. Manmode, S. Padgilwar and S. Patil, *J. Environ. Chem. Eng.*, 2014, **2**, 573–584.
48. A. Gevorgyan, K. H. Hopmann and A. Bayer, *ChemSusChem*, 2020, **13**, 2080–2088.
49. Y. L. Gu and F. Jerome, *Green Chem.*, 2010, **12**, 1127–1138.
50. J. I. Garcia, H. Garcia-Marin, J. A. Mayoral and P. Perez, *Green Chem.*, 2010, **12**, 426–434.
51. A. E. Díaz-Álvarez, J. Francos, B. Lastra-Barreira, P. Crochet and V. Cadierno, *Chem. Commun.*, 2011, **47**, 6208–6227.
52. C. Len and R. Luque, *Sustainable Chem. Processes*, 2014, **2**, 1.
53. J. I. Garcia, H. Garcia-Marin and E. Pires, *Green Chem.*, 2014, 1007–1033.

54. L. Moity, A. Benazzouz, V. Molinier, V. Nardello-Rataj, M. K. Elmkaddem, P. de Caro, S. Thiebaud-Roux, V. Gerbaud, P. Marion and J. M. Aubry, *Green Chem.*, 2015, **17**, 1779–1792.
55. A. Leal-Duaso, P. Perez, J. A. Mayoral, J. I. Garcia and E. Pires, *ACS Sustainable Chem. Eng.*, 2019, **7**, 13004–13014.
56. P. Ravichandiran and Y. Gu, in *Carbohydrate Chemistry*, ed. A. P. Rauter, T. K. Lindhorst and Y. Queneau, Royal Society of Chemistry, 2018, vol. 43, pp. 177–195.
57. V. Fischer and W. Kunz, *Mol. Phys.*, 2014, **112**, 1241–1245.
58. S. Paul, K. Pradhan and A. R. Das, *Curr. Green Chem.*, 2016, **3**, 111–118.
59. A. V. Dolzhenko, *Sustainable Chem. Pharm.*, 2020, **18**, 100322.
60. F. Diwan, M. H. Shaikh, S. Fatema and M. Farooqui, *Org. Commun.*, 2019, **12**, 188–201.
61. J. Yang, B. Zhou, M. Li and Y. Gu, *Tetrahedron*, 2013, **69**, 1057–1064.
62. W. Sheng, Y. Du, F. Tian, L. Han and N. Zhu, *Chem. Bull.*, 2012, **75**, 1026–1030.
63. B. Zhou, J. Yang, M. Li and Y. Gu, *Green Chem.*, 2011, **13**, 2204–2211.
64. A. R. Alcántara and P. Dominguez de Maria, *Curr. Green Chem.*, 2018, **5**, 85–102.
65. V. Pace, W. Holzer, P. Hoyos, M. J. Hernáiz and A. R. Alcántara, in *Encyclopedia of Reagents for Organic Synthesis [Online]*, John Wiley & Sons Ltd, http://onlinelibrary.wiley.com/book/10.1002/047084289X, accessed date, 2014.
66. V. Pace, P. Hoyos, L. Castoldi, P. Domínguez de María and A. R. Alcántara, *ChemSusChem*, 2012, **5**, 1369–1379.
67. N. Guajardo and P. Domínguez de María, *Mol. Catal.*, 2020, **485**, 110813.
68. J. Sherwood, M. De Bruyn, A. Constantinou, L. Moity, C. R. McElroy, T. J. Farmer, T. Duncan, W. Raverty, A. J. Hunt and J. H. Clark, *Chem. Commun.*, 2014, **50**, 9650–9652.
69. D. M. Alonso, S. G. Wettstein and J. A. Dumesic, *Green Chem.*, 2013, **15**, 584–595.
70. J. Wei, X. Tang, Y. Sun, X. Zeng and L. Lin, *Prog. Chem.*, 2016, **28**, 1672–1681.
71. L. Vaccaro, S. Santoro, M. Curini and D. Lanari, *Chim. Oggi*, 2017, **35**, 46–48.
72. O. Al Musaimi, A. El-Faham, A. Basso, B. G. de la Torre and F. Albericio, *Tetrahedron Lett.*, 2019, **60**, 151058.
73. F. Boissou, S. Baranton, M. Tarighi, K. De Oliveira Vigier and C. Coutanceau, *J. Electroanal. Chem.*, 2019, **848**, 113257.
74. F. Diwan, M. H. Shaikh, M. Shaikh and M. Farooqui, *Org. Commun.*, 2019, **12**, 1–13.
75. M. A. Rasool and I. F. J. Vankelecom, *Green Chem.*, 2019, **21**, 1054–1064.
76. X. Shen, D. Xia, Y. Xiang and J. Gao, *e-Polymers*, 2019, **19**, 323–329.
77. F. Aricò, *Curr. Opin. Green Sustain. Chem.*, 2020, **21**, 82–88.
78. K. L. Wilson, J. Murray, H. F. Sneddon, C. Jamieson and A. J. B. Watson, *Synlett*, 2018, **29**, 2293–2297.

79. C. Sambiagio, R. H. Munday, A. John Blacker, S. P. Marsden and P. C. McGowan, *RSC Adv.*, 2016, **6**, 70025–70032.
80. F. Russo, F. Galiano, F. Pedace, F. Aricò and A. Figoli, *ACS Sustainable Chem. Eng.*, 2020, **8**, 659–668.
81. J. B. McKinlay, C. Vieille and J. G. Zeikus, *Appl. Microbiol. Biotechnol.*, 2007, **76**, 727–740.
82. C. S. Lopez-Garzon, L. A. M. van der Wielen and A. J. J. Straathof, *RSC Adv.*, 2016, **6**, 3823–3829.
83. M. Morales, M. Ataman, S. Badr, S. Linster, I. Kourlimpinis, S. Papadokonstantakis, V. Hatzimanikatis and K. Hungerbühler, *Energy Environ. Sci.*, 2016, **9**, 2794–2805.
84. C. S. López-Garzón, L. A. M. van der Wielen and A. J. J. Straathof, *Chem. Eng. J.*, 2014, **235**, 52–60.
85. S. Sangon, N. Supanchaiyamat, J. Sherwood, C. R. McElroy and A. J. Hunt, *React. Chem. Eng.*, 2020, **5**, 1798–1804.
86. T. M. Lammens, M. C. R. Franssen, E. L. Scott and J. P. M. Sanders, *Green Chem.*, 2010, **12**, 1430–1436.
87. J. Lopez, S. Pletscher, A. Aemissegger, C. Bucher and F. Gallou, *Org. Process Res. Dev.*, 2018, **22**, 494–503.
88. A. Kumar, M. Alhassan, J. Lopez, F. Albericio and B. G. de la Torre, *ChemSusChem*, 2020, 5288–5294.
89. B. G. De La Torre, A. Kumar, M. Alhassan, C. Bucher, F. Albericio and J. Lopez, *Green Chem.*, 2020, **22**, 3162–3169.
90. M. Erny, M. Lundqvist, J. H. Rasmussen, O. Ludemann-Hombourger, F. Bihel and J. Pawlas, *Org. Process Res. Dev.*, 2020, **24**, 1341–1349.
91. J. Sherwood, H. L. Parker, K. Moonen, T. J. Farmer and A. J. Hunt, *Green Chem.*, 2016, **18**, 3990–3996.
92. F. De Schouwer, S. Adriaansen, L. Claes and D. E. De Vos, *Green Chem.*, 2017, **19**, 4919–4929.
93. C. Löser, T. Urit and T. Bley, *Appl. Microbiol. Biotechnol.*, 2014, **98**, 5397–5415.
94. S. Zhang, F. Guo, W. Yan, W. Dong, J. Zhou, W. Zhang, F. Xin and M. Jiang, *Appl. Microbiol. Biotechnol.*, 2020, **104**, 7239–7245.
95. N. Tsolakis, W. Bam, J. S. Srai and M. Kumar, *J. Cleaner Prod.*, 2019, **222**, 802–822.
96. M. Lamarche, M. T. Dang, J. Lefebvre, J. D. Wuest and S. Roorda, *ACS Sustainable Chem. Eng.*, 2017, **5**, 5994–5998.
97. N. Pourreza and T. Naghdi, *J. Ind. Eng. Chem.*, 2017, **51**, 71–76.
98. S. Yadav and C. S. Sharma, *Polym. Bull.*, 2018, **75**, 5133–5142.
99. A. K. El-Deen and K. Shimizu, *Anal. Sci.*, 2019, **35**, 1385–1391.
100. J. Ma, S. Chen, C. Ye, M. Li, T. Liu, X. Wang and Y. Song, *Phys. Chem. Chem. Phys.*, 2019, **21**, 14516–14520.
101. G. Paggiola, N. Derrien, J. D. Moseley, A. Green, S. L. Flitsch, J. H. Clark, C. R. McElroy and A. J. Hunt, *Pure Appl. Chem.*, 2020, **92**, 579–586.
102. M. Sadi, S. Zeboudj, Y. M. Azri and I. Tou, *Sep. Sci. Technol.*, 2020, **55**, 1776–1785.

103. Y. H. Bi, Z. Q. Duan, W. Y. Du and Z. Y. Wang, *Biotechnol. Lett.*, 2015, **37**, 115–119.
104. A. de Oliveira Dias, M. G. P. Gutiérrez, J. A. A. Villarreal, R. L. L. Carmo, K. C. B. Oliveira, A. G. Santos, E. N. dos Santos and E. V. Gusevskaya, *Appl. Catal., A*, 2019, **574**, 97–104.
105. S. Labua and T. Kenkhunthot, *J. Curr. Sci. Tech.*, 2020, **10**, 35–40.
106. K. J. Quinn, Y. Hu, P. J. Miller, R. T. Walsh, M. A. Caporello, M. L. Maliszewski and J. H. Markowski, *Tetrahedron Lett.*, 2019, **60**, 1773–1776.
107. A. Banach, J. Scianowski, M. Uzarewicz-Baig and A. Wojtczak, *Eur. J. Org. Chem.*, 2015, **2015**, 3477–3485.
108. M. Boariu, L. M. Nica, A. Marinescu, E. V. Ganea, O. Velea, D. M. Pop, I. D. Bretean and L. E. Cirugeriu, *Rev. Chim.*, 2015, **66**, 907–910.
109. J. F. Campos and S. Berteina-Raboin, *Catal. Today*, 2020, **358**, 138–142.
110. J. F. Campos and S. Berteina-Raboin, *Catalysts*, 2019, **9**, 840.
111. G. Knothe and K. R. Steidley, *Ind. Eng. Chem. Res.*, 2011, **50**, 4177–4182.
112. M. B. da Roza Costa, A. Nicolau, R. Guzatto, L. M. Angeloni and D. Samios, *Polym. Bull.*, 2017, **74**, 2365–2378.
113. R. Kaur, P. Khullar, A. Gupta, G. K. Ahluwalia and M. S. Bakshi, *Biofuels*, 2019, DOI: 10.1080/17597269.2019.1594593.
114. J. Hu, Z. Du, Z. Tang and E. Min, *Ind. Eng. Chem. Res.*, 2004, **43**, 7928–7931.
115. K. Srinivas, T. M. Potts and J. W. King, *Green Chem.*, 2009, **11**, 1581–1588.
116. S. Wildes, *Chem. Health Saf.*, 2002, **9**, 24–26.
117. S. Monticelli, L. Castoldi, I. Murgia, R. Senatore, E. Mazzeo, J. Wackerlig, E. Urban, T. Langer and V. Pace, *Monatsh. Chem.*, 2017, **148**, 37–48.
118. V. Rapinel, O. Claux, M. Abert-Vian, C. McAlinden, M. Bartier, N. Patouillard, L. Jacques and F. Chemat, *Molecules*, 2020, **25**, 3417.
119. C. S. Slater, M. J. Savelski, D. Hitchcock and E. J. Cavanagh, *J. Environ. Sci. Health, Part A: Toxic/Hazard. Subst. Environ. Eng.*, 2016, **51**, 487–494.
120. X. He and D. Yu, *Environ. Impact Assess. Rev.*, 2020, **85**, 106461.
121. H. H. Khoo, L. L. Wong, J. Tan, V. Isoni and P. Sharratt, *Resour., Conserv. Recycl.*, 2015, **95**, 174–182.
122. K. Bluhm, T. B. Seiler, N. Anders, J. Klankermayer, A. Schaeffer and H. Hollert, *Sci. Total Environ.*, 2016, **566**, 786–795.
123. K. Bluhm, S. Heger, R. Redelstein, J. Brendt, N. Anders, P. Mayer, A. Schaeffer and H. Hollert, *Environ. Toxicol. Pharmacol.*, 2018, **64**, 131–138.
124. V. Antonucci, J. Coleman, J. B. Ferry, N. Johnson, M. Mathe, J. P. Scott and J. Xu, *Org. Process Res. Dev.*, 2011, **15**, 939–941.
125. P. Parris, J. N. Duncan, A. Fleetwood and W. P. Beierschmitt, *Regul. Toxicol. Pharmacol.*, 2017, **87**, 54–63.
126. A. G. Sicaire, M. A. Vian, A. Filly, Y. Li, A. Bily and F. Chemat, in *Alternative Solvents for Natural Products Extraction*, ed. F. Chemat and M. A. Vian, Springer-Verlag Berlin, Berlin, 2014, pp. 253–268.
127. D. Prat, A. Wells, J. Hayler, H. Sneddon, C. R. McElroy, S. Abou-Shehada and P. J. Dunn, *Green Chem.*, 2015, 4848.
128. V. Pace, *Aust. J. Chem.*, 2012, **65**, 301–302.

129. M. Fairley, L. J. Bole, F. F. Mulks, L. Main, A. R. Kennedy, C. T. O'Hara, J. Garcia-Alvarez and E. Hevia, *Chem. Sci.*, 2020, **11**, 6500–6509.
130. F. F. Mulks, L. J. Bole, L. Davin, A. Hernán-Gómez, A. Kennedy, J. García-Álvarez and E. Hevia, *Angew. Chem., Int. Ed.*, 2020, **59**, 19021–19026.
131. E. Bisz and M. Szostak, *ChemSusChem*, 2018, **11**, 1290–1294.
132. K. Y. Ding, F. Zannat, J. C. Morris, W. W. Brennessel and P. L. Holland, *J. Organomet. Chem.*, 2009, **694**, 4204–4208.
133. S. De Angelis, M. De Renzo, C. Carlucci, L. Degennaro and R. Luisi, *Org. Biomol. Chem.*, 2016, **14**, 4304–4311.
134. P. Lei, Y. Ling, J. An, S. P. Nolan and M. Szostak, *Adv. Synth. Catal.*, 2019, **361**, 5654–5660.
135. J. Zhang, Y. Liu, Q. Q. Jia, Y. Wang, Y. M. Ma and M. Szostak, *Org. Lett.*, 2020, **22**, 6884–6890.
136. A. A. Rajkiewicz, K. Skowerski, B. Trzaskowski, A. Kajetanowicz and K. Grela, *ACS Omega*, 2019, **4**, 1831–1837.
137. M. Smoleń, W. Kosnik, R. Gajda, K. Wozniak, A. Skoczen, A. Kajetanowicz and K. Grela, *Chem. - Eur. J.*, 2018, **24**, 15372–15379.
138. M. Smolen, A. Marczyk, W. Kosnik, B. Trzaskowski, A. Kajetanowicz and K. Grela, *Eur. J. Org. Chem.*, 2019, **2019**, 640–646.
139. Q. Q. Zhen, L. P. Chen, L. J. Qi, K. Hu, Y. L. Shao, R. H. Li and J. X. Chen, *Chem. - Asian J.*, 2020, **15**, 106–111.
140. K. Nakamura, M. Kinoshita and A. Ohno, *Tetrahedron*, McNeil-PPC, Inc., USA, 1994, vol. 50, pp. 4681–4690.
141. US5445951A, 1995.
142. Y. Simeó, J. V. Sinisterra and A. R. Alcantara, *Green Chem.*, 2009, **11**, 855–862.
143. E. Peris, R. Porcar, M. Isabel Burguete, E. Garcia-Verdugo and S. V. Luis, *ChemCatChem*, 2019, **11**, 1955–1962.
144. W. B. Wu, J. S. Yu and J. Zhou, *ACS Catal.*, 2020, **10**, 7668–7690.
145. X. P. Zeng, J. C. Sun, C. Liu, C. B. Ji and Y. Y. Peng, *Adv. Synth. Catal.*, 2019, **361**, 3281–3305.
146. P. Bracco, H. Busch, J. von Langermann and U. Hanefeld, *Org. Biomol. Chem.*, 2016, **14**, 6375–6389.
147. Universitaet Bielefeld, *WO Pat.*, WO2019197571A1, Pharmazell GmbH, Germany, 2019.
148. F. L. Scott, B. Clemons, J. Brooks, E. Brahmachary, R. Powell, H. Dedman, H. G. Desale, G. A. Timony, E. Martinborough, H. Rosen, E. Roberts, M. F. Boehm and R. J. Peach, *Br. J. Pharmacol.*, 2016, **173**, 1778–1792.
149. A. Pellis, F. P. Byrne, J. Sherwood, M. Vastano, J. W. Comerford and T. J. Farmer, *Green Chem.*, 2019, **21**, 1686–1694.
150. G. Englezou, K. Kortsen, A. A. C. Pacheco, R. Cavanagh, J. C. Lentz, E. Krumins, C. Sanders-Velez, S. M. Howdle, A. J. Nedoma and V. Taresco, *J. Polym. Sci.*, 2020, **58**, 1571–1581.
151. H. Seyednejad, A. H. Ghassemi, C. F. van Nostrum, T. Vermonden and W. E. Hennink, *J. Controlled Release*, 2011, **152**, 168–176.

152. R. Gerardy, D. P. Debecker, J. Estager, P. Luis and J. C. M. Monbaliu, *Chem. Rev.*, 2020, **120**, 7219–7347.
153. X. Liu, D. C. Y. Leong and Y. J. Sun, *Green Chem.*, 2020, **22**, 6531–6539.
154. S. De, T. Kumar, A. Bohre, L. R. Singh and B. Saha, *Bioorg. Med. Chem.*, 2015, **23**, 791–796.
155. S. Chen, R. Wojcieszak, F. Dumeignil, E. Marceau and S. Royer, *Chem. Rev.*, 2018, **118**, 11023–11117.
156. J. N. Wei, T. Wang, P. F. Tang, X. Tang, Y. Sun, X. H. Zeng and L. Lin, *Curr. Org. Chem.*, 2019, **23**, 2155–2167.
157. X. Tang, J. N. Wei, N. Ding, Y. Sun, X. H. Zeng, L. Hu, S. J. Liu, T. Z. Lei and L. Lin, *Renewable Sustainable Energy Rev.*, 2017, **77**, 287–296.
158. L. Hu, A. Y. He, X. Y. Liu, J. Xia, J. X. Xu, S. Y. Zhou and J. M. Xu, *ACS Sustainable Chem. Eng.*, 2018, **6**, 15915–15935.
159. Z. H. Xia, M. H. Zong and N. Li, *Enzyme Microb. Technol.*, 2020, **134**, 5.
160. Z. H. Xu, A. D. Cheng, X. P. Xing, M. H. Zong, Y. P. Bai and N. Li, *Bioresour. Technol.*, 2018, **262**, 177–183.
161. Y. M. Li, X. Y. Zhang, N. Li, P. Xu, W. Y. Lou and M. H. Zong, *ChemSusChem*, 2017, **10**, 372–378.
162. K. S. Arias, J. M. Carceller, M. J. Climent, A. Corma and S. Iborra, *ChemSusChem*, 2020, **13**, 1864–1875.
163. M. A. Lăcătuș, L. C. Bencze, M. I. Tosa, C. Paizs and F. D. Irimie, *ACS Sustainable Chem. Eng.*, 2018, **6**, 11353–11359.
164. M. A. Lăcătuş, A. J. Dudu, L. C. Bencze, G. Katona, F. D. Irimie, C. Paizs and M. I. Tosa, *ACS Sustainable Chem. Eng.*, 2020, **8**, 1611–1617.
165. I. T. Horvath, H. Mehdi, V. Fabos, L. Boda and L. T. Mika, *Green Chem.*, 2008, **10**, 238–242.
166. M. C. Bryan, P. J. Dunn, D. Entwistle, F. Gallou, S. G. Koenig, J. D. Hayler, M. R. Hickey, S. Hughes, M. E. Kopach, G. Moine, P. Richardson, F. Roschangar, A. Steven and F. J. Weiberth, *Green Chem.*, 2018, **20**, 5082–5103.
167. G. Strappaveccia, E. Ismalaj, C. Petrucci, D. Lanari, A. Marrocchi, M. Drees, A. Facchetti and L. Vaccaro, *Green Chem.*, 2015, **17**, 365–372.
168. G. Strappaveccia, L. Luciani, E. Bartollini, A. Marrocchi, F. Pizzo and L. Vaccaro, *Green Chem.*, 2015, **17**, 1071–1076.
169. E. Ismalaj, G. Strappaveccia, E. Ballerini, F. Elisei, O. Piermatti, D. Gelman and L. Vaccaro, *ACS Sustainable Chem. Eng.*, 2014, **2**, 2461–2464.
170. D. Rasina, A. Kahler-Quesada, S. Ziarelli, S. Warratz, H. Cao, S. Santoro, L. Ackermann and L. Vaccaro, *Green Chem.*, 2016, **18**, 5025–5030.
171. X. Tian, F. Yang, D. Rasina, M. Bauer, S. Warratz, F. Ferlin, L. Vaccaro and L. Ackermann, *Chem. Commun.*, 2016, **52**, 9777–9780.
172. F. Ferlin, L. Luciani, S. Santoro, A. Marrocchi, D. Lanari, A. Bechtoldt, L. Ackermann and L. Vaccaro, *Green Chem.*, 2018, **20**, 2888–2893.
173. S. Tabasso, E. Calcio Gaudino, L. Rinaldi, A. Ledoux, P. Larini and G. Cravotto, *New J. Chem.*, 2017, **41**, 9210–9215.
174. F. Ferlin, S. Santoro, L. Ackermann and L. Vaccaro, *Green Chem.*, 2017, **19**, 2510–2514.

175. A. Bechtoldt, M. E. Baumert, L. Vaccaro and L. Ackermann, *Green Chem.*, 2018, **20**, 398–402.
176. Q. Bu, T. Rogge, V. Kotek and L. Ackermann, *Angew. Chem., Int. Ed.*, 2018, **57**, 765–768.
177. K. C. Jiang, L. Wang, Q. Chen, M. Y. He, M. G. Shen and Z. H. Zhang, *Synth. Commun.*, 2021, **51**, 94–102.
178. P. Gandeepan, T. Müller, D. Zell, G. Cera, S. Warratz and L. Ackermann, *Chem. Rev.*, 2019, **119**, 2192–2452.
179. P. Gandeepan, N. Kaplaneris, S. Santoro, L. Vaccaro and L. Ackermann, *ACS Sustainable Chem. Eng.*, 2019, **7**, 8023–8040.
180. N. Sauermann, R. Mei and L. Ackermann, *Angew. Chem., Int. Ed.*, 2018, **57**, 5090–5094.
181. P. Gandeepan, L. H. Finger, T. H. Meyer and L. Ackermann, *Chem. Soc. Rev.*, 2020, **49**, 4254–4272.
182. Q. Bu, E. Gońka, K. Kuciński and L. Ackermann, *Chem. - Eur. J.*, 2019, **25**, 2213–2216.
183. S. J. Zhu, X. Q. Ma, E. Z. Su and D. Z. Wei, *Green Chem.*, 2015, **17**, 3992–3999.
184. A. Iemhoff, J. Sherwood, C. R. McElroy and A. J. Hunt, *Green Chem.*, 2018, **20**, 136–140.
185. Z. Q. Duan and F. Hu, *Green Chem.*, 2012, **14**, 1581–1583.
186. J. E. Camp, *ChemSusChem*, 2018, **11**, 3048–3055.
187. V. L. Budarini, K. J. Milkowski, P. Shuttleworth, B. Lanigan, J. H. Clark, D. J. Macquarrie and A. Wilson, *US Pat.*, US20110219679A1, University of York, 2011.
188. CCG. IL Bioeconomista, An interview with Tony Duncan, the Most Innovative Bioeconomy CEO, 2017, https://ilbioeconomista.com/2018/02/19/an-interview-with-tony-duncan-ceocirca-group-the-most-innovative-bioeconomy-ceo-2017/, accessed 14th May 2018.
189. J. F. Zhang, G. B. White, M. D. Ryan, A. J. Hunt and M. J. Katz, *ACS Sustainable Chem. Eng.*, 2016, **4**, 7186–7192.
190. https://echa.europa.eu/substance-information/-/substanceinfo/100.234.612, accessed 18th July 2018.
191. S. Kudo, Z. W. Zhou, K. Norinaga and J. Hayashi, *Green Chem.*, 2011, **13**, 3306–3311.
192. J. A. P. Coutinho, D. O. Abranches, J. Benfica and S. Shimizu, *Ind. Eng. Chem. Res.*, 2020, **59**, 18649–18658.
193. D. O. Abranches, J. Benfica, S. Shimizu and J. A. P. Coutinho, *Ind. Eng. Chem. Res.*, 2020, **59**, 18247–18253.
194. M. De Bruyn, V. L. Budarin, A. Misefari, S. Shimizu, H. Fish, M. Cockett, A. J. Hunt, H. Hofstetter, B. M. Weckhuysen, J. H. Clark and D. J. Macquarrie, *ACS Sustainable Chem. Eng.*, 2019, **7**, 7878–7883.
195. A. Alves Costa Pacheco, J. Sherwood, A. Zhenova, C. R. McElroy, A. J. Hunt, H. L. Parker, T. J. Farmer, A. Constantinou, M. De bruyn, A. C. Whitwood, W. Raverty and J. H. Clark, *ChemSusChem*, 2016, **9**, 3503–3512.

196. T. Brouwer and B. Schuur, *ACS Sustainable Chem. Eng.*, 2020, **8**, 14807–14817.
197. J. Sherwood, M. De Bruyn, A. Constantinou, L. Moity, C. R. McElroy, T. J. Farmer, T. Duncan, W. Raverty, A. J. Hunt and J. H. Clark, *Chem. Commun.*, 2014, **50**, 9650–9652.
198. H. J. Salavagione, J. Sherwood, M. De Bruyn, V. L. Budarin, G. J. Ellis, J. H. Clark and P. S. Shuttleworth, *Green Chem.*, 2017, **19**, 2550–2560.
199. D. H. Gharib, S. Gietman, F. Malherbe and S. E. Moulton, *Carbon*, 2017, **123**, 695–707.
200. S. Lawrenson, M. North, F. Peigneguy and A. Routledge, *Green Chem.*, 2017, **19**, 952–962.
201. K. L. Wilson, A. R. Kennedy, J. Murray, B. Greatrex, C. Jamieson and A. J. B. Watson, *Beilstein J. Org. Chem.*, 2016, **12**, 2005–2011.
202. L. Mistry, K. Mapesa, T. W. Bousfield and J. E. Camp, *Green Chem.*, 2017, **19**, 2123–2128.
203. K. L. Wilson, J. Murray, C. Jamieson and A. J. B. Watson, *Synlett*, 2018, **29**, 650–654.
204. K. L. Wilson, J. Murray, C. Jamieson and A. J. B. Watson, *Org. Biomol. Chem.*, 2018, **16**, 2851–2854.
205. A. G. Lanctot, T. M. Attard, J. Sherwood, C. R. McElroy and A. J. Hunt, *RSC Adv.*, 2016, **6**, 48753–48756.
206. H. A. L. Phuong, L. Cseri, G. F. S. Whitehead, A. Garforth, P. Budd and G. Szekely, *RSC Adv.*, 2017, **7**, 53278–53289.
207. A. G. Lanctot, T. M. Attard, J. Sherwood, C. R. McElroy and A. J. Hunt, *RSC Adv.*, 2016, **6**, 48753–48756.
208. G. de Gonzalo, *Biocatal. Biotransform.*, 2021, DOI: 10.1080/10242422.2021.1887150.
209. M. Bačić, A. Ljubić, M. Gojun, A. Šalić, A. J. Tušek and B. Zelić, *Energies*, 2021, **14**, 403.
210. M. R. Monteiro, C. L. Kugelmeier, R. S. Pinheiro, M. O. Batalha and A. D. Cesar, *Renewable Sustainable Energy Rev.*, 2018, **88**, 109–122.
211. M. Ladero, *Catalysts*, 2021, **11**, 103.
212. M. R. Karimi Estahbanati, M. Feilizadeh, F. Attar and M. C. Iliuta, *React. Chem. Eng.*, 2021, **6**, 197–219.
213. A. Wolfson, C. Dlugy and Y. Shotland, *Environ. Chem. Lett.*, 2007, **5**, 67–71.
214. A. Wolfson, A. Snezhko, T. Meyouhas and D. Tavor, *Green Chem. Lett. Rev.*, 2012, **5**, 7–12.
215. S. Tagliapietra, L. Orio, G. Palmisano, A. Penoni and G. Cravotto, *Chem. Pap.*, 2015, **69**, 1519–1531.
216. P. Ravichandiran and Y. Gu, in *Bio-based Solvents*, John Wiley & Sons, Ltd, 2017, pp. 1–28.
217. S. Thumula, *Asian J. Chem.*, 2019, **31**, 255–260.
218. S. Thumula, V. Srinivasadesikan, R. K. Kottalanka, S. R. J. Rajkumar and B. Ramchandran, *Asian J. Chem.*, 2020, **32**, 1343–1351.
219. N. Yadav, V. B. Yadav, M. D. Ansari, H. Sagir, A. Verma and I. R. Siddiqui, *New J. Chem.*, 2019, **43**, 7011–7014.

220. D. K. Jamale, S. S. Undare, N. J. Valekar, A. P. Sarkate, G. B. Kolekar and P. V. Anbhule, *J. Heterocycl. Chem.*, 2019, **56**, 608–618.
221. L. K. Soares, A. M. Barcellos, J. S. S. Neto, D. Alves, E. J. Lenardão, O. Rosati, C. Santi and G. Perin, *ChemistrySelect*, 2020, **5**, 9813–9819.
222. O. S. Zaky, M. A. Selim, M. M. Ebied and K. U. Sadek, *J. Heterocycl. Chem.*, 2019, **56**, 2796–2803.
223. S. S. Kotalwar, A. D. Kale, R. B. Kohire and V. B. Jagrut, *Asian J. Chem.*, 2019, **31**, 993–996.
224. R. Kordnezhadian, M. Shekouhy and A. Khalafi-Nezhad, *Mol. Diversity*, 2020, **24**, 737–751.
225. A. Serrano-Maldonado, T. Dang-Bao, I. Favier, I. Guerrero-Ríos, D. Pla and M. Gómez, *Chem. - Eur. J.*, 2020, **26**, 12553–12559.
226. F. Pazoki, S. Bagheri, M. Shamsayei, M. J. Nejad and A. Heydari, *Mater. Chem. Phys.*, 2020, **253**, 123327.
227. L. Moity, V. Molinier, A. Benazzouz, B. Joossen, V. Gerbaud and J. M. Aubry, *Green Chem.*, 2016, **18**, 3239–3249.
228. L. Moity, A. Benazzouz, V. Molinier, V. Nardello-Rataj, M. K. Elmkaddem, P. de Caro, S. Thiebaud-Roux, V. Gerbaud, P. Marion and J. M. Aubry, *Green Chem.*, 2015, **17**, 1779–1792.
229. P. Bracco and P. D. de María, in *Bio-based Solvents*, John Wiley & Sons, Ltd, 2017, pp. 115–130.
230. S. Kumaravel, P. Thiruvengetam and S. Kundu, in *Green Sustainable Process for Chemical and Environmental Engineering and Science*, ed. Inamuddin, R. Boddula, M. I. Ahamed and A. M. Asiri, Elsevier, 2021, pp. 105–149.
231. M. C. Marques, N. T. Lourenço, P. Fernandes and C. C. R. de Carvalho, in *Green Solvents I*, ed. A. Mohammad, Springer Netherlands, 2012, pp. 121–146.
232. J. Sherwood, J. H. Clark, A. J. Hunt, C. Topi and G. Paggiola, in *Sustainable Solvents: Perspectives from Research, Business and International Policy*, Royal Soc Chemistry, Cambridge, 2017, vol. 49, pp. 87–135.
233. A. Wolfson, C. Dlugy, D. Tavor, J. Blumenfeld and Y. Shotland, *Tetrahedron: Asymmetry*, 2006, **17**, 2043–2045.
234. C. Cheng and Y. C. Nian, *J. Mol. Catal. B: Enzym.*, 2016, **123**, 141–146.
235. T. Fischer and J. Pietruszka, *Adv. Synth. Catal.*, 2012, **354**, 2521–2530.
236. M. A. Emmanuel, N. R. Greenberg, D. G. Oblinsky and T. K. Hyster, *Nature*, 2016, **540**, 414–417.
237. M. Burns, C. A. Martinez, B. Vanderplas, R. Wisdom, S. Yu and R. A. Singer, *Org. Process Res. Dev.*, 2017, **21**, 871–877.
238. L. Huang, J. P. Bittner, P. D. de Maria, S. Jakobtorweihen and S. Kara, *ChemBioChem*, 2020, **21**, 811–817.
239. M. Perez, J. V. Sinisterra and M. J. Hernaiz, *Curr. Org. Chem.*, 2010, **14**, 2366–2383.
240. M. Sandoval, E. Ferreras, M. Perez-Sanchez, J. Berenguer, J. V. Sinisterra and M. J. Hernaiz, *J. Mol. Catal. B: Enzym.*, 2012, **74**, 162–169.

241. M. Perez-Sanchez, M. Sandoval and M. J. Hernaiz, *Tetrahedron*, 2012, **68**, 2141–2145.
242. M. Perez-Sanchez, M. Sandoval, A. Cortes-Cabrera, H. Garcia-Marin, J. V. Sinisterra, J. I. Garcia and M. J. Hernaiz, *Green Chem.*, 2011, **13**, 2810–2817.
243. C. Bayon, A. Cortes, A. Aires-Trapote, C. Civera and M. J. Hernaiz, *RSC Adv.*, 2013, **3**, 12155–12163.
244. C. Bayon, M. Moracci and M. J. Hernaiz, *RSC Adv.*, 2015, **5**, 55313–55320.
245. P. Hoyos, T. Bavaro, A. Perona, A. Rumbero, S. Tengattini, M. Terreni and M. J. Hernaiz, *ACS Sustainable Chem. Eng.*, 2020, **8**, 6282–6292.

CHAPTER 10

Supercritical Solvents

MAURIZIO SELVA*[a], GIULIA FIORANI[a] AND DAVIDE RIGO[a]

[a]Dipartimento di Scienze Molecolari e Nanosistemi, Università Ca' Foscari Venezia, Via Torino,155, 30172, Venezia Mestre, Italy
*E-mail: selva@unive.it

10.1 Definition of Supercritical State

According to Gibbs' phase rule the physical state of a pure substance at thermodynamic equilibrium can be described by three distinct phases (solid, liquid and gas), described as a function of independent intensive variables. The complete set of accessible equilibrium states is defined by a three-dimensional *state surface* as depicted in Figure 10.1 with p (pressure), ρ (mass density) and T (temperature) as state variables. Observing Figure 10.1 (centre), it can be noticed that the three states of matter are separated by *coexistence curves*. If the values of p and T are located inside a coexistence curve, then a pure component is described as two coexisting phases. Interestingly, the liquid–vapour coexistence curve is not infinite, but presents a maximum, meaning that the liquid and vapour states cannot be considered as two separate states, but as the extremes of the same continuum (the dotted arrows in Figure 10.1, left and Figure 10.1, right: in both projections a continuous transition between vapour and liquid is possible): the liquid–vapour coexistence curve is hence defined as the *critical point*.[1]

When selecting T and p as independent state variables, the physical state of a pure substance is effectively described using a bidimensional *phase diagram*, as reported in Figure 10.2 for the case of CO_2.

Sustainable Organic Synthesis: Tools and Strategies
Edited by Stefano Protti and Alessandro Palmieri

Published by the Royal Society of Chemistry, www.rsc.org

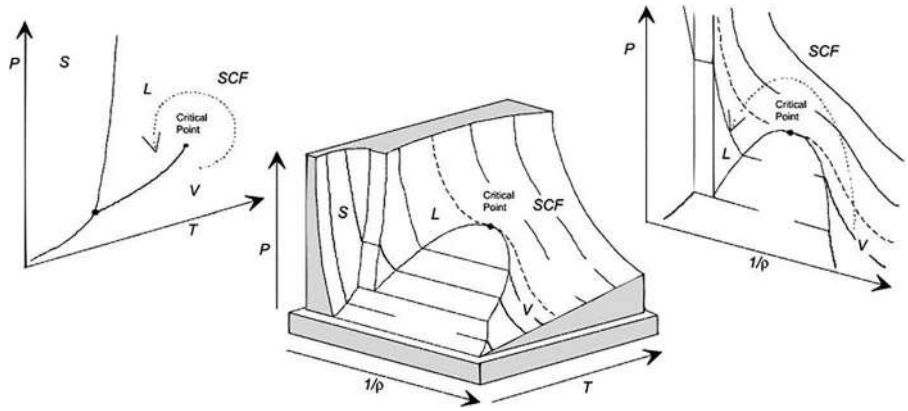

Figure 10.1 State surface of a pure component (S = solid; L = liquid; V = vapour; SCF = supercritical fluid). Left: projection on the p, T plane, centre: three-dimensional curve, right: projection on the p, $1/\rho$ plane. Reproduced from ref. 1 with permission from Elsevier, Copyright 2010.

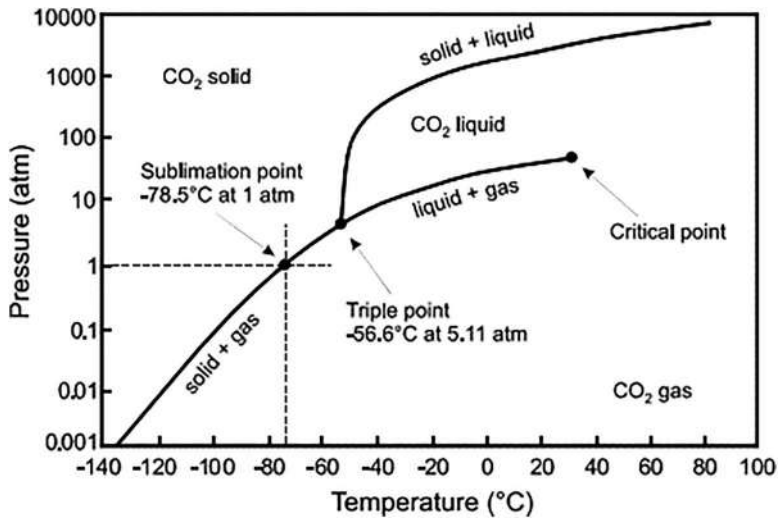

Figure 10.2 Pressure–Temperature phase diagram for CO_2. Reproduced from ref. 2 with permission from Elsevier, Copyright 2013.

The phase diagram comprises areas where the substance exists as a single solid, liquid, or gas phase or as two distinct phases, for example, as a liquid–gas if evaporation occurs or a solid–gas when sublimation takes place. Each pure substance is also characterized by a *triple point*, which is defined as a specific value of temperature and pressure where the three

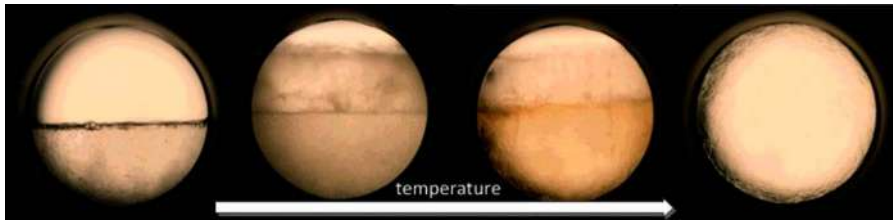

Figure 10.3 Changes in the physical state of propane as a function of temperature, from left to right, liquid, liquid–gas mixtures and supercritical fluid. Reproduced from ref. 3, with permission from American Chemical Society, Copyright 2018.

phases coexist. In the pressure–temperature diagram of Figure 10.2, each curve represents the coexistence between two of the phases. Interestingly, the gas–liquid equilibrium curve, which is a plot of vapor pressure *vs.* temperature, appears interrupted as both temperature and pressure increase. The point at which this interruption occurs is the *critical point*, which has been defined above in Figure 10.1. At the *critical point*, the densities of the two phases become identical and the distinction between gas and liquid disappears: as the temperature increases the liquid becomes less dense because of thermal expansion, while the gas becomes denser as the pressure rises. This means that above the critical point, the substance is more correctly described as a fluid that displays physical properties of both the liquid and the gas states. As depicted in Figure 10.3 for the case of propane, the critical point is reached when the gas and liquid phases coexist and become indistinguishable.[3]

A fluid, in particular, is in its *supercritical state*, once its temperature T exceeds its *critical temperature* T_c, while its pressure p exceeds the *critical pressure* p_c but stays below the pressure needed for condensation.[4] In particular, supercritical fluids (SCFs) possess liquid-like densities, gas-like viscosities and diffusivities intermediate to that of a liquid and a gas. Most pure substances can reach the critical state: some common examples are reported in Table 10.1, which also shows the corresponding values of T_c and p_c.

It should, however, be noted that practical and technological applications using supercritical substances (*i.e.* extraction, fractionation, separations, polymers, synthetic chemistry, materials processing, food processing and analytical applications), are more often focused on supercritical CO_2 ($scCO_2$) and supercritical H_2O (scH_2O). The former reaches the supercritical state under easily attainable T/p conditions, while obtaining scH_2O is far more challenging, especially in a research laboratory setup. Both $scCO_2$ and scH_2O offer many advantages that will be discussed in detail in the next sections.

Table 10.1 Critical properties of pure substances. Adapted from ref. 3 with permission from American Chemical Society, Copyright 2015.

	Critical conditions	
Pure substance	T_c (°C)	p_c (bar)
Ethylene	9.5	50.8
Carbon dioxide (CO_2)	31	73.8
Ethane	32.2	48.8
Propylene	91	46.1
Propane	96.6	42.5
1,1,2,2-Tetrafluoroethane	101	101.6
Ammonia	132.3	112.8
1-Hexene	230.8	31.7
Acetone	234.9	47.0
Methanol	240.0	79.6
Ethanol	243.1	63.8
1-Propanol	263.6	50.6
Dimethyl carbonate (DMC)[a]	284	490.8
Toluene	318.6	41.1
Water	374.2	221.2

[a]Taken from ref. 4.

Table 10.2 Comparison of physical and transport properties of gases, SCFs and liquids. Reproduced from ref. 5 with permission from The Royal Society of Chemistry.

Property	Density (kg m^{-3})	Viscosity (cp)	Diffusivity (cm^2 s^{-1})
Gas	10^{-3}	$10^{-3} - 10^{-2}$	10^{-1}
SCF[a]	0.7	10^{-2}	10^{-3}
Liquid	1.0	10^{-1}	10^{-5}

[a]CO_2 under 305 K and 13.78 MPa.

10.2 Properties of Supercritical Fluids as Pure Substances

Pure supercritical substances are characterized by distinct physical and transport properties which, as mentioned before, are often in-between those of a gas and a liquid. Table 10.2 summarizes this behaviour by comparing average values of density, viscosity, and diffusivity for gases, liquids, and sc-phases.[5]

A supercritical fluid can therefore provide efficient heat and mass transfer compared with that in the liquid state or gas state. For example, a supercritical fluid behaves as a dense gas phase and has neither a surface tension nor an enthalpy (heat) of vaporization. Although the properties

of a supercritical fluid can vary greatly applying small changes in temperature and/or pressure, some general trends have been observed. These include:

i. *High diffusion coefficient*. The solute diffusion coefficient of supercritical fluids is higher than that of pure liquids and lower than that of gases, meaning that the overall mass transfer is improved for sc-compounds. This has been well recognised for example, in chromatographic separation and multiphase extractions mediated by $scCO_2$.[6]
ii. *Low viscosity*. The low "gas-like" viscosity of supercritical fluids implies that SCFs can penetrate matrices with low permeability more readily than conventional solvents, thereby favouring extraction and chromatographic separation.[7–9]
iii. *High compressibility factor (Z)*. Z can be interpreted as a measure of molecular interactions and it varies significantly when shifting from sub- to supercritical conditions and *vice versa*.[10,11] In general, a supercritical fluid may well be characterized as an ideal gas ($Z = 1$) for $T > 2T_c$ and $p < 3p_c$.
iv. *Low dielectric constant*. This property is useful for the selective dissolution/extraction of non-polar components of a complex mixture. Even polar solvents like H_2O ($\varepsilon_r = 78$ at 25 °C) are characterized by low relative permittivity and poor hydrogen-bonding abilities under supercritical conditions (sc-H_2O: $\varepsilon_r = 6$).[12] Solubility can be fine-tuned by adding small amounts of polar or non-polar co-solvents to the supercritical fluid (*vide infra*).
v. *Low solubility parameter*. This is correlated to both the neglectable enthalpy of vaporization and low relative permittivity of supercritical fluids. The solubility parameter decreases dramatically (by several orders of magnitude) when the fluid is depressurized at constant temperature below its critical pressure. This behaviour is at the basis of most supercritical fluid based extraction processes: the compound(s) of interest are first selectively extracted by the supercritical fluid and then precipitated by changing the T/p conditions (for example, by depressurization), thus obtaining a quantitative physical fluid-solute separation. This is especially relevant for applications of supercritical fluids in food industry.[13]

Compared with properties of the gas state, a supercritical fluid is characterized by:

i. *High thermal conductivity/low thermal diffusivity*. This property is of paramount importance for mass transfer processes mediated by supercritical fluids, *e.g.* within heat exchangers, compressors, flow meters, distillation columns, and extractors. Nevertheless, since measures of SCF thermal conductivity in specific temperature ranges are still technologically and experimentally challenging, computational

prediction methods have been developed to ensure equipment design and perform a reliable life cycle analysis for the energetic and economic viability of a given process.[14]

ii. *High heat capacity*. The heat capacity of SCFs reaches its maximum at the critical point. Modelling of the heat capacity variation as a function of other physico-chemical parameters (*e.g.* density, viscosity, or thermal conductivity) is essential to design and implement experimental and/or process operative conditions.[15]

These unique thermal properties make SCFs suitable for a number of industrial and technical applications. Among recent examples, $scCO_2$ is gaining importance as a sustainable refrigerant for automotive air-conditioners and heat pump systems, while, in modern power plants, heat is transferred to supercritical water. Rockets and military aircrafts are cooled using fuels at supercritical pressure thanks to the superconductivity effects observed for some fluids near their critical point. Similarly, highly charged machine elements, *e.g.* gas turbine blades, supercomputer elements, magnets and power transmission cables can be cooled with SCFs.[16] Nevertheless, it should be stressed that determination of the thermal properties of SCFs is still challenging, owing to the dramatic changes observed in the proximity of the critical point. A more detailed discussion of this aspect is beyond the scope of this overview; the reader, however, is referred to recent publications for further in-depth analysis.[1,16,17]

10.2.1 SCFs in Practice

Processes based on SCFs are generally considered sustainable, environmentally friendly and cost efficient and SCFs are considered "green solvents for the future". The main advantages associated with the use of SCFs as reaction media are summarised in Table 10.3.

As mentioned above, a crucial advantage is the product separation/drying that can be achieved in a single step, simply by SCF depressurization and expansion, and includes gas recovery and recycling without the need for further purification. Examples of commercially relevant $scCO_2$ extractions include the seminal work of Kurt Zosel on coffee bean decaffeination,[19] hop extraction and wine cork cleaning to prevent unwanted cork taint. Recently, Evonik developed an industrial batch process for the selective extraction of caffeine from tea leaves at T = 35–38 °C and $p(CO_2)$ = 248 bar, using a 7003 L extractor.[20] Using SCFs in industrial processes is characterised by several environmental advantages, in particular low energy consumption during operation, strengthening their potential compared to more toxic and polluting conventional organic solvents. As summarized in Table 10.1, a number of pure substances characterized by different polarities and/or solvent strength can, in principle, be employed as SCFs. However, the range of SCFs currently used in laboratory and industrial scale processes is much more limited. This can be ascribed to specific practical reasons: for example, sc-*ammonia* is

Table 10.3 Advantages of using SCFs rather than liquids as reaction media. Adapted from ref. 18 with permission from John Wiley and Sons, Copyright 2009.

Category	Advantage	SCF
Environment	Do not contribute to smog	Most
	Do not damage ozone layer	Most
	No acute ecotoxicity	CO_2, H_2O
	No liquid wastes	CO_2 and other volatile SCFs
Health and safety	Non-carcinogenic	Most SCFs, except C_6H_6
	Non-toxic	Most (but not HCl, HBr, HI, NH_3)
	Non-flammable	CO_2, N_2O, H_2O, Xe, Kr, CHF_3
Process	No solvent residues	CO_2 and other volatile SCFs
	Facile product separation	CO_2 and other volatile SCFs
	High diffusion rates	All
	Low viscosity	All
	Adjustable solvent power	All
	Adjustable density	All
	Inexpensive	CO_2, H_2O, NH_3, Ar, hydrocarbons
Chemical	High miscibility with gases	All
	Variable dielectric constant	Polar SCFs
	High compressibility	All
	Local density augmentation	All
	High diffusion rates	All
	Altered cage strength	All

highly toxic. Similarly, although light hydrocarbons and, in particular, liquefied propane (p_c = 4.25 MPa; T_c = 96.7 °C), are much better solvent for lipids compared to $scCO_2$ (*vide infra*), they are rarely employed as SCFs due to their high explosion hazard potential. *Hydrofluorocarbons (HFCs)* are a class of chemically inert halogenated polar organic compounds, neither toxic nor flammable, which are currently considered environmentally acceptable. As SCFs, they are suitable for the extraction of polar compounds, but their practical use is seldom described due to their limited thermal stability (*e.g.* decomposition into highly toxic gases when subjected to a flame in the temperature range between 150 and 350 °C) and their cost.[21] *Methanol* is another polar compound characterised by a high solvent strength: being a flammable compound, it is generally not employed as a SCF due to the rather high T_c required to reach the supercritical state. However, it is commonly used as a modifier of other SCFs (*vide infra*).

The most common SCFs, *e.g.* $scCO_2$ and SCW are instead, harmless and thermodynamically stable substances. $scCO_2$ is the most widely employed SCF for a number of practically relevant reasons: (i) it is very inexpensive, abundant and easily available in pure form (food grade) worldwide; (ii) it can be considered a renewable-based compound; (iii) it is not flammable, not toxic, and environmentally friendly; (iv) its critical point (p_c = 7.38 MPa and T_c = 31 °C) is easily attainable at near-ambient temperature and mild overpressures. Compared to $scCO_2$, supercritical conditions of water are much harsher (p_c = 22.1 MPa, T_c = 374 °C), but SCW exhibits very distinct properties,

of which the exceptional drop of the dielectric constant of common liquid water to a value for SCW comparable to non-polar supercritical fluid is probably the most interesting characteristic to dissolve organic compounds and precipitate salts.[13]

The main laboratory and industrial processes involving the use of SCFs are:

- *Solid and liquid extractions*: SCF-based extraction of renewable-based matrixes and/or natural sources is a timely research approach, achievable both on laboratory and/or industrial scale. SCF-based extractions target selectively the apolar fraction of biomass, employing $scCO_2$ or the more lipophilic super-critical hydrocarbons (although in the latter case, process safety can be an issue, *vide supra*) as fluids. SCF-based extractions are rapid processes compared to conventional extraction techniques (*e.g.* extractions with solvents, solid–liquid Soxhlet extractions, steam distillation) and do not require additional solvents. Nevertheless, the solvent properties can be tuned by adding small amounts of co-solvent (*vide infra*) or by fine-tuning the SCF density. $scCO_2$-based extractions occur in mild conditions and are therefore fully relevant for the extraction of thermally labile compounds, which would be inevitably destroyed/decomposed when employing conventional extraction techniques. $scCO_2$-based extractions require a harmless extractant and are relatively inexpensive to run and, therefore, commonly employed in the food and fragrance industry: at an industrial level, $scCO_2$ extractions are mainly used for tea and coffee decaffeination as well as for the large scale production of hop extracts.[20,22] Another interesting example is the extraction of lycopene, which is a lipidic (apolar) carotenoid naturally occurring in red fruits and vegetables. Lycopene has been selectively obtained (in up to 86% yield) *via* continuous flow $scCO_2$ extraction of tomato skins and leaves[23] at $T = 60$ °C, $p(CO_2) = 300$ bar and $F(CO_2)$ between 0.16 and 0.41 g min^{-1}. Indeed, $scCO_2$-based extraction can also target polar compounds, such as polyphenol extraction from grape marc, providing that a binary mixture composed of $scCO_2$ + 15% w/w H_2O is used as an extraction medium. In this case, the polyphenol fraction was obtained in yields up to 7% at $T = 60$ °C and $p(CO_2) = 100$ bar for $t = 300$ min. Interestingly, proanthocyanidins were quantitatively recovered with a further $scCO_2$ + 15% w/w EtOH extraction in the same experimental conditions. Additionally, the extraction could be performed in a semi-quantitative scale starting from 0.1 kg of grape marc.[24] Supercritical fluid technology based on CO_2 was successfully used by KD-Pharma in a semi-continuous apparatus to refine fish oils and concentrate long-chain ω-3 polyunsaturated fatty acids (PUFAs), which are among the most popular dietary supplements. This patented technology, known as the KD-Pür® protocol, coupled supercritical fluid extraction (SFE) and supercritical fluid chromatography (SFC) with compressed CO_2 to extract PUFAs at 35–50 °C and 140 bar. Such gentle conditions made it possible to preserve the integrity of natural fish oils and obtain a highly pure (>99%) product.[25]

- *Polymer synthesis, processing and purification*: SCFs (mostly $scCO_2$) have been extensively employed in polymer chemistry. The presence of SCFs as polymerization solvents and/or antisolvents strongly affects the resulting polymers' morphology. Tuning the polymerization process parameters (*e.g.* pressure, temperature, rate of depressurization, nozzle diameters) results in different particle size, obtaining selectively different polymeric structures ranging from nanoparticles to microparticles and foams.[26] Moreover, thanks to its unique array of physicochemical properties, $scCO_2$ has also been used in polymer processing as a solvent, antisolvent or plasticizer.[21,22] Regardless of the type of polymerization (*e.g.* step-growth *vs.* chain-growth polymerization), $scCO_2$ can have a limited number of established roles: (i) *polymerization solvent:* this is the less common application, requiring a complete solubility of the monomers, resulting polymer and catalyst and/or initiator. It should be noted that the critical point of $scCO_2$ rises sharply on increasing the solute size, which means that high MW molecules and polymers are typically characterized by a very limited solubility in carbon dioxide. By contrast, some classes of polymers which include polyalkene oxides, perfluorinated polypropylene oxide, polymethyl acrylate, polyvinyl acetate, polyalkyl siloxanes, and polyether carbonates, exhibit a relatively high solubility in carbon dioxide. Structures of these polymers are depicted in Figure 10.4: all solids are characterized by common features such as flexible backbones, high free volumes (resulting in low glass transition temperatures, T_g), weak interactions between the polymer segments, and weakly basic interaction sites (*e.g.* carbonyl groups),[26] which greatly help their solubility

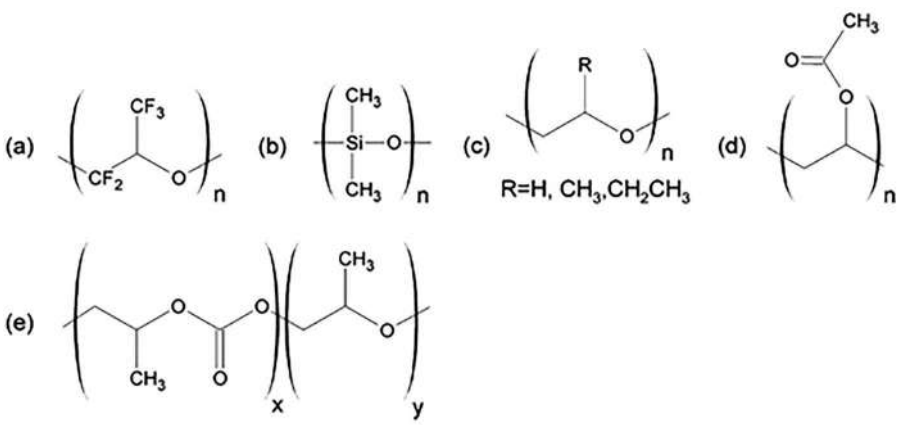

Figure 10.4 Polymeric structures soluble in $scCO_2$. (a) Perfluoropoly(propylene oxide), (b) polydimethylsiloxane, (c) poly(ethylene, propylene and butylene oxide), (d) polyvinylacetate, and (e) poly(ether carbonate). Reproduced with permission from ref. 27. Copyright 2006 John Wiley and Sons Ltd.

in dense CO_2. For example, poly(hexafluoropropylene oxide) carboxylic acid (MW = 2500) and sodium poly(hexafluoropropylene oxide) carboxylate (MW = 2500) were fully miscible with CO_2 at T = 40 °C and pressures above 16 MPa,[28] while high molar mass homopolymers (>250 000 g mol^{-1}) of a variety of fluorinated acrylic monomers were soluble in CO_2 up to 25% (w/v) at pressures and temperatures of 20–30 MPa and 50–60 °C, respectively.[29] $scCO_2$ is also particularly suitable for radical polymerization processes thanks to its inertness towards radicals.

- (ii) *Precipitation/dispersion agent*: as a precipitation agent, $scCO_2$ allows an efficient recovery of the polymer product, while when acting as a dispersion agent it improves the MW and narrows the polydispersity of the resulting polymer. These features are important for commercially relevant polymers, as in the case of poly(acrylic acid) (PAA), whose global production, estimated at 1.58×10^6 T $year^{-1}$ in 2008, has constantly increased with a CAGR (compound annual growth rate) of *ca.* 5%. PAA finds applications in different industrial sectors: high MW PAA (>1 MDa) is used as a superabsorbent polymer for hygiene products and agriculture, mid-high MW PAA (0.1–1 MDa) is employed in textiles and the paper industry, mid-low MW PAA (20–80 KDa) is used as a dispersant in paints, while low MW PAA (<20 KDa) is an effective sequestrant and/or scale inhibitor for water treatment. The large-scale production of PAA is carried out by free-radical polymerization in aqueous solutions (homogeneous conditions),[27] or in the presence of organic solvents (heterogeneous conditions) especially for preparing PAA nano- and/or microspheres. PAA heterogeneous polymerization, however, requires additional stabilizers (*e.g.* surfactants) which must be removed at the end of the process, along with unreacted AA and solvent traces. To avoid this tedious and costly purification step, PAA can be synthesised *via* precipitation polymerization, during which both the monomer and initiator are soluble in the polymerization medium, while the resulting polymer is not and can be therefore isolated *via* precipitation.[30] Precipitation polymerization processes do not require stabilizers[31,32] and they can be conveniently performed in $scCO_2$. The results of kinetic studies comparing PAA precipitation polymerization in toluene and $scCO_2$ are summarized in Table 10.4.[31] Experiments were carried out using 2,2-azobisisobutyronitrile (AIBN) as a radical initiator in both solvents/dispersants.

  The observed polydispersity ($Đ$) values are similar due to the occurrence of chain-transfer processes during the polymerization. Interestingly, however, an extensive chain transfer to the solvent occurs in toluene, resulting in low PAA MW. By contrast, in $scCO_2$, chain transfer to the polymer occurs producing significant amounts of water insoluble cross-linked PAA. This compound is lost during sample recovery and characterization, in agreement with the observed low sample recovery value (48%, last line, Table 10.4).

Table 10.4 PAA synthesis by precipitation polymerization: comparison between toluene and $scCO_2$ as polymerization media (data taken from ref. 31).

	Toluene	$scCO_2$
T **(°C)**	62	62
p **(bar)**	160	160
t **(min)**	113	220
$[AA]_0$ **(M)**	1.73	0.71
$[AIBN]_0$ **(mM)**	6.38	6.38
AA Conv. (%)	99.6	91.2
MW (g mol^{-1})	4.2×10^5	1.3×10^6
Đ	2.2	2.5
Sample recovery (%)	83	48

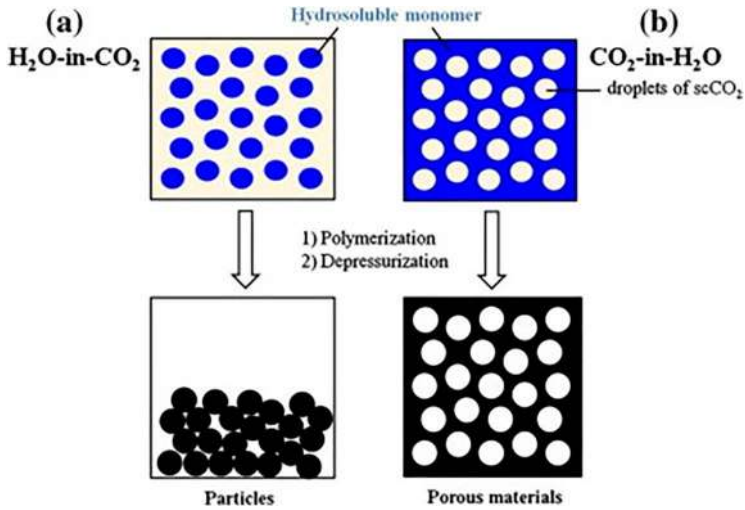

Figure 10.5 Schematic representation of heterogeneous microemulsion polymerizations in (a) water-in-CO_2 (W/C) and (b) CO_2-in-water (C/W) systems leading to particles and porous materials, respectively. Reproduced from ref. 33 with permission from Elsevier, Copyright 2014.

- (iii) *Medium for suspension and emulsion polymerizations*: these are conceptually similar heterogeneous polymerization processes. Choosing an aqueous biphasic polymerization medium allows for an improved monomer(s) conversion and resulting polymer properties, since the growing chains remain contained in particles at low concentration and are not dependent on molecular weight. Emulsion polymerization typically requires specific surfactants bearing a CO_2-philic part and the polymerization can be tuned by varying the emulsion composition.[33] As depicted in Figure 10.5a, polymerization of a hydrophilic monomer in a H_2O-in-CO_2 (W/C, CO_2 rich) emulsion system is going to produce water-soluble polymer particles, while performing the same polymerization in a CO_2-in-H_2O (C/W, water rich) system results in the formation of porous polymer matrices, as shown in Figure 10.5b.

- *Drying/cleaning*: SCFs are capable of removing liquids from solids without altering the solids' structure, thanks to the liquid-like properties of SCFs and their capacity of dissolving organic solvents. By passing a SCF through a wet solid, the solvent is removed without the occurrence of surface tension at the liquid–gas–solid interface; furthermore, the drying process occurs at relatively low temperatures. Therefore supercritical drying was applied to aerogel production,[34] set up of microelectromechanical systems,[35] and preparation of biological specimens for scanning electron microscopy.[36] It was also employed to remove biological contaminants from biobased residues, *via* $scCO_2$-based low temperature sterilization, and extensively used as a cleaning agent in the field of microelectronics. Thanks to the solvent properties of $scCO_2$, its low surface tension and its ability to infiltrate into microcavities with complex geometry, this SCF can permeate and dissolve organic contaminants, which are then removed by depressurization/gas expansion. This method is particularly suitable for cleaning small or delicate parts, or complex assemblies where the major concern is organic contamination removal, which can be performed in a more environmentally friendly fashion compared to the traditional approaches based on sulfuric acid/hydrogen peroxide mixtures or organic solvents.[26] A relevant example in this context was reported in 2014 by Lawandy and Smuk, who employed $scCO_2$ for cleaning banknotes. Banknote soiling is the main cause of rejection for automatic sorters, which are used worldwide by central banks. The soiling is primarily due to human sebum, which is transferred to the banknote surface. The oxidation of sebum results in a yellowish product that absorbs in the visible region of the spectrum and interferes with the banknotes' optical fitness sensors. Thanks to its properties (*vide supra*), $scCO_2$ is an ideal cleaning medium. As depicted in Figure 10.6, $scCO_2$ at T = 60 °C and $p(CO_2)$ = 348 bar was effective in removing human sebum and other common soiling agents, such as motor oil and organism colonies, without any damage to the printed features at all spatial levels or to the expensive security features in banknotes. Under the same conditions, the procedure proved feasible to clean conventional 100 note straps of banknotes, which typically circulate in the commercial and central bank environment. Data on the distribution of banknote soiling levels before and after cleaning in straps showed a significant decrease in soiling levels on both sides of the notes.[35]
- *Chemical/biochemical processes*: SCFs are mainly employed as sustainable reaction media, acting as replacements of toxic and volatile organic solvents. At an industrial scale, SCF-based processes are also characterized by lower operational costs. Use of SCFs as reaction media is highly desirable in pharmaceutical industry processes for the production of intermediates (*e.g.* chiral) and final products. Selected examples of recently reported SCF-based processes will be covered in the next section (*vide infra*).[37]

Figure 10.6 Banknotes before sebum treatment (top), after sebum treatment (centre), and after cleaning with $scCO_2$ at T = 60 °C with ultrasonic agitation (bottom). Reproduced from ref. 38 with permission from American Chemical Society, Copyright 2013.

- *Energy applications*: the peculiar heat transfer and thermodynamic properties of SCFs allowed for their application as heat transfer fluids (*e.g.* air conditioning, heat pump and refrigeration systems), power cycles for energy production, carbon capture and storage (CCS) and SCW-based biomass reforming liquefaction.[37]

The use of SCFs in the above-mentioned processes is characterized by several desirable sustainability features, which are summarised in Table 10.5.

Table 10.5 Green aspects of supercritical fluid technologies for material processes. Adapted from ref. 39 with permission from The Royal Society of Chemistry.

Process	Advantages of SCFs	Green aspects
Extraction/ fractionation	Selective solubility, No residual solvent	No organic solvent, complete solvent recycle
Cleaning	Good solvent power	No VOCs, no toxic organic solvents
Drying	No capillary force	Increasing production yield
Polymerization	No residual solvent	No organic solvent
Hydrothermal synthesis	No organic solvent needed Nanoparticle synthesis	Reduce
Plating	Good solubility of H_2 in $scCO_2$	No wastewater generation
Biomass conversion	No acid/base catalyst needed	Simple process without heavy wastewater generation
Recycling	No acid/base catalyst needed	No secondary contamination Less wastewater generation
Recovery of materials by SCWO	No mass transfer resistance	Valuable inorganic compounds can be recycled
Heavy metals extraction (radioactive materials)	Selective extraction of uranium	No secondary contamination
Dying	Easy to penetration	No wastewater generation
SCF deposition	No capillary force	Increasing production yield

10.3 Tailoring SCF Properties

SCF solvent properties may be modulated by alterations in temperature and pressure conditions, as well as by adding modifiers or co-solvents. In the former case, it has been observed that the density and, likewise, the solubility parameter of a given SCF can be strongly affected by pressure and temperature variations in the critical region, as depicted in Figure 10.7 for CO_2. In the latter case, a co-solvent and/or modifiers are often added to improve the solubility of polar molecules in SCFs: this is important in extraction processes based on natural, complex matrices, biomass treatment and synthesis and purification of active pharmaceutical ingredients.

As stated in the previous sections, thanks to its mild critical point, $scCO_2$ accounts for more than 90% of the published research in the field of supercritical fluid technology. Carbon dioxide is a relatively non-polar solvent but displays a limited affinity with polar molecules due to its large molecular quadrupole. Therefore, adding suitable co-solvents and modifiers can improve the solubility of polar molecules. In particular, $scCO_2$-based extraction processes often include the addition of various co-solvents and modifiers, such as isopropyl alcohol and ethanol, *n*-hexane, heptane, pentane, toluene,

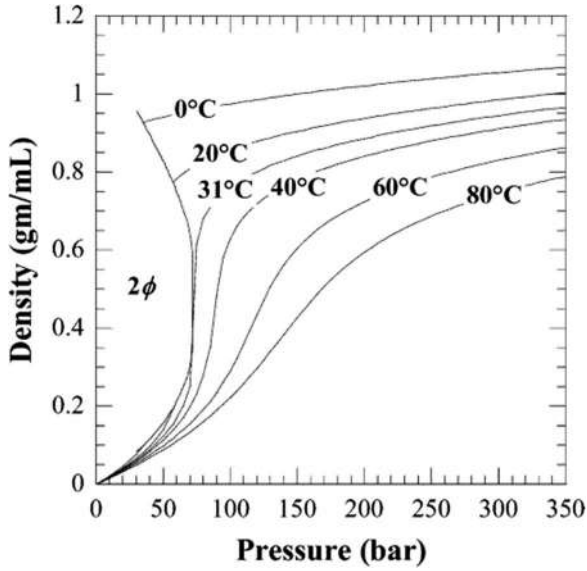

Figure 10.7 Carbon dioxide density as a function of pressure and temperature. Reproduced from ref. 40 with permission from American Chemical Society, Copyright 2004.

methanol, acetone and formic acid with ammonium formate in methanol to enhance the extraction process performance.[41] A relevant application of such extractant mixtures has been described for the valorisation of spent coffee grounds (SCG), which is a biowaste available in large amounts (9.4 MT in 2018 only) and rich in compounds suitable for food, pharmaceutical and cosmetic industry applications (*e.g.* fatty acids, amino acids, lignin, cellulose, hemicellulose and other polysaccharides, and, to a minor extent, bioactive compounds, such as alkaloids and polyphenols, caffeine, tannins, flavanols, flavones and phenolics acids). SCG oil fractionation is typically performed using organic solvents. In order to develop sustainable extraction processes, Corazza and co-workers optimized the lipid extraction from SCG in a semi-batch process using $scCO_2$ plus ethanol (EtOH; Figure 10.8). These mixtures made it possible to reduce the extraction time (20 min *vs.* > 60 min) and improve the recovered oil fraction yield by adding increasing quantities of EtOH.[42]

An alternative approach to improve the solubility of polar solutes in $scCO_2$ as well as to increase its viscosity (which is very important for carbon capture and storage, CCS, applications) is based on adding polar and ionic substances, *e.g.* surfactants, as modifiers.[43] Seminal studies by Consan and Smith highlighted the limitations associated with the use of commercially available surfactants as $scCO_2$ modifiers. Most of the 130 commercially available surfactants were insoluble in $scCO_2$, except for a few examples characterised by

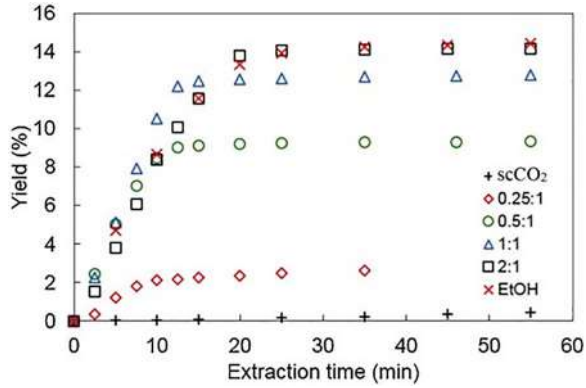

Figure 10.8 Experimental overall extraction curves for spent coffee ground oil with $scCO_2$ + EtOH at T = 60 °C, $p(CO_2)$ = 15 MPa and different EtOH/$scCO_2$ w/w ratios (EtOH/$scCO_2$ ratio = 0.25 : 1, 0.5 : 1, 1 : 1 and 2 : 1 w/w). Reproduced from ref. 42 with permission from Elsevier, Copyright 2019.

marginal solubility (*e.g.* fluorinated hydrocarbons and surfactants bearing morpholinium cations or carboxylates anions).[44] More recently, efforts have been directed towards the development of CO_2-soluble additives, often combined with $scCO_2$/water emulsions. Alternative systems were proposed, such as ionic liquid-in-CO_2 systems,[45–47] and microstructures such as lamellar and/or bicontinuous phases.[48,49]

10.3.1 Selected Applications of Supercritical Solvents in Organic Synthesis

It is well known that the global increase in environmental awareness is spreading in almost each field of our everyday life and, as far as chemistry is concerned, an ever-increasing control over the use and disposal of hazardous materials is a key aspect for chemical processes. This, in turn, means that efforts at both research and application levels must be continually addressed to find innovative "cleaner" alternatives to current protocols. One obvious target area refers to the use of new solvents able to mitigate or rule out the enormous impact that the disposal or accidental release of billions of ton/year of organic liquid solvents brings about in all terrestrial or aquatic ecosystems. Excellent candidates in this respect are SCFs, particularly but not exclusively $scCO_2$.

The second part of this chapter is intended to provide an overview of recent applications of SCFs in organic synthesis, by analysing some representative examples taken from the literature. It should be noted that although the use of SCFs as solvents in place of traditional organic solvents represents an improvement towards sustainability, by itself it is not necessarily an innovation. It becomes such only when SCF usage improves other features of the

analysed chemical transformations (*e.g.* yield enhancement, improved selectivity, milder operating conditions), representing a feasible solution to overcome physico–chemical and/or technological issues.

Each example discussed here will include a brief introduction on the reaction of interest and a description of the main features of the process. Emphasis has been placed on transformations of general interest to the green organic chemistry community, including the use of SCF solvents for: (i) metathesis of alkenes; (ii) glucose conversion; (iii) biodiesel production, promoted by methanol and ethanol; (iv) esterification of levulinic acid. For the latter example, a comparative (SCF *vs.* conventional) green metrics evaluation was also performed.

10.3.2 Olefin Metathesis Using $scCO_2$ as a Solvent

The metathesis of olefins is a powerful and elegant means of constructing complex carbon frameworks.[50–52] First discovered in the 1950s, thanks to the work of Yves Chauvin, Robert Grubbs and Richard Schrock who shared the 2005 Nobel Prize in Chemistry for their work on carbene complexes,[53–55] olefin metathesis has become over time an established green, clean, and highly atom efficient transformation, characterized by low waste generation. Scheme 10.1 provides a general description of the reaction by which the redistribution of substituents in reactant olefins takes place through the scission and regeneration of carbon–carbon double bonds.

The applications of the reaction span from the preparation of linear high olefins to polymers [*e.g.* polynorbornene and poly(dicyclopentadiene)] *via* ring-opening-metathesis polymerization and fine chemicals. Olefin metathesis has been included in this chapter not only as it represents a powerful synthetic protocol for a variety of products, but also because it is an archetype green chemistry reaction, due to the reduced emissions of hazardous waste to the environment. With the aim of further improving the potential, scope, and eco-compatibility of the process, the use of alternative safer and *greener* solvents has been investigated to replace media typically used for the metathesis reaction, *i.e.* hydrocarbons (hexane and toluene) or light chlorinated compounds (dichloromethane and carbon tetrachloride). However,

Scheme 10.1 General reaction scheme for the metathesis of olefins. AE of the reaction is intrinsically 100%.

relatively few patents and papers have been reported on the application of dense CO_2 or ionic liquids as solvents for RCM and ROMP (ring-closing and opening metathesis polymerization, respectively) processes in the presence of either Grubbs homogeneous complexes or transition metal salts [$RuCl_3$, $Ru(H_2O)_6(tos)_2$, and WCl_6/Ph_4Sn],[56–60] while heterogeneous catalysts have been even less mentioned. A comparative analysis of the self-metathesis of different α-olefins (1-hexene, 1-heptene, and 1-octene) catalysed by Re_2O_7 supported on γ-Al_2O_3 demonstrated that not only did the reaction occur efficiently and selectively in $scCO_2$, but it was even faster than in classic liquid media (*n*-heptane and toluene).[61] Scheme 10.2 illustrates the model metathesis of 1-octene.

Initially, the reaction was investigated in a static reactor (autoclave). Formation of the self-metathesis product (7-tetradecene) was accompanied by isomerization of 1-octene into 2-, 3-, and 4-octene (promoted by the acidity of the support) and the cross-metathesis process, which produced linear C_9–C_{13} olefins. However, optimization of the conditions allowed the synthesis of 7-tetradecene in ≥95% selectivity. A key aspect of the study was the comparison of $scCO_2$ to different liquid solvents, which was required to investigate the effect of the substrate concentration. Indeed, while the molar concentration was a convenient parameter to examine kinetic profiles in conventional liquid media, it was not suitable for $scCO_2$ as it did not consider that the operating pressure directly affected the density of the supercritical solvent and its solvation properties. The mole fraction of the reactant olefin

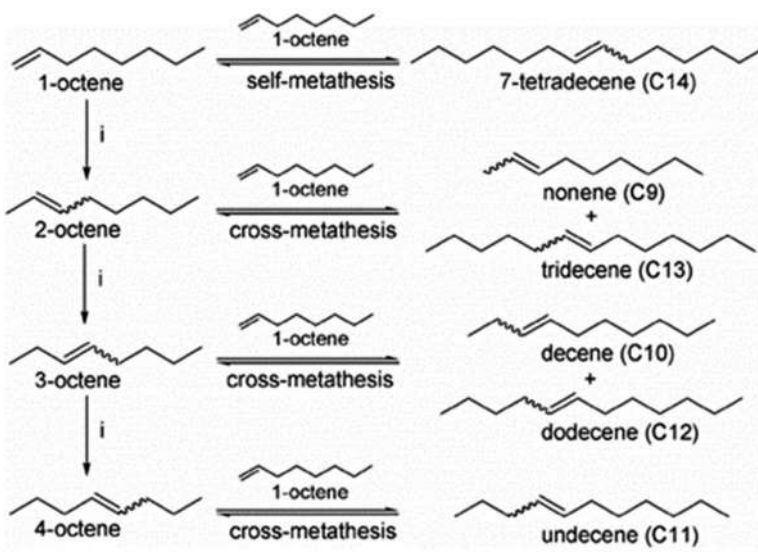

Scheme 10.2 Self- and cross-metathesis reactions were catalyzed by supported Re_2O_7. Isomerization (i) of 1-octene was promoted by the support (γ-Al_2O_3). Reproduced from ref. 61 with permission from The Royal Society of Chemistry.

$\{X = [\text{mol}_{\text{Substrate}}]/([\text{mol}_{\text{Substrate}}] + [\text{mol}_{\text{solvent}}])\}$ appeared like a more appropriate parameter for a coherent comparison, since it was related to the overall number of molecules (substrate + solvent) present in the mixture.

Accordingly, if metathesis experiments were carried out using the same mole fraction of the olefin (*e.g.* 1-octene) in $scCO_2$ (35 °C, 90 bar), *n*-heptane and toluene, the conversion was 40%, 36%, and 71%, respectively, after 2 h (Entries 1–3, Table 10.6).[61]

Similar results were obtained for the self-metathesis of 1-hexene and 1-heptene: the conversions were 61% and 63% and the corresponding selectivity towards 5-decene and 6-dodecene was 95%, respectively.

Thereafter, the metathesis of 1-octene was investigated under continuous-flow (CF) conditions.[62,63] The results confirmed the superior capability of $scCO_2$ as a solvent/carrier with respect to *n*-hexane and toluene (Entries 4–7, Table 10.6). Interestingly, it was observed that within the first five minutes of reactant feed, the conversions (*ca.* 65–70%) and selectivity towards the metathesis product (≥90%) were similar in each of the tested solvents. However, with *n*-hexane and toluene, the catalytic bed abruptly deactivated to become completely inefficient for the metathesis in less than 15 and 30 min, respectively (Entries 4 and 5, Table 10.6), while the reaction proceeded without changes for up to 1 hour in $scCO_2$ (Entry 6, Table 10.6). It was also demonstrated that after the reaction with liquid solvents (*n*-hexane and toluene), the spent catalyst could recover an activity comparable to the initial one, only when it (the catalyst) was reused in $scCO_2$. $scCO_2$ not only did not deactivate the catalytic bed, but allowed the restoration of the deactivated catalyst used with conventional solvents.

Table 10.6 Comparison of $scCO_2$ *vs.* conventional liquid solvents in the metathesis of 1-octene catalyzed Re_2O_7 supported on γ-Al_2O_3.

Entry	Operating conditions	Cat.	Solvent	$X_{1\text{-octene}}$ ($\times 10^{-2}$)[b] (mol : mol)	*T*/*p*/*t* (°C/bar/h)	Conv. (%)	Sel. (%)[d]
1	Batch[a]	Re_2O_7/γ-Al_2O_3,	*n*-heptane	1.1	35/1/2	40	95
2		(Re: 6.7 wt%)	Toluene		35/1/2	36	95
3			$scCO_2$		35/90/2	71	97
4	Continuous-	Re_2O_7/γ-Al_2O_3,	*n*-hexane	n.d.[e]	100/1/0.3	18	<1
5	flow (CF)[c]	(Re: 6.9 wt%)	Toluene		100/1/0.3	22	25
6			$scCO_2$		100/90/0.3	53	≥95
7			$scCO_2$		35/90/0.3	23	

[a]Conditions: 1-octene (5 mmol), catalyst (0.56 g) in a olefin/Re molar ration = 23.7.
[b]$X_{1\text{-octene}}$ = molar fraction of the olefin in each solvent. $scCO_2$: $p(CO_2)$ = 90 bar (V = 30 mL, d = 0.66 g mL^{-1} at 35 °C).
[c]Conditions: a catalytic bed of Re/γ-Al_2O_3 (1.4 g) in all cases; reactants feed time = 15 min in all cases; 1-octene was fed to the reactor at 0.05 mL min^{-1}, while flow rates of CO_2, *n*-hexane and toluene were 1, 2.98 and 2.45 mL min^{-1}, respectively. In this way the solutions of 1-octene in the three tested solvents have the same molar ratio of substrate.
[d]Selectivity of 7-tetradecene (% by GC: total of *cis*- and *trans*-isomers).
[e]n.d.: not determined.

The enhancement of the reaction rate and/or the improvement of the reaction outcome observed under both batch and CF-conditions was related to the capability of $scCO_2$ to overcome the mass transfer limitations associated with heterogeneous catalysis in conventional liquid solvents. In particular, this was due to the gas-like diffusivity and viscosity and the liquid-like density of the supercritical medium $scCO_2$, which allowed an efficient penetration of the reactant solution within the mesoporous solid support of the catalyst. Peculiar solvation phenomena of SCFs, known as local density enhancements (LDEs), whereby the density and the composition of the local environment around the solute molecules are modified with respect to the bulk of the supercritical solvent, were also considered.[64] It should be noted here that dilute supercritical solutions are typically classified into attractive or repulsive mixtures depending on whether the solute–solvent attraction is stronger or weaker than the solvent–solvent attraction, respectively.[64] Most of the industrial and technological applications of SCFs include attractive mixtures within which theoretical studies often invoke the occurrence of LDE phenomena related to unusually good solvation properties of supercritical solvents.

Besides the multiple advantages in terms of fast kinetics and high reaction productivity (especially under CF-conditions) described for the chosen example of the metathesis of olefins in $scCO_2$, some general critical aspects cannot be disregarded when SCFs are used. These mostly include: (i) the potential safety hazard due to high-pressure equipment and (ii) more specifically for $scCO_2$, the low dielectric constant (generally between 1.1 and 1.5), the reactivity with Lewis bases, the hydrogenation to poisonous CO over noble metals, and the formation of acidic solutions with water (pH ≈ 2.85),[65] can be both a process disadvantage and a chemical disadvantage with respect to conventional solvents.

10.3.3 Platform Chemicals from Glucose in SCW

Water can be considered as the "greenest" naturally occurring solvent. Albeit its critical point (T_c = 374 °C, p_c = 218 bar) is highly energy demanding, the use of sc-water (SCW) has become increasingly popular for several applications in organic synthesis, since it is characterized by a low dielectric constant which enables the solubilization of many organic compounds, even low polar species (*vide supra*). Gases are also miscible in SCW, thus giving further opportunities to limit or overcome mass transfer issues during multiphase processes. In addition, in proximity of the critical point, the water ion product dissociation constant (K_w) is about 3 orders of magnitude higher than that for ambient liquid water: the corresponding H^+/OH^- concentration is high enough to be effective for acid- and base-catalyzed reactions of organic compounds. In this paragraph, such properties of SCW will be explored for the conversion of glucose into valuable biobased platform chemicals in near-/super-critical water.

Glucose is the monomer unit of cellulose and it is one of the most attractive biomass-derived starting materials. For instance, its acid-catalyzed isomerization to fructose is of paramount importance, since fructose allows the selective preparation of key intermediates such as 5-hydroxymethylfurfural (HMF) and levulinic acid (LA) (Scheme 10.3) to access the synthesis of biofuels, renewable plastics and chemicals, green solvents, and lubricants.[66–68]

The overall isomerization reaction is described by the Lobry de Bruyn–van Ekenstein (LBE) process by which the two sugars may convert into each other (Scheme 10.4).

Fructose is an expensive reagent and unlike glucose, it cannot be conveniently employed as a starting substrate. However, since the involved equilibria are favoured by hydrothermal conditions,[69] SCW has been considered as an environmentally benign medium for glucose conversion. Several other reactions have been described by using glucose in hot compressed water; these include: (a) isomerization of glucose to fructose, (b) dehydration of glucose to 1,6-anhydroglucose (AHG) and dehydration of fructose to 5-hydroxymethyl-2-furaldehyde (HMF), and (c) retro-aldol condensation of fructose to glycolaldehyde (GA) and dihydroxyacetone (DHA) (Scheme 10.5).[70] In addition, the formation of gas products, char particles, and other liquid products has been observed under SC conditions.[71]

Studies published so far have reported not only on the different reactions of glucose (Scheme 10.4), but also on the effects of SCW on the product distribution.[72–78] It has been clearly highlighted that tuning the water density

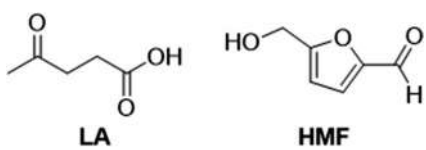

Scheme 10.3 Levulinic acid (LA) and 5-hydroxymethylfurfural (HMF): key intermediates from biomass-derived sugars.

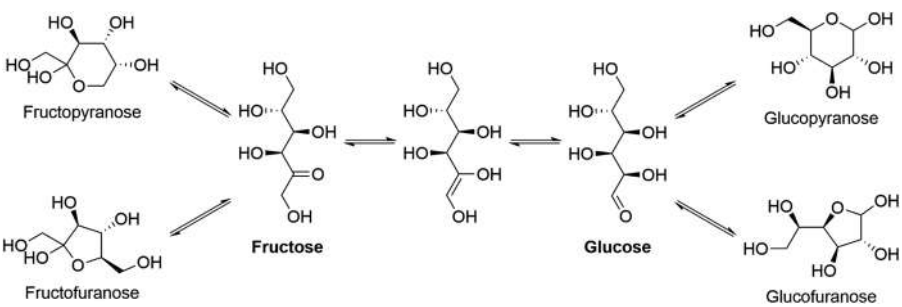

Scheme 10.4 Lobry de Bruyn-van Ekenstein (LBE) transformations of glucose and fructose.

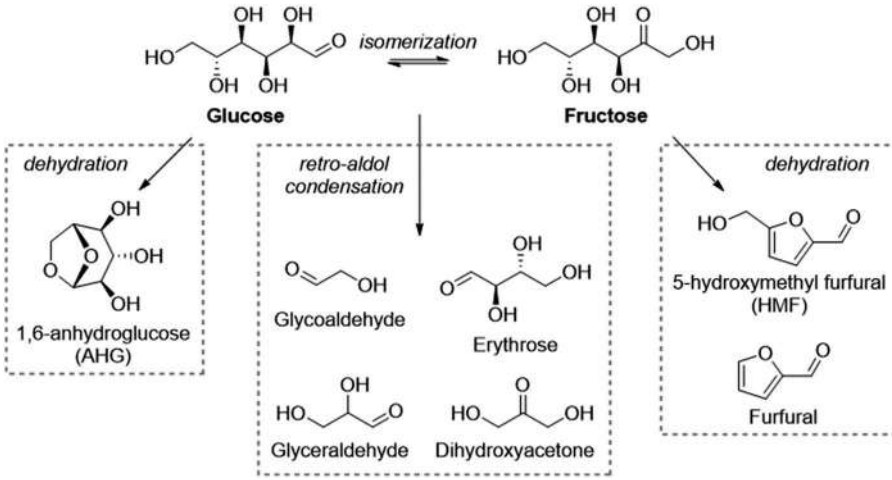

Scheme 10.5 Isomerization of glucose to fructose and possible side reactions. Adapted from ref. 72 with permission from Elsevier, Copyright 2019.

Table 10.7 Selected examples of glucose valorisation reactions in near- and/or supercritical water.

Entry	Conditions	*T*/*p*/*t* (°C/bar/s)	Conv.[a] (%)	Products, yields (%)				Reference
				Fructose	HMF	Others[b]	Total[c]	
1	*Near-critical*	200/250/300	20	5	3	3	11	70
2[d]		200/250/300	42	14	5	3	22	70
3[e]		200/250/300	80	2	20	2	24	70
4		300/250/10	61	7	20	20	47	71
5	*Super-critical*	400/250/10	99	1	13	66	80	71
6[f]		420/340/10	98	2	1	57	60	81

[a]Glucose conversion.
[b]Others includes all water-soluble products (glycolaldehyde, 1,6-anhydroglucose, furfural, mannose, pyruvaldehyde, *etc.*) different from fructose and HMF.
[c]Total yield of products was composed of fructose, HMF and all water-soluble products.
[d]ZrO_2 was employed as a catalyst.
[e]TiO_2 (anatase) was employed as a catalyst.
[f]Continuous-flow conditions.

(density variations of SCW are proportionally higher than in the subcritical state of water) and the ionic properties of the medium by changing the temperature and pressure was fundamental to control the relative extent of competitive reactions of glucose. For instance, it was noticed that dehydration pathways (C–O bond splitting) were dominant at lower temperatures (p = 250–400 bar; T = 250–350 °C), while retro-aldol condensation (C–C bond breaking) mainly occurred at higher temperatures (p = 250–400 bar, T = 400–500 °C).[78–80] Examples are illustrated in Table 10.7.

In all cases, the reactions were very fast (10–300 s). Under near-critical conditions, the main products were fructose and HMF with yields up to 14% and 20%, respectively (Entries 1–4, Table 10.7). The reaction formed also different water-soluble compounds including but not limited to glycolaldehyde, 1,6-anhydroglucose, furfural, mannose, and pyruvaldehyde (see also Scheme 10.4). These were obtained with a total yield variable from 3% to 20% ("Others" in Entries 1–4, Table 10.7). Increasing the temperature from 200 to 300 °C and decreasing the reaction time from 300 to 10 s, favoured the formation of HMF at the expense of fructose. However, both conversion and selectivity were affected by the addition of catalysts: in the presence of basic ZrO_2, glucose was primarily converted into fructose (14%, Entry 2, Table 10.7), while anatase TiO_2 enabled dehydration and condensation reactions of glucose yielding HMF as the main product (20%, Entry 4, Table 10.7). The latter result was ascribed to the amphoteric properties of anatase TiO_2 in coherence with other findings that, starting from glucose, reported the synthesis of fructose (key intermediate for HMF production) under basic conditions,[69] and the formation of HMF under acid catalysis.[81]

Under supercritical conditions at T = 400 °C and p = 250 bar, the glucose conversion was substantially quantitative, but the reaction favoured products other than fructose and HMF (Others: 66%, Entry 5, Table 10.7). A further increase of both T and p (420 °C and 340 bar, respectively) allowed the selective formation of glycolaldehyde in up to 45% yield (Entry 6, Table 10.7). All of the reactions also produced char, whose amount, however, was suppressed in supercritical rather than near-critical water.[70]

The kinetics of glucose decomposition under sub-/super-critical water was also investigated.[71] The glucose decomposition followed the Arrhenius equation, while the rates of other reactions decreased in the supercritical region plausibly because of a change of the mechanism, from an ionic to a free-radical one, which followed a non-Arrhenius and an Arrhenius behaviour, respectively.

Overall, these studies proved the potential of sub- and super-critical water to steer the selectivity of a complex network of processes such as that depicted in Scheme 10.4. On a final general note, the harsh temperature and pressure conditions required to work with supercritical water imply not only severe safety measures for SCW-plant operators, but also expensive and custom-made reactors built-up with selected materials, such as Ca, Mg, Y and Sc-doped ceramic ZrO_2, and doped (Ni, Ti, Zr, Cr) ferritic-martensitic steels,[82] necessary to withstand the highly corrosive properties of SCW.[83]

10.3.4 Biodiesel Production in SC-Methanol/Ethanol

The catalytic transesterification of natural triglycerides with short-chain alcohols, such as methanol or ethanol, is one of the best and cost-effective reactions available to produce biodiesel (Scheme 10.6).

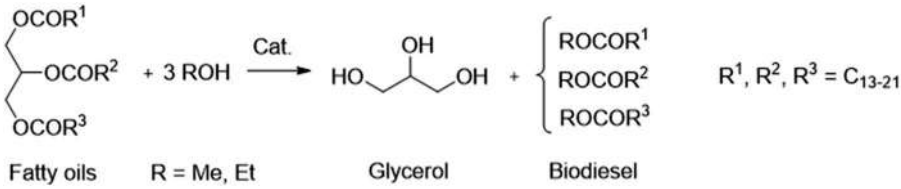

Scheme 10.6 The catalytic transesterification of triglycerides. Adapted from ref. 84 with permission from Elsevier, Copyright 2009.

Table 10.8 Variation of polarity of light alcohols from liquid to supercritical state.

		ε (dielectric constant)		
Entry	Alcohols	Liquid	Supercritical	Reference
1	MeOH	32.6 (25 °C, 1 bar)	7.2 (250 °C, 200 bar)	86
2	EtOH	25.3 (25 °C, 1 bar)	4.2 (241 °C, 61.4 bar)	87

Under conventional liquid-phase conditions, however, this process shows some relevant drawbacks of which the two most common are: (i) the reaction kinetics are disfavoured by the lack of mutual miscibility of reactants (apolar natural oils and polar alcohols), which form a biphasic system; (ii) the use of either basic or acid catalysts (sometimes added in stoichiometric amounts) brings about a complex separation of biodiesel from saline by-products, which need also to be disposed of. A promising approach to overcome these problems has been proposed by performing the reaction in supercritical alcohols.[85] Indeed, the dielectric constants of sc-ROH remarkably decrease from the liquid to the supercritical state (Table 10.8), thereby allowing the formation of homogeneous solutions with oils and avoiding the use of additional catalysts.

Fundamental studies on the transesterification of oils in supercritical methanol/ethanol have been reported from different starting substrates.[84,85] For example, a comparative analysis was described for the transesterification of rapeseed oil using: (i) liquid methanol and sodium hydroxide as a catalyst at T = 35–60 °C and ordinary pressure (typical conditions for base-catalyzed esterification), and (ii) supercritical methanol at 350–400 °C for *ca.* 240 s, in the absence of any catalyst. The investigation firstly demonstrated that the composition of the final mixture of methyl esters composed of methyl palmitate ($C_{16,0}$), methyl stearate ($C_{18,0}$), methyl oleate ($C_{18,1}$), methyl linoleate ($C_{18,2}$) and methyl linolenate ($C_{18,3}$), was substantially unchanged regardless of the (liquid or sc) method used. Only at the highest explored T (400 °C) under sc-conditions, the onset of decomposition and dehydrogenation reactions were plausibly responsible for the obtainment of lighter methyl esters. Thereafter, it was proved that the overall yield of biodiesel (mixture of methyl esters) was slightly higher (98.5%) in sc-MeOH compared to the liquid phase

reaction (97%). This result (improved yield) was related to the selective conversion of free fatty acids (FFAs), naturally occurring in the rapeseed starting oil, to their methyl esters under sc-conditions; by contrast, FFAs were saponified (not yielding the corresponding esters) in liquid methanol in the presence of a base catalyst.[88] Finally, after the transesterification process, the sc-procedure allowed a much simpler post reaction treatment based on gravity/centrifugation separation (to remove the by-product glycerol) and distillation of MeOH, with respect to the conventional method that required additional purification steps of dry washing (with silicates such as Magnesol or Trisyl, ion exchange resins, activated clay, or activated carbon) to remove residual methanol, glycerine, metals and soaps, and filtration.[89,90] Figure 10.9 compares the overall sequences of reaction and product separation involved for the sc- and the liquid-phase (catalytic) protocols.

A brief comment is placed here also on "crude glycerol", the major by-product in biodiesel production, which is also a valuable source of renewable carbon. This compound comes in the form of a complex mixture with water, alcohol and salts when it is obtained from the liquid-phase transesterification of oils. Despite the overpowering efforts devoted over the years to the direct conversion of crude glycerol into value added chemicals, limited results have been achieved in most cases. In other words, the synthetic exploitation of glycerol becomes possible if it (glycerol) is in a highly pure form, which requires energy demanding steps of salt filtration

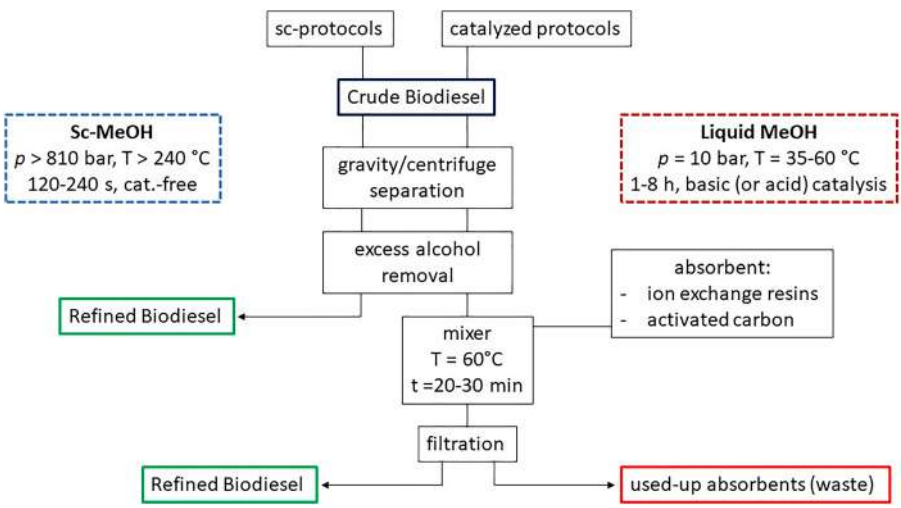

Figure 10.9 Comparison between biodiesel purification methodologies: sc-method derived biodiesel *vs.* catalyzed protocol derived biodiesel. Dry-washing technology was considered.

and distillation of the crude starting mixture. Most of these problems are avoided by the above discussed sc-protocols where oil transesterification is a catalyst-free process.

Attention has been focused also on the use of supercritical ethanol (sc-EtOH) for transesterification of natural oils. Indeed, EtOH being available from the transformation of biomass (fermentation processes), it appears a more sustainable choice than methanol that is mainly derived from fossil sources such as petroleum and natural gas.[84,91] The major advantages of supercritical conditions with EtOH are the same as those mentioned for methanol, *i.e.* very high reaction rates, applicability to various types of oil, no need of a catalyst, no waste generation (neither salt nor water to be disposed of), ease of separation, and high biodiesel yields. Nonetheless, the requirement of severe pressure and temperature (see Table 10.9) implies a high energy demanding process, which becomes competitive to conventional liquid phase methods only if heat recovery solutions are provided. Improved engineering approaches have been designed *via* continuous-flow (CF) reactors. For example, using a spiral reactor (φ = 2.17 mm; L = 10 m) integrated with a heat exchanger (2.5 m), the CF-transesterification of canola oil in supercritical ethanol proceeded with almost quantitative conversion and 94% yield of FAEEs (fatty acid ethyl esters as biodiesel) at 350 °C, 200 bar, and a residence time (τ) of 30 min.[92] Interestingly, it was demonstrated that the total energy supply to this CF-setup amounted to 0.0659 MJ day^{-1} and was nearly 7-times lower than that (0.454 MJ day^{-1}) of a conventional flow reactor without heat recovery. Another recent paper has reported on the excellent performance of a microtube reactor of 1.85 mL (φ: 0.9 mm) by which the conversion of refined palm oil into superior quality biodiesel was optimised using a response surface methodology: in the presence of sc-EtOH at 370 °C and 80 bar (τ = 5.2 min), the yield of FAEEs was >98% with a total productivity as high as 474.8 Kg h^{-1} m^{-3}. Ethyl acetate was added in this case, to improve the homogeneity of the oil/sc-EtOH mixture.[93]

Table 10.9 reports the main features of two other examples of CF-transesterification of natural oils with sc-EtOH.

Table 10.9 Protocols for biodiesel production *via* sc-ethanol mediated CF-transesterification of natural oils.

			Reactions conditions						
Entry	Oil	CF-reactor (mL)	T (°C)	p (bar)	τ (min)	Ethanol : oil (mol mol^{-1})	Yield (%)	P_o (Kg h^{-1} m^{-3})	Reference
1	Sunflower	Tubular (260)	345	160	28	40 : 1	91	292	94
2	Rapeseed	Fixed-bed (160)	350	300	n.d.	12 : 1	97.4	n.d.	95

10.3.5 The Enzyme-catalyzed Synthesis of Butyl Levulinate from Levulinic Acid and Butanol: Green Metrics Evaluation

The concluding paragraph of this chapter will further compare the use of SCFs, particularly $scCO_2$, to conventional organic solvents, by the application of modern green metrics such as *E*-Factor, Carbon Efficiency (CE), Mass Intensity (MI), Mass Productivity (MP) and Mass Yield (MY). For the reader's convenience, the definitions of such metrics are summarized here.[96,97]

E-factor refers to the mass of waste produced per unit mass of the desired product.

$$E-\text{Factor} = \frac{\text{mass of total waste}}{\text{mass of product}}$$

Carbon Efficiency (CE) is the ratio between the carbon mass of product per mass of all reagents. CE refers to the greenness of a process by considering how the carbon mass of reactants contributes to the product, but it does not provide information about the waste.

$$\text{CE} = \frac{\text{carbon mass} \in \text{product}}{\sum \text{mass of all reagents}}$$

Mass intensity (MI) includes not only the reagent amount present in the product, but also the amounts of all other compounds (such as catalysts, solvents, *etc.*) involved in the reaction step.

$$\text{MI} = \frac{\sum \text{reagents} + \text{catalysts} + \text{solvents} + \text{others}}{\text{mass of product}}$$

Mass Productivity (MP) is a measure of mass of reactants (A+B) actually present in the product.

$$\text{MP} = \frac{\text{MW of the product}}{\text{MW of reagent A} + \left\{\text{MW of reagent B} \cdot \left(\text{molar ratio}\frac{\text{B}}{\text{A}}\right)\right\}} \cdot \text{Mass Yield}$$

Mass Yield (MY) is the time-honoured chemical yield of the reaction.

The bio-catalyzed synthesis of butyl levulinate (BL) from levulinic acid and butanol is the model reaction chosen from the literature to compare the use of $scCO_2$ and a conventional solvent such as ethyl methyl ketone (EMK) (Scheme 10.7: procedure A and B, respectively).[98] Indeed, levulinate esters have vast potential applications as biomass-derived energy products, particularly as diesel-blending components.

Experiments proved that procedure A (in $scCO_2$) of Scheme 10.7 allowed BL to be obtained in 99% yield after 5 h [the addition of EMK (BuOH : EMK = 1 : 2 mol mol^{-1}) as a co-solvent was, however, necessary to overcome issues of

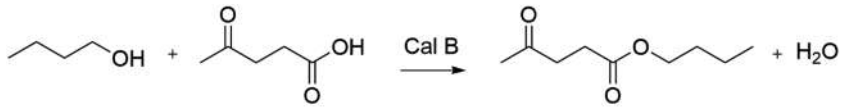

1. Procedure A: $scCO_2$ medium at 48 °C and 8.8 MPa
2. Procedure B: EMK medium at 48 °C and 0.1 MPa; [BuOH]=0.3 M

Cal B: Candida antarctica immobilized on acrylic resin (Novozyme 435)

Scheme 10.7 Bio-catalyzed synthesis of levulinate esters.

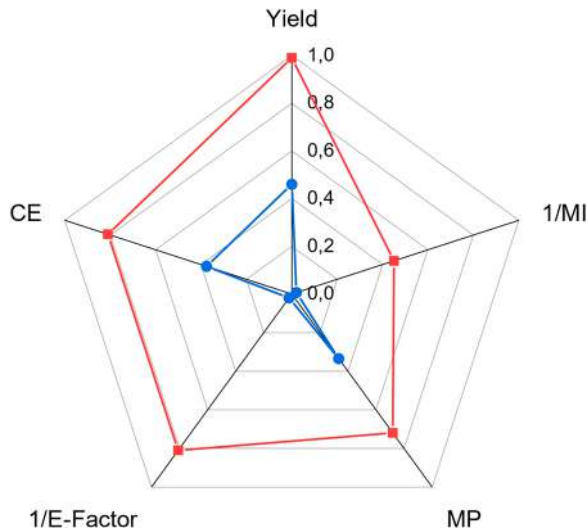

Figure 10.10 Comparative pentagonal diagram for the synthesis of butyl levulinate in $scCO_2$-medium *vs.* ethyl methyl ketone (EMK) as a solvent. (-●-) EMK as a solvent; (-■-) $scCO_2$ medium. Reaction conditions in $scCO_2$ solvent for the present study: levulinic acid (0.014 mol); butanol (0.010 mol); co-solvent: EMK 1.8 cm^3; biocatalyst (Novozyme 435): 230 mg; pressure: 88 bar; temperature: 48 °C; time 5 h. For the reaction in EMK all the parameters were equal, except for the removal of $scCO_2$. The metrics values are taken from ref. 98.

mutual solubility of reactants]; while, in EMK (procedure B), the mass yield of the product did not exceed 46%. This remarkable difference was ascribed to a higher diffusivity of $scCO_2$ compared to EMK, which favored the mass transfer of reactants towards the active sites of the enzyme and improved the reaction rate.[99]

Thereafter, the comparison of procedures A and B was refined according to the analysis proposed by Andraos where graphical outputs exemplified the performances of the above-described five metrics through radial pentagonal diagrams for the two individual reactions (Figure 10.10).[100,101] The esterification carried out in $scCO_2$ (red irregular polygon) was much closer to the green ideality (regular pentagon with five equal sides) than the same process run in

EMK (blue irregular polygon), meaning that procedure A was superior to procedure B not only for a higher chemical yield (Y), but also for a lower production of waste (*E*-factor, MI, and MP) and in general, for a better incorporation of reagents into the final product (CE) and use of all reaction auxiliaries (MI and MP). The greater product yield achieved in $scCO_2$ obviously enhanced both CE and MP, while the release of $scCO_2$ (not harmful to the environment) by depressurization did not imply any solvent/waste to be recycled/disposed of and simplified the product isolation. Although this assessment did not consider the overall energy balance, from the chemical standpoint, the analysis of green metrics demonstrated that $scCO_2$ was efficient at improving the sustainability of the described biocatalytic protocol compared to a liquid medium such as EMK.

References

1. P. Carlès, *J. Supercrit. Fluids*, 2010, **53**, 2–11.
2. P. Staša, K. Chovancová, V. Kebo, J. Chovanec and O. Kodym, *Procedia Earth Planet. Sci.*, 2013, **6**, 14–23.
3. A. R. C. Morais, A. M. da Costa Lopes and R. Bogel-Łukasik, *Chem. Rev.*, 2015, **115**, 3–27.
4. Y. Zhou (周永), J. Wu (吴江涛) and E. W. Lemmon, *J. Phys. Chem. Ref. Data*, 2011, **40**, 043106.
5. T. Yan, J. Xu, L. Wang, Y. Liu, C. Yang and T. Fang, *RSC Adv.*, 2015, **5**, 75129–75140.
6. I. Medina, *J. Chromatogr. A*, 2012, **1250**, 124–140.
7. *Applications of Supercritical Fluids in Industrial Analysis*, ed. J. R. Dean, Springer Netherlands, Dordrecht, 1993.
8. A. P. Abbott and C. A. Eardley, *J. Phys. Chem. B*, 1999, **103**, 2504–2509.
9. J. A. Branch and P. N. Bartlett, *Philos. Trans. R. Soc., A*, 2015, **373**, 20150007.
10. F. Maxim, C. Contescu, P. Boillat, B. Niceno, K. Karalis, A. Testino and C. Ludwig, *Nat. Commun.*, 2019, **10**, 4114.
11. G. Guevara-Carrion, S. Ancherbak, A. Mialdun, J. Vrabec and V. Shevtsova, *Sci. Rep.*, 2019, **9**, 8466.
12. S. Deguchi and N. Ifuku, *Angew. Chem., Int. Ed.*, 2013, **52**, 6409–6412.
13. M. Perrut and V. Perrut, in *Gases in Agro-food Processes*, Academic Press, London, 2019, pp. 483–509.
14. *Supercritical Fluids*, ed. Y. Arai, T. Sako and Y. Takebayashi, Springer Berlin Heidelberg, Berlin, Heidelberg, 2002.
15. M. P. E. Ishmael, M. Z. Lukawski and J. W. Tester, *J. Supercrit. Fluids*, 2016, **117**, 72–79.
16. X. L. Cao, Z. H. Rao and S. M. Liao, *Appl. Therm. Eng.*, 2011, **31**, 2374–2384.
17. D. Bolmatov, V. V. Brazhkin and K. Trachenko, *Nat. Commun.*, 2013, **4**, 2331.
18. *Chemical Synthesis Using Supercritical Fluids*, ed. P. G. Jessop and W. Leitner, Wiley, 1st edn, 1999.

19. K. Zosel, *Angew. Chem.*, 1978, **90**, 748–755.
20. K.-Y. Khaw, M.-O. Parat, P. N. Shaw and J. R. Falconer, *Molecules*, 2017, **22**, 1186.
21. X. Dai, L. Shi, Q. An and W. Qian, *Appl. Therm. Eng.*, 2018, **128**, 1095–1101.
22. A. Capuzzo, M. Maffei and A. Occhipinti, *Molecules*, 2013, **18**, 7194–7238.
23. B. P. Nobre, L. Gouveia, P. G. S. Matos, A. F. Cristino, A. F. Palavra and R. L. Mendes, *Molecules*, 2012, **17**, 8397–8407.
24. C. Da Porto, D. Decorti and A. Natolino, *J. Supercrit. Fluids*, 2014, **87**, 1–8.
25. T. Maschmeyer, R. Luque and M. Selva, *Chem. Soc. Rev.*, 2020, **49**, 4527–4563.
26. P. Yadav, M. Agrawal, A. Alexander, R. Patel, S. Siddique, S. Saraf and Ajazuddin, in *Green Sustainable Process for Chemical and Environmental Engineering and Science*, Elsevier, 2020, pp. 1–16.
27. M. F. Kemmere, in *Supercritical Carbon Dioxide*, ed. M. F. Kemmere and T. Meyer, Wiley-VCH Verlag GmbH & Co. KGaA, Weinheim, FRG, 2006, pp. 1–14.
28. T. Hoefling, D. Stofesky, M. Reid, E. Beckman and R. M. Enick, *J. Supercrit. Fluids*, 1992, **5**, 237–241.
29. J. M. DeSimone, Z. Guan and C. S. Elsbernd, *Science*, 1992, **257**, 945–947.
30. F. Florit, P. Rodrigues Bassam, A. Cesana and G. Storti, *Processes*, 2020, **8**, 850.
31. J.-N. Ollagnier, T. Tassaing, S. Harrisson and M. Destarac, *React. Chem. Eng.*, 2016, **1**, 372–378.
32. T. J. Romack, E. E. Maury and J. M. DeSimone, *Macromolecules*, 1995, **28**, 912–915.
33. C. Boyère, C. Jérôme and A. Debuigne, *Eur. Polym. J.*, 2014, **61**, 45–63.
34. Y. Medina-Gonzalez, S. Camy and J.-S. Condoret, *Int. J. Sustainable Eng.*, 2012, **5**, 47–65.
35. S. Zheng, X. Hu, A.-R. Ibrahim, D. Tang, Y. Tan and J. Li, *Recent Pat. Chem. Eng.*, 2010, **3**, 230–244.
36. J. R. Williams, A. A. Clifford and S. H. R. Al-Saidi, *Mol. Biotechnol.*, 2002, **22**, 263–286.
37. Ž. Knez, E. Markočič, M. Leitgeb, M. Primožič, M. Knez Hrnčič and M. Škerget, *Energy*, 2014, **77**, 235–243.
38. N. M. Lawandy and A. Y. Smuk, *Ind. Eng. Chem. Res.*, 2014, **53**, 530–540.
39. T. Adschiri, Y.-W. Lee, M. Goto and S. Takami, *Green Chem.*, 2011, **13**, 1380.
40. P. S. Shah, T. Hanrath, K. P. Johnston and B. A. Korgel, *J. Phys. Chem. B*, 2004, **108**, 9574–9587.
41. S. D. Manjare and K. Dhingra, *Mater. Sci. Energy Technol.*, 2019, **2**, 463–484.
42. M. N. Araújo, A. Q. P. L. Azevedo, F. Hamerski, F. A. P. Voll and M. L. Corazza, *Ind. Crops Prod.*, 2019, **141**, 111723.
43. J. Peach and J. Eastoe, *Beilstein J. Org. Chem.*, 2014, **10**, 1878–1895.
44. K. A. Consan and R. D. Smith, *J. Supercrit. Fluids*, 1990, **3**, 51–65.

45. J. Eastoe, S. Gold, S. E. Rogers, A. Paul, T. Welton, R. K. Heenan and I. Grillo, *J. Am. Chem. Soc.*, 2005, **127**, 7302–7303.
46. J. Liu, S. Cheng, J. Zhang, X. Feng, X. Fu and B. Han, *Angew. Chem., Int. Ed.*, 2007, **46**, 3313–3315.
47. A. Chandran, K. Prakash and S. Senapati, *J. Am. Chem. Soc.*, 2010, **132**, 12511–12516.
48. M. Klostermann, R. Strey, T. Sottmann, R. Schweins, P. Lindner, O. Holderer, M. Monkenbusch and D. Richter, *Soft Matter*, 2012, **8**, 797–807.
49. M. Sagisaka, S. Iwama, S. Ono, A. Yoshizawa, A. Mohamed, S. Cummings, C. Yan, C. James, S. E. Rogers, R. K. Heenan and J. Eastoe, *Langmuir*, 2013, **29**, 7618–7628.
50. K. J. Ivin and J. C. Mol, *Olefin Metathesis and Metathesis Polymerization*, Academic Press, San Diego, 1997.
51. M. Schuster and S. Blechert, *Angew. Chem., Int. Ed. Engl.*, 1997, **36**, 2036–2056.
52. A. M. Thayler, *Chem. Eng. News*, 2007, **85**, 37–47.
53. Y. Chauvin, *Angew. Chem., Int. Ed.*, 2006, **45**, 3740–3747.
54. R. R. Schrock, *Angew. Chem., Int. Ed.*, 2006, **45**, 3748–3759.
55. R. H. Grubbs, *Angew. Chem., Int. Ed.*, 2006, **45**, 3760–3765.
56. J. M. DeSimone and C. D. Mistele, *US Pat.*, 5840820, 1998.
57. A. Fürstner, L. Ackermann, K. Beck, H. Hori, D. Koch, K. Langemann, M. Liebl, C. Six and W. Leitner, *J. Am. Chem. Soc.*, 2001, **123**, 9000–9006.
58. A. Fürstner, W. Leitner, D. Koch, K. Langemann and C. Six, *US Pat.*, 6348551, 2002.
59. W. Leitner, N. Theyssen, Z. Hou, K. W. Kottsieper, M. Solinas and D. Giunta, *US Pat.*, 20060252951, 2006.
60. A. Stark, M. Ajam, M. Green, H. G. Raubenheimer, A. Ranwell and B. Ondruschka, *Adv. Synth. Catal.*, 2006, **348**, 1934–1941.
61. M. Selva, A. Perosa, M. Fabris and P. Canton, *Green Chem.*, 2009, **11**, 229–238.
62. M. Selva, S. Guidi, A. Perosa, M. Signoretto, P. Licence and T. Maschmeyer, *Green Chem.*, 2012, **14**, 2727.
63. R. Duque, E. Öchsner, H. Clavier, F. Caijo, S. P. Nolan, M. Mauduit and D. J. Cole-Hamilton, *Green Chem.*, 2011, **13**, 1187.
64. S. A. Egorov, A. Yethiraj and J. L. Skinner, *Chem. Phys. Lett.*, 2000, **317**, 558–566.
65. E. J. Beckman, *J. Supercrit. Fluids*, 2004, **28**, 121–191.
66. M. J. Climent, A. Corma and S. Iborra, *Green Chem.*, 2014, **16**, 516.
67. R.-J. van Putten, J. C. van der Waal, E. de Jong, C. B. Rasrendra, H. J. Heeres and J. G. de Vries, *Chem. Rev.*, 2013, **113**, 1499–1597.
68. T. Wang, M. W. Nolte and B. H. Shanks, *Green Chem.*, 2014, **16**, 548–572.
69. M. Möller, F. Harnisch and U. Schröder, *Biomass Bioenergy*, 2012, **39**, 389–398.
70. M. Watanabe, Y. Aizawa, T. Iida, R. Nishimura and H. Inomata, *Appl. Catal., A*, 2005, **295**, 150–156.

71. C. Promdej and Y. Matsumura, *Ind. Eng. Chem. Res.*, 2011, **50**, 8492–8497.
72. S. Souzanchi, L. Nazari, K. T. V. Rao, Z. Yuan, Z. Tan and C. Xu, *Catal. Today*, 2019, **319**, 76–83.
73. B. M. Kabyemela, T. Adschiri, R. M. Malaluan and K. Arai, *Ind. Eng. Chem. Res.*, 1997, **36**, 1552–1558.
74. B. M. Kabyemela, T. Adschiri, R. M. Malaluan, K. Arai and H. Ohzeki, *Ind. Eng. Chem. Res.*, 1997, **36**, 5063–5067.
75. B. M. Kabyemela, T. Adschiri, R. Malaluan and K. Arai, *Ind. Eng. Chem. Res.*, 1997, **36**, 2025–2030.
76. B. M. Kabyemela, T. Adschiri, R. M. Malaluan and K. Arai, *Ind. Eng. Chem. Res.*, 1999, **38**, 2888–2895.
77. A. Sinag, A. Kruse and V. Schwarzkopf, *Eng. Life Sci.*, 2003, **3**, 469–473.
78. M. Sasaki, K. Goto, K. Tajima, T. Adschiri and K. Arai, *Green Chem.*, 2002, **4**, 285–287.
79. Z. Srokol, A.-G. Bouche, A. van Estrik, R. C. J. Strik, T. Maschmeyer and J. A. Peters, *Carbohydr. Res.*, 2004, **339**, 1717–1726.
80. K. Goto, K. Tajima, M. Sasaki, T. Adschiri and K. Arai, *Kobunshi Ronbunshu*, 2001, **58**, 685–691.
81. D. Klingler and H. Vogel, *J. Supercrit. Fluids*, 2010, **55**, 259–270.
82. C. Sun, R. Hui, W. Qu and S. Yick, *Corros. Sci.*, 2009, **51**, 2508–2523.
83. P. Kritzer, *J. Supercrit. Fluids*, 2004, **29**, 1–29.
84. M. M. Gui, K. T. Lee and S. Bhatia, *J. Supercrit. Fluids*, 2009, **49**, 286–292.
85. S. Saka and D. Kusdiana, *Fuel*, 2001, **80**, 225–231.
86. Y. Warabi, D. Kusdiana and S. Saka, *Bioresour. Technol.*, 2004, **91**, 283–287.
87. Y. Hiejima and M. Yao, *J. Chem. Phys.*, 2003, **119**, 7931–7942.
88. J. K. Satyarthi, D. Srinivas and P. Ratnasamy, *Energy Fuels*, 2009, **23**, 2273–2277.
89. I. M. Atadashi, M. K. Aroua, A. R. A. Aziz and N. M. N. Sulaiman, *Appl. Energy*, 2011, **88**, 4239–4251.
90. I. J. Stojković, O. S. Stamenković, D. S. Povrenović and V. B. Veljković, *Renewable Sustainable Energy Rev.*, 2014, **32**, 1–15.
91. Y. Isayama and S. Saka, *Bioresour. Technol.*, 2008, **99**, 4775–4779.
92. O. Farobie, K. Sasanami and Y. Matsumura, *Appl. Energy*, 2015, **147**, 20–29.
93. N. Akkarawatkhoosith, A. Kaewchada and A. Jaree, *Energy Fuels*, 2019, **33**, 5322–5331.
94. A. Velez, G. Soto, P. Hegel, G. Mabe and S. Pereda, *Fuel*, 2012, **97**, 703–709.
95. S. V. Mazanov, A. R. Gabitova, R. A. Usmanov, F. M. Gumerov, S. Labidi, M. B. Amar, J.-P. Passarello, A. Kanaev, F. Volle and B. L. Neindre, *J. Supercrit. Fluids*, 2016, **118**, 107–118.
96. L. Soh and M. J. Eckelman, *ACS Sustainable Chem. Eng.*, 2016, **4**, 5821–5837.
97. J. Andraos, *ACS Sustainable Chem. Eng.*, 2018, **6**, 3206–3214.

98. K. C. Badgujar and B. M. Bhanage, *Biomass Bioenergy*, 2016, **84**, 12–21.
99. P. Lozano, E. García-Verdugo, R. Piamtongkam, N. Karbass, T. De Diego, M. I. Burguete, S. V. Luis and J. L. Iborra, *Adv. Synth. Catal.*, 2007, **349**, 1077–1084.
100. J. Andraos, *Pure Appl. Chem.*, 2011, **83**, 1361–1378.
101. J. Andraos and A. Hent, *J. Chem. Educ.*, 2015, **92**, 1820–1830.

CHAPTER 11

Challenges of Using Fluorous Solvents for Greener Organic Synthesis

HIROSHI MATSUBARA*[a], TAKUJI KAWAMOTO[b] AND ILHYONG RYU*[a,c]

[a]Department of Chemistry, Graduate School of Science, Osaka Prefecture University, Sakai, Osaka 599-8531, Japan; [b]Department of Applied Chemistry, Yamaguchi University, Ube, Yamaguchi 755-8611, Japan; [c]Department of Applied Chemistry, National Yang Ming Chiao Tung University (NYCU), Hsinchu 30010, Taiwan
*E-mail: ryu@c.s.osakafu-u.ac.jp, matsu@c.s.osakafu-u.ac.jp

11.1 Introduction

The term "fluorous" expresses philicity to perfluoroalkanes, which is analogous to the term "aqueous" expressing philicity to water. The term fluorous was first introduced by Horváth and Rábai in 1994 in their landmark work in fluorous chemistry.[1] The fluorous reactions, which are based on fluorous reagents and catalysts, naturally require fluorous solvents and fluorinated organic solvents.[2,3] Interestingly, developments of fluorous chemistry over a quarter of a century[4] have also encouraged organic chemists to find and use fluorous solvents that will work in "non-fluorous" ordinary organic reactions. Researchers are familiar with traditional fluorous solvents, such as trifluoroacetic acid (CF_3CO_2H: TFA) and hexafluoroisopropanol ($CF_3CHOHCF_3$: HFIP), but these have found more specific uses as

Sustainable Organic Synthesis: Tools and Strategies
Edited by Stefano Protti and Alessandro Palmieri

Published by the Royal Society of Chemistry, www.rsc.org

acidic reagents or additives, because of the notable presence of electron-withdrawing trifluoromethyl groups.

Among fluorous solvents, the use of perfluorinated hydrocarbons, such as perfluorohexanes (FC-72™), in synthetic reactions has been limited. Rather than as a reaction solvent, FC-72 is used conveniently as an extractive solvent for precious fluorous reagents and catalysts. Perfluorocarbons are generally immiscible with water and organic solvents at room temperature, except for some low molecular weight solvents such as pentane and ether. When perfluorocarbons are mixed with water or organic solvents, the water or organic phases take a position at the upper layer, while the denser fluorous phase is relegated to the lower layer. In many cases, however, a mixed-solvent system composed of perfluorinated and organic solvents can become homogeneous when heated. This thermomorphic behaviour in a fluorous/organic mixed system was applied successfully by Horváth and Rábai in hydroformylation reactions of alkenes with fluorous Rh-catalysts,[1] in which a binary solvent system composed of toluene and perfluoroheptane was used. After the reaction, upon cooling, these two solvents are separated again, which enables the facile separation of an Rh-catalyst with a fluorous phosphine ligand in the fluorous layer from organic products in the organic layer. Thermomorphic behaviours are among the most attractive aspects of fluorous chemistry, and these form the basis of the fluorous-tagged method and fluorous mixture synthesis that was developed by Curran.[5]

The rapid progress in fluorous chemistry has shed light on the use of fluorous-organic hybrid solvents, such as benzotrifluoride (BTF)[6] and the fluorous organic hybrid ether F-626 ($C_6F_{13}CH_2CH_2OCH(CH_3)CH_2CH(CH_3)CH_3$).[7] These hybrid solvents possess modest polarity and have the potential to be applied as solvents in non-fluorous organic reactions. Unfortunately, F-626 is yet to be commercially available, but lower-boiling hybrid ethers such as Novec 7100 ($CH_3OC_4F_9$) and 7200 ($C_2H_5OC_4F_9$) are available from 3M. Despite the limited number of applications, fluorous polyethers, commercially provided as Galden from Solvay, have boiling points that range upwards of 270 °C, and have shown potential for use as green solvents in terms of low volatility, thermal stability, and recyclability. In this chapter, we focus mainly on typical fluorous solvents and their use in organic reactions. Fluorous solvents are denser than either organic solvents or water, and they are capable of creating multiphasic liquid layers. Such a unique property has been exploited in phase-vanishing (PV) methods,[8] which take advantage of spontaneous reactions based on diffusion, and represent a low-energy green process. The efforts towards using fluorous media as a green substitute for organic solvents have grown steadily after we published our review on fluorous-organic-hybrid solvents in 2012.[9] It should be noted that an excellent review was published by Lo and Horváth in 2015.[10] That study provides a guide to the variety of fluorous ether solvents, and we encourage readers to refer to their work for further understanding.

11.2 Perfluorinated Solvents

11.2.1 Physical Properties of Perfluorocarbons and Perfluorinated Polyethers

In the present review, four types of perfluorocarbons, FC-72, PFMC, FC-77, and PFD, are highlighted together with their corresponding hydrocarbon counterparts in Table 11.1. The spectral polarity index (Ps) is a guide to the polarity of solvents, boiling points and densities of the four types of perfluorocarbons, together with those of the corresponding hydrocarbons. Since perfluorocarbons have only a slight polarity, as shown in the Table, they are generally immiscible with water and organic solvents, with the exception of some low molecular weight solvents such as pentane and ether, at room temperature and tend to form an independent phase (fluorous phase). The densities of these perfluorocarbons (d = 1.670 to 1.908) are even larger than those of "heavy organic solvents" such as chloroform (d = 1.480) and carbon tetrachloride (d = 1.584). Thus, when perfluorocarbons are mixed with organic solvents, the two layers generally show a lighter organic phase that forms the upper layer, and the denser fluorous phase makes up a lower layer. Such biphasic-phasic systems are available for biphasic extraction and unique multi-phasic synthetic methods, such as phase-vanishing (PV) (*vide infra*, see Chapter 11.4).

There are many cases wherein a mixed solvent system composed of perfluorinated solvents and organic solvents becomes homogeneous upon heating. Miscible temperatures of typical combinations between perfluorocarbon and organic solvents are listed in Table 11.2. Such thermomorphic behaviours are among the most attractive aspects of fluorous technologies and were initially used in fluorous-tagged methods.[3–5]

Table 11.1 Physical properties of perfluorocarbons and the corresponding hydrocarbons.

Perfluorocarbons	bp/°C	Ps	d	Hydrocarbons	bp/°C	Ps	d
C_6F_{14}(FC-72)	58–60	0.00	1.670	C_6H_{14}	69.0	2.56	0.655
c-$C_6F_{11}CF_3$(PFMC)	76.0	0.46	1.787	*c*-$C_6H_{11}CH_3$	101	3.34	0.765
C_8F_{18}(FC-77)	100–105	0.55	1.766	C_8H_{18}	125–127	2.86	0.703
Perfluorodecalin (PFD)	142	—	1.908	Decalin	190	—	0.883

Table 11.2 Thermomorphic behaviour of perfluorocarbons.[11]

Perfluorocarbons	Organic solvents	Mixing temp. °C
PFMC	$CHCl_3$	50.1
PFMC	C_6H_6	84.9
PFMC	Toluene	88.6
PFD	Toluene	64.0
PFMC	Hexane	RT
PFMC	Ether	RT

Table 11.3 Properties of perfluorinated polyethers.

	Galden HT135	Galden HT200	Krytox GPL101	Krytox GPL103
Usable temperature/°C	−70~+100	−50~+160	−70~104	−60~155
Density/g cm^{-3}	1.73	1.79	1.89	1.92
Kinetic viscosity (25 °C)/cSt	1.0	2.4	8	30

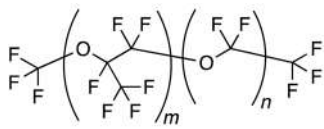

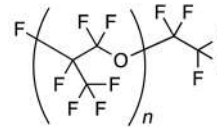

A wide variety of perfluorinated polyethers are commercially available as Galden (Solvay Inc.) and Krytox (Krytox Inc.), and these have found industrial utility as thermally durable lubricants. The physical properties of the four perfluorinated polyethers are listed in Table 11.3. Perfluorinated polyethers can be used at higher temperatures and some are even designed for use at temperatures approaching 260 °C. The densities of perfluorinated polyethers are similar to those of perfluorocarbons, while their viscosities are higher than those of monomer-type solvents, which is inherent to the increased molecular weight. Perfluorinated polyethers have shown excellent potential as "greener solvents," in terms of heat durability, low vapor pressures, and recyclability.

11.2.2 Organic Synthesis Using Perfluorinated Solvents

Otera and co-workers carried out aldol reaction of silyl enolates with benzaldehyde in the presence of fluorous stannoxane as a catalyst (Scheme 11.1).[12] The use of a 5/1 mixture of FC-72 (pefluorohexanes) with CH_2Cl_2 as a solvent gave the best results.

Jung and Bräse reported the synthesis of fluoroarenes from either diazonium salts or triazenes *via* a Sandmeyer-type fluoride introduction (Scheme 11.2).[13] When ordinary organic solvents, such as THF, DMF, and MeOH, were used, undesirable reactions occurred, whereas FC-72 returned good yields of fluoroarenes.

Itoh and co-workers reported that photo-oxidative oxylactonization of oxocarboxylic acids was affected by trifluoroacetic anhydride (Scheme 11.3).[14] While FC-72 gave a good yield, ordinary organic solvents were less efficient. This can be explained *via* the high solubility of oxygen gas by FC-72.

Shimizu and co-workers reported a Diels–Alder reaction using a hexameric capsule of resorcinarene bearing fluorous feet in FC-72 (Scheme 11.4). Separation of the capsule could be conveniently carried out by simple decantation.[15]

A convenient method for the *o*-perfluoroalkylation of aromatic triazines was developed by Bräse and co-workers (Scheme 11.5).[16] While the use of either DMF or acetonitrile as a solvent suffers from the formation of byproducts, the use of FC-72 gave good yields of the desired trifluoromethylated products.

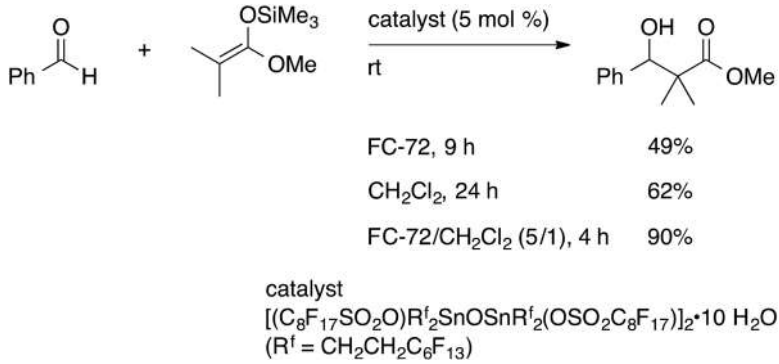

Scheme 11.1 Aldol reaction in the presence of fluorous stannoxane as a catalyst.

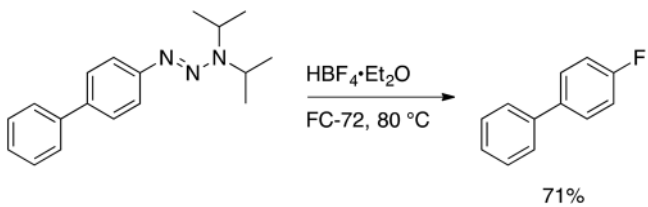

Scheme 11.2 Synthesis of fluoroarenes from either diazonium salts or triazenes *via* a Sandmeyer-type fluoride introduction.

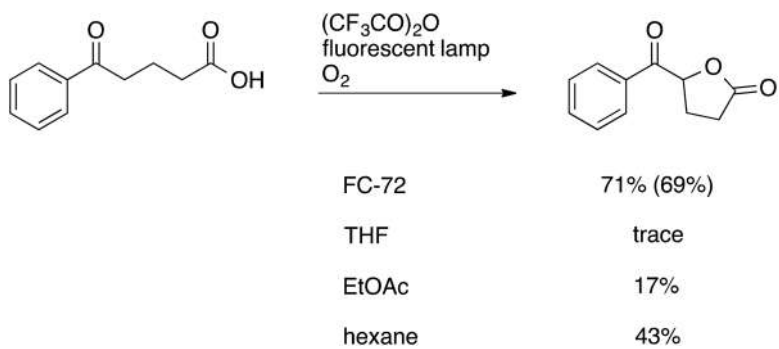

Scheme 11.3 Photo-oxidative oxylactonization of oxocarboxylic acids.

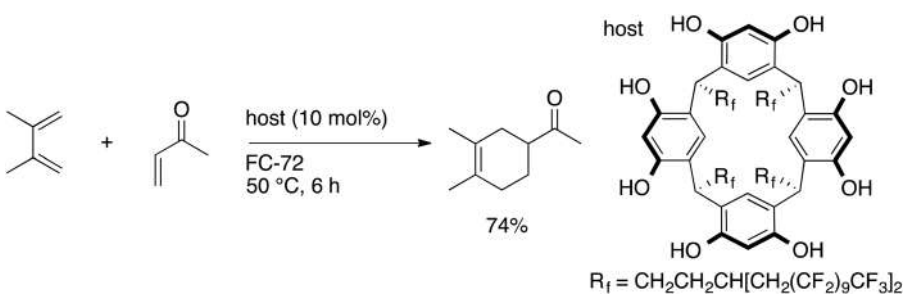

Scheme 11.4 Diels–Alder reaction using a hexameric capsule of resorcinarene bearing fluorous feet.

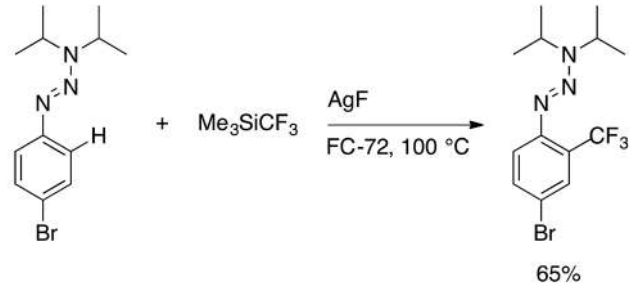

Scheme 11.5 o-Trifluoromethylation of an aromatic triazine.

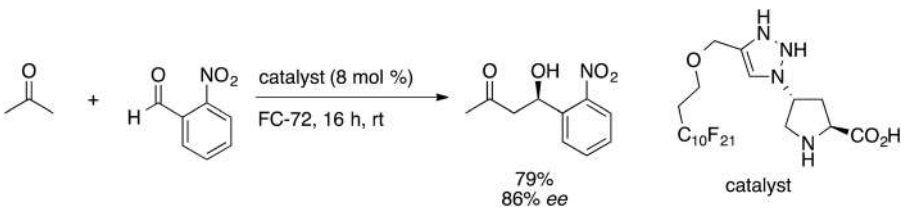

Scheme 11.6 Enantioselective aldol reaction using a fluorous proline catalyst.

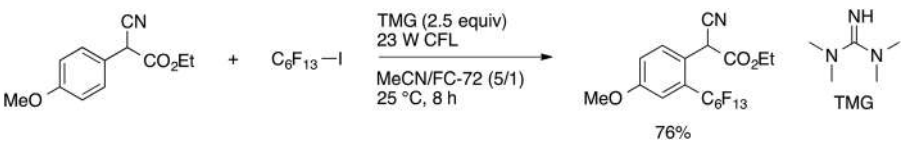

Scheme 11.7 Aromatic perfluoroalkylation of α-cyano aryl acetate.

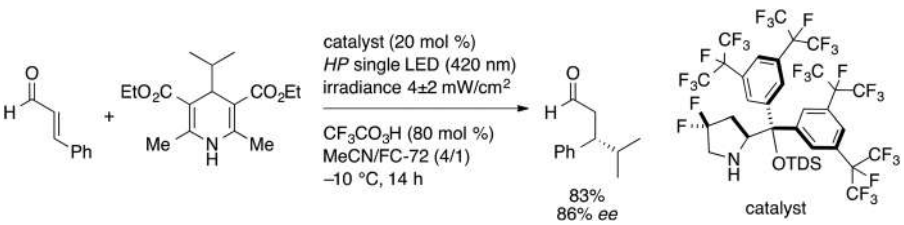

Scheme 11.8 Enantioselective radical β-alkylation of α,β-enal.

Pericàs reported enantioselective aldol reaction using a fluorous proline catalyst. Both the chiral catalyst and the FC-72 solvent are easily recycled for reuse (Scheme 11.6).[17]

Melchiorre and co-workers reported the aromatic perfluoroalkylation of α-cyano aryl acetate (Scheme 11.7).[18] To prevent inhibition of the desired reaction by the products, a biphasic system using FC-72 and acetonitrile was employed. A high stirring speed improved the overall yield.

Melchiorre and co-workers have also reported enantioselective radical β-alkylation of α,β-enals (Scheme 11.8).[19] Due to the improvement of the

solubility of a highly fluorinated chiral catalyst, FC-72 was used as a co-solvent with acetonitrile.

11.3 Fluorous-organic Hybrid Solvents

11.3.1 Physical Properties of Fluorous-organic Hybrid Solvents

Due to their amphiphilic nature, fluorous-organic hybrid solvents are expected to have utility in ordinary non-fluorous organic reactions.[9] Some physical properties of the known hybrid solvents, hydrofluorocarbon **1**–**3**, fluorous ether **4**–**6**, and fluorous DMF **7**, are listed in Table 11.4. These hybrid solvents are miscible with both perfluorocarbons and organic solvents and are often employed as co-solvents for fluorous reactions; however, they are also useful for ordinary non-fluorous organic reactions.[9] These hybrid solvents are generally more expensive than organic solvents, but they could attract more attention as designer solvents with proven green potential due to characteristics such as excellent recyclability ensured by easy separability from the reaction mixtures, easy purification by distillation, and an overall lower environmental burden.

Benzotrifluoride (BTF) **1** is a clear, low-viscosity liquid with a boiling point of 102 °C, a melting point of −29 °C, and a density of 1.190 g mL^{-3}. When considering the absorption spectra of pyridinium *N*-phenolate betaine dye, BTF is slightly more polar than THF and slightly less polar than dichloromethane (Table 11.5). The approximate partition coefficients of BTF, F-626, and F-DMF are listed in Table 11.6, which reflects the degree of the fluorous nature of these hybrid solvents.

Table 11.4 Physical data of fluorous organic hybrid solvents.[20]

Solvent	Molecular formula	Bp (°C)	Mp (°C)	n_D	d	wt% of F
1: BTF	$C_6H_5CF_3$	102[a]	−29[b]	1.413[c]	1.182[c]	39.0
2: Solkane 356mfc	$CF_3CH_2CF_2CH_3$	40[e]	−36[e]	1.282[f]	1.267[f]	64.2
3: Vertrel XF[d]	$CF_3CHFCHFCF_2CF_3$	55	−80	—	1.580	75.4
4: F-626[g]	$C_4F_9(CH_2)_2OCH(CH_3)CH_2CH(CH_3)_2$	214	−110	1.342	1.354	49.1
5: Novec7100[h]	$CH_3OC_4F_9$	61	−135	1.270	1.520	68.4
6: Novec7200[h]	$C_2H_5OC_4F_9$	76	−138	1.280	1.430	68.9
7: F-DMF[i]	$C_6F_{13}(CH_2)_3N(CH_3)CHO$	110/0.75 mm Hg	−38	1.359	1.563	58.9

Table 11.5 Solvent E_T values of BTF and other organic solvents.[21a,a]

	THF	BTF	CH_2Cl_2	DMF	CH_3CN
E_T^{30}/kcal mol^{-1}	37.4(37.4)	39.3	41.0(40.7)	43.3(43.2)	45.7(45.6)
$E_T^N \times 100$	20.7(20.7)	26.5	31.8(30.9)	38.9(38.6)	46.3(46.0)

[a]Values taken from ref. 21b are shown in parentheses.

Table 11.6 Approximate partition coefficients of BTF, F-626, and F-DMF.

	Organic solvent/FC-72		
	BTF[a]	F-626[a]	F-DMF[b]
CH_3CN	1/0.13	1/7.3	1/0.078
CH_3OH	1/0.21	1/3.8	1/0.05
C_6H_6	1/0.18	1/1.6	1/1.13
Cyclohexane	—[c]	—[c]	1/8.30
$CHCl_3$	1/0.16	1/0.85	1/0.13
AcOEt	1/0.13	1/0.85	1/0.20
Acetone	1/0.08	1/1.1	1/0.10

[a]Ref. 7.
[b]Ref. 34.
[c]Not measured.

11.3.2 Organic Synthesis Using Fluorous-organic Hybrid Solvents

BTF is often used as a substitute for toxic dichloromethane. This was originated by Curran and Ogawa, who reported several notable cases in which BTF served as a useful alternative solvent to CH_2Cl_2 (Scheme 11.9).[6] For example, Swern oxidation of secondary alcohols was performed using BTF as a solvent.

Obora and Ishii reported intermolecular oxidative allylic amination of simple alkenes with amines (Scheme 11.10).[22] BTF and FC-72 are suitable solvents for the formation of allylic amines.

Solkane 365mfc (1,1,3,3-pentafluorobutane, **2**) is a low-viscosity liquid with a boiling point of 40 °C and a melting point of −36 °C. Its density is 1.267 g mL^{-3}, which is slightly heavier than 1,2-dochloroethane. Vertrel XF (2*H*,3*H*-perfluoropentane, **3**) is also a low-viscosity liquid with a boiling point of 55 °C and a melting point of −80 °C. Its density is 1.580 g mL^{-3}, which approximates that of carbon tetrachloride. Because the ozone depletion potential of these solvents is zero, they are expected to be viable green alternatives for traditional chlorinated organic solvents.

Shibata and co-workers reported the trifluoromethylation of aldehydes or ketones using a Ruppert-Prakash reagent (Me_3SiCF_3) with Solkane 365mfc as a solvent (Scheme 11.11).[23] Although bases such as LiOAc and P(*t*-Bu)$_3$ are commonly used for reactions in DMF and THF, they were not effective in this reaction, and the use of catalytic amounts of KOH or CsF in Solkane 365mfc at room temperature produced the desired reaction.

Solkane 365mfc is a suitable solvent for Friedel–Crafts alkylation of indoles with ethyl trifluoropyruvate and glyoxylate (Scheme 11.12). Whereas, in the absence of a catalyst, Friedel–Crafts alkylation of indole

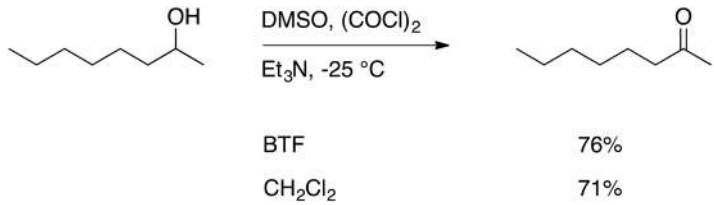

Scheme 11.9 Swern oxidation in BTF.

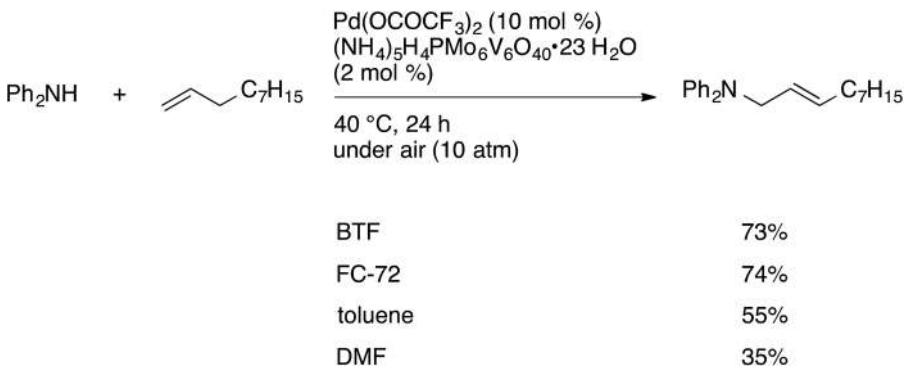

Scheme 11.10 Intermolecular oxidative allylic amination.

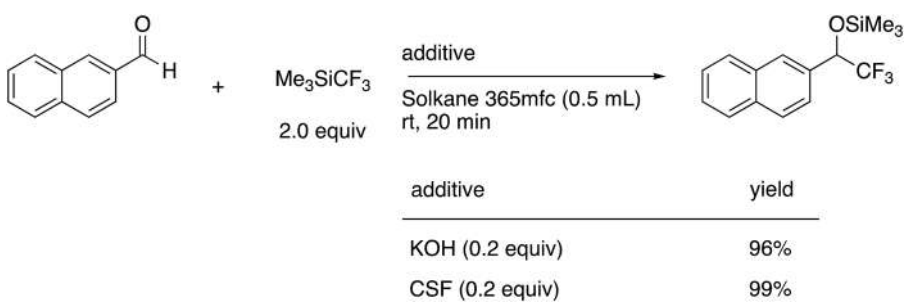

Scheme 11.11 Nucleophilic trifluoromethylation in Solkan 365mfc.

with ethyl trifluoropyruvate proceeds sluggishly in ether (reaction time: 24 h), they accomplished a similar reaction in 1 h using Solkane 365mfc as a solvent.[24]

A Glaser type of homo coupling of terminal alkynes was conducted using Solkane 365mfc as a solvent (Scheme 11.13).[25]

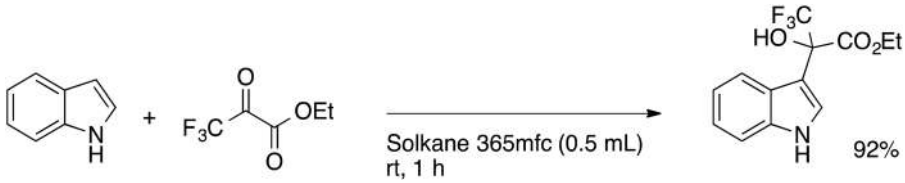

Scheme 11.12 Friedel–Crafts alkylation of indol with ethyl trifluoropyruvate and glyoxylate in Solkane 365mfc.

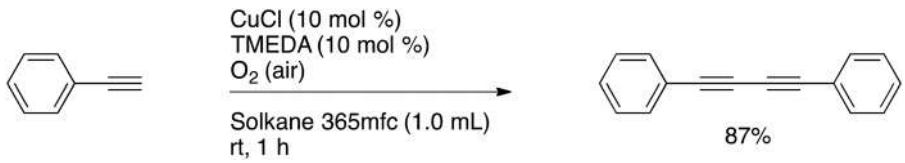

Scheme 11.13 Glaser-type homo coupling of a terminal alkyne in Solkane 365mfc.

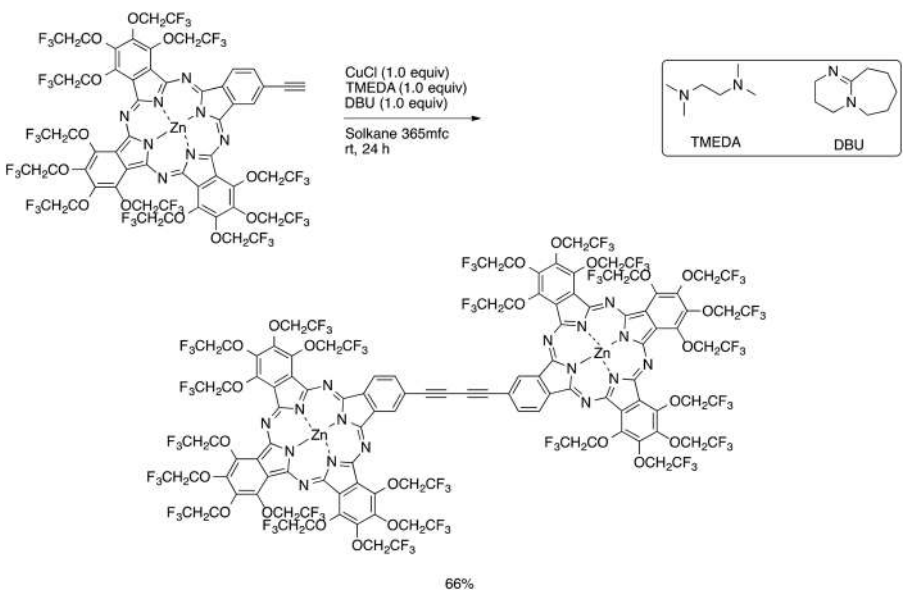

Scheme 11.14 Glaser-type coupling to synthesize trifluoroethoxy-substituted binuclear phthalocyanine.

The same group reported a Glaser-type coupling to synthesize trifluoroethoxy-substituted binuclear phthalocyanine using Solkane 365mfc as the solvent (Scheme 11.14).[26]

Blended Solkanes [93/7 mixture of Solkane 365mfc and 227 (1,1,1,2,3,3,3-heptafluoropropane)] are known to have no flash point and work as well as Solkane 365 mfc. Shibata reported the trifluoromethanesulfonylation of indoles leading to indole triflones, in which the blended Solkanes are comparable to dichloromethane or nitromethane (Scheme 11.15).[27]

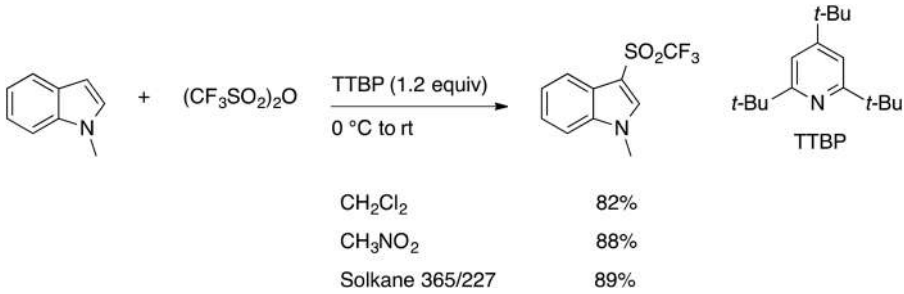

Scheme 11.15 Trifluoromethanesulfonylation of *N*-methyl indole using blended Solkanes.

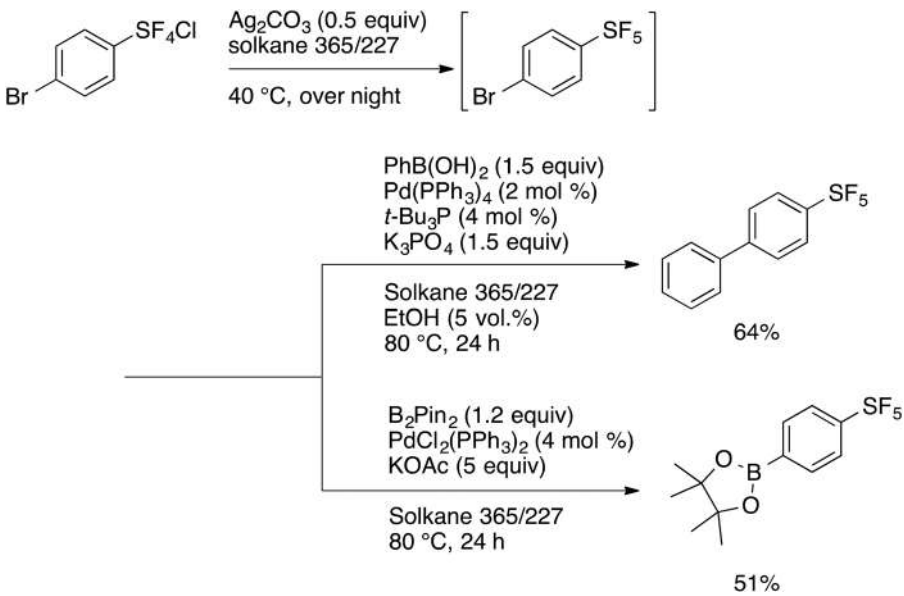

Scheme 11.16 Silver carbonate-induced Cl–F exchange of arylsulfur chlorotetrafluoride in blended Solkanes.

A silver carbonate-induced Cl–F exchange of arylsulfur chlorotetrafluorides was reported by the same group (Scheme 11.16). The reaction of *p*-bromophenylsulfur chlorotetrafluoride with silver carbonate in blended Solkanes 365/227 generates Ar-SF_5. Palladium-catalyzed coupling reactions, such as Suzuki coupling and Miyaura borylation, were successfully carried out in a one-pot reaction using the same solvent system.[28]

F-626 **4** (1*H*,1*H*,2*H*,2*H*-perfluorooctyl-1,3-dimethylbutyl ether) is an ether-type fluorous/organic hybrid solvent (bp 214 °C, glass transition −110 °C). F-626 is a colourless, clear, slightly viscous liquid, and is miscible with common organic solvents, but it is barely soluble in water. F-626 can be used as a solvent for fluorous reactions, such as fluorous tin hydride-based radical reactions[7] and Mizoroki–Heck reactions[29] using a fluorous Pd catalyst, but

it can also be used for ordinary non-fluorous reactions. For example, when F-626 was used either in the LAH reduction of esters or in Pd/C catalyzed hydrogenation, the desired products were obtained in similar yields to those using ether (Scheme 11.17). Then, the used F-626 is easily recovered by fluorous/organic biphasic workup and reused.

Standard high temperature reactions are performed using high-boiling-point organic solvents such as diethylene glycol, DMF, ortho-dichlorobenzene, diphenyl ether, *etc.* In these reactions, high-boiling-point organic solvents are generally removed from the product by aqueous treatment and/or distillation. However, aqueous treatment produces waste and distillation requires a high level of energy. In contrast, due to its fluorous nature, F-626 can be easily removed in a fluorous/organic biphasic workup and used as a reusable solvent. This has been demonstrated *via* Vilsmeier formylation (Scheme 11.18, Eqn (11.1)), Wolff-Kishner reduction (Scheme 11.18, Eqn (11.2)), Diels–Alder reaction (Scheme 11.18, Eqn (11.3)), and retro-aldol reaction (Scheme 11.18, Eqn (11.4)).[30]

The fluorous organic hybrid ether solvents Novec 7100 **5** (isomeric mixtures of methyl perfluorobutyl ether, $C_4F_9OCH_3$) and Novec 7200 **6** (isomeric mixtures of ethyl perfluorobutyl ether, $C_4F_9OC_2H_5$) are commercially available from 3M Ltd. Novec-7100 was successfully used as a co-solvent for electrophilic fluorination of aryl Grignard reagents with *N*-fluoro-2,4,6-trimethylpyridinium tetrafluoroborate (Scheme 11.19).

Crousse and co-workers reported the synthesis of ethylene carbonate from epoxide and CO_2 using Novec-7500 as a solvent (Scheme 11.20).[31] Due to the high solubility of CO_2 in Novec-7500, the ethylene carbonates were obtained in good yields even under atmospheric pressure of CO_2.

Zhang and co-workers reported a three-step synthetic sequence for biaryl-substituted oxazabicyclo[3.3.1]nonanes from fluorous benzaldehyde (Scheme 11.21).[32] Fluorous intermediates are easily purified using a solid-phase extraction (F-SPE) technique.[33] The removal of the fluorous linker and introduction of the biaryl functional groups was accomplished *via* a microwave-assisted Suzuki–Miyaura coupling reaction using Novec-7200 as a co-solvent, in which Novec-7200 increased the solubility of the starting material.

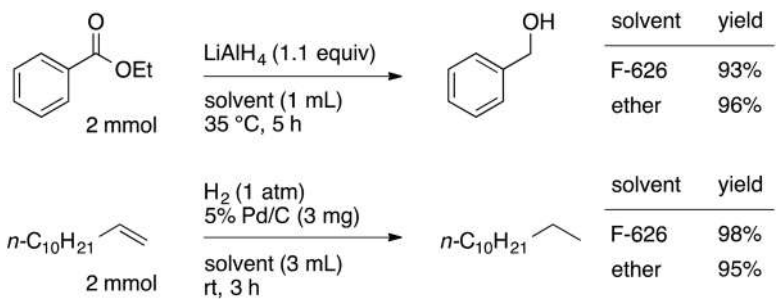

Scheme 11.17 LAH reduction of ester and hydrogenation of alkene using F-626 as a solvent.

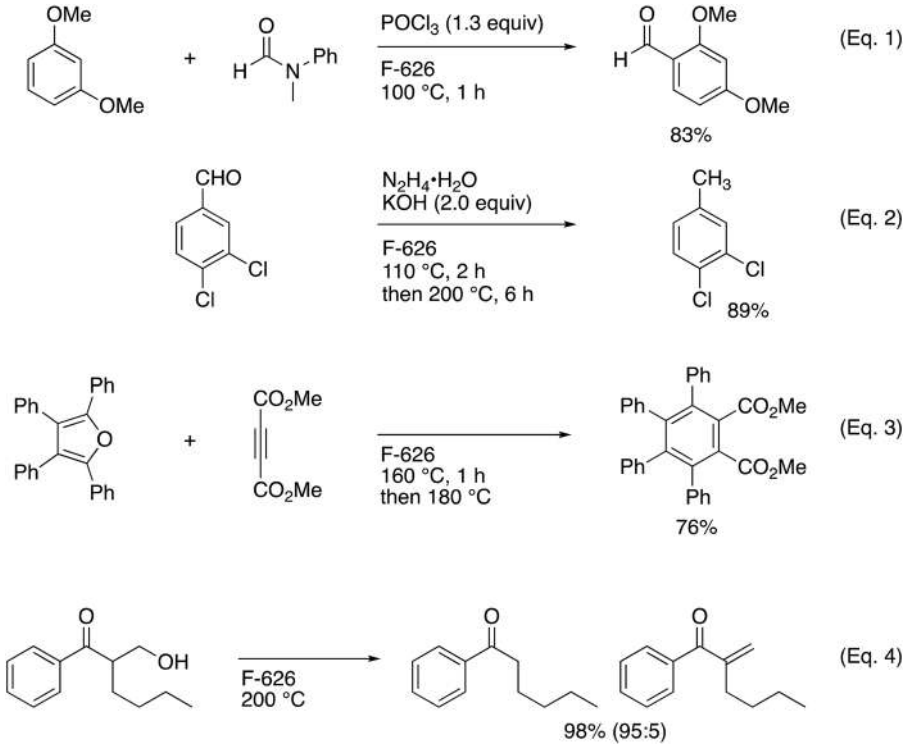

Scheme 11.18 Vilsmeier formylation (Eq. 1), Wolff-Kishner reduction (Eq. 2), Diels–Alder reaction (Eq. 3), and retro-aldol reaction (Eq. 4).

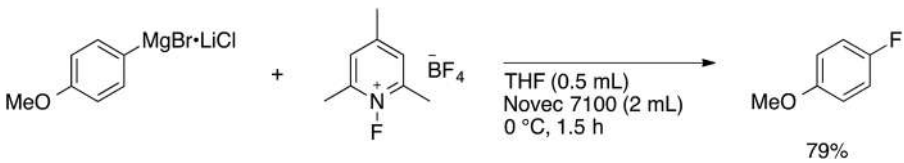

Scheme 11.19 Electrophilic fluorination of aryl Grignard reagent with *N*-fluoro-2,4,6-trimethylpyridinium tetrafluoroborate using Novec 7100.

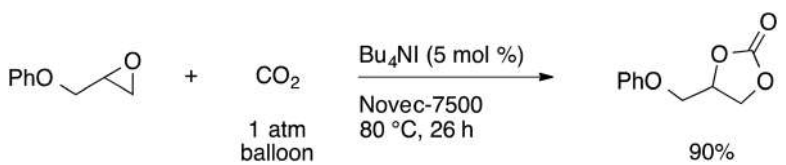

Scheme 11.20 Synthesis of ethylene carbonate from epoxide and carbon dioxide.

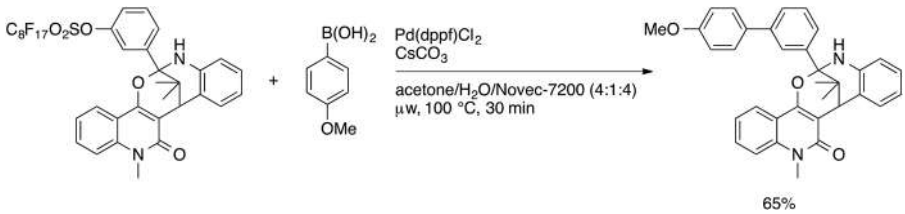

Scheme 11.21 Synthesis of biaryl-substituted oxazabicyclo[3.3.1]nonane.

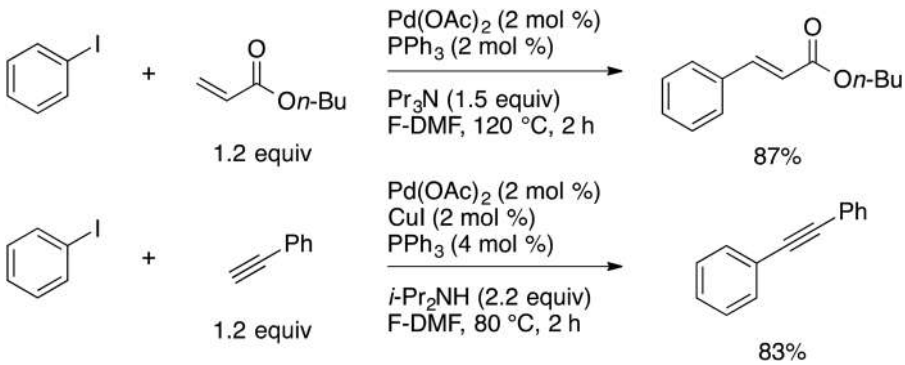

Scheme 11.22 Mizoroki–Heck and Sonogashira reactions using F-DMF.

Fluorous DMF 7 (*N*-(1*H*,1*H*,2*H*,2*H*,3*H*,3*H*-perfluorononanyl)-*N*-methyl formamide, F-DMF) is a colourless, slightly viscous liquid with a density of 1.544 g cm^{-3} (25 °C), which was developed by Matsubara, Maeda, and Ryu as part of the repertoire of recyclable DMFs.[34] The boiling point of F-DMF is 110 °C at 0.75 Torr and F-DMF does not freeze at −35 °C, but transforms to a glassy state at −40 °C. F-DMF is miscible with a wide range of organic solvents, such as hexane, benzene, chloroform, ether, acetone, ethyl acetate, and ethanol, but it is barely soluble in cyclohexane and water. F-DMF was tested for the Mizoroki–Heck and Sonogashira reactions, which worked well to afford the corresponding coupling products in good yields (Scheme 11.22). The recycling use of the catalyst and F-DMF was achieved by biphasic workup using cyclohexane and FC-72, and a second reaction using the recovered catalyst and F-DMF produced almost the same yield as the first.

11.4 Phase-vanishing (PV) Methods Using a Fluorous Solvent as a Liquid-phase Membrane

11.4.1 Concept of PV Methods

Fluorous solvents are generally not miscible either with most organic solvents or with water, creating an independent phase (fluorous phase). The densities of fluorous solvents are greater than those of organic solvents.

By utilizing these unique features of fluorous solvents, we developed a synthetic methodology using fluorous solvents as a phase screen, which is known as the phase-vanishing (PV) method.[8] Earlier results are summarized in a review jointly authored with Curran and Nakamura.[35] The concept of the PV reaction is shown in Figure 11.1. PV reactions can be carried out in a common test tube (Type A) using reagents that are denser than fluorous solvents ($d > 1.7$), while a U-tube (Type B) is employed for the PV method with lighter reagents ($d < 1.7$). The PV system involves a triphasic reaction system, in which fluorous solvents such as FC-72 and Galden (polyperfluoroalkyl ethers) serve as a phase screen between two separated phases containing substrates and reagents, respectively. In the PV method, the fluorous phase regulates the transport of reagents to a substrate-bearing organic layer by passive diffusion. The PV system allows simple and easy control of heat evolution in exothermic reactions. Indeed, many reactions can be carried out without the need for either cooling equipment or dropping funnels using the PV method.

The feasibility of the PV method was first demonstrated in 2002 by the bromination of alkenes with Br_2[8] and the demethylation of methoxy groups with BBr_3[8]. Since then, various PV reactions have been developed by our group[36] and others.[37,38] PV Friedel–Crafts acylation was carried out by placing $SnCl_4$ in the bottom layer.[36a] The four-layered PV method using an additional aqueous layer was invented for α-bromination of methyl ketones with Br_2.[36c] Cyclopropanation with CH_2I_2[36d] and an aldol reaction with $TiCl_4$[36e] both also accommodated the PV method.

The PV bromination system was successfully combined with photoirradiation, in which both alkane bromination and hydrobromination of alkenes using the resulting HBr are carried out (*vide infra*).[39] The PV system is applicable to reactions involving chlorine gas[37a] through a U-tube. Modified PV methods have been developed. For example, PV oxidation using *m*-CPBA, with 1,2-dibromoethane as the solvent of the reagent layer, was achieved,[37b] for which Curran and Werner[37c] later confirmed that the PV reaction occurs by an extractive mechanism. A U-tube variant[36b] was used for applying lighter reagents, such as thionyl chloride and phosphorous trichloride, in the PV method. In addition, Dragojlovic and co-workers carried out PV reactions employing PTFE (Teflon tape) as a phase screen.[37h,37i]

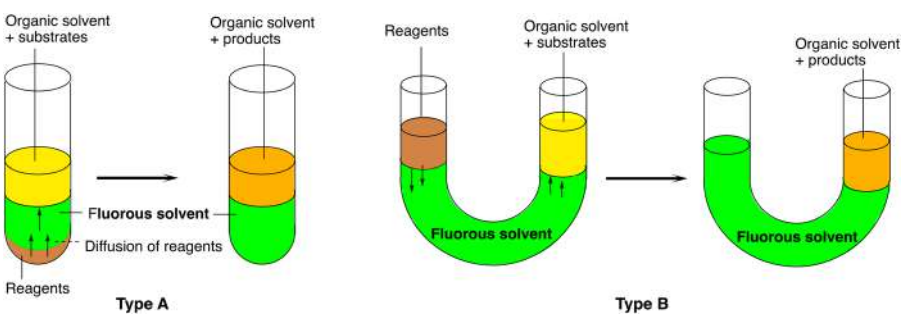

Figure 11.1 General concept of the phase-vanishing methods.

Since the original work of phase-vanishing reactions was already detailed in our previous review,[35] in this chapter we highlight three novel types where active species are generated *in situ* from reagents and are diffused to react with substrates to afford the desired products: (1) Photo-irradiative PV hydrobromination of alkenes; (2) PV Grignard reactions using MeI and EtI; and, (3) PV reactions using *in situ*-generated gaseous reagents such as acetylene, hydrogen sulfide, carbon monoxide, and borane.

11.4.2 PV Method Accompanied by Photo Irradiation

In the original PV bromination method,[8] alkenes spontaneously reacted with Br_2 to afford 1,2-dibromoalkanes. The concept of the photo-irradiative PV bromination reaction is demonstrated in Figure 11.2. In this system, hydrogen bromide (HBr) is generated by photo-bromination of isooctane by molecular bromine. This occurs in the fluorous layer, in which dissolved isooctane encounters upcoming Br_2 to undergo radical-mediated C–H bromination. Dry HBr formed in this way undergoes photo-induced radical addition to 1-alkenes in the organic phase to afford terminal bromides.[39] The thickness of the fluorous layer is double that in the usual PV bromination, which ensures the complete reaction of Br_2 with isooctane in the fluorous phase. Various terminal alkenes are subjected to photo-irradiative PV conditions to afford the corresponding anti-Markovnikov monobromides in good yields (Scheme 11.23).

Mizuno and co-workers carried out the bromination of carbohydrates using the photo-irradiative PV method (Scheme 11.24).[40] For example, a glucose derivative underwent bromination under photo-irradiative PV conditions to afford the corresponding glycosyl bromide in 91% yield. In this reaction, ethyl acetate is the best solvent in the organic phase, as it reacts with bromine to generate HBr.

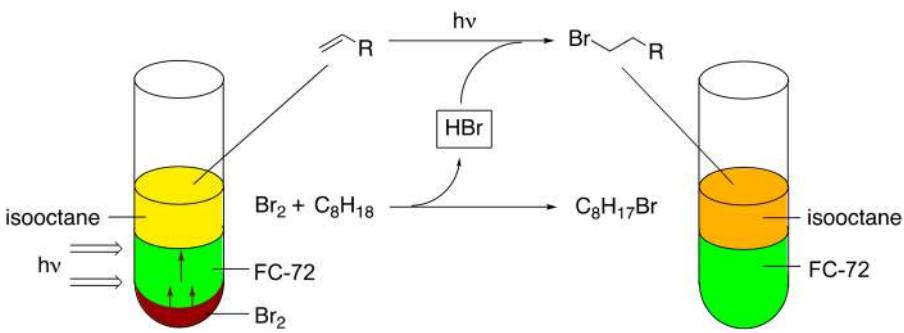

Figure 11.2 Concept of photo-irradiative PV hydrobromination of alkenes.

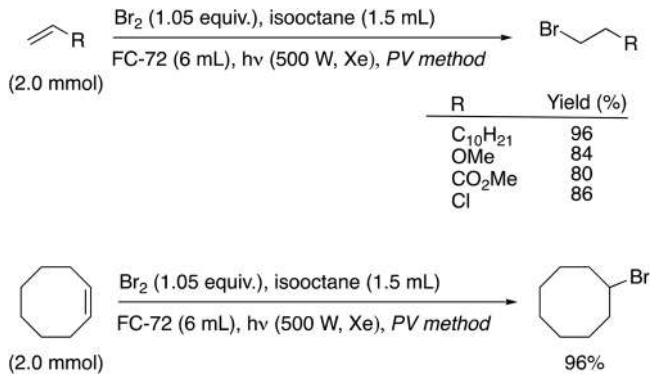

Scheme 11.23 Hydrobromination of alkenes using the photo-irradiative PV method.

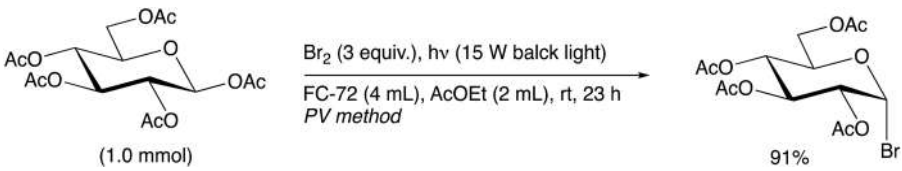

Scheme 11.24 Bromination of carbohydrates using the photo-irradiative PV method.

11.4.3 Grignard-type Reaction Using the PV Method

Recent advances have shown that the PV method is applicable to the facile preparation of Grignard reagents using magnesium particles.[41] The concept of the PV Grignard reaction is shown in Figure 11.3. Methylmagnesium iodide and ethylmagnesium iodide were prepared under the PV conditions using iodomethane or iodoethane, respectively. Initially these alkyl iodides were placed in the bottom reagent layer, since they were denser than fluorous solvents. Diethyl ether was employed as the top organic phase, in which carbonyl compounds were dissolved. Tuning of the fluorous layer was critical to place magnesium particles afloat at the border of organic and fluorous phases. FC-72 is miscible with diethyl ether and was not suitable, and perfluoropolyethers (Galden) were tested for use in the fluorous phase. Galden HT-135 (ρ = 1.72 g cm^{-3}) was not suitable in the fluorous phase due to it having a density that is less than that of magnesium (ρ = 1.74 g cm^{-3}), but Galden HT-200 (ρ = 1.79 g cm^{-3}) maintained the magnesium between the two phases. However, Galden HT-200 was too viscous to diffuse iodoalkanes from the bottom. Consequently, we found that a 1 : 1 blended solvent system (ρ = 1.75 g cm^{-3}) of Galden HT-135 and HT-200 could float magnesium at the border position and also smoothly transport iodoalkane to the magnesium phase.

Using the blended fluorous solvents, Grignard reagents in the forms of iodomethane or iodoethane were successfully prepared and the subsequent

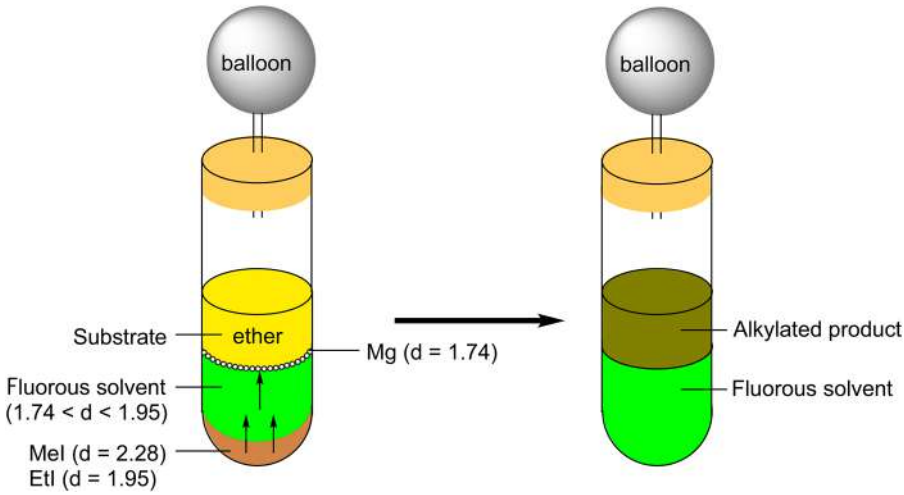

Figure 11.3 PV Grignard reaction using a blended solvent system.

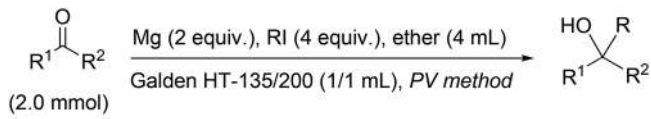

Entry	R^1	R^2	RI	Yield (%)
1	C_8H_{17}	Me	MeI	93
2	C_5H_{11}	C_5H_{11}	MeI	87
3	C_5H_{11}	C_5H_{11}	EtI	80
4	$C_{11}H_{23}$	H	MeI	30[b]
5[a]	$C_{11}H_{23}$	OEt	MeI	81
6[a]	$C_{11}H_{23}$	OEt	EtI	77

[a]Mg (4 equiv.), MeI (4 equiv.).
[b]1-Dodecanol (47%) was also obtained.

Scheme 11.25 PV Grignard alkylation of carbonyl compounds.

addition of Grignard reagents to various carbonyl compounds in the top ether layer was examined. As summarized above, ketones and esters afforded the corresponding alkylated alcohols in good yields (Scheme 11.25, entries 1–3, 5–6). The reactivity of iodoethane was slightly lower than that of iodomethane (Scheme 11.25, entries 2, 3 and 5, 6). Unfortunately, a PV reaction of dodecanal with MeMgI met with limited success due to the reduction of aldehyde by the remaining magnesium (Scheme 11.25, entry 4).

11.4.4 PV Method Accompanied by *in situ* Gas Evolution

The photo-irradiative PV and Grignard-type PV reactions provide a methodology whereby reactive chemical species, such as dry HBr and methyl and ethyl magnesium iodides, can be generated in the fluorous phase, and

then utilized in subsequent reactions. We then focused on another PV system, where gaseous reagents, such as acetylene, hydrogen sulfide, and carbon monoxide, evolved in the fluorous phase, and the gases generated were simultaneously used in subsequent reactions. As illustrated in Figure 11.4, the passive diffusion of water into the fluorous solvent was exploited to allow these gaseous reagents to evolve gently.

The procedure for the Sonogashira coupling of iodobenzenes using the PV method with acetylene gas evolution[42] is described below (Scheme 11.26). In a common test tube, calcium carbide was placed as the reagent phase (bottom layer) and THF was employed as the organic phase (top layer). Galden HT-135 was used as the fluorous phase, and water, serving as the reagent for acetylene generation, was placed onto the fluorous layer. To the top layer, 4-iodotoluene, $Pd(PPh_3)_4$, CuI, and triethylamine were added, and then the air in the test tube was removed using a syringe. The bottom layer was gently stirred at 55 °C, taking care not to mix the four layers. Continuous acetylene gas evolution was observed, and after 20 h both the reagent phase and water phase had vanished. The organic layer was taken and an aqueous workup followed by column chromatography on silica gel afforded diphenylacetylenes

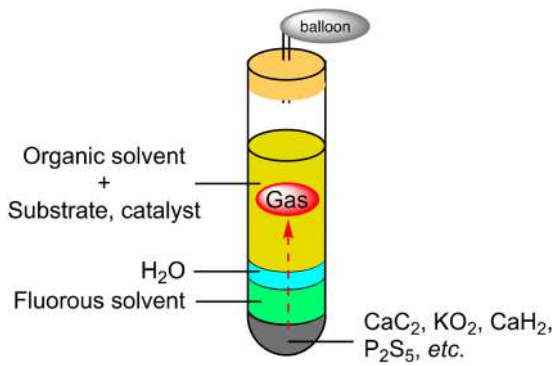

Figure 11.4 PV method with *in situ* gas evolution.

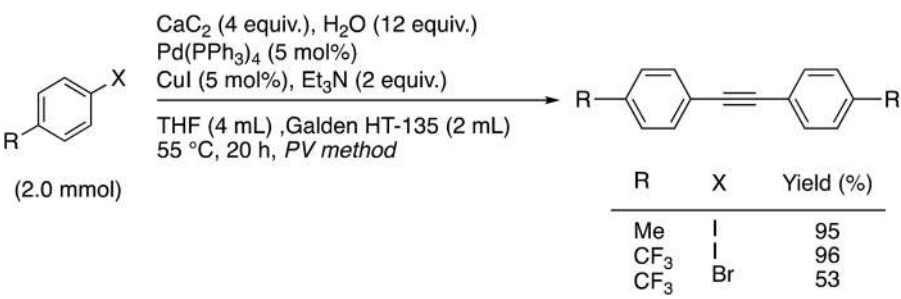

Scheme 11.26 Sonogashira coupling using acetylene evolved in the PV method.

in good yields. The yield of aryl bromide was a bit inferior to that of aryl iodide.

Some other reactions involving acetylene were also demonstrated using the PV method. A copper-catalyzed azide–alkyne cycloaddition (CuAAC) was carried out using benzyl azide to afford triazole in an 85% yield (Scheme 11.27, Eqn (11.15)). In addition, a three-component aldehyde-alkyne-amine (A^3) coupling reaction using benzaldehyde and pyrrolidine was performed to afford the desired product in a 75% yield (Scheme 11.27, Eqn (11.6)). In these reactions, the product yields using the PV system with *in situ* acetylene evolution are similar to those using traditional batch methods.

The PV method with gas evolution has been applied to reactions involving other gaseous reagents. Dihydrogen and dioxygen were generated from calcium hydride and potassium peroxide *via* the PV system and used for hydrogenation (Scheme 11.28, Eqn (11.7)) and Wacker oxidation (Scheme 11.28, Eqn (11.8)), respectively.[43]

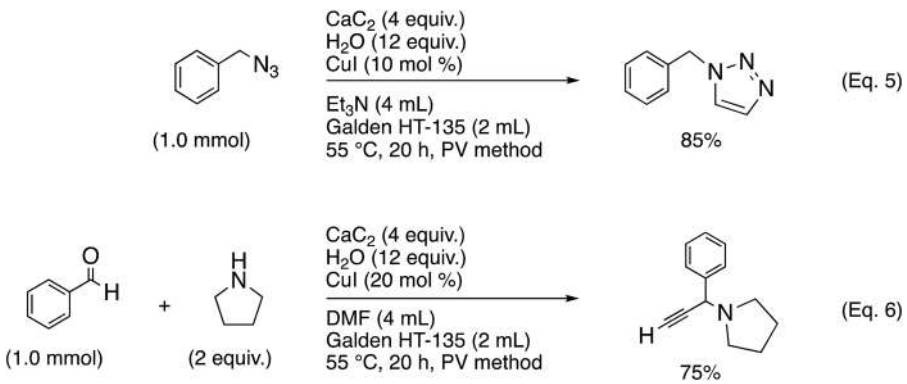

Scheme 11.27 PV reaction with acetylene evolution.

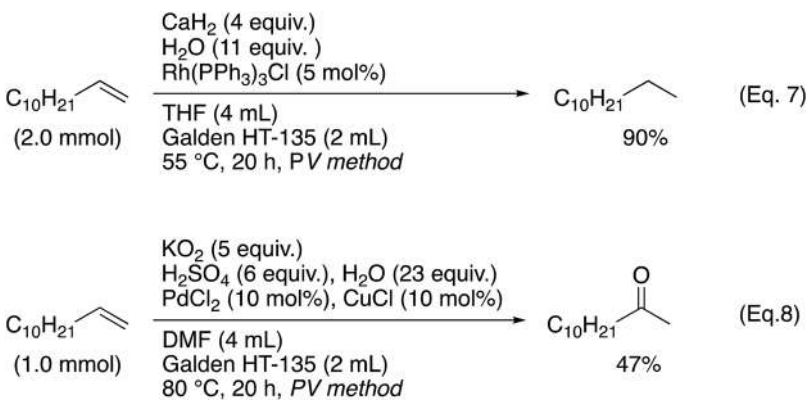

Scheme 11.28 Hydrogenation and oxidation of alkenes using H_2 and O_2 evolved in the PV method.

Hydrogen sulfide was also generated form phosphorous pentasulfide using the PV method and consumed in the preparation of sulfur-containing compounds (Scheme 11.29). Interestingly, as shown below, sulfide was a major product when DBU was used as the base, while disulfides were exclusively afforded with a weaker base such as TEA.

We performed carbonylation reactions using the PV method with carbon monoxide (CO) evolution.[44] In this case, CO gas was generated from sulfuric acid and ammonium formate and used in the palladium-catalyzed aminocarbonylation of iodobenzenes. Using an H-shaped reactor (Figure 11.5) such as that produced by COware,[45,46] we successfully carried out the PV carbonylation reaction (Scheme 11.30, Eqn (11.9)). Several reactions such as the carbonylative Sonogashira reaction (Scheme 11.30, Eqn (11.10)) and xanthone synthesis (Scheme 11.30, Eqn (11.11)) were also performed using a U-shaped reactor.

Very recently, the evolution of borane (BH_3) was also examined *via* a similar PV method,[46] in which borane was generated from sodium borohydride by treatment with oxidizing reagents such as sulfuric acid, iodine, and ethyl

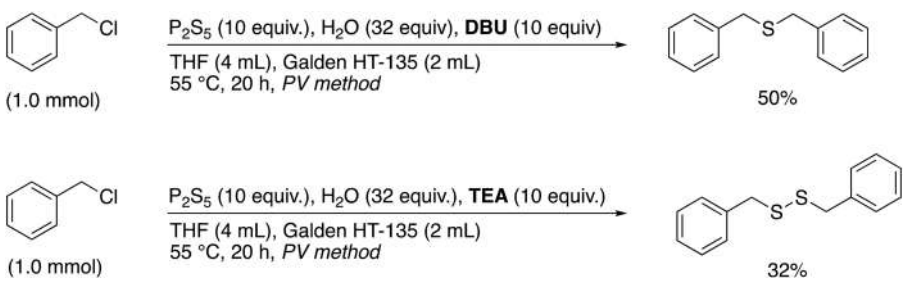

Scheme 11.29 PV reaction with H_2S gas evolution.

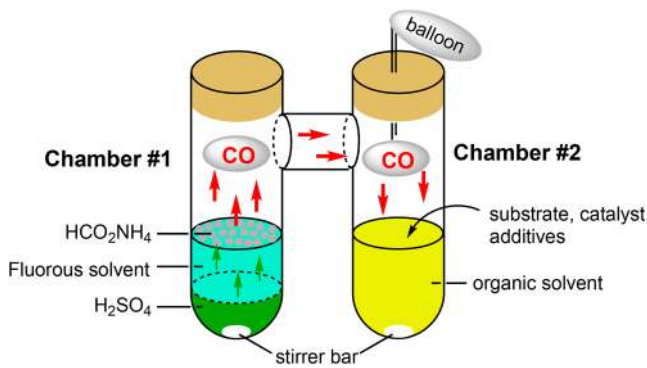

Figure 11.5 Concept of the PV method with CO gas evolution using an H-shaped reactor.

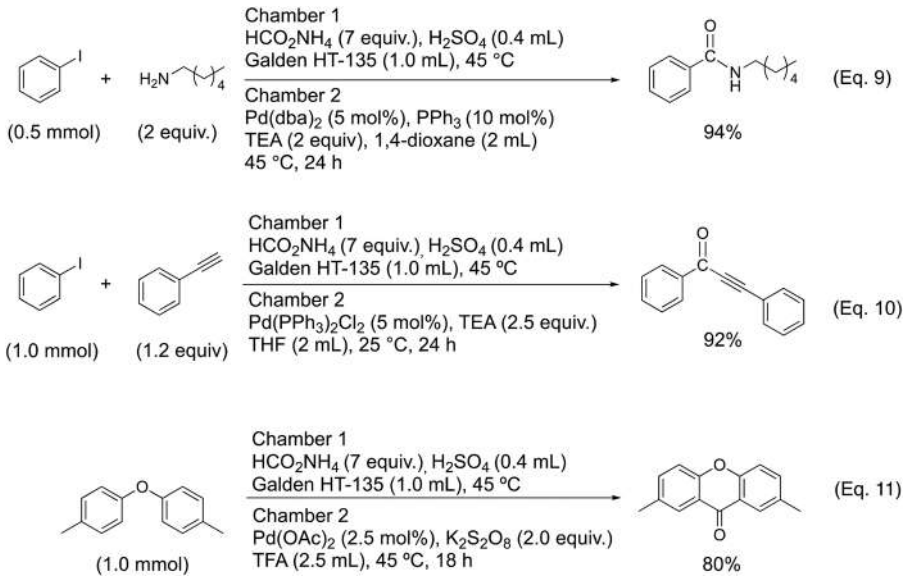

Scheme 11.30 PV reaction with CO gas evolution.

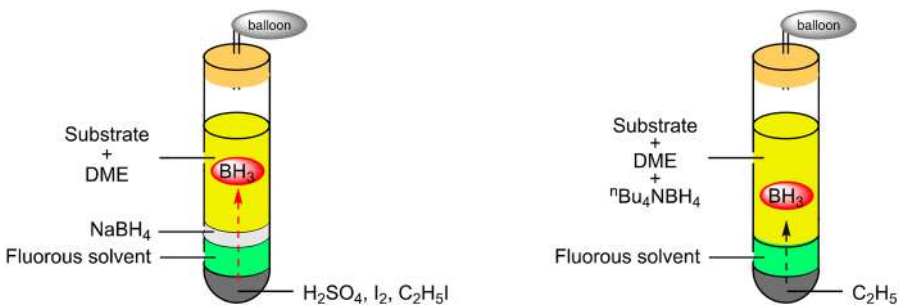

Figure 11.6 Concept of the PV method with borane evolution (borane source, left: $NaBH_4$, right: $^nBu_4NBH_4$).

iodide (Figure 11.6, left). Tetrabutylammonium borohydride was also used as a borane source (Figure 11.6, right). Using the PV system, alkenes underwent hydroboration with the evolved borane, followed by oxidation to afford the desired alcohols in good yields (Scheme 11.31). The selective reduction of carboxylic acids with borane evolved from $^nBu_4NBH_4$, and ethyl iodide was achieved under the PV conditions (Scheme 11.32, Eqn (11.12)) while the organoboranes generated by hydroboration successfully underwent Suzuki–Miyaura coupling with iodobenzene in the same test tube (Scheme 11.32, Eqn (11.13)).

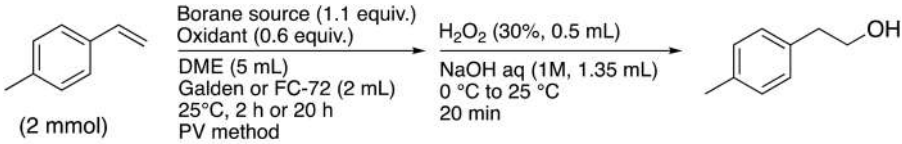

Boran source	Oxidant	Time (h)	Yield (%)
$NaBH_4$	H_2SO_4	20	74
$NaBH_4$	I_2	20	63
$NaBH_4$	EtI	20	91
$^nBu_4NBH_4$	EtI	2	85

Scheme 11.31 Hydroboration of alkenes using borane evolved in the PV method.

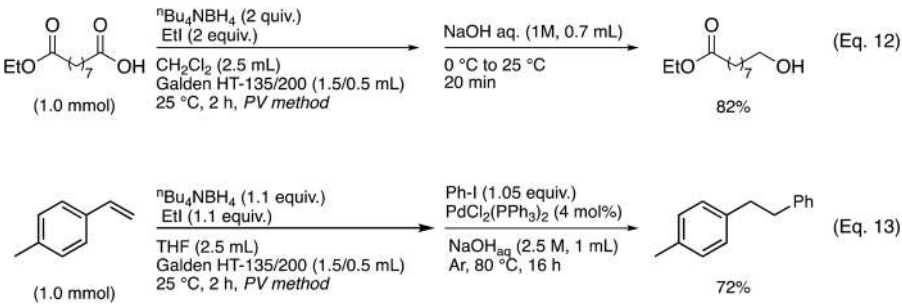

Scheme 11.32 Borane reduction of carboxylic acids and hydroboration of alkenes followed by Suzuki-Miyaura coupling using the PV method.

11.5 Conclusions

This chapter highlights recent advances in the use of fluorous solvents in organic synthesis. It is obvious that commercially available fluorous solvents are becoming the standard repertoire of organic chemists. Increasing demands for greener reactions and processes have shed light on greener substitutes for volatile and harmful organic reagents. In this regard, fluorous solvents, and high-boiling hybrid versions in particular, seem to offer more promise. Despite the fact that cost is always an issue, we nonetheless encourage chemists to design, prepare, and examine new fluorous solvents, as we have done for F-DMF. At the same time, the development of novel procedures that could attain a minimal use of solvents is highly required.

Two unique characteristics of fluorous solvents, immiscibility with water or organic solvents and higher density than usual organic solvents, are smartly capitalized on in the first-generation-PV systems, in which fluorous solvents act as a liquid membrane to regulate reactions by passive diffusion of reagents. The second-generation-PV systems enable the combination of *in situ*-generated active species in the fluorous phase, which ultimately diffuse

to the top layer to react with stored substrates, affording the desired products. In this way, toxic gaseous reagents, such as HBr, H_2S, acetylene, CO, and BH_3, are safely generated and consumed step-by-step. These are regarded as spontaneous "molecular level" flow reaction systems, which occur in very simple apparatus, such as a common test tube or modified glassware reactors. Examples of the *in situ* generation of MeMgI and EtMgI *via* the PV system would also stimulate efforts for easy access to a wide range of reactive species, which govern modern organic syntheses.

References

1. I. T. Horváth and J. Rábai, *Science*, 1994, **266**, 72.
2. (a) K. Uneyama, *Organofluorine Chemistry*, Blackwell Publishing, Oxford, 2006; (b) P. Kirsch, *Modern Fluoroorganic Chemistry: Synthesis, Reactivity, Applications*, Wiley-VCH, Weinheim, 2013.
3. *Handbook of Fluorous Chemistry*, ed. J. A. Gladysz, D. P. Curran and I. T. Horváth, Wiley-VCH, Weinheim, 2004.
4. *Fluorous Chemistry in Topics in Current Chemistry*, ed. I. T. Horváth, Springer, Heidelberg, 2011, p. 135.
5. Z. Luo, Q. Zhang, Y. Oderaotoshi and D. P. Curran, *Science*, 2001, **291**, 1766.
6. (a) A. Ogawa and D. P. Curran, *J. Org. Chem.*, 1997, **62**, 450; (b) J. J. Maul, P. J. Ostrowski, G. A. Ublacker, B. Linclau and D. P. Curran, *Top. Curr. Chem.*, 1999, **206**, 79.
7. H. Matsubara, S. Yasuda, H. Sugiyama, I. Ryu, Y. Fujii and K. Kita, *Tetrahedron*, 2002, **58**, 4071.
8. I. Ryu, H. Matsubara, S. Yasuda, H. Nakamura and D. P. Curran, *J. Am. Chem. Soc.*, 2002, **124**, 12946.
9. H. Matsubara and I. Ryu, *Top. Curr. Chem.*, 2012, **308**, 135.
10. A. S. W. Lo and I. T. Horváth, *Green Chem.*, 2015, **17**, 4701.
11. L. P. Barthel-Rosa and J. A. Gladysz, *Coord. Chem. Rev.*, 1999, **190–192**, 587.
12. A. Orita, S. Tanabe, T. Ono and J. Otera, *Adv. Synth. Catal.*, 2010, **352**, 1419.
13. M. Döbele, S. Vanderheiden, N. Jung and S. Bräse, *Angew. Chem., Int. Ed.*, 2010, **49**, 5986.
14. N. Tada, L. Cui, T. Ishigami, K. Ban, T. Miura, B. Uno and A. Itoh, *Green Chem.*, 2012, **14**, 3007.
15. S. Shimizu, A. Usui, M. Sugai, Y. Suematsu, S. Shirakawa and H. Ichikawa, *Eur. J. Org. Chem.*, 2013, 4734.
16. A. Hafner and S. Bräse, *Angew. Chem., Int. Ed.*, 2012, **51**, 3713.
17. P. O. Miranda, P. Llanes, L. Torkian and M. A. Pericàs, *Eur. J. Org. Chem.*, 2013, 6254.
18. M. Nappi, G. Bergonzini and P. Melchiorre, *Angew. Chem., Int. Ed.*, 2014, **53**, 4921.
19. C. Verrier, N. Alandini, C. Pezzetta, M. Moliterno, L. Buzzetti, H. B. Hepburn, A. Vega-Peñaloza, M. Silvi and P. Melchiorre, *ACS Catal.*, 2018, **8**, 1062.

20. (a) J. E. Baldwin and R. A. Smith, *J. Am. Chem. Soc.*, 1967, **89**, 1886; (b) Ref. 6; (c) Z. Atik, *J. Chem. Eng. Data*, 2007, **52**, 1128; (d) K. Tochigi, C. Kikuchi, K. Kurihara, K. Ochi, J. Mizukado and K. Otake, *J. Chem. Eng. Data*, 2005, **50**, 784; (e) H.-J. Frohn, M. Giesen, D. Welting and V. V. Bardin, *J. Fluorine Chem.*, 2010, **131**, 922; (f) A. L. Henne and J. B. Hinkamp, *J. Am. Chem. Soc.*, 1945, **67**, 1194; (g) Ref. 7; (h) https://www.3m.com/, accessed February 2021; (i) Ref. 34.
21. (a) E. Hasegawa, Y. Ogawa, K. Kakinuma, H. Tsuchida, E. Tosaka, S. Takizawa, H. Muraoka and T. Saikawa, *Tetrahedron*, 2008, **64**, 7724; (b) C. Reichardt, *Chem. Rev.*, 1994, **94**, 2319.
22. Y. Shimizu, Y. Obora and Y. Ishii, *Org. Lett.*, 2010, **12**, 1372.
23. A. Kusuda, H. Kawai, S. Nakamura and N. Shibata, *Green Chem.*, 2009, **11**, 1733.
24. S. Okusu, H. Kawai, X.-H. Xu, E. Tokunaga and N. Shibata, *J. Fluorine Chem.*, 2012, **143**, 216.
25. A. Kusuda, X.-H. Xu, X. Wang, E. Tokunaga and N. Shibata, *Green Chem.*, 2011, **13**, 843.
26. S. Mori and N. Shibata, *Beilstein J. Org. Chem.*, 2017, **13**, 2273.
27. X.-H. Xu, G.-K. Liu, A. Azuma, E. Tokunaga and N. Shibata, *Org. Lett.*, 2011, **13**, 4854.
28. B. Cui, S. Jia, E. Tokunaga, N. Saito and N. Shibata, *Chem. Commun.*, 2017, **53**, 12738.
29. T. Fukuyama, M. Arai, H. Matsubara and I. Ryu, *J. Org. Chem.*, 2004, **69**, 8105.
30. T. Fukuyama, T. Kawamoto, T. Okamura, A. Denichoux and I. Ryu, *Synlett*, 2010, 2193.
31. M. Mamone, T. Milcent and B. Crousse, *Chem. Commun.*, 2015, **51**, 12736.
32. S. Ding, M. Le-Nguyen, T. Xu and W. Zhang, *Green Chem.*, 2011, **13**, 847.
33. Q. Zhang, Z. Luo and D. P. Curran, *J. Org. Chem.*, 2000, **65**, 8866.
34. H. Matsubara, L. Maeda and I. Ryu, *Chem. Lett.*, 2005, **34**, 1548.
35. I. Ryu, H. Matsubara, H. Nakamura and D. P. Curran, *Chem. Rec.*, 2008, **8**, 351.
36. (a) H. Matsubara, S. Yasuda and I. Ryu, *Synlett*, 2003, 247; (b) H. Nakamura, T. Usui, H. Kuroda, I. Ryu, H. Matsubara, S. Yasuda and D. P. Curran, *Org. Lett.*, 2003, **5**, 1167; (c) M. T. Rahman, N. Kamata, H. Matsubara and I. Ryu, *Synlett*, 2005, 2664; (d) H. Matsubara, M. Tsukida, S. Yasuda and I. Ryu, *J. Fluorine Chem.*, 2008, **129**, 951; (e) Y. Adachi, K. Kuniyoshi and H. Matsubara, *J. Fluorine Chem.*, 2017, **197**, 100.
37. (a) J. Iskra, S. Stavber and M. Zupan, *Chem. Commun.*, 2003, 2496; (b) N. K. Jana and J. G. Verkade, *Org. Lett.*, 2003, **5**, 3787; (c) D. P. Curran and S. Werner, *Org. Lett.*, 2004, **6**, 1021; (d) A. Podgoršek, S. Stavber, M. Zupan and J. Iskra, *Eur. J. Org. Chem.*, 2006, 483; (e) N. Windmon and V. Dragojlovic, *Tetrahedron Lett.*, 2008, **49**, 6543; (f) N. Windmon and V. Dragojlovic, *Beilstein J. Org. Chem.*, 2008, **4**, 29; (g) K. Ma, S. Li and R. G. Weiss, *Org. Lett.*, 2008, **10**, 4155; (h) N. J. van Zee and V. Dragojlovic, *Org. Lett.*, 2009, **11**, 3190; (i) K. Pels and V. Dragojlovic, *Beilstein J. Org. Chem.*, 2009, **5**, 75.

38. (a) J. Iskra, *Lett. Org. Chem.*, 2006, **3**, 170; (b) N. J. Van Zee and V. Dragojlovic, *Chem. - Eur. J.*, 2010, **16**, 7950.
39. H. Matsubara, M. Tsukida, D. Ishihara, K. Kuniyoshi and I. Ryu, *Synlett*, 2010, 2014.
40. M. Tojino, Y. Hirose and M. Mizuno, *Tetrahedron Lett.*, 2013, **54**, 7124.
41. H. Matsubara, Y. Niwa and R. Matake, *Synlett*, 2015, **26**, 1276.
42. R. Matake, Y. Niwa and H. Matsubara, *Org. Lett.*, 2015, **17**, 2354.
43. R. Matake, Y. Niwa and H. Matsubara, *Tetrahedron Lett.*, 2016, **57**, 672.
44. Y. Adachi and H. Matsubara, *J. Fluorine Chem.*, 2018, **216**, 89.
45. P. Hermange, A. T. Lindhardt, R. H. Taaning, K. Bjerglund, D. Lupp and T. Skrydstrup, *J. Am. Chem. Soc.*, 2011, **133**, 6061.
46. C. Brancour, T. Fukuyama, Y. Mukai, T. Skrydstrup and I. Ryu, *Org. Lett.*, 2013, **15**, 2794.
47. N. Soga, T. Yoshiki, A. Sato, T. Kawamoto, I. Ryu and H. Matsubara, *Tetrahedron Lett.*, 2021, **69**, 152977.

CHAPTER 12

Ionic Liquids and Deep Eutectic Solvents

LORENZO GUAZZELLI[a] AND CHRISTIAN SILVIO POMELLI*[a]

[a]Department of Pharmacy, University of Pisa, Via Bonanno Pisano 33, 56126 Pisa, Italy
*E-mail: christian.pomelli@unipi.it

12.1 A Very Short Introduction

In this chapter, the authors present the state of the art of ILs and DESs with emphasis on their application to sustainable organic synthesis. These two topics are in different stages of development. ILs is a mature research field where research is mostly focused on applications. DESs are still in full development. We present here ILs and DESs in two separate sections as "parallel lives" toward the same goal of sustainable chemistry, highlighting affinity and divergences.

12.2 Ionic Liquids

12.2.1 Ionic Liquid Structure, Synthesis and Basic Properties: A Brief Survey

The chemistry of ionic liquids (ILs) has attracted increasing interest in the last twenty years, as shown by the number of peer reviewed papers from the year 2000 (Figure 12.1). The total number of papers is approaching 1 00 000.

Sustainable Organic Synthesis: Tools and Strategies
Edited by Stefano Protti and Alessandro Palmieri

Published by the Royal Society of Chemistry, www.rsc.org

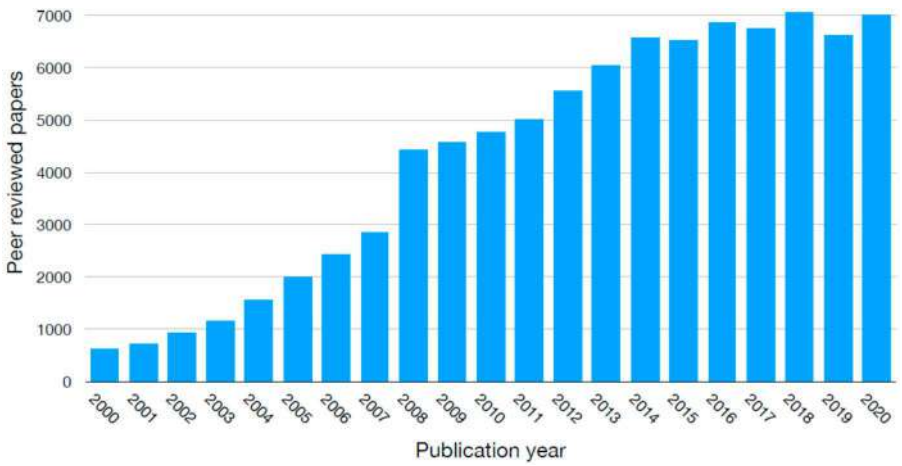

Figure 12.1 Number of peer reviewed papers on ionic liquids published from 2000 to 2020. Data obtained by searching the keyword "ionic liquids" in Scopus (8/2/2021).

After a fast initial rise, the topic seems to have reached its maturity in the last seven years. Looking at these figures, it is evident that it is impossible for anyone to be updated on the whole subject or to follow the entire literature about ILs.

For the same reason, it is impossible to cite all the papers about a given aspect of ILs. In this section, we will refer mainly to review papers in which the reader can retrieve the relevant literature about a given subtopic and/or to some, when possible, recent examples of application. Two detailed reviews, covering the use of ILs as solvents in synthesis and catalysis, have been published in 1999[1] and 2011.[2]

An operative definition of ILs[3,4] is that they are a class of ionic compounds that are in the liquid state below 100 °C.[5] Therefore, they must be liquid using one of the simplest experimental setups of a chemistry laboratory: an oil bath and a heating plate. As natural in the evolution of the topic, these constraints have been loosened, especially for the upper temperature limit.

The guideline for the molecular design of ILs is to sketch and pair a cation and an anion that, for their geometrical structures, cannot efficiently pack in a crystal lattice. The most common solution is a spherical top (or at least globular) anion and a stick shaped cation. Some of the most common structures of anions and cations are reported in Figure 12.2.

Cations are usually obtained by quaternarization of a heteroatom. The imidazolium based cations were one of the first classes to be extensively investigated and are still the most diffused in practice and in the literature. The anions are often inorganic, but there are also organic examples, such as bis(trifluoromethane)sulfonimide. Thus, one of the most common schemes is organic cation–inorganic anion, but there are also examples of ILs containing monoatomic inorganic cations like Na^+.[6]

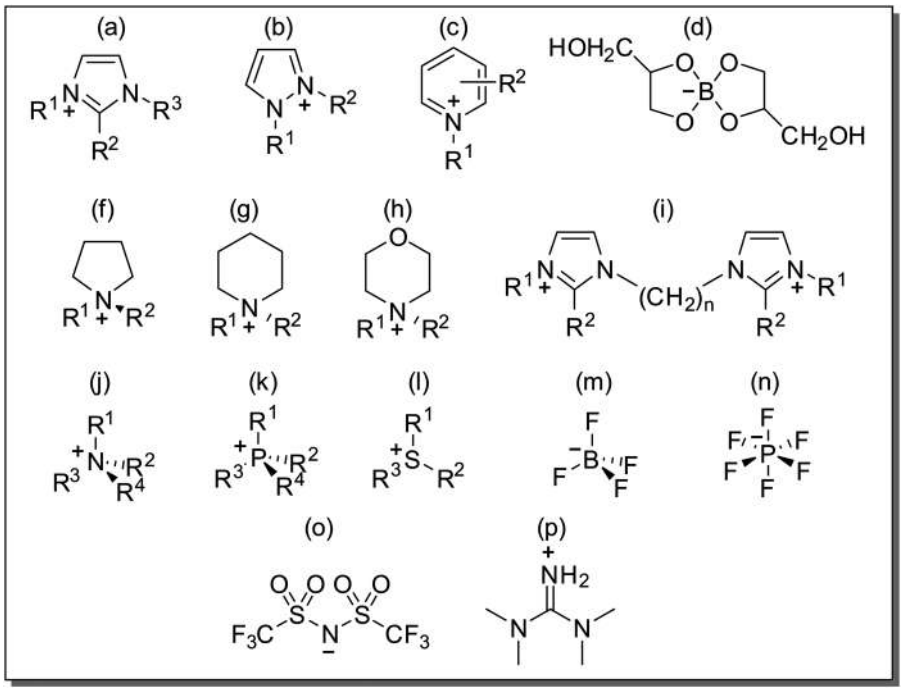

Figure 12.2 Some typical structures of IL cations and anions. (a) Alkylimidazolium. Often R^2 = H, R^3 = CH_3, R^1 = a longer chain. (b) Alkylpyrazolium. (c) Alkylpyridinium. (d) Glyceroborate, an example of an organic anion, (e) Alkylpyrrolidinium. (f) Alkylpiperidinium. (g) Alkylmorpholinium. In b, e, f and g R^1 and R^2 are of different lengths. (h) An example of an imidazolium-based dication. (i) Tetraalkylammonium. (l) Tetraalkylphosphonium. (m) Trialkylsolphonium; in i, l and m three (two) sidechains are generally the same, and the 4th (3rd) of very different length. C (n) tetrafluoroborate. (o) Hexaflurophosphate. (p) Bis (trifluoromethane)sulfonimide, short name Bistriflimide, acronyms: Tf_2N, TFSI; a very common anion. (p) Tetramethylguanidinium. Also common are small organic/inorganic ions like Cl^-, Br^-, $RCOO^-$, $-OOC(CH_2)_nCOO^-$, RSO_3^-, Na^+, K^+, *etc.*

A large number of variants can be obtained by changing the sidechain length. More specialized structures can be designed introducing a functional group on a sidechain, thus obtaining a point-functionalized IL.[7]

ILs belonging to the above defined class are designed for specialized uses. "Simple" ILs planned to be used as solvents must be easy to synthesize with a reasonable price.

A typical synthesis of a common IL is reported in the Scheme 12.1.

First, a S_N2 reaction between 1-methylimidazole and bromobutane leads to 1-methyl-3-butylimidazolium bromide; then, the bromide anion is replaced by hexafluorophosphate in an ion-exchange reaction. This synthesis is so routine as to be proposed in student's laboratories.[8]

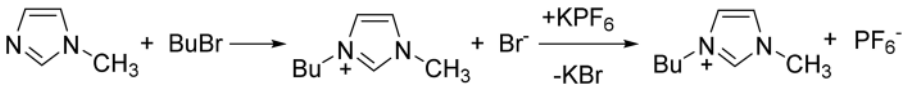

Scheme 12.1 Synthesis of butylmethylimidazolium hexafluorophosphate *via* S_N^2 and ion exchange.

This scheme is extremely modular: the entering group, carbon chain, nucleophile, leaving group and exchanging anion can be easily replaced, leading to a very large number of possible ILs. However, some of the reactions may not work, and some of the products may be solid ("stones" in jargon), unstable and/or not useful for some reason, but a large number have been synthesized and successfully used as reaction media. It is also worth mentioning two different classes of ILs, namely protic ILs, obtained through an acid-base neutralization reaction,[9,10] and switchable ILs, which are systems able to turn from molecular-to-ionic and *vice versa* when a triggering compound is added or removed.[11] These classes of ILs are not of common use in organic synthesis, but for instance in CO_2 capture and biomass processing.[12]

At least for some applications, the high viscosity of an IL can represent an issue.[13] The value of this physical property for ILs is extremely variable[14] ranging from values comparable to those of molecular solvents to values of the order of 10^5 mPa • s. Its value is sensitive to the presence of impurities like water or halides.[13]

An intrinsic characteristic of ILs, related to their ionic nature, is a rather high hygroscopicity.[15] Since a thorough drying process can be a demanding task, sometimes of limited benefit,[16] the water content must be measured and controlled in order to ensure reproducibility of the experimental results. Some fundamental properties of ILs, like viscosity, electrochemical window, and density, depend on their water content.[15] However, confirming their flexibility, hydrophobic ILs can also be prepared.[16,17]

Polarity is a common concept used in solvent classification and choice. Extending this concept from molecular solvents to ILs is not trivial.[18] The dielectric constant, the physical property more directly related to the concept of polarity, cannot be measured easily for ILs.[19] Several polarity scales have been developed for molecular solvents, but for ILs, they lead to divergent values.[20]

In fact, the process of selection of an IL for a given application is more complex than for a molecular solvent.

A recurring concept is the tailor made or task-specific design of ILs.[21,22] While the number of molecular solvents with given characteristics is limited, the extreme flexibility of the molecular structure of ILs leads to the possibility of tuning and designing their properties in order to fit perfectly to the desired application.

12.2.2 Sustainable Physical Properties

Some physical properties of ILs grant them an intrinsic sustainability. The meaning of this statement is: since the dispersion and/or the degradation of this kind of solvent is not easy, they are easily recyclable and re-usable; therefore, they are more sustainable than other systems.

One of the traditional channels of dispersion of molecular solvents, especially for not polar ones, is through their evaporation. In ILs, the strong charge–charge interactions, which do not exist in molecular solvents, annihilate their vapour pressure and thus their volatility. Actually, there are studies at low pressures (of the order of mPa) that show that the evaporation of ILs, probably as ionic pairs, is still possible,[23] but these conditions are far beyond the standard laboratory operative conditions. Furthermore, ILs combine with a negligible volatility another very attractive feature, that of non-flammability.

ILs present high resistance against some of the most common threats to the stability of a chemical compound.

Imidazolium-based ILs present, usually, an onset temperature over 300 °C, except when the cation is paired to a thermolabile anion or there exist specific anion–cation degradation reactions.[24] Similar values are typical for other common ILs, like ammonium and phosphonium-based ones.

The degradation process can follow several reactive paths. Often, they are the reverse reaction of the one used in the synthetic procedure. A selection of degradation paths is presented in Figure 12.3.[25]

ILs are, generally, stable *versus* oxidation and reduction. Given their ionic nature, their electrochemical window limits are determined by anion, oxidation, and cation, reduction.[26] Among the anions, the, not too green, halogenated anions, like $[BF_4]^-$, $[PF_6]^-$, or $[Tf_2N]^-$, are the most resistant. For cations, good examples are aliphatic and acyclic with sterically hindered

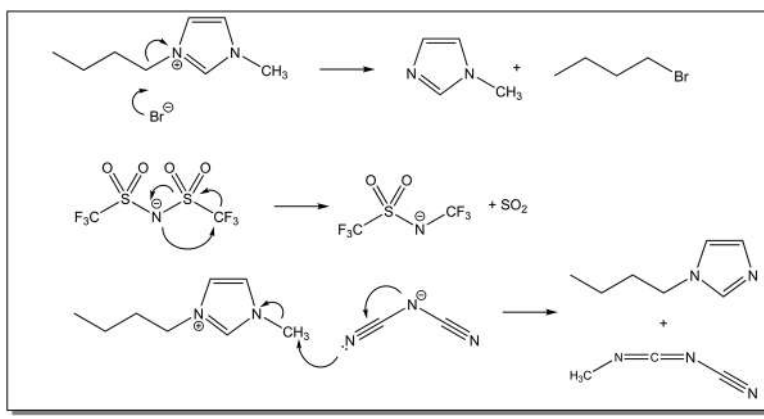

Figure 12.3 Some examples of thermal degradation reactions of ILs.[24]

charge centres, like tetraalkylammonium and phosphonium, but also alkylimidazolium.

This feature has led to an intense investigation of the possible use of ILs in batteries, but also as media in electrochemical synthesis.[13,26]

Some ILs are vulnerable *versus* strong Brønsted bases.[27] Imidazolium cations, with R_2 = H, can be deprotonated giving a hybrid carbene-ylide neutral molecule.[27] This feature can be exploited for organic synthesis (see 12.2.3). Ammonium and phosphonium-based cations are more resistant to bases.[27]

12.2.3 Solvent Intrinsic Catalysis

Most molecular solvents are chemically inert, like hydrocarbons, or can act as hydrogen bond donors and/or acceptors. Furthermore, their electrostatic features do not go beyond the dipole. The repertoire of chemical features of ILs is larger. Therefore, the intrinsic catalytic effects of ILs when used as solvents often dispense with the use of additional catalysts, an implicit sustainability feature.

Imidazolium-based ILs have been widely used as solvents for organic synthesis. The protons on the imidazolium ring and the protons in the side-chains in the α position with respect to one of the two nitrogen atoms give rise to very strong hydrogen bonds.[28] This can be depicted from a simple analysis of imidazolium ring resonance structures and confirmed by *ab initio* calculations,[29] FTIR spectroscopy[30,31] and the chemical reactivity in these media. Other kinds of ILs, like ammonium and pyridinium ones, present similar properties.[28]

The Diels–Alder reaction, the archetype of cycloaddition reactions, a useful tool for creating carbon–carbon bonds, has been extensively studied in ILs, since their rate and selectivity are considerably enhanced in these media.[32,33] If the dienophile has polar groups like a carbonyl, then it can establish a hydrogen bond with the cation, which causes an increase of the *endo*/*exo* selectivity.[33,34] The presence of Lewis acids like $AlCl_3$, stabilized by IL anions, further enhances the reaction rate and the selectivity.[32]

Another chemical feature of imidazolium-based cations is their possibility to act as N-heterocyclic carbenes (NHCs).[35] There is evidence that the formation of carbenes can be spontaneous, in the presence of a sufficiently basic anion (Scheme 12.2).[36,37]

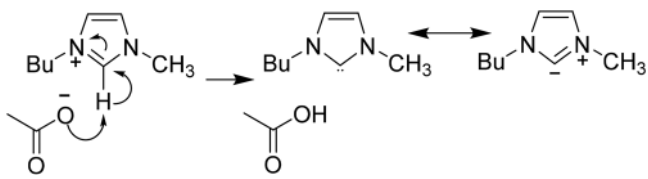

Scheme 12.2 Formation, and stabilization by resonance of NHC carbene from butylmethylimidazolium.

This mechanism is confirmed by the fact that when a methyl group is present on the carbon between the two nitrogen atoms, the reaction does not take place.[36]

Carbene formation in ILs can be induced, also, by traditional methods like heat, bases or electrochemically.[38]

Carbenic ILs can activate carbonyl groups *via* the formation of the Breslow intermediate (Scheme 12.3).[39,40]

In a paper by Vedachalam *et al.*,[41] a task-specific IL based on the thiazolium ring is used as a catalyst in combination with an imidazolium-based IL as the bulk solvent. This experimental setup allows for the green synthesis of a set of complex functionalized chromones with anticancer activity. The study was supported by a DFT study of the mechanism.

The use of imidazolium ILs with $[WO_4]^{2-}$ anions allows for a base-free oxidative synthesis of substituted benzoxazinones and benzoxazoles. Carbenes are obtained by thermal activation. Furthermore, there is no need to add an oxidant since air is sufficient.[42]

ILs may present intrinsic Brønsted acid and basic properties. However, it is possible to use conventional acids or bases in ILs. Standard mineral or organic acids show a behaviour in ILs not too different from the one they show in water.[43] However, this is not a green option: the green option is to use the built-in acid/base properties of some IL systems.

Brønsted acidic ILs are usually functionalized with acidic groups ($-SO_3H$ or $-CH_2COOH$ are typical examples). An anion similar to the acidic moiety can enhance the acidity.[44] A typical synthetic approach is the nitrogen quaternization by 1,4-butane or 1,3 propane sultones (Scheme 12.4).[44]

A wide variety of reactions can be performed in these task-specific ILs: addition or elimination of water, oxidation, transesterification, *etc.*[44]

Imidazolium cations functionalized by a carboxylic function efficiently catalyse the regioselective opening of epoxides by NaN_3.[45] The reaction takes place in mild conditions. The catalyst has been recycled five times with yields higher than 90%.

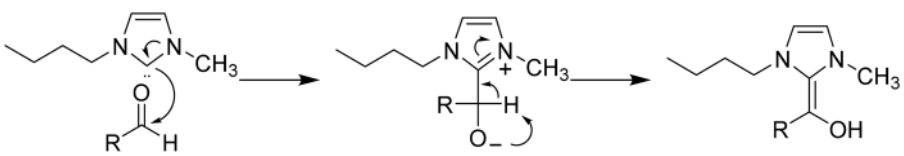

Scheme 12.3 Formation of the Breslow intermediate from IL-derived NHC carbene.

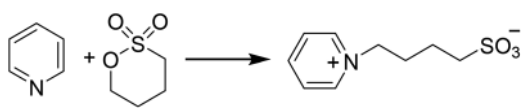

Scheme 12.4 Synthesis of a Brønsted acidic IL.

ILs with an acetate or propionate anion can be used to synthetize nitrile functionalized derivatives of malonic acid in mild conditions and short reaction times (room temperature, 20′). It is interesting that the reaction does not work with the not so green $[CF_3COO]^-$ anion.[46]

On the other hand, the basic potential of ILs is represented by ammine, phenate, or similar functional groups.[46,47] Single alkylated DABCO-based (where basicity is implicitly furnished by the not-quaternized nitrogen atom) and 4-*N*,*N*-dimethylamminepyridium-based cations can be used to perform esterification of triterpenic acids.[47] A base-free synthesis of functionalized 3-iodothiophenes can be performed in ILs with the $[EtSO_4]^-$ anion, which plays an active role in interacting with the proton of the –SH group, thus promoting the formation of the heterocyclic ring. The basic IL used in the reaction can be recycled up to seven times.[48]

12.2.4 Ionic Liquids as a Nice Environment for Metal-based Catalysts

The IL environment is a nice place for metal ions. Indeed, they can easily coordinate to anions (50% of each IL system) forming complex ions. Main groups and transition metal ions in ILs are exploited in a wide range of applications, which span from electrochemistry (batteries, coating, *etc.*), to metal extraction and/or concentration, *etc.* Furthermore, defining their potential role in green organic synthesis has been a subject of intense research.

If a salt with the same anion is solvated in an IL and the ratio of ion:IL is stoichiometric, this leads to new ILs with metal containing anions. Among the first examples are chloroaluminates (Scheme 12.5).[49]

Also, higher order polynuclear ions are possible. Similar systems exist for a larger number of other ions, like iron.[50] Speciation and system properties can vary along with the variation of the proportions between IL and metal salt.[52] The whole range of reactions catalysed by $AlCl_3$ and other group IIIA halogenides can be transferred in these media.[49] For example, esterification of acetic acid with a range of alcohols can be carried out in 1-butylpyridinium chloride, in the presence of $AlCl_3$, avoiding the traditional use of sulphuric acid. Furthermore, the produced esters separate spontaneously from the reaction media.[51] CuBr/IL systems can be used for the synthesis of 2-oxazolidinones from aminoalcohols using CO_2 as a source of C1. The reaction can be carried out with a very low salt loading (0.0125–0.5 M) reaching a remarkable value of 2960 as the turnover number.[52] A similar reaction can be carried out using Ag(I) salts instead of Cu(I).[53]

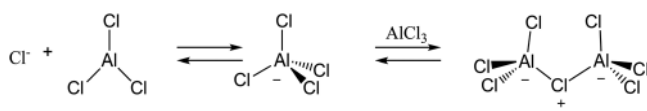

Scheme 12.5 Formation of chloroaluminate ions.

Switching from simple salts to complexes, 2,4,6-tris(di-4-chlorobenzamido)-1,3,5-triazine palladium(II) chloride, a palladium metallodendrimer, can be used in tetra-*n*-butylammonium bromide IL to efficiently synthesize functionalized benzothiophenes.[54] The yields are high (75% to 96%) and the catalyst can be recycled up to five times.

The commercial NHC-Pd-2 catalyst can be used in coupling reactions between acetylenic oximes and inactivated long-chain enols, leading to substituted isoxazoles, using 1-carboxymethyl-3-methyl-imidazolium chloride IL. The IL has an active role in the reaction: it eliminates HCl from the product in the last stage of the reaction.[55] With respect to traditional reactions in molecular solvents like dichloroethane, the conditions are milder, the catalyst loading is lower, and the number of steps is decreased.

Metal nanoparticles in ILs are generally stable and present catalytic properties.

ILs can be supported on metal or metal oxide nanoparticles[56,57] leading to efficient and sustainable catalytic systems for a wide range of reactions. In a large number of these multi-component systems, ILs do not have a prevalent role, like solvent, but are only a part of complex systems.[57] To have an idea of these complex systems, gold nanoparticles can be stabilized by trinuclear imidazolium cations with PEG-like sidechains.[58] The resulting catalytic system can efficiently promote A^3 coupling and cycloisomerization reactions. These systems are often employed in applications not directly related to organic synthesis, such as petroleum derivatives[59] and biomass processing.[60]

12.2.5 How Sustainable are ILs?

In the previous section, a rapid survey of IL properties and applications to sustainable synthesis has been presented. These systems have been proposed from the beginning as sustainable systems. However, their sustainability has been centred on the fact that they lack some of the classic dispersion channels of molecular solvents, mainly by volatility. However, other ways of dispersion are possible: container washing, accidental leaks, *etc.* Toxicity tests show that ILs, especially those containing halogens, can be toxic when released in the environment.[61–63]

To address this issue, research in the IL area has moved in recent years towards new systems prepared from natural and renewable sources, mainly biomasses, in order to increase their sustainability, and improve their green profile in terms of biodegradability and toxicity.[64,65] An interesting emerging topic, related to the biological activity of ILs, is their use as active pharmaceutical ingredients:[66,67] the transformation of traditional drugs in ILs. This is not so unexpected since a large number of drugs are chlorohydrates or sodium salts. Furthermore, ILs have shown great potential as antimicrobials[68,69] and antifungals.[70]

12.3 Deep Eutectic Solvents

12.3.1 Deep Eutectic Solvents (DESs): General Overview

Deep eutectic solvents (DESs) are binary mixtures of Brønsted/Lewis acids and bases characterized by a decrease of their freezing temperatures at the eutectic point, which are lower than those otherwise expected for ideal mixtures.[71] The strong interactions between the DES partners, most often hydrogen bonds between a hydrogen bond donor (HBD) and a hydrogen bond acceptor (HBA), can cause impressive freezing temperature decrement at a specific, albeit not fixed molar ratio. Quaternary ammonium salts, and in particular choline chloride (ChCl), are often found as HBA components in DESs together with different HBDs such as urea, alcohols or organic acids (Figure 12.4).

However, the first examples proposed by Abbott *et al.* in 2001 (type I DES)[72] do not actually belong to this type of DES. Since then, a classification system for DESs has been proposed, which is summarized in Table 12.1.

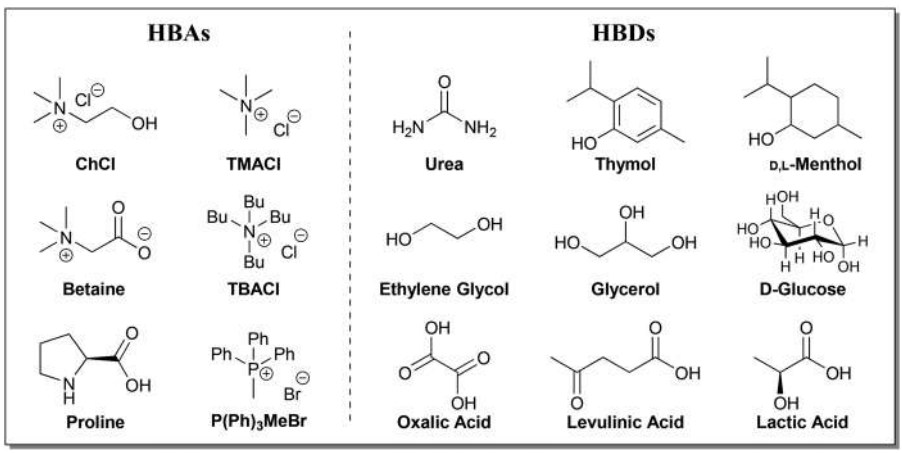

Figure 12.4 Common hydrogen bond acceptor (HBA) and hydrogen bond donor (HBD) DES partners.

Table 12.1 Different types of DESs classified on the basis of the constituting components. Reproduced from ref. 73 with permission from the Royal Society of Chemistry.

DES type	Acid	Base
I	Lewis	Lewis
	MCl_x; M = Zn, Sn, Fe, Al, Ga, In	R_4NCl
II	Lewis	Lewis
	$MCl_x{\cdot}yH_2O$; M = Cr, Co, Cu, Ni, Fe	R_4NCl
III	Brønsted	Lewis
	RZ; Z = $CONH_2$, COOH, OH	R_4NCl
IV	Lewis	Lewis
	MCl_x or $MCl_x{\cdot}yH_2O$; M = Al, Zn, Cr	RZ; Z = $CONH_2$, COOH, OH
V	Brønsted	Lewis
	ROH; Z = COOH	RZ; Z = $CONH_2$, COOH, OH

A particular kind of DES is represented by the so-called Natural DESs (NaDESs), which are mixtures composed solely by naturally occurring partners (such as organic acids, plant metabolites, sugars or amino acids).[74] It is worth stressing that DESs containing bio-based derivatives, such as those obtainable from natural compounds, cannot be considered NaDESs with full rights. Another peculiar class of DESs appeared in the literature in 2015 and comprises hydrophobic, water immiscible DESs. Members of this DES class can, in some cases, also be NaDESs.[75,76]

12.3.2 Preparation of DESs and Overview of their Properties and Applications

The ease of preparation of DESs is one of the main advantages over the synthesis and manipulation of the related materials ILs. Indeed, no reaction is required in this case as the production of these species only entails the combination of the selected DES components. Three strategies are usually pursued:

- Heating the two partners (often at 80 °C) until a homogeneous liquid is formed (thermal procedure).
- Freeze drying aqueous solutions of the two partners.
- Ball milling a mixture of the two partners.

Related to the last point, the mechanochemical approach was proved to be feasible in a large scale DES preparation by Crawford *et al.*[77] by means of a twin screw extrusion (TSE) process. Indeed, the archetypical DES composed of ChCl:urea (1 : 2 molar ratio) was produced on a 6.54 Kg h^{-1} scale. The space time yield (STY) output was found to be as high as 3 250 000 Kg m^{-3} day^{-1}, an improvement of 4 orders of magnitude when compared to the batch preparation. Furthermore, the authors highlighted further advantages of the TSE process, such as the suppression of thermal decomposition of sensitive DES components (*e.g.* D-fructose) thanks to the short residence time and the avoidance of the collection and transfer issues related to the handling of viscous DESs. Although the ease of DES preparation, good (Environmental)[78] factor = 0 in two of the strategies listed above (if water from the freeze drying is considered waste) and 100% atom economy are very attractive aspects of these media, a word of warning is needed about possible side reactions that can occur between the DES partners. For instance, in DESs containing ChCl and a carboxylic acid, a self-esterification reaction can take place during the preparation step and in some cases continue to reach 30% conversion after eleven months.[79]

Moving from preparation to physicochemical properties, quite often DESs are said to possess negligible vapor pressure and to be thermally stable. These assertions caused the misleading belief that DESs and ILs are interchangeable regarding these aspects. However, DES vapor pressures can be significantly higher than those observed for typical ILs. Ravula *et al.* ranked low-volatility fluids in the following decreasing vapor pressure order: triglyme,

short-chain PEGs > long-chain PEGs > DESs > protic ILs > polymeric ILs > conventional, aprotic ILs > dicationic ILs.[80] The same discrepancy between DESs and ILs holds true for their thermal stability. It has been shown for a set of ChCl-based DESs, studied by means of TGA coupled with FTIR, that the nature of the HBD component represents the limiting factor in terms of the thermal stability of the system.[81] In this series, the first decomposition step was related to the HBD part (in some cases a simple evaporation process was observed) followed by the formation of decomposition products ascribable to the entire DES system and finally completed with events associated with the more thermally stable HBA.

An updated, detailed survey of the physicochemical properties of DESs can be found in the highlighted ref. 82. One of the main messages of this report is that several pieces of the puzzle are still missing (especially in terms of phase diagrams) and that more studies are needed to fully understand the relationship between DES structure and their behaviour. However, at least for the most well-known DESs, Kamlet–Taft solvatochromic parameters, pH values, conductivity, thermal stability and viscosity data are available. The latter property is a relevant one: high viscosity values have a negative effect on mass transfers, which is crucial for solvent applications. DESs are known to be quite viscous fluids, with for instance ChCl-ethylene glycol (1 : 2 molar ratio) presenting a viscosity of 52 cP at 20 °C against 1 cP for water. Furthermore, viscosity values are even higher for polyhydroxylated HBDs (*e.g.* glycerol and sugars). A working solution for making DESs into better solvents has been the use of additives that could, however, modify the interaction of the DES components at the molecular level and change the physicochemical properties of the bulk material beyond viscosity. In this context, the case of water as an additive is particularly interesting. Indeed, it has been shown that some DES systems are able to tolerate substantial amounts of water before losing their properties and acting as water solutions. This is somewhat counterintuitive on account of the dual HBA-HBD nature of water, which would be expected to disrupt the hydrogen bonding pattern of the pristine DES, even if present in small amounts. However, the above behaviour, which has been highlighted only in specific cases, should not be taken as generally valid for all DESs.

A similar analysis should be done for the (eco)toxicological profile of DESs, a feature which is praised in several publications. Indeed, the number of systems available is so large that caution is required when making general statements about DESs. Studies in this area are still in their infancy and only recently has a multilevel evaluation to assess the overall impact of DESs been proposed.[83] It is fair to state, when dealing with NaDESs, that their profile is likely to be more benign concerning toxicity and biodegradability. However, a very recent metabolomic study focusing on ChCl-based DESs highlighted that using safe DES partners does not necessarily result in safe DESs.[84]

As mentioned at the very beginning of this chapter, tunability gives DESs considerable potential as materials and constitutes their main shared feature

with ILs. In the former class, from a single HBA several liquid mixtures can be prepared selecting different HBDs, while in the latter class a single cation can give rise to related families of ILs *via* a metathesis reaction. In both cases, a solvent/material with specific application-driven characteristics can be designed and obtained, with a clear advantage for DESs in terms of preparation protocols and green metrics.

Taking into account the ease of preparation and low cost compared to ILs, (Na)DESs are regarded as the 21st century solvents for the development of sustainable chemistry.[74] Other key features that make these materials extremely attractive are their favorable physicochemical properties (and the possibility to modulate them easily) as well as their benign (eco)toxicological profiles, especially when compared with traditional organic solvents. Historically, DESs were firstly employed in metal processing applications,[85] while nowadays they find use in a rather wide range of different research areas, which include biomass treatment,[86–88] high value added compound extraction,[89–91] biocatalysis reactions[92] and biomedical engineering.[93]

12.3.3 DESs in Organic Synthesis

A research area where DESs have experienced continuously growing interest in the last ten years is that of organic chemistry. Indeed, the quest for safer, renewable and environmentally friendlier media for organic reactions is boosting the search for alternatives to conventional solvents. In this context, DESs have first been considered just as green innocent solvents, capable of dissolving both hydrophilic and lipophilic reacting partners, while over time being increasingly appreciated for their ability to function as both a solvent and catalyst. The active role of DESs in organic reactions is for example highlighted in works where they are exclusively used as a catalyst, even a supported catalyst, rather than solvents. It is also worth mentioning that the effect on reaction outcomes of combining alternative technologies, such as microwaves[94,95] or ultrasound,[96] with the use of DESs is nowadays an active topic of research.

Before considering specific examples, a brief description of the solutions adopted to date to address one of the major issues encountered in running a reaction in DESs, namely the separation of the reaction products from the DES medium avoiding the use of traditional organic solvents, is provided. In the simplest scenario, the reaction product precipitates or gives rise to a separate layer, thus allowing for its physical separation. If this is not the case, the reaction mixture can be treated with water, which will selectively dissolve the DES components and leave the reaction products behind. Alternatively, a more classical extraction process can be pursued with the latest generation of (bio-based) organic solvents (*e.g.* 2-Me-THF, dimethyl isosorbide, cyrene), which are endowed with a benign environmental and toxicity impact. Both approaches are characterized by drawbacks, and hence a case-by-case evaluation needs to be performed in order to select the option that best fits our reaction of interest. Indeed, the addition of water requires

a drying step for the DES recovery, which costs energy and poses practical considerations for large industrial setups. Also, DES side reactions can occur during this thermal treatment, while residual water in the DES can change its physiochemical properties and thus its performance. On the other hand, the use of organic solvents, although of low impact, partially counterbalances the benefits related to the use of DESs, especially if their final removal to isolate the products is hampered by low volatility.

Although usually a few consecutive cycles are carried out to prove that these systems still work with only minor yield decrements, an in depth study of the recovered DES focusing on the determination of the HBA/HBD molar ratio, as well as on the presence of residual reagents or water, is often missing. It is therefore clear that the recovery of the reaction products still represents an open challenge for the development of efficient and sustainable DES-based large scale organic reactions.

In the following part of this section, a few examples of organic reactions in DESs are presented with the intention to provide an overview of possible options and open questions. A comprehensive survey of organic reactions carried out in DESs is beyond the scope of the present analysis and the reader is invited to refer to excellent dedicated reviews[73,97–101] on the topic.

12.3.3.1 Consecutive Reactions in DESs

The possibility to perform sequential transformations, either one-pot in the same DES, or even in two different DESs, represents an intriguing option toward the goal of multistep synthesis in these new media.

The one-pot azidation/cyclisation of phenyl acyl bromide has been performed in ChCl : glycerol (1 : 2 molar ratio) for the preparation of 2,5-diaryl pyrazines (yields up to 95%, Scheme 12.6).[102] The utility of the intermediate phenyl acyl azide has also been further highlighted by studying its transformation into functionalized imidazole and pyrimidine derivatives (same DES or in ChCl : urea, 1 : 2 molar ratio).[103]

The one-pot preparation of several (*E*)-4-benzylidenylacridin-1(2*H*)-one derivatives, including also various (*E*)-2-styryl quinoline-3-carboxamides has been reported by the group of Khan.[104] In this case, after completion of the first reaction in K_2CO_3 : glycerol (1 : 1 wt/wt), a different DES (dimethyl urea : tartaric acid; 7 : 3 wt/wt) was added together with the required reagents.

This approach, although appealing, will need further investigation to ensure the recovery of the DES system employed.

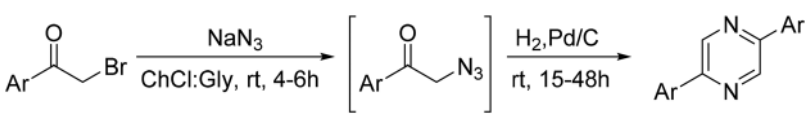

Scheme 12.6 One-pot azidation/cyclisation of phenyl acyl bromide in DESs.

12.3.3.2 Unveiling the Role Played by the DES

As mentioned previously, the role played by DESs in reactions can vary substantially: they can behave just as solvents, as participating catalysts (*e.g.* L-proline-based DESs) or as active species. The hydrogen bond acceptor and donor nature of the DES components is often advocated to play a key part during the course of a reaction and reaction mechanisms based on this assumption have been proposed. However, only in a handful of works are these hypotheses corroborated by additional investigations.

Gutierrez-Henandez *et al.* reported a six-step, enthalpy-controlled mechanism for the aza-Michael reaction of arylamines and maleimide performed in ChCl:TsOH and ChCl:TsOH:H_2O.[105] The presence of the DES and DES plus water has a clear beneficial effect in stabilizing complexes, intermediates, transition states, and products (Figure 12.5). Beyond the computational study, the reaction mechanism was further validated by H/D exchange NMR experiments. This work highlights well how a deep investigation into the role of both DES partners and of any additional components can be instrumental in understanding these systems and help to fully exploit their potential.

12.3.3.3 The Case of Reactive DESs

Beyond an active role as a catalyst, DES components can act as a solvent and substrate at the same time.

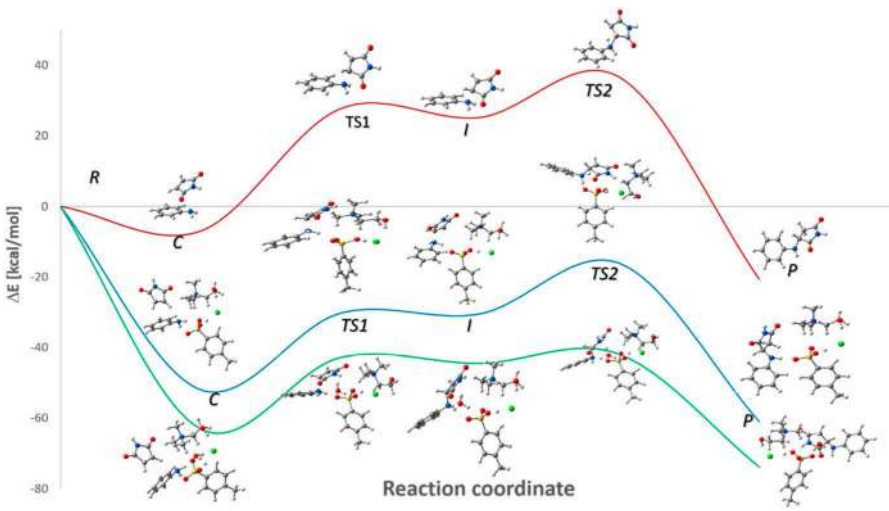

Figure 12.5 Energy profiles for the addition of arylamines to maleimide. The top, middle, and bottom lines show the addition in the absence of solvent (including water) and in the presence of ChCl:TsOH and ChCl:TsOH:H_2O, respectively. Reproduced with permission from ref. 105 Copyright 2021 The American Chemical Society.

Karimi *et al.* studied the conversion of sucrose into 5-(hydroxymethyl) furfural (HMF), which is a biobased platform chemical, employing a newly developed, magnetically recoverable solid catalyst and making use of a series of Type III DESs as solvents (Scheme 12.7).[106] The authors observed that, when they moved to a Type V DES composed of sucrose and fructose, a higher yield of the desired product was obtained. A conceptually similar example has been reported by Wang *et al.*[107] In this case, the preparation of caffeoyl alkyl esters was carried out by combining the appropriate alcohol and a cation exchange resin with a DES composed of ChCl and caffeic acid.

This almost unexplored approach is particularly intriguing as it allows for treating solid substances as liquid materials when the partner of a DES. This possibility could well inspire novel transformations of naturally occurring solid compounds.

12.3.3.4 Grignard and Organolithium Chemistry in DESs

In 2014, ChCl-based DESs were for the first time used as media for the addition of Grignard and organolithium reagents to ketones (Scheme 12.8).[108] This chemoselective transformation is also remarkable as it can be carried out in air and at room temperature.

After comparing the results obtained in DESs against those in water as a solvent, the authors rationalized their data invoking a kinetic activation of the alkylating reagents, which would favour the nucleophilic addition over the competing hydrolysis. The latter process would be normally expected to rapidly take place in the presence of the hydrogen bond network of the DES system. This ground-breaking work paved the way for several related developments. For instance, directed *ortho*-metalation or nucleophilic acyl substitution reactions have been chemoselectively performed on an aromatic

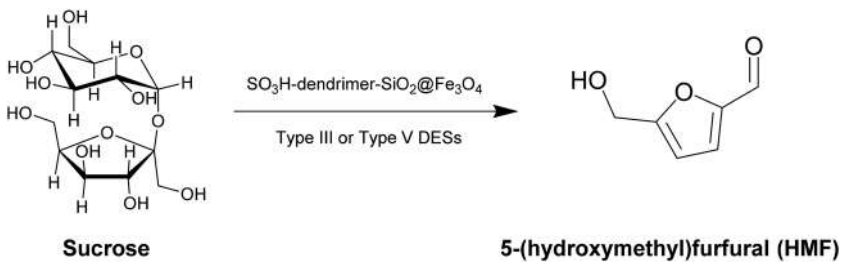

Scheme 12.7 Preparation of HMF in DESs exploiting a magnetically recoverable acid solid catalyst.

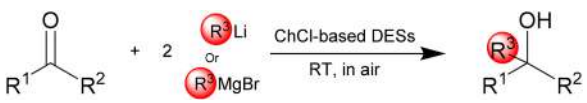

Scheme 12.8 Chemoselective addition of Grignard and organolithium reagents to ketones in DESs.

carboxylic acid amide carried out in ChCl-based DESs, combined in some cases with cyclopentyl methyl ether. The optimised conditions also allowed for a one-pot, telescoped *ortho*-lithiation/Pd-catalyzed Suzuki–Miyaura coupling reaction.[109] Two reviews by Hevia, Garcıa-Alvarez and Capriati summarize well recent advancements, challenges and opportunities in this research area.[110,111]

12.3.3.5 To What Extent are the Green Metrics of Reactions in DESs Investigated?

Reactions in DESs are often ranked against those performed in conventional organic solvents and evaluated through traditional synthetic parameters (*e.g.* conversion, yield, regioselectivity). Conversely, very few green metrics analyses have been reported to date. For instance, the E-factor has been calculated for a series of metal catalyzed cross coupling reactions (Suzuki–Miyaura, E-factor = 8.74;[112] Sonogashira, E-factor = 24.4;[113] Ullmann, E-factor = 13.8;[114] Hiyama, E-factor = 25.6 [115]) and Nazarov cyclization (E-factor = 19.5 [116]).

A deeper analysis has been performed and published in two key papers by Kouznetsov and Ochoa-Puentes.[117,118] The results obtained for different green metrics in the preparation of tetrahydroquinolines through aza Diels–Alder reaction in ChCl : $ZnCl_2$ are summarized in Figure 12.6.[118] The

Process	Number of steps	Yield (%)	AE(%)	AEf(%)	CE(%)	RME(%)	OE(%)	MP(%)
A	1	85	95	81	85	81	85	4.73
B	1	52	95	49	45	43	45	0.25
C	1	55	95	52	47	45	47	0.87

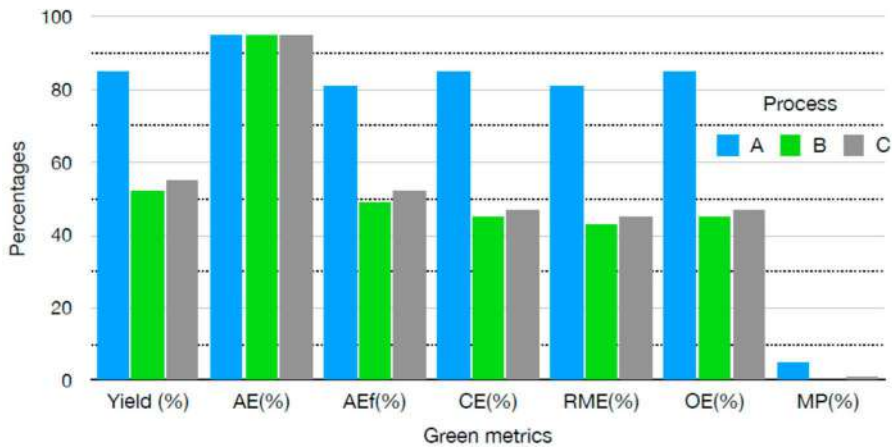

Figure 12.6 Green metrics for the preparation of a tetrahydroquinoline in a DES (process A) against two literature methods (processes B and C). Adapted from ref. 118 with permission from American Chemical Society, Copyright 2021.

optimized reaction conditions (process A) compared favourably with two literature methods (processes B and C) regarding atom efficiency (AEf), carbon efficiency (CE), reaction mass efficiency (RME), optimum efficiency (OE) and mass productivity (MP). Atom economy (AE) had similar values in the three processes considered.

The authors also reported the comparative evaluation of the E-factor, the solvent intensity, the process mass intensity and the water intensity, which again confirmed the greener character of their method.

Recently, a clear trend can be seen whereby green metric analyses are becoming essential tools for assessing the sustainability of a process. This is in sharp contrast with the current, traditional approach, where the environmental impact is determined solely by looking at the nature of the selected medium. This novel attitude, though, is yet to become a routine process when planning reactions performed in DESs.

12.3.4 Future Perspective

The use of DESs as reaction media for organic reactions holds great promise towards the goal of sustainability in the chemical industry. Several research groups are becoming interested in exploiting the potential of these materials: a steady increase in the research activity in this area is expected in the coming years, in combination also with alternative green technologies. However, it is highly desirable that the future synthetic challenges will be tackled following a multilevel perspective. Indeed, building knowledge on DES systems from the reactivity point of view should not come at the price of overlooking their (eco)toxicity profiles. Other aspects that must not be neglected are the overall environmental impact of the reaction systems, as well as the possible alterations of the DES partner interactions, due for example to the presence of a third component, reagents or reaction products. The fundamental tools needed to tackle these issues are still limited or missing, and several research groups are working with this aim in mind.[119]

From the synthetic perspective, while several organic reaction types have been studied in DESs, the DES types used are often limited to the prototypical ChCl-based ones. It can be therefore anticipated that broadening the type of DESs investigated, and thus exploiting the DES tunability potential, will provide further unexpected results and reaction outcomes. At the same time, the study of the relevant reaction mechanisms by means of multiple techniques will enable a clear understanding of the role played by each DES component.

Finally, as mentioned above, there is an urge to explore new strategies for the recovery of reaction products or at least a need for gaining an in-depth understanding of the parameters that allow for an efficient retrieval of the newly formed compounds. These investigations are of great importance for improving the green metrics analyses of the reactions carried out in these new media. The final goal is to assess the entire life-cycle impact of such processes, as well as evaluating the technical and economic feasibility in large scale setups.

12.4 Author Credits

C.S. Pomelli edited Section 12.2 on Ionic Liquids, while L. Guazzelli edited Section 12.3 on Deep Eutectic Solvents.

References

1. T. Welton, *Chem. Rev.*, 1999, **99**, 2071.
2. T. Welton and J. P. Hallet, *Chem. Rev.*, 2011, **111**, 3508.
3. T. Welton, *Biophys. Rev.*, 2018, **10**, 691.
4. J. P. Hallett and T. Welton, *Chem. Rev.*, 2011, **111**, 3508.
5. *Green Industrial Applications of Ionic Liquids*, ed. R. D. Rogers, K. R. Seddon and S. Volkov, NATO Science Series, Kluwer, Dordrecht, 2002.
6. C. Chiappe, F. Signori, G. Valentini, L. Marchetti, C. S. Pomelli and F. Bellina, *J. Phys. Chem. B*, 2010, **114**, 508.
7. S. K. Singh and A. W. Savoy, *J. Mol. Liq.*, 2020, **297**, 112038.
8. S. V. Dzyuba, K. D. Kollar and S. S. Sabnis, *J. Chem. Educ.*, 2009, **86**, 856.
9. T. L. Graves and C. J. Drummond, *Chem. Rev.*, 2008, **108**, 206.
10. J. Zhang, X. Zhang, M. Yang, S. Singh and G. Cheng, *Bioresour. Technol.*, 2021, **322**, 124522.
11. P. G. Jessop, S. M. Mercer and D. J. Heldebrandt, *Energy Environ. Sci.*, 2012, **5**, 7240.
12. P. Dominguez de Maria, *J. Chem. Technol. Biotechnol.*, 2014, **89**, 11.
13. S. Bonermann and S. T. Handy, *Molec*, 2011, **16**, 5963.
14. S. Jiang, Y. Hu and Y. Wang, *J. Phys. Chem. Ref. Data*, 2019, **48**, 033101.
15. A. Maiti, A. Kumar and R. D. Rogers, *Phys. Chem. Chem. Phys.*, 2012, **14**, 5139.
16. M. O Mahony, D. S. Silvestor, L. Aldous, C. Hardacare and R. G. Compton, *J. Chem. Eng. Data*, 2008, **53**, 2884.
17. M. G. Freire, C. M. S. S. Neves, P. J. Carvalho, R. L. Gardas, A. M. Fernandes, I. M. Marrucho, L. M. N. B. F. Santos and J. A. P. Coutinho, *J. Phys. Chem. B*, 2007, **111**, 13082.
18. C. Chiappe, M. Malvaldi and C. S. Pomelli, *Pure Appl. Chem.*, 2009, **81**, 767.
19. A. Rybinska-Fryca, A. Sosnowska and T. Puzyn, *J. Mol. Liq.*, 2018, **260**, 57.
20. X. Wang, K. Chen, J. Yao and H. Li, *Sci. China: Chem.*, 2016, **59**, 517.
21. W. Miao and T. H. Chan, *Acc. Chem. Res.*, 2006, **39**, 897.
22. P. Chandra, S. S. Shinde and A. V. Biradar, *Curr. Org. Chem.*, 2015, **19**, 728.
23. S. Horike, M. Ayano, M. Tsuno, T. Fukushima, Y. Koshiba, M. Misaki and K. Ishida, *Phys. Chem. Chem. Phys.*, 2018, **20**, 21262.
24. C. Maton, N. De Vos and C. V. Stevents, *Chem. Soc. Rev.*, 2013, **42**, 5963.
25. P. Anirban, M. Sriram and P. Shalini, *J. Electrochem. Soc.*, 2020, **167**, 037511.
26. M. Kathiresan and D. Velayutham, *Chem. Commun.*, 2015, **51**, 17499.
27. S. Raiguel, W. Dehanen and K. Binnermans, *Green Chem.*, 2020, **22**, 5225.

28. K. Dong, S. Zhang and J. Wang, *Chem. Commun.*, 2016, **52**, 6744.
29. P. A. Hunt and I. R. Gould, *J. Phys. Chem. A*, 2006, **110**, 2269.
30. K. Fumino, A. Wulfa and R. Ludwig, *Phys. Chem. Chem. Phys.*, 2009, **11**, 8790.
31. K. Fumino, K. Wittler and R. Ludwig, *J. Phys. Chem. B*, 2012, **116**, 9507.
32. G. R. Gupta, T. R. Girase and A. R. Kapdi, Ionic Liquid as a Sustainable Reaction Medium for Diels-Alder Reaction, in *Encyclopedia of Ionic Liquids*, ed. S. Zhang, Springer, Singapore, 2019.
33. C. Chiappe, M. Malvaldi and C. S. Pomelli, *Green Chem.*, 2010, **12**, 1330.
34. R. Bini, C. Chiappe, V. L. Mestre, C. S. Pomelli and T. Welton, *Theor. Chem. Acc.*, 2009, **123**, 347.
35. O. Hollóczki, D. Gerhard, K. Massone, L. Szarvas, Ba. Németh, T. Veszprémi and L. Nyulászi, *New J. Chem.*, 2010, **34**, 3004.
36. M. N. A. N. Daud, E. Bakis, J. P. Hallet, C. C. Weber and T. Welton, *Chem. Commun.*, 2017, **53**, 11154.
37. I. Chiarotto, L. Mattiello, F. Pandolfi, D. Rocco and M. Feroci, *Frontiers*, 2018, **6**, 355.
38. F. Vetica, M. Bortolami, R. Petrucci, D. Rocco and M. Feroci, *Chem. Rec.*, 2021, **21**, 1.
39. O. Bortolini, C. Chiappe, M. Fogagnolo, P. P. Giovannini, A. Massi, C. S. Pomelli and D. Ragno, *Chem. Commun.*, 2014, **50**, 2008.
40. O. Bortolini, C. Chiappe, M. Fogagnolo, A. Massi and C. S. Pomelli, *J. Org. Chem.*, 2017, **82**, 302.
41. N. Murugesh, J. Haribabu, K. Arumugan, C. Balachandran, R. Swaathy, S. Aori, A. Sreekanth, R. Karvembu and S. Vedachalam, *New J. Chem.*, 2019, **43**, 13509.
42. Y. Zhoua, W. Liub, Y. Liua, J. Guana, J. Yana, J. Yuana, D. Taoa and Z. Songa, *Mol. Catal.*, 2020, **492**, 111013.
43. A. P. Abbott, S. S. M. Alabdullah, A. Y. M. Al-Murshedi and K. S. Ryder, *Faraday Discuss.*, 2018, **206**, 365.
44. M. Vafaeezadeh and H. Alinezhad, *J. Mol. Liq.*, 2016, **218**, 95.
45. S. Rezayati, E. Salehi, R. Hajinasiri, S. Afshari and S. Abad, *C. R. Chim.*, 2017, **20**, 554.
46. A. Ajay, A. Ansari, S. Nandi, N. Gupta, N. H. Khan and R. Kureshy, *ChemistrySelect*, 2017, **2**, 11346.
47. A. K. Ressmann, M. Schneider, P. Gaertner, M. Weil and K. Bica, *Monatsh. Chem.*, 2017, **148**, 139.
48. R. Mancuso, C. S. Pomelli, C. Chiappe, R. C. Larock and B. Gabriele, *Org. Biomol. Chem.*, 2014, **12**, 651.
49. R. Kore, P. Berton, S. P. Kelley, P. Aduri, S. S. Katti and R. D. Rogers, *ACS Catal.*, 2017, **7**, 7014.
50. E. Santos, J. Albo and A. Irabien, *RSC Adv.*, 2014, **4**, 40008.
51. Y. Deng, F. Shi, J. Beng and K. Qiao, *J. Mol. Catal. A: Chem.*, 2001, **16**, 33.
52. C. Bu, Y. Gong, M. Du, C. Chen, S. Chaemchuen, J. Hu, Y. Zhang, H. D. Velàsquez, Y. Yuan and F. Verpoort, *Catalysts*, 2021, **11**, 233.

53. M. Du, Y. Gong, C. Bu, J. Hu, Y. Zhang, C. Chen, S. Chaemchuen, Y. Yuan and F. Verpoort, *J. Catal.*, 2021, **393**, 70.
54. M. Sayedul Islam and M. Abu Sayid Mia, *ChemistrySelect*, 2020, **5**, 14632.
55. M. Hu, Z. Lin, J. Li, W. Wu and H. Jiang, *Green Chem.*, 2020, **22**, 5584.
56. P. Migowski and J. Dupont, *Chem. - Eur. J.*, 2007, **13**, 32.
57. S. Li, W. Zhao, Y. Liu, Z. Liu and A. Ying, *Chin. J. Org. Chem.*, 2020, **40**, 1835.
58. G. Fernández, L. Bernardo, A. Villanueva and R. Pleixats, *New J. Chem.*, 2020, **44**, 6130.
59. F. Liu, J. Yu, A. B. Qazi, L. Zhang and X. Liu, *Environ. Sci. Technol.*, 2021, **55**, 1419.
60. Y. Zhao, K. Lu, H. Lu, L. Zhu and S. Wang, *Renewable Sustainable Energy Rev.*, 2021, **139**, 110706.
61. T. P. T. Pham, C. Cho and Y. Yun, *Water Res.*, 2010, **44**, 352.
62. C. Pretti, C. Chiappe, I. Baldetti, S. Brunini, G. Monni and L. Intorre, *Ecotoxicol. Environ. Saf.*, 2009, **72**, 1170.
63. J. Flieger and M. Flieger, *Int. J. Mol. Sci.*, 2020, **21**, 6267.
64. J. Feder-Kubis, P. Czerwoniec, P. Lewandowski, H. Pospieszny and M. Smiglak, *ACS Sustainable Chem. Eng.*, 2020, **8**(2), 842.
65. M. Longhi, S. Arnaboldi, E. Husanu, S. Grecchi, I. F. Buzzi, R. Cirilli, S. Rizzo, C. Chiappe, P. R. Mussini and K. Guazzelli, *Electrochim. Acta*, 2019, **298**, 194.
66. K. S. Egorova, E. G. Gordeev and V. P. Ananikov, *Chem. Rev.*, 2017, **117**, 7132.
67. A. Gamboa, N. Scüßler, E. Soto-Bustamante, R. Romero-Hasler, L. Meinel and J. O. Morales, *Eur. J. Pharm. Biopharm.*, 2020, **156**, 203.
68. W. Florio, S. Becherini, F. D'Andrea, A. Lupetti, C. Chiappe and L. Guazzelli, *Mater. Sci. Eng., C*, 2019, **104**, 109907.
69. J. Suchodolski, J. Feder-Kubis and A. Krasowska, *Microbiol. Res.*, 2017, **197**, 56.
70. C. Croituru and I. C. Roata, *Molecules*, 2020, **25**, 4289.
71. M. A. R. Martins, S. P. Pinho and J. A. P. Coutinho, *J. Solution Chem.*, 2019, **48**, 962.
72. A. P. Abbott, G. Capper, D. L. Davies, H. L. Munro, R. K. Rasheed and V. Tambyrajah, *Chem. Commun.*, 2001, 2010.
73. G. Di Carmine, A. P. Abbott and C. D'Agostino, *React. Chem. Eng.*, 2021, **6**, 582–598.
74. A. Paiva, R. Craveiro, I. Aroso, M. Martins, R. L. Reis and A. R. C. Duarte, *ACS Sustainable Chem. Eng.*, 2014, **2**, 1063.
75. D. J. G. P. van Osch, C. H. J. T. Dietz, S. E. E. Warrag and M. C. Kroon, *ACS Sustainable Chem. Eng.*, 2020, **8**, 10591.
76. C. Florindo, L. C. Branco and I. M. Marrucho, *ChemSusChem*, 2019, **12**, 1549.
77. D. E. Crawford, L. A. Wright, S. L. James and A. P. Abbot, *Chem. Commun.*, 2016, **52**, 4215.

78. R. A. Sheldon, *Green Chem.*, 2017, **19**, 18.
79. N. R. Rodriguez, A. van den Bruinhorst, L. J. B. M. Kollau, M. C. Kroon and K. Binnemans, *ACS Sustainable Chem. Eng.*, 2019, **7**, 11521.
80. S. Ravula, N. E. Larm, M. A. Mottaleb, M. P. Heitz and G. A. Baker, *Chem. Eng.*, 2019, **3**, 42.
81. J. González-Rivera, E. Husanu, A. Mero, C. Ferrari, C. Duce, M. R. Tinè, F. D'Andrea, C. S. Pomelli and L. Guazzelli, *J. Mol. Liq.*, 2020, **300**, 112357.
82. B. B. Hansen, S. Spittle, B. Chen, D. Poe, Y. Zhang, J. M. Klein, A. Horton, L. Adhikari, T. Zelovich, B. W. Doherty, B. Gurkan, E. J. Maginn, A. Ragauskas, M. Dadmun, T. A. Zawodzinski, G. A. Baker, M. E. Tuckerman, R. F. Savinell and J. R. Sangoro, *Chem. Rev.*, 2021, **121**, 1232–1285.
83. J. Torregrosa-Crespo, X. Marset, G. Guillena, D. J. Ramón and R. M. Martínez-Espinosa, *Sci. Total Environ.*, 2020, **704**, 135382.
84. D. Jung, J. B. Jung, S. Kang, K. Li, I. Hwang, J. H. Jeong, H. S. Kim and J. Lee, *Green Chem.*, 2021, **23**, 1300–1311.
85. E. L. Smith, A. P. Abbott and K. S. Ryder, *Chem. Rev.*, 2014, **114**, 11060.
86. G. Colombo Dugoni, A. Mezzetta, L. Guazzelli, C. Chiappe, M. Ferro and A. Mele, *Green Chem.*, 2020, **22**, 8680.
87. E. S. Morais, A. M. Da Costa Lopes, M. G. Freire, C. S. R. Freire and A. J. D. Silvestre, *ChemSusChem*, 2021, **14**, 686.
88. E. S. Morais, M. G. Freire, C. S. R. Freire, J. A. P. Coutinho and A. J. D. Silvestre, *ChemSusChem*, 2020, **13**, 784.
89. E. Husanu, A. Mero, J. Gonzalez Rivera, A. Mezzetta, J. Cabrera Ruiz, F. D'Andrea, C. Silvio Pomelli and L. Guazzelli, *ACS Sustainable Chem. Eng.*, 2020, **8**, 18386.
90. A. A. Redha, *J. Agric. Food Chem.*, 2021, **69**, 878.
91. G. Grillo, V. Gunjević, K. Radošević, I. Radojčić Redovniković and G. Cravotto, *Antioxidants*, 2020, **9**, 1069.
92. M. Pätzold, S. Siebenhaller, S. Kara, A. Liese, C. Syldatk and D. Holtmann, *Trends Biotechnol.*, 2019, **37**, 943.
93. M. S. Rahman, R. Roy, B. Jadhav, M. N. Hossai, M. A. Halim and D. E. Raynie, *J. Mol. Liq.*, 2021, **321**, 114745.
94. G. Colombo Dugoni, A. Sacchetti and A. Mele, *Org. Biomol. Chem.*, 2020, **18**, 8395.
95. F. Curti, M. Tiecco, V. Pirovano, R. Germani, A. Caselli, E. Rossi and G. Abbiati, *Eur. J. Org. Chem.*, 2019, **9**, 1904.
96. S. Marullo, A. Meli and F. D'Anna, *ACS Sustainable Chem. Eng.*, 2020, **8**, 4889.
97. P. Liu, J.-W. Hao, L.-P. Mo and Z.-H. Zang, *RSC Adv.*, 2015, **5**, 48675.
98. J. Garcia-Alvarez, *Eur. J. Inorg. Chem.*, 2015, **31**, 5147.
99. S. Khandelwal, Y. K. Tailor and M. Kumar, *J. Mol. Liq.*, 2016, **215**, 345.
100. D. A. Alonso, A. Baeza, R. Chinchilla, G. Guillena, I. M. Pastor and D. J. Ramon, *Eur. J. Org. Chem.*, 2016, **4**, 612.
101. S. E. Hooshmand, R. Afshari, D. J. Ramón and R. S. Varma, *Green Chem.*, 2020, **22**, 3668.

102. P. Vitale, L. Cicco, F. Messa, F. M. Perna, A. Salomone and V. Capriati, *Eur. J. Org. Chem.*, 2019, 5557.
103. P. Vitale, L. Cicco, I. Cellamare, F. M. Perna, A. Salomone and V. Capriati, *Beilstein J. Org. Chem.*, 2020, **16**, 1915.
104. S. Prameela and F.-R. N. Khan, *Eur. J. Org. Chem.*, 2020, 2888.
105. A. Gutierrez-Hernandez, A. Richaud, L. Chacon-García, C. J. Cortes-García, F. Mendez and C. A. Contreras-Celedon, *J. Org. Chem.*, 2021, **86**, 223.
106. S. Karimi, H. Shekaari, A. Z. Halimehjani and M. Niakan, *ACS Sustainable Chem. Eng.*, 2021, **9**, 326.
107. X. Wang, S. Sun and X. Hou, *ACS Omega*, 2020, **5**, 11131.
108. C. Vidal, J. Garcia-Alvarez, A. Hernan-Gomez, A. R. Kennedy and E. Hevia, *Angew. Chem., Int. Ed.*, 2014, **53**, 5969.
109. S. Ghinato, G. Dilauro, F. M. Perna, V. Capriati, M. Blangetti and C. Prandi, *Chem. Commun.*, 2019, **55**, 7741.
110. J. Garcia-Alvarez, E. Hevia and V. Capriati, *Eur. J. Org. Chem.*, 2015, **1**, 6779.
111. J. Garcia-Alvarez, E. Hevia and V. Capriati, *Chem. - Eur. J.*, 2018, **24**, 14854.
112. G. Dilauro, S. Mata Garcia, D. Tagarelli, P. Vitale, F. M. Perna and V. Capriati, *ChemSusChem*, 2018, **11**, 3495.
113. F. Messa, G. Dilauro, P. Vitale, F. M. Perna, V. Capriati and A. Salomone, *ChemCatChem*, 2020, **12**, 1979.
114. A. F. Quivelli, P. Vitale, F. M. Perna, V. Capriati and A. Salomone, *Front. Chem.*, 2019, **7**, 723.
115. X. Marset, S. De Gea, G. Guillena and D. J. Ramon, *ACS Sustainable Chem. Eng.*, 2018, **6**, 5743.
116. S. Nejrotti, M. Iannicelli, S. S. Jamil, D. Arnodo, M. Blangetti and C. Prandi, *Green Chem.*, 2020, **22**, 3668.
117. D. Pena-Solorzano, V. V. Kouznetsov and C. Ochoa-Puentes, *New J. Chem.*, 2020, **44**, 7987.
118. A. Penaranda Gomez, O. Rodriguez Bejarano, V. V. Kouznetsov and C. Ochoa-Puentes, *ACS Sustainable Chem. Eng.*, 2019, **7**, 18630.
119. For valuable examples, please refer to the virtual issue on Deep Eutectic solvents at, https://pubs.acs.org/page/jpcbfk/vsi/deep-eutectic-solvents?ref=vi_journalhome&.

CHAPTER 13

Environmentally Benign Media: Water, AOS, and Water/Organic Solvent Azeotropic Mixtures

RUCHITA R. THAKORE[a] AND BALARAM S. TAKALE*[a]

[a]Department of Chemistry and Biochemistry, University of California Santa Barbara, California 93106, USA
*E-mail: balaram_takale@ucsb.edu

13.1 Introduction

Use of organic solvents[1,2] to carry out the synthesis of chemicals remains a critical issue in various industries.[3] The waste stream generated during synthesis consists of ~56% organic solvents. Most importantly, water also contributes ~32% waste. The treatment of ~88% of this waste stream is responsible for almost 50% of greenhouse gas emissions[4] in pharmaceutical manufacturing.[5] Apart from the waste stream, solvents like dichloromethane, dioxane, dimethylformamide, benzene, *etc.* pose a serious health risk to chemists and workers exposed to these chemicals. Additionally, the severe threats posed by organic solvents, not only due to their limited availability but also their negative footprint on the environment, such as climate change, has brought attention from several private as well as government institutions to limit, if not ban, the usage of toxic organic solvents.[2] There has been significant interest in finding alternative solvents that are not only less toxic, but also renewable (see Figure 13.1).[6] Pioneering research by several scientists on using water with a trace amount of additives could

Sustainable Organic Synthesis: Tools and Strategies
Edited by Stefano Protti and Alessandro Palmieri

Published by the Royal Society of Chemistry, www.rsc.org

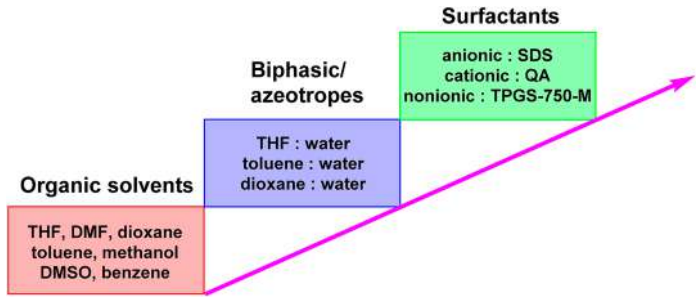

Figure 13.1 Evolution of technologies for greening organic synthesis.

significantly remove organic solvents from chemical reactions that were previously assumed to require dry conditions.[7–10] The American Chemical Society honoured Earth day in 2008 with "Water: Streaming Chemistry".[11] If one looks at the properties of water, the heat capacity is 4.181 kJ/(kg K), heat of vaporization is 40.65 kJ mol^{-1}, boiling point is 100 °C and melting point is 0 °C. It is transparent above 200 nm and has a dielectric constant of 78 (at 25 °C). One would question the importance of these properties in organic synthesis. However, if we compare it with one of the most widely used organic solvents, tetrahydrofuran (THF), THF has a heat capacity of 1.77 kJ/(kg K), heat of vaporisation of 29.6 kJ mol^{-1}, boiling point of 66 °C and melting point of −108 °C. Firstly, water provides a range of reaction temperatures between 0 and 100 °C, and the heat capacity is quite a bit higher, which avoids rapid exotherms in reaction. Apart from this, many organic solvents are flammable, but water is non-flammable. It should be mentioned that given the heterogeneity of reactant-water mixtures, the pK_a value is also not quite the same in bulk water and at the oil-water interface; in fact, the pK_a is at least a unit higher near this interface, which could also provide additional opportunities for chemical reactivity.[12] However, one challenge that is often encountered, especially for the scale-up of organic reactions in water, is the insolubility of organic reactants in water. This leads to poor agitation and a heterogeneous reaction mixture, which subsequently not only impacts the reactivity but creates several hurdles in process safety evaluation. An immediate solution to this problem is to use a small amount of organic solvents for the dissolution of organic reactants. However, the overall purpose of greenness becomes obliterated if such organic "co-solvents" are used in a higher ratio. To overcome these problems, several additives are used. Ionic surfactants are one of the initial discoveries in the category of such additives; these include anionic surfactants such as alpha-olefin sulfonate,[13] alkyl sulfates (AS), primary alkane sulfonates (PAS),[14] cationic surfactants such as quaternary ammonium salts (QA), and neutral/non-ionic surfactants such as TPGS-750-M, Brij-30, PS-750-M, *etc.*[15] This chapter will highlight discoveries based on these categories both from academia and industrial labs.[16] It has been arranged in sections for easy understanding.

13.2 Water and Biphasic/Azeotropic Mixtures as Reaction Solvents

13.2.1 Organic Synthesis Exclusively Performed in Water

Several initial results[17] of doing organic reactions in water[18] suggested that many reactions could in-fact be performed in water in an efficient way. One of the first pioneering examples was reported by Rideout and Breslow,[19] dealing with Diels–Alder reaction in water. A remarkable difference in reactivity was observed in a comparative solvent study. The rate of reaction was increased more than two orders of magnitude when methanol was replaced with water as a reaction solvent. The notion of hydrophobicity was the major focus, while the importance of hydrogen bonding and phase boundaries was not realized in this work. Perhaps, the reaction conditions limit its synthetic utility (see Scheme 13.1). The next breakthrough truly in terms of application to synthetic chemistry with water as a solvent was disclosed by Narayan, Sharpless and co-workers.[20] They were able to show the concept of "on water"[21] reactions for several classes of reactions, including Diels–Alder reaction. Remarkably, in all cases, not only faster reaction rates but also excellent chemical yield of the desired product was obtained (see Scheme 13.2). This work gives greater understanding about the "on water" phenomenon;[22] however, much remains to be understood, including why exactly the rate of reaction on water is higher? Also, its extension to other reactions will be important. The challenges and solutions when all reactants are solid should not be overlooked, especially for large scale synthesis. A question still remains to be answered regarding the true notion of these reactions occurring "in water", "on water", or in the presence of water.[23] Although, mechanistic details at the molecular level for reactions carried out in water are relatively unknown,[24] Jung and

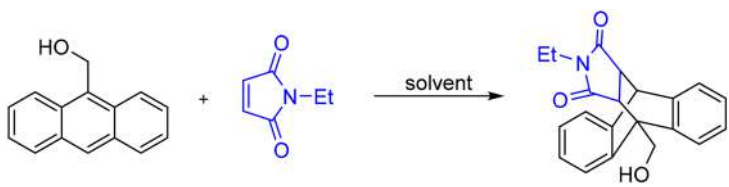

solvent	rate constant of Diels-Alder Reaction k_2 X 10^5, M^{-1} S^{-1}
MeOH	75.5
H_2O	4400
H_2O + LiCl (4.86 M)	10800

Scheme 13.1 Kinetics of Diels–Alder reactions using aqueous reaction media.

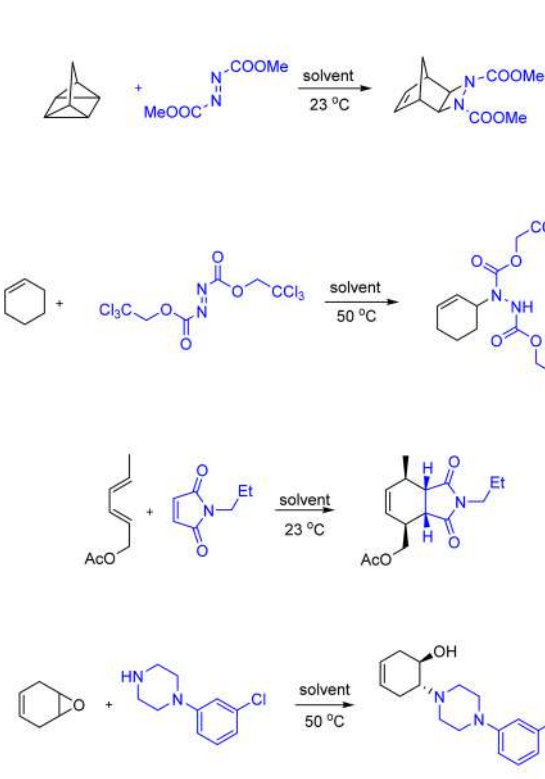

(eq. 1: cycloaddition)

solvent	time	yield (%)
neat	2 h	0
toluene	24 h	74
"on water"	**10 min**	**82**

(eq. 2: ene reaction)

solvent	time	yield (%)
neat	36 h	62
benzene	24 h	70*
"on water"	**8 h**	**91**

* performed at 80 °C

(eq. 3: Diels-Alder reaction)

solvent	time	yield (%)
neat	10 h	82
toluene	144 h	79
"on water"	**8 h**	**81**

(eq. 4: epoxide opening)

solvent	time	yield (%)
neat	72 h	76
toluene	120 h	<10
"on water"	**12 h**	**88**

Scheme 13.2 Reaction rate differences for on-water and in toluene reactions.

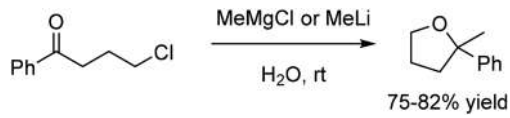

Scheme 13.3 Addition of organometallic reagents onto ketones using water as a solvent.

Marcus used a computational study and proposed that free hydroxyl groups from water help in hydrogen bonding and subsequent reactivity.[25] However, the exploration of chemistries remains the forefront of the research, and reactants such as alkyllithium or alkylmagnesium, which were kept at safe distance from water, are now used for reactions performed on water (see Scheme 13.3 and 13.4).[26,27]

Some scientists have asked questions about the reactions performed in water that required extraction with organic solvents (at least on a small scale), and hence the whole purpose of greening the process became debatable.[28] However, such commentary would not generate a wider perspective

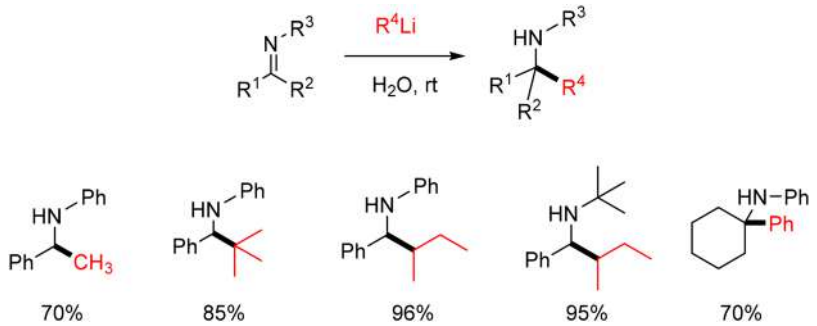

Scheme 13.4 Addition of alkyl lithium onto imines in water as a solvent.

about how someone prefers to call a process "green". For example, if a reaction solvent as hazardous as dimethylformamide is replaced with water, and the product from the reaction is extracted with a greener solvent such as ethylacetate, then it totally defeats the above debate, because the toxicity of DMF is much higher compared to ethyl acetate.[29] In fact, in many large-scale processes, it is possible to crystallize or filter the product directly from the aqueous phase. Also, given the heat capacity of water, potential runaway reactions are minimized. Yes, the waste-water treatment is a costly process, and uncleaned water could not be simply dumped in a biological treatment plant.[30] However, such a question also remains valid when reactions are performed in organic solvents where aqueous work up is required. In fact, several of such aqueous work-ups use more water in purification than pure water-based chemistries. Nevertheless, it has always been brought to attention that handling of reactions in water could be easy on a small scale, but it becomes much more complicated for large scale processes. The heterogeneity of the reaction mixture could make it difficult to provide a uniform data point in safety assessment of the process,[31] and this becomes a unique challenge for process safety evaluation labs (PSEL). The agitation of a reaction could be a problem as insoluble organic reactants start to form clumps, leading to severe setbacks in terms of reaction profile and reproducibility. The immediate and straightforward solution to this problem could be the addition of a small amount of organic solvent for the dissolution of the organic reactant. This will be discussed below in further detail.

13.2.2 Organic Reactions in Aqueous Organic Solvents or a Biphasic System

Use of biphasic systems is valuable when organic reactants are insoluble in water. Use of a small amount of organic co-solvent could significantly enhance the reaction performance. However, the initial complex phenomenon of the reaction on water becomes more complex to understand when co-solvents[32,33] are added in such systems.[34] The choice of co-solvent has

prime importance depending on the nature of the reaction. For example, S_N2 reactions of alkyl halides performed using an alcoholic co-solvent led to the formation of ether products along with the desired hydrolysis products.[35] Nevertheless, one of the earliest reports based on using an organic co-solvent in a reaction was disclosed by Waldmann for aza-Diels–Alder reaction between an amino acid methyl ester and diene. Moderate to good yields of the desired cyclized products were obtained when ~10 vol% THF was used for the reaction (see Scheme 13.5).[36]

1,4-Addition of nitro alkanes on to unsaturated compounds was performed in a biphasic solvent of $H_2O:CHCl_3$ (9:1) in the presence Sodium Lauryl Sulfate (SLS) at 25 °C.[37] It was found that using chiral catalyst **L1**, remarkable enantiomeric as well as diastereomeric ratios were obtained (see Scheme 13.6). The authors also demonstrated that this reaction could be easily scaled up to prepare the desired product in over a gram.

Buchwald's group recently used a mixture of solvents, such as THF and water (1:5), to perform cyanation of aryl halides (see Scheme 13.7).[38] The Pd-catalyzed coupling seems to work well only when such a mixture of solvents is used, and failed to give a satisfactory yield of the desired product when performed in either of these solvents. The utility of the reaction was

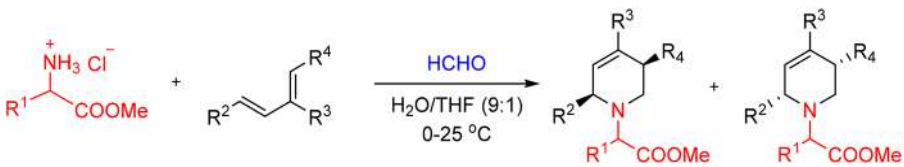

Scheme 13.5 Aza Diels–Alder reaction in an aqueous organic solvent.

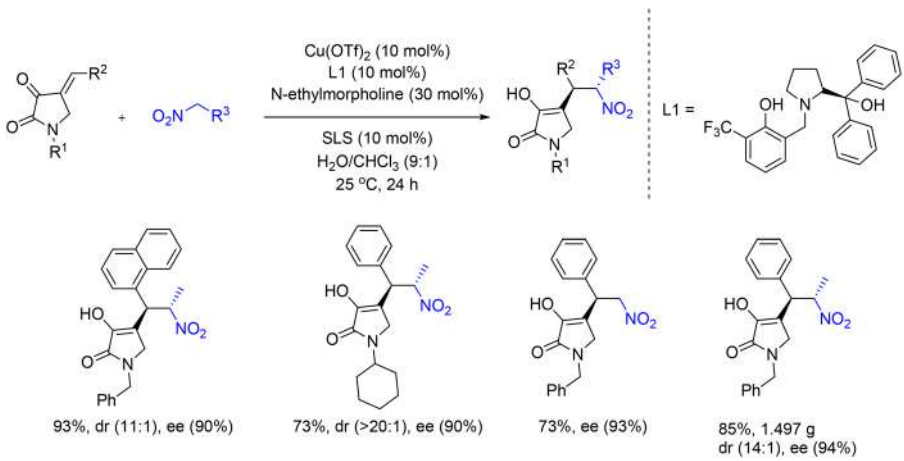

Scheme 13.6 Addition of nitroalkanes onto unsaturated ketones in an aqueous organic solvent.

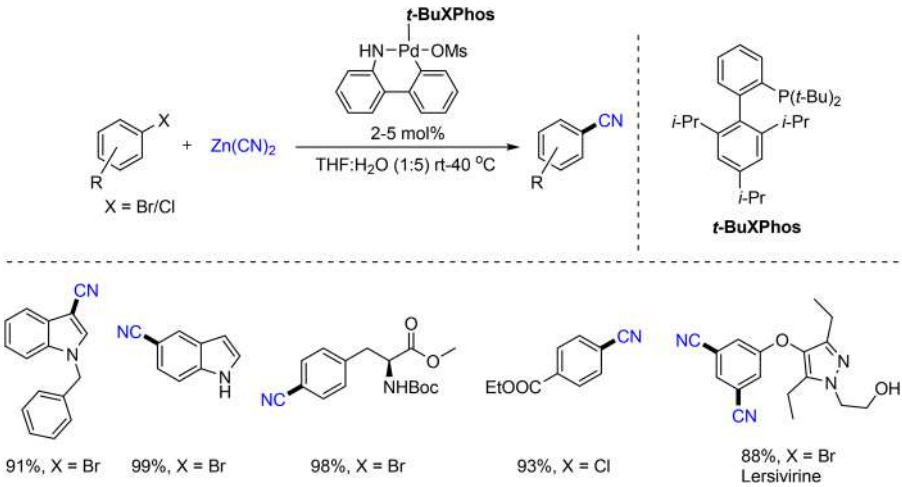

Scheme 13.7 Cyanation of aryl halides in an aqueous organic solvent.

wide, and several heteroaryl halides were cyanated efficiently at room temperature, although they required a high Pd–catalyst loading. Nevertheless, the reaction was also explored for double cyanation of a dibromide, leading to the synthesis of lersivrine, a reverse transcriptase inhibitor.

13.3 Surfactants as an Additive for Chemistry in Water

13.3.1 Anionic Surfactants

Sodium dodecyl sulfate (SDS) and sodium lauryl sulfate (SLS) are widely used surfactants that form micelles in water. One of the earliest reports on the use of these surfactants for chemical reactions was disclosed by Jaeger and Robertson[39] for electrophilic halogenation of aryl ethers. It was observed that the surfactant SDS played a crucial role to increase the chemical yield as well as regioselectivity of the reaction. Chlorination performed in a micellar solution of SDS resulted in a 94% yield and ~3 : 1 ratio of para : ortho chlorination compared to 1.6 : 1 in pure water. A similar effect was observed for bromination, in which the use of SDS led to 79% yield with a para : ortho ratio of 114 : 1, which dropped to 21% yield and a 21 : 1 ratio when performed in pure water (see Scheme 13.8).

The remarkable reactivity after combining a surfactant, a single walled carbon nanotube (SWNT) ligand and $Ni(DS)_2$, a nickel catalyst called Lewis acid-surfactant-combined catalyst (LASC)[40] was observed in the case of addition of hydroxyl amines to unsaturated compounds. It is worth mentioning that the reaction only carried out in the presence of water led to both high chemical yield and enantioselectivity, while an organic solvent failed to give an acceptable amount of the desired product (see Scheme 13.9).[41]

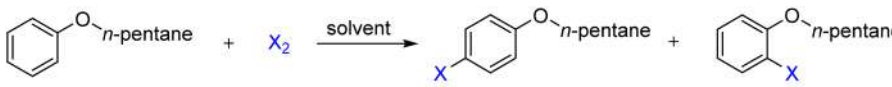

solvent	X	yield (%)	ratio (para:ortho)
SDS in H_2O	Cl	94	3.1:1
H_2O	Cl	15	1.6:1
SDS in H_2O	Br	79	114:1
H_2O	Br	21	21:1

Scheme 13.8 Halogenation of aryl ethers using SDS in water.

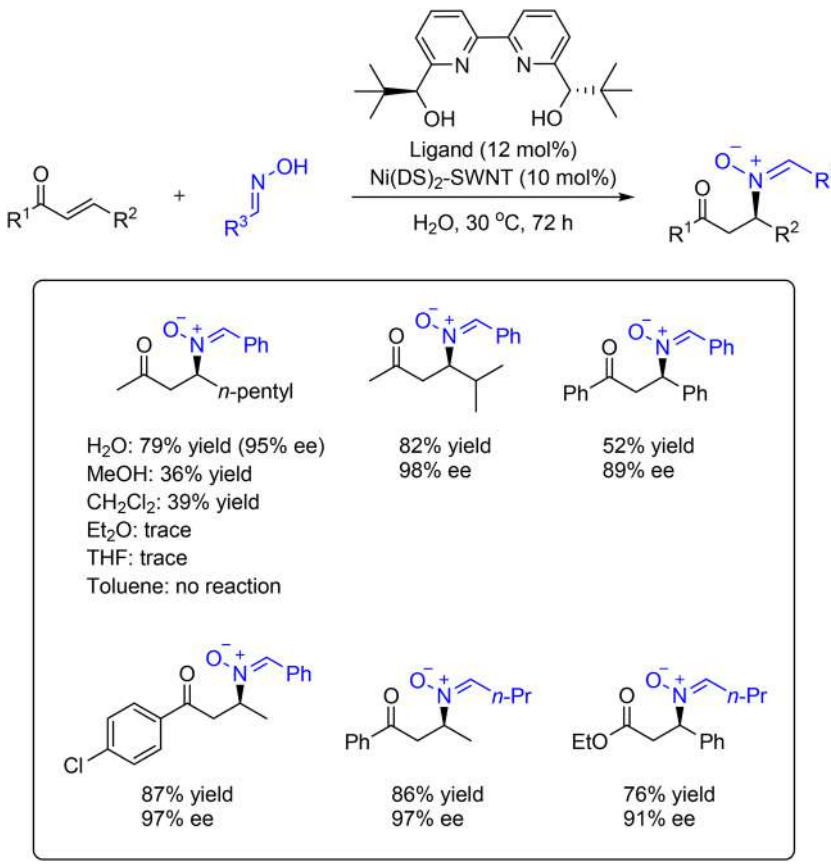

Scheme 13.9 Addition of hydroxylamines onto unsaturated compounds in water.

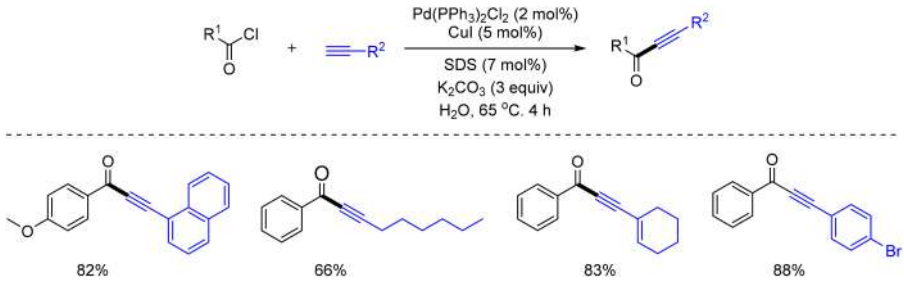

Scheme 13.10 Pd-catalyzed coupling of aroyl chlorides with alkynes in water.

Li's group[42] has demonstrated an interesting application of SDS for the coupling of acid chlorides with alkynes to prepare various ynones in good chemical yields. It should be mentioned that acid chlorides are mostly sensitive towards moisture leading to effective deactivation to the corresponding acid. Given the nature of the reaction conditions, these acid chlorides were quickly attacked by alkynyl-copper species before hydrolysis to the acid could take place (see Scheme 13.10).

13.3.2 Amphiphilic Surfactants

Lipshutz and co-workers[43] have pioneered the use of amphiphilic surfactant additives to perform several organic transformations. It is believed that these surfactants form aggregates of size 25–50 nm, called nano-micelles. It is indeed made-up of a lipophilic core obtained from the hydrocarbon portion, and a hydrophilic shell obtained from polyethylene glycol. Given the special properties of these micelles, most of the reactions were performed efficiently in bulk water just by adding ~2 wt% of amphiphilic surfactant. From a variety of surfactants studied for several reactions, the most widely used is TPGS-750-M (Tocopherol-PolyethyleneGlycol-Succinate) to date.[44] Although this surfactant is only used in a trace amount (2 wt%), several efforts have been put forth to make TPGS-750-M using green processes. The more recent of such an approach is removal of the succinic acid linker (Figure 13.2), which not only helped in atom economy but also the step economy, and now TPG-lite can be made using a two-step sequence in a much more environmentally friendly manner compared to the original TPGS-750-M.[45] On some occasions, when free –OH is not a problem in the reaction, Brij-30 or Brij L4, a commercially available surfactant supplied by Croda Chemicals, has also shown promising results in chemical reactions. The cryoTEM images suggested that both TPGS-750-M and TPG-lite have a similar size as well as arrangement of the nano-micelles; however, Brij-30, owing to its free-OH group, likes to form clusters of nano-micelles (Figure 13.2). Nevertheless, this micellar technology has been applied to most of the well-known reactions, as shown in Scheme 13.11.

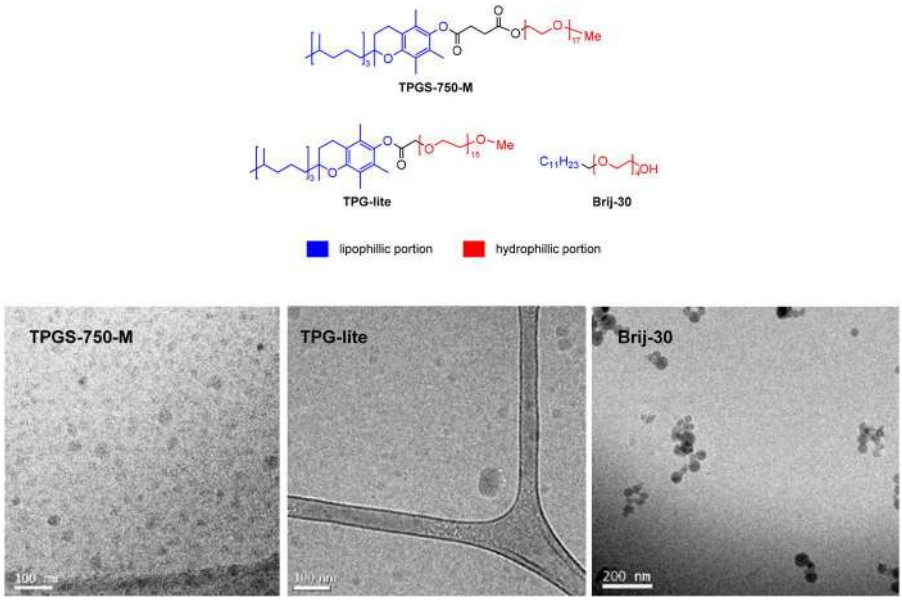

Figure 13.2 Chemical structures (top) and cryoTEM images of TPGS-750-M, TPG-lite, and Brij-30 sequentially.

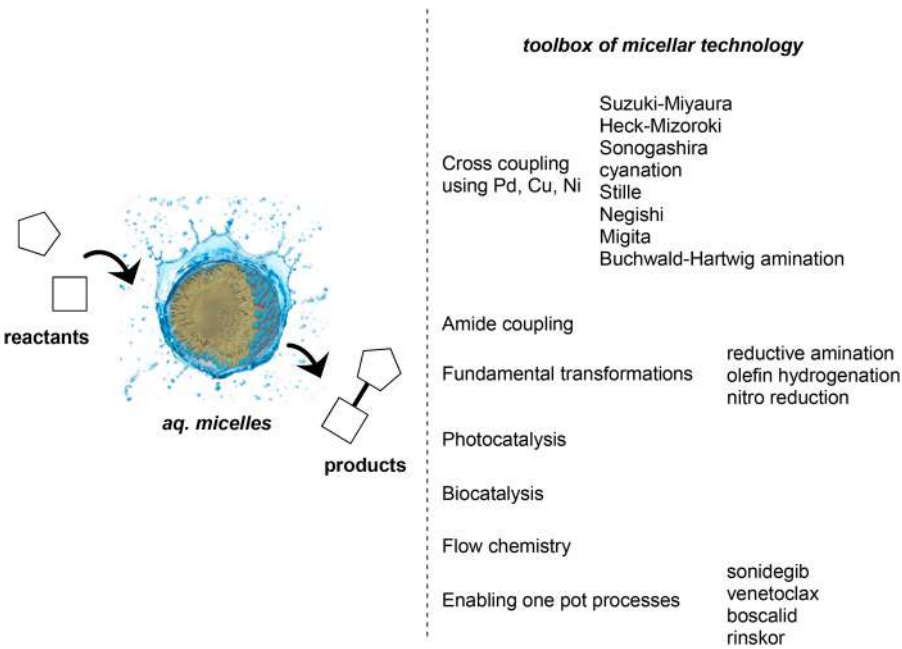

Scheme 13.11 Toolbox of reactions performed in aqueous micelles.

This system is quite different than just using water as a solvent. In this case, reactions are taking place in these nano-micelles that involve an inner lipophilic core (vitamin-E portion) and outer hydrophilic shell (polyethylene glycol portion), which technically still means that reactions are happening in organic solvents, and it is nothing but this tiny amount of surfactant forming nano-reactors. This phenomenon also gives an opportunity to design new catalysts or reagents that could be more lipophilic, and hence partition easily within these micelles, for better reactivity (Figure 13.3). For example, a highly effective Suzuki–Miyaura cross coupling reaction could be performed using only 0.03 mol% of Pd-precatalyst **P2.**[46] The presence of an isopropyl group (for lipophilicity) in this catalyst seems to be particularly useful for effective cross coupling. Nonetheless, without this substitution (**P1**), the reactivity was poor (see Scheme 13.12).

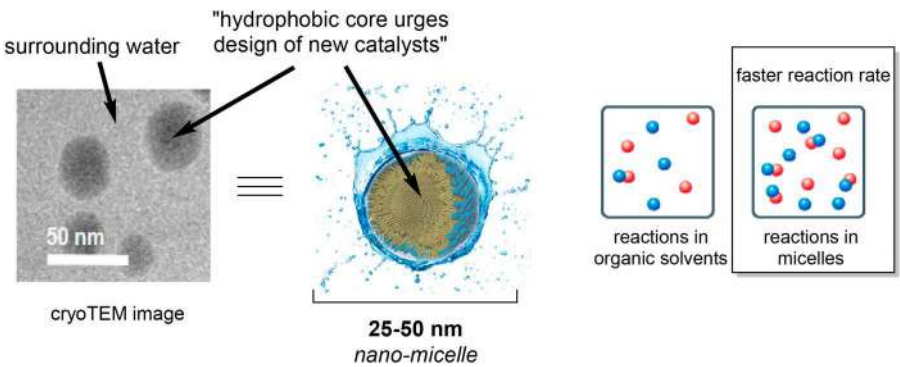

Figure 13.3 Simulated structure of nanomicelles formed by TPGS-750-M in water and its impact on chemical reactions.

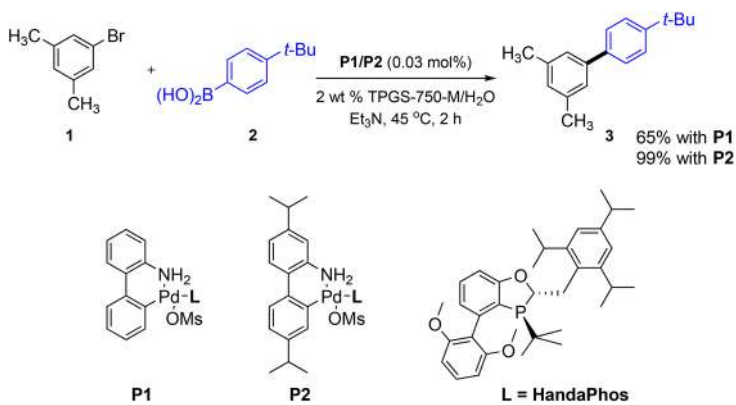

Scheme 13.12 Importance of the designed lipophilic catalyst for Suzuki–Miyaura coupling.

Drug discovery is becoming more and more challenging, with new diseases or increased complexity of old diseases, requiring highly complex molecules, and hence complex chemical synthesis. Efficient preparation of these molecules is more challenging than ever. Many of the lab-based processes discovered at academic level fail when applied to real world molecules. Lipshutz, Takale and co-workers[47] recently demonstrated that Stille coupling could be employed to make not only active pharmaceutical intermediates (APIs) but also other highly complex heterocyclic molecules. The most interesting factor of this discovery was the use of pre-catalyst **P3**, which is based on an economical as well as easily available ligand, PPh_3, such that this protocol was also scalable to make API intermediate OSU6162 on a multigram scale (see Scheme 13.13). The presence of ammonium salt, tetrabutylammonium chloride (TBAC), and CuI was an essential part of this reaction recipe.

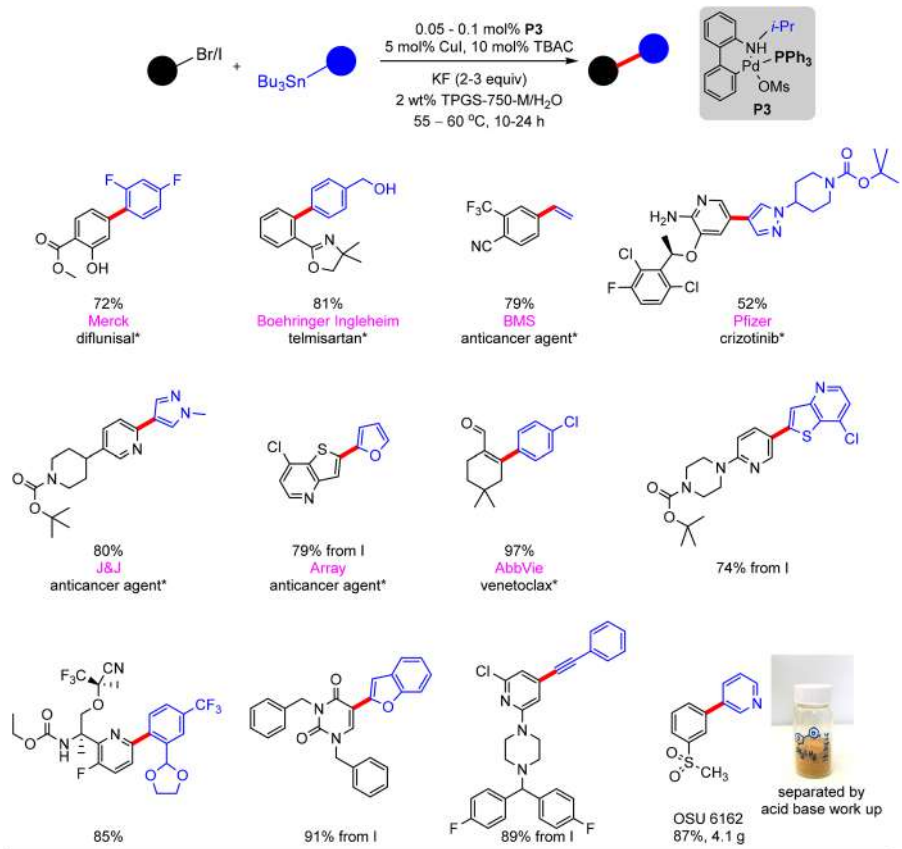

Scheme 13.13 Synthesis of pharmaceutical intermediates using Stille coupling in water.

Exploring avenues of complexity of molecules that could be prepared using cross coupling reactions in aqueous micelles, the same group was recently able to disclose another widely used industrial reaction, cyanation of aryl halides from the Merck informer library (see Scheme 13.14).[48] It should be noted that due to the presence of a large number of heteroatoms, previously these aryl halides required the use of a stochiometric amount of Pd for cross coupling. Under the newly developed cyanation reaction conditions, most of these halides were coupled using only ~0.7 mol% **P4** when polymethylhydrosiloxane (PMHS) was used as a reductant.

The toolbox was not only limited to the cross-coupling reactions, but several other fundamental transformations such as hydrogenation,[49] reductive amination,[50] nitro reduction,[51] and amide coupling could also be performed.[52] These aqueous micelles have been recently explored for photocatalysis,[53] biocatalysis[54] and flow chemistry.[55] A particularly interesting aspect of this technology is performing several types of reactions in one-pot using the same solvent, which is "water". One of such examples is the complete synthesis

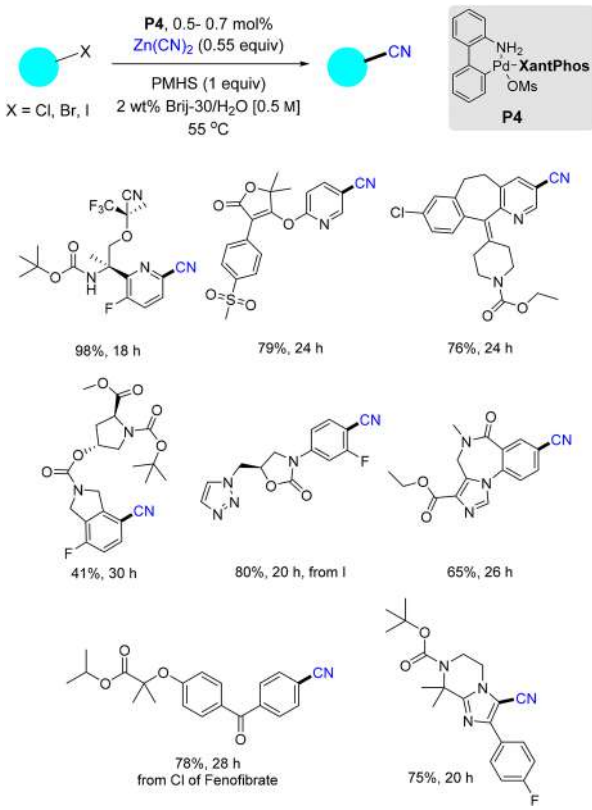

Scheme 13.14 Cyanation of drug-like molecules in water.

of Novartis's anticancer agent sonidegib (see Scheme 13.15).[56] This API was prepared *via* convergent synthesis in 5 steps and 3-pots. The individual steps were high yielding, giving the respective intermediates **A** and **B**. In fact, a key Suzuki–Miyaura coupling was not only performed under milder reaction conditions, but required an order of magnitude low Pd catalyst loading compared to the literature route.[57]

In the category of amphiphilic surfactants, Handa's group[58] from the University of Louisville developed a proline-based surfactant, PS-750-M, that forms nano-micelles and helps to drive several organic transformations efficiently.[59] Most importantly, the group has shown that through a shielding effect and high solubilization of the reactants by micelles, highly selective monofluorination of aryl as well as heteroaryl molecules could be performed.[60] A detailed study through dynamic light scattering (DLS) suggested the swelling of the nano-micelles from 237 nm to 845 nm due to the encapsulation of the reactants inside the micelles. Nevertheless, the reaction could be performed on a wide variety of indoles and benzene derivatives to achieve high selectivity, and good to moderate chemical yields (see Scheme 13.16).

The Buchwald group has shown that[61] the Negishi coupling in water initially discovered by Lipshutz[62] could also be performed using surfactants such as octanoic acid. However, the reaction required a stoichiometric amount of octanoic acid, which might limit its use for large-scale processes due to the generation of a large amount of carbon-based waste. Nevertheless, using 5 mol% of palladacycle **P5** made up of modular ligand VPhos was efficiently able to give a high chemical yield of the desired cross coupled product (see Scheme 13.17).

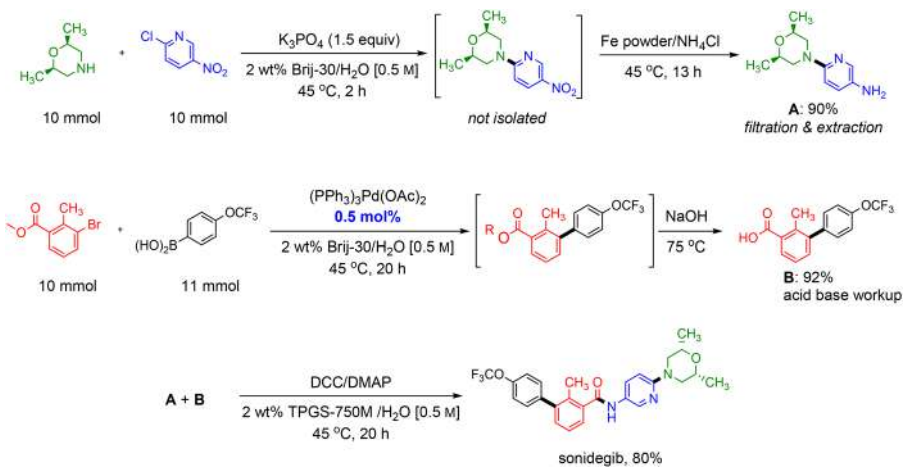

Scheme 13.15 Complete synthesis of sonidegib in aqueous micelles.

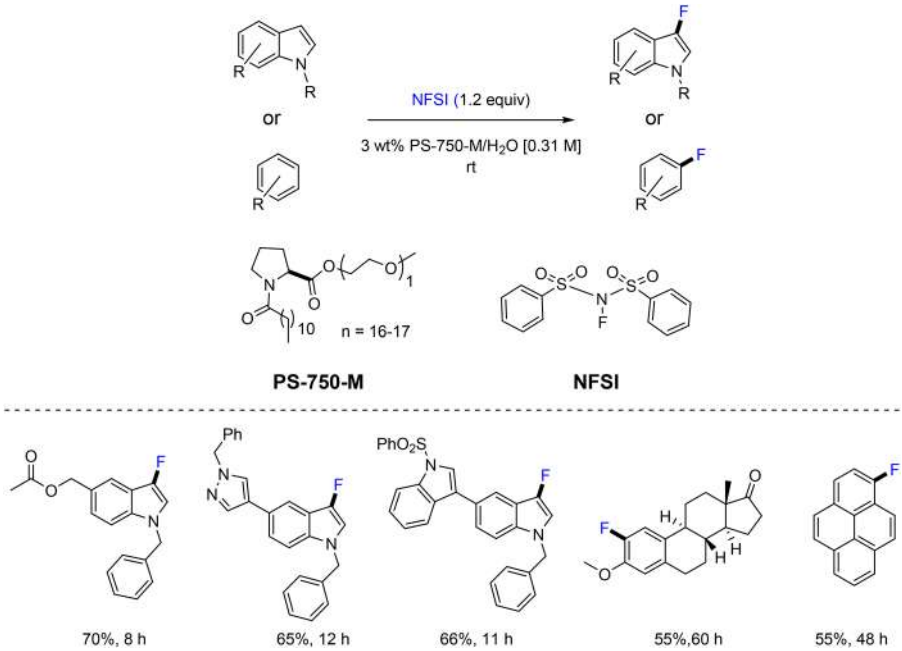

Scheme 13.16 Regioselective fluorination of (het)arene in aqueous micelles.

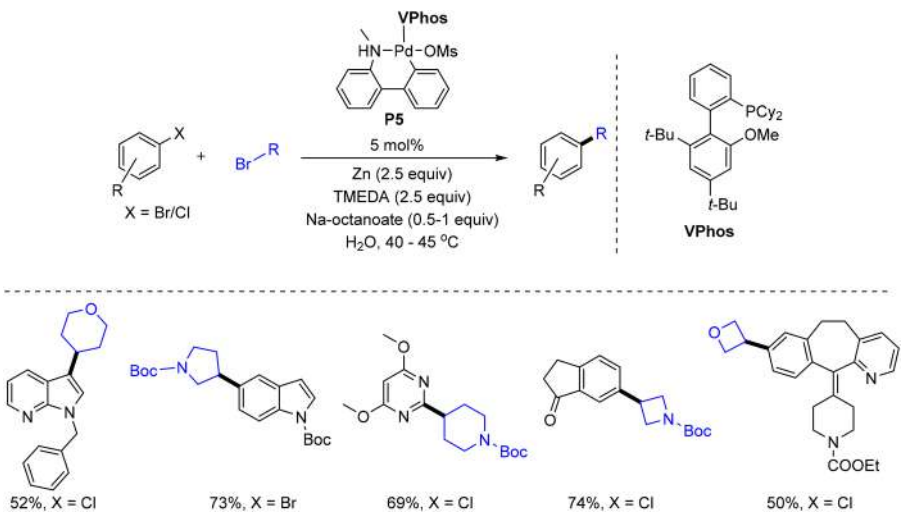

Scheme 13.17 Negishi coupling in water.

13.4 Use of Aqueous Reaction Media for Industrial Applications

It has been believed that the reactions based on aqueous systems pose several issues when scaled up at an industrial level. However, the presence of the tiny amount of surfactant which forms micelles has shown tremendous potential to be used in actual pharmaceutical synthesis. There are a variety of reports that have recently appeared in the literature by big pharma companies such as Takeda, Novartis, *etc.* who demonstrated that an aqueous micellar system was equally efficient in large scale synthesis. The Takeda team has synthesized the API[63] TAK-954 using a multi-step procedure all in water, and most of these steps were performed using aqueous micelles. Using this process, the waste solvent stream, illustrated by the process mass intensity (PMI), was significantly reduced to 11.8 (see Scheme 13.18).

Novartis in Basel[64] was very successful in efficient amide coupling on a larger scale. It was found that the typical reaction that was carried out in a highly undesirable polar aprotic solvent could be efficiently performed in an aqueous surfactant system with an organic co-solvent (see Scheme 13.19). The reaction profile was much better in the presence of a surfactant compared to just run in organic solvent. Similarly, an additional example from Novartis, China[65] suggested that the Suzuki–Miyaura cross coupling reaction

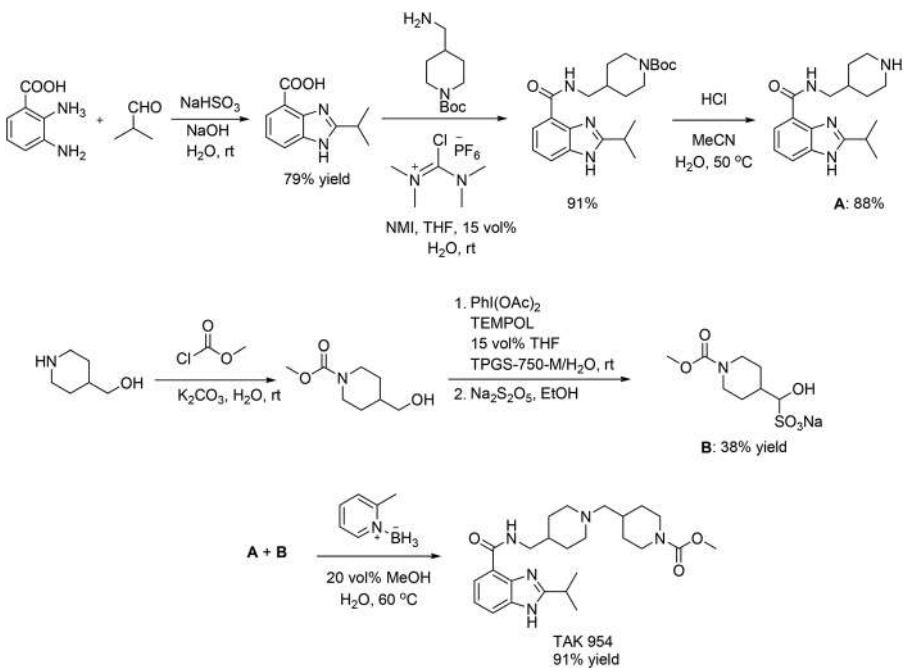

Scheme 13.18 Total synthesis of TAK-954 in water.

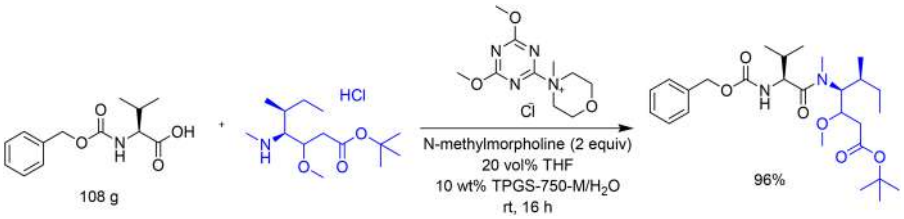

Scheme 13.19 Amide coupling in aqueous micelles by Novartis.

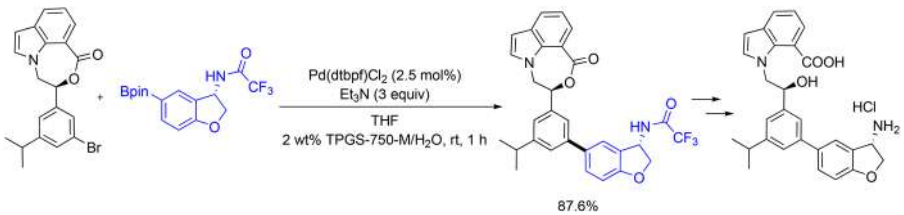

Scheme 13.20 Suzuki Miyaura coupling by Suzhou-Novartis in aqueous micelles.

could be easily scaled up (multi-kilo) to get 87.6% yield of the desired product (see Scheme 13.20).

A featured discovery from AbbVie's medicinal chemistry team has appeared recently. Quite unique in nature, capsules made-up of hydroxypropyl methylcellulose (HPMC)[66] were used to encapsulate the catalyst or reagents required for the reaction. Exploring their own previous results of HPMC,[67] the authors have now demonstrated that, if the reagents and catalyst can be pre-weighed and encapsulated in the capsules, then cross coupling reactions could be performed under glovebox free conditions. Nevertheless, the solubility of HPMC in water provided an additional opportunity to use water as a reaction medium, which also helps with dissolution of the capsule for subsequent release of the reaction materials for Buchwald-Hartwig amination (see Scheme 13.21).

Boehringer Ingelheim[68] was not far behind in applying aqueous surfactant-based chemistry for Suzuki–Miyaura coupling to make 11-β-HSD1 inhibitor on a 50 g scale in excellent chemical yield. It was obviously less waste-generating, even after considering aqueous waste. For example, the reaction carried out in water generated an *E* factor of 11 (kg of waste/kg of the desired product). On the other hand, a similar reaction in organic solvents generated an almost 3 times higher waste stream, where the *E* factor was 33. Interestingly, the actual Suzuki–Miyaura reaction was easily performed by using only 0.05 mol% Pd catalyst (see Scheme 13.22).

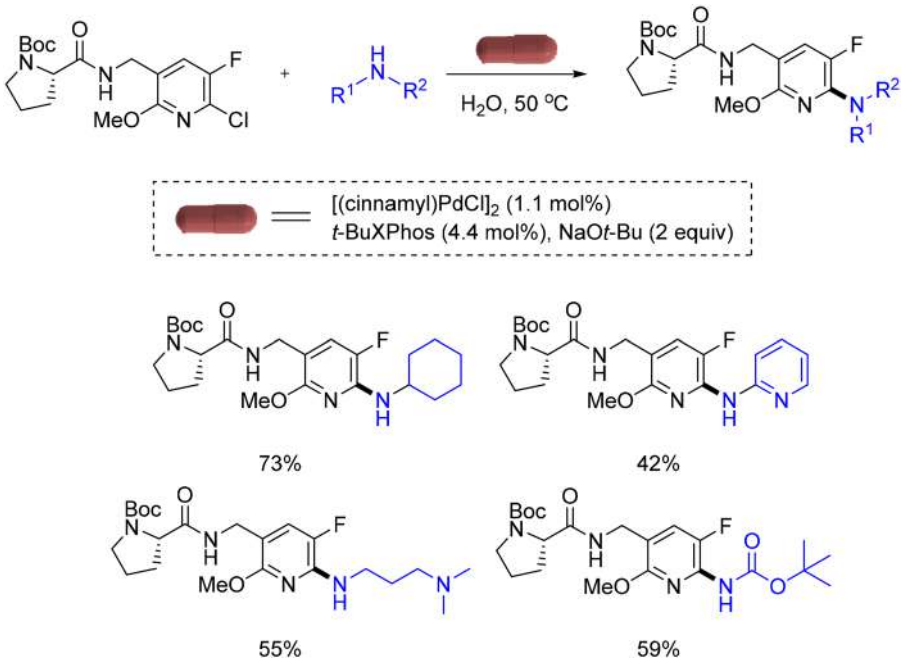

Scheme 13.21 Readily made capsules for Buchwald-Hartwig amination in water.

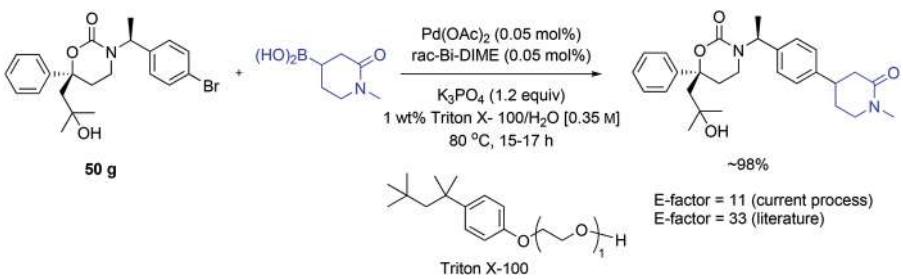

Scheme 13.22 Suzuki–Miyaura coupling in water by Boehringer Ingelhiem.

13.5 Academic Incorporation of Chemistry in Water

Although there was some resistance to the incorporation of water as a solvent in undergraduate courses in the United States, recently tremendous efforts and focus have been given by the ACS and ACS-Green Chemistry Institute to incorporate laboratory chemistry experiments that use water as a solvent for organic reactions.[69] The Wittig–Horner

or Horner–Wadsworth–Emmons reaction is one of the earlier reactions introduced in chemistry courses. The reaction was initially incorporated at the University of Toronto to demonstrate the synthesis of methyl cinnamate esters, an intermediate to make sunscreen.[70] The reaction could be performed with *p*-anisaldehyde and trimethylphosphonoacetate in the presence of environmentally benign base, K_2CO_3 in water. The product was precipitated after cooling and diluting with water, making easy isolation possible. Further purification could be performed by recrystallizing from ethanol. The most important feature of this reaction was the 15–20 minute reaction time (see Scheme 13.23). There are several other types of reactions that have been performed at undergraduate level, and these seem to work fine although they require a slightly high reaction temperature. The Undergraduate lab at University of California Santa Barbara recently introduced the S_NAr reaction between a heteroaryl fluoride or bromide and benzyl amine (see Scheme 13.24).[71] This reaction was performed under milder reaction conditions in water that contains a surfactant, TPGS-750-M. The reaction was complete in ~30 min at 45 °C. The crude product was removed by filtration and recrystallized using an ethyl acetate and heptane mixture.

Chemistry in water has been expanding rapidly in recent years,[72–80] and several efforts have been put forward towards making processes green. Researchers have shown that almost all reactions can be performed in water, in fact in very efficient ways compared to organic solvents. In Table 13.1, a summary of the different types of reactions that have been explored recently using water as a solvent are summarized.

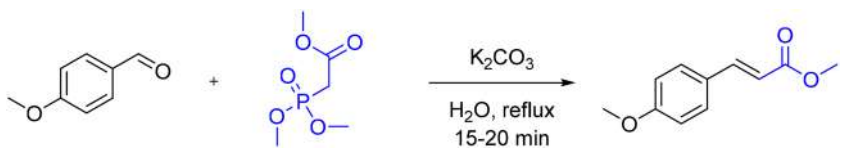

Scheme 13.23 Horner–Wadsworth–Emmons in water at undergraduate lab level.

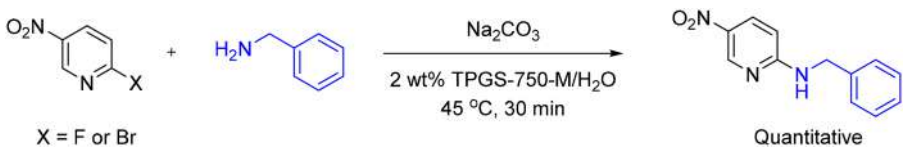

Scheme 13.24 S_NAr reaction in water at undergraduate lab level.

Table 13.1 Recently reported reactions in water.

Reaction type	Solvent (ratio)	Temp. (°C)	Product	year[ref]
Oxidation of alcohols	H_2O with 5 mol% fluorous surfactant	25	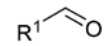	2015 [81]
Fehling's reaction	H_2O	50	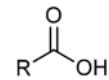	2016 [82]
Oxidation of keto alcohol	H_2O	50	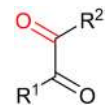	2016 [83]
Epoxidation of alkenes	H_2O	rt	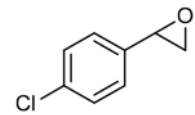	2016 [84]
Condensation	H_2O	100	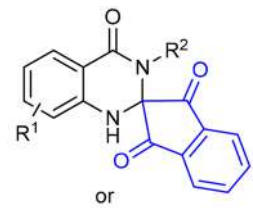 or 	2016 [85]
C–H function-alization of indoles	H_2O	rt		2016 [86] 2020 [87] 2020 [88]
Asymmetric Michael reaction	H_2O	rt	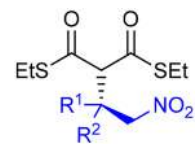	2017 [89]
C–O bond formation	H_2O with 10 mol% SDS	80	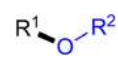	2017 [90]
C–H activation	H_2O	100		2017 [91]

(*continued*)

Table 13.1 (*continued*)

Reaction type	Solvent (ratio)	Temp. (°C)	Product	year[ref]
Azide alkyne cycloaddition	H_2O	rt	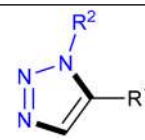	2017 [92]
Asymmetric Barbier-type reaction	H_2O	0	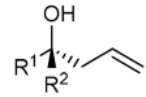	2017 [93]
Photocatalytic oxidation of alcohol	H_2O	rt	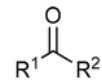	2017 [94]
Reduction of nitro	H_2O with ~ 0.7% SMPS	rt	Ar-NH_2	2017 [95]
Hydroxysulfenylation of alkenes	H_2O with 2 wt% Brij L4	rt	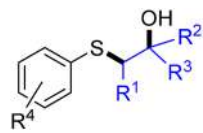	2018 [96]
Oxidative coupling	H_2O	100	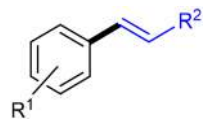	2020 [97]
Spirocyclization	H_2O:DMSO: AcOH (8:1:2)	60	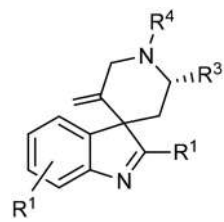	2020 [98]

13.6 Conclusion

Sustainability will be of prime importance in the decades to come, where businesses, investors, and the community will continuously demand clean energy. Chemistry will play an enormous role by employing sustainable practices at ground level, not only to prepare green end products, but also by following green practices to make products like materials, plastics, agrochemicals, pharmaceuticals, and much more. Nevertheless, some of the forefront green chemistry research has been discussed in this review, and these are great options to replace a century old chemistry practice with green and clean chemistry performed in water. Support to accomplish green chemistry

research is already provided by scientific institutions such as the American Chemical Society-Green Chemistry Institute (ACS-GCI),[99] the pharma round table,[100] the International Consortium for Innovation & Quality in Pharmaceutical Development (IQ), and the European REACH program.[101] More emphasis, support and encouragement will definitely change the mindset of scientists both in academic institutions and industries to think beyond using unsustainable organic solvents for process development.

References

1. T. Welton, Solvents and sustainable chemistry, *Proc. R. Soc. A*, 2015, **471**, 20150502.
2. Organic solvents, https://www.cdc.gov/niosh/topics/organsolv/default.html, accessed on 15 January 2021.
3. C. S. Ashcroft, P. J. Dunn, J. D. Hayler and A. S. Wells, Survey of Solvent Usage in Papers Published in Organic Process Research & Development 1997–2012, *Org. Process Res. Dev.*, 2015, **19**, 740.
4. The Paris Agreement, https://unfccc.int/process-and-meetings/the-paris-agreement/the-paris-agreement, accessed on 20 January 2021.
5. C. J. Gonzalez, A. D. Curzons, D. J. C. Constable and V. L. Cunningham, *Clean Technol. Environ. Policy*, 2005, **7**, 42–50.
6. (a) D. C. Cook, R. H. Jones, H. Kabir, D. J. Lythgoe, I. M. McFarlane, C. Pemberton, A. A. Thatcher, D. M. Thompson and J. B. Walton, Process Development of the PDE IV Inhibitor 3-(Cyclopentyloxy)-*N*-(3,5-dichloropyrid-4-yl)-4-methoxybenzamide, *Org. Process Res. Dev.*, 1998, **2**, 157; (b) Y. Tao, D. W. Widlicka, P. D. Hill, M. Couturier and G. R. Young, A Scalable Synthesis of CE-157119 HCl Salt, an SRI/5-HT_{2A} Antagonist, *Org. Process Res. Dev.*, 2012, **16**, 1805.
7. D. B. G. Williams and M. Lawton, Drying of Organic Solvents: Quantitative Evaluation of the Efficiency of Several Desiccants, *J. Org. Chem.*, 2010, **75**, 8351.
8. S. Banerjee, Calculation of water solubility of organic compounds with UNIFAC-derived parameters, *Environ. Sci. Technol.*, 1985, **19**, 369.
9. *Organic Reactions in Water: Principles, Strategies and Applications*, ed. U. M. Lindström, Blackwell, Oxford, 2007.
10. (a) A. P. Dicks, A review of aqueous organic reactions for the undergraduate teaching laboratory, *Green Chem. Lett. Rev.*, 2009, **2**, 9; (b) B. H. Lipshutz, Synthetic Chemistry in a Water World. New Rules Ripe for Discovery, *Curr. Opin. Green Sustain. Chem.*, 2018, **11**, 1; (c) C. J. Li, Organic Reactions in Aqueous Media with a Focus on Carbon–Carbon Bond Formations: A Decade Update, *Chem. Rev.*, 2005, **105**, 3095.
11. (a) J. W. Moore, Streaming Chemistry, *J. Chem. Educ.*, 2008, **85**, 171; (b) J. H. Tomasik, News from Online: Water, Streaming Chemistry, *J. Chem. Educ.*, 2008, **85**, 185; (c) E. K. Jacobsen, JCE Resources for Chemistry and Water, *J. Chem. Educ.*, 2008, **85**, 188.

12. M. P. Andersson, M. H. M. Olsson and S. L. S. Stipp, Predicting the pK_a and Stability of Organic Acids and Bases at an Oil–Water Interface, *Langmuir*, 2014, **30**, 6437.
13. K. H. Raney, P. G. Shpakoff and D. K. Passwater, Use of high-active alpha olefin sulfonates in laundry powders, *J. Surfactants Deterg.*, 1998, **1**, 361.
14. J. R. Wechsler and A. M. Koberda, Primary alkane sulfonates, *J. Am. Oil Chem. Soc.*, 1983, **60**, 2012.
15. (a) B. H. Lipshutz, When Does Organic Chemistry Follow Nature's Lead and "Make the Switch"?, *J. Org. Chem.*, 2017, **82**, 2806; (b) B. H. Lipshutz, F. Gallou and S. Handa, Evolution of Solvents in Organic Chemistry, *ACS Sustainable Chem. Eng.*, 2016, **4**, 5838; (c) M. Bihani, T. N. Ansari, J. D. Smith and S. Handa, The magical but endangered metal: searching for sustainable palladium catalysis, *Curr. Opin. Green Sustain. Chem.*, 2018, **11**, 45.
16. S. Sharma, J. Das and S. Handa, A Glimpse on Green Chemistry Practices in the Pharmaceutical Industry, *ChemSusChem*, 2020, **13**, 2859.
17. (a) J. An, L. Bagnell, T. Cablewski, C. R. Strauss and R. W. Trainor, Applications of High-Temperature Aqueous Media for Synthetic Organic Reactions, *J. Org. Chem.*, 1997, **62**, 2505; (b) C.-J. Li, Aqueous Barbier-Grignard type reaction: Scope, mechanism, and synthetic applications, *Tetrahedron*, 1996, **52**, 5643; (c) C.-J. Li, Organic reactions in aqueous media - with a focus on carbon-carbon bond formation, *Chem. Rev.*, 1993, **93**, 2023; (d) U. Pindur, G. Lutz and C. Otto, Acceleration and selectivity enhancement of Diels-Alder reactions by special and catalytic methods, *Chem. Rev.*, 1993, **93**, 741; (e) A. Lubineau, J. Auge and Y. Queneau, Water-Promoted Organic Reactions, *Synthesis*, 1994, **8**, 741; (f) P. A. Grieco, Organic chemistry in unconventional solvents, *Aldrichimica Acta*, 1991, **24**, 59.
18. U. M. Lindström, Stereoselective Organic Reactions in Water, *Chem. Rev.*, 2002, **102**, 2751.
19. D. C. Rideout and R. Breslow, Hydrophobic acceleration of Diels-Alder reactions, *J. Am. Chem. Soc.*, 1980, **102**, 7816.
20. S. Narayan, J. Muldoon, M. G. Finn, V. V. Fokin, H. C. Kolb and K. B. Sharpless, "On Water": Unique Reactivity of Organic Compounds in Aqueous Suspension, *Angew. Chem., Int. Ed.*, 2005, **44**, 3275.
21. J. E. Klijn and J. B. F. N. Engberts, Organic chemistry: Fast reactions 'on water', *Nature*, 2005, **435**, 746.
22. R. N. Butler and A. G. Coyne, Organic Synthesis Reactions On Water at the Organic–liquid Water Interface, *Org. Biomol. Chem.*, 2016, **14**, 9945.
23. (a) Y. Hayashi, In Water or in the Presence of Water?, *Angew. Chem., Int. Ed.*, 2006, **45**, 8103; (b) Y. J. Zuo and J. Qu, How Does Aqueous Solubility of Organic Reactant Affect a Water-Promoted Reaction?, *J. Org. Chem.*, 2014, **79**, 6832.
24. J. K. Beattie, C. S. P. McErlean and C. B. W. Phippen, The Mechanism of On-Water Catalysis, *Chem. - Eur. J.*, 2010, **16**, 8972.

25. (a) Y. Jung and R. A. Marcus, On the Theory of Organic Catalysis "on Water", *J. Am. Chem. Soc.*, 2007, **129**, 5492; (b) R. A. Marcus, Interaction between Experiments, Analytical Theories, and Computation, *J. Phys. Chem. C*, 2009, **113**, 14598.
26. L. Cicco, S. Sblendorio, R. Mansueto, F. M. Perna, A. Salomone, S. Florio and V. Capriati, Water Opens the Door to Organolithiums and Grignard Reagents: Exploring and Comparing the Reactivity of Highly Polar Organometallic Compounds in Unconventional Reaction Media towards the Synthesis of Tetrahydrofurans, *Chem. Sci.*, 2016, **7**, 1192.
27. G. Dilauro, M. Dell'Aera, P. Vitale, V. Capriati and F. M. Perna, Unprecedented Nucleophilic Additions of Highly Polar Organometallic Compounds to Imines and Nitriles Using Water as a Non-Innocent Reaction Medium, *Angew. Chem., Int. Ed.*, 2017, **56**, 10200.
28. D. G. Blackmond, A. Armstrong, V. Coombe and A. Wells, Water in Organocatalytic Processes: Debunking the Myths, *Angew. Chem., Int. Ed.*, 2007, **46**, 3798.
29. K. Alfonsi, J. Colberg, P. J. Dunn, T. Fevig, S. Jennings, T. A. Johnson, H. P. Kleine, C. Knight, M. A. Nagy, D. A. Perry and M. Stefaniakc, Green chemistry tools to influence a medicinal chemistry and research chemistry based organization, *Green Chem.*, 2008, **10**, 31.
30. A. Adewuyi, Chemically Modified Biosorbents and Their Role in the Removal of Emerging Pharmaceutical Waste in the Water System, *Water*, 2020, **12**, 1551.
31. A. D. Allian, N. P. Shah, A. C. Ferretti, D. B. Brown, S. P. Kolis and J. B. Sperry, Process Safety in the Pharmaceutical Industry—Part I: Thermal and Reaction Hazard Evaluation Processes and Techniques, *Org. Process Res. Dev.*, 2020, **24**, 2529.
32. C. M. Gabriel, N. R. Lee, F. Bigorne, P. Klumphu, M. Parmentier, F. Gallou and B. H. Lipshutz, Effects of Co-solvents on Reactions Run under Micellar Catalysis Conditions, *Org. Lett.*, 2017, **19**, 194.
33. (a) W. Blokzijl and J. B. F. N. Engberts, Hydrophobic Effects. Opinions and Facts, *Angew. Chem., Int. Ed. Engl.*, 1993, **32**, 1545; (b) S. Salmar, J. Järv, T. Tenno and A. Tuulmets, Role of water in determining organic reactivity in aqueous binary solvents, *Cent. Eur. J. Chem.*, 2012, **10**, 1600.
34. M. H. Abraham, J. C. Dearden and G. M. Bresnen, Hydrogen bonding, steric effects and thermodynamics of partitioning, *J. Phys. Org. Chem.*, 2006, **19**, 242.
35. (a) T. W. Bentley, I. S. Koo, H. Choi and G. Llewellyn, A kinetic model for water reactivity (avoiding activities) for hydrolyses in aqueous mixtures– selectivities for solvolyses of 4-substituted benzyl derivatives in alcohol–water mixtures, *J. Phys. Org. Chem.*, 2008, **21**, 251; (b) T. W. Bentley, H. C. Harris, Z. H. Ryu, G. T. Lim, D. D. Sung and S. R. Szajda, Mechanisms of Solvolyses of Acid Chlorides and Chloroformates. Chloroacetyl and Phenylacetyl Chloride as Similarity Models, *J. Org. Chem.*, 2005, **70**, 8963.

36. H. Waldmann, Amino Acid Methyl Esters as Chiral Auxiliaries in Aza–Diels-Alder Reactions in Aqueous Solution, *Angew. Chem., Int. Ed. Engl.*, 1988, **27**, 274.
37. Y. Huang, Z. Zha and Z. Wang, Copper Catalyzed Diastereo- and Enantioselective 1,4-Addition Michael Reaction of 2,3-Dioxopyrrolidines with Nitroalkanes in Aqueous Media, *Org. Lett.*, 2020, **22**, 2512.
38. D. T. Cohen and S. L. Buchwald, Mild Palladium-Catalyzed Cyanation of (Hetero)aryl Halides and Triflates in Aqueous Media, *Org. Lett.*, 2015, **17**, 202.
39. D. A. Jaeger and R. E. Robertson, Micellar effects on the monohalogenation of n-pentyl phenyl ether, *J. Org. Chem.*, 1977, **42**, 3298.
40. (a) T. Kitanosono and S. Kobayashi, Reactions in Water Involving the "On-Water" Mechanism, *Chem. - Eur. J.*, 2020, **26**, 9408; (b) K. Manabe, Y. Mori, T. Wakabayashi, S. Nagayama and S. Kobayashi, Organic Synthesis Inside Particles in Water: Lewis Acid–Surfactant-Combined Catalysts for Organic Reactions in Water Using Colloidal Dispersions as Reaction Media, *J. Am. Chem. Soc.*, 2000, **122**, 7202.
41. T. Kitanosono, P. Xu and S. Kobayashi, Chiral Lewis acids integrated with single-walled carbon nanotubes for asymmetric catalysis in water, *Science*, 2018, **362**, 311.
42. L. Chen and C. J. Li, A Remarkably Efficient Coupling of Acid Chlorides with Alkynes in Water, *Org. Lett.*, 2004, **6**, 3151.
43. B. H. Lipshutz, S. Ghorai and M. Clerget, The Hydrophobic Effect Applied to Organic Synthesis: Recent Synthetic Chemistry "in Water", *Chem. - Eur. J.*, 2018, **24**, 6672.
44. B. H. Lipshutz, S. Ghorai, A. R. Abela, R. Moser, T. Nishikata, C. Duplais, A. Krasovskiy, R. D. Gaston and R. C. Gadwood, TPGS-750-M: A Second-Generation Amphiphile for Metal-Catalyzed Cross-Couplings in Water at Room Temperature, *J. Org. Chem.*, 2011, **76**, 4379.
45. R. R. Thakore, B. S. Takale, Y. Hu, J. Kostal, F. Gallou and B. H. Lipshutz, "TPG-lite": A new, simplified "designer" surfactant for general use in synthesis under micellar catalysis conditions in recyclable water, *Tetrahedron*, 2021, **87**, 132090.
46. B. S. Takale, R. R. Thakore, S. Handa, F. Gallou, J. Reilly and B. H. Lipshutz, A new, substituted palladacycle for ppm level Pd catalyzed Suzuki–Miyaura cross couplings in Water, *Chem. Sci.*, 2020, **10**, 8825.
47. B. S. Takale, R. R. Thakore, G. Casotti, X. Li, F. Gallou and B. H. Lipshutz, Mild and robust Stille reactions in water using ppm levels of a new triphenylphosphine-based palladacycle, *Angew. Chem., Int. Ed.*, 2021, **60**, 2.
48. R. R. Thakore, B. S. Takale, V. Singhania, F. Gallou and B. H. Lipshutz, Late-stage Pd-catalyzed cyanations of aryl/heteroaryl halides in aqueous micellar media, *ChemCatChem*, 2021, **13**, 212.
49. B. S. Takale, R. R. Thakore, E. S. Gao, F. Gallou and B. H. Lipshutz, Environmentally responsible, safe, and chemoselective catalytic hydrogenation of olefins: ppm level Pd catalysis in recyclable water at room temperature, *Green Chem.*, 2020, **22**, 6055.

50. R. R. Thakore, B. S. Takale, G. Casotti, E. S. Gao, H. S. Jin and B. H. Lipshutz, Chemoselective Reductive Aminations in Aqueous Nanoreactors Using Parts per Million Level Pd/C Catalysis, *Org. Lett.*, 2020, **22**, 6324.
51. N. R. Lee, A. A. Bikovtseva, M. Cortes-Clerget, F. Gallou and B. H. Lipshutz, Carbonyl Iron Powder: A Reagent for Nitro Group Reduction Under Aqueous Micellar Catalysis Conditions, *Org. Lett.*, 2017, **19**, 6518.
52. C. M. Gabriel, M. Keener, F. Gallou and B. H. Lipshutz, Amide and Peptide Bond Formation in Water at Room Temperature, *Org. Lett.*, 2015, **17**, 3968.
53. M.-j. Bu, C. Cai, F. Gallou and B. H. Lipshutz, PQS-enabled Visible-Light Iridium Photoredox Catalysis in Water at Room Temperature, *Green Chem.*, 2018, **20**, 1233.
54. M. Cortes-Clerget, N. Akporji, J. Zhou, F. Gao, P. Guo, M. Parmentier, F. Gallou, J.-Y. Berthon and B. H. Lipshutz, Bridging the gap between transition metal- and bio-catalysis *via* aqueous micellar catalysis, *Nat. Commun.*, 2019, **10**, 2169.
55. A. B. Wood, K. Y. Nadiwale, Y. Mo, B. Jin, A. Pomberger, V. L. Schultz, F. Gallou, K. F. Jensen and B. H. Lipshutz, Continuous Flow Suzuki-Miyaura Couplings in Water Under Micellar Conditions in a CSTR Cascade Catalyzed by Fe/ppm Pd Nanoparticles, *Green Chem.*, 2020, **22**, 3441.
56. B. S. Takale, R. R. Thakore, F. Y. Kong and B. H. Lipshutz, An environmentally responsible 3-pot, 5-stepsynthesis of the antitumor agent sonidegib using ppm levels of Pd catalysis in water, *Green Chem.*, 2019, **21**, 6258.
57. A. Fritze, K. Corcelle and M. E. Grubesa, *WO Pat.*, WO2011009852A2, 2011.
58. J. Brals, J. D. Smith, F. Ibrahim, F. Gallou and S. Handa, Micelle-Enabled Palladium Catalysis for Convenient sp^2-sp^3 Coupling of Nitroalkanes with Aryl Bromides in Water Under Mild Conditions, *ACS Catal.*, 2017, **7**, 7245.
59. (a) U. T. Duong, A. B. Gade, S. Plummer, F. Gallou and S. Handa, Reactivity of Carbenes in Aqueous Nanomicelles Containing Palladium Nanoparticles, *ACS Catal.*, 2019, **9**, 10963; (b) J. Brals, J. D. Smith, F. Ibrahim, F. Gallou and S. Handa, Micelle-Enabled Palladium Catalysis for Convenient sp2-sp3 Coupling of Nitroalkanes with Aryl Bromides in Water Under Mild Conditions, *ACS Catal.*, 2017, **7**, 7245; (c) M. Bihani, T. N. Ansari, L. Finck, P. P. Bora, J. B. Jasinski, B. Pavuluri, D. K. Leahy and S. Handa, Ultrasmall Pd Nanoparticles in Aqueous Micelles for Scalable α-Arylation of Nitriles: Surprising Formation of Carbanions, *ACS Catal.*, 2020, **10**, 6816; (d) T. N. Ansari, A. Taussat, A. Clark, M. Nachtegaal, S. Plummer, F. Gallou and S. Handa, Insights on Bimetallic Micellar Nanocatalysis for Buchwald-Hartwig Aminations, *ACS Catal.*, 2019, **9**, 10389.
60. P. P. Bora, M. Bihani, S. Plummer, F. Gallou and S. Handa, Shielding Effect of Micelle for Highly Effective and Selective Monofluorination of Indoles in Water, *ChemSusChem*, 2019, **12**, 3037.

61. V. R. Bhonde, B. T. O'Neill and S. L. Buchwald, An Improved System for the Aqueous Lipshutz–Negishi Cross-Coupling of Alkyl Halides with Aryl Electrophiles, *Angew. Chem., Int. Ed.*, 2016, **55**, 1849.
62. A. Krasovskiy, C. Duplais and B. H. Lipshutz, Zn-Mediated, Pd-Catalyzed Cross-Couplings in Water at Room Temperature *Without* Prior Formation of Organozinc Reagents, *J. Am. Chem. Soc.*, 2009, **131**, 15592.
63. J. D. Bailey, E. Helbling, A. Mankar, M. Stirling, F. Hicksa and D. K. Leahy, Beyond organic solvents: synthesis of a 5-HT4 receptor agonist in water, *Green Chem.*, 2021, **23**, 788.
64. F. Gallou, P. Guo, M. Parmentier and J. Zhou, A General and Practical Alternative to Polar Aprotic Solvents Exemplified on an Amide Bond Formation, *Org. Process Res. Dev.*, 2016, **20**, 1388.
65. B. Wu, S. Zhang, T. Hong, Y. Zhou, H. Wang, M. Shi, H. Yang, X. Tian, J. Guo, J. Bian, J. Roache, P. Delgado, R. Mo, C. Fridrich, F. Gao and J. Wang, Merging Biocatalysis, Flow, and Surfactant Chemistry: Innovative Synthesis of an FXI (Factor XI) Inhibitor, *Org. Process Res. Dev.*, 2020, **24**, 2780.
66. N. Borlinghaus, J. Kaschel, J. Klee, V. Haller, J. Schetterl, S. Heitz, T. Lindner, J. D. Dietrich, W. M. Braje and A. Jolit, Reagent and Catalyst Capsules: A Chemical Delivery System for Reaction Screening and Parallel Synthesis, *J. Org. Chem.*, 2021, **86**, 1357.
67. D. Petkova, N. Borlinghaus, S. Sharma, J. Kaschel, T. Lindner, J. Klee, A. Jolit, V. Haller, S. Heitz, K. Britze, J. Dietrich, W. M. Braje and S. Handa, Hydrophobic Pockets of HPMC Enable Extremely Short Reaction Times in Water, *ACS Sustainable Chem. Eng.*, 2020, **8**, 12612.
68. N. D. Patel, D. Rivalti, F. G. Buono, A. Chatterjee, B. Qu, S. Braith, J. N. Desrosiers, S. Rodriguez, J. D. Sieber, N. Haddad, K. R. Fandrick, H. Lee, N. K. Yee, C. A. Busacca and C. H. Senanayake, Effective BI-DIME Ligand for Suzuki–Miyaura Cross-Coupling Reactions in Water with 500 ppm Palladium Loading and Triton X, *Asian J. Org. Chem.*, 2017, **6**, 1285.
69. A. P. Dicks, A review of aqueous organic reactions for the undergraduate teaching laboratory, *Green Chem. Lett. Rev.*, 2009, **2**, 921.
70. L. L. W. Cheung, R. J. Lin, J. W. McIntee and A. P. Dicks, Expeditious Horner-Wadsworth–Emmons Synthesis of Methyl Cinnamate Esters under Aqueous Conditions, *Chem. Educ.*, 2005, **10**, 300.
71. E. B. Landstrom, M. Nichol, B. H. Lipshutz and M. J. Gainer, Discovery-Based SNAr Experiment in Water Using Micellar Catalysis, *J. Chem. Educ.*, 2019, **96**, 2668.
72. T. Lorenzetto, G. Berton, F. Fabris and A. Scarso, Recent designer surfactants for catalysis in water, *Catal. Sci. Technol.*, 2020, **10**, 4492.
73. T. Kitanosono, K. Masuda, P. Xu and S. Kobayashi, Catalytic Organic Reactions in Water toward Sustainable Society, *Chem. Rev.*, 2018, **118**, 679.
74. T. Kitanosono and S. Kobayashi, Reactions in Water Involving the "On-Water" Mechanism, *Chem. - Eur. J.*, 2020, **26**, 9408.

75. R. N. Butler and A. G. Coyne, Water: Nature's Reaction Enforcer—Comparative Effects for Organic Synthesis “In-Water” and “On-Water”, *Chem. Rev.*, 2010, **110**, 6302.
76. R. N. Butler and A. G. Coyne, Organic Synthesis reactions on-water at the organic liquid water interface, *Org. Biomol. Chem.*, 2016, **14**, 9945.
77. A. Chanda and V. V. Fokin, Organic synthesis “On Water”, *Chem. Rev.*, 2009, **109**, 725.
78. C. J. Li and L. Chen, Organic chemistry in water, *Chem. Soc. Rev.*, 2006, **35**, 68.
79. M. O. Simon and C. J. Li, Green chemistry oriented organic synthesis in water, *Chem. Soc. Rev.*, 2012, **41**, 1415.
80. A. Steven, Micelle-Mediated Chemistry in Water for the Synthesis of Drug Candidates, *Synthesis*, 2019, **51**, 2632.
81. B. T. Chen, K. V. Bukhryakov, R. Sougrat and V. O. Rodionov, Enzyme-Inspired Functional Surfactant for Aerobic Oxidation of Activated Alcohols to Aldehydes in Water, *ACS Catal.*, 2015, **5**, 1313.
82. M. Liu and C. J. Li, Catalytic Fehling's Reaction: An Efficient Aerobic Oxidation of Aldehyde Catalyzed by Copper in Water, *Angew. Chem., Int. Ed.*, 2016, **55**, 10806.
83. Y. Yu, C. Lin, B. Li, P. Zhao and S. Zhang, Dendrimer-like core cross-linked micelle stabilized ultra-small gold nanoclusters as a robust catalyst for aerobic oxidation of α-hydroxy ketones in water, *Green Chem.*, 2016, **18**, 3647.
84. T. Omagari, A. Suzuki, M. Akita and M. Yoshizawa, Efficient Catalytic Epoxidation in Water by Axial N-Ligand-Free Mn-Porphyrins within a Micellar Capsule, *J. Am. Chem. Soc.*, 2016, **138**, 499.
85. R. V. Devi, A. M. Garande, D. K. Maity and P. M. Bhate, A Serendipitous synthesis 11a-Hydroxy-11,11a-dihydrobenzo[*e*]indeno[2,1-*b*][1,4]diazepine-10,12-dione Derivatives by Condensation of 2-Aminobenzamides with Ninhydrin in Water, *J. Org. Chem.*, 2016, **81**, 1689.
86. T. Kitanosono, M. Miyo and S. Kobayashi, Surfactant-Aided Chiral Palladium(II) Catalysis Exerted Exclusively in Water for the C–H Functionalization of Indoles, *ACS Sustainable Chem. Eng.*, 2016, **4**, 6101.
87. T. Kitanosono, T. Hisada, Y. Yamashita and S. Kobayashi, Hydrogen-Bonding-Assisted Cationic Aqua Palladium(II) Complex Enables Highly Efficient Asymmetric Reactions in Water, *Angew. Chem., Int. Ed.*, 2020, **59**, 1.
88. X. Liang, Y. Gui, K. Li, J. Li, Z. Zha, L. Shi and Z. Wang, A novel chiral surfactant-type metallomicellar catalyst for asymmetric Michael addition in water, *Chem. Commun.*, 2020, **56**, 11118.
89. J. H. Sim and C. E. Song, Water-Enabled Catalytic Asymmetric Michael Reactions of Unreactive Nitroalkenes: One-Pot Synthesis of Chiral GABA-Analogs with All-Carbon Quaternary Stereogenic Centers, *Angew. Chem., Int. Ed.*, 2017, **56**, 1835.

90. D. Ahanthem and W. S. Laitonjam, C(sp^2)-O Bond Formation through a Nickel-Catalyzed Cross-Coupling Reaction in Water Enabled by Micellar Catalysis, *Asian J. Org. Chem.*, 2017, **6**, 1492.
91. H. Wang, M. M. Lorion and L. Ackermann, Air-Stable Manganese(I)-Catalyzed C−H Activation for Decarboxylative C−H/C−O Cleavages in Water, *Angew. Chem., Int. Ed.*, 2017, **56**, 6339.
92. W. G. Kim, M. E. Kang, J. B. Lee, M. H. Jeon, S. Lee, J. Lee, B. Choi, P. M. S. D. Cal, S. Kang, J.-M. Kee, G. J. L. Bernardes, J.-U. Rohd, W. Choe and S. Y. Hong, *J. Am. Chem. Soc.*, 2017, **139**, 12121.
93. S. Nakamura, Y. Hara, T. Furukawaa and T. Hirashitaa, Enantioselective Barbier-type allylation of ketones using allyl halide and indium in water, *RSC Adv.*, 2017, **7**, 15582.
94. L. -M. Zhao, Q. -Y. Meng, X. -B. Fan, C. Ye, X. -B. Li, B. Chen, V. Ramamurthy, C. -H. Tung and L. -Z. Wu, Photocatalysis with Quantum Dots and Visible Light: Selective and Efficient Oxidation of Alcohols to Carbonyl Compounds through a Radical Relay Process in Water, *Angew. Chem., Int. Ed.*, 2017, **56**, 3020.
95. J. Kothandapani, S. Megarajan, B. A. A. Khan, P. Marimuthu, V. Anbazhagan and S. S. Ganesan, Stearyl MethoxyPEGglycol Succinate-A Designer Micellar Medium for Diverse Aniline Derivatives Synthesis, *ACS Sustainable Chem. Eng.*, 2017, **5**, 5740.
96. B. Zhang, T. Liu, Y. Bian, T. Lu and J. Feng, Micelle Enhanced Auto-Oxidative Hydroxysulfenylation of Alkenes, *ACS Sustainable Chem. Eng.*, 2018, **6**, 2651.
97. S. Hazra, V. Tiwari, A. Verma, P. Dolui and A. J. Elias, NaCl as Catalyst and Water as Solvent: Highly E-Selective Olefination of Methyl Substituted N-Heteroarenes with Benzyl Amines and Alcohols, *Org. Lett.*, 2020, **22**, 5496.
98. N. Sabat, F. Soualmia, P. Retailleau, A. Benjdia, O. Berteau and X. Guinchard, Gold-Catalyzed Spirocyclization Reactions of N-Propargyl Tryptamines and Tryptophans in Aqueous Media, *Org. Lett.*, 2020, **22**, 4344.
99. Explore Resources in Green and Sustainable Chemistry and Engineering for Industry Professionals, Educators and Students, https://www.acs.org/content/acs/en/greenchemistry.html, accessed on 25 January 2021.
100. About the Roundtable, https://www.acsgcipr.org, accessed on 25 January 2021.
101. REACH, https://ec.europa.eu/environment/chemicals/reach/reach_en.htm, accessed on 25 January 2021.

CHAPTER 14

Solvent-free Conditions

KOICHI TANAKA*

Department of Chemistry and Materials Engineering, Faculty of Chemistry, Materials and Bioengineering, Kansai University, Suita, Osaka 564-8680, Japan
*E-mail: ktanaka@kansai-u.ac.jp

14.1 Introduction

Solvent-free reactions have become increasingly popular in recent years, resulting in the publication of excellent books and reviews.[1–14] Solvent-free reactions can be conducted using the reactants alone or incorporating them with a solid-support, supramolecular templates (co-crystals), or metal–organic frameworks (MOFs) to achieve high degrees of chemo-, regio-, stereo-, and enantioselectivity in the products, and reducing reaction byproducts and harmful wastes. Various protocols have been developed and improved over the last two decades. This chapter aims to highlight research in the field of solvent-free reactions mostly reported in the last 10 years. Accordingly, solvent-free neat reactions, MOF-catalyzed reactions, thermal solid-state reactions, topochemical reactions, solid-state melt reactions, mechanochemical reactions, photochemical reactions, asymmetric reactions, and continuous flow twin-screw extrusions are described.

14.2 Solvent-free Organic Reactions

14.2.1 Neat Reactions

The self-aldol condensation of aldehydes to form α,β-conjugated aldehydes is an important reaction in synthetic organic chemistry that has been employed to prepare useful synthetic intermediates. However, controlling the reactions

Sustainable Organic Synthesis: Tools and Strategies
Edited by Stefano Protti and Alessandro Palmieri

Published by the Royal Society of Chemistry, www.rsc.org

of the substrates with low boiling points is difficult. Silica-gel-mediated self-aldol reactions of highly volatile aldehydes under organic solvent-free conditions were recently reported. For example, a mixture of propionaldehyde **1** (bp. 49 °C, 2 mmol), piperidine (0.2 mmol), and silica gel (63–200 mm, spherical, 2 g) was heated at 80 °C under N_2 for 1 h without a reflux condenser to give α,β-conjugated aldehyde **2** in 80% yield (Scheme 14.1).[15] In contrast, **2** was obtained in only 2% yield in the reaction without silica gel.

CBr_4 has been employed as a halogen bond donor catalyst for the synthesis of α,β-unsaturated ketones (Scheme 14.2).[16] It has been postulated that ketone **3** generates the corresponding enol, which then reacts with activated aldehyde **4** through halogen-bonding with CBr_4 to yield chalcone **5** in 86%. This methodology performed better under neat conditions than in organic solvent.

Nitrile-containing derivatives of N-heteroarenes are widely used in the pharmaceutical and agrochemical industries. A one-pot regioselective heteroaromatic C–H cyanation that proceeds without metal catalyst, base and solvent has recently been reported. When a mixture of quinoline *N*-oxide **6** and Me_3SiCN (3 equiv.) was heated at 80 °C under solvent-free conditions, quinoline-2-carbonitrile **7** was obtained in 90% yield (Scheme 14.3).[17]

Recently, a visible-light-promoted, catalyst-free, and solvent-free, one-pot multicomponent synthetic strategy has become a powerful tool for the synthesis of heterocyclic compounds. For example, a mixture of 2-aminopyridine

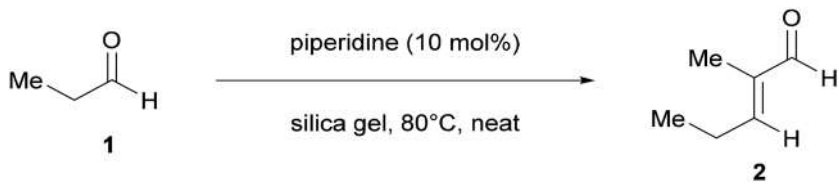

Scheme 14.1 Solvent-free self-aldol reaction of a highly volatile aldehyde.

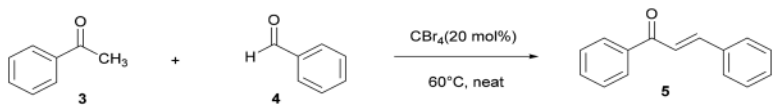

Scheme 14.2 Solvent-free chalcone synthesis catalyzed by CBr_4.

Scheme 14.3 Solvent-free cyanation of quinoline *N*-oxides with trimethylsilyl cyanide.

8 (1 mmol), benzaldehyde **9** (1 mmol), and isonitrile **10** (1 mmol) was stirred in a sealed round bottom flask under visible light irradiation (white compact fluorescent light, 24 W) for 3 h to give 3-aminoimidazo-fused heterocyclic compound **11** in excellent yield (~97%) (Scheme 14.4).[18] When the reaction was performed without the compact fluorescent light, only a trace amount of the product was formed.

2,4-Dienones **12** undergo visible-light-promoted, photocatalyst-free dimerization under neat conditions at ambient temperature to furnish cyclohexene derivatives **13** *via* s-*trans* to s-*cis* isomerization, regioselective *E*/*Z* isomerization, and Diels–Alder cycloaddition, while in nitromethane solution, regioselective *E*/*Z* isomerization of **12** to **14** occurs exclusively (Scheme 14.5).[19] Notably, the reaction is highly regio- and diastereoselective, and does not require any organic solvent or photocatalyst.

A highly efficient, room-temperature double hydroboration of nitriles under transition-metal-free and solvent-free conditions was recently reported. The hydroboration of nitriles **15** proceeded using 2.5–4.0 equivalent of pinacolborane (HBpin) and sodium triethylborohydride ($NaHBEt_3$) as a catalyst to afford bis(boryl)amines **16** in excellent isolated yields of up to 95% (Scheme 14.6).[20] The key advantage of this protocol was that no metal waste and no byproducts were generated.

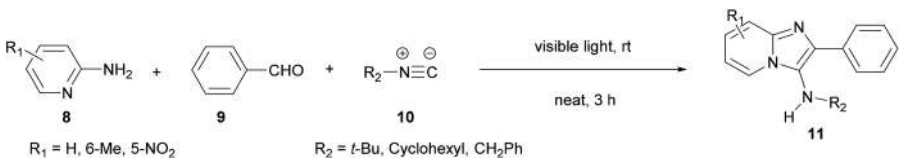

Scheme 14.4 Solvent-free Groebke–Biackburn–Bienaymé reaction promoted by visible-light irradiation.

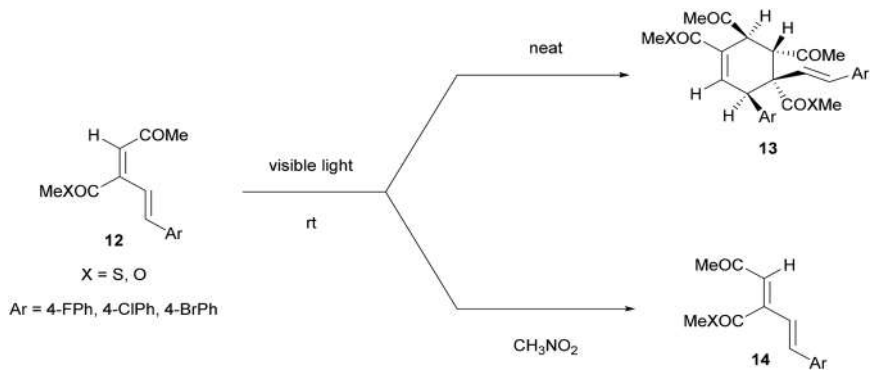

Scheme 14.5 Solvent- and photocatalyst-free dimerization of neat dienone promoted by visible-light irradiation.

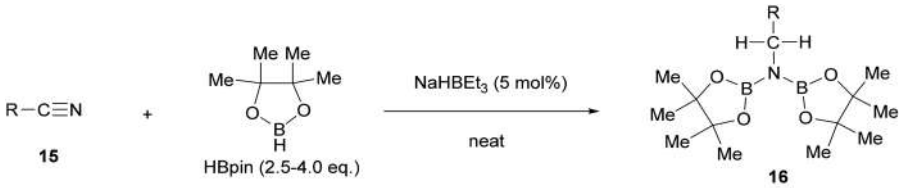

R = Et; *n*-Pr; *i*-Pr; cyclopropyl, cyclohexyl, Ph, 2-MePh, 3-MePh, 4-FPh, 4-ClPh, 4-BrPh, 4-MeOPh, 1-Napthyl

Scheme 14.6 Solvent- and transition metal-free double hydroboration of nitriles.

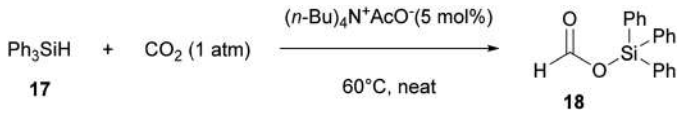

Scheme 14.7 Hydrosilylation of CO_2 under solvent-free conditions.

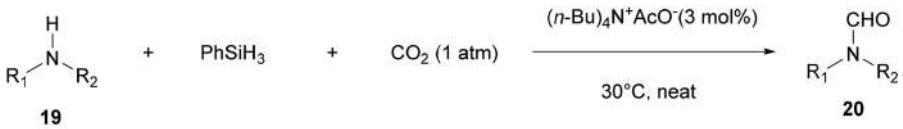

R_1 = Ph, 4-ClPh, 4-BrPh, 4-MeOPh, 4-MePh, $PhCH_2$, Me
R_2 = Me, Et, *n*-Pr, OMe, $CH_2CH{=}CH_2$

Scheme 14.8 *N*-Formylation of amines under solvent-free conditions.

Carbon dioxide is an inexpensive chemical feedstock that has attracted much research attention. Among various methods for CO_2 fixation, catalytic CO_2 reduction with hydrosilanes gives valuable substances. Tetrabutylammonium acetate (TBAA) acted as a catalyst for the solvent-free hydrosilylation of CO_2 (1 atm). Ph_3SiH **17**, a solid at room temperature, was melted at 60 °C, and the reaction proceeded to give the corresponding silyl formate **18** in 78% yield (Scheme 14.7).[21] TBAA was also effective for the *N*-formylation of amines **19** with CO_2 (1 atm) and $PhSiH_3$ at 30 °C, affording various formamides **20** (Scheme 14.8).

Polyhexahydrotriazines (PHT) **24** are promising high-performance thermosets exhibiting enhanced thermal and mechanical properties. However, these systems require a solvent for their synthesis, which creates voids and leads to material shrinkage during processing. A novel solvent-free PHT polymerization addressed many of these challenges using liquid or low-melting-point monomers. The reaction of 4-aminobenzylamine **21** with paraformaldehyde **22** in the absence of solvent led to initial formation of poly(hemiaminal) network **23**, which formed PHT **24** upon heating to 200 °C (Scheme 14.9).[22]

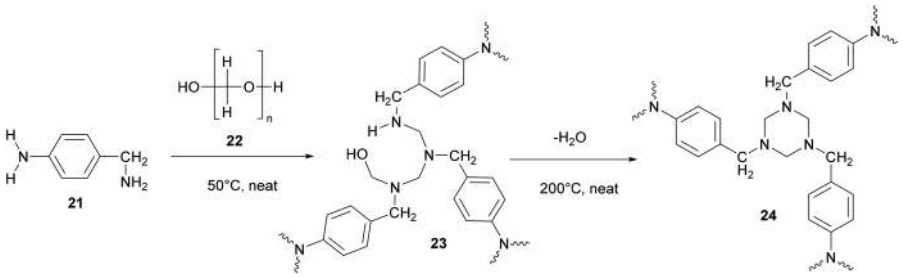

Scheme 14.9 Solvent-free synthesis of polyhexahydrotriazine.

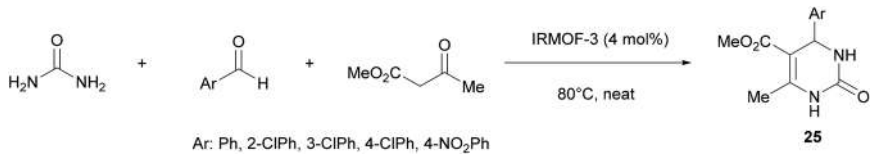

Scheme 14.10 IRMOF-3-catalyzed Biginelli coupling under solvent-free conditions.

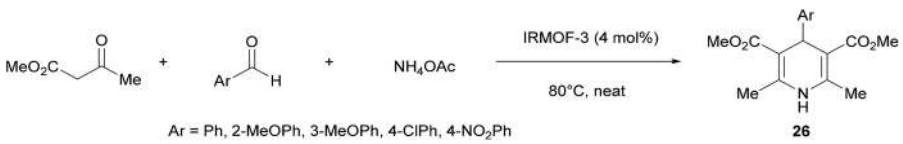

Scheme 14.11 IRMOF-3-catalyzed Hantzsch coupling under solvent-free conditions.

14.2.2 MOF-catalysed Reactions

The channels of metal–organic frameworks (MOFs) have been used as nanoscale reaction vessels in recent years.[23–25] IRMOF-3 acts as a suitable green catalyst for the one-pot synthesis of dihydropyrimidinone **25** and dihydropyridine derivatives **26** through Biginelli (Scheme 14.10) and Hantzsch (Scheme 14.11) reactions, with the desired products obtained in high yields from short reaction times under mild solvent-free conditions.[26] These MOFs can be isolated from the reaction mixture and reused four times.

IRMOF-3 is also an active, selective, and stable solid catalyst for three-component one-pot reactions of amines **27**, aldehydes **28**, and dimethyl phosphite **29** to form the corresponding α-aminophosphonates **30** in high yields (Scheme 14.12).[27] The catalyst can be isolated from the reaction mixture and reused at least four times.

MOF-199 has been utilized as a novel heterogeneous catalyst for the synthesis of imines **32** from primary amines **31** in excellent conversions of up to 96% under mild reaction conditions (Scheme 14.13).[28] This method uses

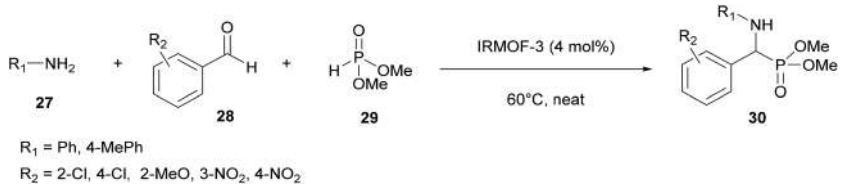

Scheme 14.12 IRMOF-3-catalyzed Kabachnik–Fields reaction under solvent-free conditions.

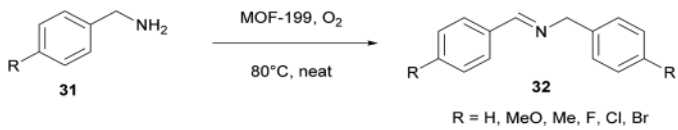

Scheme 14.13 MOF-199-catalyzed conversion of benzyl amine to imine under solvent-free conditions.

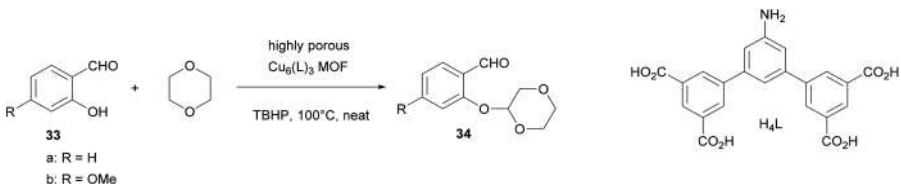

Scheme 14.14 $Cu_6(L)_3$-MOF-catalyzed oxidative C–O coupling under solvent-free conditions.

O_2 as an environmentally friendly oxidant at 80 °C without a solvent, and the MOF can be reused in up to five cycles without loss of reactivity. Lewis acid sites present on the MOF played a key role in the formation of imines **32** from amines **31** under aerobic oxidative conditions.

A robust paddle-wheel $Cu_6(L)_3$ MOF bearing Lewis acid and basic sites has been explored as a heterogeneous catalyst for cross-dehydrogenative coupling reactions by direct C–H activation of 1,4-dioxane with 2-carbonyl-substituted phenols **33** under solvent-free conditions using *tert*-butyl hydroperoxide (TBHP) as an oxidant, affording the desired product **34** in up to 96% yield (Scheme 14.14).[29] The reaction proceeded with a short reaction time and minimum waste, and the catalyst was easily recovered and recycled up to five times without a significant loss of catalytic activity.

A highly efficient method for the synthesis of pyrroles **37** from amines **35** and acetonylacetone **36** using MIL-53(Al) as a catalyst has been developed using solvent-free sonication (Scheme 14.15).[30] This reaction showed a broad substrate scope and high yields (~96%) within a short reaction time. MIL-53(Al) was recovered and reused several times without a significant loss of catalytic activity.

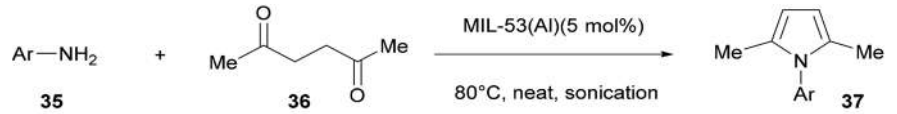

Ar = Ph, 2-MePh, 4-OHPh, 4-IPh, 2,5-Cl_2Ph, 3,4-Cl_2Ph, 3,5-Cl_2Ph, 2,5-Br_2Ph, 4-NO_2Ph, 4-CNPh

Scheme 14.15 MIL-53(Al)-MOF-catalyzed Paal–Knorr reaction under solvent-free conditions.

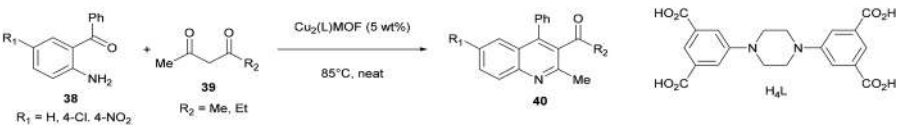

Scheme 14.16 Cu_2(L)-MOF-catalyzed Friedländer reaction under solvent-free conditions.

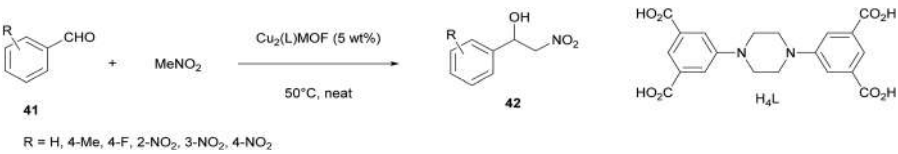

R = H, 4-Me, 4-F, 2-NO_2, 3-NO_2, 4-NO_2

Scheme 14.17 Cu_2(L)-MOF-catalyzed Henry reaction under solvent-free conditions.

A three-dimensional NbO-type porous MOF, Cu_2(L), containing both tertiary amine groups and paddle wheel secondary building units, was used as an efficient heterogeneous catalyst for the synthesis of quinoline derivatives **40** by the Friedländer reaction between aromatic 2-aminobenzophenones **38** and β-diketones **39** (Scheme 14.16), and the synthesis of β-nitroalcohols **42** by the Henry reaction of benzaldehydes **41** with nitromethane (Scheme 14.17).[31] This MOF catalyst was easily recycled and reused for at least four runs without loss of catalytic activity.

An MOF-5-catalyzed coupling reaction was developed as an efficient synthesis of quinolines **46** *via* a one-pot three-component reaction of aromatic amines **43**, aldehydes **44**, and alkynes **45** in good to excellent yields (Scheme 14.18).[32] The catalyst was easily recovered by simple filtration and reused at least five times without loss of catalytic activity.

NH_2-MIL-53(Al) MOF, with coordinative unsaturated aluminium sites, was active in a Groebke–Blackburn–Bienaymé multicomponent coupling reaction for the synthesis of 3-aminoimidazo[1,2*a*]pyridines **50** by condensation of isocyanide **47**, benzaldehyde **48**, and 2-aminepyridine **49** (Scheme 14.19).[33] This reaction proceeded under solvent-free conditions with a high yield (~95%), with the NH_2-MIL-53(Al) MOF recovered and reused for five reaction cycles, affording a total turnover number of 455.

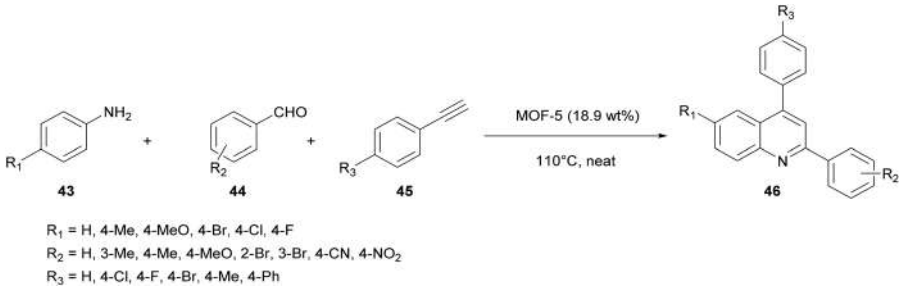

Scheme 14.18 MOF-5-catalyzed one-pot synthesis of 2,4-disubstituted quinolines under solvent-free conditions.

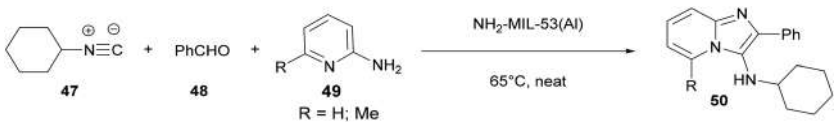

Scheme 14.19 NH_2-MIL-53(Al)-MOF-catalyzed Groebke–Blackburn–Bienaymé reaction under solvent-free conditions.

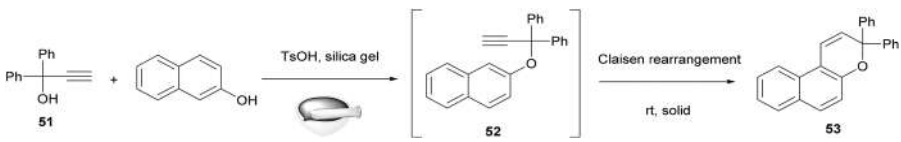

Scheme 14.20 One-pot synthesis of naphthopyran in the solid-state.

14.3 Solid-state Reactions

Organic solid-state reactions date back to 1828, when Friedrich Wöhler discovered that ammonium cyanate rearranged to urea in the solid-state. In the 1970s, Schmidt studied the solid-state photodimerization of *trans*-cinnamic acid derivatives, discovering why they reacted highly regio- and stereoselectively, and more efficiently than in solution.[34] This is often cited as the starting point of intensive research in organic solid-state chemistry.[35–41]

14.3.1 Thermal Solid-state Reactions

Naphthopyran derivatives are well known as photochromic compounds. *p*-TsOH-catalyzed condensation reactions of 1,1-diaryl-2-propyn-1-ol **51** and 2-naphthol by grinding using a mortar and pestle in the solid-state gave photochromic naphthopyran **53** in 56% yield *via* Claisen rearrangement of propargyl ether **52** (Scheme 14.20).[42] When the reaction was carried out in CH_2Cl_2

solution, the product **52** was obtained in 39% yield. This protocol provides a simple, efficient and environmentally friendly one-pot synthesis of photochromic naphthopyrans without using harmful halogenated solvents.

Heating colourless crystals of the 1 : 2 complex of tetraallene derivative **54a** and toluene at 180 °C on a hot plate for 30 min gave yellow crystals of anthrodicyclobutene derivative **55a** in quantitative yield (Scheme 14.21).[43] Differential scanning calorimetry (DSC) measurements showed an exothermic peak at 189 °C, which is attributable to the thermal cyclization of **54a** to **55a** in the crystal without melting.

When colourless prisms of propargylallene **56** were heated at 190–200 °C, dark copper-brown crystals of furofuran derivative **57** were formed quantitatively (Scheme 14.22).[44] This reaction occurred without any melting and DSC measurement of a crystal of **56a** showed a sharp exothermic peak at 198 °C resulting from the transformation. The melting temperature of the product **57a** (>300 °C) was significantly higher than the reaction temperature.

A vinylogous pinacol rearrangement of thienothienyl-substituted 9,10-dihydroxy-9,10-dihydroanthracene **58**, involving intramolecular 1,4-migration of the bulky thienothienyl substituent, was thermally induced in the solid state. When heated at around 240 °C, the crystals were transformed quantitatively, accompanied by dehydration, affording crystals of anthrone derivatives **59** without wetting or melting (Scheme 14.23).[45]

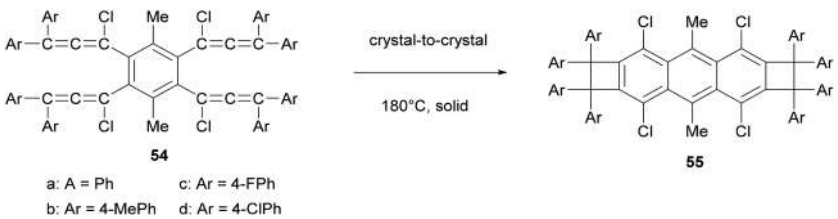

Scheme 14.21 Thermal cyclization of tetraallene to anthrodicyclobutene in the solid-state.

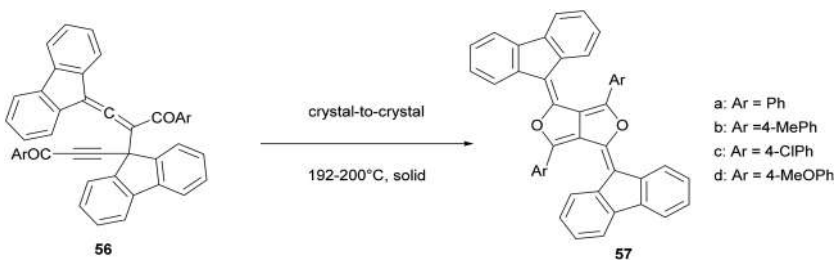

Scheme 14.22 Thermal rearrangement of propargylallene to furofuran in the solid-state.

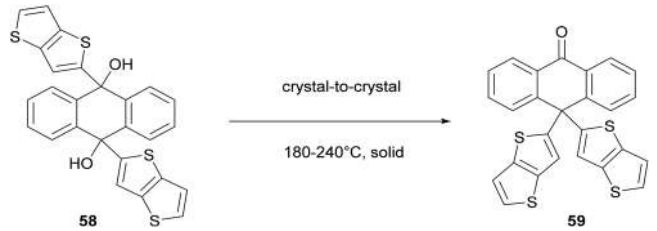

Scheme 14.23 Thermal pinacol rearrangement in the solid-state.

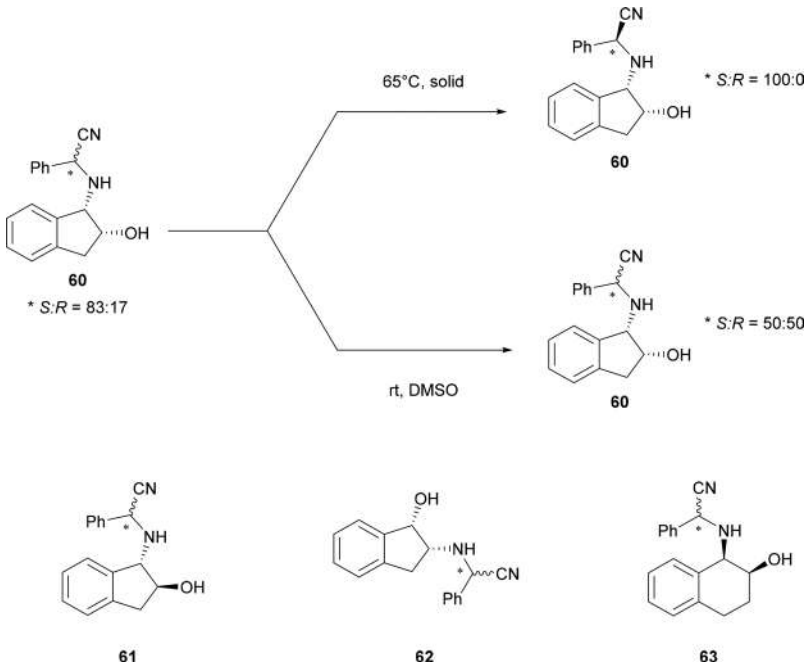

Scheme 14.24 Thermal epimerization of α-amino nitrile in the solid-state.

A diastereomeric mixture ($S:R$ = 83:17) of α-amino nitrile **60** thermally epimerized in the solid-state to give a single diastereomer ($S:R$ = 100:0) at the α-position of the nitrile moiety in (*S*)-**60** (Scheme 14.24).[46] This was in stark contrast to the reaction conducted in DMSO solution at room temperature, which gave a 1:1 mixture ($S:R$ = 50:50) of α-amino nitrile **60**. Notably, complete diastereomeric enrichment was also achieved for (*R*)-amino nitriles prepared similarly from racemic *trans*-1-aminoindan-2-ol **61**, *cis*-2-aminoindan-1-ol **62** and tetrahydronaphthalene derivative **63** as the amine components.

14.3.2 Topochemical Reactions

A single-crystal-to-single-crystal solid-state Diels–Alder reaction of the 1 : 2 charge–transfer complex of bis(*N*-cyclobutylimino)-1,4-dithiin **64** and 9-bromoanthracene **65** at 30 °C led to a 1 : 1 co-crystal composed of cycloadduct **66** and unreacted 9-bromoanthracene **65** (Scheme 14.25).[47] The distances between the reacting atoms of dienophile **64** and diene **65** are within Schmidt's criterion (less than 4.2 Å).

Heating crystals of *rac*-1,2 : 3,4-di-*O*-isopropylidene-*myo*-inositol **67** at 110 °C for 10 min resulted in 92–95% isomerization to *rac*-1,2 : 5,6-di-*O*-isopropylidene-*myo*-inositol **68** (Scheme 14.26).[48] The crystal structures of **67** and **68** showed that the C5–OH moiety in each molecule was facing the *trans*-ketal carbon of a neighboring molecule from a close distance, resulting in a *pseudo*-trigonal-bipyramidal arrangement.

The *rac*-4-*O*-phenoxycarbonyl derivative **69a** (mp:166–167 °C) and 4-*O*-phenoxythiocarbonyl derivative **69b** (mp:162–164 °C) of *myo*-inositol orthoformate underwent thermal intramolecular cyclization in the crystalline form to afford the corresponding 4,6-bridged carbonate **70a** in 85% yield and thiocarbonate **70b** in 84% yield, respectively (Scheme 14.27).[49] The crystal structures of these two carbonates and a thiocarbonate showed that the relative orientations of the electrophile and nucleophile in the crystal lattice facilitated the intramolecular cyclization reaction.

Slow annealing of a single crystal of stacked macrocycle monomer **71**, bearing two parallel diacetylene functionalities, at 40 °C for 35 days achieved single-crystal-to-single-crystal thermal polymerization, which afforded

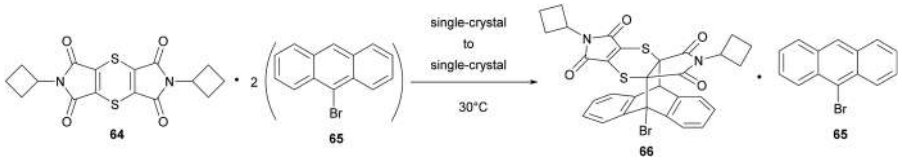

Scheme 14.25 Single-crystal-to-single-crystal Diels–Alder reaction in the solid-state.

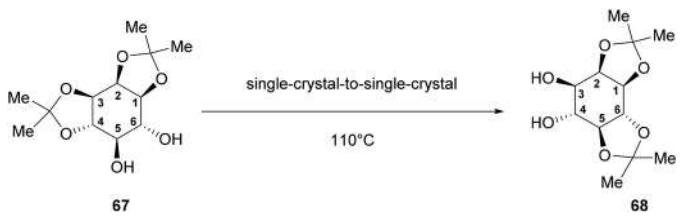

Scheme 14.26 Single-crystal-to-single-crystal transketalization reaction in the solid-state.

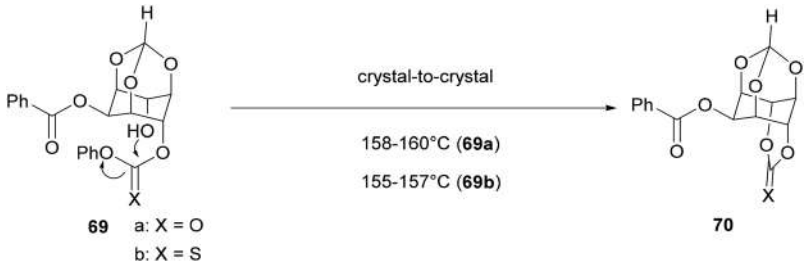

Scheme 14.27 Intramolecular acyl transfer reaction in the solid-state.

Scheme 14.28 Single-crystal-to-single-crystal polymerization of a diacetylene-containing macrocycle in the solid-state.

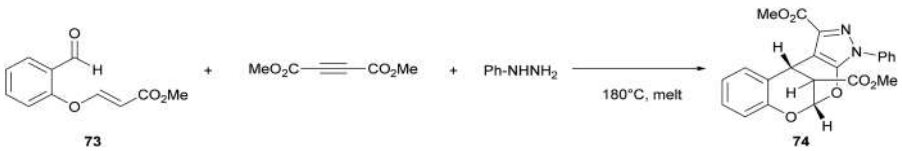

Scheme 14.29 Synthesis of tetracyclic chromene fused pyranopyrazole in the solid-state melt reaction.

tubular addition polymer **72** (Scheme 14.28).[50] The crystal structure showed that compound **71** crystallized with structural parameters suitable for topochemical polymerization.

14.3.3 Solid-state Melt Reactions

Efficient multicomponent domino reaction for the synthesis of novel tetracyclic pyrazole-fused 2,8-dioxabicyclo[3.3.1]nonane **74**, starting from methyl-3-(2-formylphenoxy)acrylate **73** and involving hydrazone formation, amidation, Knoevenagel condensation, and intramolecular hetero Diels–Alder reactions in one pot was reported (Scheme 14.29).[51] The best result was observed when the reaction was carried out at 180 °C providing a single product in 91% yield.

Similar one-pot assembly of benzo[*a*]phenazinone-fused chromene bicyclic scaffolds **78** *via* a one pot multicomponent domino Knoevenagel intramolecular hetero-Diels–Alder strategy using a solid-state melt reaction of *o*-phenylenediamine **75**, 2-hydroxynaphthalene-1,4-dione **76** and *O*-allyl salicylaldehyde derivative **77** was reported (Scheme 14.30).[52]

14.3.4 Mechanochemical Reactions

In recent years, reactions performed by grinding with a mortar and pestle and mechanochemical ball milling under solvent-free conditions have been used in organic synthesis. The ball milling technique has also been applied to a wide range of organic reactions, including metal-catalyzed reactions, condensation reactions, and nucleophilic addition reactions.[53–63]

Silver and copper foil were found to be effective, versatile, and selective heterogeneous catalysts for the cyclopropenation of terminal and internal alkynes under solvent-free mechanochemical milling conditions. The copper-foil-catalyzed cyclopropenation of phenyl acetylene **79a** with methyl phenyldiazoacetate **80** afforded cyclopropene **81a** in 88% yield. Meanwhile, the silver-foil-catalyzed mechanochemical reaction of 1-phenyl-propyne **79b** afforded cyclopropene **81b** in 90% yield (Scheme 14.31).[64]

A rapid and environmentally benign method for the synthesis of 2,3-dihydroquinazolin-4(1*H*)-one has been achieved by grinding in a mortar

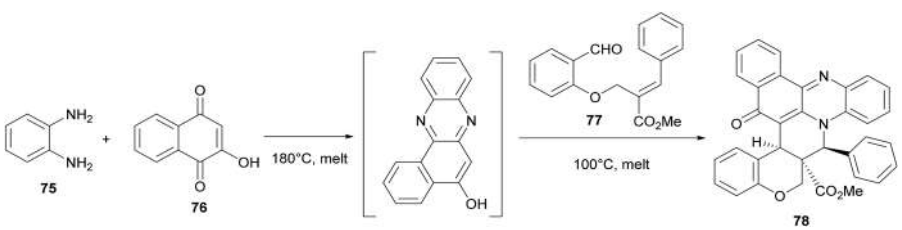

Scheme 14.30 Synthesis of heptacyclic chromene fused benzo[*a*]phenazinone in the solid-state melt reaction.

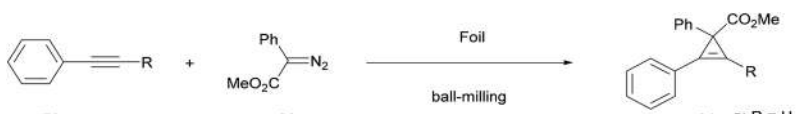

Foil	R	Yield (%)
Cu	H	88
Ag	Me	90

Scheme 14.31 Metal foil-catalyzed cyclopropanation of alkyne under ball-milling conditions.

and pestle. Using 10 mol% of *p*-TsOH, the reaction between anthranilimide **82** and *p*-nitrobenzaldehyde **83** (R = NO_2) smoothly furnished the desired product **84** (R = NO_2) in 90% yield after grinding for 10 min (Scheme 14.32).[65]

The zinc-mediated solvent-free reaction of [60]fullerene **85** with chalcone **86** and water, and subsequent treatment with triethylamine, afforded [60] fullerene-fused cyclopentanol **87** in 66% yield under ball-milling conditions (Scheme 14.33).[66]

Ball milling enabled the alkynylation of ketones using calcium carbide (CaC_2). This was achieved by simply co-milling CaC_2 with organic substrates in a tungsten carbide jar without additives or catalyst. For example, benzophenone **88** was converted to give terminal alkyne **89** and central alkyne **90** in 75% yield with a 1 : 2 **89**/**90** ratio after 40 min (Scheme 14.34).[67] This method provided a practical alternative to established procedures for introducing ethynyl functionalities.

An operationally simple one-step mechanochemical Reformatsky reaction, using *in situ* generated organozinc intermediates under neat grinding conditions, has been developed. A solution-based reaction of benzaldehyde **91** and ethyl 2-bromoacetate **92** in dry THF under a nitrogen atmosphere

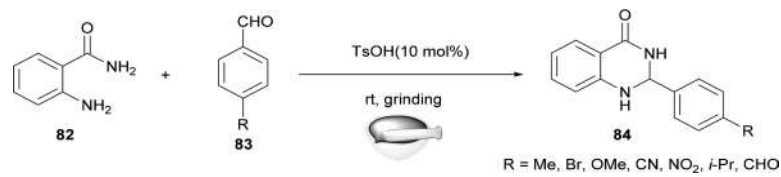

Scheme 14.32 Synthesis of 2,3-dihydroquinazolin-4(1*H*)-one under grinding with a mortar and pestle.

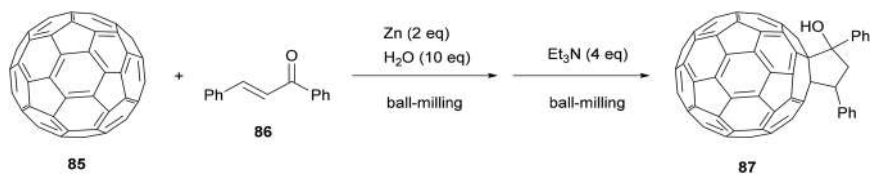

Scheme 14.33 Zinc-mediated reductive cyclization of [60]fullerene with enone under ball-milling conditions.

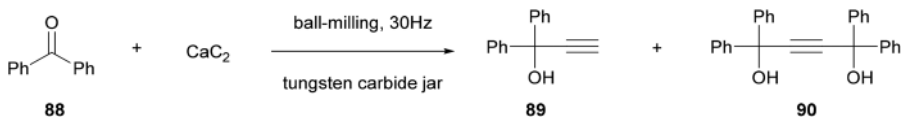

Scheme 14.34 Alkynylation of benzophenone using calcium carbide under ball-milling conditions.

at 50 °C using zinc flakes afforded product **93** in only 7% yield. In contrast, the reaction proceeded smoothly under ball-milling conditions without any solvent, inert gas, or additive, affording the product **93** in up to 87% yield (Scheme 14.35).[68]

A mechanochemical zinc-mediated Barbier-type allylation reaction of allyl halide with aldehydes **94** under ball-milling conditions is reported (Scheme 14.36).[69] This process, which was operationally simple and did not require an inert atmosphere or dry solvents, produced versatile homoallylic alcohol products **95** in moderate to good yields.

A SUS-304 ball-milling mediated continuous H_2 generation reaction from H_2O along with the hydrogenation reaction has been reported. SUS-304 and mechanochemical processing played crucial roles in the development of these reactions. Notably, zero-valent Cr, a constituent of SUS304, was found to be involved in H_2 generation, while Ni acted as a catalyst for the hydrogenation. Alkyne, alkene, aromatic bromide, nitro, azide and carbonyl functionalities were all efficiently reduced under these reaction conditions (Scheme 14.37).[70] These environmentally benign hydrogenation reactions using H_2O as the hydrogen source are highly attractive.

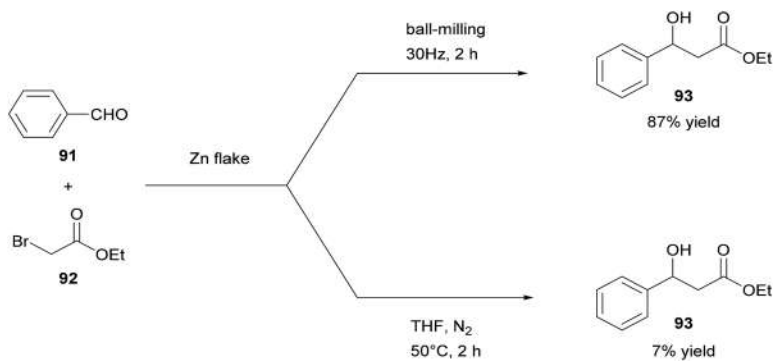

Scheme 14.35 Reformatsky reaction with unactivated zinc flakes under ball-milling conditions.

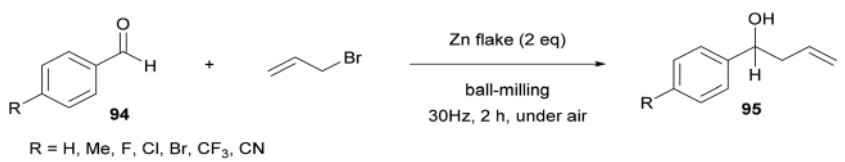

Scheme 14.36 Zinc-mediated Barbier-type allylation reaction under ball-milling conditions.

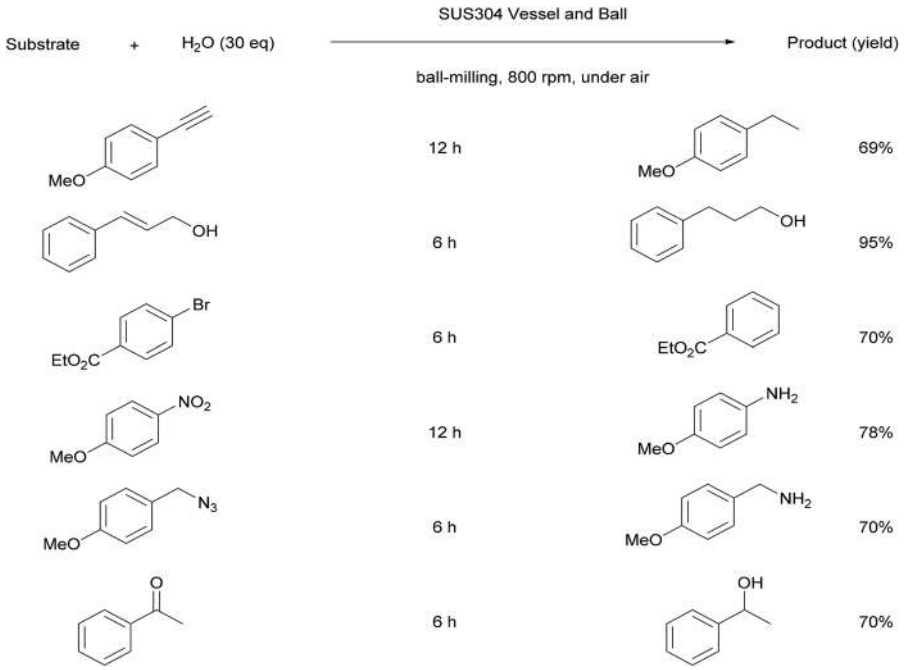

Scheme 14.37 Stainless-steel-mediated hydrogenation using H_2O under ball-milling conditions.

14.3.5 Photochemical Reactions

The [2 + 2]-photocycloaddition of olefins is a useful reaction in synthetic organic chemistry for obtaining cyclobutene derivatives. This reaction occurs more efficiently and selectively when performed in the crystalline state compared with homogeneous solution owing to the tight and regular molecular arrangement in the crystal. To date, many strategies have been employed to control the stacking arrangements of the reactant in the reaction. These include weak intermolecular interactions between reactant olefins by co-crystallization with hydrogen-bond or halogen-bond templates.[71–84]

3-Arylindenones **96** exhibited different photochemical behaviours in solution and in the solid-state. Irradiation of **96** in benzene solution exclusively gave *anti*-head-to-head dimers **97** in good yields. In contrast, photolysis in the solid-state, strongly influenced by the molecular arrangement in the crystal lattice, afforded *syn*-head-to-head dimers **98** exclusively (Scheme 14.38).[85]

The photoirradiation of crystalline powders of *S,S*-dioxobenzothiophene-2-methanol **99** led to *syn*-head-to-tail dimer **100** as the major product in *ca.* 9.6 : 0.4 diastereomeric ratios with conversions >95%, while photoreactions in $CHCl_3$ solution in the presence of a triplet sensitizer (benzophenone) yielded exclusively *anti*-head-to-tail dimer **101** (Scheme 14.39).[86]

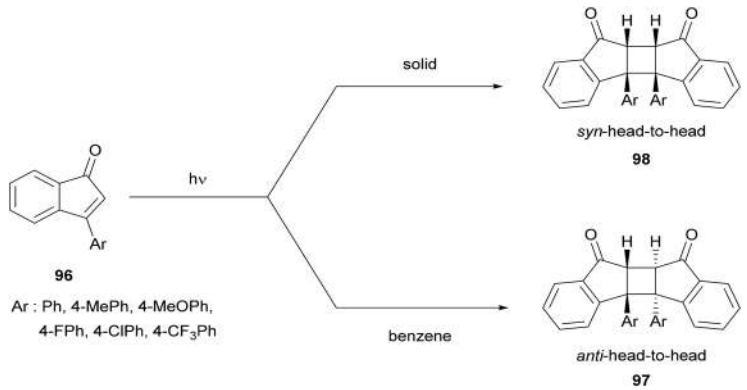

Scheme 14.38 Stereoselective photodimerization of 3-arylindenone in the solid-state.

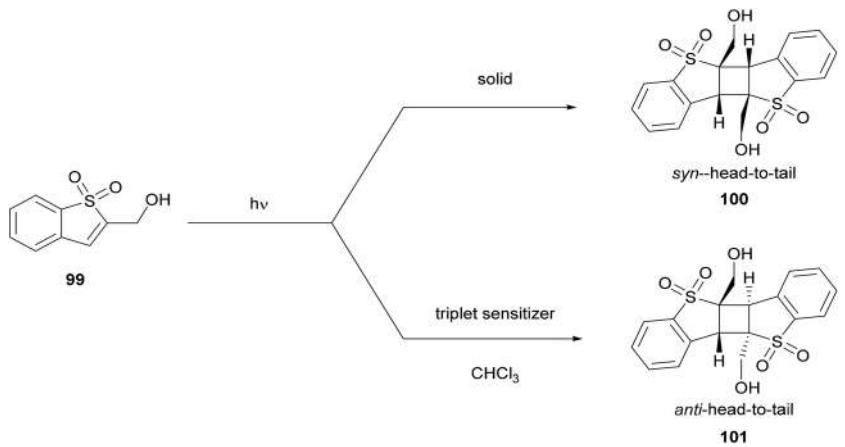

Scheme 14.39 Stereoselective photodimerization of *S*,*S*-dioxo-benzothiophene in the solid-state.

Halogen bonds have been employed to direct solid state organization of alkenes to facilitate [2 + 2] photocycloaddition reactions. For example, upon exposure to UV light, 2:1 cocrystals of 1,4-diiodoperchlorobenzene and *trans*-1,2-bis(4-pyridyl)ethylene **102** underwent a stereoselective [2 + 2] cycloaddition reaction to produce *tetrakis*(4-pyridyl)cyclobutane **103** in 89% yield (Scheme 14.40).[87]

Cocrystals 1,4-diiodoperchlorobenzene·(*E*)-methyl-3-(pyridine-4-yl)prop-2-enoate **104** and 1,4-diiodoperchlorobenzene·(*E*)-methyl-3-(pyridine-3-yl) prop-2-enoate **105** both underwent a regioselective [2 + 2] photocycloaddition reaction to yield corresponding head-to-head dimers **106** and **107**,

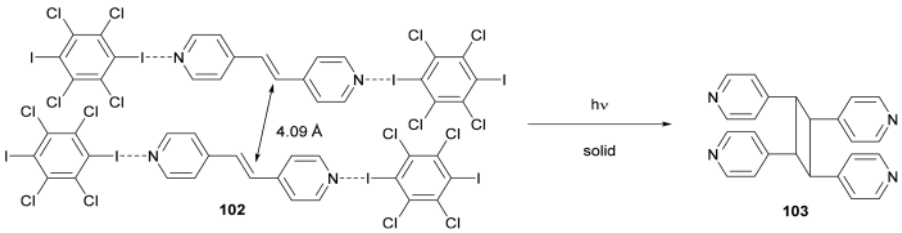

Scheme 14.40 Photodimerization reaction of a co-crystal of *trans*-1,2-bis(4-pyridyl) ethylene with 1,4-diiodoperchlorobenzene in the solid-state.

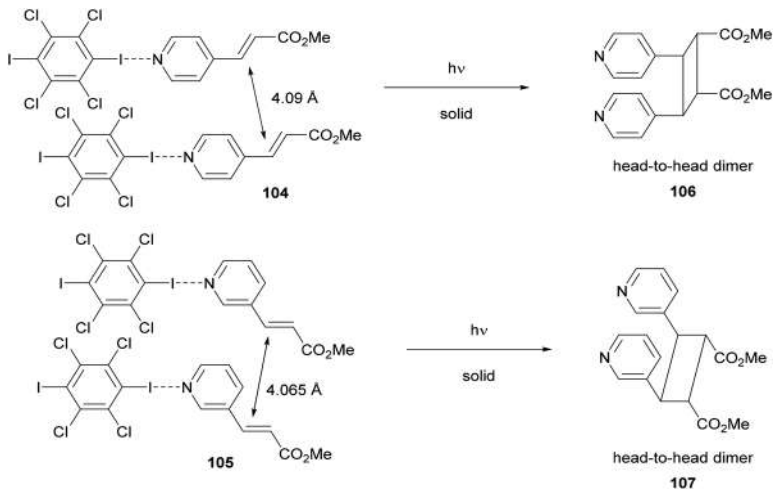

Scheme 14.41 Photodimerization reaction of a co-crystal of isomeric pyridine vinyl esters with 1,4-diiodoperchlorobenzene in the solid-state.

respectively (Scheme 14.41).[88] In both cases, the photoreaction did not proceed *via* a single-crystal-to-single-crystal transformation, as the crystalline state was lost upon exposure to UV light.

Hydrogen-bond-donor templates based on 4-chlororesorcinol complete the supramolecular construction of *ortho*- and *meta*-[2.2]cyclophanes in the solid-state (Scheme 14.42).[89] When a finely ground crystalline sample of 2(4-Cl-resorcinol)·2(*ortho*-di-[2-(4-pyridyl)ethenyl]) **108** was exposed to UV light for 75 h, *exo,exo-ortho*-cyclophane **109** was formed in quantitative yield. In contrast, crystals of 2(4-Cl-resorcinol)·2(*meta*-di-[2-(4-pyridyl) ethenyl]) **110** were highly photoreactive under ambient light, undergoing a single-crystal-to-single-crystal transformation to form *exo,exo-meta*-cyclophane **111**.

The 2 : 1 cocrystals formed from *N,N′*-diacetyl-1,4-dihydropyrazine **112** and thiourea underwent dimerization to afford *syn*-dimer **113** in 90% yield. This was followed by intramolecular [2 + 2]-cycloaddition to give cage dimer **114**

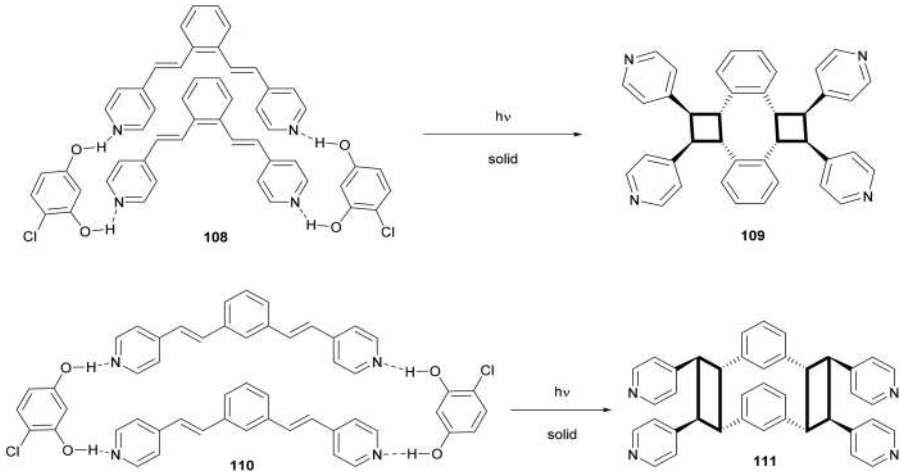

Scheme 14.42 Synthesis of *ortho*- and *meta*-[2.2]cyclophanes using cocrystals with 4-chlororesorcinol in the solid-state.

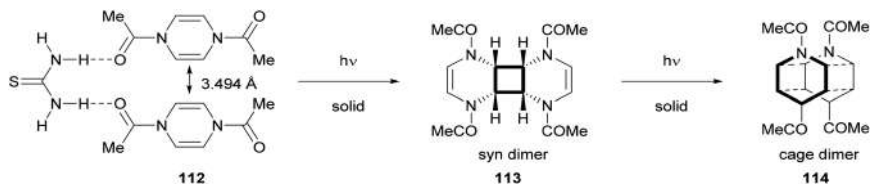

Scheme 14.43 [2 + 2] Photocycloaddition of a 1,4-dihydropyrazine derivative using cocrystals with thiourea in the solid-state.

in 100% yield. The successful photodimerization of **112** was attributed to the short distance between them (3.494 Å) and appropriate overlap of the p-orbitals of the reactive double bonds. Additionally, two double bonds in *syn*-dimer **113** are separated by a centroid distance of 3.568 Å for generation of a cage dimer **114** (Scheme 14.43).[90]

14.4 Asymmetric Reactions

Asymmetric solvent-free reactions using chiral organocatalysts, organometallic catalysts, and homochiral MOFs under neat or ball-milling conditions have been reported.[91–100]

The organocatalytic Michael reaction of cyclohexanone **115** with γ-monohalonitrodienes **116** catalyzed by chiral prolinethiol ether **117** under solvent-free conditions was developed. This method affords a novel approach to accessing highly functionalized optically active monohaloalkenes **118** with up to >95% yield, >99% ee and >99 : 1 regioselectivities (Scheme 14.44).[101]

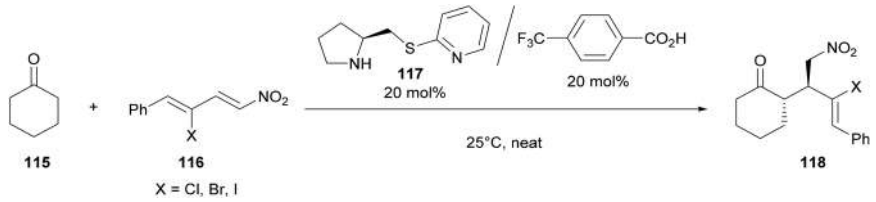

Scheme 14.44 Solvent-free asymmetric Michael reaction catalyzed by prolinethiol ether.

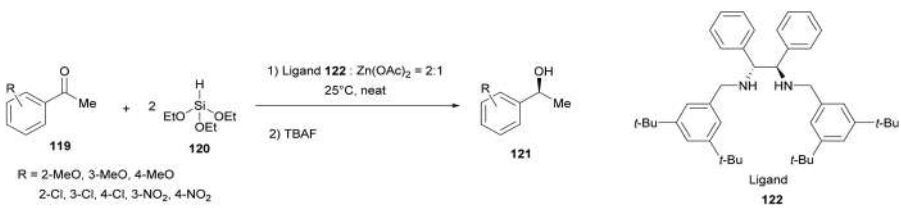

Scheme 14.45 Solvent-free asymmetric hydrosilylation of ketones promoted by a chiral diamine-$Zn(OAc)_2$ complex.

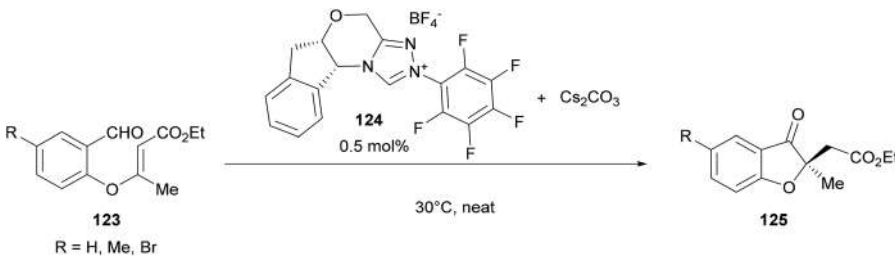

Scheme 14.46 Solvent-free asymmetric Stetter reaction catalyzed by chiral N-heterocyclic carbene.

The zinc-acetate-promoted asymmetric hydrosilylation of various ketones under solvent-free conditions has been examined. Exposing acetophenone derivatives **119** to a Zn complex of chiral diamine **122** (0.05 mol%) in the presence of triethoxysilane **120** afforded optically active *sec*-alcohols **121** with excellent yields (up to 98%) and enantioselectivities (up to 97% ee) (Scheme 14.45).[102]

The solvent-free intramolecular asymmetric Stetter reaction of aldehyde **123** proceeded efficiently using chiral N-heterocyclic carbene **124** (0.2–1 mol%) as a catalyst to give product **125** with excellent yields (up to 99%) and enantioselectivities (up to 98% ee). These solvent-free reactions are green, efficient, and practical, using approximately 10 to 100 times less catalyst than typical literature protocols (Scheme 14.46).[103]

A 1:2 complex of (*S,S,S,S,S,S*)-**129** with $CoBr_2$ was an excellent catalyst for the asymmetric aldol reaction between cyclohexanone **126** and benzaldehydes **127** under solvent-free conditions using a planetary ball mill. The resulting *anti*-aldol adducts (1′*R,* 2*S*)-**128** were obtained with high enantioselectivity (up to 93% ee) compared with the same reaction performed in solution or neat liquid with traditional magnetic stirring (Scheme 14.47).[104]

An efficient solvent-free protocol has been developed for the asymmetric Michael addition of α-nitrocyclohexanone **130** to nitroalkenes **131** using chiral thiourea derivatives **132** as hydrogen bonding catalysts. By performing these organocatalytic reactions in a planetary ball mill, the corresponding addition products **133** were obtained in high yields (up to 97%) with excellent enantioselectivities (up to 96% ee) in short reaction times with low catalyst loadings (Scheme 14.48).[105]

Optically active propargylamines **138** were synthesized in excellent yields (up to 99%) with high enantioselectivity (up to 99% ee) using $Cu(OTf)_2$-pybox **137** (10 mol%) as a catalyst in the solvent-free three-component asymmetric coupling of aldehydes **134,** amines **135,** and alkynes **136** by ball-milling for 60 min. This catalytic system was reused several times without losing activity (Scheme 14.49).[106]

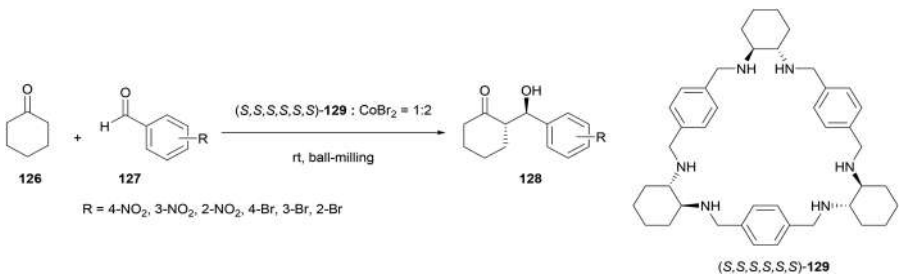

Scheme 14.47 Asymmetric Aldol reaction catalyzed by a chiral triangleamine-$CoBr_2$ complex under ball-milling conditions.

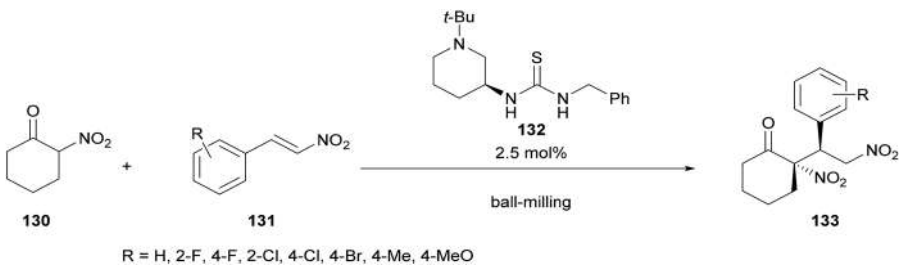

Scheme 14.48 Asymmetric Michael reaction catalyzed by chiral piperidine-based thiourea under ball-milling conditions.

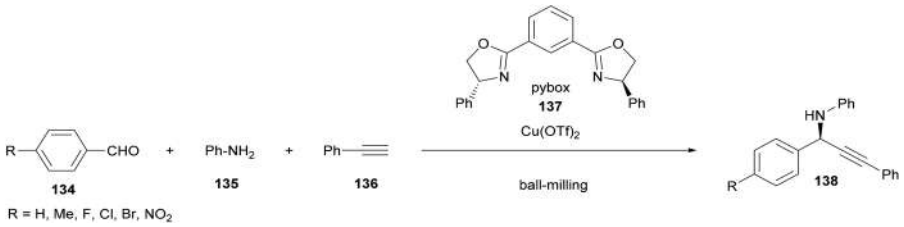

Scheme 14.49 Asymmetric synthesis of propargylamines catalyzed by the chiral Cu(II)pybox complex under ball-milling conditions.

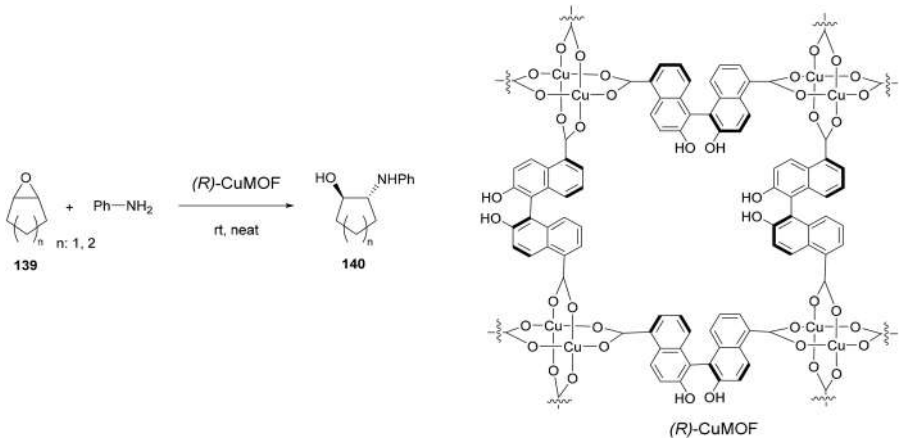

Scheme 14.50 Asymmetric ring–opening reaction of epoxides with aniline catalyzed by (*R*)-CuMOF under solvent-free conditions.

A novel homochiral MOF, (*R*)-CuMOF, has been synthesized and structurally characterized. In the presence of this chiral MOF, asymmetric ring opening reactions of epoxides **139** with aniline proceeded to give optically active β-amino alcohols **140** (up to 51%ee) under solvent-free conditions (Scheme 14.50).[107]

14.5 Continuous Flow Twin-Screw Extrusion

Extrusion is a well-established technique with vital roles in the manufacturing processes of polymers, pharmaceuticals, and food products. Recently, this technique has been applied to solvent-free continuous organic synthesis,[108] including aldol condensations, Biginelli reactions, Knoevenagel condensations, and Michael reactions.[109]

Twin-screw extrusion has also been successfully used in the solvent-free synthesis of various naphthalic imides **142** and perylene diimides **144** (Scheme 14.51).[110] A mixture of **141** (5.0 g, 25 mmol) and 4-ethoxyaniline

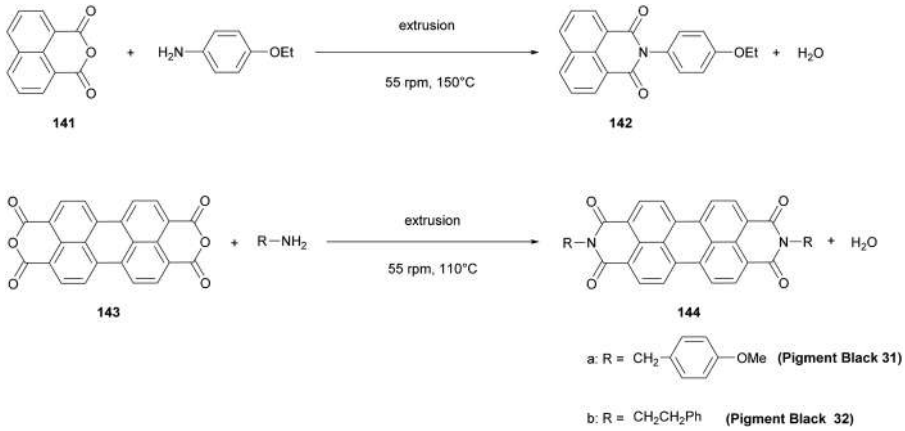

Scheme 14.51 Continuous flow synthesis of imides by twin-screw extrusion.

(3.46 g, 25 mmol) was fed manually into an extruder over 8 min, with a screw rotation rate of 55 rpm at 110 °C for 30 min yielding naphthalic imide **142** in >99% yield. Similar extrusion of a mixture of perylene-3,4,9,10-tetracarboxylic dianhydride **143** and various amines under similar conditions resulted in the formation of commercial pigments, Pigment Black 31 **144a** in 93% yield and Pigment Black 32 **144b** in 96% yield, respectively.

14.6 Conclusion

Solvent-free reactions have become increasingly popular and appealing in the field of green chemistry because they can minimize the amount of hazardous waste. Various strategies and protocols have been developed and improved over the last two decades. Furthermore, numerous reviews have revealed how solid reactants can be ground, heated, or irradiated to favour transformations that may be more efficient and selective than those obtained using traditional methods involving organic solvents. Mechanochemistry is the paradigm of solvent-free reactions because operations such as grinding or ball milling are simple and can be performed using low-cost devices. In addition, mechanochemistry has emerged as a valuable tool for organic synthesis. However, solvent-free mechanochemical reactions may not be applicable to industrial continuous-flow reactors owing to the possible formation of highly viscous solids. Reactive extrusion has recently emerged as a powerful technique that can overcome this limitation. Reagents and reactants are mixed and processed on a kilogram scale in highly efficient extruders using single or double rotating screws. Thus, in recent years, solvent-free reactive extrusion has gained considerable interest in the large-scale production of pharmaceuticals. The use of visible light irradiation as a novel, green, and simple protocol in solvent-free reactions has also been developed. Generally, compact fluorescent light and white light emitting diodes are used

as sources of visible light for various organic transformations. The use of catalyst-free and solvent-free conditions, and direct work-up without chromatographic separation are among the notable advantages of this green and simple protocol. Since 2000, chemical educators have published a wide range of procedures to elucidate the advantages of green chemistry through their undergraduate laboratory experiments, wherein they illustrate some examples of solvent-free organic reactions.[111,112]

References

1. F. Toda, *Trends Org. Chem.*, 1992, **3**, 323.
2. F. Toda, *Synlett*, 1993, 303.
3. F. Toda, *Acc. Chem. Res.*, 1995, **28**, 480.
4. R. S. Varma, *Green Chem.*, 1999, **1**, 43.
5. K. Tanaka and F. Toda, *Chem. Rev.*, 2000, **100**, 1025.
6. D. Bradley, *Chem. Br.*, 2002, **38**, 42.
7. K. Tanaka, *Solvent-free Organic Synthesis*, Wiley-VCH, Weinheim, 2003, p. 1.
8. K. Bougrin, A. Loupy and M. Soufiaoui, *J. Photochem. Photobiol., C*, 2005, **6**, 139.
9. K. Tanaka, *Solvent-free Organic Synthesis*, 2nd Completely Revised and Updated Edition, Wiley-VCH, Weinheim, 2009, p. 1.
10. M. A. P. Martins, C. P. Frizzo, D. N. Moreira, L. Buriol and P. Machado, *Chem. Rev.*, 2009, **109**, 4140.
11. M. S. Singh and S. Chowdhury, *RSC Adv.*, 2012, **2**, 4547.
12. M. B. Gawande, V. D. B. Bonifácio, R. Luque, P. S. Branco and R. S. Varma, *ChemSusChem*, 2014, **7**, 24.
13. A. Sarkar, S. Santra, S. K. Kundu, A. Hajra, G. V. Zyryanov, O. N. Chupakhin, V. N. Charushin and A. Majee, *Green Chem.*, 2016, **18**, 4475.
14. M. Obst and B. König, *Eur. J. Org. Chem.*, 2018, 4213.
15. K. Tanemura, *Tetrahedron Lett.*, 2019, **60**, 1924.
16. I. Kazi, S. Guha and G. Sekar, *Org. Lett.*, 2017, **19**, 1244.
17. B. K. Sarmah, M. Konwar, D. Bhattacharyya, P. Adhikari and A. Das, *Adv. Synth. Catal.*, 2019, **361**, 5616.
18. K. N. Shivhare, M. K. Jaiswal, A. Srivastava, S. K. Tiwari and I. R. Siddiqui, *New J. Chem.*, 2018, **42**, 16591.
19. S. Naskar, S. R. Chowdhury, S. Mondal, D. K. Maiti, S. Mishra and I. Das, *Org. Lett.*, 2019, **21**, 1578.
20. D. Bedi, A. Brar and M. Findlater, *Green Chem.*, 2020, **22**, 1125.
21. T. Murata, M. Hiyoshi, M. Ratanasak, J. Hasegawa and T. Ema, *Chem. Commun.*, 2020, **56**, 5783.
22. R. Kaminker, E. B. Callaway, N. D. Dolinski, S. M. Barbon, M. Shibata, H. Wang, J. Hu and C. J. Hawker, *Chem. Mater.*, 2018, **30**, 8352.
23. A. Dhakshinamoorthy and H. Garcia, *Chem. Soc. Rev.*, 2014, **43**, 5750.
24. A. Dhakshinamoorthy, A. M. Asiri, M. Alvaro and H. Garcia, *Green Chem.*, 2018, **20**, 86.

25. K. Tanaka in *Advances in Organic Crystal Chemistry*, ed. M. Sakamoto and H. Uekusa, Springer Nature, Singapore, 2020, p. 477.
26. S. Rostamnia and A. Morsali, *RSC Adv.*, 2014, **4**, 10514.
27. S. Rostamnia, H. Xin and N. Nouruzi, *Microporous Mesoporous Mater.*, 2013, **179**, 99.
28. B. Venu, V. Shirisha, B. Vishali, G. Naresh, R. Kishore, I. Sreedhar and A. Venugopal, *New J. Chem.*, 2020, **44**, 5972.
29. V. Sharma, D. De and P. K. Bharadwaj, *Inorg. Chem.*, 2018, **57**, 8195.
30. H. T. Nguyen, L. H. T. Nguyen, T. L. H. Doan and P. H. Tran, *RSC Adv.*, 2019, **9**, 9093.
31. A. K. Gupta, D. De and P. K. Bharadwaj, *Dalton Trans.*, 2017, **46**, 7782.
32. S. Xiao, C. Ma, J. Di and Z. Zhang, *New J. Chem.*, 2020, **44**, 8614.
33. S. Rostamnia and M. Jafari, *Appl. Organomet. Chem.*, 2017, **31**, e3584.
34. G. M. J. Schmidt, *Pure Appl. Chem.*, 1971, **27**, 647.
35. I. C. Paul and D. Y. Curtin, *Acc. Chem. Res.*, 1973, **6**, 217.
36. J. M. Thomas, *Pure Appl. Chem.*, 1979, **51**, 1065.
37. A. Gavezzotti and M. Simonetta, *Chem. Rev.*, 1982, **82**, 1.
38. V. Ramamurthy, *Tetrahedron*, 1986, **42**, 5753.
39. K. Tanaka and F. Toda, in *Organic Solid-state Reactions*, ed. F. Toda, Kluwer Academic Publishers, Dordrecht, 2002, p. 1.
40. F. Toda, in *Topics in Current Chemistry*, ed. F. Toda, Springer, Berlin, 2005, p. 1.
41. G. Kaupp, in *Encyclopedia of Physical Organic Chemistry*, ed. Z. Wang, John Wiley & Sons, 2017, vol. 2, p. 1.
42. K. Tanaka, H. Aoki, H. Hosomi and S. Ohba, *Org. Lett.*, 2000, **2**, 2133.
43. K. Tanaka, N. Takamoto, Y. Tezuka, M. Kato and F. Toda, *Tetrahedron*, 2001, **57**, 3761.
44. K. Tanaka, A. Tomomori and J. L. Scott, *Eur. J. Org. Chem.*, 2003, 2035.
45. R. Sekiya, K. Kiyo-oka, T. Imakubo and K. Kobayashi, *J. Am. Chem. Soc.*, 2000, **122**, 10282.
46. R. Sakurai, S. Suzuki, J. Hashimoto, M. Baba, O. Itoh, A. Uchida, T. Hattori, S. Miyano and M. Yamamura, *Org. Lett.*, 2004, **6**, 2241.
47. S. Khorasani and M. A. Fernandes, *Chem. Commun.*, 2017, **53**, 4969.
48. K. M. Sureshan, T. Murakami, T. Miyasou and Y. Watanabe, *J. Am. Chem. Soc.*, 2004, **126**, 9174.
49. M. I. Tamboli, M. S. Shashidhar, R. G. Gonnade and S. Krishnaswamy, *Chem. - Eur. J.*, 2015, **21**, 13676.
50. T. Hsu, F. W. Fowler and J. W. Lauher, *J. Am. Chem. Soc.*, 2012, **134**, 142.
51. M. Bakthadoss, S. Jayakumar, S. Raman, A. Devaraj and D. S. Sharada, *Org. Biomol. Chem.*, 2019, **17**, 3884.
52. M. Bakthadoss, J. Srinivasan, M. A. Hussain and D. S. Sharada, *RSC Adv.*, 2019, **9**, 24314.
53. A. Stolle, T. Szuppa, S. E. S. Leonhardt and B. Ondruschka, *Chem. Soc. Rev.*, 2011, **40**, 2317.

54. S. L. James, C. J. Adams, C. Bolm, D. Braga, P. Collier, T. Friščić, F. Grepioni, K. D. Harris, G. Hyett, W. Jones, A. Krebs, J. Mack, L. Maini, A. G. Orpen, I. P. Parkin, W. C. Shearouse, J. W. Steed and D. C. Waddell, *Chem. Soc. Rev.*, 2012, **41**, 413.
55. G. Wang, *Chem. Soc. Rev.*, 2013, **42**, 7668.
56. D. Tan, L. Loots and T. Friščić, *Chem. Commun.*, 2016, **52**, 7760.
57. T. K. Achar, A. Bose and P. Mal, *Beilstein J. Org. Chem.*, 2017, **13**, 1907.
58. M. Leonardi, M. Villacampa and J. C. Menéndez, *Chem. Sci.*, 2018, **9**, 2042.
59. J. L. Howard, Q. Cao and D. L. Browne, *Chem. Sci.*, 2018, **9**, 3080.
60. J. Andersen and J. Mack, *Green Chem.*, 2018, **20**, 1435.
61. A. Bose and P. Mal, *Beilstein J. Org. Chem.*, 2019, **15**, 881.
62. C. Bolm and J. G. Hernández, *Angew. Chem., Int. Ed.*, 2019, **58**, 3285.
63. T. Friščić, C. Mottillo and H. M. Titi, *Angew. Chem., Int. Ed.*, 2020, **59**, 1018.
64. L. Chen, D. Leslie, M. G. Coleman and J. Mack, *Chem. Sci.*, 2018, **9**, 4650.
65. G. Yashwantrao, V. P. Jejurkar, R. Kshatriya and S. Saha, *ACS Sustainable Chem. Eng.*, 2019, **7**, 13551.
66. H. Liu, H. Xu, G. Shao and G. Wang, *Org. Lett.*, 2019, **21**, 2625.
67. A. Hosseini and P. R. Schreiner, *Eur. J. Org. Chem.*, 2020, 4339.
68. Q. Cao, R. T. Stark, I. A. Fallis and D. L. Browne, *ChemSusChem*, 2019, **12**, 2554.
69. J. Yin, R. T. Stark, I. A. Fallis and D. L. Browne, *J. Org. Chem.*, 2020, **85**, 2347.
70. Y. Sawamura, T. Kawajiri, M. Niikawa, R. Goto, Y. Yabe, T. Takahashi, T. Marumoto, M. Itoh, Y. Kimura, Y. Monguchi, S. Kondo and H. Sajiki, *ChemSusChem*, 2015, **8**, 3773.
71. V. Ramamurthy and K. Venkatesan, *Chem. Rev.*, 1987, **87**, 433.
72. H. E. Zimmerman and E. E. Nesterov, *Acc. Chem. Res.*, 2002, **35**, 77.
73. K. Tanaka and F. Toda, in *Organic Solid-State Reactions*, ed. F. Toda, Kluwer Academic Publishers, Dordrecht, 2002, p. 109.
74. D. Bučar, G. S. Papaefstathiou, T. D. Hamilton, Q. L. Chu, I. G. Georgiev and L. R. MacGillivray, *Eur. J. Inorg. Chem.*, 2007, 4559.
75. I. G. Georgiev and L. R. MacGillivray, *Chem. Soc. Rev.*, 2007, **36**, 1239.
76. M. Nagarathinam, A. M. P. Peedikakkal and J. J. Vittal, *Chem. Commun.*, 2008, 5277.
77. L. R. Macgillivray, G. S. Papaefstathiou, T. Friščić, T. D. Hamilton, D. Bucar, Q. Chu, D. B. Varshney and I. G. Geogiev, *Acc. Chem. Res.*, 2008, **41**, 280.
78. L. R. MacGillivray, *J. Org. Chem.*, 2008, **73**, 3311.
79. C. Yang and W. Xia, *Chem.–Asian J.*, 2009, **4**, 1774.
80. K. Biradha and R. Santra, *Chem. Soc. Rev.*, 2013, **42**, 950.
81. R. Medishetty, I. Park, S. S. Lee and J. J. Vittal, *Chem. Commun.*, 2016, **52**, 3989.
82. V. Ramamurthy and J. Sivaguru, *Chem. Rev.*, 2016, **116**, 9914.

83. J. J. Vittal and H. S. Quah, *Dalton Trans.*, 2017, **46**, 7120.
84. J. Yu, M. M. Gan, S. Bai and Y. Han, *CrystEngComm*, 2019, **21**, 4675.
85. N. Uemura, H. Ishikawa, N. Tamura, Y. Yoshida, T. Mino, Y. Kasashima and M. Sakamoto, *J. Org. Chem.*, 2018, **83**, 2256.
86. C. O'Hara, C. Yang, A. J. Francis, B. S. Newell, H. Wang and M. J. E. Resendiz, *J. Org. Chem.*, 2019, **84**, 9714.
87. E. Bosch, S. J. Kruse, H. R. Krueger Jr and R. H. Groeneman, *Cryst. Growth Des.*, 2019, **19**, 3092.
88. S. J. Kruse, E. Bosch, F. Brown and R. H. Groeneman, *Cryst. Growth Des.*, 2020, **20**, 1969.
89. T. Friščić, E. Elacqua, S. Dutta, S. M. Oburn and L. R. MacGillivray, *Cryst. Growth Des.*, 2020, **20**, 2584.
90. Q. Fan, X. Duan and H. Yan, *CrystEngComm*, 2018, **20**, 1151.
91. B. S. Green, M. Lahav and G. M. J. Schmidt, *Mol. Cryst. Liq. Cryst.*, 1975, **29**, 187.
92. B. S. Green and M. Lahav, *J. Mol. Evol.*, 1975, **6**, 99.
93. M. Sakamoto, *Chem. - Eur. J.*, 1997, **3**, 684.
94. E. Brunet, *Chirality*, 2002, **14**, 135.
95. J. R. Scheffer and W. Xia, in *Topics in Current Chemistry*, Springer, Berlin, 2005, 254, p. 233.
96. M. Sakamoto, *J. Photochem. Photobiol., C*, 2006, **7**, 183.
97. P. J. Walsh, H. Li and C. Anaya de Parrodi, *Chem. Rev.*, 2007, **107**, 2503.
98. C. Yang and W. Xia, *Chem.–Asian J.*, 2009, **4**, 1774.
99. I. N. Egorov, S. Santra, D. S. Kopchuk, I. S. Kovalev, G. V. Zyryanov, A. Majee, B. C. Ranu, V. L. Rusinov and O. N. Chupakhin, *Green Chem.*, 2020, **22**, 302.
100. M. Tavakolian, S. Vahdati-Khajeh and S. Asgari, *ChemCatChem*, 2019, **11**, 2943.
101. A. Xia, C. Wu, D. Xu, Y. Wang, X. Du, Z. Li and Z. Xu, *J. Org. Chem.*, 2013, **78**, 1254.
102. M. Szewczyk, A. Bezłada and J. Mlynarski, *ChemCatChem*, 2016, **8**, 3575.
103. T. Ema, Y. Nanjo, S. Shiratori, Y. Terao and R. Kimura, *Org. Lett.*, 2016, **18**, 5764.
104. K. Tanaka, A. Asakura, T. Muraoka, P. Kalicki and Z. Urbanczyk-Lipkowska, *New J. Chem.*, 2013, **37**, 2851.
105. M. Jörres, S. Mersmann, G. Raabe and C. Bolm, *Green Chem.*, 2013, **15**, 612.
106. Z. Li, Z. Jiang and W. Su, *Green Chem.*, 2015, **17**, 2330.
107. K. Tanaka, S. Oda and M. Shiro, *Chem. Commun.*, 2008, 820.
108. D. E. Crawford, C. K. Miskimmin, J. Cahir and S. L. James, *Chem. Commun.*, 2017, **53**, 13067.
109. D. E. Crawford, C. K. G. Miskimmin, A. B. Albadarin, G. Walker and S. L. James, *Green Chem.*, 2017, **19**, 1507.
110. Q. Cao, D. E. Crawford, C. Shi and S. L. James, *Angew. Chem., Int. Ed.*, 2020, **59**, 4478.

111. A. P. Dicks, *Green Chem. Lett. Rev.*, 2009, **2**, 87.
112. For selected recent example, see: (a) M. Touaibia, A. Selka, N. A. Levesque and P. A. St-Onge, *J. Chem. Educ.*, 2020, **97**, 2296; (b) Y. M. Omar, N. G. Mohamed, A. N. Boshra and A. M. Abdel-Aal, *J. Chem. Educ.*, 2020, **97**, 1134; (c) E. Colacino, G. Dayaker, A. Morère and T. Friščić, *J. Chem. Educ.*, 2019, **96**, 766.

Section 3

Sustainable Approaches in Organic Synthesis

CHAPTER 15

Biomass-derived Platform Chemicals

THOMAS J. FARMER[a] AND MARK MASCAL*[b]

[a]Green Chemistry Centre of Excellence, Department of Chemistry, University of York, Heslington, York, YO10 5DD UK; [b]Department of Chemistry, University of California Davis, 1 Shields Avenue, Davis, California 95616, USA
*E-mail: thomas.farmer@york.ac.uk, mjmascal@ucdavis.edu

15.1 The Platform Molecules

The chemical industry represents one of the greatest modern achievements of mankind. We have developed countless highly optimised pathways for the creation of a vast array of products that form the very fabric of our everyday lives. Organic synthesis, the field which utilises carbon as a focal atom, is at the foundation of the most significant and successful technologies that drive the chemical industry. The manufacture of plastics, textiles, paints and coatings, adhesives, detergents, agrichemicals, dyes, pharmaceuticals, and food ingredients are just some of the many examples where synthetic organic chemistry has served the needs of mankind. Perhaps even more remarkable is that the majority of the aforementioned products have ultimately been produced from just a small set of simple chemical building blocks, known as the base chemicals. Base chemicals represent the first functional molecules prepared from the initial processing of crude oil and natural gas. "Functional" in this instance refers to each of the base chemicals containing

Sustainable Organic Synthesis: Tools and Strategies
Edited by Stefano Protti and Alessandro Palmieri

Published by the Royal Society of Chemistry, www.rsc.org

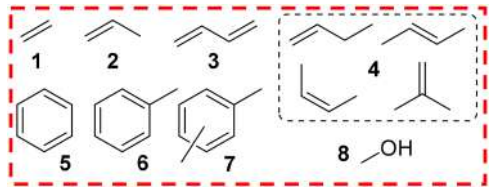

Figure 15.1 The base chemicals. Ethene **1**; propene **2**; 1,3-butadiene **3**; butenes **4** (1-butene, *cis*- and *trans*-2-butene and isobutene); benzene **5**; toluene **6**; xylenes **7** (*ortho*-, *meta*- and *para*-); methanol **8**.

functional groups that a chemist would see as a point for synthetic modification. Although what exactly constitutes the base chemicals may be argued, they are generally accepted to be those given in Figure 15.1.

Starting from the base chemicals, reactions such as oxidations (*e.g.* ethene to oxirane), polymerisations (*e.g.* ethene to polyethene), or reactions between two base chemicals (*e.g.* ethene + benzene to form ethylbenzene) produce the bulk and commodity chemicals, with further modification leading to fine and specialty chemicals. With base, bulk, commodity, fine, and specialty chemicals we have a diverse toolkit of compounds from which are made the plethora of commercial products delivered by industry.

There is, however, a fundamental problem with the long-term sustainability of the chemical industry: its overreliance on non-renewable fossil feedstocks. In 1925, petroleum derivatives contributed less than 0.1% to the production of organic chemicals in the US. By 1946, that number had increased to 28%,[1] and by the end of the 20th century petroleum achieved nearly full dominance of the chemicals sector. Although projections for a resurgence of biomass and comprehensive recycling are robust,[2] meaningful statistics are few and far between. What bioeconomy advocates generally agree on, however, is that the potential exists to ultimately achieve 100% renewable energy, chemicals, and materials through a combination of biomass utilization and non-fossil-based power sources.

The sheer abundance of crude oil and natural gas as feedstocks put the chemical industry into overdrive from about the middle of the 20th century. It has, however, been recognized for years that economically accessible reserves of crude oil and natural gas are diminishing, although so-called Peak Oil, in terms of supply, appears still to be distant.[3] The term, however, has recently taken on a new significance in the post covid-19 world, where demand has been significantly impacted.[4] Given these uncertainties, it is of paramount importance that the chemical industry undergoes a shift towards the utilisation of biomass. Unlike fossil resources, biomass is replenished globally on a timescale measured in years, not millennia. Of course, it should be recognized that crude oil and natural gas are formally products of biomass, though geological processes over many thousands of years were needed for their conversion to the fossil reserves we have today. We cannot of course wait for more crude oil and natural gas to be created, but we can

accelerate the process, so to speak, in the laboratory. In biomass, we therefore have access to a renewable feedstock that has the potential to supply our chemical industry sustainably for the long term, if managed correctly. The future biobased chemical industry we seek to create can learn lessons from the many successes of the petrochemical industry. Some of these lessons include economies of scale, the minimisation of waste, consideration of energetics for reactions performed at industrial scales, and the value in having a set of established fundamental building blocks that bring stability to downstream chemistry. It is this last point where platform molecules have a clear role to play.

Many publications have covered the concept of platform molecules or platform chemicals (the terms are used interchangeably),[5] with the majority agreeing that they generally can be defined as:

> "...the fundamental building blocks of a biobased chemical industry, representing the first small functional chemicals readily accessed from biomass feedstocks."[6]

Based upon this definition, and through our own experience and opinions of candidates of great promise, the authors have prepared a representative list of platform molecules (Figure 15.2). The list is of course not exhaustive, but instead attempts to provide a depiction of the diverse toolbox of biobased building blocks that are already accessible to the synthetic organic chemist. At the end of the chapter, twelve platform molecules of exceptional promise are singled out and profiled as candidates for a new "Top 12" list.[7]

Some differences of opinion exist as to whether scale of production should be an aspect of the definition of platform molecules. However, there is no doubt that if platform molecules are to displace base and bulk chemicals in the chemical industry, then scale is indeed a major consideration. Base chemicals vary in scale of global annual production from ~10 MT for butadiene to >100 MT for ethene. Commodity chemicals often exceed global productions of 1 MT. It is therefore reasonable to attach a condition of scale for consideration as a platform molecule, but as we cannot yet be sure which biobased building blocks will be produced in excess of 1 MT per annum, it seems premature to attach a scale to the definition at this point. We can, however, appreciate that only platform molecules derivable from the most abundant streams of biomass can ultimately achieve large global annual production volumes. Those components include cellulose, hemicellulose, lignin, starches, and related, common polysaccharides such as alginic acid (from macroalgae). Other abundant plant extracts, including monoterpenes and triglycerides, will also contribute, but cannot compete in terms of tonnage with the major structural components of plants.

There are also differences of opinion regarding the relevance of the term "small" when defining a platform molecule. Again, if we consider a comparison to base and bulk chemicals, then building blocks of low molecular mass (<200 g mol^{-1}) would seem appropriate, but this risks ignoring the potential

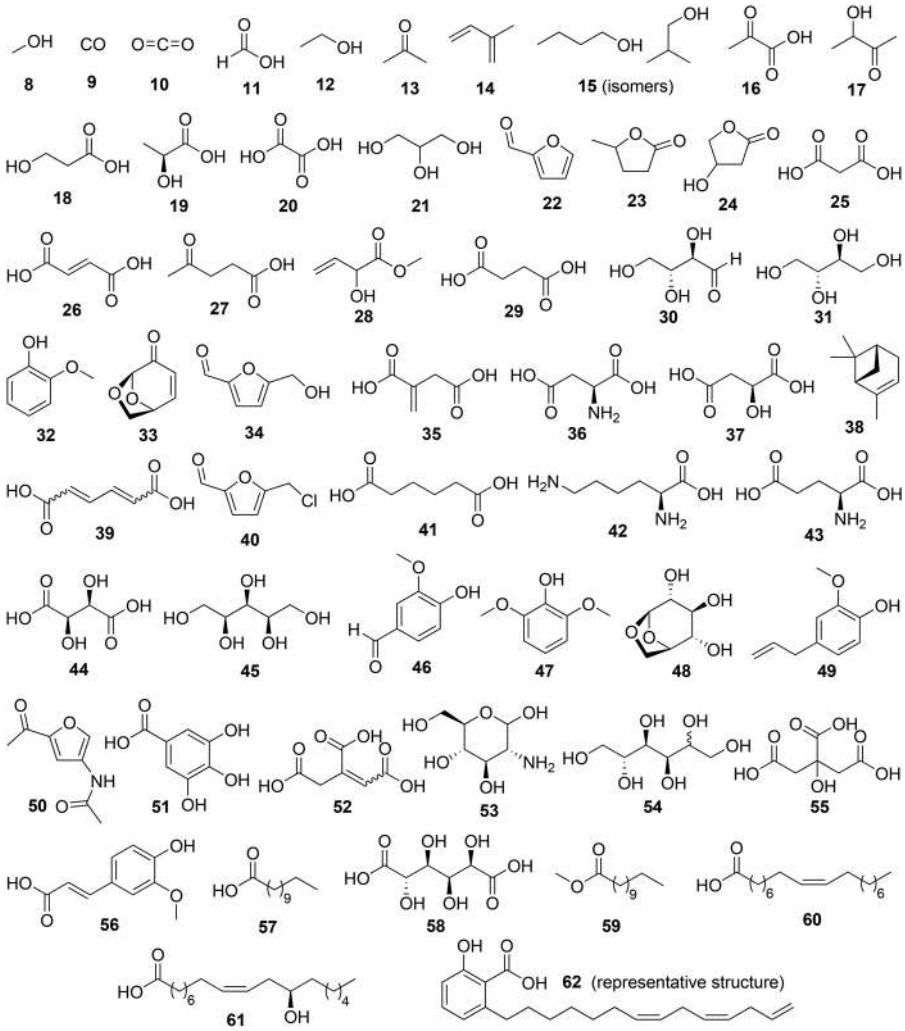

Figure 15.2 The authors' list of key platform molecules. Methanol **8**; carbon monoxide **9**: carbon dioxide **10**; formic acid **11**; ethanol **12**; acetone **13**; isoprene **14**; butanol (*n*-, iso-) **15**; pyruvic acid **16**; acetoin **17**; 3-hydroxypropanoic acid **18**; lactic acid **19**; oxalic acid **20**; glycerol **21**; furfural **22**; γ-valerolactone **23**; 3-hydroxybutyrolactone **24**; malonic acid **25**; fumaric acid **26**; levulinic acid **27**; methyl vinyl glycolate **28**; succinic acid **29**; erythrose **30**; erythritol **31**; guaiacol **32**; levoglucosenone **33**; 5-(hydroxymethyl)furfural **34**; itaconic acid **35**; aspartic acid **36**; malic acid **37**; monoterpenes (*e.g.* α-pinene) **38**; muconic acid **39**; 5-(chloromethyl)furfural **40**; adipic acid **41**; L-lysine **42**; glutamic acid **43**; tartaric acid **44**; xylitol and arabitol **45**; vanillin **46**; syringol **47**; levoglucosan **48**; eugenol **49**; 3-acetamido-5-acetylfuran **50**; gallic acid **51**; aconitic acid **52**; glucosamine **53**; sorbitol and mannitol **54**; citric acid **55**; ferulic acid **56**; saturated fatty acids (*e.g.* lauric acid) **57**; glucaric **58**; fatty acid alkyl esters (*e.g.* methyl laurate) **59**; oleic acid **60**; ricinolelic acid **61**; anacardic acid **62**.

for plants to produce some larger compounds with genuine potential as key building blocks, such as oleic acid (**60**, 282.5 g mol^{-1}) and similar fatty acids.

Others have undertaken to define lists of platform molecules, often with the intention to highlight those deemed to be of greatest commercial potential. The most influential to date was published in 2004 by the US Department of Energy (DOE).[7] It compiled a list (Figure 15.3) of what at that time were considered the most promising building block chemicals derivable from biomass carbohydrates (including glycerol) and syngas. This list omitted molecules obtainable from lignin, which was covered in a later report.[8]

There is no doubt that this report influenced research on platform molecules in the years that followed. Of note is that the US DOE at the time did not use the term "platform molecule," instead detailing the most promising biomass-derived chemicals and so contained 2,5-furandicarboxylic (FDCA), which is arguably only a "second generation" platform molecule as it is itself derived from either HMF **34** or glucaric acid **58**. Most research articles and reviews on biobased chemicals reference this seminal publication, although time has proven the DOE report inaccurate in some of their predictions. For example, 3-hydroxypropanoic acid **18** and 3-hydroxybutyrolactone **24** have progressed little since their mention in the report.

In 2010, Bozell reassessed the DOE report in his highly cited *Technology development for the production of biobased products from biorefinery carbohydrates–the US Department of Energy's "Top 10" revisited*, and by applying a modified selection process he established an alternative list.[9] Bozell added ethanol and lactic acid, which did not appear in the DOE report as they were already seen as advanced biobased chemicals, while including the popular biobased chemical furfural **22**. Bozell also added "biohydrocarbons" with a direct focus on isoprene and monoterpenes, while removing all of the diacids except succinic acid **29** as well as the aforementioned 3-hydroxybutyrolactone **24**. Possibly the best ongoing oversight of the DOE

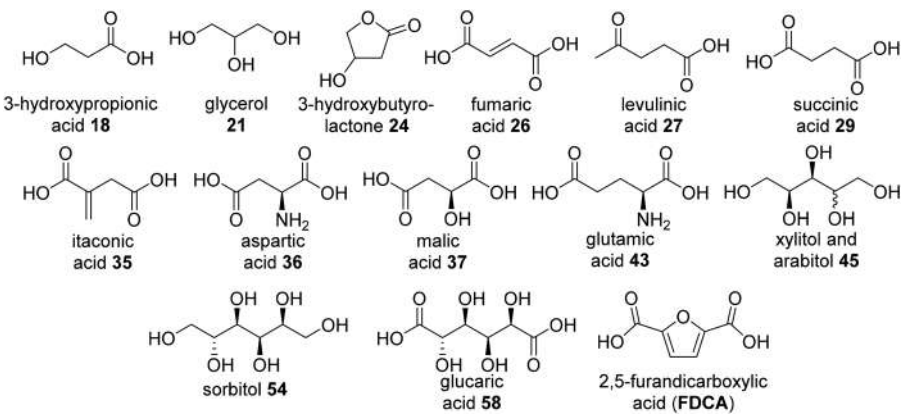

Figure 15.3 US Department of Energy Top Value-Added Chemicals from Biomass 2004 List.[7]

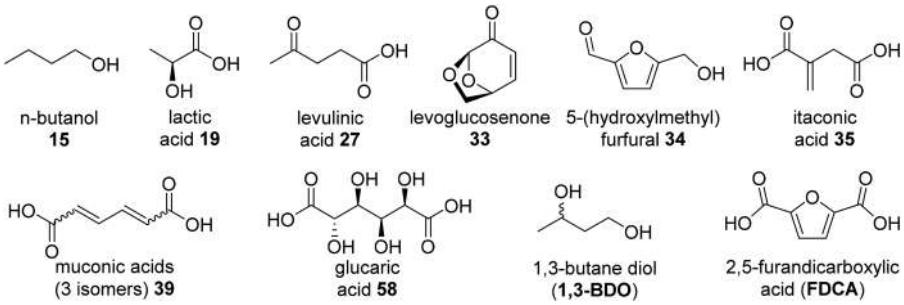

Figure 15.4 UK Lignocellulosic Biorefinery Network (LBNet) UKBioChem10 2018 List (http://ukbiochem10.co.uk/wp/wp-content/uploads/2019/01/UKBioChem10_Report.pdf).

list, and other promising platform molecules, can be found in the work and presentations of Doris De Guzman. The Green Chemicals Blog curated by De Guzman remains one of the most informative sites for an up-to-date narrative on biobased building blocks.[10] In 2019 the Lignocellulosic Biorefinery Network (LBNet) led an initiative to establish its own list of platform molecules with specific potential for development within the UK, the so-called UKBioChem10. This list (Figure 15.4) sought to achieve a similar outcome to the US DOE report from fifteen years earlier, in an attempt to focus research effort on small biobased building blocks where the UK could take a leading role in their development. Of particular note in the UKBioChem10 is the emergence of levoglucosenone **33** as a prominent biobased chemical, and the inclusion of *n*-butanol **15**, 1,3-butanediol, and muconic acids **39** on the basis of strong research into their production *via* industrial biotechnology. What this and the other lists demonstrate is both a clear appreciation that platform molecules have a fundamental role to play in a future biobased chemical industry and that academia, industry, and governments seemingly all agree that there is value in focusing on a small, manageable set of compounds, at least in the near term.

15.2 Rich Diversity Across the Platforms

Looking at the base chemicals (Figure 15.1) in comparison to the platform molecule lists of Figures 15.2–15.4 instantly highlights a major difference between a petroleum- and bio-derived chemical industry in terms of building block chemistry. The base chemicals of the present chemical industry, except methanol **8**, have no heteroatoms, being instead comprised wholly of hydrocarbons. The current petrochemical industry adds functional complexity to base chemicals usually *via* incorporation of heteroatoms in oxidation processes. In comparison, the biobased platform molecules are rich in heteroatoms, especially O, this stemming from the fact that their feedstock is already heteroatom rich. It logically follows that heteroatoms in the biobased

platform molecules lead to greater synthetic diversity and that we should seek to maximally exploit this diversity, as recently highlighted by Hülsey.[11] Indeed, the present list contains examples of alcohols (including several polyols), carboxylic acids (mono-, di- and tri-), aldehydes, ketones, esters (including lactones), alkenes (both electron rich and electron deficient), dienes, furans, aromatics, acetals, amines, amides, bicyclic compounds, and even a halogenated molecule (CMF **40**). Perhaps most significant is that many of the platform molecules listed here contain combinations of more than one of the above functions. It is thus apparent that these platforms offer a veritable feast of molecules from which to build a future sustainable chemical industry, with most of the functional groups most widely exploited by synthetic chemists being present.

Chirality is also well represented in the list, with sixteen molecules having one or more chiral centres and a further three (**17**, **24** and **28**) with the potential to be single stereoisomers if appropriate methods are used in their production. This defined stereochemistry has obvious utility in the synthesis of pharmaceuticals and agrochemicals. Potentially cheap access to stereodefined molecules could also bring additional value to higher volume, lower value products of a bioeconomy. For example, the isohexides isosorbide, isomannide, and isoidide represent an interesting group of molecules whereby the initial stereochemistry of the feedstock results in structurally distinct diols. As shown in Figure 15.5, differences in intramolecular hydrogen bonding of the hydroxyl groups to the oxygens

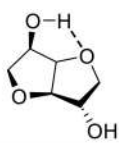

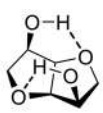

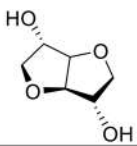

Isohexide	isosorbide	isomannide	isoidide
Feedstock	glucose (very abundant)	mannose, mannitol (fairly abundant)	idose, iditol (very rare)
Designation	exo-endo	endo-endo	exo-exo
-OH reactivity	1 high, 1 low	both low	both high
Adipate polyester Tg	21 °C	28 °C	45 °C

Adipate polyester =

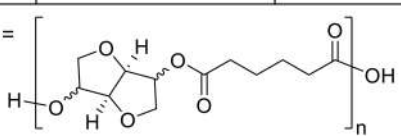

Figure 15.5 Influence of biomass-derived stereochemistry of the isohexides on their adipate polyesters.[13]

of the oxolane rings affect the reactivity of these groups. In the case of isomannide, both OH groups participate in hydrogen bonding which reduces their reactivity, while for isoidide the opposite is observed. Stereochemistry thus affects the materials properties of the resultant adipate polyesters of the isohexides, with the glucose-derived isosorbide possessing the lowest glass transition temperature (T_g), while isoidide polyesters have the highest.[12]

The occurrence of the chiral centres in some platform molecules, and the diverse range of functional groups seen in them, harkens back to another key point of consideration, that is, that the structure is dictated *both* by the component of the feedstock from which it is derived *and* the process by which it is produced. Some of the common components of biomass that can lead to platform molecules at scale have already been highlighted, with cellulose, hemicellulose, and lignin widely seen as the most significant due to their abundance. Broadly speaking, there are four conversion pathways that a biorefinery would employ to produce platform molecules from biomass:

(1) **Extraction**: generally mild and often assisted *via* solvent and/or mechanical processing, resulting in isolation of compounds naturally present in biomass (*e.g.* monoterpenes **38**).
(2) **Biocatalytic conversion**: generally mild conditions involving the use of enzymes, bacteria, or yeast (*e.g.* glucose to ethanol **12**).
(3) **Chemocatalytic conversion**: may involve more forcing conditions than (1) or (2) by the application of elevated temperatures and/or pressures as well as the use of homogeneous or heterogeneous catalysts, acids, bases, water, oxygen, hydrogen, or other chemicals (*e.g.* reduction of glucose to sorbitol **54**)
(4) **Thermal (or thermochemical) conversions**: extreme conditions involving multiple bond cleavages by the application of temperatures >200 °C, leading to bio-oil, a chemically mobile mixture which may contain up to hundreds of compounds, or bio-gas (mainly H_2, CO, CO_2, H_2O, CH_4 and other small hydrocarbons). Thermochemical refers to the use both of high temperatures and chemical agents such as acid catalysts which can lead to better selectivity (*e.g.* acid catalysed pyrolysis of cellulose leading to levoglucosenone **33**)

Figure 15.6 demonstrates how for the monosaccharides glucose and fructose it is possible to produce widely differing structures depending upon whether biological, chemical, or thermal conversions are applied. Many of the acids and diacids are accessed by fermentation, though some involve chemocatalytic methods. All three conversion approaches can produce compounds where some chirality from the monosaccharide is maintained. The key point here is that even from the same component of biomass a variety of molecular structures and functional groups are accessible because of the extensive conversion toolkit available in the biorefinery.

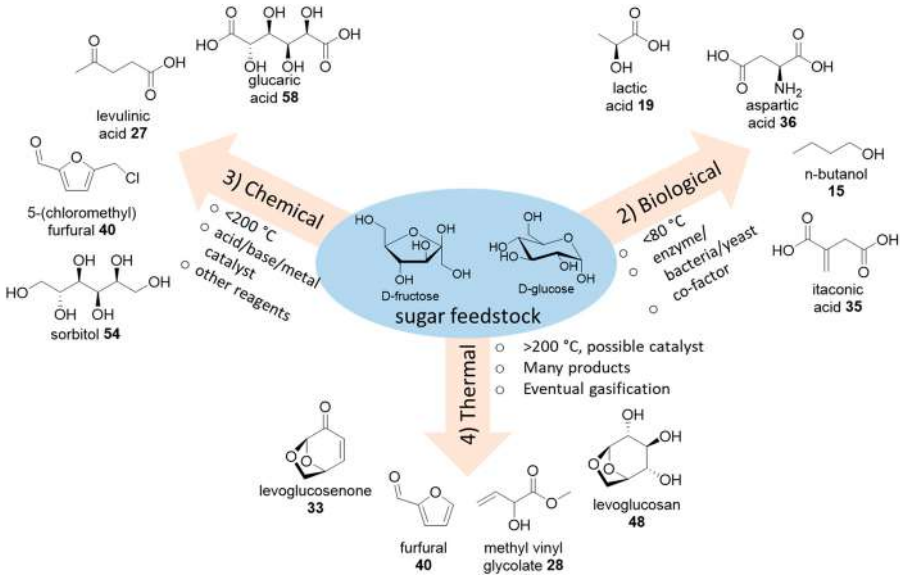

Figure 15.6 Influence of different conversion technologies (biological, chemical and thermal) on the molecular structure of platform molecules derived from common monosaccharide feedstocks.

15.3 Heteroatom Content

Several authors have attempted to map the rich functional diversity in the platform molecules, with the aim of both comparing with petrochemicals and ultimately developing a means of ranking or selecting the most promising biobased building blocks. Van Krevelen diagrams, originally developed as a means of mapping the composition of kerogen and petroleum, are a logical starting point for this comparison, being a plot of the atomic ratios of H:C *versus* O:C.[13] The use of van Krevelen diagrams for assessing biomass components has already been demonstrated and shows some merit when plotting biomass against fossil resources.[14,15] Unfortunately, conventional van Krevelen plots have shortcomings when used for platform molecules, the most significant being that they consider only oxygen and ignore other heteroatoms, and that platform molecules are generally of a higher molecular mass than the base chemicals. Rivas-Ubach *et al.* refined the van Krevelen plot for classification of organic matter in environmental studies by considering other heteroatoms such as N and P in biological samples.[16] However, their classification was still based on atomic ratios (O:C, H:C, N:C, P:C and N:P) and therefore omitted the influence of different functional groups. Dusselier *et al.* noted these shortcomings and developed an alternative approach based on functionality scoring.[17] Lie *et al.* also sought to refine van Krevelen diagrams for platform molecules and subsequently established *BioLogicTool* plots, which map percent heteroatoms by mass

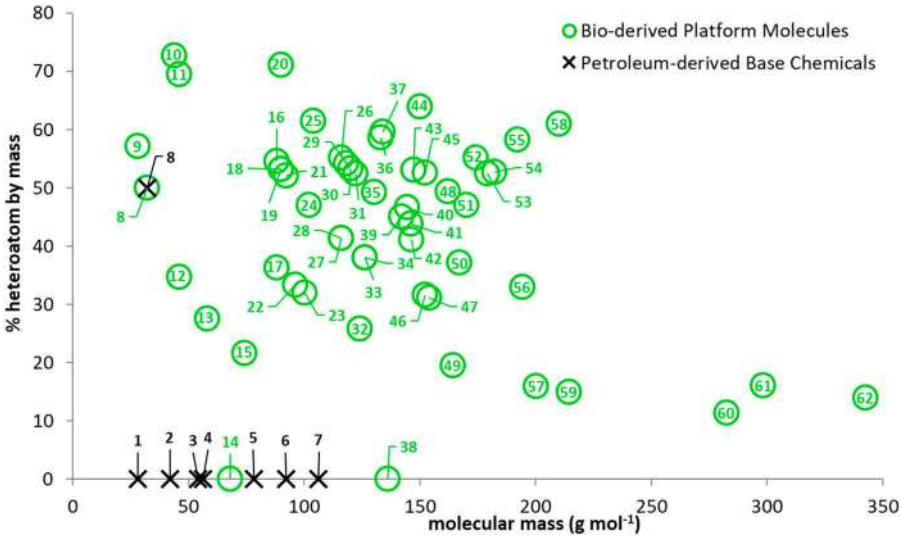

Figure 15.7 BioLogicTool plot (% heteroatom by mass *vs.* molar mass *M*) of the base chemicals (**1-8**) and our selected list of platform molecules (**8-62**). Numbers match those for the structures in Figures 15.1 and 15.2. Figure modified from the original BioLogicTool article of Lie *et al.*[18]

(*y*-axis) against compound molar mass (*x*-axis).[18] The original *BioLogicTool* study capped molecular mass at 220 g mol^{-1}, but for plotting our list of platform molecules here (Figure 15.7) we have extended the range to 350 g mol^{-1} to allow for compounds **60-62** to also be considered. The value in using percent heteroatom by mass over O : C is apparent as six molecules in our list contain heteroatoms other than oxygen (aspartic acid **36**, lysine **42**, glutamic acid **43**, 3-acetamido-5-acetylfuran **50**, glucosamine **53** and 5-(chloromethyl)furfural **40**). Compounds **36**, **42** and **43** were selected as example amino acids but many more are abundant in biomass and all contain at least one non-O heteroatom. It is possible that other heteroatom-containing platform molecules may become prevalent in the future, including compounds containing S (*e.g.* cysteine and methionine), P (*e.g.* phospholipids), or other halogens. Figure 15.7 clearly highlights the significant difference between base chemicals **1-8** and the platform molecules **8-62**; the former are confined mainly to the bottom left corner to indicate no heteroatom content and low molecular mass. The platform molecules described here however occupy a much wider space, ranging from high heteroatom content combined with low mass, for example CO_2 **10**, formic acid **11**, and oxalic acid **20**, through to some examples of low heteroatom with high mass, such as the fatty acids lauric acid **57**, oleic acid **60** and ricinoleic acid **61**. Other molecules of notably high heteroatom content include **25**, **36**, **37**, **44**, **55** and **58**, all of which are diacids where most bear additional amino or hydroxyl groups. The broad distribution of platform molecules across the plot in Figure 15.7 further reinforces their potential value to

synthetic chemists, this great chemical diversity being a consequence of the variety of structural motifs and functional groups present in feedstocks.

15.4 Functional Groups/Level of Functionality

Figures 15.2 and 15.7 showcase the potential of this set of platform molecules in terms of their diverse chemical functionality. It was noted by Dusselier that not all functional groups in platform molecules are equal; some present greater utility to the synthetic chemist than others.[17] Key observations made by Dusselier were that the use of simple van Krevelen diagrams fails to distinguish carbohydrates from one another, and that formaldehyde occupies the same location, thus overlooking the greater reactivity of this aldehyde relative to the acetals of sugars. Dusselier proposed instead the use of a new parameter, *F*, to score the *molecular functionality* of platform molecules. Each functional group is assigned a contribution value towards a molecule's overall *F*, with some bond types or groups scoring more highly than others. C–C and C–H σ-bonds contribute nothing, while σ-bonds to heteroatoms score +1. Pi-bonds add +1, and the effects are cumulative, for example a carboxylic acid scores +3 for the 2 × C–O σ-bonds and 1 × C–O π-bond. We have chosen here to modify and extend the scoring further, with details of our modifications to Dusselier's approach described in Table 15.1.

Table 15.1 Modified "Contribution to Molecular Functionality *F*" originally used by Dusselier *et al.* New or modified values from the original concept shown in bold.

Type of functional group/bond	Contribution to molecular functionality *F*
–C–X(H_n) (*e.g.* alchohols, thiols, primary amines, chloromethyl in CMF **40**)	+1
–C=X (*e.g.* aldehydes, ketones)	+2
–C–X–C (*e.g.* ethers, secondary amines)	+2
–CO_2H (carboxylic acids)	+3
–C=C– (alkenes)	+1
–C=C–C=C– (dienes)	**+3** (acknowledges extra use in [4+2] cycloadditions)
Furans	**+5** (2 × C=C, +1 for diene as above, 2 × C–O)
Benzene ring	**+4** (3 × C=C and additional +1 for aromatic chemistry)
1,3-dicarbonyl (*e.g.* malonic acid)	**+7** (2 × acids gives +6, +1 for additional enolate chemistry)
–C=C–C(=O or O_2H)	**+4/+5** (+3 for acid or +2 for aldehyde/ketone, +1 for C=C and additional +1 for conjugate addition reactivity)
Cyclic hydrocarbon	**+1** (acknowledges structure diversity offered)
Chirality (applies to whole molecule)	**+1** (acknowledges potential value in exploiting chirality already present, only scored once per molecule)
Hydrocarbon chain ≥C6	**+1** (acknowledges value of biobased hydrophobes)

Primarily, we chose that certain functional groups would score higher if they offered a greater number of synthetic transformations, such as for example dienes in Diels–Alder cycloadditions or double bonds α,β to a carbonyl group in conjugate addition. We also added a point for chiral centres as these could potentially negate a costly stereoselective synthesis. The ratio of *F* to the number of carbons (*C*) gives the *functionality index* (*F*:*C*), which describes the density of functionality in the molecule. Dusselier plotted *F*:*C* against several different property axes, but for the sake of comparing our list of platform molecules the number of carbons (*C*) has been selected as the *x*-axis (Figure 15.8). At first glance, the application of *F*:*C* reinforces the point that platform molecules have a clear benefit in available chemical functionality over base chemicals. This level of chemical functionality in platform molecules makes them comparable to commodity and specialty chemicals of the present chemical industry, where the diversity of functional groups enhances their utility for synthesis. Closer inspection of Figure 15.8 shows that the presence of carboxylic acid groups, especially in the di- and tri- acids (highlighted in **blue**), results in higher *F*:*C* values. The prevalence of di- and tri-acids leads to platform molecules having potential as monomers for polyester and polyamide synthesis, a point reinforced by several reviews on this topic.[19–22] Arguably, an aldehyde group offers greater utility to synthetic chemists than a carboxylic acid, the former being easily manipulated chemically (redox, reaction with nucleophiles, *etc.*). The aldehyde-containing platform molecules (highlighted in **red**, compounds **22**, **30**, **34**, **40** and **46**) are

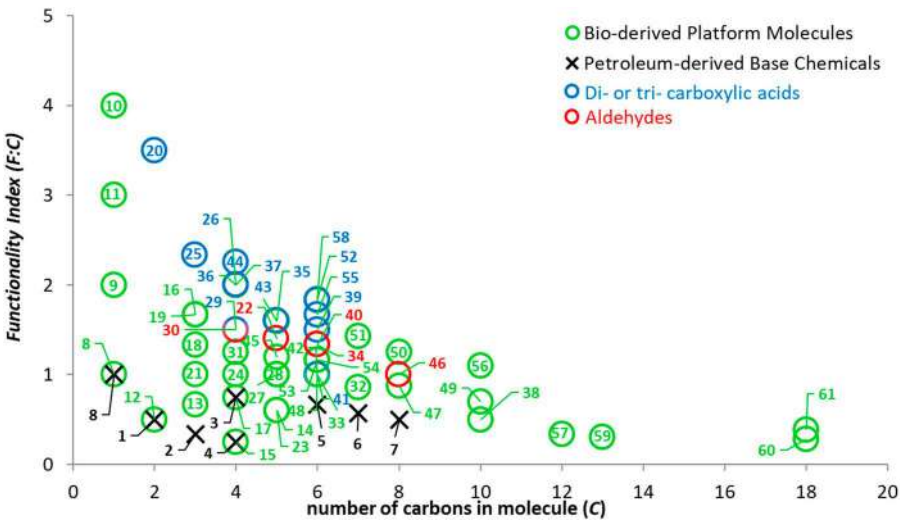

Figure 15.8 Comparing platform molecules and base chemicals using Functionality Index (*F*:*C*) *versus* number of carbons (*C*). Di- and tri-carboxylic acids in **blue**, and aldehyde containing compounds in **red**. Number labels match those for the structures in Figures 15.1 and 15.2. Plot prepared by adapting the methodology of Dusselier *et al.*[17]

"less functional" than carboxylic acids and are therefore positioned around the center of the plot, but as noted above, their synthetic potential should not be underestimated.

15.5 The Challenge of Hydrophobic Platform Molecules

Although the chemist needs functional groups to make synthetic use of a molecule, there is often also a need for hydrophobicity, and this characteristic is generally linked to low or zero heteroatom content. Hydrophobes are necessary in the production of surfactants, coatings, adhesives, and some pharmaceuticals, to name but a few examples. The petrochemical industry, starting from a feedstock built around hydrophobic base chemicals, can easily access higher linear, branched, and cyclic alkanes. Indeed, the simplest plastics, polyethene and polypropene, derive useful material properties from their hydrophobicity. Few platform molecules, on the other hand, are hydrophobic (Figure 15.9), with the monoterpenes (**38**) and fatty acids (**57**, **59-61**) being the only exceptions. Other hydrophobic compounds are potentially available from natural sources. For example, many non-polar compounds

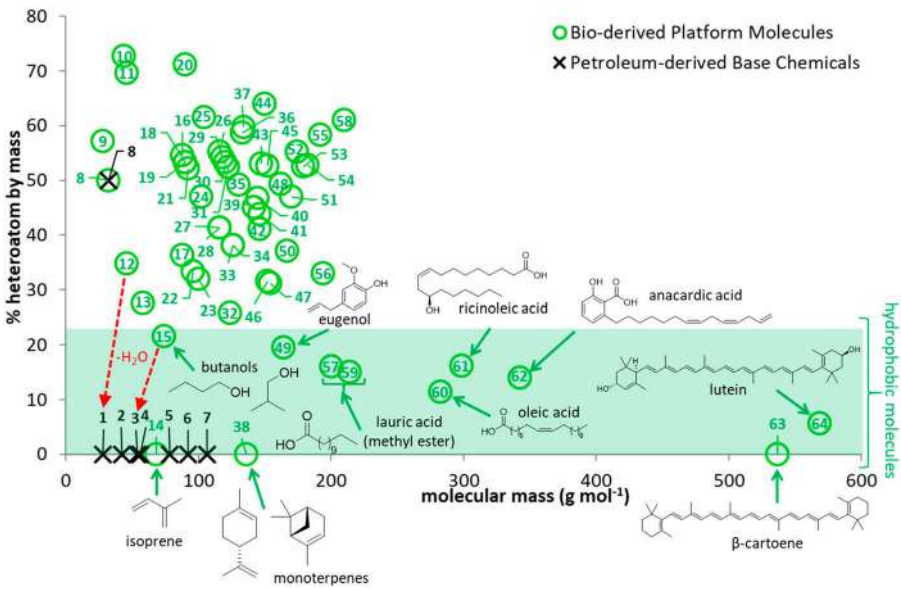

Figure 15.9 Modified BioLogicTool plot from Figure 15.7, extending the mass range and highlighting the small number of hydrophobic platform molecules. Numbers match those for the structures in Figures 15.1 and 15.2, β-carotene (**63**) and lutein (**64**) given as examples of hydrophobic carotenoids. Figure modified from the supplementary information of the original BioLogicTool article of Lie *et al.*[18]

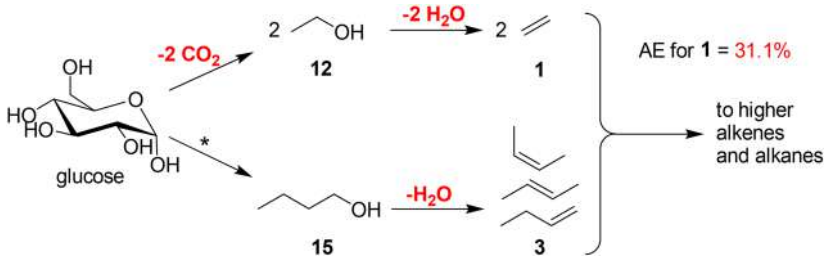

Figure 15.10 Conversion of glucose-derived platform molecules ethanol (**12**) and butanol isomers (**15**) to biobased alkenes ethene (**1**) and butene (**3**), highlighting potential issues with atom economy. **via* ABE fermentation and therefore complete mass balance and AE calculation is not possible.

occur as plant extractives, such as anacardic acid (**62**) from cashew nutshell liquid, carotenoids (**63** and **64**, Figure 15.9), and waxes, but these are only available in small quantities. Indeed, the future sustainable biobased chemical industry will need to a find a means of producing hydrophobic compounds on an industrial scale, and this cannot easily be achieved from monoterpenes and fatty acids alone as these are only available in biomass in comparatively small quantities (relative to the whole of their parent plants). One possibility is to use dehydration of biobased alcohols such as ethanol **12** and the butanols **15**, to create drop-in replacements for the ethene (**1**) and butene (**3**) base chemicals. From **1** and **3**, higher alkanes and alkenes can be accessed through well-established refinery processes currently used for petrochemicals. However, this pathway comes at an expense to atom economy (Figure 15.10), with the pathways from monosaccharides through to eventual alkenes requiring complete loss of all oxygen and some carbon (*via* CO_2). This pathway also suffers from the need to use fermentable sugars that could potentially divert food production towards chemicals, a long held concern of a large-scale biobased economy.[23] In recent years an emphasis has been placed on the use of lignocellulose to produce hydrocarbon fuels,[24] and this emerging field of research could ultimately allow for large volumes of biobased hydrophobes to be produced at scale without competing with food production. Like all carbohydrate conversions to molecules with low or no functionality, these pathways suffer from a low overall AE, which must simply be the sacrifice for obtaining hydrocarbons from these feedstocks. Ultimately, the large-scale production of hydrophobes from non-food feedstock is a key challenge for researchers to address in the coming years.

15.6 Time for a New Top Twelve

As mentioned above, in 2004, the U.S. National Renewable Energy Laboratory (NREL) undertook a detailed screening of most of the recognized platform molecules at the time.[7] Starting with a list of more than 300 candidates,

a shortlist of 30 was produced following an iterative review process based on petrochemical building block models, chemical and physical data, market data, and the prior industry experience of the teams at PNNL and NREL. From these 30, a top tier of 12 molecules was selected, which consisted of the C_4 diacids (succinic, fumaric acid, malic), arabinitol/xylitol, aspartic acid, 2,5-furandicarboxylic acid, glucaric acid, glutamic acid, glycerol, 3-hydroxybutyrolactone, 3-hydroxypropanoic acid, itaconic acid, levulinic acid, and sorbitol.

The revised 2010 list of Bozell and Petersen generated new rankings based on a set of criteria including literature attention, potential to serve as "drop-in" petrochemical substitutes, flexibility for derivatization, overall synthetic utility, potential for production in industrially relevant volumes, current developmental status (bench, pilot, demonstration scale), and the current market status of the molecule.[9] This list consisted of ethanol, furfural, 5-(hydroxymethyl)furfural, **2,5-furandicarboxylic acid**, **glycerol**, isoprene, lactic acid, **succinic acid**, **3-hydroxypropanoic acid**, **levulinic acid**, **sorbitol**, and **xylitol**.

The compounds in bold represent overlaps with the original NREL list. As mentioned above, while some of these platforms rose to prominence in the literature, others received less attention. In any case, interest in this topic remains strong, as witnessed by the number of citations that the revised Bozell & Petersen list has received (currently ~2300).[25] Now, a decade later, we propose further revisions based not on an extensive set of analytical parameters which, in any case, have not always correlated well to commercial success in ventures involving these chemicals, but in terms of "grand challenges," where successful translation to the mass commodity market could be considered a major win for sustainable chemistry and process engineering in general. A brief commentary on the candidates chosen for inclusion on this list is given below.

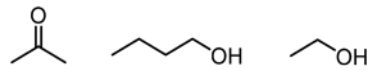

***Candidate 1**: acetone–butanol–ethanol (ABE)*. Although fermentation products will always be disadvantaged relative to chemocatalytically produced platforms in terms of space-time yields, the sheer utility of these three products of *Clostridium acetobutylicum*/*Clostridium beijerinckii* fermentation is simply unbeatable in terms of industrial utility. ABE fermentation has been described as one of the largest scale biotechnological operations ever undertaken industrially, second only to bioethanol.[26] Various aspects of the process continue to be advanced in order to manage issues associated with low productivity, product inhibition, and downstream isolation.[27] Genetic and metabolic pathway engineering strategies promise to deliver continued performance enhancements that will promote widespread industrial adoption.

It can well be said that if one had essentially unlimited access to the alcohol products of this fermentation (isopropanol from acetone, ethanol, and *n*-butanol), the mainstream petrochemical repertory would be covered, since

dehydration gives propylene, ethylene, and the butylenes, respectively. The range of industrial products that flow from these three streams, *via* refinery technologies, is extensive. These alcohols are also straight-up replacements for gasoline in spark-ignition engines,[28] and can also be used to power fuel cells. Acetone itself is a low-toxicity solvent, and both a nucleophile and electrophile for building up carbon chains to make fuels or renewable monomers *via* condensation reactions. It is also a precursor of methyl isobutyl ketone, another key industrial solvent. ABE thus embodies, in itself, one concept of the idealized biorefinery. The feed for ABE is glucose, which is Candidate 4 below.

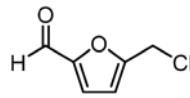

***Candidate 2**: 5-(chloromethyl)furfural*. For decades, the premier platform representing the cellulosic fraction of biomass was 5-(hydroxymethyl)furfural (HMF), to the extent that it needs virtually no introduction.[29] However, as described above, one test of the value of a platform molecule is industrial translation, and to date, no commercial technology has been developed based on the direct conversion of biomass to HMF. Indeed, HMF pilot processes have used fructose as the feed, both a foodstuff itself and sourced from grains. On the other hand, 5-(chloromethyl)furfural (CMF) can be produced directly from raw biomass in high yield.[30,31] It is easier to isolate than HMF, more stable than HMF and, with a halogen replacing the hydroxy group, more synthetically versatile than HMF. Origin Materials, part of an alliance of companies commercializing CMF for the production of biobased poly(ethylene terephthalate) (PET), recently became the first publicly traded pure-play carbon negative materials company.[32]

The derivative chemistry of CMF has been covered in reviews,[33,34] but suffice it here to say that the synthetic versatility offered by the combination of an aldehyde, a chloromethyl group, and the furan ring offers nearly limitless potential for derivative production. Indeed, a wide range of biofuels, renewable monomers, industrial products like agrochemicals and dyes, as well as value-added products have been described. Importantly, CMF is also an excellent source of levulinic acid (Candidate 7) by hydrolysis of the furan ring.[35]

To complete the picture, when raw biomass is fed into the CMF process, a lignin-humic composite exits the reactor as a fine black solid. This textured, high-carbon product has been analyzed using a range of techniques. A key aspect of interest of this material, which is referred to as a structured hydrothermal carbon (SHC), is that it possesses a remarkable degree of porosity straight out of the reactor.[36] Pyrolysis increases porosity even further. This material also has a range of potential commercial applications, including catalyst supports, absorbent solids and, most recently, for the production of asphalt.[37]

***Candidate 3**: CO_2*. The potential of carbon dioxide as a source of renewable carbon for the biobased economy is virtually unlimited. It represents 0.041% of earth's atmosphere, which is estimated to amount to a total of about 3000 gigatonnes which, for all practical purposes, is a limitless resource, particularly considering the fact that ~40 gigatons more are currently being released into the atmosphere every year. Developing this platform serves the dual purpose of supporting the circular economy while at the same time remediating the greenhouse gas effect in the atmosphere, which is of course a global imperative. For this reason, no portfolio involving the exploitation of renewable carbon should be without it.

Several technologies have been engineered for the capture of CO_2 directly from the atmosphere or from industrial effluent, where concentrations are higher. These involve scrubbing to form complexes with CO_2 that can be isolated and from which the CO_2 can be liberated in a concentrated form. New developments seem to appear weekly, and solution-based methods, solid sorbents, and membrane technologies have all been advanced.[38] Solution approaches typically involve the reaction of CO_2 with hydroxide or amines to form carbonate or carbamates in a process that can be thermally reversed.[39] Sorbent matrices include metal–organic frameworks covalent organic frameworks, zeolites, silica, activated carbon, and polymers.[40]

For CO_2 valorization, the direct targets are reduction to carbon monoxide, methanol, and methane or other hydrocarbons by various forms of electron transfer,[41] with an emphasis on photocatalysis on semiconductor surfaces,[42] and even hydrogenation using a metal catalyst.[43] It is interesting to note that, with reduction of CO_2 to methanol, the system can be linked with the classic concept of the methanol economy famously advanced by George Olah.[44]

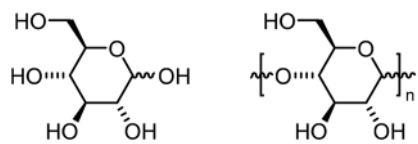

***Candidate 4**: glucose, including cellulose pulps, microcellulose and nanocelluloses*. An enduring challenge that has engaged the chemical community in various ways over the years is the conversion of plant matter efficiently and economically into glucose, clean cellulose pulps, and micro/nanostructured cellulose. The saccharification of lignocellulose has been practiced for over a century.[45] Wood, the principal feed in most studies, has been deconstructed under a broad variety of conditions, including acid and base-catalyzed hydrolysis,[46] solid acid catalysis,[47] chemical processing,[48] mechanical defibrillation,[49] and enzymatic breakdown.[50] Although some of these technologies have already advanced to the point of industrialization, since they feed into Candidates 1, 2, 6, 7, 8, 10, and 12, either through glucose or cellulose, the better they are able to compete with mass production of glucose from starch sources, the closer the concept of the global biorefinery[51] comes to realization.

Similarly, the separation of cellulose pulp from lignin and hemicellulose is of strategic importance to biorefinery practice, particularly where there is the intention to fully valorize these streams. Multiple volumes have been written on the subject of wood pulping,[52] and yet, like saccharification, there remains much room for improvement, and significant advances have been made for example in the separation of cellulose from biomass by simple dissolution and regeneration by adding antisolvent.[53] The pulse of the biorefinery movement is sustained by continued advancement in these technologies.

Finally, a comparative newcomer to the biorefinery product field is nanocellulose. Cellulose nanocrystals and nanofibrils are a sustainable platform for a variety of technical applications, including reinforcing agents and rheology modifiers for biodegradable polymer nanocomposites, scaffolds for enzyme immobilization and tissue regeneration, excipients for drug delivery, biocompatible hydrogels, and environmental remediation.[54] Their abundance, unique morphology, low toxicity, high modulus, low density, chirality, ability to self-assemble, and versatility for chemical manipulation suggests that the current applications are just the beginning of a technological revolution based around these platforms,[55] and to the extent that advanced materials add value to biomass, they merit inclusion in any priority list for biorefinery development.

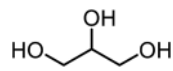

***Candidate 5**: glycerol*. This platform molecule is directly linked with Candidate 11 (fatty acids), since both derive from lipids. Although the volumetric production of triglycerides from biomass generally falls far behind that of carbohydrates and lignin, continuing efforts to boost oil production in microalgae and the development of oilseed crops that can be grown on marginal land means that both candidates have a place in this list. The sheer bulk of research in the potential applications of this platform is extraordinary,[56] initially stimulated by the large volumes of glycerol generated by transesterification of fatty acids for biodiesel production. Glycerol can also be produced by fermentation,[57] and can itself be a substrate for fermentation for the production of ethanol, butanol, and succinic acid,[58] all of which also appear in this list.

Although a deep dive into the derivative chemistry of glycerol is beyond the remit of this commentary, a search of Chemical Abstracts finds nearly 50 recent reviews of glycerol with ≥100 citations each, while the leading reviews have >1000 citations.[59,60] Topping the list of products are acrolein, propanediols, ethylene glycol, and useful derivatives of glycerol itself (acetals, carbonate, ethers, polymers, *etc.*). Also of strong interest is the reforming of glycerol to hydrogen or syngas.[61]

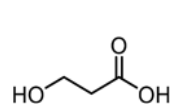

***Candidate 6**: 3-hydroxypropanoic acid*. 3-Hydroxypropanoic acid (HPA), like succinic acid (Candidate 12), is a molecule of high promise that has thus far struggled to enter the biobased product market due to its expensive derivation using biotechnological methods. It has two main application manifolds: (1) as a monomer for homopolymer or co-polymer production,[62,63] and (2) dehydration to bioacrylic acid,[64] the market for which is of course massive. Recently, more efficient chemocatalytic approaches to HPA have been described starting from levulinic acid, where oxidation with hydrogen peroxide gives HPA in high yields,[65,66] which should stimulate further commercial interest in this renewable platform and its derivatives.

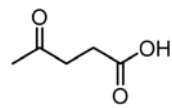

***Candidate 7**: levulinic acid*. Levulinic acid (LA) is formally an HMF decomposition product that is much more stable than HMF itself. A major advantage of LA over HMF is that it can be produced in 70–80% yield directly from raw biomass using the commercial Biofine method, or as noted above, by hydrolysis of CMF.[36] The Biofine process involves two-stage thermolysis in the presence of an acid catalyst and co-produces formic acid, furfural (from the hemicellulose present), and a carbonaceous char.[67] Simply stated, with its ketone and carboxylic acid functional groups, LA is essentially on equal par with HMF and CMF (Candidate 2) in terms of synthetic versatility and hence derivative reach.[68] Thus LA and its cyclodehydration product angelica lactone have variously been used to make a wide range of fuels, monomers, industrial chemicals, and value-added products.[69–71] One of its derivatives, γ-valerolactone, is considered a platform molecule in its own right.[72,73]

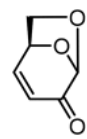

***Candidate 8**: levoglucosenone*. Levoglucosenone (LGO) is a multifaceted platform molecule that rivals the furfurals in its synthetic versatility, having an α,β-unsaturated ketone functional group and a glycosidic center for derivatization. It is generated by the pyrolysis of cellulose or even raw biomass, which translates to a high production rate and operational simplicity. In a typical run, cellulose and a catalytic quantity of acid are heated to *ca.* 300 °C to give an oil from which the product can be isolated by distillation. The bottleneck so far has been to produce LGO in high yields. Although a number of innovations have been reported, including solvent assisted pyrolysis,[74] isolated yields on preparative scales have typically been <20%.

LGO is also a chiral building block, which lends it a broad scope of applications in asymmetric synthesis.[75] While many creative studies involving LGO derivatization have been reported,[76] to date, its main practical application relevant to sustainable chemistry involves hydrogenation of the double bond to give dihydrolevoglucosenone or cyrene; a nontoxic, polar aprotic solvent with properties comparable to DMF and sulfolane, although somewhat more limited in scope due to its reactivity.[77]

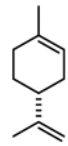

Candidate 9*: limonene and other monoterpenes*. Like LGO, these chiral molecules have unsaturations and/or oxygen functionality that can be exploited for a wide range of synthetic purposes. The highest volume monoterpene is limonene, a by-product of the citrus industry. Both *R*-(shown) and *S*-limonene are available, depending on the source. Total citrus production worldwide is about 100 million tonnes,[78] which means the potential supply of limonene is of practical interest. Given that citrus waste also contains sugars, pectin, cellulose, and hemicellulose, the concept of the "limonene biorefinery" has been advanced.[79–81] Beyond this, biosynthetic approaches to the production of monoterpenes using metabolically engineered organisms,[82] or in cell-free processes,[83] are gaining momentum. Finally, wood terpenes, which make up between 0.2 and 0.8% of softwood on a dry weight basis,[84] may ultimately also contribute to the overall supply.

In terms of present applications, similar to cyrene, limonene can serve as an effective, nontoxic solvent. Limonene oxide has also been advanced as a renewable monomer.[85] Dehydrogenation to *p*-cymene, a major petrochemical, is yet another option. However, perhaps the most intriguing recent application of limonene and terpenes in general has been in the production of energy dense jet fuels. Limonene and other monoterpenes such as pinene can be hydrogenated to menthane and pinane, respectively, which have volumetric net heats of combustion higher than jet A-1 and excellent low-temperature flow properties.[86]

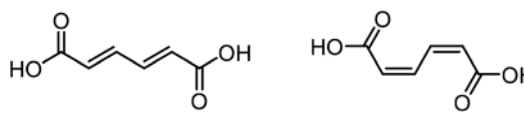

Candidate 10*: muconic acids*. In 1997, evidence of the formation of muconic acid and muconolactones was reported during the oxidative delignification and bleaching of wood.[87] This was later confirmed by an in-depth 2D NMR study.[88] The oxidative cleavage of aromatic rings associated with lignin

however didn't attract much further attention until recent work from NREL described the use of an engineered strain of the microorganism *Pseudomonas putida* to "biologically funnel" lignin directly towards *cis–cis* muconic acid.[89–91] This work is attractive from the perspective of sustainable chemistry first in that lignin is being selectively exploited, which is an accomplishment in its own right. But more significantly, *cis–cis*-muconic acid can be hydrogenated to adipic acid, or isomerized to *trans–trans*-muconic acid, esters of which undergo Diels–Alder cycloaddition with ethylene to give tetrahydrophthalate esters, the catalytic dehydrogenation of which gives terephthalates. Thus, two giants of the chemical industry can, in principle, be derived from this otherwise difficult to exploit biomass stream. That said, significant technical advancements will be needed to make lignin-to-muconate pathways commercially attractive.[92]

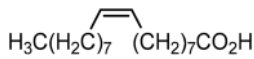

Candidate 11*: oleic acid and fatty acids in general*. Broadly speaking, the lipid fraction of biomass has had less appeal than carbohydrates and lignin due to its generally much lower yield per unit mass of whole plant material, but also because its use for chemicals and fuels can, like sugars, run afoul of the food-fuel debate. Indeed, edible oils can be sold into the consumer market generally at a much higher premium than would be possible if converted into chemicals. For this reason, early interest centred largely on spent cooking oil, the available volumes of which are however not sufficient to drive a renewable chemical economy. A popular answer to this issue has been the development of strains of microalgae that overproduce and even excrete oil. Although the concept has been around since the 1990s,[93] it has struggled to gain industrial traction. There has, on the other hand, been a growing interest in tall oil, which contains a mixture of lipids that makes up *ca.* 3–5% of the dry weight of softwoods.[94,95] Assuming that the future global biorefinery makes strong use of arboriculture, even this minor fraction can be advantageously developed.

The principal use of lipids to date has been in the production of biodiesel, about which hundreds of reviews have been written in the last decade, and a wide plethora of transesterification methods to generate fatty acid methyl esters have been described.[96] There remains a consistent market for biodiesel, which however to date has been dependent on government subsidies and tax credits to remain competitive with petroleum diesel.

While fuels can take advantage of the chemically heterogeneous nature of the fatty acid composition of biomass, the production of polymers and chemicals generally favours single components. On this count, oleic acid, the most abundant of the monosaturated fatty acids, bears singling out. Although polymers and chemicals based around this platform have been reported,[97,98] a recent paper that appeared in *Nature* showed that the C_{18} diacid and diol derived from oleate metathesis could be used to prepare polyesters and polycarbonates with properties closely analogous to those of

high-density polyethylene, but with a much more straightforward recycling path by simple chemical solvolysis, unlocking a potential multibillion dollar global market.

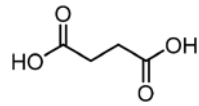

***Candidate 12**: succinic acid*. Like HPA (Candidate 6), succinic acid (SA) is a monomer of strong commercial interest which has nevertheless thus far failed to make it to the forefront due to unsuccessful attempts to produce it using biotechnology in a way that could be competitive with petrochemical routes. This said, chemocatalytic routes have been described starting from levulinic acid, furfural, or glucose similar to those used to access HPA.[99–101] Assuming one of these advances to commercial translation, biosuccinic acid-based materials could become part of the plastics mainstream. Indeed, a plethora of biodegradable co-polymers have been described for SA over the years. Of particular interest has been poly(butylenesuccinate), which has properties comparable both to polyethylene and polypropylene.[102]

Although the above twelve candidates are considered to represent exceptional opportunities for development in the context of the global biorefinery, many of the other platform molecules described in this chapter also hold significant promise in that regard. As new research emerges and continues to favour industrially practical routes to biobased chemicals, a new generation of technologies and products that can compete head-to-head in the petrochemical market will emerge. As petroleum reserves diminish or, in the nearer term, fossil fuel exploitation is limited either by market forces or government intervention, we will see these various new biobased products introduced into the commodity and ultimately consumer marketplace.

References

1. G. Egloff, *Chem. Eng. News*, 1947, **25**, 3634–3637.
2. M. Kircher, *Biofuels, Bioprod. Biorefin.*, 2012, **6**, 369–375.
3. U. Bardi, *Energy Res. Soc. Sci.*, 2019, **48**, 257–261.
4. M. Jefferson, *Energy Res. Soc. Sci.*, 2020, **68**, 101669.
5. S. H. Shinde, A. Hengne and C. V. Rode, in *Recent Advances in Development of Platform Chemicals*, ed. S. Saravanamurugan, A. Pandey, H. Li and A. Riisager, Chapter 1 – Lignocellulose-derived platform molecules: An introduction, Elsevier B.V., Amsterdam, 1st edn, 2020, pp. 1–31.
6. T. J. Farmer and M. Mascal, in *Introduction to Chemicals from Biomass*, ed. J. Clark and F. Deswarte, Wiley, Chichester, 2nd edn, 2015, Ch. 4, pp. 89–156.
7. T. Werpy and G. Petersen, *Top Value Added Chemicals from Biomass. Volume I – Results of Screening for Potential Candidates from Sugars and Synthesis Gas*, United States Department of Energy, 2004, www.osti.gov/biblio/15008859-top-value-added-chemicals-from-biomass-volume-results-screening-potential-candidates-from-sugars-synthesis-gas.

8. J. E. Holladay, J. J. Bozell, J. F. White and D. Johnson, *Top Value Added Chemicals from Biomass – Volume II, Results of Screening for Potential Candidates from Biorefinery Lignin*, United States Department of Energy, 2007, www.pnnl.gov/main/publications/external/technical_reports/PNNL-16983.pdf.
9. J. J. Bozell and G. R. Petersen, *Green Chem.*, 2010, **12**, 539–554.
10. https://greenchemicalsblog.com/author/greenchemicalsblog/.
11. M. J. Hülsey, H. Yang and N. Yan, *ACS Sustainable Chem. Eng.*, 2018, **6**, 5694–5707.
12. F. Fenouillot, A. Rousseau, G. Colomines, R. Saint-Loup and J.-P. Pascault, *Prog. Polym. Sci.*, 2010, **35**, 578–622.
13. D. W. van Krevelen, *Fuel*, 1950, **29**, 269–284.
14. N. Hertkorn, M. Frommberger, M. Witt, B. P. Koch, P. Schmitt-Kopplin and E. M. Perdue, *Anal. Chem.*, 2008, **80**, 8908–8919.
15. S. Kim, R. W. Kramer and P. G. Hatcher, *Anal. Chem.*, 2003, **75**, 5336–5344.
16. A. Rivas-Ubach, Y. Liu, T. S. Bianchi, N. Tolić, C. Jansson and L. Paša-Tolić, *Anal. Chem.*, 2018, **90**, 6152–6160.
17. M. Dusselier, M. Mascal and B. F. Sels, in *Selective Catalysis for Renewable Feedstocks and Chemicals*, ed. K. M. Nicholas, Top Chemical Opportunities from Carbohydrate Biomass: A Chemist's View of the Biorefinery, Springer, New York, 2014, pp. 1–40.
18. Y. Lie, P. Ortiz, R. Vendamme, K. Vanbroekhoven and T. J. Farmer, *Ind. Eng. Chem. Res.*, 2019, **58**, 15945–15957.
19. F. H. Isikgor and C. R. Becer, *Polym. Chem.*, 2015, **6**, 4497–4559.
20. T. J. Farmer, J. W. Comerford, A. Pellis and T. Robert, *Polym. Int.*, 2018, **67**, 775–789.
21. K. H. Zia, A. Noreen, M. Zuber, S. Tabasum and M. Mujahid, *Int. J. Biol. Macromol.*, 2016, **82**, 1028–1040.
22. R. P. Babu, K. O'Connor and R. Seeram, *Prog. Biomater.*, 2013, **2**, 8.
23. S. Prasad and A. P. Ingle, *Sustainable Bioenergy Advances and Impacts*, 2019, ch. 12, pp. 327–346.
24. M. Mascal and S. Dutta, *Fuel Process. Technol.*, 2020, **197**, 106192.
25. Ref. 9 searched on the Chemical Abstracts database using SciFinder April 2021.
26. J. Zhang, S. Wang and Y. Wang, *Adv. Bioenergy*, 2016, **1**, 1–68.
27. H. Amiri, *Biofuel Res. J.*, 2020, **7**, 1256–1266.
28. Y. Li, L. Meng, K. Nithyanandan, T. H. Lee, Y. Lin, C. F. Lee and S. Liao, *Fuel*, 2016, **184**, 864–872.
29. L. Hu, A. He, X. Liu, J. Xia, J. Xu, S. Zhou and J. Xu, *ACS Sustainable Chem. Eng.*, 2018, **6**, 15915–15935.
30. M. Mascal and E. B. Nikitin, *Angew. Chem., Int. Ed.*, 2008, **47**, 7924–7926.
31. M. Mascal and E. B. Nikitin, *ChemSusChem*, 2009, **2**, 859–861.
32. https://www.originmaterials.com/investors, accessed April 2021.
33. M. Mascal, *ACS Sustainable Chem. Eng.*, 2019, **7**, 5588–5601.
34. M. Mascal, *ChemSusChem*, 2015, **8**, 3391–3395.
35. M. Mascal and E. B. Nikitin, *Green Chem.*, 2010, **12**, 370–373.

36. V. L. Budarin, J. H. Clark, J. Henschen, T. J. Farmer, D. J. Macquarrie, M. Mascal, G. K. Nagaraja and T. H. M. Petchey, *ChemSusChem*, 2015, **8**, 4172–4179.
37. https://www.originmaterials.com/press-releases/press-release-1-1-1.
38. E. S. Sanz-Perez, C. R. Murdock, S. A. Didas and C. W. Jones, *Chem. Rev.*, 2016, **116**, 11840–11876.
39. I. M. Bernhardsen and H. K. Knuutila, *Int. J. Greenhouse Gas Control*, 2017, **61**, 27–48.
40. J. Wang, L. Huang, R. Yang, Z. Zhang, J. Wu, Y. Gao, Q. Wang, D. O'Hare and Z. Zhong, *Energy Environ. Sci.*, 2014, **7**, 3478–3518.
41. Q. Lu and F. Jiao, *Nano Energy*, 2016, **29**, 439–456.
42. B. Kumar, M. Llorente, J. Froehlich, T. Dang, A. Sathrum and C. P. Kubiak, *Annu. Rev. Phys. Chem.*, 2012, **63**, 541–569.
43. M. D. Porosoff, B. Yan and J. G. Chen, *Energy Environ. Sci.*, 2016, **9**, 62–73.
44. G. A. Olah, A. Goeppert and G. K. S. Prakash, *J. Org. Chem.*, 2009, **74**, 487–498.
45. C. F. Cross and C. Doree, *Researches on Cellulose*, Longmas, Green & Co, London, 1922.
46. R. Rinaldi and F. Schueth, *ChemSusChem*, 2009, **2**, 1096–1107.
47. L. Hu, L. Lin, Z. Wu, S. Zhou and S. Liu, *Appl. Catal., B*, 2015, **174–175**, 225–243.
48. B. R. Caes, M. J. Palte and R. T. Raines, *Chem. Sci.*, 2013, **4**, 196–199.
49. Q. Zhang and F. Jerome, *ChemSusChem*, 2013, **6**, 2042–2044.
50. V. Juturu and J. C. Wu, *Renewable Sustainable Energy Rev.*, 2014, **33**, 188–203.
51. The concept of the global biorefinery is an analogy to common technologies that have worldwide diffusion. For example, various productive infrastructures, like the conversion of ores into metals, or sand into glass, trees into lumber, or crude oil into finished petrochemicals, are routinely practiced throughout the world. Likewise any country with the raw material (biomass) has the potential to adopt what will, in the future, become common, fully sustainable biorefinery technologies.
52. Pulping Chemistry and Technology, in *Pulp and Paper Chemistry and Technology*, ed. M. Ek, G. Gellerstedt and G. Henriksson, De Gruyter, 2009, vol. 2.
53. C. Olsson and G. Westman, *Direct Dissolution of Cellulose: Background, Means and Applications, Cellulose – Fundamental Aspects*, Theo van de Ven and Louis Godbout, IntechOpen, 2013.
54. T. Abitbol, A. Rivkin, Y. Cao, Y. Nevo, E. Abraham, T. Ben-Shalom, S. Lapidot and O. Shoseyov, *Curr. Opin. Biotechnol.*, 2016, **39**, 76–88.
55. A. Dufresne, *Mater. Today*, 2013, **16**, 220–227.
56. P. S. Kong, M. K. Aroua and M. A. W. D. Wan, *Renewable Sustainable Energy Rev.*, 2016, **63**, 533–555.
57. Z. Wang, J. Zhuge, H. Fang and B. A. Prior, *Biotechnol. Adv.*, 2001, **19**, 201–223.
58. J. M. Clomburg and R. Gonzalez, *Trends Biotechnol.*, 2013, **31**, 20–28.

59. C.-H. Zhou, J. N. Beltramini, Y.-X. Fan and G. Q. Lu, *Chem. Soc. Rev.*, 2008, **37**, 527–549.
60. M. Pagliaro, R. Ciriminna, H. Kimura, M. Rossi and C. Della Pina, *Angew. Chem., Int. Ed.*, 2007, **46**, 4434–4440.
61. Y. C. Lin, *Int. J. Hydrogen Energy*, 2013, **38**, 2678–2700.
62. B. Andreessen, N. Taylor and A. Steinbuechel, *Appl. Environ. Microbiol.*, 2014, **80**, 6574–6582.
63. D. B. Hazer, E. Kilicay and B. Hazer, *Mater. Sci. Eng., C*, 2012, **32**, 637–647.
64. C. Li, Q. Zhu, Z. Cui, B. Wang, Y. Fang and T. Tan, *Chem. Eng. Sci.*, 2018, **183**, 288–294.
65. L. Wu, S. Dutta and M. Mascal, *ChemSusChem*, 2015, **8**, 1167–1169.
66. D. Carnevali, M. G. Rigamonti, T. Tabanelli, G. S. Patience and F. Cavani, *Appl. Catal., A*, 2018, **563**, 98–104.
67. D. J. Hayes, S. Fitzpatrick, M. B. H. Hayes and J. R. H. Ross, *The Biofine Process–production of Levulinic Acid, Furfural, and Formic Acid from Lignocellulosic Feedstocks. Biorefineries–Industrial Processes and Products*, ed. B. Kamm, P. R. Gruber and M. Kamm, 2006, vol. 1, pp. 139–164.
68. F. D. Pileidis and M.-M. Titirici, *ChemSusChem*, 2016, **9**, 562–582.
69. M. Mascal and S. Dutta, *Top. Curr. Chem.*, 2014, **353**, 41–84.
70. J. Zhang, S. Wu, B. Li and H. Zhang, *ChemCatChem*, 2012, **4**, 1230–1237.
71. L. Yan, Q. Yao and Y. Fu, *Green Chem.*, 2017, **19**, 5527–5547.
72. S. Dutta, I. K. M. Yu, D. C. W. Tsang, Y. H. Ng, Y. S. Ok, J. Sherwood and J. H. Clark, *Chem. Eng. J.*, 2019, **372**, 992–1006.
73. U. Omoruyi, S. Page, J. Hallett and P. W. Miller, *ChemSusChem*, 2016, **9**, 2037–2047.
74. F. Cao, T. J. Schwartz, D. J. McClelland, S. H. Krishna, J. A. Dumesic and G. W. Huber, *Energy Environ. Sci.*, 2015, **8**, 1808–1815.
75. M. B. Comba, Y. Tsai, A. M. Sarotti, M. I. Mangione, A. G. Suarez and R. A. Spanevello, *Eur. J. Org. Chem.*, 2018, 590–604.
76. S. Fadlallah, L. M. M. Mouterde, G. Garnier, K. Saito and F. Allais, *ACS Symp. Ser.*, 2020, **1373**, 77–97.
77. J. E. Camp, *ChemSusChem*, 2018, **11**, 3048–3055.
78. Citrus: World Markets and Trade, United States Department of Agriculture report, January 2021, https://apps.fas.usda.gov/psdonline/circulars/citrus.pdf.
79. A. Satira, C. Espro, E. Paone, P. S. Calabrò, M. Pagliaro, R. Ciriminna and F. Mauriello, *Catalysts*, 2021, **11**, 387.
80. R. Ciriminna, M. Lomeli-Rodriguez, P. Demma Cara, J. A. Lopez-Sanchez and M. Pagliaro, *Chem. Commun.*, 2014, **50**, 15288–15296.
81. I. John, K. Muthukumar and A. Arunagiri, *Int. J. Green Energy*, 2017, **14**, 599–612.
82. Z. Zebec, J. Wilkes, A. J. Jervis, N. S. Scrutton, E. Takano and R. Breitling, *Curr. Opin. Chem. Biol.*, 2016, **34**, 37–43.
83. T. P. Korman, P. H. Opgenorth and J. U. Bowie, *Nat. Commun.*, 2017, **8**, 15526.
84. T. Stevanovic, *Lignocellulosic Fibers and Wood Handbook*, ed. Belgacem, N. and Pizzi, A., 2016, pp. 49–106.

85. F. Parrino, A. Fidalgo, L. Palmisano, L. M. Ilharco, M. Pagliaro and R. Ciriminna, *ACS Omega*, 2018, **3**, 4884–4890.
86. J.-D. Woodroffe and B. G. Harvey, *Energy Fuels*, 2020, **34**, 5929–5937.
87. D. V. Evtuguin and D. Robert, *Wood Sci. Technol.*, 1997, **31**, 423–431.
88. D. V. Evtuguin, G. Rocha and B. J. Goodfellow, *Holzforschung*, 2009, **63**, 675–680.
89. D. R. Vardon, M. A. Franden, C. W. Johnson, E. M. Karp, M. T. Guarnieri, J. G. Linger, M. J. Salm, T. J. Strathmann and G. T. Beckham, *Energy Environ. Sci.*, 2015, **8**, 617–628.
90. A. Rodriguez, D. Salvachua, R. Katahira, B. A. Black, N. S. Cleveland, M. Reed, H. Smith, E. E. K. Baidoo, J. D. Keasling, B. A. Simmons, G. T. Beckham and J. M. Gladden, *ACS Sustainable Chem. Eng.*, 2017, **5**, 8171–8180.
91. D. Salvachua, C. W. Johnson, C. A. Singer, H. Rohrer, D. J. Peterson, B. A. Black, A. Knapp and G. T. Beckham, *Green Chem.*, 2018, **20**, 5007–5019.
92. S. Choi, H.-N. Lee, E. Park, S.-J. Lee and E. S. Kim, *Biomolecules*, 2020, **10**, 1238.
93. P. G. Roessler, L. M. Brown, T. G. Dunahay, D. A. Heacox, E. E. Jarvis, J. C. Schneider, S. G. Talbot and K. G. Zeiler, Enzymatic Conversion of Biomass for Fuels Production, *ACS Symp. Ser.*, 1994, **566**, 255–270.
94. P. Bajpai, Kraft Spent Liquor Recovery, in *Biermann's Handbook of Pulp and Paper*, Raw Material and Pulp Making, 3rd edn, 2018, vol. 1, pp. 425–451.
95. T. Aro and P. Fatehi, *Sep. Purif. Technol.*, 2017, **175**, 469–480.
96. D. Y. C. Leung, X. Wu and M. K. H. Leung, *Appl. Energy*, 2010, **87**, 1083–1095.
97. P.-J. Roumanet, F. Lafleche, N. Jarroux, Y. Raoul, S. Claude and P. Guegan, *Eur. Polym. J.*, 2013, **49**, 813–822.
98. T. Hayes, Y. Hu, S. A. Sanchez-Vazquez, H. C. Hailes, A. E. Aliev and J. R. G. Evans, *J. Polym. Sci., Part A*, 2016, **54**, 3159–3170.
99. Y. Wan and J.-M. Lee, *ACS Catal.*, 2021, **11**, 2524–2560.
100. J. Iglesias, I. Martinez-Salazar, P. Maireles-Torres, D. Martin Alonso, R. Mariscal and M. Lopez Granados, *Chem. Soc. Rev.*, 2020, **49**, 5704–5771.
101. P. L. Arias, J. A. Cecilia, I. Gandarias, J. Iglesias, M. López Granados, R. Mariscal, G. Morales, R. Moreno-Tost and P. Maireles-Torres, *Catal. Sci. Technol.*, 2020, **10**, 2721–2757.
102. J. Xu and B.-H. Guo, *Biotechnol. J.*, 2010, **5**, 1149–1163.

CHAPTER 16

Sustainable Tools for Flow Chemistry

FRANCESCO FERLIN[a] AND LUIGI VACCARO*[a]

[a]Laboratory of Green S.O.C., Dipartimento di Chimica, biologia e Biotecnologie, Università degli Studi di Perugia, Via Elce di Sotto 8, 06123, Perugia, Italy
*E-mail: luigi.vaccaro@unipg.it

16.1 Introduction

The field of organic synthesis has deeply changed in the last two decades and terms such as sustainability, waste-minimization and pot-economy have become very frequent in the literature. This transition toward a more sustainable chemistry is nowadays recognized in different areas both at academic and industrial levels and the *leitmotiv* is that applied processes need to be based on a mindful evaluation of the environmental impact.[1] However, based on the truly multifaceted nature of the chemical research, it is difficult, and somehow wrong, to define a unique strategy to face and solve the sustainability issues. On the contrary, case-by-case evaluation is required depending on the issues to solve and the limitations imposed by local policies and regulations.[2,3] In the past century, chemistry has been the strategic science that furnishes effective tools to achieve added-value materials. In addition, nowadays, it is of primary importance to define protocols consuming minimal energy while respecting the environmental cost, and featuring a good balance between waste produced and amount of the target material obtained. Waste, in fact, clearly impacts on the economy of the overall applied process

Sustainable Organic Synthesis: Tools and Strategies
Edited by Stefano Protti and Alessandro Palmieri

Published by the Royal Society of Chemistry, www.rsc.org

as its cost is seriously affected by its disposal. At the end of the 90's, Anastas and Warner gave a fundamental direction to steer the shift to a more sustainable chemistry by disclosing the "12 Green Chemistry principles"[4] in which the priorities for the implementation of innovative and environmentally friendly synthetic processes are indicated.[5–7] To date, the definition of efficient and sustainable chemical transformations can benefit from modern tools that in different ways influence the minimization of waste and energy consumption, while increasing the safety hazard prevention.[8] Among these, the use of a heterogeneous catalyst,[9–11] the adoption of flow conditions[12–14] and the utilization of safer/recyclable reaction media[15–17] are of principal interest. This chapter will highlight the improvements in the application of the above-described tools and their role in the development of new and efficient synthetic methodologies.

16.1.1 Flow Chemistry as a Key Tool in Green and Sustainable Chemistry

Flow chemistry combines different areas of interest spanning from fundamental research to process chemistry and chemical engineering.[18] The growing interest in reactions performed in flow conditions is proven by the many scientific contributions that have appeared in the last decade. They describe the use of flow reactors in a wide variety of processes, including examples of organic synthetic chemistry,[19,20] organometallic chemistry,[21,22] photochemistry[23,24] and many others.

Among the most peculiar features associated with flow chemistry, the unique possibility of accessing new process windows allowing innovative synthetic pathways[25] otherwise not accessible with the classic batch reactors is always mentioned.

Flow conditions are also proving to be an innovative technology that if properly implemented can enable efficient solutions to sustainability issues.[26,27]

Therefore to realize efficient and sustainable processes in flow, adequate tools need to be developed to minimize waste while increasing chemical efficiency.

One of the most common issues in a process is related to the proper selection of a reaction medium and in fact the "solvent selection"[28] has a tremendous impact due to their use in very large volumes. While flow conditions normally require the use of diluted conditions, taking into account the sustainability of a process, flow reactors should be adequately developed to operate using minimal amounts of solvents or be associated with automated continuous solvent recovery and reuse.

Efficient chemical processes are based on the use of catalytic conditions to replace highly reactive and unsafe reagents. From the sustainability point of view, heterogeneous recoverable and reusable catalytic systems are highly desirable. Flow technology can actually be a very effective technology

for preserving and prolonging the efficiency of a heterogeneous catalyst, as this can be packed into a flow reactor facilitating its separation from the reaction mixture and improving its stability.[29,30] In general, the adoption of flow conditions is also very useful to handle hazardous reagents such as pressurized gases or highly reactive species.[31] Indeed, the reagents in flow are generally subjected to reaction conditions for a shorter time, their handling being operatively safer than in batch procedures. In the following subchapters, several different approaches will be presented paying particular attention to those tools developed to realize efficient and sustainable processes in flow.

16.2 Heterogeneous and Recyclable Catalytic Systems

The development of catalytic systems has always attracted many researchers for the possibility to develop efficient transformations in which the reactivity is controlled by an external agent (the catalyst) that possibly also influences the reaction pathway, therefore opening up the possibility to perform chemical reactions, which would otherwise require high activation energies, under milder conditions. Moreover, in certain cases, the use of a catalyst can allow a completely new reactivity. Ideally, the best catalytic system should be durable for many catalytic cycles and if based on metals, it should have the ability not to pollute the reaction products with metal impurities.[32] The chemical industry, especially when dealing with fine chemicals, is always looking for new, more selective and more efficient catalysts.[33] Generally, homogeneous catalysts are therefore considered highly reliable and when possible, techniques for their separation and recovery from the reaction mixture have been defined.[34] These techniques include phase transfer separation or ion-exchange resins. The use of homogeneous catalysts is therefore generally desirable in terms of selectivity and chemical efficiency, but it is not always economically or environmentally convenient often resulting in the inevitable release of waste and metal catalysts into the environment. A greener approach for the recovery and reuse of a catalyst involves the development of effective heterogeneous catalytic systems exploiting a variety of possible supports.[35] Aside from their reusability, these catalysts may be easily removed facilitating the processing of the final mixture and therefore simplifying the work-up procedures.[36,37] This field of research is the subject of many studies based on the identification of different supports, either organic and inorganic, such as carbon/silicon-based,[38] metal–organic framework,[39] or a large variety of polymeric supports.[40] In the following subchapters, selected examples of the use of heterogeneous metal catalysts will be given in order to understand the differences in terms of sustainability based on the quantification of the Environmental Factor (*E*-factor), which is an intuitive yet effective green metric able to quantify the mass (Kg) of waste per mass (Kg) of target product achieved.

16.2.1 Pd/C Catalyzed Arylation of Indoles in a Recoverable Polarclean/Water Mixture as the Reaction Medium

Among the most used and diffused supports, charcoal is commonly applied to the synthesis of heterogeneous metal-based catalysts and widely used in industry. The stability of these catalysts is strongly dependent on mainly two factors: (i) the temperature and (ii) the solvent used as reaction medium. These types of catalyst can be produced on a large scale and can be loaded with different metals in various weight percentages. The extremely high versatility of these catalyst can offer a wide applicability in different types of reaction from hydrogenation reaction to more complex selective activation of inert C–H bonds.[41–45]

As previously mentioned, the efficiency of a heterogeneous catalyst, both in terms of catalytic activity and in terms of sustainability, depends on the selection of the reaction medium. In the following examples, the authors reported a C-2 selective arylation of indoles, catalyzed by Pd/C using Polarclean/water as the reaction mixture (see Figure 16.1).[46]

Polarclean is a promising solvent that can be used as an alternative to toxic dipolar aprotic solvents (NMP, DMF, and DMA). It is produced by Solvay, in a circular-economy based process utilizing 2-methylglutaronitrile as the starting material (see Figure 16.2).[47] 2-Methylglutaronitrile itself is the major waste produced in the synthesis of Nylon-6,6. Polarclean is composed of a

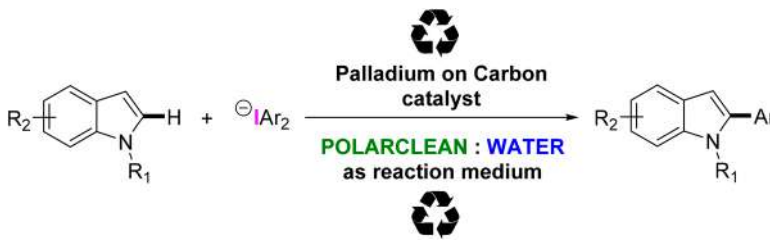

Figure 16.1 Palladium on carbon (Pd/C)-catalysed indole C-2 arylation.

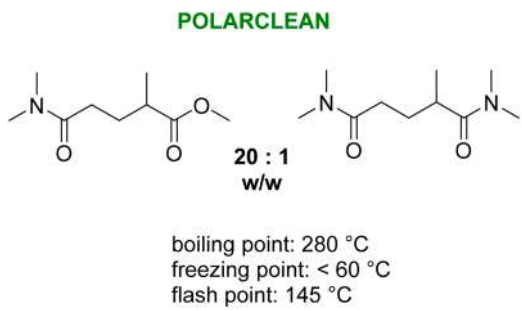

Figure 16.2 Polarclean composition and physical properties.

20 : 1 mixture of an ester amide and a diamide, and is water-miscible, non-toxic and highly biodegradable.

Due to its solvation properties, Polarclean is largely used as a solvent for agrochemical formulation and crop protection,[48] while its use as a reaction medium for chemical reactions is to date restricted to a few applications.[49,50] The authors exploited the peculiar properties of Polarclean, combined with the use of a Pd/C catalyst, to achieve waste minimization in the C–H activation reaction of the C-2 proton of differently substituted indoles with diphenyliodonium tetrafluoroborate as an aryliodonium source. After an initial screening of solvents, a 1 : 4 mixture of Polarclean and water was found to be a suitable reaction mixture. Importantly, this mixture allows very limited palladium leaching to be achieved in the reaction mixture and therefore both the catalyst and the solvent mixture can be recycled up to five times without loss of efficiency. A comparative approach between different methods for the isolation of the product led to the assessment of a very low *E*-factor value of 5, which represents an important reduction compared to the values reported in the literature (ranging from 66 to over 383). Furthermore, a comprehensive analysis of the heterogeneous nature of the catalyst in the reaction mixture selected has also been reported, highlighting the important role of Polarclean in general in the selection of an appropriate medium.

16.2.2 Heterogenized Palladium-based Catalytic Systems

Another very useful strategy to achieve waste minimization by recycling together the catalyst and the reaction medium may fall under the classification of "heterogenization strategies".[51] These strategies implicate the initial use of a homogeneous catalyst, which is supported *in situ* during the reaction. Recently, the dehydrogenative aerobic C–H arylation of 1,2,3-triazoles has been reported following this strategy.[52] Polyethylene glycol (PEG) has been used as a non-toxic reaction medium for this oxidative transformation (see Figure 16.3).

PEG has a very low vapor pressure, and a solid thermal stability, and therefore has already found different applications as an efficient reaction medium

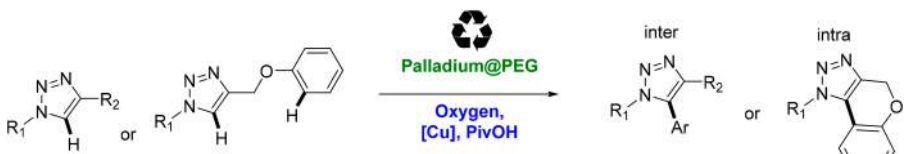

run	Yield	Pd loading in PEG
1	72%	0.2 % w/w
2	74%	0.2 % w/w
3	70%	0.2 % w/w
4	68%	0.2 % w/w

Figure 16.3 Pd@PEG C–H arylation of 1,2,3-triazoles.

for chemical reactions.[53,54] After optimization of the reaction conditions, the authors found that the initial catalytic system composed by palladium acetate, a substoichiometric amount of copper acetate, pivalic acid, PEG and molecular oxygen as a sacrificial oxidant is very efficient in promoting the envisaged C–H arylation. The improvements in terms of sustainability become evident at the end of the reaction; indeed, the output reaction mixture, upon cooling, appears as a solid. This solid mixture can be easily extracted using green cyclopentyl methyl ether (CPME) to isolate the product. The remaining solid is just solvent (PEG) and the catalyst and it can be readily re-used for further reactions. To gain more insight into the operative mechanism of the reaction, the authors have also performed a deep investigation into the palladium content in the solvent-catalyst mixture. As a result, it can be concluded that a stable catalytic system is formed *in situ via* reduction of the starting palladium acetate to Pd nanoparticles with the help of PEG as a stabilizer. Importantly, environmental advantages were obtained in terms of step-economy by the intrinsic nature of the C–H activation reactions,[55] and in terms of waste thanks to the use of the heterogenized palladium system and oxygen as a sacrificial oxidant leaving water as the sole by-product.

16.2.3 Polymer-supported Catalytic Systems

Immobilized catalytic systems should be adequately designed considering that the reagents, dissolved in the reaction medium, need to access the catalytic sites. Therefore, the solid support plays a central role in the definition of effective catalytic systems able to operate in the presence of a novel green medium. A clear example of this is given by the design and preparation of specific polymer supported ionic tags (see Figure 16.4).

These molecular entities can be tuned for basic[56,57] or acid catalysis,[58] or alternatively to immobilize ligands for metal-catalysts.[59,60] A very recent example of the use of a polymeric ionic-tag (POLITAG) to support palladium(II) species is found in the C2-selective olefination of quinoline and quinoxaline

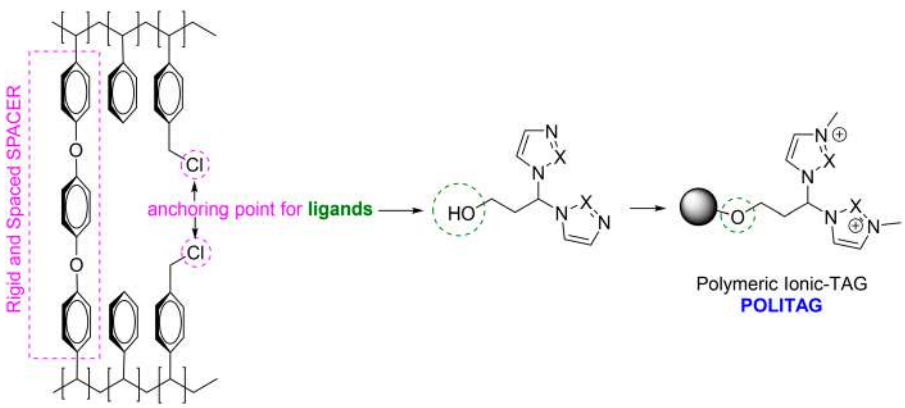

Figure 16.4 Polymeric ionic tag (POLITAG) synthesis overview.

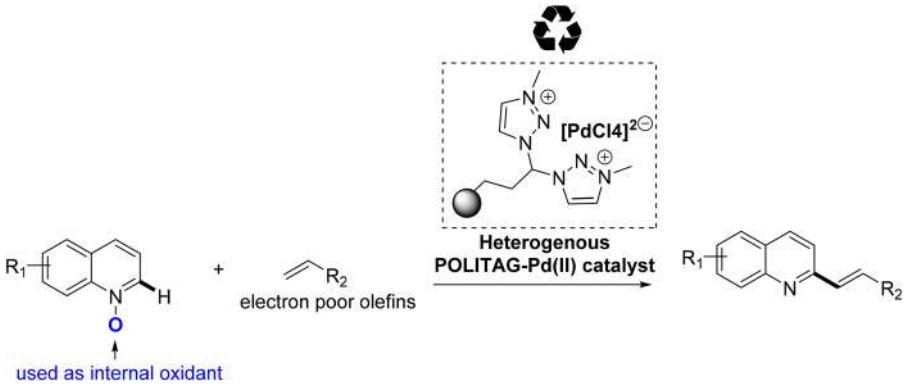

Figure 16.5 POLITAG-Pd(II)-catalysed quinoline-*N*-oxide alkenylation.

N-oxide moieties.[61] It is noteworthy that heterogeneous POLITAG-Pd catalysts, with heterocyclic pincer type ligands, have already proven to be effective in biomass-derived GVL as a reaction medium for the Mizoroki–Heck reaction,[62] exploiting high chemical efficiency and a low leaching of metal, reaching the lowest level known in the literature (0.05 Pd ppm). This catalytic system has only very recently been reported in C–H activation reactions and the following examples report the first utilization of a heterogeneous catalyst in the alkenylation of quinoline *N*-oxide.

The *N*-oxide functionality is known for being capable of specifically directing C–H activation processes in the metalation step, and also allowing oxidant ability to be exploited opening access to external-oxidant-free transformations. These features have led to different valuable contributions for the alkenylation of quinoline *N*-oxide, also with some interesting reactions exploiting environmentally friendly 3d metals such as iron.[63] The authors began their investigation in the synthesis of different polymeric ionic-tags designed *ad hoc* to support palladium(II) species. After a considerable screening of heterocyclic supported ligands and of the reaction conditions, the optimal catalyst was found to be the POLITAG-Pd(II)-L3 (see Figure 16.5), which is able to steer the envisaged C–H alkenylation selectively in the C-2 position.

Importantly, the catalyst designed showed a very limited leaching in solution and has been found to be recyclable for five consecutive runs with a negligible loss in its efficiency. The catalyst reported has also been found to be suitable for gram-scale synthesis of C-2 functionalized quinolines, exploiting its applicability to these types of transformations.

16.3 Selection of Safer and Recoverable Reaction Media

Solvents constitute the major percentage of the mass involved in many common chemical processes, and they are indeed used not only to execute the reactions but also and especially at the purification stages, in the

analysis or more simply to transfer reaction mixtures.[64] In addition, the selection of a proper solvent could influence the reactive pathways dramatically. For these reasons, the solvents play a pivotal role in the development of a generic chemical reaction, and become even more important in the definition of an eco-friendly transformation.[65,66] The choice of a chemical which serves as a reaction medium is tricky due to the fact that it influences not only the reagents but also the catalytic system.[67] Often, the selection of a so-called "green solvent" is a very delicate issue, as many classic unsafe solvents (DCM, DMA, DMF, NMP) exploit peculiar properties in terms of solvation of the variety of species present in the reaction pot, increasing their reactivity.[68] A thoughtful approach to this matter should always start by considering that a solvent cannot be assumed as totally green, while the evaluation can be made on the whole process and on the effective role of the solvent in the reaction examined.[69] Generally, different approaches have been revealed to be very efficient to face the issues of solvent selection. One of the most direct and efficient is the adoption of solvent-free or highly concentrated conditions; these can be very efficient in terms of "volume reduction strategies",[7] offering the possibility of also speeding-up certain reactions.[70]

If a solvent is needed anyway, a modern approach to solvent selection includes the shift from petrol-based to circular-economy-, or biomass-derived solvents.[71] The latter offer the great advantages of being generally non or less toxic compared to the petrol-based counterparts and obviously of being synthesized by renewable sources and therefore featuring a CO_2 closed cycle (see Figure 16.6).

In addition, another effective strategy is the use of an adequate recoverable aqueous azeotropic mixture. Although water is safe and possesses peculiar properties in terms of influencing the reactivity of organic molecules, it

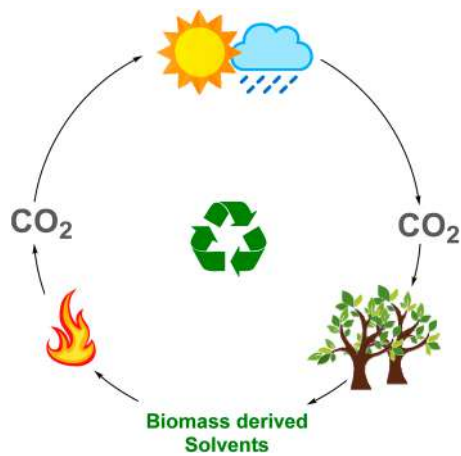

Figure 16.6 CO_2 cycle for the production of bio-based chemicals.

cannot be considered totally green if including its somehow costly disposal. Very often water is used in combination with an organic soluble solvent, and therefore by forming an aqueous azeotropic mixture, the reaction can benefit also from the properties of an organic solvent and more importantly the azeotrope can be distilled and optionally reused.

In the following subchapters selected examples of the use of bio/waste-derived solvents and recoverable azeotropic mixtures will be shown remarking on the improvements in terms of sustainability.

16.3.1 Biomass-derived Solvents

Among the various biomass-derived solvents, γ-valerolactone (GVL) certainly deserves particular attention. This solvent indeed is one of the few promising candidates to replace petrol-based dipolar aprotic solvents.[72] GVL is obtained from levulinic acid *via* hydrogenative cyclization.[73] GVL has an optimal safety profile being a high boiling point (207 °C) chemical, with low toxicity, low tendency to form peroxides and good biodegradability. Furthermore, GVL shows a dielectric constant (ε) similar to those of dimethylformamide and *N*-methylpyrrolidone (see Figure 16.7).

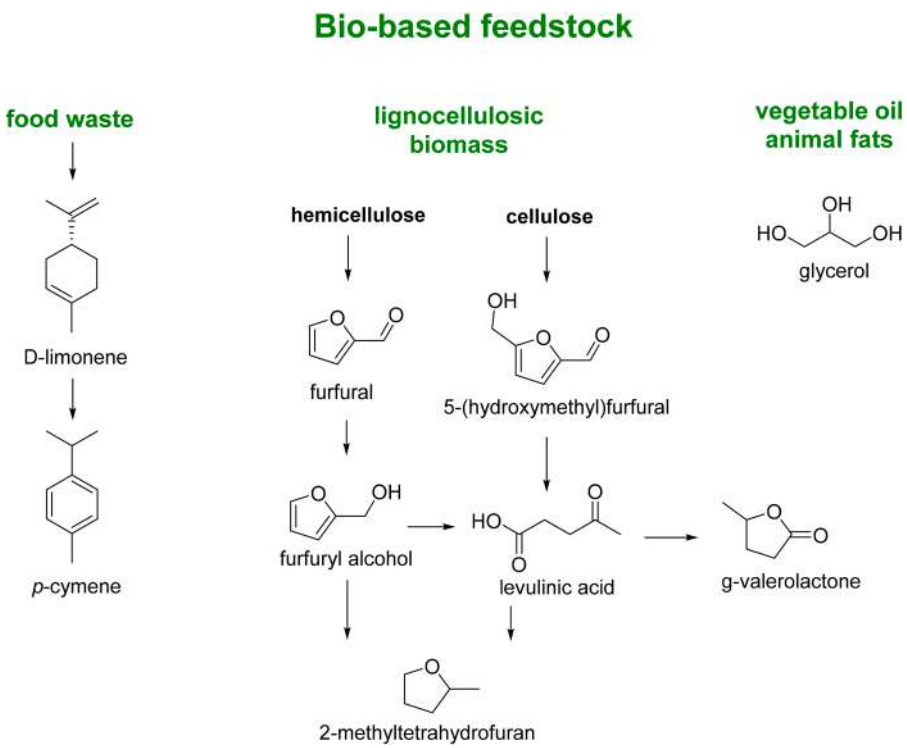

Figure 16.7 Common bio-derived chemicals used as reaction media.

However, due to the lactone functionality, GVL exploits a low coordination ability with metal centres and therefore appears useful when it is used in combination with heterogeneous catalysts, lowering their leaching in solution. To date, several examples have been reported in the literature using GVL for metal and non-metal catalyzed transformations and more importantly, in many cases its utilization has been accompanied by the *E*-factor quantification of the environmental improvements achieved.[74–78] The following examples have been selected to demonstrate how the use of GVL could be useful in promoting different approaches for waste minimization when it is used concomitantly with heterogeneous catalysts.

16.3.1.1 Heck–Mizoroki Cross-coupling in GVL

In this example, due to its generally high efficiency in different reaction conditions, the Mizoroki–Heck reaction has been taken as a model reaction to test the ability of various reaction media in controlling the metal leaching in solution of the polymer supported palladium(0) catalyst (see Figure 16.8).[79]

The reaction was carried out between iodobenzene and methyl acrylate using supported triethylamine as a base in different common dipolar aprotic solvents such us DMF, DMA, NMP and in a previously reported aqueous azeotropic mixture CH3CN/water. The polymer supported palladium(0) catalyst has been used in very low amount (0.1 mol%). In these conditions, excellent results could always be obtained in terms of conversion after 3 h of reaction time, while differences can be individuated on the purity of the reaction mixture mainly in terms of metal leached in solution, which was measure by Microwave Plasma Atomic Emission Spectroscopy (MP-AES). The results obtained by the authors must be interpreted assuming that a release and catch mechanism is operative.[80] According to this mechanism, palladium is

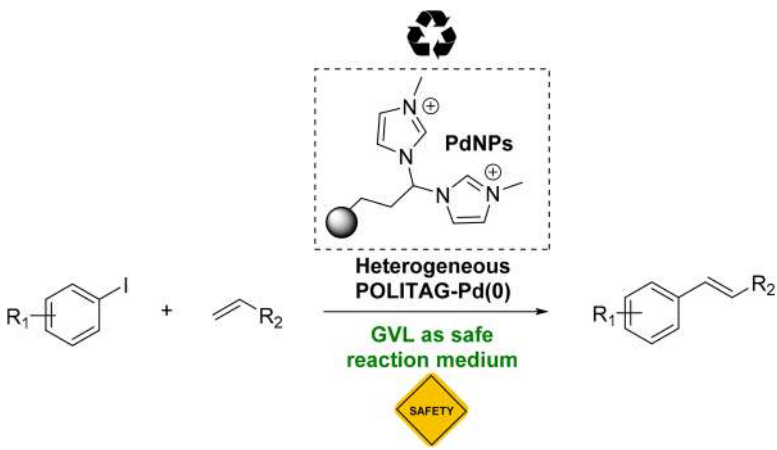

Figure 16.8 POLITAG-Pd(0)-catalysed Heck–Mizoroki reaction.

firstly released in the reaction medium in the oxidative addition of the aryl halide, and subsequently is re-caught by the support after the reductive elimination. The leaching minimization can be therefore due, in the first instance, to a lower ability of GVL in complexing the soluble palladium species released in solution. It is noteworthy that reducing the leaching means also reducing the common purification step required to remove metal impurities. In this regard, after the leaching evaluation, the authors have also quantitatively monitored the environmental impact of different work-up procedures as the physical forms of the product varies. More specifically, an extraction work-up was needed in the presence of oily products and a precipitation work-up was carried out with solid compounds. *E*-factor values in the range of 19–66 have been obtained.

16.3.1.2 Fujiwara–Moritani C–H Alkenylation in GVL

Another explicative example on the use of GVL as a reaction medium is the oxidative C–H alkenylation process catalyzed by Pd/C of aromatic C(sp^2)–H bonds;[81] in this case, acetanilides have been taken as model substrates. This reaction is also known as the Fujiwara–Moritani or dehydrogenative Heck reaction (see Figure 16.9).[82]

An initial optimization of the reaction conditions led to the selection of *p*-benzoquinone and a polymer-bound *para*-toluenesulfonic acid as an oxidant and acid additive, respectively. A series of unsubstituted and substituted acetanilides, presenting electron-withdrawing/donating groups, was tested with acrylates and styrenes using GVL as a reaction medium, leading to olefinated products in generally good yields. The reaction shows in all cases excellent selectivity, furnishing the mono-alkenylated products in the ortho position with respect to the acetamido functionality. The use of both a heterogeneous catalyst and resin-bound acid additive led to their complete easy recovery at the end of the process and to their efficient reuse for up-to five consecutive runs with negligible loss of conversion and no changes in regioselectivity. A quantitative analysis of the amount of palladium leached in solution has been carried out and it was found to be very low (4.2 ppm). Experimental mechanistic investigations have also been carried out performing a hot-filtration test and mercury poisoning test, which both stopped the reaction. These results suggested a genuinely heterogeneous or a very fast release/catch mechanism. To assess the environmental improvement derived

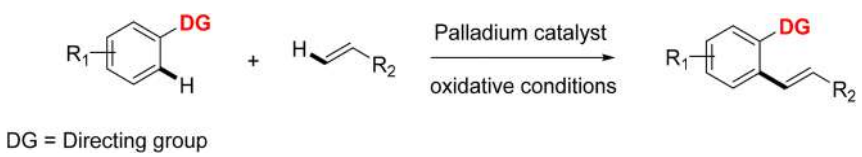

Figure 16.9 Fujiwara–Moritani reaction overview.

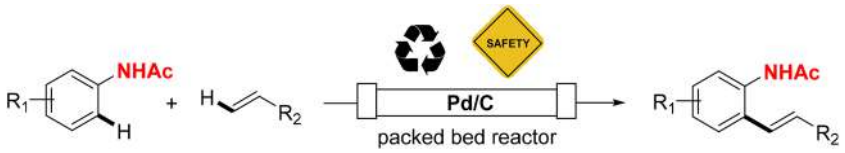

Figure 16.10 Fujiwara–Moritani reaction Pd/C-catalysed in flow.

from the use of GVL, different reactions using the optimized conditions have been conducted in conventional dipolar aprotic solvents, such as DMF and NMP. Slightly lower or almost comparable conversion has been noted, while a higher amount of metal leaching in solution occurs (80 and 31 ppm in DMF and NMP, respectively). The stability exploited by the heterogeneous Pd/C catalyst in GVL also allowed the transfer of the reaction to a tailored packed-bed flow reactor (see Figure 16.10).

The flow protocol showed very good performance in terms of catalytic efficiency, allowing the processing of more than 500 mmol of substrate with a productivity of 4 g h^{-1}. The metal species leached in solution was measure periodically and it was found to be low and stable at around a value of 4 ppm.

16.3.2 Recoverable Azeotropic Reaction Media

An effective remediation strategy to minimize the waste produced in a chemical process consists in the utilization of a reaction medium, which in some manners is recoverable and preferably reusable; the use of recoverable aqueous azeotropic mixtures appears to be an outstanding alternative to promote sustainable and waste minimized synthetic methodologies.[15] These azeotropic mixtures become even more interesting if the organic component is derived from biomass.[83] To date, different synthetic processes have been steered making use of a mixture of an organic solvent and water in order to fulfil both the solvation of inorganic (bases, additives, catalyst) and organic (substrates, products) reagents.[84,85] Usually, the water/organic solvent ratio is determined by the observed efficiency of the process rather than aiming at a reuse of the solvent mixture in order to achieve waste minimization. In this regard, the azeotropes may lead to an ideal system offering a good ability for solvation of the reactants and being reusable.

16.3.2.1 Waste Minimized Reduction of Nitrocompounds by a Heterogenous Au-based Catalyst in an EtOH/Water Azeotrope

In this example, zirconium-phosphonate layers were used to support gold nanoparticles, which have been used to catalyse the reduction of nitroarene to aniline or azoxybenzene in the presence of $NaBH_4$ as a hydride source.[86]

When the reaction was performed in an azeotropic mixture of water and ethanol (EtOH 96%) in the presence of 1 mol% of the gold catalyst and 6 equivalents of $NaBH_4$, the azoxy derivative was obtained in 99% conversion with almost complete selectivity. The authors also noted that when absolute ethanol[87] was used instead of the azeotropic mixture a completely different selectivity occurs toward the formation of aniline. This result suggested that, apart from the obvious influences of the reaction media in the mechanism of the reduction, a switchable chemoselectivity could be possible simply by changing the solvent. The heterogenous gold-catalyst was recovered and reused both in azeotrope EtOH/water and in absolute ethanol showing excellent performance for each consecutive run equal to the fresh catalyst. Inductive Coupled Plasma Optical Emission Spectroscopy (ICP-OES) has been used to determine the gold leached in solution, which is as low as 2.7 ppm. At this stage, to better evaluate the reusability of the catalyst, the authors decided to use it under flow conditions paving the opportunity to assess a sustainable large-scale production of two distinct products (aniline and azoxybenzene) with the same set-up simply by switching the solvent mixture (see Figure 16.11).

Both processes have been continuously performed on more than 10 mmol scale with a productivity of 1.45 mmol h^{-1}, and periodical measurement of the gold species in solution showed an effective reduction of the leaching, which is stable at values of 0.1 ppm. Most importantly, an environmental assessment has been performed for both processes highlighting the importance of the use of the azeotropic mixture ethanol/water. Indeed, an *E*-factor value of 2.1 comes from the almost complete recovery and reuse of the azeotropic mixture, which is lower than the value obtained when absolute ethanol has been used (5.4) due to an incomplete recovery.

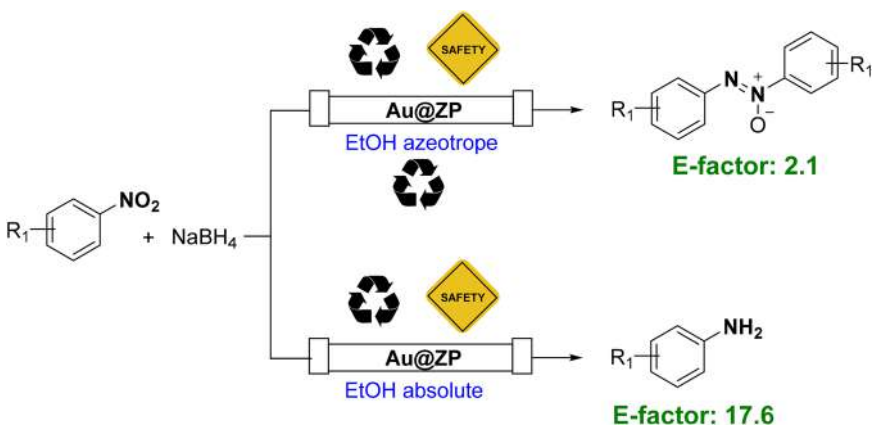

Figure 16.11 Flow system for switchable Au-catalysed reduction of nitroarene.

16.3.2.2 *Waste Minimized Ullmann-type Reaction in Biomass Derived Furfuryl Alcohol/Water Azeotrope*

Furfuryl Alcohol (FA) is a biomass derived chemical which possesses a relatively high boiling point (171 °C); it is soluble in most common organic solvents and it is miscible with water.[88] In this example, the authors have proposed the use of an azeotropic mixture of water and FA as a recoverable reaction medium for the coupling reaction of aryl iodide and aromatic or aliphatic amine (also known as Ullmann cross coupling).[89] Very interestingly, the FA/water azeotrope exploits two peculiar properties: (i) it is among the very few alcohol/water azeotropes that is prevalently formed by water (80% w/w); (ii) the boiling point of this azeotrope (98 °C) is much lower than that of pure FA and therefore is appetible for recovery *via* simple distillation. After an initial optimization of the reaction conditions aimed at finding the optimal combination of inorganic base (K_3PO_4) and catalyst (CuI), the authors studied more in depth the influence of the FA. Using the reaction between imidazole and aryl iodide as a model reaction, several combinations of solvents, water and 1,2-diols and 1,2-diol-ether ligands (see Figure 16.12) were tested.

As a result, all the tested bidentate diols, as well as their methyl ethers, gave very good results in terms of conversion to final product. This investigation confirmed the beneficial role of water as a medium for the Ullmann-type reaction and the requirement for a bidentate ligand to achieve satisfactory consumption of the starting materials. FA and tetrahydro-FA on their side, showed better results leading to complete disappearance of the starting materials and the exclusive formation of the desired product. However, FA exploits a beneficial effect as it is the only one among the ligands tested that is able to form an azeotropic mixture with water, and therefore can be recovered by distillation at the end of the process and reused for consecutive reaction runs. In order to give a quantitative evaluation of the sustainable improvements, the authors optimized a work-up procedure, in which the final reaction mixture, after cooling, was subjected to distillation to recover the azeotropic mixture,

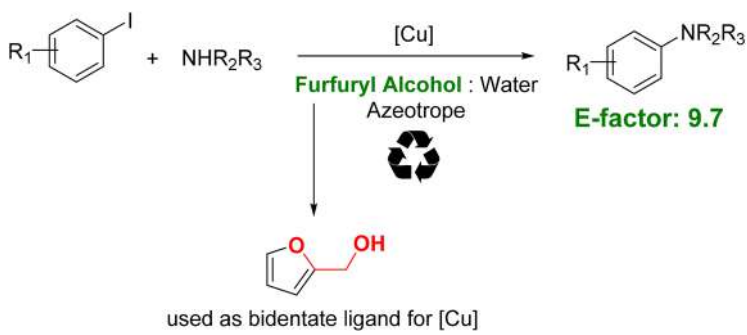

Figure 16.12 Waste-minimized Ullman-coupling in furfuryl alcohol/water azeotrope.

and the residual was dissolved in a minimal amount of ethyl acetate and filtered to recover the pure product. This procedure allows the calculation of an *E*-factor value of 9.7, which is an important reduction compared to other common methodologies present in the literature (range 71–619).

16.4 Adoption of Flow Conditions to Access Sustainable Processes

Moving towards the so-called "pot economy" concept, the adoption of flow reactors can certainly represent an ideal approach.[90,91] In this context, some concepts can be very simply summarized. The classical "pot" used to execute a reaction is replaced by channels or tubes, stirring equipment is replaced by pumps and the performance of a specific process is expressed in terms of residence time inside the flow reactor rather than a reaction time.[92] This configuration allows improvements to be obtained in terms of mass/heating/cooling transfer with consequential benefits in terms of the selectivity and general output of the reaction.[25,93,94] In addition, the confinement of reagents, catalysts, and solvents inside the reactors led to an increase in safety hazard prevention, limiting the exposure of the operators.[95,96] All these aspects have contributed to a growing interest in flow chemistry by both academia and industry offering the opportunity to connect these two areas.[97,98] Indeed, flow reactors also make it possible to simplify the industrial scale-up of a synthetic procedure and to increase the reproducibility of such processes. In simple terms, sustainable chemistry and flow chemistry are closely interlocked.[12,15,27,99] In the following sections will be given some examples that highlight the safety hazard prevention and waste-minimization using flow technology (see Figure 16.13).

16.4.1 Waste-minimized Synthesis of Questiomicyn-A and Related Compounds

In this example, a continuous flow methodology for the C–H oxidation process using molecular oxygen as both a green terminal oxidant (water being the only by-product) and as a pumping system to move the reaction mixture through a packed bed reactor has been developed.[100] A manganese-based heterogeneous catalyst (K-OMS-2) was chosen to steer this oxidative coupling by using cyclopentyl methyl ether (CPME) as a green solvent. The authors

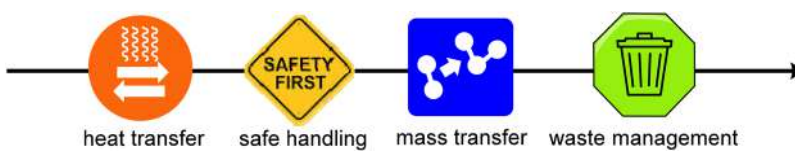

Figure 16.13 Sustainable features of flow approaches.

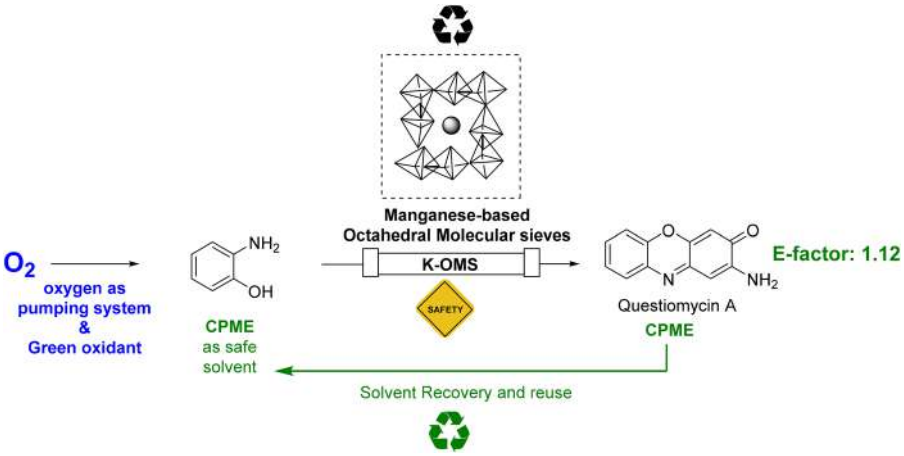

Figure 16.14 Manganese-based octahedral molecular sieve-catalysed C–H oxidation in flow.

have preliminarily studied the influence of oxygen to efficiently maintain the oxidation state of the mixed-manganese oxide during a large-scale continuous flow production of Questiomycin-A in high yields (97%) and with minimal leaching of metal species in solution (0.1–0.7 ppm of Mn), which is lower than the value obtained in other reaction media.[101] An important feature of this protocol relied on the safe management of the oxidative reaction conditions by the combination of flow chemistry and a low-peroxide formation solvent (CPME). To better evaluate the environmental improvement, a comprehensive analysis of different green metrics (AE, RME, MRP, SRP) was conducted. Notably, the flow procedure exploits an *E*-factor value of 1.4, which represents a strong reduction compared with other protocols in the literature (68–368) (see Figure 16.14).

16.4.2 Sustainable Flow Synthesis of Benzoxazoles by Heterogeneous Manganese-based Systems

The so called "pump-free" flow system should also be mentioned, where mass transfer of a gas carrier is used to replace even the mechanical pump. A telescoped approach for the synthesis of benzoxazoles has been reported.[102] The authors developed a mesofluidic flow system featuring the use of two types of heterogenous octahedral manganese-based molecular-sieves in two distinct packed-bed reactors and the use of cyclopentyl methyl ether as a reaction medium. The strategy allows for a fast and efficient production of benzoxazoles in *ca.* 1 h of total residence time. In the first section of the flow system, the CPME solution of a benzylic alcohol is pumped using oxygen pressure (5 bar) through a reactor containing a H-OMS-2 catalyst. The resulting benzaldehyde is formed almost

quantitatively, and it reacts in the following section of the flow system with *o*-aminophenols to form the corresponding imines. Finally, the reaction mixture is continuously pumped through a reactor packed with K-OMS-2 to achieve the cyclization of the imines and leading to the target benzoxazoles (see Figure 16.15).

The whole procedure has been carefully optimized to fulfil the green chemistry principles, and also achieve an efficient solvent recovery at the output of the reactor allowing the solvent to be recycled continuously without further purification. The leached manganese-species have been measured, showing a manganese content as low as 0.17 ppm. The combination of a heterogeneous catalytic system/eco-friendly solvent/flow conditions leads also to the production of an active pharmaceutical ingredient Tafamidis in high yield (92%) in a 1 h residence time and with a very low *E*-factor value (4.4). The usefulness of the flow protocol developed is also highlighted considering that similar batch protocols will have the limitations of handling the appropriate

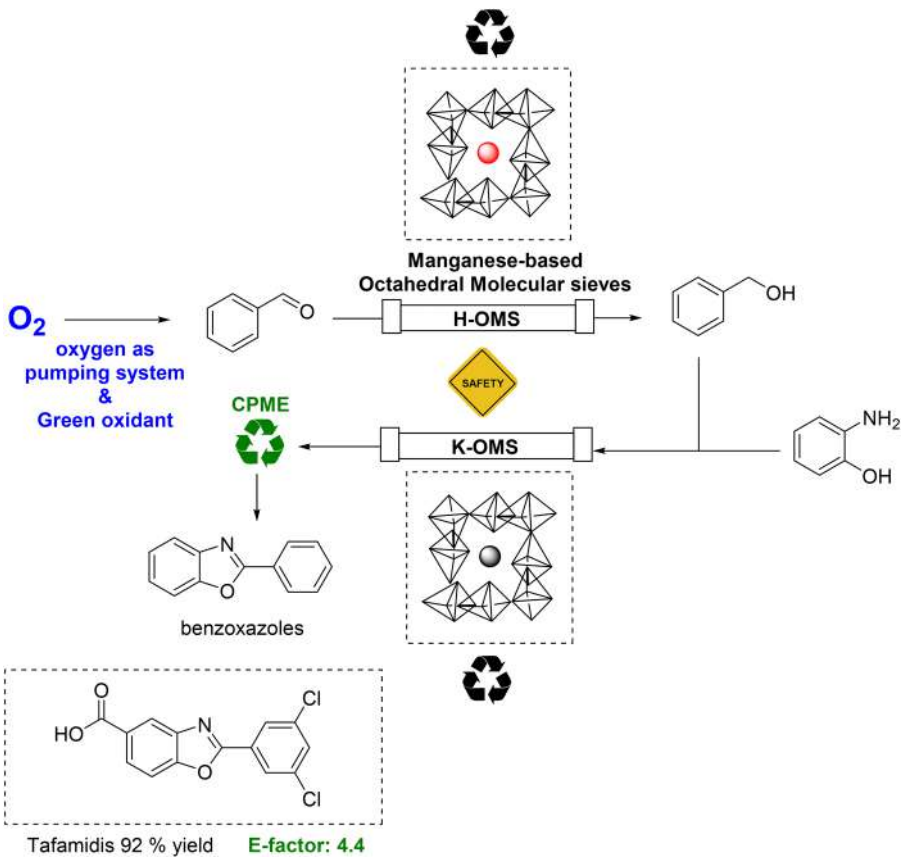

Figure 16.15 Pump-free telescoped flow system for the synthesis of benzoxazoles.

oxygen pressure needed to maintain the activity of the catalyst. Therefore, the flow conditions adopted offer both high productivity and consistent waste minimization as compared to batch processes.

16.4.3 Leaching-minimized Flow-assisted Protocol for Mizoroki–Heck Reaction

As previously mentioned, the adoption of flow conditions is among the most effective strategies to achieve a better stabilization of a heterogeneous catalyst. Indeed, it helps to preserve the catalyst integrity, also resulting in a consequent minimized leaching reduction. In the following example, the preparation of a polymer supported ionic-tag to immobilize palladium(II) species and its utilization in the Mizoroki–Heck cross-coupling reaction in a packed bed flow reactor is shown.[103] Initially, the authors designed and synthetized the heterogeneous catalyst based on a spaced and rigid polymer, which led to easy access to the catalytic sites while maintaining a good mechanical stability. Subsequent anchoring of a bis-imidazole based ligand and immobilization of the palladium(II) metal species allows the desired catalytic system to be obtained. The efficiency of the heterogenous catalyst has been preliminarily tested in batch conditions for the envisaged Mizoroki–Heck reaction between aryliodide and methyl acrylate using biomass derived GVL as the reaction medium. Reusability and leaching measurements confirmed the high stability and encouraged the authors to transfer the reaction to cyclic flow conditions in order to open the possibility for larger scale operation. The polymeric supported catalyst has been therefore packed into a stainless-steel column and the reaction mixture has been pumped through the reactor (see Figure 16.16).

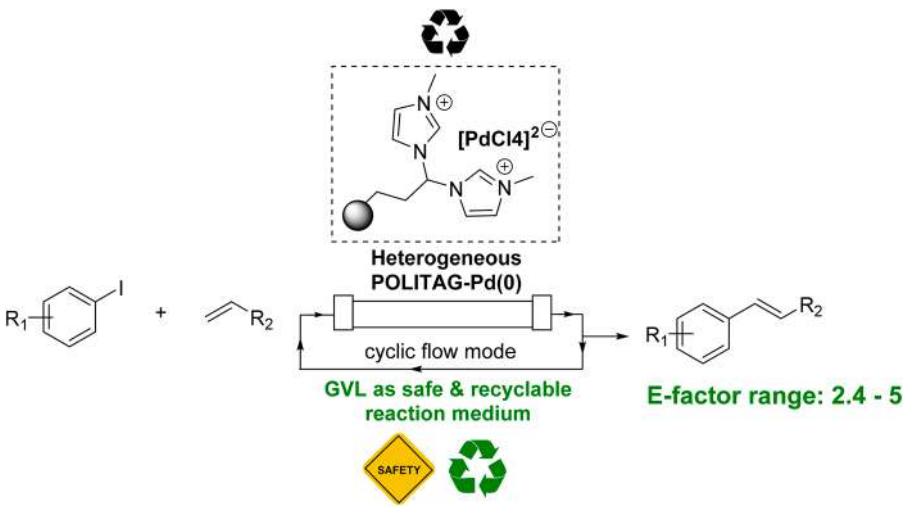

Figure 16.16 POLITAG-Pd(II)-catalysed Heck–Mizoroki reaction in flow.

As a result, the authors highlighted several improvements in terms of: (i) the catalytic activity, including TON and TOF values, has been increased in flow (5940 and 495 h^{-1}) compared to the batch conditions (4870 and 487 h^{-1}); (ii) *E*-factor minimization achieving a range of 2.4–5, which is lower than those obtained in batch conditions (21–75 range) with a consequent higher processable volume of substrates and of the implementation of a system for the recovery and reuse of the GVL; (iii) palladium leaching with a consistent reduction of one order of magnitude from the batch conditions (0.5 ppm) to the flow (0.05 ppm).

16.4.4 Continuous Flow Waste Minimized C–H Arylation of 1,2,3-triazoles

The extensive exploration of synthetic methodologies for the synthesis of 1,2,3-triaozles *via* cycloaddition reaction and subsequent functionalization through C–H activation technologies deserves a special mention, being among the most powerful tools to achieve highly added value target materials. In this example, a heterogeneous palladium catalyst has been used in a tailor-made packed-bed flow reactor using bio-derived GVL as a safe and recoverable reaction medium.[104] The thoughtful combination of the three pillars described through the whole chapter has led to the definition of the lower *E*-factor protocol in the literature to achieve functionalized 1,2,3-triazoles. An initial assessment of the reaction conditions, aimed at obtaining a homogeneous reaction mixture suitable for flow technology, has been done. Further analysis regarded the reusability of the heterogeneous catalyst and the measurement of the palladium leaching in batch conditions was performed. Subsequently, the authors implemented a 2 m packed-bed tubular flow reactor made of PTFE to screen the flow parameters. With the flow conditions optimized, different functionalized chromenes and isoindoline fused 1,2,3-triaozles were synthesized in an intramolecular fashion. The protocol was also suitable to achieve C-5 arylated 1,2,3-triaozles *via* intermolecular reaction. All the target compounds were obtained in high yields and short residence time inside the reactor (80 min). Periodical measurement of the palladium leaching during a long operation flow test (100 mmol) shows an extremely improved stability of the packed catalyst resulting in a percentage reduction of palladium loss of two orders of magnitude compared to the batch conditions (0.0015% and 0.16%, respectively). At the output of the flow reactor, a pressurized (0.3 mbar) distillation system for the recovery of the GVL has been installed, allowing the reuse of the solvent continuously (see Figure 16.17).

The resulting dried reaction mixture could be easily re-crystallized from an acetone/water mixture (1 : 20) leading to pure target compounds. The whole strategy led to an *E*-factor value of 24, which confirms a strong reduction compared to other literature known procedures (349–4825 range). More importantly, the waste-minimization has also been compared with a batch test, which replicates the exact conditions used in batch conditions showing

Figure 16.17 Pd/C-catalysed arylation of 1,2,3-triazoles in flow.

an *E*-factor of 64, corroborating the usefulness of using flow conditions to easily handle large-scale reaction mixtures and to avoid the wasteful purification steps needed to regenerate the catalyst.

16.5 Conclusions

In conclusion, this chapter offer an angle on the chemical and environmental improvements possible by the combined use of heterogenous catalytic systems, safe and recoverable reaction media, and adoption of flow conditions. The intuitive quantification of *E*-factors for the procedures reported and their comparison with known protocols is helpful to offer a better comprehension of the factors that influence the minimization of the waste. Notably, the environmental issues faced by chemistry are of widely different nature, and therefore the corresponding solutions also require a holistic approach.[105] It is of primary importance to utilize all the possible information and technological strategies, with the final guidance of the green metrics, to choose the optimal solution to a specific case.

References

1. P. T. Anastas and J. B. Zimmerman, *Green Chem.*, 2019, **21**, 6545.
2. D. Griggs, M. Stafford-Smith, O. Gaffney, J. Rockström, M. C. Öhman, P. Shyamsundar, W. Steffen, G. Glaser, N. Kanie and I. Noble, *Nature*, 2013, **495**, 305.
3. S. Latouche, in *Petit traité de la décroissance sereine*, Mille et une Nuits, Paris, 2007.
4. P. T. Anastas and J. C. Warner, in *Green Chemistry: Theory and Practice*, Oxford University Press, New York, 1998.
5. P. T. Anastas, *ChemSusChem*, 2009, **2**, 391.
6. P. T. Anastas and J. B. Zimmerman, *Curr. Opin. Green Sustainable Chem.*, 2018, **13**, 150.
7. P. J. Hessop, in *Encyclopedia of Sustainable Technologies*, 1st edn, 2017, p. 611.
8. L. Vaccaro, M. Curini, F. Ferlin, D. Lanari, A. Marrocchi, O. Piermatti and V. Trombettoni, *Pure Appl. Chem.*, 2017, **90**, 21.

9. S. Santoro, S. I. Kozhushkov, L. Ackermann and L. Vaccaro, *Green Chem.*, 2016, **18**, 3471.
10. F. Valentini, G. Brufani, L. Latterini and L. Vaccaro, in *Advanced Heterogeneous Catalysts Volume 1: Applications at the Nano-Scale*, ACS publication, 2020, ch. 17, p. 513.
11. B. Altava, M. I. Burguete, E. García-Verdugo and S. V. Luis, *Chem. Soc. Rev.*, 2018, **47**, 2722.
12. S. Santoro, F. Ferlin and L. Vaccaro, in *Sustainable Approaches to C–H Functionalization through Flow Techniques*, ed. S. V. Luis and E. Garcia-Verdugo, Royal Society of Chemistry, 2019, p. 199.
13. S. Santoro, F. Ferlin, L. Ackermann and L. Vaccaro, *Chem. Soc. Rev.*, 2019, **48**, 2767.
14. F. Ferlin, D. Lanari and L. Vaccaro, *Green Chem.*, 2020, **22**, 5937.
15. F. Valentini and L. Vaccaro, *Molecules*, 2020, **25**, 5264.
16. S. Santoro, F. Ferlin, L. Luciani, L. Ackermann and L. Vaccaro, *Green Chem.*, 2017, **19**, 1601.
17. F. Gao, R. Bai, F. Ferlin, L. Vaccaro, M. Li and Y. Gu, *Green Chem.*, 2020, **22**, 6240.
18. D. T. McQuade and P. H. Seeberger, *J. Org. Chem.*, 2013, **78**, 6384.
19. J. C. Pastre, D. L. Browne and S. V. Ley, *Chem. Soc. Rev.*, 2013, **42**, 8849.
20. R. Porta, M. Benaglia and A. Puglisi, *Org. Process Res. Dev.*, 2016, **20**, 2.
21. T. Zhao, L. Micouin and R. Piccardi, *Helv. Chim. Acta*, 2019, **102**, e1900172.
22. M. Colella, A. Nagaki and R. Luisi, *Chem. - Eur. J.*, 2020, **26**, 19.
23. Z. J. Garlets, J. D. Nguyen and C. R. J. Stephenson, *Isr. J. Chem.*, 2014, **54**, 351.
24. Y. Su, N. J. W. Straathof, V. Hessel and T. Noel, *Chem. - Eur. J.*, 2014, **20**, 10562.
25. V. Hessel, D. Kralisch, N. Kockmann, T. Noel and Q. Wang, *ChemSusChem*, 2013, **6**, 746.
26. S. G. Newman and K. F. Jensen, *Green Chem.*, 2013, **15**, 1456.
27. L. Vaccaro, D. Lanari, A. Marrocchi and G. Strappaveccia, *Green Chem.*, 2014, **16**, 3680.
28. O. M. Morales-Gonzales, C. Zhang, S. Li and V. Hessel, *Chem. Eng. Sci.: X*, 2019, **3**, 100024.
29. W.-J. Yoo, H. Ishitani, Y. Saito, B. Laroche and S. Kobayashi, *J. Org. Chem.*, 2020, **85**, 5132.
30. K. Masuda, T. Ichitsuka, N. Koumura, K. Sato and S. Kobayashi, *Tetrahedron*, 2018, **74**, 1705.
31. M. Movsisyan, E. I. P. Delbeke, J. K. E. T. Berton, C. Battilocchio, S. V. Ley and C. V. Stevens, *Chem. Soc. Rev.*, 2016, **45**, 4892.
32. R. A. Sheldon, I. W. C. E. Arends and U. Hanefeld, *GC Chemistry and Catalysis*; Wiley-VCH, Weinheim, 2007.
33. *Catalyst Immobilization: Methods and Applications*, ed. M. Benaglia and A. Puglisi, Wiley-VCH, Weinheim, 2019.
34. D. Roy and Y. Uozumi, *Adv. Synth. Catal.*, 2018, **360**, 602.

35. S. Hübner, J. G. de Vries and V. Farina, *Adv. Synth. Catal.*, 2016, **358**, 3.
36. G. Rothenberg, *Catalysis: Concepts and Green Applications*, Wiley-VCH Weinheim, 2008.
37. R. A. Sheldon, *Green Chem.*, 2017, **19**, 18.
38. J. M. Asensio, D. Bouzouita, P. W. N. M. Van Leeuwen and B. Chaudret, *Chem. Rev.*, 2020, **120**, 1042.
39. A. Bavykina, N. Kolobov, I. S. Khan, J. A. Bau, A. Ramirez and J. Gascon, *Chem. Rev.*, 2020, **120**, 8468.
40. H. Wang, Y. Shao, S. Mei, Y. Lu, M. Zhang, J.-K. Sun, K. Matyjaszewski, M. Antonietti and J. Yuan, *Chem. Rev.*, 2020, **120**, 9363.
41. F. Valentini, N. Santillo, C. Petrucci, D. Lanari, E. Petricci, M. Taddei and L. Vaccaro, *ChemCatChem*, 2018, **10**, 1277.
42. E. Petricci, C. Risi, F. Ferlin, D. Lanari and L. Vaccaro, *Sci. Rep.*, 2018, **8**, 10571.
43. X. Tian, F. Yang, D. Rasina, M. Bauer, S. Warratz, F. Ferlin, L. Vaccaro and L. Ackermann, *Chem. Commun.*, 2016, **52**, 9777.
44. G. Strappaveccia, E. Ismalaj, C. Petrucci, D. Lanari, A. Marrocchi, M. Drees, A. Facchetti and L. Vaccaro, *Green Chem.*, 2015, **17**, 365.
45. T. Wagener, A. Heusler, Z. Nairoukh, K. Bergander, C. G. Daniliuc and F. Glorius, *ACS Catal.*, 2020, **10**, 12052.
46. F. Campana, B. M. Massaccesi, S. Santoro, O. Piermatti and L. Vaccaro, *ACS Sustainable Chem. Eng.*, 2020, **8**, 16441.
47. O. Jentzer and M. Guglieri, Use of esteramides as solvents, novel esteramides and process for preparing esteramides, *US Pat.*, US20140221211, 2014.
48. http://www.solvay.com/sites/g/files/srpend221/files/tridion/documents/Polarclean.pdf/, accessed 2020.
49. L. Vaccaro, S. Santoro, L. Luciani, C. Melone and F. Ferlin, *Chem. Today*, 2019, **37**, 60.
50. F. Ferlin, L. Luciani, O. Viteritti, F. Brunori, O. Piermatti, S. Santoro and L. Vaccaro, *Front. Chem.*, 2019, **6**, 659.
51. A. E. C. Collins and I. T. Horvath, *Catal. Sci. Technol.*, 2011, **1**, 912.
52. F. Ferlin, S. R. Yetra, S. Warratz, L. Vaccaro and L. Ackermann, *Chem. - Eur. J.*, 2019, **25**, 11427.
53. N. R. Candeias, L. C. Branco, P. M. P. Gois, C. A. M. Afonso and A. F. Trindade, *Chem. Rev.*, 2009, **109**, 2703.
54. L. Ackermann and R. Vicente, *Org. Lett.*, 2009, **11**, 4922.
55. T. Gensch, M. N. Hopkinson, F. Glorius and J. Wencel-Delord, *Chem. Soc. Rev.*, 2016, **45**, 2900.
56. A. Marrocchi, P. Adriaensens, E. Bartollini, B. Barkakaty, R. Carleer, J. Chen, D. K. Hensley, C. Petrucci, M. Tassi and L. Vaccaro, *Eur. Polym. J.*, 2015, **73**, 391.
57. M. Tassi, E. Bartollini, P. Adriaensens, L. Bianchi, B. Barkakaty, R. Carleer, J. Chen, D. K. Hensley, A. Marrocchi and L. Vaccaro, *RSC Adv.*, 2015, **5**, 107200.
58. V. Trombettoni, D. Sciosci, M. P. Bracciale, F. Campana, M. L. Santarelli, A. Marrocchi and L. Vaccaro, *Green Chem.*, 2018, **20**, 3222.

59. S. Mujahed, F. Valentini, S. Cohen, L. Vaccaro and D. Gelman, *ChemSusChem.*, 2019, **12**, 4693.
60. T. Verheyen, N. Santillo, D. Marinelli, E. Petricci, W. M. De Borggraeve, L. Vaccaro and M. Smet, *ACS Appl. Polym. Mater.*, 2019, **1**, 1496.
61. D. Sciosci, F. Valentini, F. Ferlin, S. Chen, Y. Gu, O. Piermatti and L. Vaccaro, *Green Chem.*, 2020, **22**, 6560.
62. F. Valentini, H. Mahmoudi, L. A. Bivona, O. Piermatti, M. Bagherzadeh, L. Fusaro, C. Aprile, A. Marrocchi and L. Vaccaro, *ACS Sustainable Chem. Eng.*, 2019, **7**, 6939.
63. F. Ferlin, A. Zangarelli, S. Lilli, S. Santoro and L. Vaccaro, *Green Chem.*, 2021, **23**, 490–495.
64. D. Cespi, E. S. Beach, T. E. Swarr, F. Passarini, I. Vassura, P. J. Dunn and P. T. Anastas, *Green Chem.*, 2015, **17**, 3390.
65. M. C. Bryan, P. J. Dunn, D. Entwistle, F. Gallou, S. G. Koenig, J. D. Hayler, M. R. Hickey, S. Hughes, M. E. Kopach, G. Moine, P. Richardson, F. Roschangar, A. Steven and F. J. Weiberthm, *Green Chem.*, 2018, **20**, 5082.
66. C. Jiménez-González, A. D. Cur-zons, D. J. C. Constable and V. L. Cunningham, *Int. J. Life Cycle Assess.*, 2004, **9**, 114.
67. P. J. Dyson and P. G. Jessop, *Catal. Sci. Technol.*, 2016, **6**, 3302.
68. D. Prat, A. Wells, J. Hayler, H. Sneddon, C. R. McElroy, S. Abou-Shehada and P. J. Dunn, *Green Chem.*, 2016, **18**, 288.
69. P. G. Jessop, *Green Chem.*, 2011, **13**, 1391–1398.
70. D. R. Snead and T. F. Jamison, *Angew. Chem., Int. Ed.*, 2015, **54**, 983.
71. S. Santoro, A. Marrocchi, D. Lanari, L. Ackermann and L. Vaccaro, *Chem. - Eur. J.*, 2018, **24**, 13383.
72. D. Prat, A. Wells, J. Hayler, H. Sneddon, C. R. McElroy, S. Abou-Shehada and P. J. Dunn, *Green Chem.*, 2016, **18**, 288.
73. P. Pongrácz, L. Kollár and L. T. Mika, *Green Chem.*, 2016, **18**, 842.
74. C. Petrucci, G. Strappaveccia, F. Giacalone, M. Gruttadauria, F. Pizzo and L. Vaccaro, *ACS Sustainable Chem. Eng.*, 2014, **2**, 2813.
75. I. Anastasiou, N. Van Velthoven, E. Tomarelli, A. Lombi, D. Lanari, P. Liu, S. Bals, D. E. De Vos and L. Vaccaro, *ChemSusChem*, 2020, **13**, 2786.
76. E. Ismalaj, G. Strappaveccia, E. Ballerini, F. Elisei, O. Piermatti, D. Gelman and L. Vaccaro, *ACS Sustainable Chem. Eng.*, 2014, **2**, 2461.
77. G. Strappaveccia, L. Luciani, E. Bartollini, A. Marrocchi, F. Pizzo and L. Vaccaro, *Green Chem.*, 2015, **17**, 1071.
78. D. Rasina, A. Kahler-Quesada, S. Ziarelli, S. Warratz, H. Cao, S. Santoro, L. Ackermann and L. Vaccaro, *Green Chem.*, 2016, **18**, 5025.
79. F. Valentini, H. Mahmoudi, L. A. Bivona, O. Piermatti, M. Bagherzadeh, L. Fusaro, C. Aprile, A. Marrocchi and L. Vaccaro, *ACS Sustainable Chem. Eng.*, 2019, **7**, 6939.
80. C. Pavia, F. Giacalone, L. A. Bivona, A. M. P. Salvo, C. Petrucci, G. Strappaveccia, L. Vaccaro, C. Aprile and M. Gruttadauria, *J. Mol. Catal. A: Chem.*, 2014, **387**, 57.
81. F. Ferlin, S. Santoro, L. Ackermann and L. Vaccaro, *Green Chem.*, 2017, **19**, 2510.

82. Y. Fujiwara, I. Moritani, R. Asano and S. Teranishi, *J. Am. Chem. Soc.*, 1969, **91**, 7166.
83. D. Rasina, A. Lombi, F. Ferlin, S. Santoro and L. Vaccaro, *Green Chem.*, 2016, **18**, 6380.
84. V. Kozell, M. McLaughlin, G. Strappaveccia, S. Santoro, L. A. Bivona, C. Aprile, M. Gruttadauria and L. Vaccaro, *ACS Sustainable Chem. Eng.*, 2016, **4**, 7209.
85. V. Kozell, T. Giannoni, M. Nocchetti, R. Vivani, O. Piermatti and L. Vaccaro, *Catalysts*, 2017, **7**, 186.
86. F. Ferlin, M. Cappelletti, R. Vivani, M. Pica, O. Piermatti and L. Vaccaro, *Green Chem.*, 2019, **21**, 614.
87. F. Ferlin, T. Giannoni, A. Zuliani, O. Piermatti, R. Luque and L. Vaccaro, *ChemSusChem*, 2019, **12**, 3178.
88. G. Li, N. Li, M. Zheng, S. Li, A. Wang, Y. Cong, X. Wang and T. Zhang, *Green Chem.*, 2016, **18**, 3607.
89. F. Ferlin, V. Trombettoni, L. Luciani, S. Fusi, O. Piermatti, S. Santoro and L. Vaccaro, *Green Chem.*, 2018, **20**, 1634.
90. Y. Hayashi, *J. Org. Chem.*, 2021, **86**, 1.
91. R. L. Hartman, *Curr. Opin. Chem. Eng.*, 2020, **29**, 42.
92. M. B. Plutschack, B. Pieber, K. Gilmore and P. H. Seeberger, *Chem. Rev.*, 2017, **117**, 11796.
93. C. Wiles and P. Watts, *Green Chem.*, 2014, **16**, 55.
94. A. C. Bedard, A. Adamo, K. C. Aroh, M. G. Russell, A. A. Bedermann, J. Torosian, B. Yue, K. F. Jensen and T. F. Jamison, *Science*, 2018, **361**, 1220.
95. D. Dallinger, B. Gutmann and C. O. Kappe, *Acc. Chem. Res.*, 2020, **53**, 1330.
96. M. Brzozowski, M. O'Brien, S. V. Ley and A. Polyzos, *Acc. Chem. Res.*, 2015, **48**, 349.
97. K. P. Cole, J. M. Groh, M. D. Johnson, C. L. Burcham, B. M. Campbell, W. D. Diseroad, M. R. Heller, J. R. Howell, N. J. Kallman, T. M. Koenig, S. A. May, R. D. Miller, D. Mitchell, D. P. Myers, S. S. Myers, J. L. Phillips, C. S. Polster, T. D. White, J. Cashman, D. Hurley, R. Moylan, P. Sheehan, R. D. Spencer, K. Desmond, P. Desmond and O. Gowran, *Science*, 2017, **356**, 1144.
98. S. A. May, M. D. Johnson, J. Y. Buser, A. N. Campbell, S. A. Frank, B. D. Haeberle, P. C. Hoffman, G. R. Lambertus, A. D. McFarland, E. D. Moher, T. D. White, D. D. Hurley, A. P. Corrigan, O. Gowran, N. G. Kerrigan, M. G. Kissane, R. R. Lynch, P. Sheehan, R. D. Spencer, S. R. Pulley and J. R. Stout, *Org. Process Res. Dev.*, 2016, **20**, 1870.
99. C. Wiles and P. Watts, *Green Chem.*, 2014, **16**, 55.
100. F. Ferlin, P. M. L. Navarro, Y. Gu, D. Lanari and L. Vaccaro, *Green Chem.*, 2020, **22**, 397.
101. F. Ferlin, A. Marini, N. Ascani, L. Ackermann, D. Lanari and L. Vaccaro, *ChemCatChem*, 2020, **12**, 449.
102. F. Ferlin, M. K. Van der Hulst, S. Santoro, D. Lanari and L. Vaccaro, *Green Chem.*, 2019, **21**, 5298.

103. H. Mahmoudi, F. Valentini, F. Ferlin, L. A. Bivona, I. Anastasiou, L. Fusaro, C. Aprile, A. Marrocchi and L. Vaccaro, *Green Chem.*, 2019, **21**, 355.
104. F. Ferlin, L. Luciani, S. Santoro, A. Marrocchi, D. Lanari, A. Bechtoldt, L. Ackermann and L. Vaccaro, *Green Chem.*, 2018, **20**, 2888.
105. R. A. Sheldon, *ACS Sustainable Chem. Eng.*, 2018, **6**, 32.

CHAPTER 17

Step Economy

LVQI JIANG[a] AND WENBIN YI*[a]

[a]School of Chemical Engineering, Nanjing University of Science and Technology, Nanjing, China
*E-mail: yiwb@njust.edu.cn

17.1 Introduction to Step Economy

Organic synthesis plays an important role in preparing compounds and materials with desirable physical, chemical, and biological utilities. It involves many green chemistry topics, such as waste prevention, renewable feedstocks, alternative solvents, catalysis, safety, toxicity, energy, and efficiency. Among them, synthetic efficiency is especially important from both green chemistry and economic considerations.

Pot, atom, and step economy synthesis is an important tool for achieving high synthetic efficiency, and has intrinsic advantages in terms of efficiency by being easy in operation, saving energy and effort, and producing minimal amount of waste. In this chapter, we focus on introducing two types of step economy synthesis: cascade reactions (Figure 17.1) and multicomponent reactions (Figure 17.2). These two methods have similar reaction processes. Both of them are conducted in a single reaction vessel. Once the initial reaction starts, there will be no addition of new reactants or changing of conditions during the reaction. The major difference is that in multicomponent reactions, three or more reactants are added together at the beginning of the reaction.

The development of step economy synthesis is an active topic in organic synthesis. Organofluorine chemistry has been considered as "a hot topic" for more than 35 years and demand for fluorinated molecules continues to

Sustainable Organic Synthesis: Tools and Strategies
Edited by Stefano Protti and Alessandro Palmieri

Published by the Royal Society of Chemistry, www.rsc.org

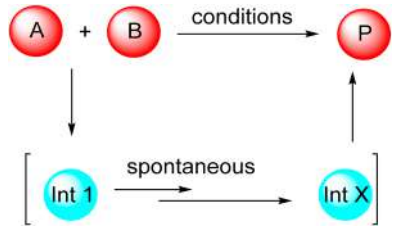

Figure 17.1 Schematic diagram of cascade reactions.

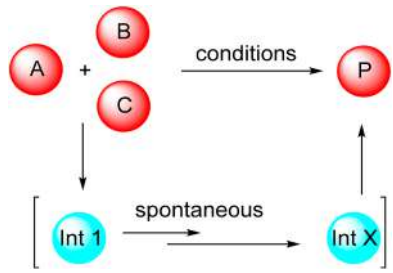

Figure 17.2 Schematic diagram of multicomponent reactions.

grow at a tremendous speed. This is because the properties of drug molecules, including fat solubility, metabolic stability, and biological activities, such as drug absorption, distribution, and donor–receptor interaction, can be significantly altered by the introduction of one or a small number of fluorine substituents.[1] Several monographies and numerous reviews about step economy have been published in recent years; however, there is no special introduction to organofluorine chemistry. Presented in this chapter are selective examples of the application of step economy synthesis in organofluorine chemistry.

17.2 Cascade Reactions

17.2.1 Introduction

In a cascade reaction process, sequential transformations take place spontaneously after the initial reaction. No new reagents or catalysts are introduced during the reactions and the reactive intermediates are usually not isolatable. Free radical reactions are the most common type of cascade reaction. Thus, a radical trapping agent can be used to quench a cascade radical reaction. In organofluorine chemistry, trifluoromethylation and trifluoromethylthiolation reactions are the two most common types of free radical reactions. Covered in this section are examples of trifluoromethylation and trifluoromethylthiolation reactions that involve less than three components.

17.2.2 Trifluoromethylation Reaction

Among the prevalent fluorine-containing moieties, the CF_3 group is the most studied and used one due to its high lipophilicity and electron-withdrawing character. Trifluoromethyl radicals can be generated from various trifluoromethylthiolation reagents, including Togni's reagent, $TMSCF_3$, CF_3I, CF_3SO_2Na, *etc.* Presented in this section are examples of radical trifluoromethylation reactions based on different trifluoromethylthiolation reagents.

Tu's group reported a free radical trifluoromethyl addition/half-pinacol rearrangement of allylic alcohols by using Togni's reagent (Scheme 17.1), which is a new and effective method to simultaneously construct a quaternary carbon center and Csp^3-CF_3 bond.[2] Togni's reagent is firstly catalyzed by copper to initiate CF_3 free radicals, and then the CF_3 free radicals attack the olefin double bond of **1** to produce intermediate **2**. Intermediate **2** is spatially conducive to 1,2-migration to produce intermediate **3**, which would produce product 4 upon further single electron transfer (SET) oxidation.

Shi's research group reported on the copper-catalyzed free radical trifluoromethyl addition/cyclization reaction of *N*-allylbenzenesulfonamide compounds with Togni's reagent, and a series of 1,2-benzothiazine dioxides were obtained, which are important structural fragments in the structure of drugs (Scheme 17.2).[3] The reaction starts with the addition of trifluoromethyl radicals and allyl double bonds, and the resulting radical intermediates are then functionalized with intramolecular C–H radicals. Then, the ring is closed to obtain the final benzo\thiazine products. At the beginning of this transformation, a single electron transfer (SET) process takes place between the Cu(I) catalyst and Togni's reagent II to generate a Cu(II) complex and a trifluoromethyl radical species, which reacts with the alkene substrate **5** to form a radical intermediate **6**, followed by a cyclization with the sulfonyl benzene ring to give another radical intermediate **7**. After aromatization, the trifluoromethylated cyclization product **8** is formed.

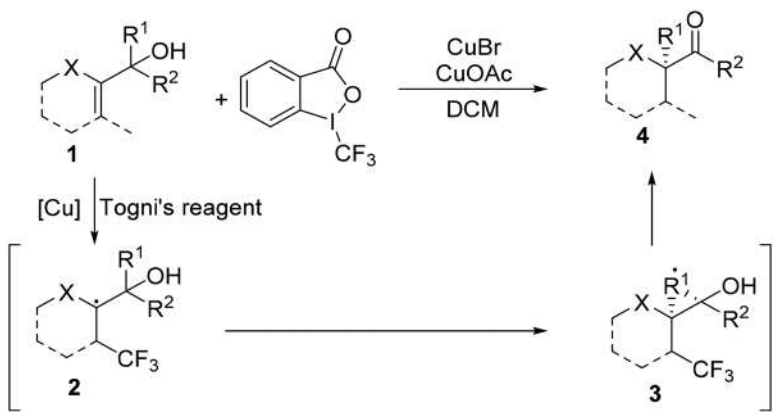

Scheme 17.1 Copper-catalyzed tandem trifluoromethylation/semipinacol rearrangement of allylic alcohols.

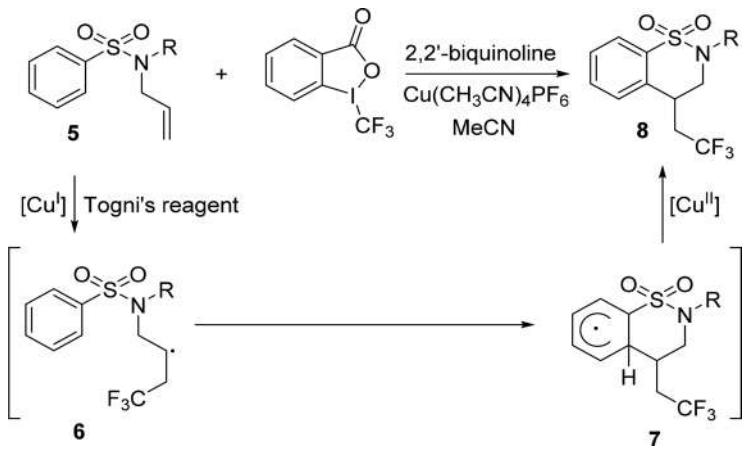

Scheme 17.2 Copper-catalyzed trifluoromethylation and cyclization of aromatic-sulfonyl-group-tethered alkenes.

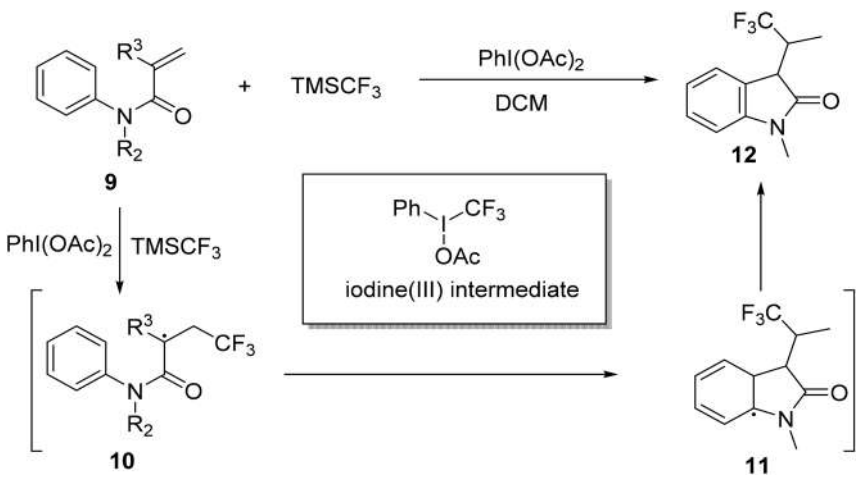

Scheme 17.3 Synthesis to CF_3-containing oxindoles by $PhI(OAc)_2$-mediated trifluoromethylation of *N*-arylacrylamides with $TMSCF_3$.

Zou's research developed a mild and efficient method for the construction of oxindoles bearing a trifluoromethyl group through oxidative trifluoromethylation of *N*-arylacrylamides with the use of $TMSCF_3$ under metal-free conditions (Scheme 17.3).[4] Initially, PIDA (phenyliodonium diacetate) reacts with $TMSCF_3$ to give an iodine(III) intermediate upon release of TMSOAc. The following homolysis generates a hypervalent iodine(III) centred radical and the $^{\bullet}CF_3$ radical. Subsequently, the addition of the $^{\bullet}CF_3$ radical to *N*-arylacrylamide **9** generates alkyl radical **10**, followed by an intramolecular

radical cyclization to give cyclized radical intermediate **11**. A single-electron oxidation of intermediate **11** by the iodine intermediate forms a cyclohexadienyl cation, which undergoes dehydrogenation to give product **12**.

In 2012, Zakarian *et al.* reported a ruthenium-catalyzed trifluoromethylation of *N*-acyloxazolidinone with the use of CF_3I (Scheme 17.4).[5] The authors speculated that the reaction mechanism was as follows: Firstly, *N*-acyl oxazolidinone **13** is attacked by the coordination of Lewis acid $ZrCl_4$ with two carbonyl groups. A proton capture then occurs under the action of Et_3N form the zirconium enolate intermediate **14**. At the same time, CF_3I is reduced by Ru^{II} to form trifluoromethyl radicals ($^{\bullet}CF_3$), and the ruthenium catalyst is oxidized to form trivalent ruthenium species. Next, the trifluoromethyl radical undergoes a stereospecific reaction under the influence of the chiral oxazolidinone auxiliary agent to form a trifluoromethyl-containing radical intermediate **15**, which is probably better represented by the resonance form **16**. The ruthenium catalyst is recovered by a SET process from intermediate **16** to form the final product **17**.

In 2013, Maiti's group discovered a direct, efficient, and general method to access CF_3-substituted ketones by using CF_3SO_2Na (Scheme 17.5).[6] Wide functional-group tolerance, mild reaction conditions, and the use of an inexpensive trifluoromethylation reagent are the key features of this reaction. The research team speculated that trifluoromethyl radicals could be generated in the presence of CF_3SO_2Na, Ag(I) and $K_2S_2O_8$. X-ray photoelectron spectroscopy (XPS) confirmed the formation of Ag^0 in the reaction mixture.

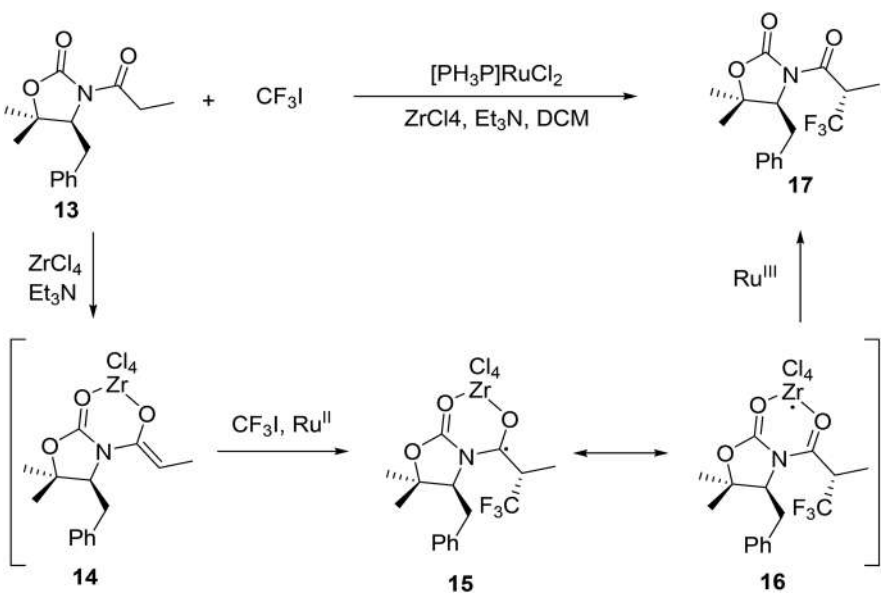

Scheme 17.4 Asymmetric trifluoromethylation of *N*-acyl oxazolidinones *via* Ru-catalyzed radical addition to zirconium enolates.

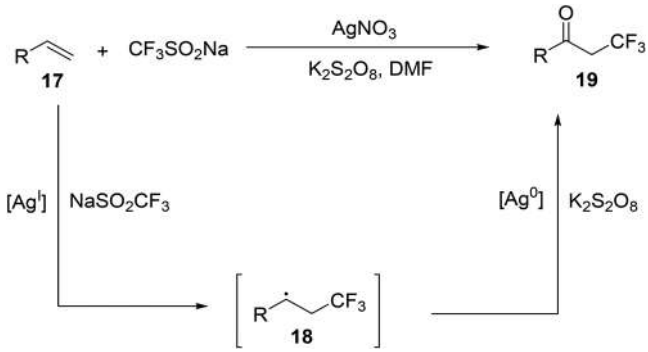

Scheme 17.5 Synthesis of α-trifluoromethyl-substituted ketones by using CF_3SO_2Na.

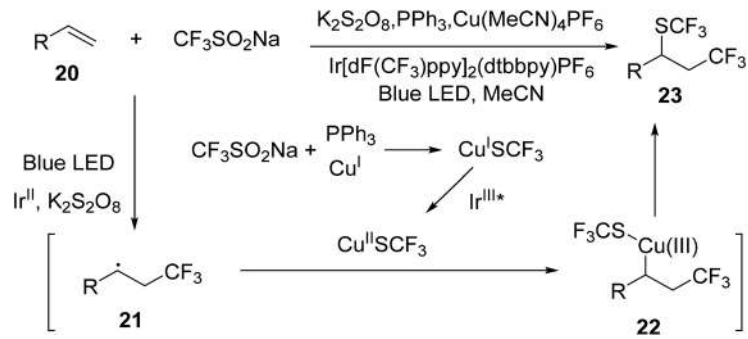

Scheme 17.6 Photocatalyzed trifluoromethylthio-trifluoromethylation of alkenes with CF_3SO_2Na.

Then trifluoromethyl radicals attack olefins **17** to form transition state **18,** and finally form a $-CF_3$ substituted ketone **19** through oxidation with O_2. An ^{18}O labelling experiment confirmed that both air and $K_2S_2O_8$ can be the source of oxygen atoms in ketones. Based on these studies, a catalytic cycle involving Ag^I/Ag^0 has been proposed.

Very recently, our group reported a photocatalyzed trifluoromethylthio-trifluoromethylation of alkenes with CF_3SO_2Na (Scheme 17.6).[7] The highlight of this work is that CF_3SO_2Na is used as both the CF_3 and SCF_3 source. A series of vicinal trifluoromethylthiotrifluoromethylated compounds were successfully synthesized, and late-stage modification based on this new method was also proved to be feasible.

Mechanistic investigations indicated that a photocatalyzed dual-oxidative process was involved in the reaction. Firstly, excited state species $Ir^{III}*$ is generated under visible-light irradiation. Then, single-electron transfer (SET) between the $Ir^{III}*$ complex and CF_3SO_2Na results in the trifluoromethyl radical $CF_3^{\bullet}$ and Ir^{II} species. The trifluoromethyl radical reacts with alkyenes

20 to generate a radical intermediate **21**. At the same time, $Cu^{I}SCF_3$ is also generated *in situ* in the presence of CF_3SO_2Na, PPh_3 and copper(I), and then oxidized to a Cu^{II} species by the Ir^{III}* through single-electron transfer. The intermediate **21** then undergoes single-electron oxidative addition to form Cu^{III} intermediate **22**. Finally, reductive elimination from intermediate **22** would yield the desired product **23**.

17.2.3 Trifluoromethylthiolation Reaction

The trifluoromethylthio (SCF_3) group has attracted increasing attention because of its special biological properties, such as enhancement of membrane permeability and absorption rate and improvement of the stability of parent molecules, due to its high electronegativity and lipophilicity.[8] Compared with nucleophilic and electrophilic trifluoromethylthiolation reagents, the $F_3CS^{\bullet}$ radical-type pathway remains less explored. Presented in this section are examples of radical trifluoromethylthiolation reactions based on the most commonly used radical trifluoromethylthiolation reagent $AgSCF_3$, and $AgSCF_3/K_2S_2O_8$ is the most reported system to produce SCF_3 radicals.

A general method to form a $C(SP^3)$–SCF_3 bond *via* copper-mediated oxidative trifluoromethylthiolation of unactivated alkenes with stable nucleophilic $AgSCF_3$ was developed (Scheme 17.7).[9]

The SCF_3 radical produced by $AgSCF_3$ attacks alkyenes **24** to afford intermediate **25**, which could be further oxidized to form cation intermediate **26** through a single electron transfer (SET) process by $Cu(OAc)_2/K_2S_2O_8$. Then intermediate **26** undergoes deprotonation to give the desired trifluoromethylthiolated allylic products **27**.

A mild and convenient oxidative radical cyclization of aryl alkynoate esters for the synthesis of 3-trifluoromethylthiolated and 3-thiocyanated coumarins has been developed (Scheme 17.8).[10] Initially, the $AgSCF_3/K_2S_2O_8$ system generates SCF_3 radicals. Regio-selective addition of the F_3CS to **28** affords vinyl radical **29**, followed by an intramolecular cyclization, which gives radical intermediate **30**. **30** is further oxidized by Ag^{II} to form intermediate **31**. Finally, a deprotonation yields the final product **32**.

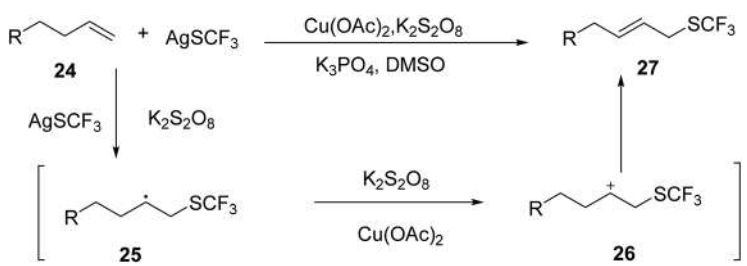

Scheme 17.7 Copper-mediated oxidative trifluoromethylthiolation of unactivated terminal alkenes.

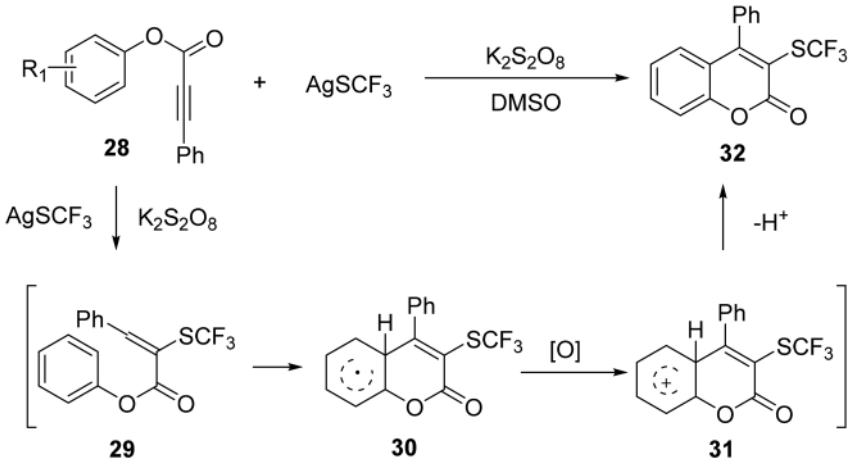

Scheme 17.8 Direct radical trifluoromethylthiolation and thiocyanation of aryl alkynoate esters.

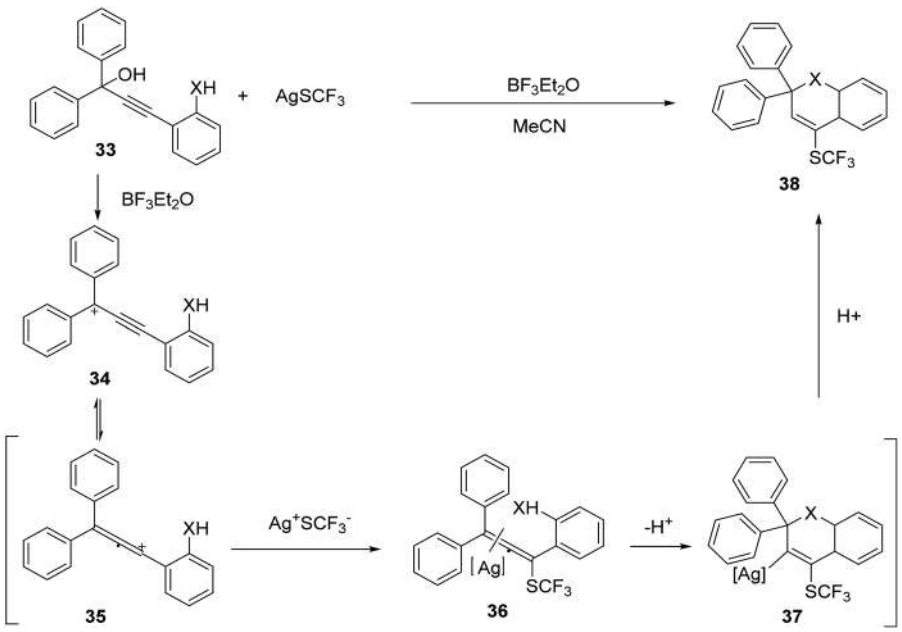

Scheme 17.9 $BF_3{\cdot}OEt_2$–$AgSCF_3$-mediated trifluoromethylthiolation/cascade cyclization of propynols.

$BF_3{\cdot}OEt_2$–$AgSCF_3$-mediated direct trifluoromethylthiolation/cascade cyclization of propynols involving the SCF_3 anion nucleophilic pathway was developed (Scheme 17.9).[11] Initially, **33** is activated by $BF_3{\cdot}OEt_2$ and generates propargylic cation **34.** Subsequently, tautomerism of **34** affords allenic cation **35,** which is attacked by the SCF_3 anion affording intermediate **36.**

Activated by Ag(I) species or a proton, intermediate **36** could give intermediate **37**. Then, the desired product **38** is obtained through a subsequent intramolecular endo attack of the phenolic hydroxy group followed by protonation.

A protocol for the elusive cyanotrifluoromethylthiolation of unactivated olefins has been described (Scheme 17.10).[12] Initially, SCF_3 radicals, which were generated by the interaction of $AgSCF_3$ and $K_2S_2O_8$, were added to the olefin part of **39** to form the alkyl radical **40**. Then, the intramolecular interception of the alkyl radical affords the iminium radical **41** *via* a five-membered transition state. Homolysis of the cyclic C–C bond of **41** led to the cyano-migrated intermediate **42**, which was then oxidised by $K_2S_2O_8$ or Ag species to generate the cation intermediate **43**. Finally, **43** furnishes the product **44** after deprotonation.

An example of $AgSCF_3$-mediated oxidative radical trifluoromethylthiolation of α,α-diaryl allylic alcohols has been presented (Scheme 17.11).[13] Firstly,

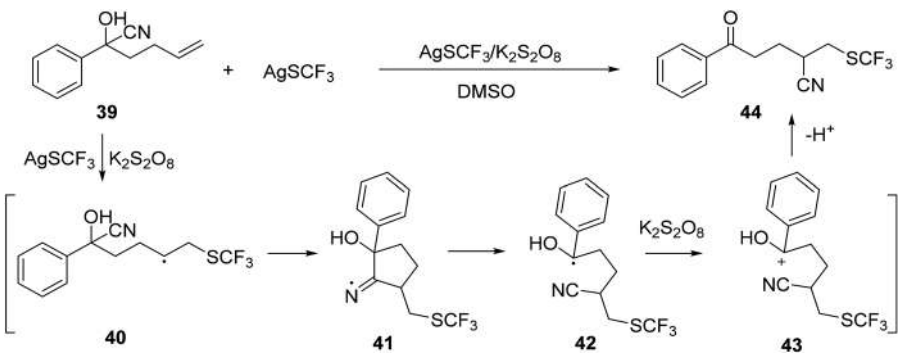

Scheme 17.10 Cyanotrifluoromethylthiolation of unactivated olefins through intramolecular cyano migration.

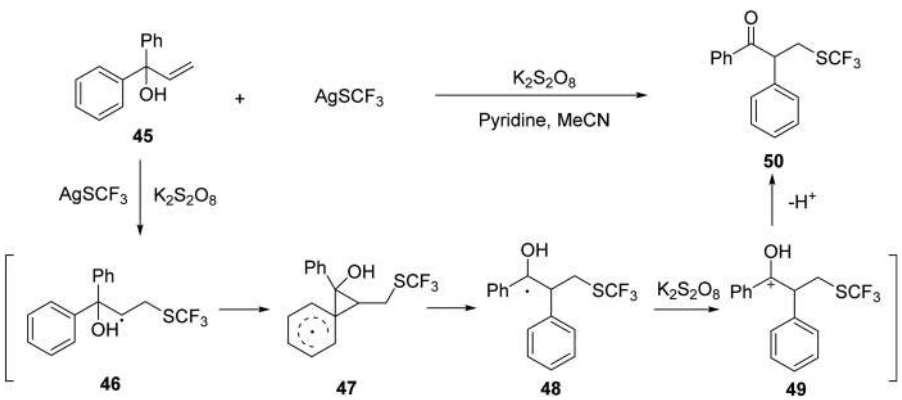

Scheme 17.11 $AgSCF_3$-mediated trifluoromethylthiolation of α,α-diaryl allylic alcohols.

the SCF_3 radical adds to the double bond of allylic alcohol **45** to afford the radical intermediate **46**. Within radical intermediate **46**, half pinacol rearrangement of the aryl group occurs *via* spiro octadienyl radical **47** to produce another radical intermediate **48**. Subsequent single electron transfer from intermediate **48** generates intermediate **49**, which then affords final product **50** by release of a proton.

17.3 Multicomponent Reactions

17.3.1 Introduction

Multicomponent reactions involve three or more components added together at the beginning of the reaction. Most components of the reactants are incorporated into the product structure. No additional reactants or catalysts are introduced during the reaction. The processes of the multicomponent reactions are similar to cascade reactions, except that the former ones involve more than two components.

Multicomponent reactions are also widely used in organic synthesis. Presented in this chapter are two classic types of multicomponent reactions in organofluorine chemistry: (1) construction of fluorine-containing functional groups involving difluorocarbene and (2) fluorinated functionalization of carbon–carbon unsaturated bonds.

17.3.2 Construction of Fluorine-Containing Functional Groups Involving Difluorocarbene

Difluorocarbene ($:CF_2$) has served as a versatile intermediate and the transformations of difluorocarbene have proved to be quite efficient for fluorine incorporation.[14] In recent years, difluorocarbene has been reported to be used to construct various fluorine-containing functional groups. Selected recent examples of the construction of a difluoromethyl group (CF_2H), trifluoromethyl group (CF_3), difluoromethylthio group (SCF_2H), trifluoromethylthio group (SCF_3), trifluoromethylseleno group ($SeCF_3$) and trifluoromethoxyl group (OCF_3) involving difluorocarbene are presented in this section.

Zhang developed a palladium-catalyzed direct difluoromethylation method for coupling $ClCF_2H$ with aryl boronic acids and esters to efficiently generate difluoromethylated aromatics (Scheme 17.12).[15] This reaction shows a very wide range of substrates and has been used for the difluoromethylation of a range of drugs and biologically active compounds. This reaction involves a difluorocarbene process. The author proposed two possible reaction pathways: the Pd(II/II) catalytic cycle (path a) and Pd(0/II) catalytic cycle (path b). In both routes, difluorochloromethane first produces difluorocarbene under alkaline conditions, and then in path a, difluorocarbene is combined with divalent palladium complexes and aryl boronic acid to produce the intermediate $[XPd^{II}(L_n)CF_2Ar]$ (**51**). This intermediate can easily produce the final product **53**. In path b, the difluorocarbene and palladium^0 catalyst obtain

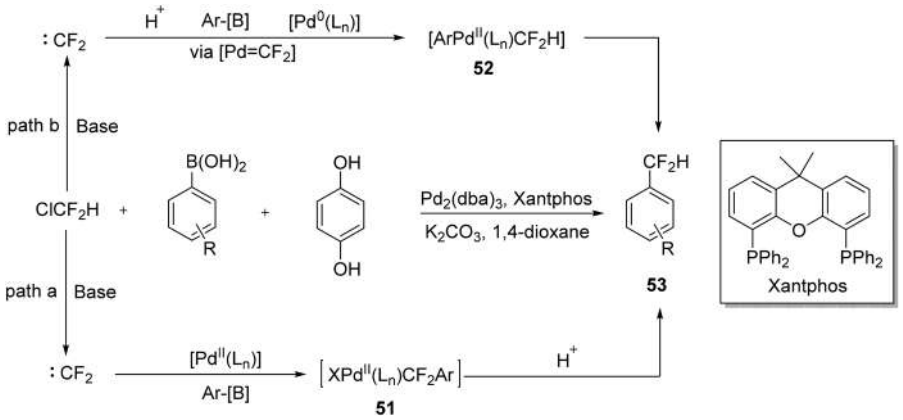

Scheme 17.12 Chlorodifluoromethane-triggered formation of difluoromethylated arenes catalyzed by palladium.

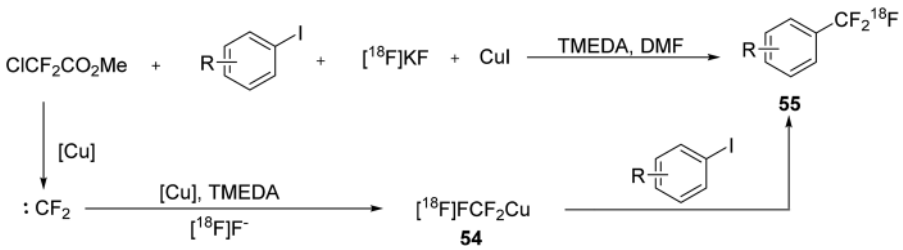

Scheme 17.13 [^{18}F]trifluoromethylation of aryl and heteroaryl iodides.

the intermediate [$ArPd^{II}(L_n)CF_2H$] (**52**) through the process of the difluorocarbene palladium complex, and finally undergo a reduction and elimination reaction to produce the desired product **53**.

The Passchier group described a no-carrier added multicomponent method for [^{18}F] trifluoromethylation, which can easily and efficiently realize aromatic and heteroaromatic systems (Scheme 17.13).[16] The key intermediate, [^{18}F]FCF_2Cu, is generated *in situ* from methyl difluorochloroacetate, CuI, TMEDA and [^{18}F]fluorine. Difluorocarbene was firstly generated from methyl difluorochloroacetate, and then fluorinated by [^{18}F]F^- and next captured by copper iodide to obtain intermediate **54**. Finally, the *in situ* [^{18}F]FCF_2Cu reacts with aryl or heteroaryl iodide and releases [^{18}F]-labelled trifluoromethyl (hetero)arene product **55**.

The Xiao group has described the synthesis of SCF_2H-substituted heterocycles from *o*-phenylenediamines *via* a tandem cyclization/difluoromethylation process (Scheme 17.14).[17] First, the PDFA/S_8 system generates thiocarbonyl fluoride, and diamine **56** undergoes cyclization reaction with its intermediate thiocarbonyl fluoride or isothiocyanate to obtain thiourea **57**.

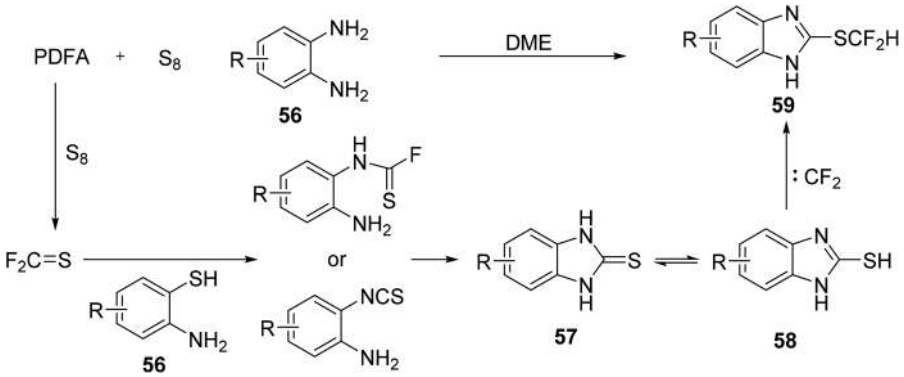

Scheme 17.14 Reaction of thiocarbonyl fluoride formed from difluorocarbene with amines.

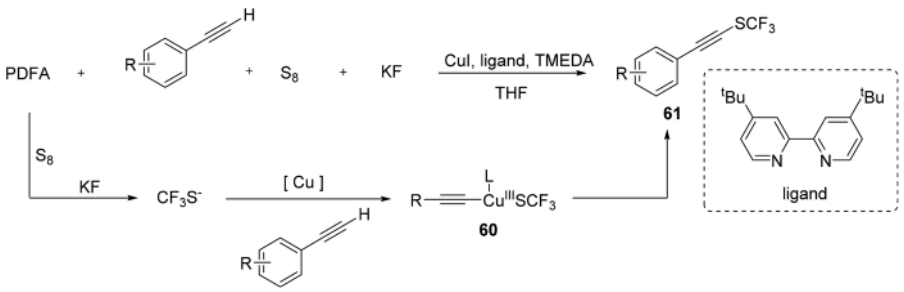

Scheme 17.15 Difluorocarbene-based trifluoromethylthiolation of terminal alkynes.

The aromatization of thiourea **57** will produce thiol **58**, and it will be difluoromethylated to obtain the final product **59** *via* difluorocarbene produced by PDFA.

A trifluoromethylthiolation reaction of terminal alkynes based on difluorocarbene was also reported by Xiao's group, which can construct C_{sp}-SCF_3 bonds through copper complexes without trifluoromethylthiolation reagents (Scheme 17.15).[18] The CF_3S^- anion is formed by the $Ph_3P^+CF_2CO_2^-/S_8/F^-$ system, and then the Cu^ISCF_3 (**60**) complex is formed with the copper center. Subsequently, the coordination of the terminal alkyne with Cu^ISCF_3 (**60**) increases the acidity of the terminal proton. It is easy to deprotonate to obtain copper acetylene, and finally S_8 oxidizes Cu^I to Cu^{III}, and produces the final product (**61**) through reduction and elimination reaction.

In 2019, Xiao's group described the trifluoromethylselenylation of benzyl halides using the $Ph_3P^+CF_2CO_2^-/Se/F^-$ system, which involves the difluorocarbene process (Scheme 17.16).[19] This is the first trifluoromethylselenylation involving CF_3Se^- anions, a key intermediate for the formation of an

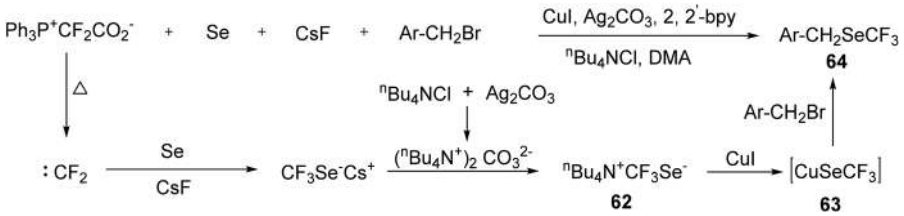

Scheme 17.16 Difluorocarbene-derived trifluoromethylselenolation of benzyl halides.

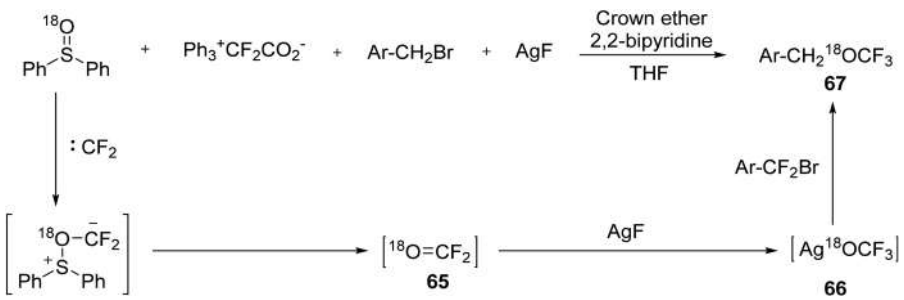

Scheme 17.17 Oxidation of difluorocarbene and subsequent trifluoromethoxylation.

external fluoride. The author believes that difluorocarbene is first captured by elemental selenium to form selenocarbonyl fluoride (CF_2=Se), which is an electrophile that will be immediately attacked by fluoride ions to obtain trifluoromethylselenide anion CF_3Se^-. The CF_3Se^- anion can be stabilized by $^nBu_4N^+$ to form another intermediate [$^nBu_4N^+CF_3Se^-$] (**62**), and finally coordinated with monovalent copper to form a key intermediate $CuSeCF_3$ (**63**), which can easily convert the benzyl halides into the final product **64.**

Xiao pointed out that difluorocarbene can be oxidized smoothly to form carbonyl fluoride, and this process was confirmed by successful trifluoromethoxylation, ^{18}O trifluoromethoxylation, the observation of $AgOCF_3$ species and DFT calculations (Scheme 17.17).[20] Among them, $Ph_2S=^{18}O$ is used as an oxidant to convert difluorocarbene into $CF_2=^{18}O$ (**65**), and then carbonyl fluoride (**65**) reacts with silver fluoride to form an important intermediate $Ag^{18}OCF_3$ (**66**), which then reacted with benzyl halides to obtain the desired trifluoromethoxylated or ^{18}O trifluoromethoxylated product **67**.

17.3.3 Fluorinated Functionalization of Carbon–Carbon Unsaturated Bonds

Due to the prevalence of C=C bonds in biomedically and synthetically relevant molecules,[21] catalytic difunctionalization of alkenes has attracted great attention from synthetic methodology.[22] Due to the unique properties of

fluorine-containing moieties, fluoroalkylation-involved difunctionalization of alkenes has been widely investigated, resulting in diverse tools to generate complex molecules with various functional groups.[23]

In 2017, Song reported a thiotrifluoromethylation of terminal alkenes (Scheme 17.18).[24] The mechanistic studies suggested that this reaction undergoes an untraditional reductive quenching cycle. In this reaction, CF_2SO_2Na was first initiated by a photocatalyst to generate CF_3 radicals, which then attacked alkenes to generate radical intermediate **68.** Next, the photoredox catalyst reduces the carbon radical generated from the addition of the CF_3 radical onto the alkene into a carbanion **69.** Finally, benzenesulfonothioates, which are good electrophiles are easily attacked by the carbanion to get the final products **70.**

In 2016, Munetaka Akita first used Hu reagent (**71**) as a radical difluoromethylation precursor under photocatalysis conditions (Scheme 17.19).[25] CF_2H radicals attack the C–C double bond to generate **72**, which is then

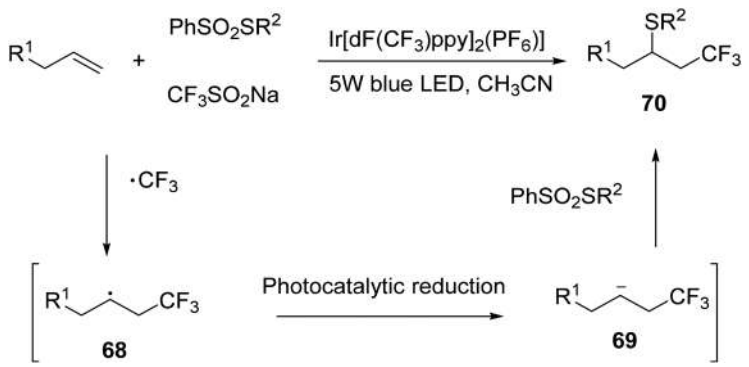

Scheme 17.18 Photocatalytic thiotrifluoromethylation of terminal alkenes.

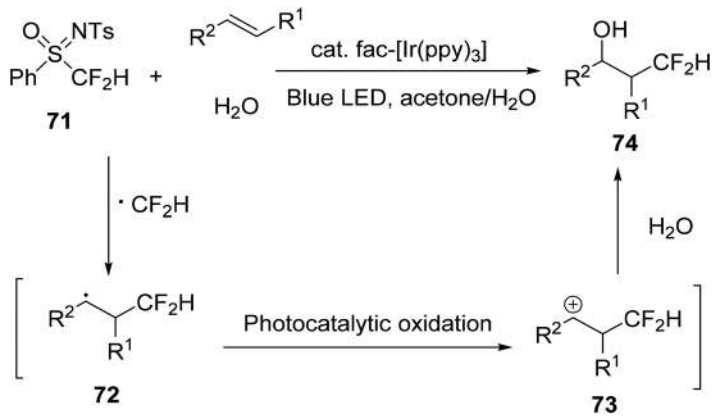

Scheme 17.19 Photocatalytic hydroxydifluoromethylation of alkenes.

oxidized by the strongly oxidizing species Ir^{IV} to generate a $-CF_2H$ carbocationic intermediate **73**. Finally, the carbocationic intermediate **73** undergoes solvolysis by H_2O to produce hydroxydifluoromethylated products **74**.

17.4 Conclusion

The step economy synthesis processes presented in this chapter, including cascade reactions and multicomponent reactions, have intrinsic efficiency due to being simple in operation and short in reaction time, using less energy, saving resources, and reducing waste by eliminating intermediate separations. As a powerful tool in the synthetic toolbox, step economy synthesis together with other green synthetic methods will play more important roles in the synthesis of complex organic molecules with biological interests and other utilities.

List of Abbreviations

DCM	Dichloromethane
DMF	Dimethylformamide
DMSO	Dimethyl sulfoxide
DME	Ethylene glycol dimethyl ether
THF	Tetrahydrofuran
TMS	Trimethylsilyl

References

1. I. Ojima, *Fluorine in Medicinal Chemistry and Chemical Biology*, Wiley-VCH, Chichester, UK, 2009.
2. Z. M. Chen, W. Bai, S. H. Wang, B. M. Yang, Y.-Q. Tu and F. M. Zhang, *Angew. Chem., Int. Ed.*, 2013, **52**, 9781.
3. X. Dong, R. Sang, Q. Wang, X. Y. Tang and M. Shi, *Chem. - Eur. J.*, 2013, **19**, 16910.
4. W. Fu, F. Xu, Y. Fu, C. Xu, S. Li and D. Zou, *Eur. J. Org. Chem.*, 2014, **4**, 709.
5. A. T. Herrmann, L. L. Smith and A. Zakarian, *J. Am. Chem. Soc.*, 2012, **134**, 6976.
6. A. Deb, S. Manna, A. Modak, T. Patra, S. Maity and D. Maiti, *Angew. Chem., Int. Ed.*, 2013, **52**, 9747.
7. S. S. Liang, J. J. Wei, L. Q. Jiang, J. Liu, Y. Mumtaz and W. B. Yi, *CCS Chem.*, 2021, **3**, 265.
8. F. Leroux, P. Jeschke and M. Schlosser, *Chem. Rev.*, 2005, **105**, 827.
9. K. Zhang, J. B. Liu and F. L. Qing, *Chem. Commun.*, 2014, **50**, 14157.
10. Y. F. Zeng, D. H. Tan, Y. Y. Chen, W. X Lv, X. G. Liu, Q. J. Li and H. G. Wang, *Org. Chem. Front.*, 2015, **2**, 1511.
11. Y. F. Qiu, X. R Song, M. Li, X. Y. Zhu, A. Q. Wang, F. Yang, Y. P. Han, H. R. Zhang, D. P. Jin, Y. X. Li and Y. M. Liang, *Org. Lett.*, 2016, **18**, 1514.

12. M. S. Ji, Z. Wu, J. J. Yu, X. B. Wan and C. Zhu, *Adv. Synth. Catal.*, 2017, **359**, 1959.
13. K. Liu, Q. Jin, Sh. Chen and P. N. Liu, *RSC Adv.*, 2017, **7**, 1546.
14. A. D. Dilman and V. V. Levin, *Acc. Chem. Res.*, 2018, **51**, 1272.
15. Z. Feng, Q. Q. Min, X. P. Fu, L. An and X. G. Zhang, *Nat. Chem.*, 2017, **9**, 918.
16. M. Huiban, M. Tredwell, S. Mizuta, Z. H. Wan, X. M. Zhang, T. L. Collier, V. Gouverneur and J. Passchier, *Nat. Chem.*, 2013, **5**, 941.
17. J. Yu, J. H. Lin and J. C. Xiao, *Angew. Chem., Int. Ed.*, 2017, **56**, 16669.
18. G. W. He, Y. H. Jiang, X. Xiao, J. H. Lin, X. Zheng, R. B. Du, Y. C. Cao and J. C. Xiao, *J. Fluorine Chem.*, 2020, **230**, 109437.
19. X. L. Chen, S. H. Zhou, J. H. Lin, Q. H. Deng and J. C. Xiao, *Chem. Commun.*, 2019, **55**, 1410.
20. J. Yu, J. H. Lin, D. H. Yu, R. B. Du and J. C. Xiao, *Nat. Commun.*, 2019, **10**, 5362.
21. J. Y. W. Mak, R. H. Pouwer and C. M. Williams, *Angew. Chem., Int. Ed.*, 2014, **53**, 13664.
22. G. Yin, X. Mu and G. Liu, *Acc. Chem. Res.*, 2016, **49**, 2413–2423.
23. C. Alonso, E. Martínez de Marigorta, G. Rubiales and F. Palacios, *Chem. Rev.*, 2015, **115**, 1847–1935.
24. W. Kong, H. An and Q. Song, *Chem. Commun.*, 2017, **53**, 8968.
25. Y. Arai, R. Tomita, G. Ando, T. Koike and M. Akita, *Chem. - Eur. J.*, 2016, **22**, 1262.

CHAPTER 18

Microwave Irradiation

SAMUELE MARAMAI[a] AND MAURIZIO TADDEI*[a]

[a]Dipartimento di Biotecnologie, Chimica e Farmacia, Università degli Studi di Siena, Via A. Moro 2, 53100 Siena, Italy
*E-mail: maramai@unisi.it, maurizio.taddei@unisi.it

18.1 Introduction to Microwaves

18.1.1 History and Theory

Using microwaves (MWs) in organic chemistry has represented a major breakthrough for synthetic methodologies and performances. Deep changes were introduced to the way a chemical route is conceived, opening up the possibility to explore new processes for faster, cleaner and higher yielding reactions. MWs allow energy to be directly transferred to the reactive species with an efficient rise of the temperature, which can be counteracted by the activation of a simultaneous cooling system, in order to perform cool MW-enhanced reactions. The development of MW technology started soon after the II World War and boomed in the 50s and 60s, with the diffusion of home MW ovens, along with more sophisticated industrial apparatuses. By the mid-90s, several companies had developed MW ovens specifically designed for laboratory use, improving these systems until the modern single–mode technology for small scale Microwave-Assisted Organic Synthesis (MAOS, see Section 18.2). To better understand how MWs engage in interactions with the matter and transfer energy, it could be useful to recall the basic theory behind them. MWs are electromagnetic waves formed by an electric and a magnetic field moving perpendicular to each other at the speed of light (Figure 18.1), and only the electric field can transfer energy and heat substances.

Sustainable Organic Synthesis: Tools and Strategies
Edited by Stefano Protti and Alessandro Palmieri

Published by the Royal Society of Chemistry, www.rsc.org

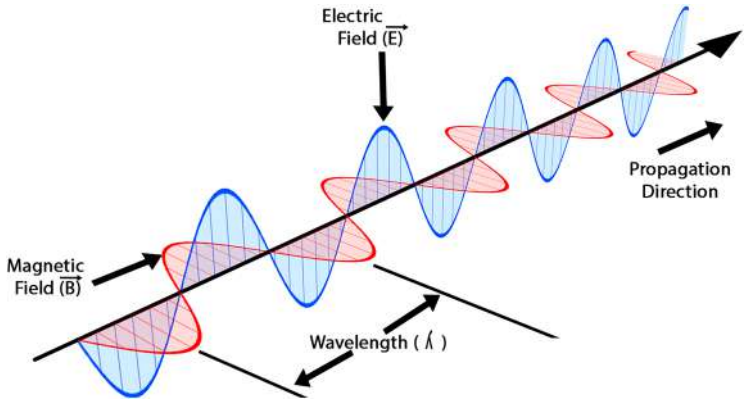

Figure 18.1 A schematic representation of an electromagnetic wave, where an electric field and a magnetic one spread perpendicularly to each other at the speed of light.

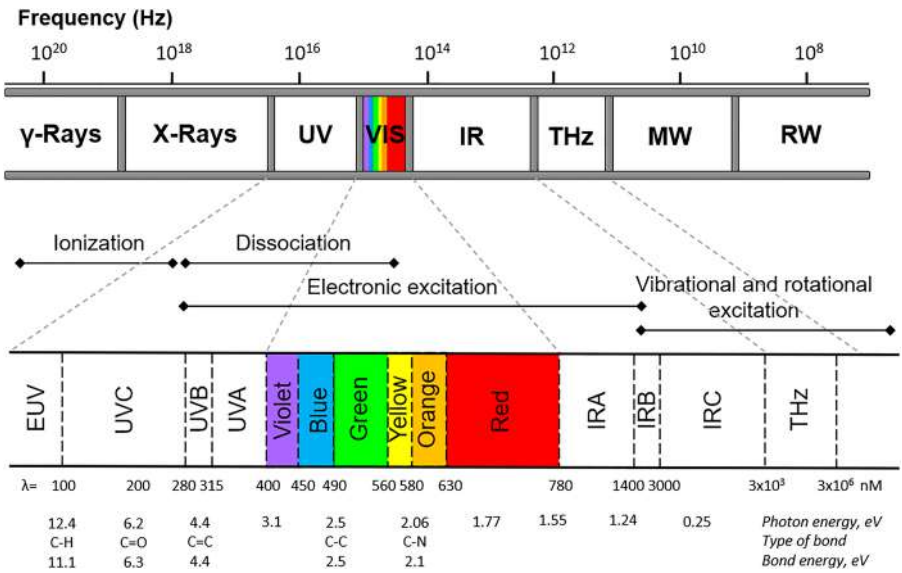

Figure 18.2 The electromagnetic spectrum.

The energy of MWs falls in the lower frequency end of the electromagnetic spectrum (300–300,000 MHz, Figure 18.2). Within this region, only molecular rotation is affected by the waves, since the energy of photons from MWs is much lower than that required to break molecular bonds, thus being ineffective in molecular structures. Dipole rotation and ionic conduction represent the only mechanisms involved in transferring energy to the substances, contributing to the so-called dielectric heating effect. In fact, the energy is transferred by dipole rotation to polar molecules because of their alignment to the rapidly changing electric field, while in ionic conduction, ionic motions are

generated by electromagnetic waves through their interaction with free ions and ionic species, making them oscillate back and forth and increasing the temperature with a superheating effect.

The most common source of heat available in organic synthesis is the conductive heating furnished by convectional thermal sources (reflux systems such as heating blocks, oil and sand baths, thermoblock systems *etc.*). However, the way heat is driven into substances has several disadvantages. Heating must penetrate through the walls of the reaction container, then spread into the solvent and reach the reactive species, making the whole method not very efficient. As heating must penetrate several materials, the result is a slow process where the temperature of the reaction vessel is higher than that of the core unit. On the other hand, dielectric heating with MW irradiation is a unique process which allows an instant rise and fall of the temperature. There is no dependence upon the thermal conductivity of the different materials and the reaction vessel can be easily sealed, therefore permitting temperatures beyond the boiling point of the solvent mixture to be reached. Fortunately, glass is transparent to MWs, such that waves are not absorbed but almost completely transmitted to the vessel content. Teflon and quarts are also suitable materials for MW reaction containers.

18.1.2 How Microwaves Enhance Organic Reactions

Classically, a reaction between reactants R1 and R2, with a generic energy level (E_{R1} + E_{R2}), occurs when these molecules collide in the correct orientation, reaching a higher activated transition state (E_T). The difference between (E_{R1} + E_{R2})–(E_T) is defined as the activation energy (E_a) and this has to be overcome by absorbing energy from other sources for the reaction to occur. The reactants furnish new products, and the system moves to a lower energy state (E_P) (Figure 18.3). MWs represent the source of external

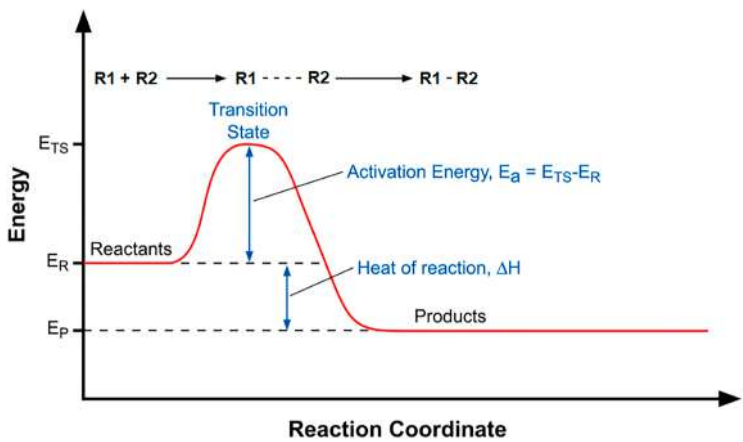

Figure 18.3 Energetic diagram for a classical organic reaction.

energy needed by the system to go over the E_a and react, yielding more stable products. MW ovens can usually transfer a relatively large amount of energy compared to that required for the system reactivity, whose kinetics are also positively affected by the high speed of energy transfer (10^{-9} sec), higher than molecule relaxation. The reaction rate is based on the Arrhenius equation:

$$k = A \cdot e^{-Ea/RT}$$

where A is the frequency of geometrically correct collisions between molecules and $e^{-Ea/RT}$ represents the fraction of molecules with enough energy to overcome the activation energy barrier.

In this equation, MWs affect the temperature parameter (T), leading to an increased number of correct collisions and faster reactions. At its best, heating by MW irradiation can increase chemical reactions rates up to 1000-fold with respect to convectional heating methods. Thanks to their ability to transfer energy directly to the reactive species, MWs are capable of reducing reaction times from days to hours, or even minutes. In addition, MW irradiation can provide a discriminant between kinetic and thermodynamic products.[1] Traditional heating systems cause a slow increase of the temperature, thus leading to the formation of the kinetic products, while MWs provide a more powerful and instantaneous source of energy, driving the reaction towards the formation of the thermodynamic products. The dielectric heating process is also influenced by the solvents where reactions are performed, in correlation with their loss tangent ($\tan\delta$) values:

$$\tan\delta = \varepsilon''/\varepsilon'$$

The term ε'' represents the dielectric loss (efficiency in converting MW irradiation into heat) and ε' is the dielectric constant of the medium (measurement of the polarizability of molecules hit by the electric field). Solvents with high values of $\tan\delta$ (>0.5) are associated with a higher ability to absorb MW energy and heating, while solvents without a dipole moment, such as toluene or *n*-hexane ($\tan\delta < 0.1$) are almost transparent to MWs (Table 18.1).[2] Although polar solvents are required for rapid heating, these are not necessarily the best choice to perform a reaction, since reagents and catalysts also contribute to the dielectric properties of the mixture. Balancing the polarity of the medium can make the system less affected by MW irradiation, therefore diminishing bulk heating but still energizing molecules.

In the presence of systems that require higher temperatures and longer times to react, there is also the possibility to enhance the process with the help of substances called "susceptors". These are inert materials that can rapidly absorb MW energy and transfer heat to other poor radiation absorbents, and will be further discussed in Section 18.2.2.

Table 18.1 Tan δ values of the most common organic solvents and water.

High (>0.5)		Medium (0.1–0.5)		Low (<0.1)	
Solvent	tan δ	Solvent	tan δ	Solvent	tan δ
Ethylene glycol	1.350	2-Butanol	0.447	Chloroform	0.091
Ethanol	0.941	Dichlorobenzene	0.280	Acetonitrile	0.062
DMSO	0.825	NMP	0.275	Ethyl acetate	0.059
2-Propanol	0.799	Acetic acid	0.174	Acetone	0.054
Formic acid	0.722	DMF	0.161	THF	0.047
Methanol	0.659	Dichloroethane	0.127	Dichloromethane	0.042
Nitrobenzene	0.589	Water	0.123	Toluene	0.040
1-Butanol	0.571	Chlorobenzene	0.101	*n*-Hexane	0.020

18.1.3 Non-thermal Effect of Microwaves

MWs may have a so-called "non-thermal" or "specific" effect in enhancing certain organic reactions.[3] At the beginning of MW-assisted chemistry, it was hypothesized that the interaction of MWs with polar transition states gave the acceleration effect.[4] Soon after, this theory was challenged, as no solid evidence accounted for it, and MWs were considered more likely to be a very efficient source of dielectric heating.[5] Although the debate is still open, it cannot be denied that some organic reactions undergo a much more powerful enhancement under MW irradiation regarding exposure to convectional heating, and this has contributed to the development of the concept of "microwave catalysis". This catalytic effect of MWs may influence the "A" parameter of the Arrhenius equation, because of rotational excitation of the collision geometry, or it may have an even greater impact by diminishing the value of the apparent activation energy. In fact, E_a (also termed ΔG) is calculated from the contribution of enthalpy and entropy to the system:

$$E_a = \Delta H - T\Delta S$$

MW catalysis could contribute to increasing the value of $T\Delta S$ as a consequence of enhancing collision probabilities because of dipolar polarization, thus lowering the value of E_a.[6] This effect finally results in a strong activation of molecules at the surface of polar MW-absorbing materials. Cross- and ring-closing metathesis (RCM) reactions have been the subject of several controversial publications for the identification of a non-thermal MW effect (Scheme 18.1).

Although some research works reported no improvement in MW-assisted RCM when compared to classical heating,[7] MW irradiation has been later re-proposed as a complementary activation mode for olefin metathesis.[8] Several examples of RCM performed at the same temperature under classical or MW-assisted protocols are described, evidencing higher efficiency under

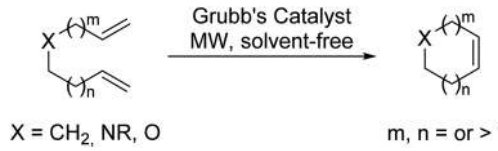

Scheme 18.1 Generic scheme of a ring-closing metathesis (RCM) reaction under MW-irradiation and solvent-free conditions.

MW-irradiation, both in terms of yields and reaction times.[9] A more recent rigorous study shows the existence of a microwave-specific effect[10] of "selective heating" of reactants in solution.[11] Studying the Claisen rearrangement of allyl *p*-nitrophenyl ether and the Friedel–Crafts benzylation of *p*-xylene using 2-benzyloxy-1-methylpyridinium tetrakis[3,5-*bis*(trifluoromethyl)-phenyl]borate, the authors found that the operative temperature under MW irradiation was lower than that under convectional heating. This gap was attributed to a MW-specific rate enhancement resulting from the energy storage of aggregated dipoles in a nanosphere produced working in nonpolar solvents.[12] This truly overall MW effect, albeit demonstrated, was quantitatively thin. In addition, the MW catalytic effect seems to be more evident in heterogeneous systems (*e.g.* solvent-free or reagent-supported reactions) rather than homogeneous ones and may also be affected by the scale of reactions. Not all organic reactions are influenced by MWs at the same rate, but MW catalysis has to be considered as a combination of thermal and specific (or non-thermal) effects, leading to increased reaction performances with respect to convectional heating.

18.1.4 Microwave Reactors

Up to the late 90s, the only available instruments for MW-assisted chemistry were domestic MW ovens. These are multimodal appliances which operate at a frequency of 2.45 GHz meant to be used for cooking and heating food, not for synthetic purposes. Back then, they represented the only choice to have a "proof of concept" about the enhancing effects of MWs on organic reactions. However, they had some significant limits:

- The power of the MWs couldn't be regulated, and inside the oven the temperature was never uniform, leading to the formation of hot spots.
- Reactions had to be run solvent-free, as no refluxing system was available, and solvents could evaporate or boil with a high risk of fire or explosions.
- The reaction flask could not be sealed, and the open-vessel mode was the only way of performing a reaction, with no possibility of a superheating effect.
- Safety and parameter control were also of great concern.

MW-assisted organic synthesis (MAOS) started in the mid-80s with the first published report on MW heating to speed up organic chemical transformations.

In this experiment (Scheme 18.2), the authors compared the hydrolysis of benzamide to benzoic acid in sulphuric acid by convectional and MW heating, evidencing an improvement in performing the MW-irradiated reaction, both in terms of yield and time, which was reduced from 1 h to 10 min.[13] Despite the promising results, these experiments were typically carried out in domestic ovens, in sealed Teflon or glass vessels, with no possibility to control internal temperature or pressure, often resulting in violent explosions. Analogously, the multicomponent Biginelli reaction performed under MW irradiation was reported by Kappe *et al.* to occur in a domestic MW oven (Scheme 18.3).[14]

In this example, the reaction times were shortened to seconds and the yields were moderate to high depending on the reactant substituents.

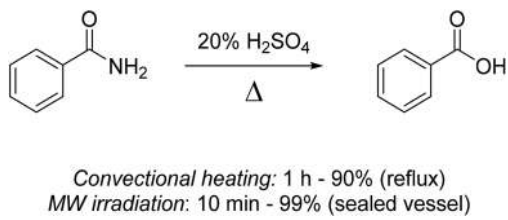

Scheme 18.2 The first reported example of MAOS by Gedye *et al.* in 1986.[13]

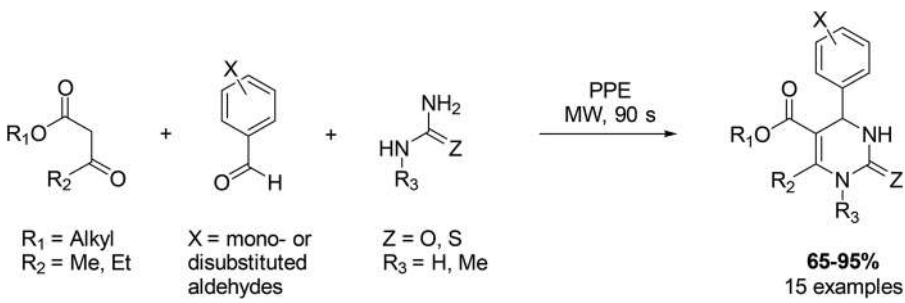

Scheme 18.3 The MW-assisted Biginelli reaction proposed by Kappe *et al.* in 1999 using a domestic MW oven.[14]

Despite the encouraging results, the authors later admitted that the reproducibility of the process was obviously affected by the lack of instruments to check the various parameters during the reaction in domestic ovens.[15] From there up to now, a great evolution has been observed in the technology of MW reactors. In 1999, a multimode MW oven equipped with a condenser for refluxing conditions and an internal temperature sensor was developed by MLS GmbH and called MLS ETHOS, which also allowed high pressure reactions to be performed in sealed PFA vessels. But the real revolution has been achieved by introducing single-mode MW reactors, which could operate on their own with no PC control, in open- or sealed-vessel mode, also endowed with temperature and pressure controls and an air-compressed cooling system. Since the early '00s, CEM Corporation, Anton Paar and Biotage have become the leading producers of MW equipment for organic synthesis and medicinal chemistry. CEM Discover released in 2001, Anton Paar Monowave 300 released in 2004, and Biotage Initiator$^+$ released in 2003 (Figure 18.4), together with their following upgrades, are still the most popular and efficient single-mode MW reactor models typically used for small-scale laboratory synthesis.

Accordingly, scientific journals only accept experiments performed with dedicated laboratory equipment, under controlled parameters, which can be easily reproduced by other operators. Most of these publications describe MAOS in sealed vessels and single-mode MW instruments, which also allow parallel and automated sequential processes and provide modern technologies for solid-phase synthesis. Along with the increase of sophistication and reliability of these MW reactors, also the price dramatically increased. These new single-mode appliances require an investment of tens of thousands of euros, thus significantly affecting the budget of a research group. However, the benefits they bring make their use mandatory in an organic synthesis laboratory.

Figure 18.4 From left to right, two models of the CEM Discover single-mode MW reactor (with a manual or automated arm for pressurized reactions), the Anton Paar Monowave 300 and the Biotage Initiator$^+$.[16]

18.2 Microwave-assisted Organic Synthesis and Green Chemistry

According to the 12 principles of green chemistry,[17] apart from the increase of energy efficiency at point 6, the use of safer solvents and reaction conditions (point 5), and the atom economy (point 2), due to higher yields and lower by-product formation, are significantly fulfilled by MW-assisted processes. Along with the ongoing debate about the specific MW effects, heating with MW irradiation has been pointed out as a "green source" of heat and may serve as an optimal method to perform high temperature green reactions. In fact, it is evident how MW activation dramatically reduces reaction times in comparison with convectional heating, while preserving or increasing reaction yields. Since the reduction of energy consumption is a crucial feature in the design of green processes, shorter reaction times are associated with a lower energy demand; thus, MW heating was automatically considered as a green process. However, the energy efficiency of MW-assisted transformations and the relative "greenness" is a complex issue involving different factors and needs to be carefully tested.

18.2.1 Energy Efficiency and Microwaves

According to the Arrhenius equation (Section 18.1), the energy consumption for a high temperature but short reaction should be lower than a low temperature but longer one. The energy conversion efficiency in MW appliances mainly depends on the internal microwave generator and cavity losses. It has been shown that the efficiency of the magnetron in a MW unit is medium-low, with a 60–65% conversion of electrical energy into electromagnetic radiation. In addition, the transformation of electromagnetic waves into heat can be hampered by the low polarity of the reaction media. Nevertheless, different studies have proven how heating by MW irradiation is a more convenient and economic process, especially when associated with continuous flow systems. Benaskar *et al.* in 2011,[18] performed a complete analysis of the overall efficiency of the MW heating process compared to oil-bath heating, where the losses are principally affected by losses of the medium to the environment, resulting in an overall efficiency of 54% for MW *vs.* 27% for the oil bath (Figure 18.5).

During the last decade, several other experiments have been dedicated to evaluating the efficiency of MAOS. The major conclusion has always been that a detailed analysis is required on a case-by-case basis. If we investigate laboratory scale experiments in classical synthetic conditions (not the flow processes) and we take into account the sole energy consumption, it could be questionable whether MW heating should be labelled as green. Moseley and Kappe performed in 2011 an interesting study about the energy efficiency

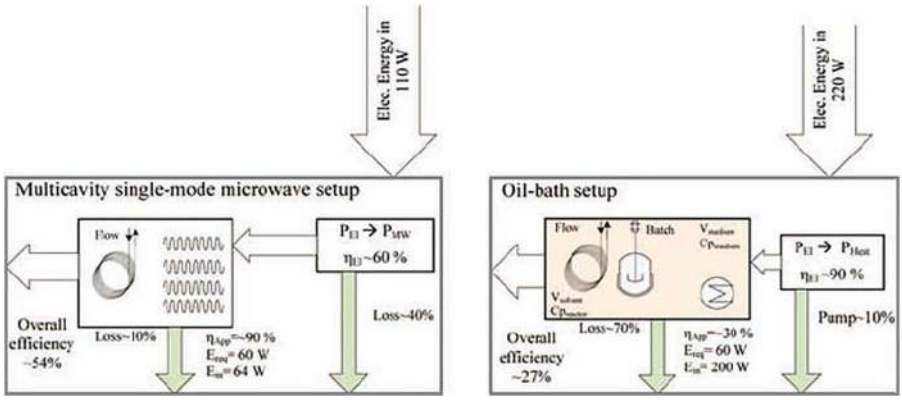

Figure 18.5 Energy flow diagram for single-mode MW and oil-bath heating processes. Reproduced with permission from ref. 18, Springer Nature, Copyright 2011.

of MAOS using different MW reactors and reaction conditions.[19] On a small scale, their results highlighted how energy consumption is not significantly affected by MW irradiation compared to classical heating. A greater improvement was observed by shifting from small to larger scales, thus increasing the greenness of the synthesis. In fact, all of the above-mentioned considerations are reliable as long as we consider laboratory scale MAOS, but they may be different for industrial transformation and scaled-up processes. To assess the energy efficiency of a heating mantle and a multimodal MW oven on batch scale, Devine and Leadbeater performed a simple experiment involving heating 1 L of water from room temperature to its boiling point.[20] The efficiency was calculated as follows:

$$\text{Efficency} = \frac{4.18 \cdot 1000 \cdot \Delta T}{\text{Whconsumed} \cdot 3600}$$

Knowing that the heat capacity of water is 4.18 J g^{-1} K^{-1} and 1 W = 1 J s^{-1}, it took 22 min with convectional heating to raise 1 L of water from 27 °C to 100 °C, consuming 184 W h and making the process 46% efficient overall. On the other hand, MW irradiation needed 4.66 min and consumed 190 W h, with a 44% of overall efficiency (Figure 18.6). These values are almost equal and comparable as the conversion of electrical energy by the heating mantle is almost quantitative (97% efficiency) while the same procedure performed by the magnetron of a MW unit has the abovementioned 65% efficiency.

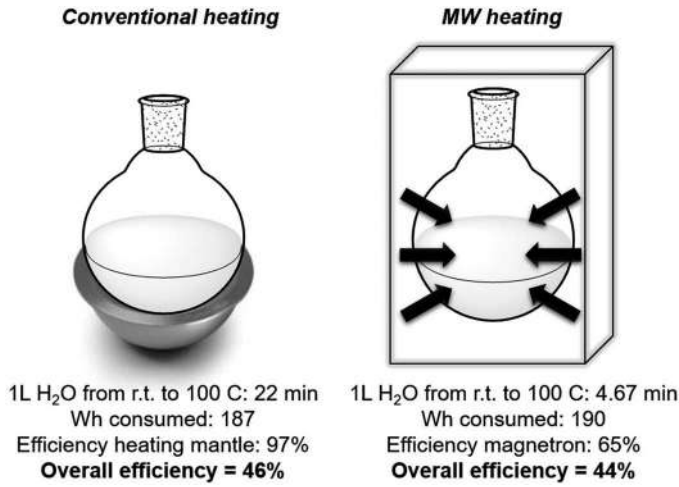

Figure 18.6 Comparison between convectional and MW-assisted heating on a batch scale.

Therefore, the two processes are equally efficient on a batch scale, and this is mainly due to the lower performance of the MW magnetron in converting energy to heat. Regardless of this latter aspect, the great difference in reaction times makes the two methods equivalent.

However, Devine and Leadbeater also reported some interesting experiments on different reactions aimed at proving the energy efficiency of MW-assisted processes.[20] They considered a MW-promoted Suzuki coupling reaction between 4-bromoanisole and phenylboronic acid (Scheme 18.4), and set different reactions at different concentrations in a single-mode MW unit, in a multimode MW unit and under convectional heating in continuous-flow mode. While on a 1 mmol scale in a sealed vessel and single-mode MW unit, they used 9.8 W h mol^{-1}, yielding the coupling product in 3 minutes and 93%, a 20 mmol scale in an open vessel single-mode unit (10 min, 90.3% yield) and a 200 mmol scale in an open vessel multimode unit (20 min, 76% yield) only required 2.0 and 1.7 W h mol^{-1}, respectively. These two latter processes were significantly more efficient if compared to convectional heating in continuous flow mode, which required at its best 3.0 W h mol^{-1} (5 min, 84–89% yield depending on scale). The results perfectly matched with the above stated assumptions, reported by Moseley and Kappe,[19] that large-scale processes are more efficient under MW irradiation while, as soon as the scale decreases, convectional heating and MW irradiation may not differ in energy consumption.

Heating by MW irradiation has undeniable advantages, not only related to the consumption of energy. The possibility of increasing reaction yields

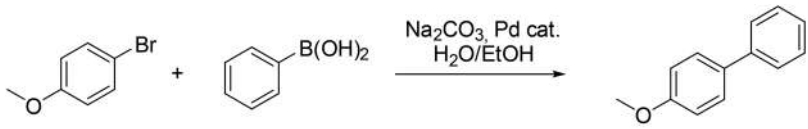

	conditions	time	yield	energy
MW single-mode	1 mmol[a]	3 min	93%	9.8 Wh/mmol
MW single-mode	20 mmol[b]	10 min	90%	2.0 Wh/mmol
MW multimode	200 mmol[b]	20 min	76%	1.7 Wh/mmol
Conventional heating	100 mmol[c]	5 min	89%	3.0 Wh/mmol

a: sealed vessel; *b*: open vessel; *c*: continuous flow mode

Scheme 18.4 The Suzuki coupling reaction between 4-bromoanisole and phenylboronic acid performed with different methodologies, in comparison with their energy consumption.

coupled with the reduction of side product formation during chemical transformations makes up a significant boost to the greenness of the whole synthetic process. The use of "unconventional" solvents such as water or ionic liquids is smoother using MW apparatus and also the "no solvent" choice is highly favored under MW heating. Recently discovered methodologies opened up also the possibility to exploit metal catalysis under MW-assisted conditions, thus implementing reaction efficiency while diminishing reagent amounts and, consequently, reaction waste. In the following sections, we describe and discuss all the methodologies that allow a MW-assisted procedure to be labelled as green, not only in correlation to energy consumption, but for the use of more sustainable reaction conditions, solvents and catalysts.

18.2.2 Solvent-free Reactions

Open-vessel solvent-free reactions under MW irradiation are a well-established method for safe, clean and efficient synthesis. Thanks to the absence of organic solvents, the safety dramatically increases, large scales can be used, and several other aspects of the reactivity are affected, including yield and selectivity. In solvent-free conditions, the MW radiation is directly absorbed by reactants, thus increasing the efficiency of the heating system and saving energy, making the procedure very attractive for sustainable synthesis. Solvent-free reactions can be classified into three categories:

Reaction between neat reactants, where at least one of the reagents has to be a liquid substance and the MW radiation is directly absorbed by the reagents. A great variety of reactions can be carried out under this condition, yielding structures useful as intermediates for the development of biologically active compounds. In 2017, the Pechmann reaction between resorcinol and ethyl acetoacetate under solvent-free conditions was proposed for obtaining 7-hydroxy-4-methylcoumarin (or 4-methylcoumarin if starting from phenol) (Scheme 18.5).[21]

Coumarins are an important family of oxygen-containing heterocycles, also found as secondary metabolites in some plants and microorganisms, with several therapeutic applications. The heterogeneous acidic catalysis of Amberlist-15, coupled with MW-irradiation at 100 °C for 20 min, in solvent-free conditions, allowed the synthesis of the desired coumarin in 97% yield. Another environmentally friendly protocol for preparing condensation products in solvent-free conditions has been recently proposed, resulting in the synthesis of chalcones, which are interesting compounds from a biological point of view. 4-Methoxyacetophenone and 4-methoxybenzaldehyde were selected as the model substrates for optimizing the reaction conditions (Scheme 18.6).[22]

Under MW-irradiation at 160 °C and employing 50 mol% of boric acid, the reaction proceeded stereoselectively furnishing the *E*-chalcone in 95% yield in 20 min. Similar results have been obtained lowering the amount of boric acid to 20 mol% in 40 min at the same temperature. The reaction conditions and the catalyst used make the entire process non-toxic and cheap, and it can have a broad application to all the base-sensitive substrates. Acetophenones can also undergo Friedlander coupling condensation with 2-aminoacetophenones in the presence of diphenylphosphate (DPP), to obtain substituted quinolines (Scheme 18.7).[23]

The preparation of a small library of these intermediates has been reported under MW-irradiation and solvent-free conditions, affording the desired

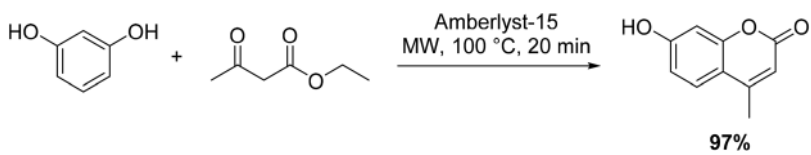

Scheme 18.5 Pechmann reaction between resorcinol and ethyl acetoacetate with heterogeneous catalysis by Amberlyst-15.

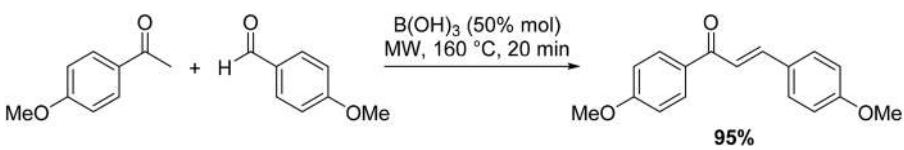

Scheme 18.6 Condensation reaction between p-substituted acetophenone and benzaldehyde in solvent-free conditions using $B(OH)_3$ as the catalyst.

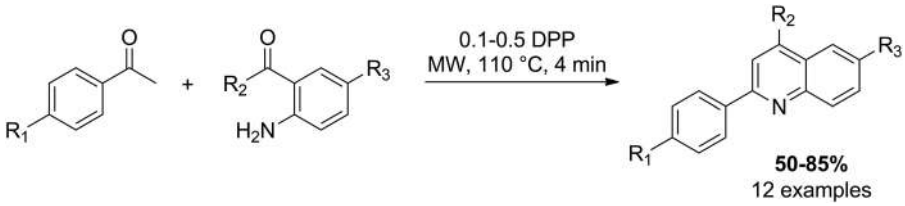

Scheme 18.7 Friedlander coupling condensation under solvent-free MW-assisted conditions for the synthesis of a small library of quinoline derivatives.

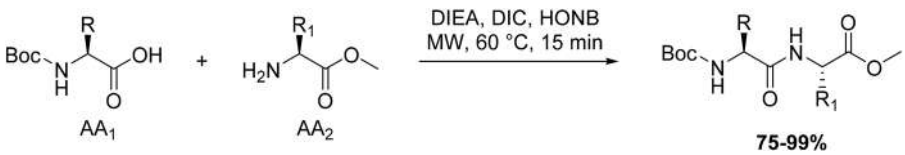

Scheme 18.8 Synthesis of peptides *via* a MW-assisted solvent-free coupling reaction.

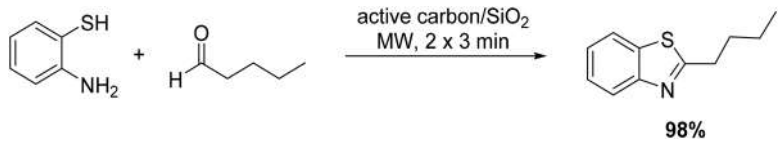

Scheme 18.9 The reaction of 2-aminothiophenol with valeraldehyde in the presence of a solid support under solvent-free and MW irradiation conditions.

products with yields ranging from 50% to 85%, in only 4 minutes at 110 °C. This represents a great improvement compared to classical heating reactions, where fewer analogues were obtained in very low yields (24% for the best performing procedure). The coupling reaction of amino acids yielding peptides with different chain lengths is also a suitable procedure under MW solvent-free conditions (Scheme 18.8).[24] Using *N*,*N*′-diisopropylcarbodiimide (DIC) and *N*-hydroxy-5-norbornene-*endo*-2,3-dicarbodiimide (HONB) as the coupling agent and auxiliary nucleophile, respectively, peptides were obtained in high yields and purity, without racemization.

Reaction using supported reagents, where the reactive species are absorbed on dry media such as silica, alumina or clay. As abovementioned, absorbing the reactive species on dry media that can interact with MWs and heat was one of the first techniques to perform MAOS. There are several advantages, including the possibility of scaling up the amount of chemicals and handling the reactions in a safer way, but it also represents a green procedure to avoid the use of organic solvents and waste formation. 2-Alkylbenzothiazoles can be synthesized from the reaction of 2-aminothiophenol with aliphatic aldehydes in the presence of active carbon/SiO_2 under solvent-free conditions and MW irradiation. For example, by using valeraldehyde, the corresponding 2-butylbenzothiazole is obtained in 6 minutes (2 MW cycles of 3 min each) in almost quantitative yield (Scheme 18.9).[25]

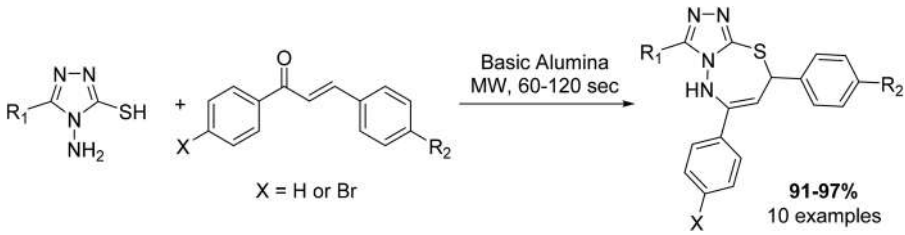

Scheme 18.10 Synthesis of 1,2,4-triazolo[3,4-*b*]-1,3,4-thiadiazepines under solid supported and MW irradiation conditions.

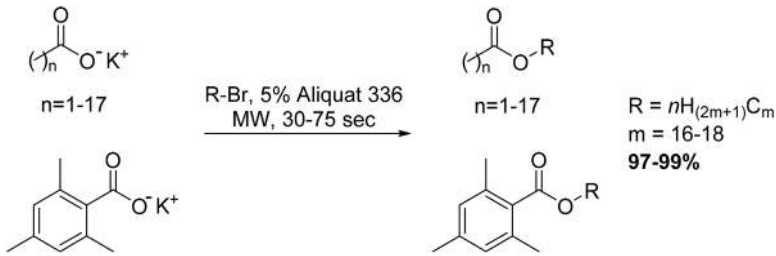

Scheme 18.11 Examples of different carboxylate alkylations using Aliquat 336 as a phase transfer catalyst under MW irradiation.

Similarly, the synthesis of antimicrobial agents based on a triazolothiazepine core has been reported in the absence of any toxic and mineral acids, bases or organic solvents (Scheme 18.10).[26] The reactive species are absorbed on basic alumina and the desired compounds are isolated in a very high yield after 60 or 120 seconds.

Reaction under phase transfer catalyst conditions, where a liquid compound acts both as the reagent and the organic phase. This is the case of some well-known procedures for carboxylate alkylation with long chain halides using Aliquat 336, a quaternary ammonium salt used as a phase transfer catalyst (Scheme 18.11).[6] Due to the polarity of Aliquat 336, MW radiation is highly absorbed and alkylation reactions occur within seconds and in almost quantitative yields. Similarly, hydrolysis of esters can be accomplished.

18.2.3 Susceptors

When the activation energy for certain reactions is too high to reach by classical MW-assisted procedures, or with a very poor MW absorbent solvent, there is the possibility to add particular substances to the reaction mixture in order to increase the absorption of MWs, also reducing the amount of energy needed for heating the system. These inert materials do not take part to the

reaction, they only provide a very efficient and rapid increment of the temperature, regardless of the reaction media, and they are called susceptors. For example, carbon powder and graphite are considered good MW susceptors, able to reach very high temperatures within minutes.

Graphite is widely used, both in catalytic amounts (Scheme 18.12)[27] or in excess compared to the reagents, thus resulting in a graphite-supported MW process (Scheme 18.13).[28]

Graphite oxide is also used in preparing graphene nanosheets. Graphene is a one-atom thick two-dimensional carbon structure with interesting applications in material science, which can behave as a susceptor in its own synthesis from graphite oxide under a hydrogen atmosphere.[29] In addition, carbon nanotubes can act as MW susceptors in epoxy matrix curing processes.[30] Silicon carbide (SiC) is another strong MW absorber, with a very low thermal expansion coefficient and no transition phases. In the presence of this material, non-polar solvents under MW irradiation can be easily heated and reach temperatures as high as 300 °C (Scheme 18.14).[31]

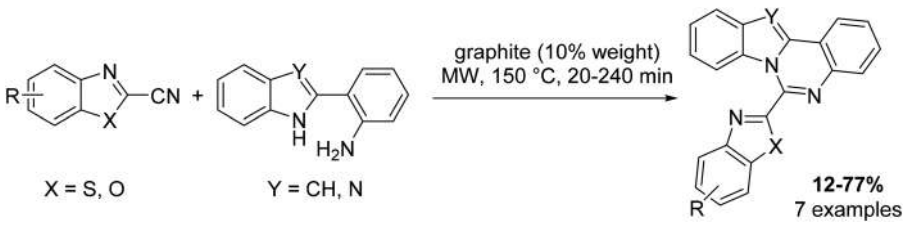

Scheme 18.12 Preparation of quinazoline derivatives with the use of catalytic graphite as a MW susceptor.

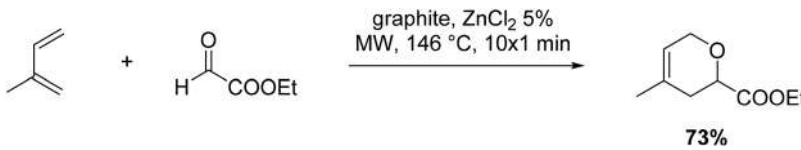

Scheme 18.13 MW-assisted cycloaddition reaction with reagents absorbed on graphite.

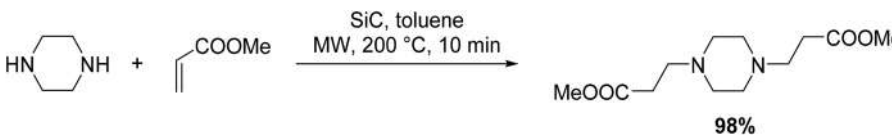

Scheme 18.14 Michael addition reaction performed in the presence of SiC as a susceptor.

Moreover, SiC is difficult to destroy and can be reused with no loss of efficiency, making it an optimal material for the production of reaction vials in place of the classical Pyrex glass. Other materials, such as metal particles of Fe or Ni, have been described as MW susceptors in different chemical transformations.

18.2.4 Heterogeneous Catalysis

A broad variety of reactions can benefit from more powerful MW enhancement, thanks to the ability of the catalysts (or their supports) to behave as susceptors. This can happen as long as we consider introducing heterogeneous systems to catalyse a chemical transformation. In this way, the efficiency of the heating medium could be higher than any other pressurized systems and the energy consumption profile might be totally different. Considering a Paal–Knorr reaction between aniline and 2,5-hexanedione in solvent-free conditions and catalysed by Montmorillonite (K-10) (Scheme 18.15),[32] the convectional heating consumed 60 W h of energy in comparison with the 10 W h of the MW-promoted reaction, and also required 30 min of reaction time against 1 min under MW irradiation. This is additional confirmation that several reactions can be improved by MAOS and result in more efficient and green processes.

Heterogeneous catalysis can positively affect not only the energy consumption, but also the yield and selectivity of product formation. The preparation of 2-substituted or 1,2-disubstituted benzimidazoles and benzoxazoles has been reported using the association of Pd/C and MW, leading to a successful hydrogen transfer-based reaction (Scheme 18.16).[33] In fact, under MW dielectric heating, it is possible to use tertiary, secondary, and even primary amines as the substrates for the palladium-mediated process with substituted *o*-phenylenediamines. The reaction is highly selective and no (poly)-alkylated phenylenediamines or cross-contaminated benzimidazoles were isolated.

Alternatively, a similar procedure for obtaining a benzimidazole core from *o*-phenylenediamine has been proposed using γ-Valerolactone (GVL) as a new biomass-derived reaction medium (Scheme 18.17).[34] The GVL heating profile under MW irradiation showed high stability and applicability in

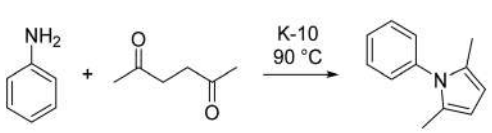

	time	yield	energy
MW	1 min	99%	10 Wh
c. heat.	30 min	97%	60 Wh

Scheme 18.15 The Paal–Knorr reaction on aniline using Montmorillonite (K-10) as a solid support under MW-irradiation.

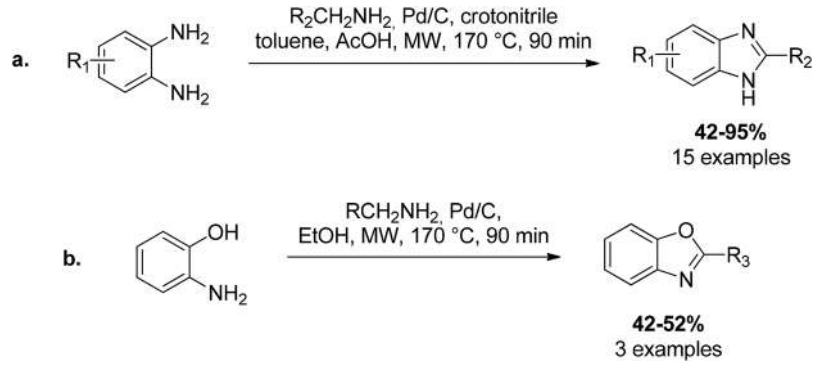

Scheme 18.16 Preparation of substituted benzimidazoles and benzoxazoles using Pd/C heterogeneous catalysis and MW dielectric heating.

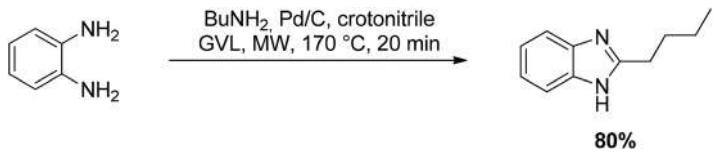

Scheme 18.17 An example of MW-assisted benzimidazole synthesis using γ-Valerolactone (GVL) as the reaction medium.

MW-assisted Pd/C catalysed reactions, avoiding the arcing phenomena frequently observed in these conditions and furnishing the desired structures in high yields.

18.2.5 Green Solvents

Most of the organic transformations occur in organic solvents. Several reasons make in-solution synthesis one of the most appealing procedures: (i) it allows an efficient mixing of the reactive species, placing them in contact at a known concentration; (ii) reagents can be easily dissolved and mixed inside the reactor; (iii) the temperature can be easily controlled for both endothermic and exothermic processes. However, solvents represent a waste part used in large excess that has to be disposed of. Organic solvents are also commonly used in the subsequent steps of product extraction, separation and purification. Therefore, they represent the most common source of impurities amongst the purified compounds and may have several other drawbacks, being toxic, ecotoxic, flammable and polluting. Last but not least, solvents are frequently volatile species that can contribute to the worsening of the greenhouse effect. Although most organic solvents can be recycled by fractional distillation at the end of the processes, their replacement with other

liquid media is the most obvious choice for increasing the sustainability of the procedure. Water is definitely a green alternative to classical solvents, but the scarce solubility of organic species represents a clear obstacle. Ionic liquids, supercritical fluids, fluorous solvents and other media are valuable alternatives for a new concept of in-solution green chemistry.

Reactions in water. Water is the green solvent *par excellence*. It is readily available in large amounts, non-toxic, and non-flammable, but the solubility of organic species in it is usually really poor, hampering its use in place of other organic media. However, the use of water at elevated temperatures, as close as possible to its critical point (or even above), completely changes the properties of this liquid, conferring unique characteristics that can be exploited under MW-assisted conditions. At high temperatures, near-critical water (NCW) can be seen as a pseudo-organic solvent. For instance, the dielectric constant of water drops from 78.5 at 25 °C to 27.5 at 250 °C, while the ionic product increases, making water a stronger base or acid. Several reactions have been performed in NCW under MW irradiation, involving both small and more complex organic species. The first applications for reactions in NCW concerned the hydrolysis or degradation of simple structures. The hydrolysis of indole 2-carboxylic ester was performed in a basic aqueous medium at 220 °C in 10 min in a quantitative yield (Scheme 18.18),[35] and by doubling the reaction time, decarboxylation also occurred.

However, different procedures arise from the use of NCW. Aryl halides can be converted into the corresponding phenols using NaOH as the base, coupled with CuI (10 mol%) and L-Proline (5 mol%) as additional catalysts (Scheme 18.19).[36]

Starting both from 4-bromo or 4-iodoacetophenone, this reaction occurs in almost quantitative yields, at 200 °C in less than 30 minutes.

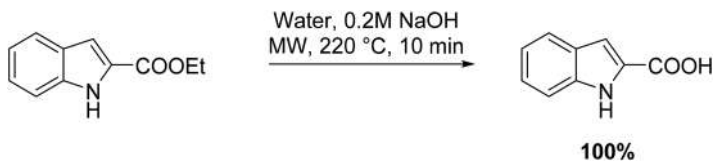

Scheme 18.18 Hydrolysis of indole 2-carboxylic ester in basic water at 220 °C.

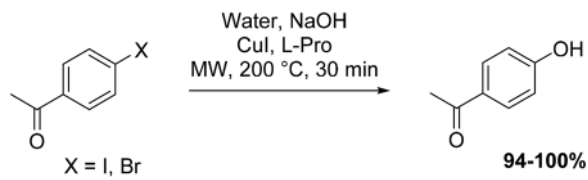

Scheme 18.19 Direct transformation of aryl halides to phenols in water at 200 °C using CuI as a catalyst, L-proline as an additive, and sodium hydroxide as a base.

4-Bromoacetophenone can also be a substrate for Suzuki coupling in NCW under MW irradiation (Scheme 18.20).[37] TBAB was used as a phase transfer agent, enhancing the solvation and reaction rate by complexing the boronate counterpart, and metal catalysis was furnished by the traces of palladium in the carbonate powder, giving the coupling product in a quantitative yield after 5 minutes at 150 °C.

Coumarin-3-carboxylic acid is another accessible structure through MW-assisted synthesis in NCW, by reaction of 2-hydroxybenzaldehyde with Meldrum's acid for a time as short as 2 minutes (Scheme 18.21).[38]

Reactions in ionic liquids. Ionic liquids represent a valid alternative to organic solvents. These liquid organic salts are non-volatile, non-flammable, highly stable (both thermally and chemically), and miscible with organic media. Moreover, they possess catalytic properties (*e.g.* Lewis acid behaviour) and a high electrical conductivity. Because of their ionic character, ionic liquids are very efficient MW radiation absorbers and transfer energy by ionic conduction, thus producing a superheating effect, although an overheating effect due to their non-volatile nature also occurs. Beckmann rearrangement of ketoximes to the corresponding amides is an important synthetic method that usually requires large amounts of H_2SO_4 as Brønsted acids, leading to the formation of ammonium sulphate as a by-product. However, the corresponding amides can be produced in high yields within 60 seconds under MW-irradiation (Scheme 18.22),[39] using a very low amount of H_2SO_4 (5 mol%) in combination with a hydrophobic ionic liquid such as 1-*n*-butyl-3-methylimidazolium hexafluorophosphate salt. Compared to classical heating, which was unable to return the desired rearrangement products at the same rate, MWs made the procedure extremely efficient. More complex procedures can be performed with the help of ionic liquids, such

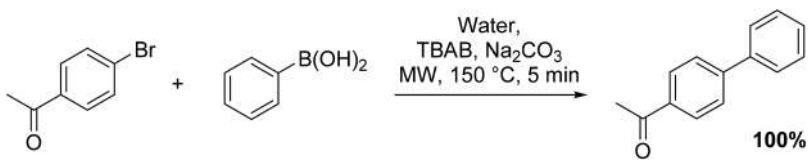

Scheme 18.20 Suzuki coupling reaction in water at 150 °C, catalysed by traces of Pd and enhanced by TBAB and MW irradiation.

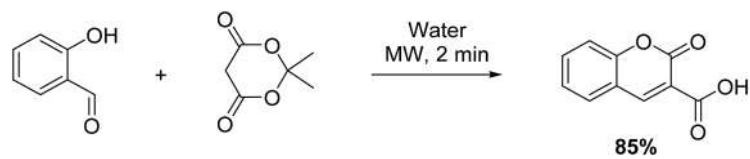

Scheme 18.21 Synthesis of coumarin-3-carboxylic acid using Meldrum's acid in water under MW irradiation.

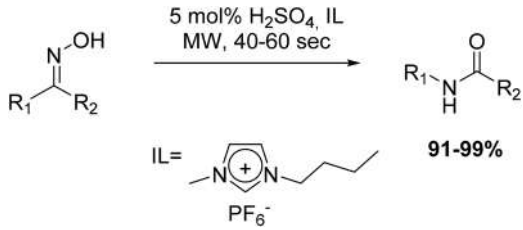

Scheme 18.22 MW-assisted Beckmann rearrangement of ketoximes in ionic liquids.

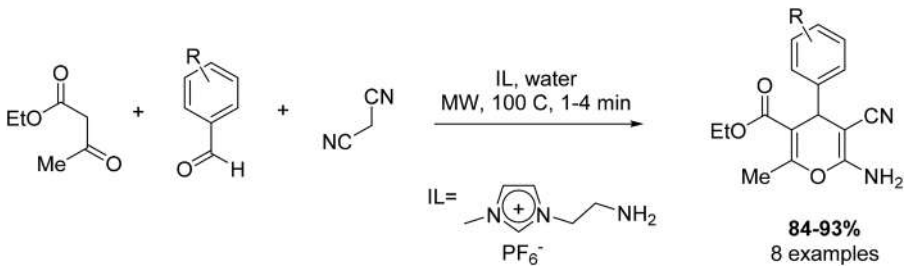

Scheme 18.23 Amino-functionalized ionic liquid as a catalytically active solvent for MW-assisted synthesis of 4H-pyrans.

as three-component reactions leading to the formation of substituted 4*H*-pyrans (Scheme 18.23).[40] It has been proposed how 1-methyl 3-(2-aminoethyl) imidazolium hexafluorophosphate can behave as a catalytically active solvent towards the achievement of 4*H*-pyrans and represents a green reaction medium and environmentally friendly alternative to available procedures. In fact, MW irradiation up to 100 °C for 1–4 min is enough to obtain these compounds in very high yield and purity.

Reactions in deep eutectic solvents. As a particular kind of ionic liquid, deep eutectic solvents (DESs) may represent another valuable alternative to organic solvents. DESs are formed from a eutectic mixture of Lewis or Brønsted acids and bases, which can contain a variety of anionic and/or cationic species and possess a melting point much lower than each single component. The most common association resulting in a DES is a mixture of choline chloride and urea (CC/U) in a 1:2 ratio, which has a melting point of 12 °C, thus being liquid at room temperature. Obviously, DESs are polar media and can be rapidly heated by MWs. Although not extensively used, a few interesting examples are reported with the association of DESs and MW dielectric heating. Aromatic nitriles were obtained from substituted benzaldehydes by treatment with hydroxylamine hydrochloride in CC/U at 100 °C for 30 minutes under MW irradiation (Scheme 18.24a).[41] Aurones synthesis was also accomplished under the same conditions, obtaining the desired products

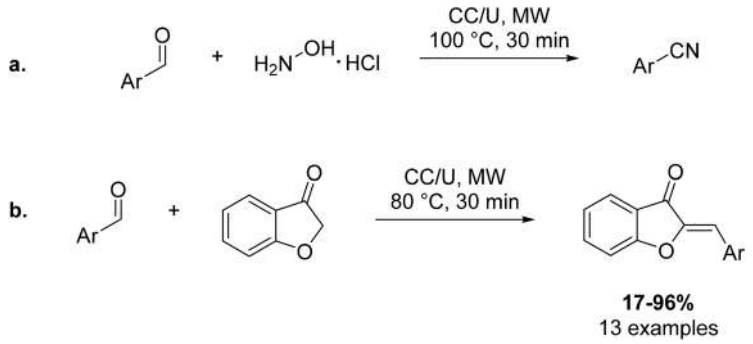

Scheme 18.24 Synthesis of benzonitriles (a) and aurones (b) using a deep eutectic solvent and MW dielectric heating.

in shorter reaction times and similar or improved yields compared to conventional heating (Scheme 18.24b).[42] In some cases, only the MW-assisted procedure afforded the aurone structure in reasonable yields.

18.2.6 Flow Chemistry and Green Scale-up

One of the major drawbacks associated with industrial scale MW-promoted processes is reproducing the same reaction conditions and efficiency of a laboratory scale experiment. As already discussed, MW-assisted reactions on a large scale still deserve attention and can significantly contribute to the greenness of an industrial process, by positively affecting energy consumption and waste generation, and by reducing the reaction times while increasing yields. However, the possibility of scaling up a reaction strictly depends on the conditions required. At the classical MW operating frequency (2.45 GHz), the major limitation is represented by the ability of the electromagnetic waves to penetrate the reaction medium, which is limited to a few centimetres of depth and highly affected by the dielectric properties. This reflects into a significant difference between the MW power density on the reaction surface and the one inside a large reactor, which could be a much smaller fraction, leading to internal heating by convection only. Exclusively reactors with a few litres of volume (or less) are suitable for batch scale MW reactions and this may represent an obstacle for applying MW technology to large industrial productions of chemical compounds. Moreover, an increase in the capacity of MW reactors directly correlates with an increase in the MW power output and involves more sophisticated extra-size cooling systems. In addition, large, pressurized vessels would not be recommended due to the heavy consequences occurring in the case of malfunctioning and explosions. An interesting solution arose from the combination of MW heating and flow chemistry, which opened up the possibility to bypass these problems. In fact, continuous or stop-flow reactors allow a relatively small amount of reaction mixture to be processed through a MW-irradiated flow cell, avoiding internal heating problems and reacting high amounts of material in time.

Several systems have been proposed since the early '90s to perform continuous flow MW-assisted reactions. Initially, these systems were specifically assembled by each research group and possibly endowed with sensors for the principal reaction parameters, such as temperature, pressure, and flow rate. Nowadays, flow systems are commercially available and can be adapted to any single- or multimodal MW reactor. However, following specific requirements, flow systems can still be designed in house for particular uses and reactions. In 2004, a microcapillary reactor was introduced for performing heterogeneous catalysed reactions inside a single mode MW cavity. Suzuki–Miyaura coupling was successfully accomplished using Pd/Al_2O_3 in a glass capillary that was coated with gold layers to enhance MW absorbance (Figure 18.7).[43]

Similarly, another custom designed microreactor has been employed to carry out reactions such as the previously reported Suzuki–Miyaura couplings or Wittig olefinations (Figure 18.8).[44] Here, a thin film of Pd was

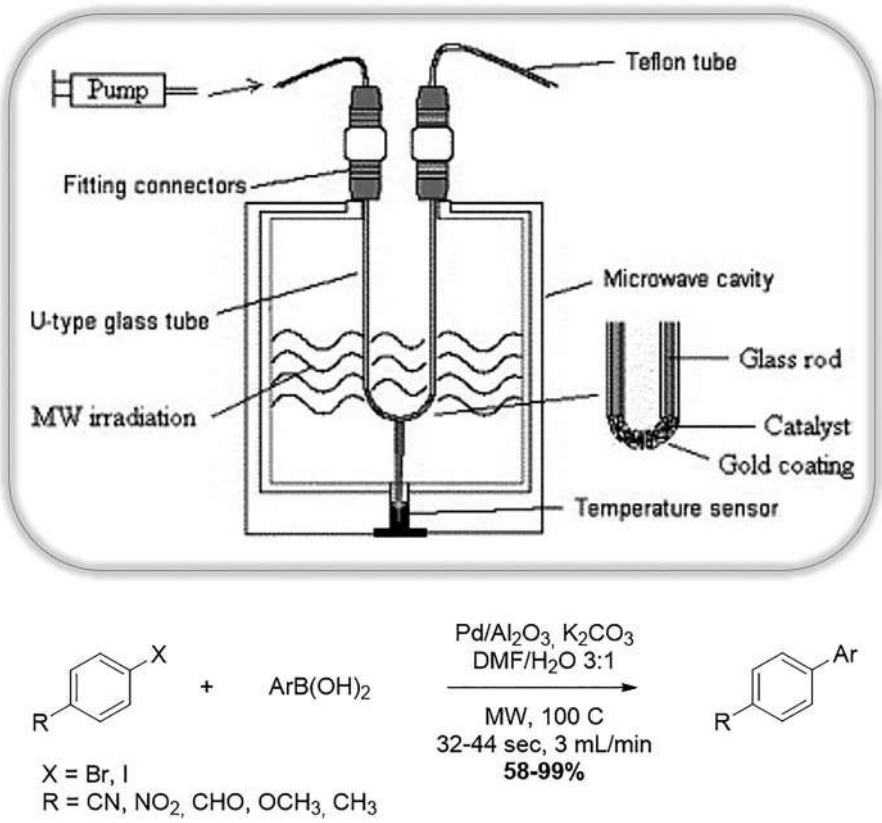

Figure 18.7 Microcapillary reactor for Suzuki–Miyaura coupling coated in gold for ensuring MW absorption on the Al_2O_3-supported catalyst area. Reproduced with permission from ref. 43, Elsevier, Copyright 2004.

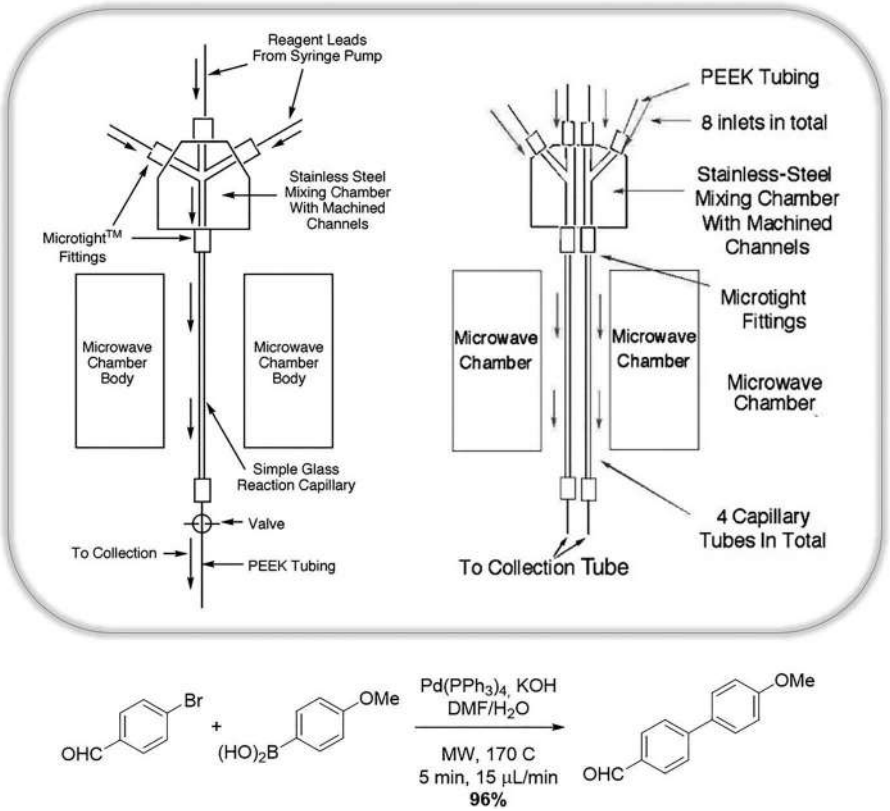

Figure 18.8 Microreactors for single (left) and combinatorial (right) MW applications. Reproduced with permission from ref. 44, American Chemical Society, Copyright 2005, and John Wiley and Sons, Copyright 2006.

used to coat the internal surface of the glass capillary, resulting in a perfect immobilized catalyst that displayed excellent reaction rate acceleration. The system was placed into the cavity of a single mode MW synthesizer and HPLC pumps were used to create a constant flow, allowing the metal-catalysed reactions to happen with no problems of clogging inside the reactor. Additional improvements on the same apparatus made it possible to perform combinatorial synthesis of small libraries of compounds. These were elegant examples of how the combination of flow chemistry, heterogeneous catalysis, and MW irradiation can lead to very efficient organic synthesis in different batch scales.

Although other examples have been reported, involving capillary systems made of Teflon coils instead of glass ones and dealing with mesofluidic systems (>1 mm of inner diameter), a different prototype has been created by filling a normal 10 mL Pyrex tube with fine sand, held by porous frits,

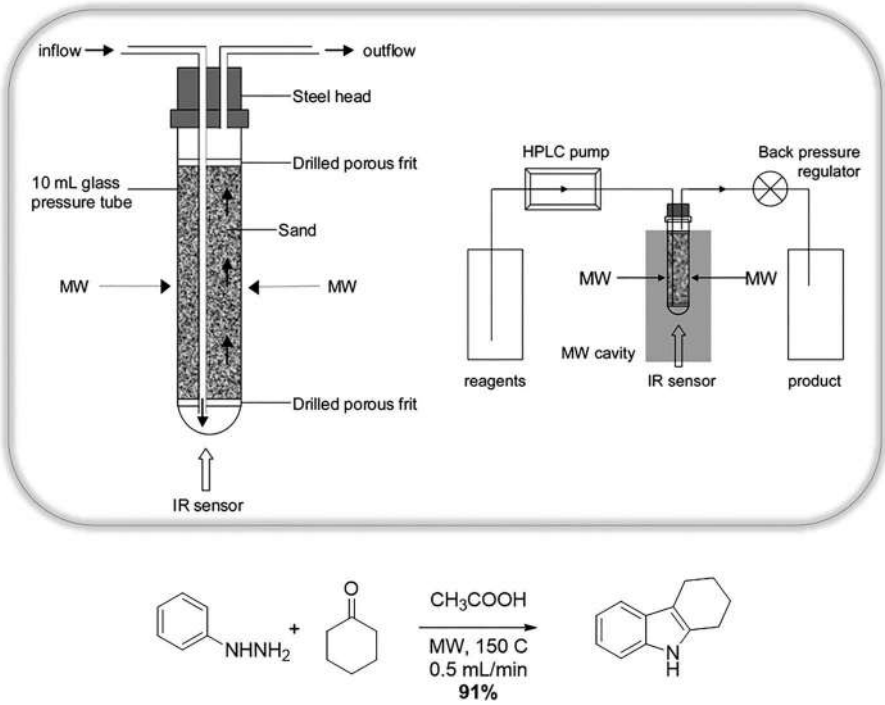

Figure 18.9 Schematic view of a sand-filled flow cell and its application in MW reactors. Reproduced with permission from ref. 45, American Chemical Society, Copyright 2005.

where the reacting mixture is forced to flow upwards through the sand layer (Figure 18.9).[45] This system can be placed into a MW cavity and used to perform organic synthesis in an efficient and scalable way, as for the Fisher indole synthesis.

Recently, beside the continuous flow method seen in the previous reactors, the stop-flow mode has been developed.[46,47] Here the reaction mixture is transferred into the MW reactor by using a powerful pump system, then reacted and pumped out into a receiving container, leaving the cavity empty for further batches. This contributed to partially solving the problems associated with continuous flow MW reactors, where clogging of the capillaries, products crystallization and the incompatibility of the heterogeneous catalysis may represent serious obstacles to accomplish the required synthesis.

18.2.7 MW-assisted Reactions and the *E*-factor

In the previous section, we gave ample space to the discussion on the environmental friendliness of MAOS. All the reported reactions possess substantial improvements when compared to previously described procedures for accomplishing similar structures. Although we proved that it is reasonable

to think about MW as a "green reaction rate accelerator", its impact on chemical processes requires further consideration in the light of quantitative parameters such as the "Environmental factor" (*E*-factor). The *E*-factor is calculated as the ratio of the total mass of all waste to the mass of the desired product and it offers a whole perspective since it accounts for product yield, stoichiometry, catalysts, solvents, and any other auxiliary masses used (Scheme 18.25). According to green metrics, increased yields and crude materials that do not require extensive purification represent a favourable starting point for expecting improved *E*-factor and greenness. And this is perfectly in accordance with the use of MW-assisted chemistry, where higher yields and lower amounts of side or undesired products are undeniable features. Therefore, we will discuss below a few examples of MAOS and related *E*-factor calculations.

In a generic reaction where A + B are the reagents and C + D are the product of interest and a possible by-product (or just wasted material) respectively, the *E*-factor will be calculated as the difference between the masses of A, B, D, and those of solvents and catalysts (or any other additional reagent), minus the mass of product C, all divided by this latter mass (Scheme 18.25). This generic calculation can apply to all organic transformations and gives a complete outline of the impact on the environment and, by simple comparison, on the atom economy and mass efficiency of the process. However, there is not a unique way to calculate the *E*-factor. Different values can be obtained if we consider waste and product masses only, including all the reagents and solvents (SYS, synthesis step), or if we add the amounts of chemicals needed for product isolation (PIS, product isolation step) and those for product purification (PPS, product purification step).[48] It is worth noting that if we add the mass of solvents for product extraction and chromatography (SYS+PIS+PPS), the value of the *E*-factor dramatically increases. Nonetheless, when product isolation and purification require extensive amounts of materials, these should be included in the calculation. The result is a lack of homogeneity in the way *E*-factors are reported, but they still represent a straight value to compare different reactions conditions and their impact on the environment.

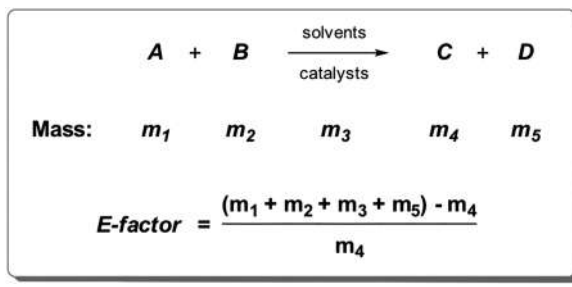

Scheme 18.25 Representation of a generic reaction between reactants A and B furnishing product C and side product (or waste) D, using specified amounts of solvents and catalysts.

As an example, we can calculate the *E*-factor (SYS) for the same Suzuki coupling reaction reported in Scheme 18.26.[37] Suzuki coupling is one of the most explored reactions under MW-assisted conditions, although it does not represent the best "green process" in terms of atom economy, since a metal catalyst, a ligand, and a base have to be added for the reaction to occur. However, in particular conditions, the process can be improved in terms of greenness to levels that are acceptable by green metrics. Considering the reaction conditions reported in Scheme 18.26, on a 1 mmol scale of aryl bromide, we can calculate two different *E*-factors for MW-assisted and oil bath heated procedures, independently from the reaction time. Yields are very high in both cases, even if the MW-promoted coupling is reported in quantitative yield, regarding the 94% yield of the convectional heating. The two *E*-factors are calculated as follow:

$$\text{MW } E-\text{factor} = \frac{0.200\text{g} + 0.158\text{g} + 2\text{g} + 0.320\text{g} + 0.402\text{g} + 0.162 - 0.196\text{g}}{0.196\text{g}} = 15.5$$

$$\text{CH } E-\text{factor} = \frac{0.200\text{g} + 0.158\text{g} + 2\text{g} + 0.320\text{g} + 0.402\text{g} + 0.174 - 0.184\text{g}}{0.184\text{g}} = 16.7$$

It is worth noting that a slight increment in the yield, as little as 6%, affects the *E*-factor by over one point. This alone would stand for preferring MAOS. Moreover, this procedure works with variously decorated aryls and only requires negligible traces of the Pd-based catalyst. Under convectional heating, on the contrary, the desired products are obtained in the absence of deactivating substituent on the aryl bromide side. Otherwise, the yields dramatically decrease and the use of increased amounts of the catalyst are required to perform this coupling, while setting the reaction time to at least 16 h. The higher amount of the catalyst would contribute to worsening the value of the *E*-factor, as additional mass would be added to its calculation.

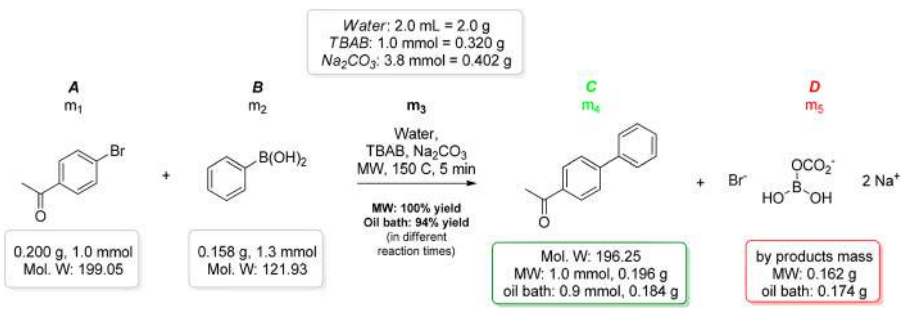

Scheme 18.26 The Suzuki coupling under MW irradiation and related amounts of reagents, solvents and (by)products for *E*-factor calculation.

This example clearly highlighted the impact of MOAS on *E*-factors, despite the little change evidenced in the reaction yield. However, if we consider an industrial scale process, dealing with kilos of reagents and products, a slight improvement in the yield and *E*-factor value would considerably affect the reduction of waste and energy consumption, thus prompting the system towards greener levels. If MW irradiation could double the reaction yield, as often happens, that would cut in half the value of the *E*-factor, with a great green enhancement for the entire process, both on small and larger scales. Another interesting example of MW-enhanced chemical transformation is the hydroformylation reaction of terminal alkenes under a H_2/CO mixture (syngas) atmosphere.

With this procedure, different terminal alkenes have been transformed into the corresponding aldehydes using syngas, a rhodium-based catalyst, Xantphos as the ligand and a mixture of toluene and an ionic liquid ([bmim][BF_4]) as the reaction medium.[49,50] In Scheme 18.27, allylbenzene has been transformed into 4-phenylbutanal (and, potentially, its branched analogue) and a comparison between MW and convectional heating was provided. It is clear how the MW-assisted procedure led to an increased yield with a reaction time as short as 4 minutes, while classical heating needed several hours to achieve a lower product yield. In addition, MW heating promoted the formation of the linear aldehyde only, and no branched derivative was isolated. As a further confirmation of the improvement brought by MW, the calculation of the *E*-factors reported a value of 48 for MW heating against one of 56 for the convectional heating (both as SYS value), thus highlighting the positive contribution of MW irradiation to the reaction greenness. Lately, this reaction has been further improved by different research groups,[51] introducing water in place of toluene and by adding different surfactants for inducing micellar catalysis. In this way, the *E*-factor value has been lowered down to 1 for the best performing processes, thanks to the possibility of recycling both the catalyst and the surfactants.

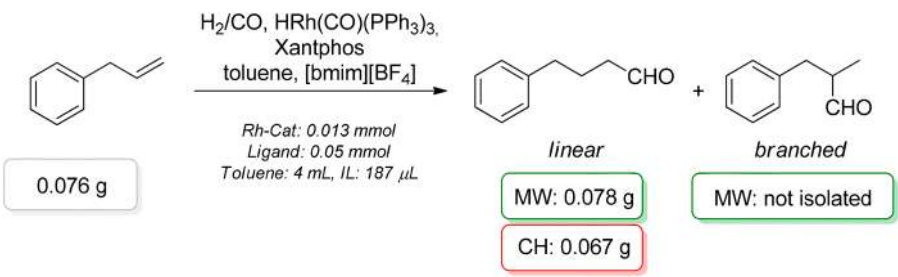

Scheme 18.27 Hydroformylation reaction under MW irradiation compared to conventional heating.

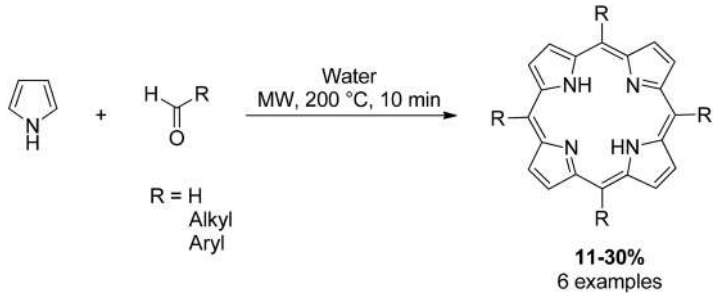

Scheme 18.28 Improved synthesis of meso-substituted porphyrins, using water as an additive, under MW irradiation at 200 °C.

The *E*-factors of several other procedures were significantly affected by the use of MW, in any case due to the high yield and purity of the obtained products. The synthesis of *meso*-substituted porphyrins from pyrrole and substituted aldehydes has been reported using water at 200 °C under MW dielectric heating and resulting in an eco-friendly process, although not very high yielding (Scheme 18.28).[52] Here, the best performing substrates furnished the desired compound in 30% yield, but the proposed method had an *E*-factor of 35, the lowest ever observed for porphyrin synthesis. In fact, the closest *E*-factor value obtained with convectional heating was 158. Moreover, this procedure made it possible to minimize the usage of organic solvent and to avoid the addition of toxic and expensive oxidants, water also being able to act as a catalyst.

bis-Pyrazolo[3,4-*b*;4'3'-*e*]pyridines have been the substrate material for bromination and nitration reactions to assess the contribution of MW to the reaction greenness.[53] In the examples reported in Scheme 18.29, it is evident how the use of MW *vs.* convectional heating led to a higher selectivity in the formation of products.

In more detail, the bromination reaction with Br_2 and catalytic amounts of Fe under classical heating furnished a polybrominated compound as the principal product, while MW allowed the insertion of bromine on the phenyl groups only at the *para*-position, with respect to their junction with the core structure. Similarly, nitration reaction led to a mixture of differently nitrated compounds, while the MW-assisted transformation returned a single tetranitro-derivative in 70% yield. The significant improvements introduced by MW irradiation are further confirmed by the calculation of the *E*-factors, which displayed values of 0.6 and 0.1 for the bromination and nitration reactions, respectively.

18.2.8 The Setup of a Green MW-assisted Chemistry Process

MW dielectric heating has introduced significant changes to the way high temperature organic transformations are designed and performed. Even if they were erroneously labelled as green by default, MWs alone represent a

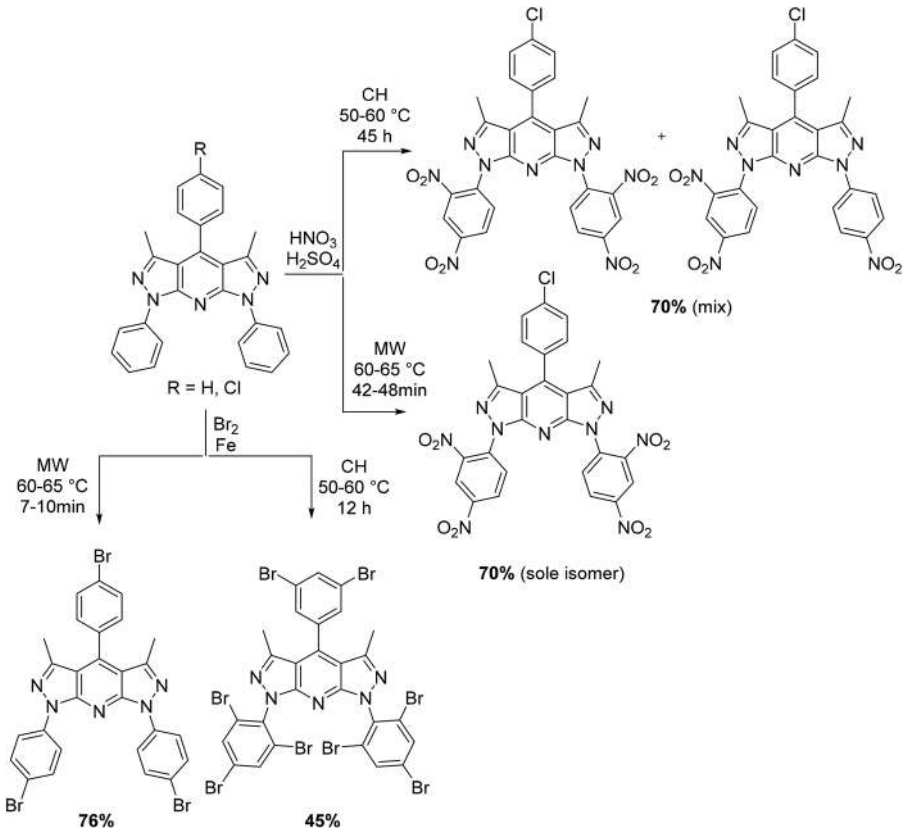

Scheme 18.29 Bromination and nitration reactions of bis-pyrazolo[3,4-*b*;4′,3′-*e*] pyridines using convectional and MW dielectric heating.

powerful source of heating rather than a proper green method, especially if we consider laboratory scale experiments and energy consumption.

However, the possibility to couple MW with different green methodologies can have a synergic effect on the greenness of the entire process, thus really affecting its eco-friendliness and sustainability (Figure 18.10). It has been showed that by increasing the scale to industrial batches, MW-assisted processes significantly differ from convectional heating, both in terms of energy consumption and reaction rate acceleration. In addition, the association with continuous-flow reactors contributes to further enhancing the greenness introduced by MW irradiation. On a laboratory scale, where MWs cannot be considered as green on their own, there are several expedients for designing a green chemistry process. First, if the reaction can be performed in solvent-free conditions, this would represent a preferred path, as the absence of organic solvents avoids the generation of toxic waste. If a liquid medium is needed, near critical water and other green solvents (ionic liquids or DESs) should be tested as an alternative. Using water may not be

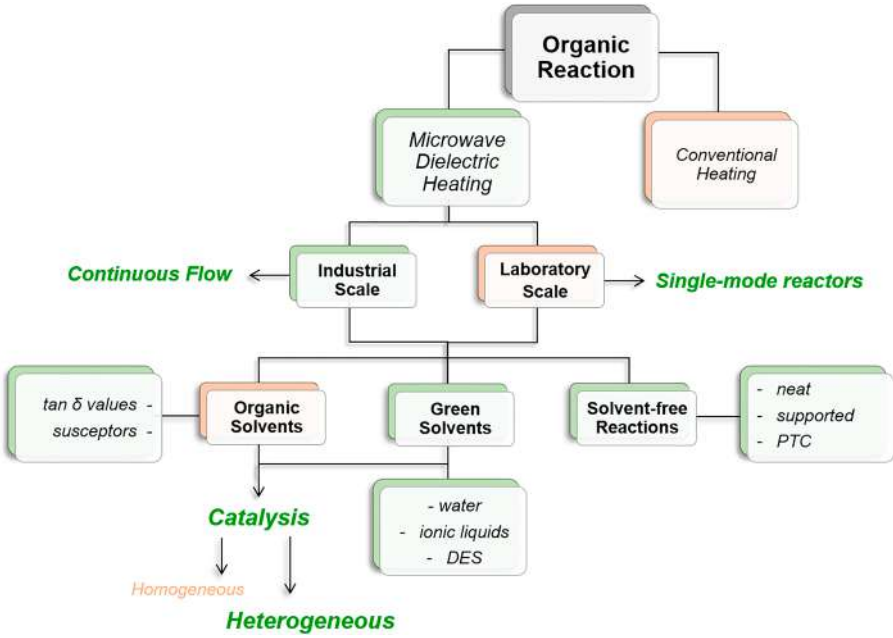

Figure 18.10 Flow diagram representing the classical cascade of procedures and methods that can be applied to move towards greener MW-assisted reactions.

compatible with all the chemical transformations, but it would represent an excellent green aspect, also affecting the *E*-factor value, since water mass can be removed from the calculation thanks to the possibility to evaporate and recycle it. If organic solvents are required to perform the experiment, then the introduction of MW susceptors and heterogeneous catalysis should be considered, improving the quality and greenness of the process. In fact, susceptors do not take part to the reaction, and only absorb and transfer heat, while a catalytic amount of metal or supported material can contribute to accelerating the reaction with little impact on the *E*-factor calculation and great enhancement of the greenness.

18.3 Conclusions

For 30 years, microwave irradiation has attracted increasing attention both as an efficient source of dielectric heating and an organic reaction rate accelerator. Although there is still a need to explore the specific effects of MWs on organic synthesis, undeniable advantages come from the use of MWs in laboratory and industrial scale reactions. MW-assisted organic synthesis agrees with the principles of green chemistry, since it beneficially affects atom economy and waste production. Moreover, the use of green solvents, heterogeneous catalysis, and

continuous flow methodologies contribute to improving the greenness of an organic reaction, thus lowering its impact on the environment. The consumption of energy for the heating process is also positively affected by MWs, as it has been shown, especially for large batch scales.

Not only the use of MWs, but its association with other methodologies has opened up a route for developing alternative processes that could have the lowest impact on the environment. The reactions reported in this chapter should be taken as successful examples of how MWs contribute to developing and improving different processes dealing with heterocyclic chemistry, natural product synthesis, industrial applications, and many other transformations for obtaining fine chemicals or pharmaceutical intermediates.

The calculation of the *E*-factor serves as a comparative value between the different procedures, helping to unveil the positive effect of green-designed processes upon the environment. Still, there is a need to work in this direction, in order to persuade both academic researchers and big companies to pursue a more sustainable and environment friendly way of performing chemical transformations.

References

1. B. L. Hayes, *Microwave Synthesis: Chemistry at the Speed of Light*, Cem Corp, 2002.
2. C. Gabriel, S. Gabriel, E. H. Grant, B. S. J. Halstead and D. M. Mingos, *Chem. Soc. Rev.*, 1998, **27**, 213.
3. A. de la Hoz, A. Díaz-Ortiz and A. Moreno, *J. Microwave Power Electromagn. Energy*, 2006, **41**, 45.
4. A. Loupy, *Microwaves in Organic Synthesis*, WILEY-VCH Verlag GmbH & Co. KGaA, 2nd edn, 2006.
5. C. O. Kappe, B. Pieber and D. Dallinger, *Angew. Chem., Int. Ed.*, 2013, **52**, 1088.
6. A. Loupy, *C. R. Chim.*, 2004, **7**, 103.
7. S. Garbacia, B. Desai, O. Lavastre and C. O. Kappe, *J. Org. Chem.*, 2003, **68**, 9136.
8. Y. Coquerel and J. Rodriguez, *Eur. J. Org. Chem.*, 2008, 1125.
9. G. Vo Than and A. Loupy, *Tetrahedron Lett.*, 2003, **44**, 9091.
10. G. B. Dudley and A. E. Stiegman, *Chem. Rec.*, 2018, **18**, 381.
11. G. B. Dudley, R. Richert and A. E. Stiegman, *Chem. Sci.*, 2015, **6**, 2144.
12. Y. Wu, J. Gagnier, G. B. Dudley and A. E. Stiegman, *Chem. Commun.*, 2016, **52**, 11281.
13. R. Gedye, F. Smith, K. Westaway, H. Ali, L. Baldisera, L. Laberge and J. Rousell, *Tetrahedron Lett.*, 1986, **27**, 279.
14. O. C. Kappe, D. Kumar and R. S. Varma, *Synthesis*, 1999, **10**, 1799.
15. C. O. Kappe, *Chem. Rec.*, 2019, **19**, 15.
16. https://cem.com/in/discover, https://www.anton-paar.com/it-it/prodotti/gruppo/sintesi-a-microonde-chimica-sintetica/ and https://www.biotage.com/product-page/biotage-initiator.

17. P. Anastas and N. Eghbali, *Chem. Soc. Rev.*, 2010, **39**, 301.
18. F. Benaskar, A. Ben-Abdelmoumen, N. G. Patil, E. V. Rebrov, J. Meuldijk, L. A. Hulshof, V. Hessel, U. Krtschil and J. C. Schouten, *J. Flow Chem.*, 2011, **1**, 74.
19. J. D. Moseley and C. O. Kappe, *Green Chem.*, 2011, **13**, 794.
20. W. G. Devine and N. E. Leadbeater, *Arkivoc*, 2011, **5**, 127.
21. S. Bouasla, J. Amaro-Gahete, D. Esquivel, I. M. López, C. Jiménez-Sanchidrián, M. Teguiche and F. J. Romero-Salguero, *Molecules*, 2017, **22**, 2072.
22. E. Brun, A. Safer, F. Carreaux, K. Bourahla, J. M. L'Helgoua'ch, J. P. Bazureau and J. M. Villalgordo, *Molecules*, 2015, **20**, 11617.
23. S. J. Song, S. J. Cho, D. K. Park, T. W. Kwon and S. A. Jenekhe, *Tetrahedron Lett.*, 2003, **44**, 255.
24. A. Mahindra, N. Patel, N. Bagraa and R. Jain, *RSC Adv.*, 2014, **4**, 3065.
25. R. Sakiyama, T. Aoyama, H. Akazawa, N. Kikuchi, K. Omura, A. Ohsaki, K. Yasukawa, T. Iida and M. Kodomari, *J. Oleo Sci.*, 2018, **67**, 1209.
26. M. Kidwai, P. Sapra, P. Misra, R. K. Saxena and M. Singh, *Bioorg. Med. Chem.*, 2001, **9**, 217.
27. S. Frère, V. Thiéry, C. Bailly and T. Besson, *Tetrahedron*, 2003, **59**, 773.
28. C. Laporte, A. Oussaid and B. Garrigues, *C. R. Acad. Sci., Ser. IIc*, 2000, **3**, 321.
29. S. H. Park, S. M. Bak, K. H. Kim, J. P. Jegal, S. I. Lee, J. Lee and K. B. Kim, *J. Mater. Chem.*, 2011, **21**, 680.
30. I. Fotiou, A. Baltopoulos, A. Vavouliotis and V. Kostopoulos, *J. Appl. Polym. Sci.*, 2013, **129**, 2754.
31. J. M. Kremsner and C. O. Kappe, *J. Org. Chem.*, 2006, **71**, 4651.
32. H. Cho, F. Töröka and B. Török, *Green Chem.*, 2014, **16**, 3623.
33. M. Pizzetti, E. De Luca, E. Petricci, A. Porcheddu and M. Taddei, *Adv. Synth. Catal.*, 2012, **354**, 2453.
34. E. Petricci, C. Risi, F. Ferlin, D. Lanari and L. Vaccaro, *Sci. Rep.*, 2018, **8**, 10571.
35. C. R. Strauss, *Aust. J. Chem.*, 1999, **52**, 83.
36. C. M. Kormos and N. E. Leadbeater, *Tetrahedron*, 2006, **62**, 4728.
37. N. E. Leadbeater and M. Marco, *Angew. Chem., Int. Ed.*, 2003, **42**, 1407.
38. D. Sharma, S. Kumar and J. K. Makrandi, *Chem. Sci. Trans.*, 2013, **2**, 403.
39. J. K. Lee, D. C. KIm, C. E. Song and S. Lee, *Synth. Commun.*, 2003, **33**, 2301.
40. Y. Peng and G. Song, *Catal. Commun.*, 2007, **8**, 111.
41. K. M. Taylor, Z. E. Taylor and S. T. Handy, *Tetrahedron Lett.*, 2017, **58**, 240.
42. U. B. Patil, S. S. Shendage and J. M. Nagarkar, *Synthesis*, 2013, **45**, 3295.
43. P. He, S. J. Haswell and P. D. Fletcher, *Appl. Catal., A*, 2004, **274**, 111.
44. (a) E. Comer and M. G. Organ, *J. Am. Chem. Soc.*, 2005, **127**, 8160; (b) G. Shore, S. Morin and M. G. Organ, *Angew. Chem., Int. Ed.*, 2006, **45**, 2761.
45. M. C. Bagley, R. L. Jenkins, M. C. Lubinu, C. Mason and R. Wood, *J. Org. Chem.*, 2005, **70**, 7003.

46. R. K. Arvela, N. E. Leadbeater and M. J. Collins Jr, *Tetrahedron*, 2005, **61**, 9349.
47. K. T. J. Loone, B. U. W. Maes, G. Rombouts, S. Hostyn and G. Diels, *Tetrahedron*, 2005, **61**, 10338.
48. R. Gilbile, R. Bhavani and R. Vyas, *Asian J. Chem.*, 2017, **29**, 1477.
49. E. Petricci, E. Cini and M. Taddei, *Eur. J. Org. Chem.*, 2020, 4435.
50. E. Petricci, A. Mann, A. Schoenfelder, A. Rota and M. Taddei, *Org. Lett.*, 2006, **8**, 3725.
51. B. Bibouche, D. Peral, D. Stehl, V. Soderholm, R. Schomacker, R. von Klitzing and D. Vogt, *RSC Adv.*, 2018, **8**, 23332.
52. C. A. Henriques, S. M. Pinto, G. L. Aquino, M. Pineiro, M. J. Calvete and M. M. Pereira, *ChemSusChem*, 2014, **7**, 2821.
53. M. Marcinkowska, D. Rasala, A. Puchala and A. Galuszka, *Heterocycl. Commun.*, 2011, **17**, 191.

CHAPTER 19

Process Intensification: From Green Chemistry to Continuous Processing

CLAUDIO BATTILOCCHIO(0000-0002-4601-8527)[a], STEVEN V. LEY(0000-0002-7816-0042)[b] AND EDOUARD GODINEAU(0000-0002-5958-4317)[a]

[a]Syngenta Crop Protection AG, Schaffauserstrasse 101, CH-4332, Stein, Switzerland; [b]Yusuf Hamied Department of Chemistry, University of Cambridge, Lensfield Road, Cambridge CB2 1EW, UK
*E-mail: claudio.battilocchio@syngenta.com, svl1000@cam.ac.uk, edouard.godineau@syngenta.com

19.1 Process Intensification & Green Approaches to Enable a Better Future

It has taken the world many years to fully embrace the issues and ramifications associated with climate change and there is still a long way to go and battles to be fought over exploitation of our planetary resources. The modern world has become very dependent upon, and demanding of, our functional materials, most of which need to be assembled (or synthesised) from primary chemical building blocks. This activity raises many concerns relating to sustainability and depletion of feedstocks (in particular oil-based feedstocks), the associated energy demands, recyclability and waste product remediation. Inevitably, this imposes ever increasing demands on the management and our responsibility in the use of these limited, precious chemical entities.

Sustainable Organic Synthesis: Tools and Strategies
Edited by Stefano Protti and Alessandro Palmieri

Published by the Royal Society of Chemistry, www.rsc.org

Also of importance, is how to best maximise the human resources in terms of innovation and creativity, while relegating more menial and repetitious tasks to machinery and the use of robotic systems. These are changing and challenging times, where decisions made now could result in long term consequences. This is particularly true in the context of the construction of the next generation of functional molecules for futuristic and unknown applications for tomorrow's novel drugs, agrochemicals, pigments, paints, polymers and perfumes.

The above statement, therefore, makes a clear case for why we need to maximise the output from our labour, whilst striving to minimise the input (doing more with less) – and this cannot be more clearly highlighted than by the topic of this chapter. These apparently conflicting views will determine the future sustainability of the science involved and suggest that there is a need for better connectivity from the initial synthesis discovery environment, through early stage process development and scale-up, and on to full scale manufacturing.

Enabling technologies and process intensification in all its forms will drive innovation, but be led by greater attention to the metrics and the circular economy of the local ecosystems. In this data-rich world, we increasingly need to live in harmony with our machines or be left to confront escalating costs and unacceptable practices. Continuous reaction processing and related enabling methods have been widely recognised to alleviate some of the issues associated with small molecule assembly. Nevertheless, these methods alone will not address all our concerns, which is why new thinking and repositioning of the Green agenda is necessary to provide a better understanding of the systems involved.

19.2 Process Intensification

Process Intensification (PI) relates to an industrial strategy that ultimately delivers chemical processes which are more sustainable and cheaper to operate. The first time that these two words were recognised as a concept was in 1995.[1–8] However, this was not the first time the principles behind the definition of PI were used in chemical processes. Since its first introduction at Imperial Chemical Industries during the 1970s,[4] PI has been associated more with a philosophy rather than a strict set of parameters. Indeed, in its very first definition, PI refers to a *general strategic approach aiming at reducing the cost burden of a chemical process*[1,2,6] (improving safety in industrial operations came in later).

In line with these definitions, PI accommodates "*any development work leading to a significantly cleaner, safer, smaller and more energy efficient manufacturing process*".[2] These principles have significant societal value, requiring our industrial output to conform to ever improving standards of manufacturing.

Within this context, in an insightful paper, Keller and Bryan pointed out that healthy worldwide industrial competition was necessary to bring about any notable changes in the way chemicals are manufactured.[9]

In general, PI encompasses the general philosophy of using compact equipment to improve the following parameters (Figure 19.1):

1. **Waste** – reduce waste generation and minimise the burden of downstream operations of the chemical process.
2. **Energy** – reduce energy consumption and make the process as energy efficient as possible.
3. **Capital costs** – reduce capital costs associated with industrial processes (*i.e.* manufacturing).
4. **Inventory** – reduce the burden of large inventories of raw materials and chemical intermediates
5. **Chemical Hazards** – reduce hazards in order to create safer and more sustainable workflows.
6. **Processing flexibility and speed** – enhance the agility of chemical processing plants, in order to create multipurpose configurations.

All these parameters contribute to the potential of a chosen PI strategy in the eventual industrialisation of a process, and in most cases, there is not one particular parameter driving the intensification strategy, but rather it is a combination of many of the parameters.

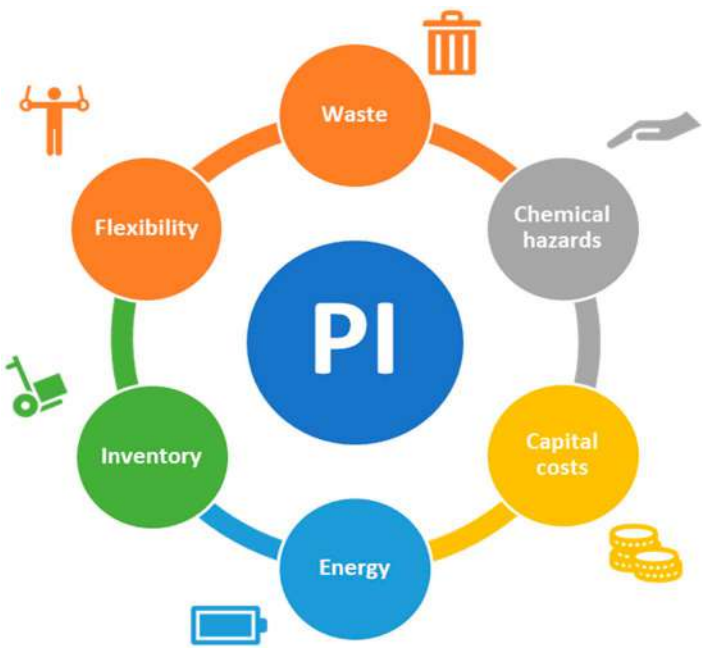

Figure 19.1 Process intensification and the interplay of contributing parameters.

We will see later how these are fundamentally connected to the principles of green chemistry and the choice of specific enabling technologies for manufacturing.

The most defining features of any intensified process are represented by the installation of a "pocket size plant" for the production of chemicals. The consequence of having this type of plant results in improved energy efficiencies and safety features, coming from the intrinsic reduction of the chemicals used at any given time. There is also a positive impact on the management of downstream unit operations of the synthesis process.

The changing mindset associated with PI often leads to greater innovation and more sustainable practices, aligning with the principles of the Green Chemistry agenda.

19.2.1 General Strategies in PI

While in the past, chemical manufacturing was generally conducted in large, centralised facilities the trend today is to use the collective output from smaller delocalised suppliers. When selecting a process for manufacturing, however, the amount of product (in kg) that can be processed per unit of reactor volume (in m^3), per unit of time (in hours) becomes an important factor whereby PI has a crucial role to play.[10]

Indeed, the two key elements of PI, namely **reduction in equipment size** (*miniaturisation*) and **total unit operations** are of primary concern.

Reducing the size of equipment can be directly coupled to capital cost investment and safety gains. Reduction in unit operations is more complex as it correlates to both energy efficiency and capital costs.

Process Intensification is achieved through application of the methods and the equipment used (Figure 19.2).

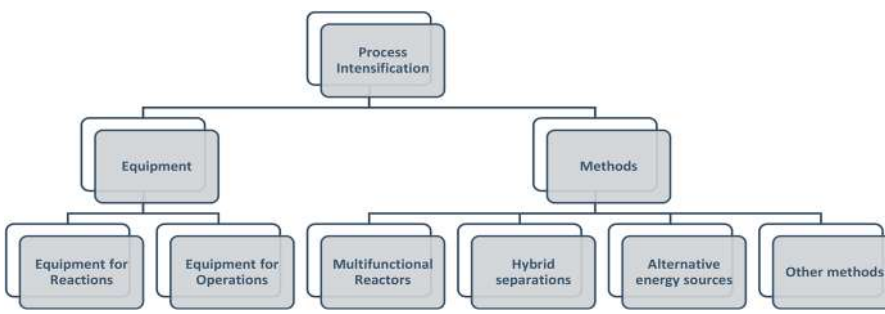

Figure 19.2 The components (equipment and methods) in PI.

19.2.2 Continuous Flow Technology: an Essential Tool for PI

As extensively described in other chapters of this book, continuous flow processing results in specific advantages over batch,[11–22] which of course makes it attractive for delivering PI.

It is prudent to properly evaluate all these technologies prior to their deployment and especially their integration with existing batch equipment. Disruptive methods will always be met with a degree of conservatism since innovation cannot be imposed upon unreceptive customers.

Consequently, to adopt these new tools of synthesis, decisions need to be based on demonstrable improvements and a strong business case. Being aware of the issues leads to a greater appreciation and a desire to find the best holistic solutions to the problems of synthesis.

Here, we highlight some further guidelines and general areas whereby process improvements can be expected through application of continuous flow methods, and which can impact considerably PI. Particularly illustrative examples will be discussed later, however a broad appreciation of some of the general components of continuous reaction processing are necessary prior to evaluating individual elements that contribute to PI.

In a typical single-step reaction sequence one can envisage a flow reaction set up whereby the input flow stream is driven by one or more external pumps and the reactive chemicals introduced directly or *via* injection coils (Figure 19.3).

These individual inputs meet at a mixing T-piece from where they then flow onto the main reaction coil (housed in a temperature-controlled zone). The reactor tubing size, length and material is chosen based on the proposed chemistries. The exiting flow stream from the reactor is subsequently passed through a heat exchanger (not shown) and onto some

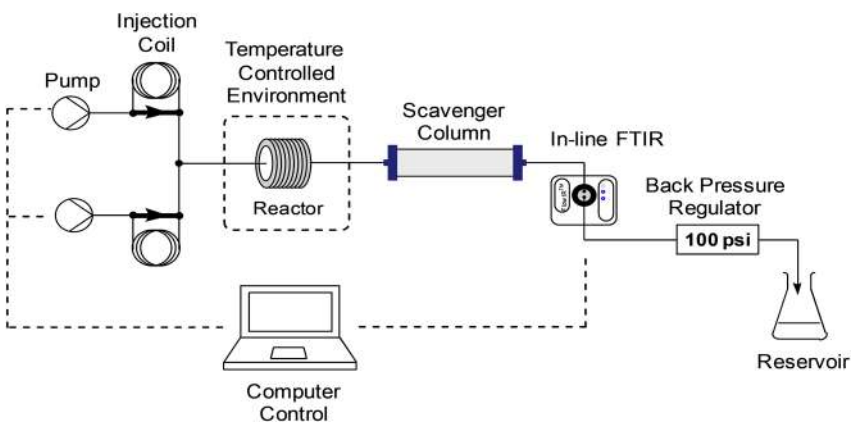

Figure 19.3 General set up of a continuous flow reaction.

downstream processing unit such as an immobilised scavenger column to remove by-products or other reaction impurities. New scavenger columns can be switched into line as needed. The flow stream can be analysed by an appropriate process analytical technology (PAT) device (in this case by FT IR). The information collected from this equipment is then fed back to a computer system that controls all modules of the flow platform. A final back pressure regulator is often inserted to accurately control the pressure in the system and can be used to provide early safety warnings of potential hazards (blockages or leakages). Products are collected in a final reservoir as appropriate. The small footprint of these reactor configurations aids in the delivery of PI over classical batch methods.

Limitations of these flow reactor arrangements often cited are problems due to solid precipitation leading to blockages. These can be ameliorated by use of agitation with ultrasound, for example, or better, by redesigning the synthesis route to avoid the problem. In multistep telescoped intensified processes (see later) the need to switch solvents can be problematic and complicate later automation. Furthermore, large viscosity changes during certain reactions may cause issues, but these too are similar to those met during traditional batch methods.

The following topics have been selected to exemplify individual aspects of how process intensification and the green agenda can be achieved through application of continuous methodologies.

19.3 Benefits and Impact of PI

All PI advances have major benefits for businesses, processes and the environment, resulting in specific positive outcomes as illustrated in Figure 19.4.

Figure 19.4 Benefits associated with process intensification practices.

19.3.1 Business Benefits: Responsive Processing

The miniaturisation of chemical plants in terms of reactors, exchangers and downstream processing units normally results in cost savings leading to more mobile and flexible arrangements, such that they can be easily reconfigured or relocated geographically. Another interesting business opportunity also arises due to a faster product launch process when using miniaturised plants. As a technique able to effectively deliver the concept of PI, continuous flow chemistry methods are becoming increasingly widespread across many industries.

19.3.1.1 On Processing Flexibility

Synthesis "on-demand" constitutes the preparation of a compound at the time it is needed in the quantity and purity it is needed. This has relevance for a number of reasons, but comes with many challenges (having a flexible supply chain being one of such challenges). Most commonly the methods are used to reduce inventories usually in the production of unstable or in some way hazardous materials.[23] The industry is also looking for greater flexibility but cannot afford to miss delivery deadlines. Properly managed, the machinery of flow chemistry can result in PI through on-demand methods operating across international borders and time zones.

A constant challenge to on-demand synthesis is the varying compound purity spectrum as the reaction scale changes.[24] With real-time, in-line analytics and information feedback, these issues are less of a problem, especially at steady state and over long reaction runs.

An insightful example of the general applications of PI is provided by the work by Jensen *et al.*[25] The report describes a chemically compatible *plug&play* system, enabling rapid realization of multiple different chemical reactions on a single platform. The authors highlight that the system has different reactor modules (*e.g.* cooling, heating, photochemical) and separators which can be interchanged by the operator, without the need to replumb any of the connections or reconfigure any part of the system, so bringing the value of flexibility to a single synthesis platform (Figure 19.5). Overall, this fully integrated system was successfully used for the automated preparation of a wide set of seven different chemical reactions, leading to more than 50 compounds in high yield.

19.3.1.2 Going from the Lab to Production Scales

The performance of today's functional molecules is constantly being challenged by industrial competition and/or by new regulations being implemented. Ultimately, this is for the good of the customer as they benefit as a consequence of these functional molecules being more effective towards their target, while remaining benign against all other species. However, the research and development costs for a given pharmaceutical or agrochemical

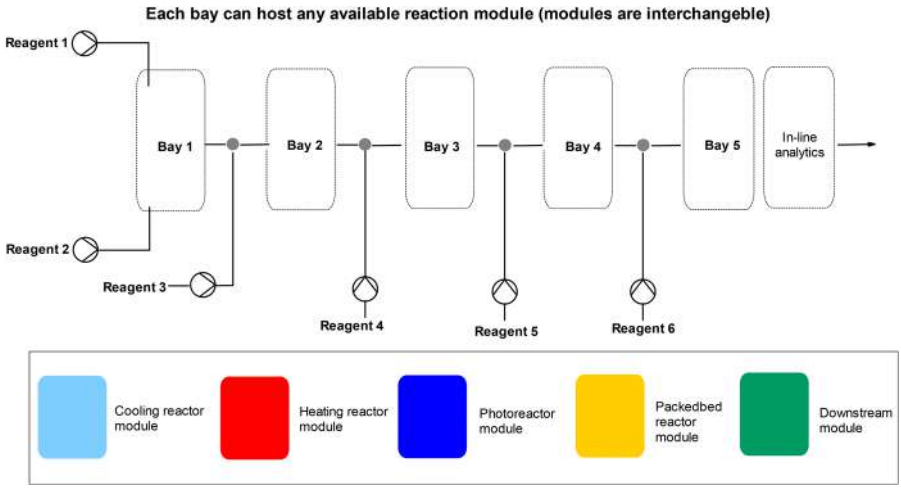

Figure 19.5 Reconfigurable flow chemistry unit from Jensen *et al.*

active ingredient have gone up substantially in the last 15 years and continue to escalate.

In the past, reaching a new product sales plateau typically took between 4 and 5 years. During this period, companies had ample time to refine the manufacturing process to a high state of maturity. Nowadays, there is a trend to ramp up this development process to cut the timelines to only 2 to 3 years. Clearly this can affect the maturation cycle, making it difficult to introduce a new second generation process involving an intensified continuous version alongside the usual batch development. This might suggest that the better approach would be to focus on the opportunities arising from the intensified process from the start, particularly as the resulting product sustainability metrics can be used in articulating the marketing of new chemical entities.

19.3.2 Sustainability Impact of PI and Continuous Flow Technology

PI can play a major role in reducing the impact of a chemical reaction on the environment and therefore will be important in achieving sustainability targets for the future. The world is facing many potentially existential challenges: the depletion of natural resources and global warming being prime concerns. It is well established that human-derived CO_2 emissions are directly impacting global warming and consequently in need of innovative human solutions to address these problems. A strategy has been agreed and coordinated by The United Nations, which has resulted in key sustainability targets for the future. Seventeen sustainable development goals[26] have been formulated that need to be achieved by 2030, Climate Action being goal #13.

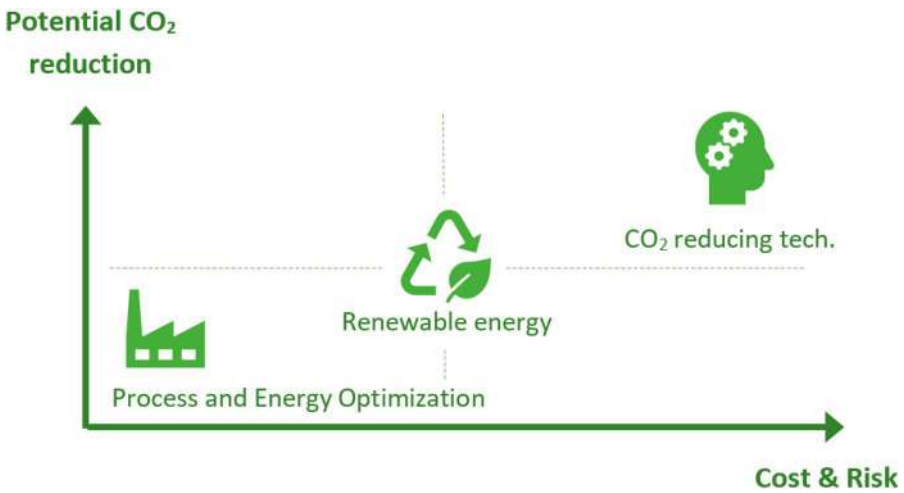

Figure 19.6 Key strategic areas for the industry to act on for substantial CO_2 reduction.

Also, the European commission who took office in late 2019 strengthened the ambitions and formulated "*A European Green Deal*"[27] which aims at having no net emissions of Greenhouse Gases (GHG) by 2050. The aim for a carbon neutral industry by 2050 has been recognised by the majority of European chemical companies. In particular, BASF has identified three main areas of interest (Figure 19.6):[28]

To reduce these CO_2 emissions, process intensification at all levels will be necessary. Indeed, for companies to comply, process intensification, which leads to greater chemical sustainability, is likely to be more important than the operational costs of the process. Arguably, improved environmental performance is not always associated with more expense.

Continuous flow technology has demonstrated substantial benefits enabling processes to contribute to improved sustainability.[29–33] The use of small reactors, with improved mixing capability and accurate temperature control, generally leads to better chemical reactions and higher quality products. There is also evidence that new chemical processes can be discovered in flow reactors due to the different dynamics and the physical design, which creates new process windows.[11] We discuss in more detail in the later sections how continuous flow technology contributes to PI and as a consequence improves processes and the quality of products, and conforms to more of the 12 Green Chemistry Principles.

19.3.2.1 Continuous Technology to Improve PI of HSE Problematic Chemistries

Safety is always of primary importance and is a strong component within the 12 Green Chemistry Principles. The general PI approach seeks to ameliorate problems, particularly those associated with the handling of hazardous

agents. Hendershot defined fundamental guidelines within the *inherent safer design* of chemical plants – which are based on four criteria: minimise, substitute, moderate, simplify (Figure 19.7).

As indicated earlier, continuous processing techniques involving reduction in size of the operating plant creates relevant opportunities for PI. The ability to miniaturise a process becomes even more useful when dealing with safety issues, especially using low volume chemical flow streams at steady state. Should blockages or sudden pressure drops occur, the system can recognise impending failure and shut-down safely with only a small material loss compared with large batch reaction vessels. Furthermore, control devices can be added to these flow reactor configurations, which promotes early intervention and improves reaction design by helping to mitigate risk through greater PI and automation. Although there is a constant desire to avoid hazardous, corrosive or toxic chemicals the real-world dictates otherwise. Consequently, on occasions, there is a need to manage and manipulate these obnoxious agents safely. Again the contained environment associated with continuous flow platforms comes to the rescue by providing an externally controlled reaction sequence whereby the hazardous agent can be generated in line, then translocated to a reaction zone where it is fully consumed and the product subsequently transferred to an integrated downstream work-up device for final product processing.[34] In this way, PI minimises any hazardous compound exposure and allows for remote external control as an additional safety benefit. Finally, through PI flow reactors can control and exploit exothermic reactions, which (noted elsewhere) can cause particular concerns when they occur in large batch reactors. Although very large quantities of dangerous chemicals are manipulated around the world on a daily basis, the risk factors are high, and history has been shocked by accidents such as Seveso in the 1970s, and Bhopal in the 1980s. Lessons from these events have

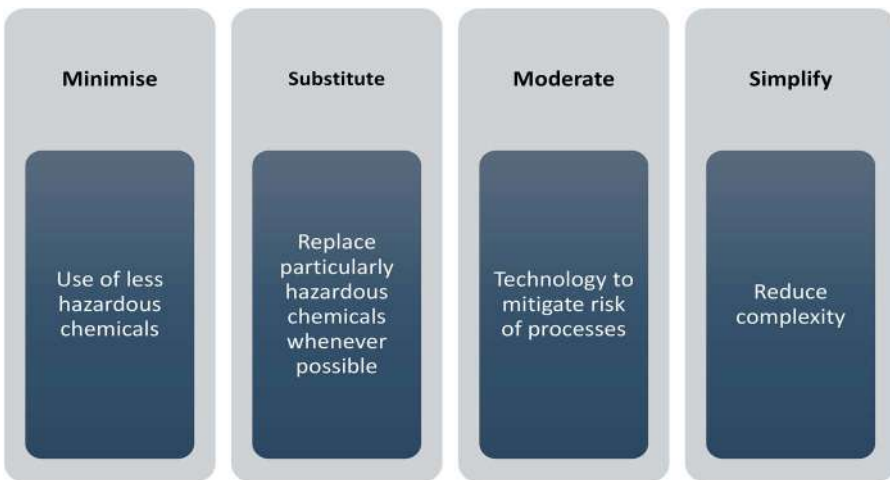

Figure 19.7 Hendershot's approach to inherent safer design of chemical plants.

resulted in the frequency of the occurrence of incidents being fortunately extremely low. Particular dangers can occur on storage of chemicals and the particularly disastrous explosion that occurred in Beirut on August 4th, 2020, is a further example of why we must always remain alert to such risks.

19.3.2.1.1 Lab Miniaturisation for Diazomethane Preparation. One illustrative example of safely handling hazardous material involves the generation and use of diazomethane. The typical batch procedure is notoriously associated with high toxicity and volatility of the reagent, combined with its explosive liability. The ***reduction in equipment size*** (miniaturisation strategy) allows PI to be used for the preparation of materials such as diazomethane. For example, scientists at Abbvie have reported an interesting research laboratory approach that continuously produces diazomethane from diazald, under basic conditions, using tube-in-tube technology (Figure 19.8).[23,35] In contrast to the batch protocol, there is no requirement for bulk storage as the product is immediately consumed on demand in the next experiment.

A related large-scale process for the continuous production of diazomethane was developed by the Phoenix company many years ago.[36] In their fully automated process, they were able produce diazomethane at a rate of 60–80 tons per year while never exceeding an inventory of over 60 g. These examples clearly show the benefits of PI towards defining safer processes.

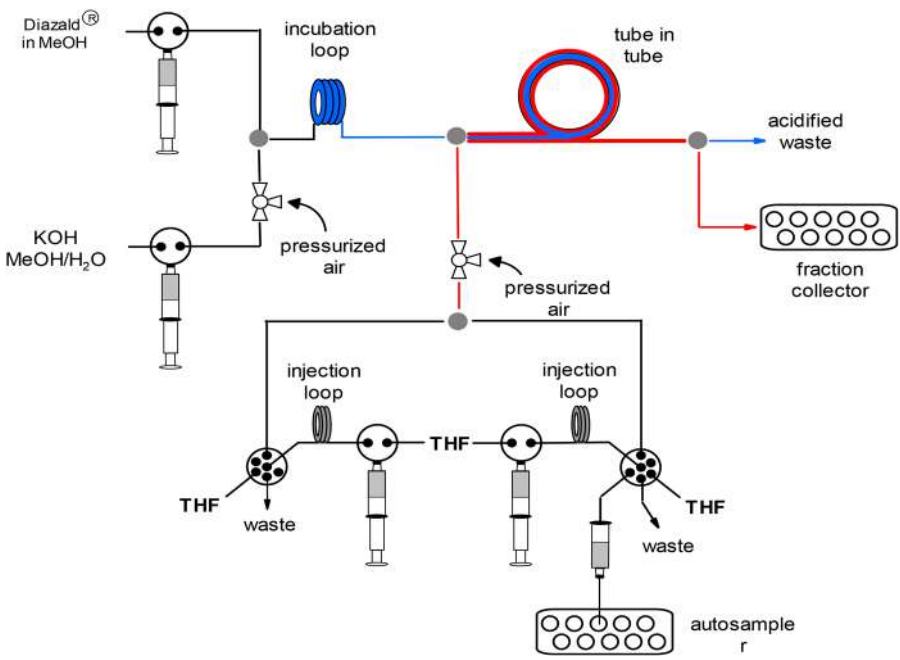

Figure 19.8 Schematic for the *in situ* generation of diazomethane using a tube-in-tube reactor. Reproduced from ref. 35 with permission from the Royal Society of Chemistry.

19.3.2.1.2 Handling Organometallics. The use of organometallics in organic synthesis programs is of fundamental importance for making carbon–carbon bonds. On a large scale, batch mode reactions of organometallics causes significant processing challenges and safety issues. These begin with the safe handling of bulk quantities of these often pyrophoric and water sensitive agents. Also, many useful reactions of organometallic compounds occur with the generation of exotherms and this again necessitates the use of specialised plants. Extensive cooling is often required in batch processes, which is both expensive and time consuming. Work-up and quenching of these highly reactive organometallic processes, on scale, is also problematic owing to the very reactive nature of the reagents involved. Their general instability on storage also often requires separate reagent generation prior to their use in coupling reactions, thereby adding further to the cost and leading to lack of process robustness. In flow systems, however, organometallics are made and reacted on demand in a limited volume reactor protected from water ingress and oxygen and where exotherms are readily controlled.[37–41] In one of the many interesting examples, Yoshida showed how the rapid dynamics of 'Flash Chemistry' can enable unexplored chemo-selective reactions using difunctional electrophiles leading to considerable improvement over the corresponding batch process (Figure 19.9).[42] Many of these improvements derive from the rapid mixing that occurs on the microflow device. The approach represents a protecting-group-free[43] use of organolithium reagents and as such can be considered as a greener process.

Researchers from Novartis reported a particularly challenging telescoped process involving lithiated species.[44] The chemical sequence described in Figure 19.10 goes through an *ortho*-lithiated intermediate (intermediate not shown), which was unstable under the reaction conditions and immediately proceeded to intermediate A *in situ*. After in-depth mechanistic investigation, it was concluded that the best conditions needed both a long dosing time for *n*-BuLi and a long holding time of intermediate A to maximize the output quality of the process. This paradox was best addressed using continuous technology, in this particular case using a series of continuous-stirred tank reactors (CSTR) and was successfully operated to deliver up to 17 kg of the final product.

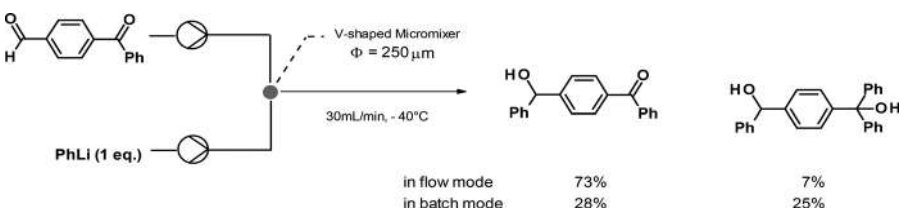

Figure 19.9 Chemoselective reactions enabled by flash chemistry.

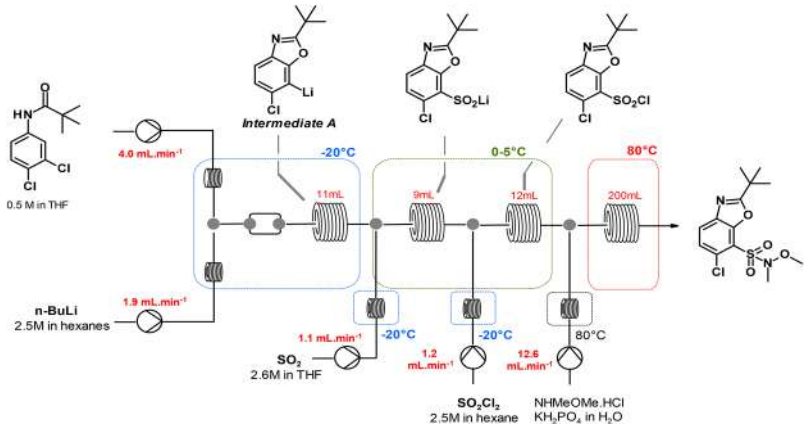

Figure 19.10 Continuous flow *ortho*-lithiation and subsequent quenching with SO_2.

19.3.2.2 Continuous Flow Technology to Improve PI vs. *Waste Minimization*

A well-known managerial phrase states: "*you can't manage what you don't measure*". Scientists therefore rightly respond by establishing metrics to monitor progress towards sustainability and generate useful tools for making informed decisions.[45–50] In terms of metrics, PI can make obvious connections to the following goals: waste prevention, less hazardous syntheses, use of benign solvents, general solvent reduction schemes, energy efficiency, real time analysis and safer chemistry. Below, the impact of PI on these topics, together with other ideas, will be evaluated.

In the early 90s, Trost formulated the concept of atom economy,[51,52] while Sheldon defined a metric termed the Environmental Impact Factor (*E*-Factor),[53–55] which enabled measurement of process performance. Some years later, the ACS GCI[56] introduced the Process Mass Intensity (PMI) factor[57] as a better reflection of the waste generated by a process, since it considers *all* inputs required in the d3 assessment of the downstream operations.

PI is a clear enabler in reducing waste and an attractive goal in any organic synthesis transformation is to minimise (or ideally eliminate) the use of solvents. In doing so a significant reduction in plant size can be expected along with reduction of associated work-up equipment. This concept leads to process intensification and compliance with the principles of Green Chemistry. In many cases, in batch mode, working at extremely high concentrations, the dosing rate of a reagent or working in the absence of a solvent, is limited by the heat absorbing capacity of the batch equipment. Further intensification is often well suited to continuous flow chemistry equipment where improved

heat transfer and in-line mixing can be best optimised. The delivery of a pure product stream in this fashion facilitates direct linkage to later chemical steps by avoiding any intermediate processing.

An example of waste reduction through PI was demonstrated in the preparation of a building block needed for the synthesis of Tiagabine (Figure 19.11).[58]

The hydrogenation process took place at very high concentrations and temperatures using the HEL FlowCAT trickle bed reactor[59] to selectively give the fully reduced piperidine product in high yield and purity at a rate of 82 g h^{-1}.

In a more recent example demonstrating the photochemical radical bromination (Figure 19.12),[60] Kappe *et al.* reported the highly exothermic *in situ*

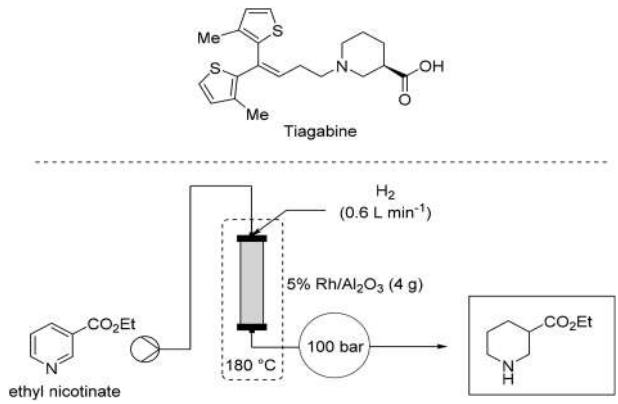

Figure 19.11 Process intensified hydrogenation preparation of a key Tiagabine building block.

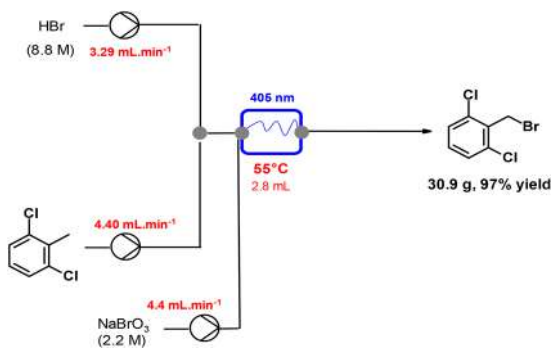

Figure 19.12 Process intensified photochemical bromination.

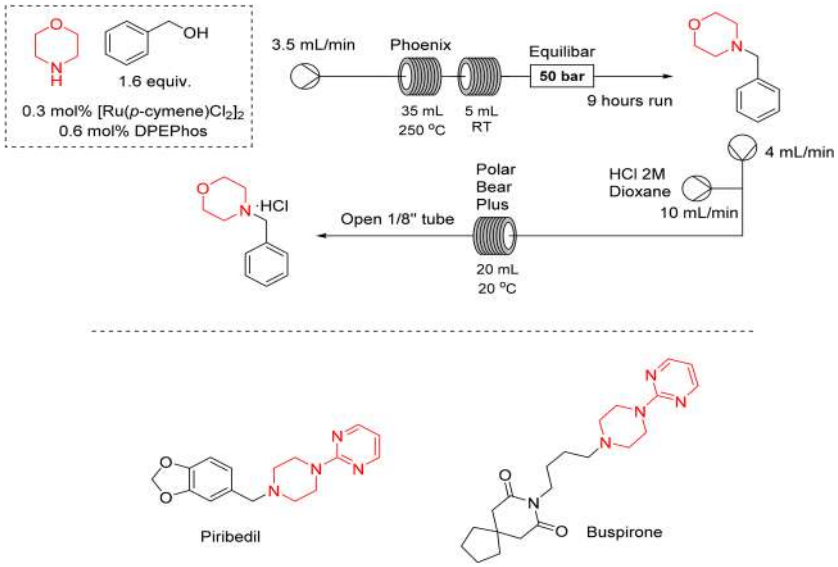

Figure 19.13 Process intensified *N*-alkylations, solvent-free at very high temperatures.

generation of Br_2 in continuous flow. The reaction proceeded in the absence of a solvent, decreasing the PMI to *ca.* 3 kg waste per kg of product made.

Another notable advantage of the flow chemistry equipment described above is that it can deliver higher quality products safely at elevated temperatures (and pressures) while maintaining liquid flow. The efficient heat transfer conditions (associated with a continuous heated flow stream) delivers PI through faster throughput kinetics often leading to improved selectivity. High temperature reactions in batch are problematic due to by-products arising from long exposure of the reaction mixture to the high temperature.

In a further interesting example employing a 'catalytic hydrogen borrowing transformation', using amines and alcohols as neat input materials was described (Figure 19.13). By combination with a Ru catalyst (*i.e.* [Ru(*p*-cymene)Cl_2]$_2$), these substrates were introduced into a high temperature flow reactor, heated at 250 °C.[61] Due to the short residence time under the flow conditions, very high yield of the coupled product amine was realised. This work highlights nicely how compact continuous flow equipment can be used to produce functionalised materials without excessive downstream processing and producing only water as the by-product under solvent free intensified conditions.

19.3.2.3 Continuous Technology to Minimize Energy Needs from Processes

On scale, energy requirements must be carefully quantified and monitored. Although popular for reactions in academic research laboratories, low temperatures (*i.e.* below −20 °C) are not considered ideal options (unless used

as a last resort) for use in commercial processes. As a consequence, there is often a very slow and reluctant take up by industry of new interesting reactions from universities operating at low temperatures (typically −78 °C). In batch, in particular when temperatures below −20 °C are required, this is understandable owing to the need for a specialised plant, the cost of cryogens, the energy needed by cryogenic devices (often prohibitively high) and the time needed to conduct these processes. Significant energy related improvements due to process intensification in moving to continuous methods can be realized. New flow equipment is now available in the form of small footprint reactors capable of accurately delivering temperatures as low as −90 °C without the need for cryogenic consumables. These devices are ideally suited to operation in research or early stage scale-up. Cooling is achieved *via* efficient transfer from a refrigerated central cylinder to a wrap-around reactor tubing. Pre-cooler coils can also be deployed in the same reactor mandrel to give better temperature control of any added reagents and avoiding water ingress, a common problem in batch mode equipment. Moreover, these small reactor units can be cooled quickly, hence avoiding the use of large quantities of cryogens over long time periods common to batch processing.

A nice illustration of dealing with organometallics was reported by scientists at Novartis (Figure 19.14).[62] In this example, the effect of equipment size reduction can be recognised to implement the PI approach.

Remarkably, this small reactor (2.4 mL volume) is able to continuously generate around 30 mmol min^{-1} of material, at −30 °C in just over a 1 s reaction time (!). The batch counterpart by comparison required very large reactor volumes (*i.e.* multi litre) to be cooled to −78 °C (very costly, time consuming and energy intensive on scale) and a much longer overall cooling and rewarming cycle (up to 1 day). The advantage of a continuous process was also reflected in the quality of material obtained (90% in flow *vs.* 21% in large batch). This result is most likely due to the improved mixing and heat transfer in the flow process, which impacts positively on the reaction kinetics.

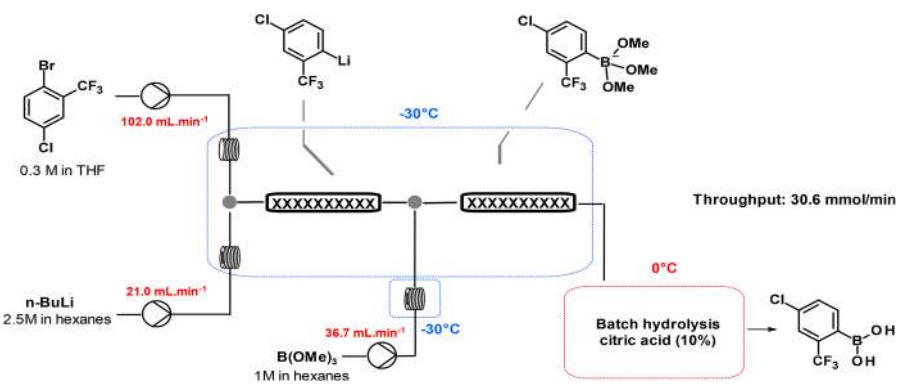

Figure 19.14 Organometallic chemistry example from Novartis.

19.3.2.4 *Continuous Technology to Minimize Intermediate Inventories by Telescoping Steps*

Intermediate product work-up operations always hamper multistep batch reaction sequences. This inevitably leads to more solvent usage and greater waste production, with a direct impact on process costs. There is also notable human manipulation necessary for multi-step reaction processing, again resulting in added costs and time. More efficient is the ability to link reactions sequentially by telescoping steps together and thereby helping to comply with the green principles and favourable PI parameters. These criteria are accommodated nicely by the use of continuous flow technology.

Manufacturing a specific chemical is always a very complex business consisting of many steps and unit operations occupying considerable plant and real estate. Moreover, transport and storage costs of bulk materials are escalating to unsustainable levels. Urgent new thinking is therefore required to massively change our approach to stock-piling of reaction intermediates. PI plays a role in reducing inventories by using continuous flow equipment to deliver chemicals 'on demand'. This becomes particularly important when safely managing a long sequence of steps involving one (or more) hazardous intermediates.

Dibromoformaldoxime (DBFO) is a chemical belonging to the family of halo-oximes and is regarded as a hazardous material. Recent work[63] highlights the toxicity and the safety risks associated with DBFO owing to autocatalytic decomposition behaviour. In addition, DBFO is significantly sensitive to basic conditions which are used in its preparation. Consequently, very careful pH control is needed to ensure a controlled generation of the intermediate bromonitrile oxide.

For the preparation of DBFO, a solution of the glyoxylic oxime was processed continuously through an improved mixer and heat exchanger system to ensure fast kinetics (Figure 19.15). By connecting the upstream (reaction) with the downstream (work up) operation, material of the quality necessary to progress directly to the next step was achieved.

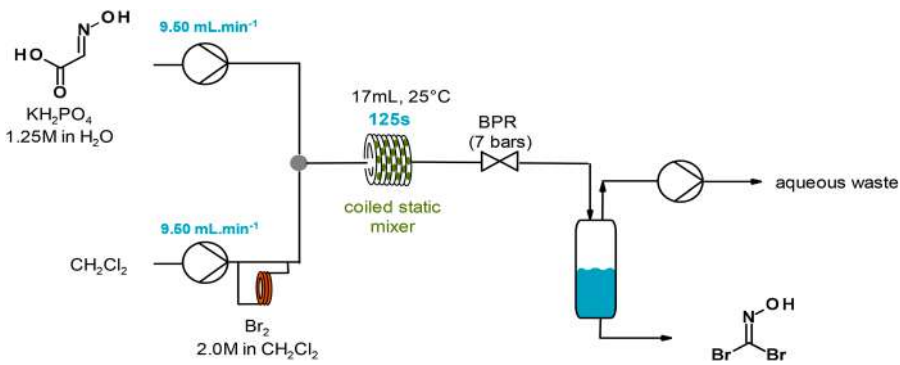

Figure 19.15 DBFO continuous synthesis.

For the next step in the sequence, the crude solution of DBFO was transferred in flow to generate the intermediate bromonitrile oxide *in situ*, in a controlled way, using a pH buffered solution and mixed vigorously with a static mixer in the presence of a trapping agent, in this case an enamide, to give the corresponding cycloaddition product in 94% yield (Figure 19.16).

In this work, further experimental observations found that the glyoxylic oxime itself also has thermal liabilities and constituted an even more serious safety hazard (*i.e.* DSC data showing >2000 J g^{-1} heat output). Owing to this, it was decided that the oxime should also be produced by a continuous process to ensure safe processing.

An overall telescoped strategy for the entire sequence was then developed (Figure 19.17).

In this example, the use of small connected reactors streamlined the 3 chemical steps leading to the safe production of the final compound 3-bromoisoxazoline at a rate of 100 g h^{-1} with minimum generation of waste products.

An equivalent batch process, due to these perceived problems was deemed too hazardous for large scale production. Clearly the PI arising from application of the continuous process is impressive.

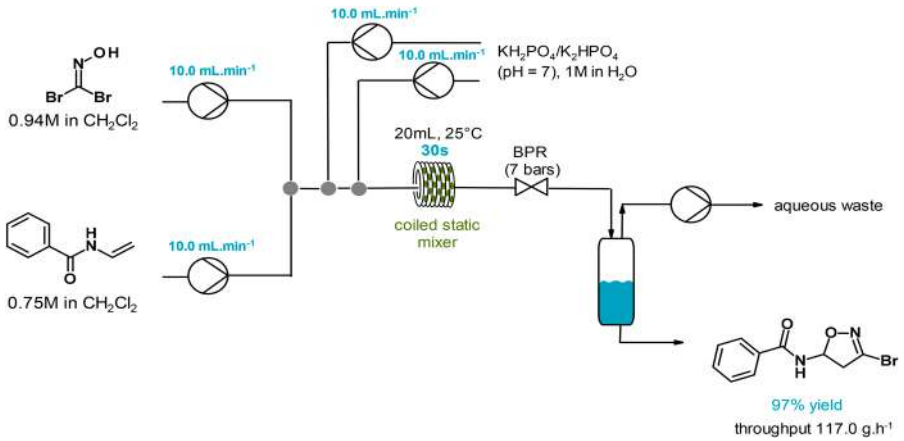

Figure 19.16 DBFO continuous controlled decomposition to the nitrile oxide and cycloaddition to yield isooxazolines.

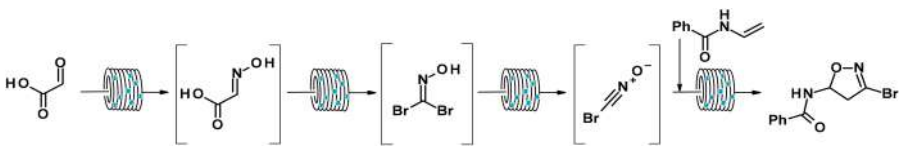

Figure 19.17 Continuous telescoped generation and use of dibromoformaldoxime.

Another example where the use of compact reactors combined with reduced work-up steps to minimise downstream processing was reported for the multistep synthesis of thiazole oximes *via* the intermediate formation of 3-bromo-2-oxopropanal *O*-methyl oxime (Figure 19.18).

The preparation of 3-bromo-2-oxopropanal *O*-methyl oxime follows a straightforward chemistry route,[64] whereby all the 3 linear steps were all run continuously. However, many of the intermediates in this synthesis displayed safety problems, making scale-up a serious issue. This was even noticeable from the first intermediate in the synthesis, which from DSC measurements was a potential explosive material. Such safety hurdles were also observed for the other intermediates in the sequence making the whole scheme particularly challenging (Figure 19.19).

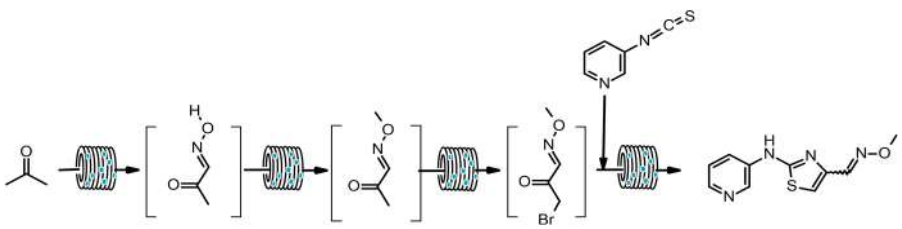

Figure 19.18 3-Bromo-2-oxopropanal *O*-methyl oxime.

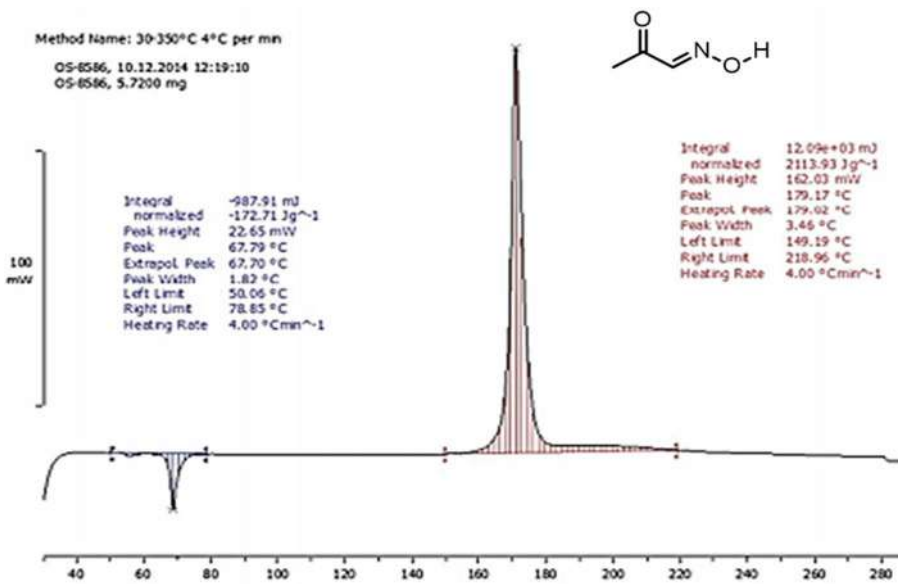

Figure 19.19 Differential scanning calorimetric data of intermediate **1**.

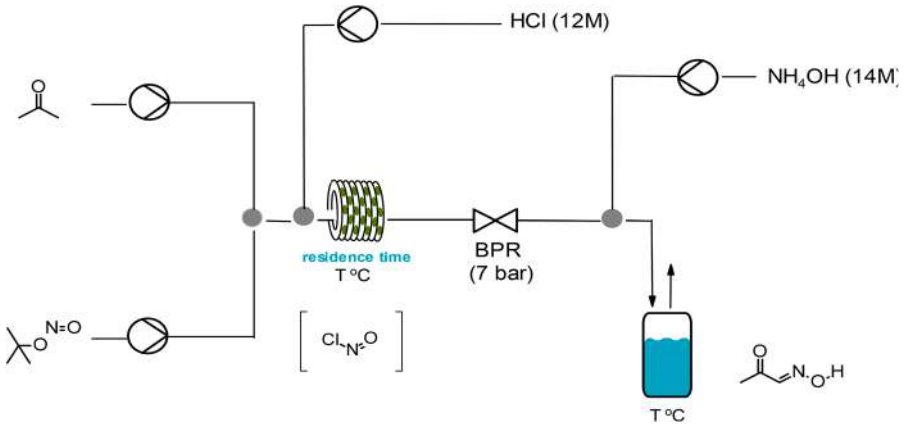

Figure 19.20 Step 1 towards the synthesis of 3-bromo-2-oxopropanal *O*-methyl oxime.

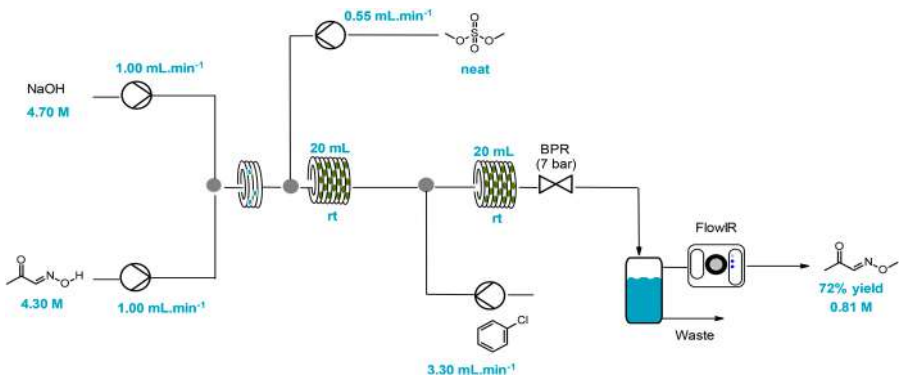

Figure 19.21 Step 2 towards the synthesis of 3-bromo-2-oxopropanal *O*-methyl oxime.

The first step[65] was known to be exothermic and also generates transient and highly reactive nitrosyl chloride as a by-product (Figure 19.20). The strategy therefore of running the chemistry under continuous flow conditions makes sense. In order to intensify the process further, higher reagent concentrations were used, which again in batch mode was unacceptable due to overheating problems.

In the second step, a methylation of a ketoxime intermediate 1 was envisaged (Figure 19.21), to give a product which was known to be volatile and thermally unstable again suggesting the need to apply flow methods. The eventual process yielded a high-quality product which did not require further purification and could be used directly in the next step.

The corresponding batch sequence is much more problematic requiring potentially hazardous distillation of intermediates.

Finally, for the last stage of the synthesis, a bromination was required prior to coupling with a thiourea to afford the required thiazole oxime. Again, one can recognise issues of using bromine as a reagent owing to its corrosive and very toxic characteristics. Once again, the flow methods provide a safe solution to the problem through the application of PI.

19.3.2.5 Continuous Flow Technology to Facilitate Catalytic Processes

Catalysis plays a major role in many modern synthesis programs and is an important component of PI and of many of the principles of Green Chemistry. While it is crucial to continue the search for new catalytic systems to build useful chemical bonds, we must be aware that there are consequences to their continued use. All chemists recognise the importance of using precious metals as catalysts for synthesis, but we must be mindful that this is a finite resource. This necessitates therefore an increased focus on downstream processing and in the recycling of catalysts in order to lower our 'precious metal footprint' along with our 'carbon footprint'. It is also where innovation and design of new catalytic systems is vital to deliver sustainable practices of the future. Areas of development will include the use of organocatalysis, bio-transformations, less expensive metals and improved recycling technologies.

Examples of using heterogeneous catalysis as a PI facilitator were discussed earlier; however, an interesting publication by Kobayashi *et al.*[66] describes a sequence of 4 chemical steps using heterogenous catalysts, one of which employed a chiral catalytic step to give (*R*)-Rolipram, a drug belonging to the family of gamma-aminobutyric acid (GABA) derivatives. The overall scheme demonstrates useful PI principles. The reaction sequence was conducted unattended for a full week without disruption and delivered (*R*)-Rolipram at a rate of 1 g day^{-1}. The approach was used to rapidly make several different pharmaceutical products (Figure 19.22).

19.3.2.6 Continuous Flow Technology to Improve the Output Quality of Processes

Quality and reproducibility are important parameters that need to be controlled in order to deliver a good manufacturing process. On scale, these issues can become complicated to manage effectively. In particular, the exact composition of an intermediate product for example can vary from one batch to another causing problems in subsequent steps. In a worst-case scenario, this can lead to out-of-specification batches which need to

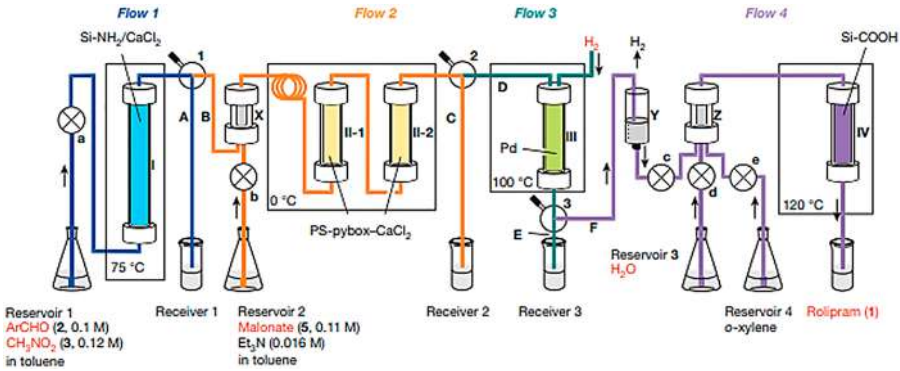

Figure 19.22 Continuous synthesis of (*R*)- and (*S*)-Rolipram. Reproduced from ref. 66 with permission from Springer Nature, Copyright 2015.

be disposed of as waste and resulting in a net substantial loss of money. It is therefore not very surprising that robustness and reproducibility criteria are often used as key performance indicators when a process route is being selected.[10] Continuous flow synthesis methods offer advantageous options to control reaction deviations, in particular owing to real-time in-line analysis, and early intervention enables processes to be aborted if out-of-spec material is detected leading to minimum loss of product compared with the equivalent batch reaction.

In a very recent example from Eli Lilly,[67] the team deployed continuous flow as a way of targeting many of the parameters to achieve PI, implementing a telescoped process to deliver multi kg quantities per hour, to produce high quality material within GMP specifications (Figure 19.23).

In step 1, the condensation step using hydrazine poses serious concerns in batch – so the choice of using continuous flow chemistry is driven by safety. Indeed, at any given time there is always a very small quantity of hydrazine present in the reaction mixture, which described a completely different scenario when compared to the need to scale up the same reaction (on kg scale) in batch (lots of hydrazine at once!) (Figure 19.24). The other parameter to consider is also the ability to shorten the reaction time under high T and high P conditions: these conditions are not feasible in batch and contribute to speeding up the reaction kinetics, increasing the intensification of the process (with the "miniaturisation" approach). The output of step 1 is continuously fed to an analytical station (*i.e.* HPLC) which is able to determine "on the fly" the quality of the reaction output so as to avoid any deviation of quality. The material processed in step 1 is directly progressed through a downstream stage, where a first liquid/liquid extraction process is followed by a solvent exchange. It is worth noticing here not only the potential for

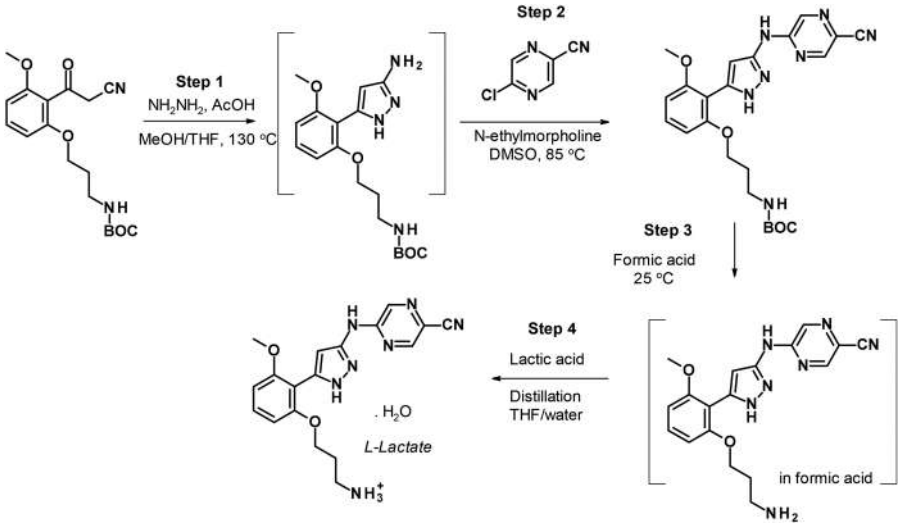

Figure 19.23 Continuous telescoped synthesis of Prexasertib monolactate monohydrate.

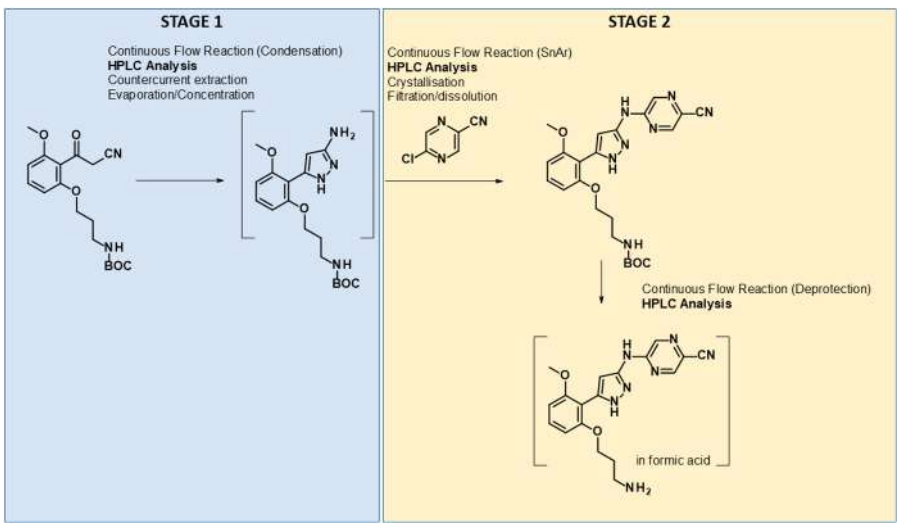

Figure 19.24 Stage 1 and stage 2 operations.

such an approach to focus on the equipment size reduction, but that it is very evident that the sequence of operations in flow accounts for a clear ***impact on operations***. Indeed, we can identify this first operation sequence as a single operation stage (stage 1). The material obtained from the first stage, is then directly used to feed the process of step 2 and step 3. Here,

both steps belong to the same operation sequence (stage 2), indicating that the sequence of operation is well connected and unified to deliver a single stage (with the advantage of ***reducing the number of unit operations***, when compared to a standard process). Throughout the different portions of the sequence in stage 2, the use of in-line PAT proved essential to "continuously" control the quality of the process, with huge implications on the intensification of the entire sequence (Figure 19.24).[68,69]

19.4 Current Barriers and Inhibitors Towards PI

We live in an uncertain and rapidly changing world. Despite being able to recognise massive opportunities by deploying PI techniques, limited budgets, time pressures and a degree of conservatism conspire to slow down development of new concepts. Clearly a more enlightened approach is necessary to drive what is often a disruptive technology but is also a considerable change in the philosophy of synthesis. To move forward, a greater investment in equipment and particularly in the recruitment of staff with the necessary skill set is vital to success. This is not as easy as it appears to be since re-education and training programs are not readily available. Furthermore, investment in equipment needs to be justified in terms of longevity and productivity. Also, further adoption requires a guarantee on safety, compliance and integration with existing plants.

Large industrial chemical synthesis operations generate information and data at an ever- increasing rate. Even today this data stream is difficult to manage. With many new technologies, concepts and approaches (with PI being just one), the system is in danger of being swamped with data unless major new thinking and financial investment occurs.

AI and machine learning as philosophies have featured in the past but have not impacted to a great extent. This situation has changed dramatically due to enhanced computer power, logistics, robotics and advanced automation. While there are inhibitors to PI, as noted above, there is an even greater danger in being 'left behind'.

In fact, the 12 principles of Green Chemistry, which have been an important charter for chemists for over 25 years, need some new interpretation and modification to respond to climate change and sustainability challenges that we all face.

References

1. D. Reay, C. Ramshaw and A. Harvey, *Process Intensification*, Butterworth-Heinemann, Oxford, 2008.
2. D. Reay, C. Ramshaw and A. Harvey, *Process Intensification*, Butterworth-Heinemann, Oxford, 2nd edn, 2013.
3. K. Boodhoo and A. Harvey, *Process Intensification for Green Chemistry*, Wiley, 2013.

4. (a) T. Grützner, D. Ziegenbalg and R. Güttel, *Chem. Ing. Tech.*, 2018, **90**, 1823; (b) C. Ramshaw, *Chem. Eng.*, 1983, **389**, 13.
5. A. Hüther, A. Geißelmann and H. Hahn, *Chem. Ing. Tech.*, 2005, **77**, 1829.
6. C. Tsouris and J. Porcelli, *Chem. Eng. Prog.*, 2003, **99**, 50.
7. S. Buchholz, *Chem. Eng. Process.*, 2010, **49**, 993.
8. A. I. Stankiewicz and J. A. Moulijn, *Chem. Eng. Prog.*, 2000, 22.
9. G. E. Keller and P. F. Bryan, *Chem. Eng. Prog.*, 2000, 41.
10. R. Dach, J. J. Song, F. Roschangar, W. Samstag and C. H. Senanayake, *Org. Process Res. Dev.*, 2012, **16**, 1697.
11. V. Hessel, *Chem. Eng. Technol.*, 2009, **32**, 1655.
12. J. Wegner, S. Ceylan and A. Kirschning, *Adv. Synth. Catal.*, 2012, **354**, 17.
13. I. R. Baxendale, *J. Chem. Technol. Biotechnol.*, 2013, **88**, 519.
14. I. R. Baxendale, L. Brocken and C. J. Mallia, *Green Process. Synth.*, 2013, **2**, 211.
15. V. Hessel, D. Kralisch, N. Kockmann, T. Noel and Q. Wang, *ChemSusChem*, 2013, **6**, 746.
16. D. T. McQuade and P. H. Seeberger, *J. Org. Chem.*, 2013, **78**, 6384.
17. B. Gutmann, D. Cantillo and C. O. Kappe, *Angew. Chem., Int. Ed.*, 2015, **54**, 6688.
18. R. Porta, M. Benaglia and A. Puglisi, *Org. Process Res. Dev.*, 2016, **20**, 2.
19. S. Kobayashi, *Chem. - Asian J.*, 2016, **11**, 425.
20. D. E. Fitzpatrick, C. Battilocchio and S. V. Ley, *ACS Cent. Sci.*, 2016, **2**, 131.
21. A. R. Bogdan and A. W. Dombrowski, *J. Med. Chem.*, 2019, **62**, 6422.
22. M. B. Plutschack, B. Pieber, K. Gilmore and P. H. Seeberger, *Chem. Rev.*, 2017, **117**, 11796.
23. Selected example: H. Yang, B. Martin and B. Schenkel, *Org. Process Res. Dev.*, 2018, **22**, 446.
24. Z. Jaman, T. J. P. Sobreira, A. Mufti, C. R. Ferreira, R. G. Cooks and D. H. Thompson, *Org. Process Res. Dev.*, 2019, **23**, 334.
25. A.-C. Bédard, A. Adamo, K. C. Aroh, M. G. Russell, A. A. Bedermann, J. Torosian, B. Yue, K. F. Jensen and T. F. Jamison, *Science*, 2018, **361**, 1220.
26. https://www.un.org/development/desa/disabilities/envision2030.html, last accessed: September 2020.
27. https://ec.europa.eu/info/strategy/priorities-2019-2024/european-green-deal_en, last accessed September 2020.
28. https://www.weforum.org/agenda/2020/01/how-to-build-a-more-climate-friendly-chemical-industry/.
29. S. G. Newman and K. F. Jensen, *Green Chem.*, 2013, **15**, 1456.
30. J.-I. Yoshida, H. Kim and A. Nagaki, *ChemSusChem*, 2011, **4**, 331.
31. J. A. M. Lummiss, P. D. Morse, R. L. Beingessner and T. F. Jamison, *Chem. Rec.*, 2017, **17**, 667.
32. S. V. Ley, *Chem. Rec.*, 2012, **12**, 378.
33. W. R. Melchert, B. F. Reis and F. R. P. Rocha, *Anal. Chim. Acta*, 2012, **714**, 8.
34. M. Movsisyan, E. I. P. Delbeke, J. K. E. T. Berton, C. Battilocchio, S. V. Ley and C. V. Stevens, *Chem. Soc. Rev.*, 2016, **45**, 4892.

35. H. F. Koolman, S. Kantor, A. R. Bogdan, Y. Wang, J. Y. Pan and S. W. Djuric, *Org. Biomol. Chem.*, 2016, **14**, 6591.
36. E. Rossi, P. Woehl and M. Maggini, *Org. Process Res. Dev.*, 2012, **16**, 1146.
37. T. Brodmann, P. Koos, A. Metzger, P. Knochel and S. V. Ley, *Org. Process Res. Dev.*, 2012, **16**, 1102.
38. F. G. J. Odille, A. Stenemyr and F. Ponten, *Org. Process Res. Dev.*, 2014, **18**, 1545.
39. M. Goldbach, E. Danieli, J. Perlo, B. Kaptein, V. M. Litvinov, B. Bluemich, F. Casanova and A. L. L. Duchateau, *Tetrahedron Lett.*, 2016, **57**, 122.
40. T. Noel, Y. Su and V. Hessel, *Top. Organomet. Chem.*, 2016, **57**, 1.
41. L. Huck, A. de la Hoz, A. Diaz-Ortiz and J. Alcazar, *Org. Lett.*, 2017, **19**, 3747.
42. A. Nagaki, K. Imai, S. Ishiuchi and J.-I. Yoshida, *Angew. Chem., Int. Ed.*, 2015, **54**, 1914.
43. T. Gaich and P. S. Baran, *J. Org. Chem.*, 2010, **75**, 4657.
44. F. Susanne, B. Martin, M. Aubry, J. Sedelmeier, F. Lima, S. Sevinc, L. Piccioni, J. Haber, B. Schenkel and F. Venturoni, *Org. Process Res. Dev.*, 2017, **21**, 1779.
45. C. R. McElroy, A. Constantinou, L. C. Jones, L. Summerton and J. H. Clark, *Green Chem.*, 2015, **17**, 3111.
46. F. Roschangar, R. A. Sheldon and C. H. Senanayake, *Green Chem.*, 2015, **17**, 752.
47. F. Roschangar, Y. Zhou, D. J. C. Constable, J. Colberg, D. P. Dickson, P. J. Dunn, M. D. Eastgate, F. Gallou, J. D. Hayler, S. G. Koenig, M. E. Kopach, D. K. Leahy, I. Mergelsberg, U. Scholz, A. G. Smith, M. Henry, J. Mulder, J. Brandenburg, J. R. Dehli, D. R. Fandrick, K. R. Fandrick, F. Gnad-Badouin, G. Zerban, K. Groll, P. T. Anastas, R. A. Sheldon and C. H. Senanayake, *Green Chem.*, 2018, **20**, 2206.
48. D. Kaiser, J. Yang and G. Wuitschik, *Org. Process Res. Dev.*, 2018, **22**, 1222.
49. H. Loureiro, M. Prem and G. Wuitschik, *Chimia*, 2019, **73**, 724.
50. J. Li and M. D. Eastgate, *React. Chem. Eng.*, 2019, **4**, 1595.
51. B. M. Trost, *Science*, 1991, **254**, 1471.
52. B. M. Trost, *Angew. Chem., Int. Ed.*, 1995, **34**, 259.
53. R. A. Sheldon, *Chem. Ind.*, 1992, 903.
54. R. A. Sheldon, *Green Chem.*, 2007, **9**, 1273.
55. http://www.sheldon.nl/roger/efactor.html, last accessed: September 2020.
56. https://www.acs.org/content/acs/en/greenchemistry.html, last accessed September 2020.
57. C. Jimenez-Gonzalez, C. S. Ponder, Q. B. Broxterman and J. B. Manley, *Org. Process Res. Dev.*, 2011, **15**, 912.
58. T. Ouchi, C. Battilocchio, J. M. Hawkins and S. V. Ley, *Org. Process Res. Dev.*, 2014, **18**, 1560.
59. https://helgroup.com/products/catalytic-processes/flowcat-high-pressure-flow-chemistry-in-a-compact-unit/, last accessed September 2020.

60. A. Steiner, J. D. Williams, O. de Frutos, J. A. Rincón, C. Mateos and C. O. Kappe, *Green Chem.*, 2020, **22**, 448.
61. R. Labes, C. Mateos, C. Battilocchio, Y. Chen, P. Dingwall, G. R. Cumming, J. A. Rincón, M. J. Nieves-Remacha and S. V. Ley, *Green Chem.*, 2019, **21**, 59.
62. A. Hafner, P. Filipponi, L. Piccioni, M. Meisenbach, B. Schenkel, F. Venturoni and J. Sedelmeier, *Org. Process Res. Dev.*, 2016, **20**, 1833.
63. C. Battilocchio, F. Bosica, S. M. Rowe, B. L. Abreu, E. Godineau, M. Lehmann and S. V. Ley, *Org. Process Res. Dev.*, 2017, **21**, 1588.
64. E. Godineau, C. Battilocchio, M. Lehmann, S. V. Ley, R. Labes, L. Birnoschi, S. Subramanian, C. S. Prasanna, A. Gorde, M. Kalbagh, V. Khade, A. Scherrer and A. C. O'Sullivan, *Org. Process Res. Dev.*, 2018, **22**, 955.
65. D. Lyn, H. Williams, and V. Sikervar, *Nitrosyl Chloride in Encyclopedia of Reagents for Organic Synthesis*, 2014.
66. T. Tsubogo, H. Oyamada and S. Kobayashi, *Nature*, 2015, **520**, 329.
67. K. Cole, *et al.*, *Science*, 2017, **356**, 1144.
68. Y. Xiang, J. Lucas, J. Van Alsten, B. Li, B. Preston, M. Lovdahl and C. M. Hayward, *Am. Pharm. Rev.*, 2012, **15**, 56.
69. H. Wu, M. A. Khan and A. S. Hussain, *Chem. Eng. Commun.*, 2007, **194**, 760.

CHAPTER 20

The Contribution of Green Chemistry to Industrial Organic Synthesis

FABIO BUCCIOL[a] AND GIANCARLO CRAVOTTO*[a]

[a]Department of Drug Science and Technology, University of Turin, Turin, Italy
*E-mail: giancarlo.cravotto@unito.it

20.1 Green Chemistry: Opportunities and Driving Forces

We live in a world where natural resources are becoming scarcer, the climate is changing, and public opinion is moving towards green choices in life and business. Chemical processes can be found at the foundations of all societal progress, and only the greener design of industrial production will facilitate the future of humankind. Green chemistry, and its complete merger with industry 4.0 strategies,[1] will have an inalienable role in shaping the next generation of the chemical industry. The 2020 European "Green Deal" has created the conditions for innovation toward greener and more sustainable production models.[2] So-called "Fourth Industrial Revolution" technologies will help industries and businesses to achieve sustainable growth, while green chemistry models will increase industrial competitiveness. The challenge here is the switch to renewable feedstocks without changing the chemistry of a process, as in the cases of bio-based ethanol, ethyl acetate, acetone and other biotech solvents.

Sustainable Organic Synthesis: Tools and Strategies
Edited by Stefano Protti and Alessandro Palmieri

Published by the Royal Society of Chemistry, www.rsc.org

The current bottlenecks for green chemistry are the high costs of non-oil-based reagents and solvents and the need for new technologies to efficiently transfer laboratory protocols to large-scale production. Organic carbonates, which are non-toxic solvents/reagents that can decompose to CO_2 and alcohol, display a low carbon footprint. This is because CO_2 can be used in their synthesis *via* insertion into an oxirane, or direct dehydrative condensation with the alcohol,[3,4] making them carbon neutral (Figure 20.1).

They can substitute halogenated reagents and solvents in a variety of industrial organic reactions, such as alkylation (often methylation) and carbonylation.[5,6] Halogenated compounds, such as phosgene, may be replaced with organic carbonates,[7] which, besides their intrinsic safety, may also improve selectivity. The use of dimethyl carbonate (DMC) in the green synthesis of dimethyl isosorbide is an interesting example.[8] Although DMC may be a valid alternative, the size of the chloroform market is still much larger. The reasons behind this are the higher costs and boiling points of carbonates that complicate reaction workup.

Greener industries will also require new technologies at their core. Of the emerging enabling technologies in organic synthesis, microwaves (MWs) and cavitation treatments, such as ultrasound (US) and hydrodynamic cavitation (HC), have proven themselves to be the most valid tools for process intensification. Unlike conductive heating, MWs induce fast volumetric dielectric heating and temperature rises with gradients that start from the inside of the reaction vessel. MWs are now relatively common in academic laboratories, and both batch and flow reactors are suitable for the design of pilot-scale applications.[9] Some authors have even reported larger-scale reactors that approach the pilot scale: Cambrex have successfully applied its CaMWave KiloLab flow reactor for a Suzuki coupling reaction with an output of 0.7 kg h^{-1} of product.[10]

In 2014, BASF's Performance Materials division and the Japanese company Microwave Chemical Co., Ltd. (MWCC) signed a joint development agreement on the use of microwave technology to improve energy efficiency in the polymer-product manufacturing process. This led to the world's first industrial continuous-flow microwave reactor, which can boast of an annual processing capacity of 1000 metric tons, in the field of polymers. A few years earlier (2010), another Japanese group used MW in the polycondensation of lactic acids at a scale of up to 20 L. At these reaction scales, polylactic acid polymers, with average molecular weights of approximately 10 000, were obtained in 5 hours. The total MW power per mole consumed by the 20 L scale reaction decreased to 1/18 of its value for the 0.2 L-scale reaction. In other words, scaling-up MW heating in chemical production saves energy.[11]

Figure 20.1 Synthesis of organic carbonates using CO_2.[3]

In the same time period, Clariant AG, a Swiss multinational speciality chemicals company, installed a biodiesel production plant using a semi-industrial continuous-flow microwave reactor in collaboration with Püschner GmbH, a German MW manufacturer. This hybrid reactor is based on the superposition of MWs between the magnetron and a reflector at the end of the waveguide. This creates a pseudo-standing wave that allows heat-transfer efficiency of up to 81% to be achieved, and the reactor has been successfully used for the production of biodiesel on a 500 L per day scale.[12]

However, true scale-up to industrial plants is often not achieved, even when the advantages of the technology are clear on paper. This is due to the difficulties involved in scaling-up microwave reactors while maintaining the promised efficiency; the results often worsen in the pilot plant and the project is abandoned. This may have several causes: the scale of the reaction; the penetration depth of the microwaves; and the design of the reactor. Improving the scale of the reactor will sometimes impact upon the distribution of the field in counterintuitive ways, meaning that a computational approach to reactor design is needed. These difficulties make it hard to plan a microwave plant and mean that it is often inconvenient to switch from a conventional reactor.

Industry should not be left alone when facing these obstacles. An important, although perhaps not crucial role, is played by public institutions, which can impose new rules on production. When old, hazardous reagents and technologies are banned from the market, industries are forced to innovate. Public funding and incentives can also be introduced to help them transition to newer plants, and to boost the market for greener alternatives that normally would be outcompeted by cheaper reagents. New regulations, in short, help green processes to become competitive and cost effective; they also speed up the transition to new technologies that would otherwise require decades before seeing widespread use. In the European Union (EU), the two main actors in this are the European Chemical Agency (ECHA) and the European regulation on Restriction, Evaluation, Authorisation and Restriction of Chemicals (REACH). REACH has been implemented since 2007 and its scope, aside from simplifying the exchange of chemical goods across Europe, is to restrict dangerous chemicals (the so called "Substances of Very High Concern", SVHC) and enhance competitiveness and innovation in chemical industries. The ECHA, working in tandem with the European Commission, uses this tool to propose that dangerous substances be restricted or pulled from the market altogether. Using restricted substances has an economic impact on industries that can range from fines to paying for permissions and the sheer cost of the time spent on compiling paperwork. It is only natural then that businesses look for greener alternatives to lighten the weight of bureaucracy. Aside from new regulations, public funding also plays a key role, as mentioned above. The most recent example of this is the European project Horizon 2020, which has only recently ended having mobilised over 900 billion euros towards the promotion of academic excellence and the application of new and greener processes in industries. The European

Union partnered with universities, but also with private companies, to create shared know-how and translate new laboratory procedures and reactions into industrial reality. Horizon 2020 is likely to be surpassed by the new European Green Deal, a project started in 2019, but whose objectives span over two decades. Given the ambitious plan to make Europe carbon neutral by 2050, it is obvious that a great amount of money will be needed, and the participation of industry and private players in the project is of high importance.

Green chemistry is a great opportunity for business and public institutions are willing to implement it on large-scale markets. Researchers have, for years, designed and proposed alternatives for chemical industries, and it is now time to translate them into reality. This is a work in progress, but examples of this change and its economic results already exist. An easy way to spot such examples exists in the winners of the Green Chemistry Challenge, set up by the United States Environmental Protection Agency (EPA) in 1996. Merck & Co. (which was also awarded a prize in 2017) was among the 2019 winners as it was awarded the prize "*for greener synthetic pathways*", while WSI won the prize "*for greener reaction conditions*".

Merck & Co. implemented a radical change in the synthesis of Zerbaxa™, an antibiotic mixture for resistant gram-negative bacteria. The purification step had previously been performed *via* chromatographic separation, but, with the switch to the direct crystallisation of one of its components (ceftolozane sulfate), the company claims to save 14 million litres of water per year, lowering the product's environmental impact and carbon footprint while increasing the yield by 50%.[13] WSI introduced its TRUpath™ technology for industrial laundry; it removes phosphates, phenols and EDTA from the formulation while maintaining the efficacy of the product, thus saving 2 billion litres of wastewater per year, by removing the harsh regeneration, and reducing overall costs per load by 50%.[14] Another prize-winning green synthesis was reported back in 2009 for the production, on a manufacturing scale, of Sitagliptin, which is a potent antihyperglycemic agent for treatment of type 2 diabetes.[15] The synthesis was performed in one pot using a homogeneous Rh-based catalyst for the asymmetrical hydrogenation step, and the catalyst was later recovered *via* adsorption onto a solid polymer matrix. This allowed for a final purity >99.9% and a yield of 65%. It also led to a five-fold reduction in the expected waste, compared to the previous process for the same pharmaceutical. This result, however, was recently enhanced with the introduction of a bioengineered transaminase biocatalyst used for the reductive amination step, and the selectivity towards the target enantiomer was improved from 95% to 99.95%. This cascaded into a 13% yield improvement, a 53% productivity improvement and an additional 19% waste reduction in a pilot-scale application.[16] Another biocatalyst was successfully used for an asymmetric reduction in the synthesis of Montelukast, which is an intermediate for anti-asthma drug Singulair (a leukotriene inhibitor). This led to a 95% yield with a purity of 98.5% at the 200 kg scale.[17]

These examples highlight how much of an impact the application of green chemistry can have on industry; tons of materials and millions of euros

saved, and significant reductions in pollution, all in processes for products that reach millions of people every day all over the world. By applying green chemistry to their processes, these companies, and many others, have improved their economic results while lowering their environmental impact, and they have rightfully been publicized for taking this *win–win* path.

Thus, given that the transition to greener processes is desirable both ethically and economically and that institutions will make it happen anyway: what makes a process greener? It is helpful to start by keeping in mind the twelve principles of green chemistry,[18] and the principles of process intensification (PI),[19] to set the targets for the desired industrial production. Then, as discussed in previous chapters, different metrics exist to uphold a quantitative approach in the matter: the life cycle assessment (LCA) of a product; its carbon footprint; mass index; and the atom economy of the reaction.[20–22] These points are not only guidelines for researchers and industrial chemists, but also challenges that can make our chemistry better and more efficient. Although they can be translated into many different results and breakthroughs, we herein try to rationalise them in the most common examples of what green chemistry can mean and bring to industrial processes.

20.2 Green Solvents as Building Blocks for Sustainable Industrial Synthesis

The first thing that comes to mind when thinking about green chemistry is the use of non-toxic reagents and solvents, which should preferably derive from renewable feedstocks. The market share of bio-based chemicals and chemical products in Europe has been estimated at around 3.0% of the total in 2019, with bio-based platform chemicals and solvents being 0.3% and 1.5% of their respective total markets.[23] This share is expected to grow and, from 2014 to 2015, the manufacture of bio-based chemicals generated a 26% income surplus.[24] However, there is still work to do, and it is clear that industry will never be truly green until this paradigm shifts.

The EU was, in 2018, the second largest manufacturer of chemicals, with a market share of 16.9%, second only to China; as shown in Figure 20.2, polymer production accounted for 21.3% of this share.[25] The polymer industry is essential to modern society, and combines huge production volumes with fine chemistry R&D. However, it currently still predominantly depends on oil refineries for all of its essential ingredients: monomers, solvents, surfactants and additives. Over 340 million tonnes of plastics were produced worldwide in 2017, with Europe accounting for 18.5% of the output, second only to China, which accounted for 29.4%.[26] However, the production of bio-based plastics from wool or biomasses in the EU was estimated to be only 1.0% of the total in 2017,[27] and only 23.2% of this 1.0% output was made up of biodegradable plastics such as polylactic acid (PLA) and polyhydroxyalkanoates (PHAs). Although aiming for a "bio" product is appealing, it is only part of the problem for a chemist.

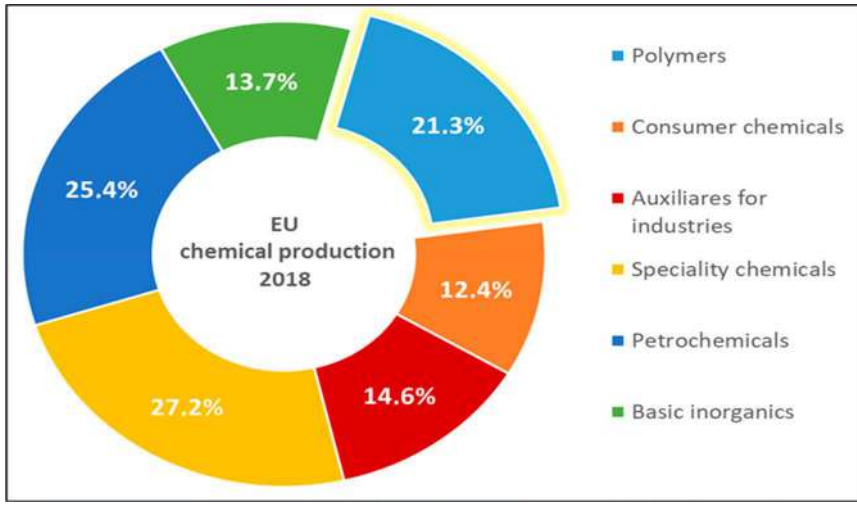

Figure 20.2 Manufacturing of chemical goods in the EU in 2018 (see ref. 25).

The need for green solvents in the polymer industry, for example, is pressing given its high consumption volumes. A green solvent should have low toxicity, low VOC content and be easily recovered.

20.2.1 Supercritical CO_2

The use of supercritical fluids as solvents has a wide array of advantages, most of which have been discussed in previous chapters, and supercritical CO_2 ($scCO_2$) has already been applied as a medium for polymerisation processes.[28] $scCO_2$ can be considered a green solvent because it is non-hazardous, naturally abundant and can easily be removed from final products, thus reducing the costs and environmental impact of purification procedures. Its use, instead of production, lowers the carbon footprint of a process. $scCO_2$ can be used in viscosity-dependant processes such as step-growth and chain-growth polymerisation,[29,30] as it has plasticiser properties and because its physical properties can be tuned by changing the experimental conditions. $scCO_2$ is also inert towards radicals, making it an ideal solvent for such a mechanism.[31] Although not many monomers and oligomers are soluble in $scCO_2$, limiting the scope of its applications somewhat, several works have demonstrated its suitability for the polymerisation of fluorinate monomers, which show good solubility in the medium. Emulsion polymerisation may be another appealing application as $scCO_2$ is insoluble with another green solvent, water. Ideally, using a water-soluble monomer, we can design two kinds of products; polymer droplets are produced in a H_2O-in-$scCO_2$ system after depressurisation, while a porous material is isolated in a $scCO_2$-in-H_2O system.[32] This, however, calls for research into practical stabilisers for such emulsions, which has been the mayor pushback for these processes so far.

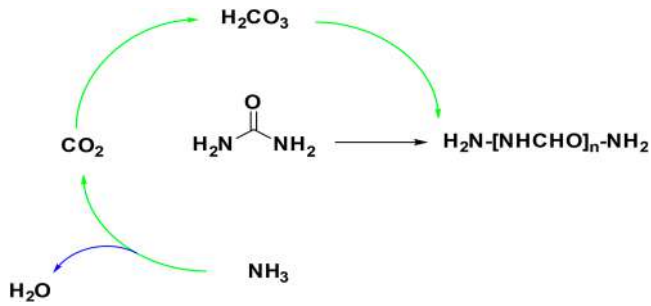

Figure 20.3 Synthesis of Nylon1 in $scCO_2$.[33]

Yuan D. *et al.* have reported the synthesis of Nylon 1 using $scCO_2$ as the medium for the reaction (Figure 20.3). In their reaction design, urea polymerises with the elimination of one molecule of ammonia. However, $scCO_2$ and ammonia can react to regenerate urea so that the only theoretical final waste is water. The reaction was conducted in a 250 mL microreactor with 210 bar CO_2 at 155 °C for 8 h, and 200 °C for an additional 2 hours.

The yield was reported to be 63% from 30 g of urea.[33] The reaction itself has high atom economy, even if we do not consider the secondary reaction between carbonic acid and urea, which is more speculative, and the use of $scCO_2$ lowers the temperature compared to a classical molten state polymerisation process. However, this is only a proof-of-concept investigation; Nylon 1 has limited industrial applicability and a 63% yield leaves room for improvement. When its direct use as a solvent for a reaction is not suitable, $scCO_2$ can still be used for polymer processing. As mentioned before, $scCO_2$ displays plasticiser properties that can allow lower processing temperatures to be set and limit the use of toxic plasticisers and co-solvents.[34] It can be used as a blowing agent to obtain polymer foams;[35] blowing or foaming agents are typically molecules that decompose to gaseous products, such as sodium bicarbonate, ammonium carbonate and ethylene diurea. Some of these decompose to CO_2 anyway, making the use of $scCO_2$ advantageous. The use of CO_2 as a blowing agent actually dates back to 1996, when recycled CO_2 from another synthetic process was used by Dow Chemicals for the processing of polystyrene as a substitute for the CFCs that were used previously.[36]

20.2.2 Ionic Liquids

The use of green solvents is not limited to $scCO_2$, nor to the polymer industry, even if it makes for a clear example. Solvent production in 2018 exceeded 20 million tons worldwide, with the EU contributing 25% to the market share,[37] meaning that the potential applications are huge in number. Often what makes a solvent appealing for an industrial process is its VOC content, as this aspect is strictly monitored and regulated by the ECHA in Europe. Ionic liquids (ILs) have often been regarded as green solvents and catalysts for a

wide array of applications, given their extremely low volatility and flammability, easy recovery and extended reusability.[38–41] ILs are, by definition, liquids below 100 °C and exist in ionic forms with a small quantity of water (usually around 10 wt%) homogenising the two counterions. They are part of the category of, so-called, deep eutectic solvents (DES), which are physical mixtures of components that show lower T_{fus} (and usually viscosity) than their starting materials. When bio-based components are used, they are referred to as natural deep eutectic solvents (NaDES).[42] A number of organic reactions have been conducted in ILs under mild conditions.[43] There are also examples of their application in radical polymerisation processes where fast propagation and low termination rates were found in poly(methyl methacrylate) (PMMA) synthesis.[44]

Kowsari *et al.* have reported an interesting methodology for the synthesis of a number of quinolines promoted by ultrasound in a ionic–liquid medium.[45] Quinolines are important platform chemicals for the synthesis of several pharmaceuticals. In this study, a basic ionic liquid (1-butyl-3-methylimidazolium hydroxide) served as a catalyst for the reaction, while water was used as the true solvent. A general structure is provided in Figure 20.4.

The reaction was run both under thermal and US activation in order to compare the results; the yield increased when US was applied, with the best result being a 95% yield, while thermal activation gave 80%. Furthermore, the reaction time decreased from 8 hours to 2 hours. To summarise, the reaction proceeded in a green solvent (water) under mild conditions with an innovative catalyst, which was recovered and reused five times without activity loss. The catalyst even exhibited superior activity to potassium hydroxide, which was used for the sake of comparison. Although energy savings are also plausible if we consider the reductions in reaction times, they are difficult to estimate as the power output of the US equipment was not stated, as is the case for the temperature progress in the two-hour window. These new methodologies have clearly improved the results for this kind of reaction, as well as its feasibility, but larger scale tests are needed. Being somewhat similar to molten salts, ILs also show a particular synergy with dielectric heating thanks to their strong polarity. Hasaninejad *et al.* have reported the MW-assisted one-pot synthesis of polysubstituted imidazoles in 1-butyl-3-methylimidazolium bromide.[46] The model reaction proceeded at 150 °C for 5 minutes with MW irradiation, instead of in 2.5 hours with conventional heating, reaching an 89% yield. The procedure was tested, with reproducible results for other compounds, giving high yields and considerable energy and time savings. MWs have also successfully been applied to the synthesis of ILs and have

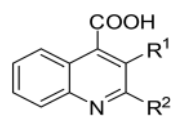

Figure 20.4 Basic structure of synthesised quinolines.[45]

been seen to speed up the reactions and even allow solvent-free conditions to be used;[47–49] this is important as one of the main criticisms aimed at ILs being "green" is that their synthesis often requires large volumes of organic solvents.

The features of ILs as green solvents and catalysts have been exploited in industrial organic synthesis. One of their most famous industrial applications is in the BASIL (Biphasic Acid Scavenging utilising Ionic Liquids) process by BASF,[50] which was awarded the "Innovation and growth award 2004" by ECN (European Chemical News). In their synthesis of diethoxyphenylphosphine (a photo-initiator intermediate), hydrochloric acid was produced as a by-product of the substitution reaction between dichlorophenylphosphine and ethanol. The use of triethylamine as a scavenger would normally form a viscous slurry, which was avoided with the use of 1-methylimidazole and an IL was created instead. It not only decreased the viscosity of the medium, but also acted as a nucleophilic catalyst, which increased the yield per unit volume from 8 to 690 000 kg m^{-3} h^{-1}.

20.2.3 Bio-based Solvents

But what about solvents that are "truly" green; those derived from renewable feedstocks? On that front, levulinic acid (LA) has been in the spotlight of academic research over the last decade. It can be derived from cellulose hydrolysis and can then serve as a platform chemical for a great number of useful products. Gamma-valerolactone (GVL) can be synthesised from LA *via* hydrogenation and subsequent cyclisation[51,52] (Figure 20.5).

It has applications as an additive for biofuels, namely bio ethanol, but also as a solvent for several organic reactions. However, its high viscosity and boiling point limit its applications. 2-Methyltetrahydrofuran (2-MTHF) is more interesting and is synthesised *via* the reduction and dehydration of GVL. It displays low polarity and boiling point, meaning that it can be used in a wide variety of syntheses as a solvent, usually replacing toxic solvents and tetrahydrofuran. However, its price is still quite high compared to other non-polar solvents; this is because its synthesis from cellulose or biomass is a multistep process that involves noble metal-based catalysts (usually ruthenium or palladium) in the hydrogenation steps.[53]

Lactate esters are another valid entry in this list of examples. Lactic acid can be derived from the conversion of biomass,[54] or, most commonly, *via* fermentation.[55] The lactic acid market has seen important growth in recent years thanks to the rising demand for polylactic acid (PLA), which is a cheap

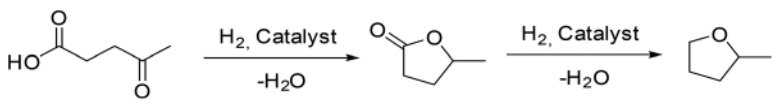

Figure 20.5 General scheme of the hydrogenation of levulinic acid to GVL and 2-MTHF.

bio-derived and bio-degradable polymer. However, the use of lactic acid as a solvent and in other industrial applications accounted for 13.0% of its total market,[56] as early as 2013, and it has been growing ever since. Methyl, ethyl and butyl lactates are all biodegradable and non-volatile. They can be used as substituents for *N*-methyl-2-pyrrolidone, acetone and toluene in paint and adhesive formulations.[57] Ethyl lactate is already used as a food and perfume additive, but its use as a solvent for paints and organic reactions is becoming more prominent (Figure 20.6).

Bennett *et al.* have demonstrated the feasibility of a green synthesis of aryl aldimines without the need for a catalyst or thermal activation.[58] The use of ethyl lactate as a solvent led to excellent yields and low reaction times, compared to other methods in the literature, and products could be crystallised directly from the reaction mixture without further purification. The use of either water or D-limonene as co-solvents also allowed the synthesis of less soluble products to be performed, and, as such, a large number of aryl amines with activating and deactivating substituents were tested with yields all above 90%. Another interesting study by Planer *et al.* has used ethyl lactate as a solvent for the ring-closing metathesis and cross metathesis of a wide number of olefins.[59] The reactions were performed at 70 °C and numerous homogeneous ruthenium-based catalysts were tested; most of the yields were above 80–90%, and were either comparable or better than those obtained using other organic solvents, such as dimethyl chlorine and toluene. The experiments were run with and without an inert atmosphere, and the products, some of which are of pharmaceutical interest, were precipitated and recovered *via* the addition of water. The direct precipitation of the target molecules is interesting, but it is fair to point out that removing water from the crystals and from ethyl acetate will have a higher energy consumption than the direct removal of other organic solvents. However, the advantages of the elimination of toluene and dimethyl chloride from the reaction should outweigh this limitation.

An ideal green solvent must not only be safe and non-toxic, but its synthesis must also have a low carbon footprint, otherwise the problem is simply moved upstream. In recent years, a lot of effort has been invested in the treatment of lignocellulosic biomasses to synthesise useful molecules.

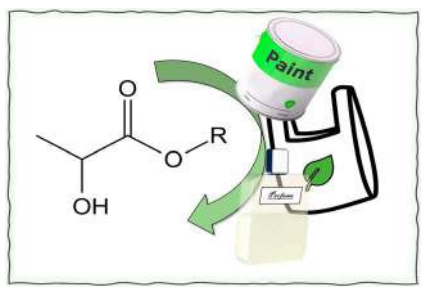

Figure 20.6 Uses of lactate esters in current markets.

This effort needs to be sustained and enhanced if we wish to supply industries with green solvents in appropriate quantities and at suitable prices. Once we achieve this goal, there is plenty of choice for organic chemists to develop greener synthesis, even on industrial scales.

20.3 Purification and Wastewater Treatments Under Acoustic and Hydrodynamic Cavitation

Besides solvents, the design of green and sustainable syntheses must consider feedstocks, experimental conditions, downstream processes, product features and waste management. The formation of secondary products is sometimes unavoidable, and the complete recovery of targets is not always possible. We must address these problems.

20.3.1 Sonocrystallisation

Besides promoting chemical reactions, especially *via* the electron-transfer mechanism, US can contribute to product purification and wastewater treatment.[60] Low-power US (usually below 50 W) is known to promote crystallisation in supersaturated solutions. This is called sonocrystallisation;[61] nuclei are formed with the compression induced by the propagation of the US in the liquid medium. Sonocrystallisation is faster than other common crystallisation techniques as it can start precipitation in minutes or even seconds, and is known to diminish the metastable zone width, which enables the technique to work at lower levels of supersaturation. This requires less energy than the evaporation of the solvent or the deep cooling of the solution to induce precipitation and can sometimes substitute the use of antisolvents. We have already discussed the advantages that direct crystallisation can provide to industrial and experimental processes; the possible application of sonocrystallisation may be able to improve those results even further. Despite considerable amounts of research, we do not yet have a fundamental understanding of sonocrystallisation, especially its mechanism of action.

Vera *et al.* have applied antisolvent-assisted sonocrystallisation for the recovery of α-glycine. A solution of 0.27 wt% of a-glycine in water at 30 °C was supplemented with ethanol, which was used as an antisolvent, to a final concentration of 0.05 wt% ethanol in water and sonicated at different power outputs at 20 kHz.[62] The sonication time to complete yield was lower using US than the respective crystallisation time under silent conditions. Increasing the US power from 0 to 40 W caused a decrease in experiment time from 2 hours to 40 minutes, and smaller crystal sizes and thinner distributions were achieved when US was applied.

Different ethanol flow rates were also tested, and it was shown that slow addition diminished the metastable zone width, and US lowered it even further at the same addition rate under all conditions. Similar results were also obtained when pulsed US was applied, with a US-to-silence ratio of 1 : 1, which

increased the efficiency of the process by lowering the power consumption and the temperature increase. Although water and ethanol are cheap and benign solvents, the addition of an antisolvent should be avoided, if possible, as it can be an additional source of contamination for the crystals and makes it more difficult to regenerate and reuse the solvents for another run. The sonocrystallisation of α-lactose without an antisolvent was performed by Sànchez-Garcìa *et al.*[63] A solution of lactose 25 wt% was pumped inside a sonication chamber where it was exposed to 20 kHz US for 107 seconds at 30 °C. The solution was then collected and cooled to 10 °C for the incubation step. The whole process took 48 hours, which is less than the average 72 hours reported in other literature manipulations without US, and gave a yield of about 20 wt%. The crystallisation of lactose was also feasible in the presence of impurities such as carrageenan and whey proteins; US was proven to speed up the crystallisation and improve the size distribution of the crystals. Hussain *et al.*, however, made the point that antisolvent crystallisation is already common in pharmaceutical companies, and, since it can operate at constant temperature, is ideal for flow processes, as it requires less parameter control and equipment complexity. In their work, these principles are applied to the flow sonocrystallisation of acetyl salicylic acid (ASA) in ethanol with the addition of water as an antisolvent.[63] The experiments were run at 25 °C, with the ASA and water solution meeting in a Y connection before reaching the sonication chamber (Figure 20.7).

Different starting concentrations and supersaturation levels were tested, with and without US. In silent conditions, no crystallisation was ever obtained under the experimental conditions. However, with US, crystallisation was

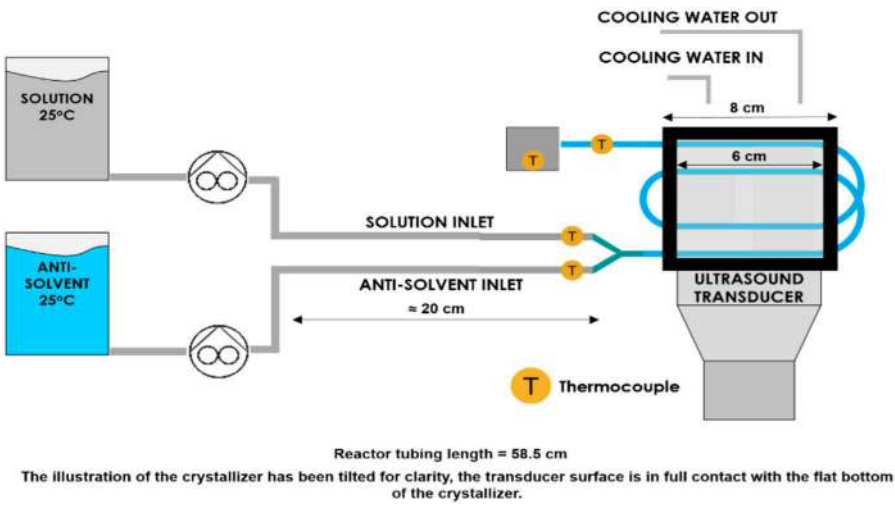

Figure 20.7 Experimental set-up for the flow sonocrystallisation of acetylsalicylic acid. Reproduced from ref. 63 with permission from American Chemical Society, Copyright 2015.

observed both with initial concentrations of 150 ppm and 70 wt% of antisolvent, and at 300 ppm and 48 wt%, after 15 minutes of sonication. An average yield of above 30 wt% was obtained. The study also underlined some pivotal aspects of sonocrystallisation. A waiting time of 18 residence times was necessary to start the experiments in a steady-state condition, otherwise the induction times would not be reproducible. Furthermore, both US and the mixing of water with ethanol induced a temperature rise despite the presence of an ice bath; at low supersaturation levels, this caused the redissolution of the formed crystals and lowered the final yields. This problem can be overcome without yield loss by using lower power levels. These are all crucial aspects for the industrial application of the technology.

Furthermore, tuning power output and impulse duration can regulate the crystal size and sometimes, depending to the specific molecule, control selectivity towards one crystal form over the others, which is a topic of paramount importance for the pharmaceutical industry. Studies on the dependence between US exposure and the size and polymorphism of the final crystals have already been performed for several molecules of pharmaceutical interest.[64–68]

The industrial use of sonocrystallisation increased during the 1980s thanks to advances in ultrasonic reactors that bore several high-intensity probes, either mounted around pipes or in the bottom of baths.[64] The pharmaceutical and fine-chemical sectors are currently using sonocrystallisation on a full-scale, and several patents have been filed by chemical, pharmaceutical and food industries for the application of sonocrystallisation in a range of production lines, as reported in Table 20.1.

Prosonix Ltd (UK) is certainly worthy of being mentioned among technology suppliers for industrial applications as they successfully applied sonocrystallisation for the production of micronised particles as inhalable medicines to treat asthma.[76]

Table 20.1 Sonocrystallisation-related patents and their applications.

Application	Company	Patent
Lipid sonocrystallisation	Thomas J Lipton Co	US20020031577A1[69]
Crystalline particles of fluticasone, beclomethasone, salmeterol and salbutamol	Glaxo Group Ltd	EP20020770107[70]
Sonocrystallisation of glucagon receptor antagonist	Merck Sharp & Dohme Co	PCT/US2008/010473[71]
Powder sonocrystallisation for inhalable medicaments	Boehringer Ingelheim, Pharma Gmbh &Co	WO2004034943[72]
Sonocrystallisation of pharmaceutical compounds	Bristol-Myers, Squibb Co	WO2000044468[73]
Sonocrystallisation of amino acids	Abbott Gmbh &Co	WO200603057717[74]
Sonocrystallisation of zeolites in continuous flow	Arkema and KU Leuven	WO2019138069A1[75]

20.3.2 Wastewater Purification

US can also be used to treat organic residues in industrial mother liquors, both to facilitate solvent recycling and to meet environmental standards for disposal. This is a relevant matter for any kind of industry: wastewater has a huge impact on the environment and on the financial balance of any production cycle. In 2016, the FAO estimated that 54% of water uptake can be traced to industry.[77] At the end of the process, it is plausible that the water used in a chemical plant will require pH adjustment and the removal of metals and organic pollutants, the latter of which create so-called "persistent organic content" that is usually reduced *via* ozonation. Ozonation is often required in pharmaceutical industries to reduce the content of pharmaceuticals, pesticides and microorganisms that derive from fermentation processes.[78,79] Both US and HC can be efficiently combined with ozone to enhance oxidative degradation. The power levels must be kept low since high cavitation can create physical barriers between O_3 and the pollutants, while the radicals formed where the bubbles collapse can act as a scavenger for ozone. US is an elastic tool and has been used in the oxidative degradation of a wide variety of compounds, including dyes and antibiotics. US is potent enough to be used both on its own, with the radicals produced at high frequencies being able to degrade pollutants, and in combination with other agents such as O_3, H_2O_2 and UV light with synergistic effects.[80–82] These processes are called "Advanced Oxidation Techniques".

Jing *et al.* have reported a pilot-scale flow system for the removal of atrazine (Figure 20.8) from pesticide-production wastewater using a combination of US, O_3 and UV light operating at 1.7 L h^{-1}.[83]

Given the complexity of the system, a Monte Carlo simulation was used to calculate the weight of the various parameters on process results and to

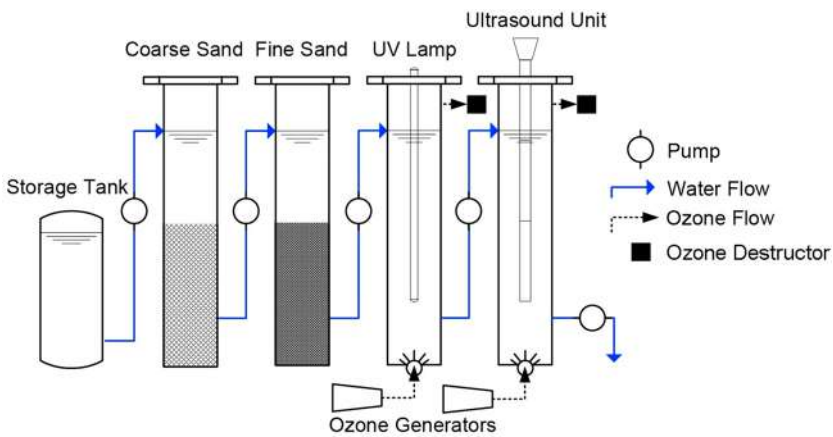

Figure 20.8 Scheme of the pilot-scale wastewater-treatment system. Reproduced from ref. 83 with permission from Elsevier, Copyright 2017.

optimise the overall protocol. As expected, the O_3 flow rate was the dominant factor for atrazine removal. However, US plays a significant role in enhancing the oxidation kinetics; US contributed to suitable mixing, and the right cavitation intensity both activated O_3 for the reaction and degraded atrazine itself *via* the formation of new radicals. High US power, however, inhibits the process as excessive cavitation impedes US penetration and scavenges O_3 from the solution. Finally, US was employed at 20 kHz and 142.5 W of power. The optimised result gave a 96% atrazine removal rate from the eluting solution, even in the presence of ionic interferents, such as chloride, carbonates and nitrates.

Promising as it is, US is currently quite costly compared to ozonation and H_2O_2 oxidations. An in-depth cost estimation for the removal of three model compounds from wastewater (phenol, an azo-dye and trichloroethylene) has been performed by Mahamuni *et al.*[84] Their conclusion was that, at the time of the study, US technologies were ten times as expensive as conventional competitors, despite the removal of the target compounds being effective. This was mainly because of their high energy consumption. However, the final cost of the process was highly dependent on a number of factors; combination with other techniques, such as O_3 and UV, always reduced costs, the treatment of lipophilic molecules had considerably lower costs and, finally, where degradation mechanisms took place inside the cavitation bubbles, such as for trichloroethylene, US was more effective and thus cheaper. The industrial CAPEX for these technologies is expected to drop in coming years.

We must therefore put together all the building blocks for a greener chemical process. Besides efficient synthesis design with green solvents and heavy-metal-free heterogeneous catalysts, a pivotal role will be played by the applied technology. A well-suited downstream process enables cost-effective product isolation if solvents are fully recycled.

20.4 Innovative Reactors for Smart Chemistry

Designing a green synthesis is the first step for a successful process, but we also need to set it into motion, and reactors are where chemistry takes place. The words “set into motion” are used for a reason as green chemistry on a large scale is likely to happen in motion, through flow reactors. To all those who have some knowledge of chemical engineering, it is clear how a flow reactor can provide higher productivity than batch and fed-batch systems; you can drastically reduce the dead times involved in charging, heating, cooling and cleaning the reactor. Of course, there are reasons behind the fact that not all chemistry is performed in flow reactors yet. Flow reactors tend to have higher installation costs and need a well-built continuous chain of provision and shipping. Furthermore, for some types of specific smaller-scale production, it is simply more convenient to use batch reactors as they are easier to handle and can perform a wider variety of reactions. However, flow chemistry provides much more than a simple increase in productivity, although

that is certainly appealing on its own. Flow chemistry allows industries to exploit hazardous chemistry that would be too difficult to control in large batches. Nitration processes, which can lead to explosions if the temperature and reaction rate are not strictly controlled, are a well-known example of this. Other interesting examples can be found in reactions with organometallic,[85] and diazo compounds,[86] which have been successfully run in flow on different scales. Flow chemistry offers advantages when it comes to speed, safety and selectivity as reactions are run in smaller volumes (without sacrificing productivity), and thus parameters such as residence time, temperature and concentration can be carefully controlled. Moreover, as the residence time and ambient conditions can be tailored, handling reactive intermediates becomes much easier and more selective than in batch chemistry.

20.4.1 Photoreactors

Flow chemistry works particularly well in photochemistry. In recent years, many have looked to photochemistry as a green and cost-effective way of activating chemical reactions, rather than using conventional heating or organic reagents to generate radicals.[87,88] The introduction of light emitting diodes (LEDs) onto the mainstream market has given this field new prospects, as they offer many advantages over the commonly known Hg vapour lamps. LEDs function thanks to electronic transitions that can be tailored to provide practically monochromatic light emissions, which minimises energy loss and parasitic reactions. LEDs consume less power than other light sources meaning that heating is also minimised. Finally, their small size allows for easier integration into reactors, even allowing them to be positioned internally; this is a pivotal aspect of reactor design since one of the drawbacks of photochemistry is the low penetration depth of ultraviolet and visible light in liquid media (Figure 20.9).

This limitation, however, can be overcome using flow microreactors. The use of small-scale transparent channels allows complete and homogeneous irradiation to be performed, which maximises heat dispersion at the same time.[89] A study on the matter has been performed by Elliott *et al.* who compared the results of several cyclisations that were run in batch and flow photochemical reactors[90] (Figure 20.10). The authors decided to compare the yields at the end of the reactions rather than considering the residence time for the flow reactor. The results showed that although the final yields were the same for all the reactors, flow reactors consistently showed higher productivity. Moreover, their inherent safety, due to the quantity of reagents undergoing a transformation in a flow reactor being lower than in a batch of the same capacity, means that it was possible to use a flow reactor to scale up the potentially explosive ring-opening reaction of [1.1.1] propellane, producing 51.8 g of product in 70 minutes.

Another interesting application of flow photochemistry can be found in the synthesis of artemisinin, an antimalarial drug with a large market worldwide. It can be extracted from *Artemisia Annua*, but the plant only contains

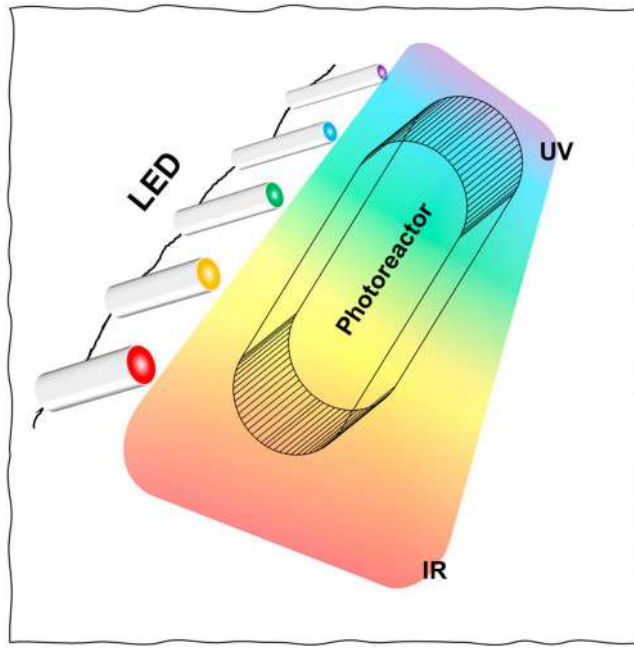

Figure 20.9 LEDs emit monochromatic light with low heat emissions.

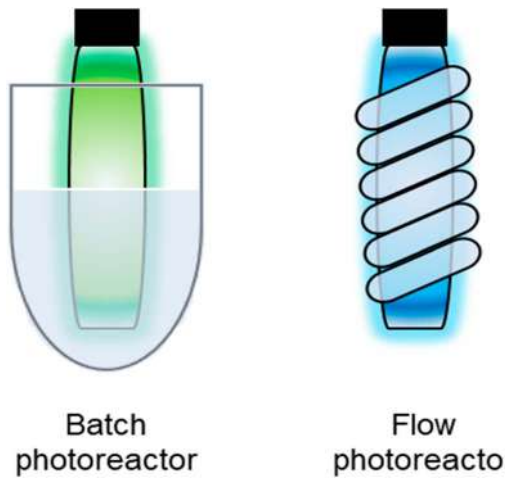

Figure 20.10 Batch and flow photoreactor configurations used.[90]

1 wt% active principle and its harvesting cycle impacts drug prices, meaning that its chemical synthesis has become of great interest. In 2012, Lévesque and Seeberg reported the first complete flow photochemical synthesis of artemisinin from artemisinic acid.[91] The highlight of the work was the photochemical oxidation of dihydroartemisinic acid *via in situ* generated singlet

oxygen. This step was performed using a medium-pressure 450 W Hg lamp with 91% conversion and a 75% yield. The reaction then proceeded *via* a Hock-cleavage and oxidation with the addition of trifluoroacetic acid (TFA) and bubbling oxygen gas. The authors successfully combined these synthetic steps into a single flow process (overall yield 39%) with a daily output of 200 g artemisinin.

This remarkable step ahead for the industrial production of artemisinin was later implemented by Sanofi. One drawback here is the use of dichloromethane (which is non-flammable) and TFA which are both toxic, while the low selectivity means that there are technical difficulties in the purification of the drug. Moreover, conventional Hg lamps require large cooling chillers as low temperatures are necessary to improve selectivity, and this adds up to the costs of the process.

Many authors have tried to design greener strategies for this methodology. Amara *et al.* have reported two different approaches in which dichloromethane and TFA were replaced by sc-CO_2, as a poorly flammable and gas-dissolving solvent, and an aqueous mixture.[92] For the sc-CO_2-based approach, ethyl acetate was used as a co-solvent for the reagents, while scCO_2 had the benefits of being inert to oxygen singlets and easily dissolving O_2 gas. They also used a heterogeneous double catalyst to immobilise commercial porphyrins (which act as photo initiators) onto Amberlist-15 resin (which adds the acid functionality to replace TFA). The reaction was performed in a fixed-bed photoreactor powered by LEDs at 5 °C, 180 bar of pressure and 2 mol% of O_2, providing 100% conversion in a single passage and a 50% yield.

Mixtures of H_2O/tetrahydrofuran and H_2O/EtOH were also tested after it was observed that traces of water did not impede the photoreaction in the screening tests. The use of water is a greener improvement that allows the reaction to run even at 30 °C. However, the best result (60% yield) was still obtained using THF and TFA in the mixture, and water-soluble ruthenium-based photocatalysts were also needed. The hydroalcoholic mixture is more appealing from a green chemistry perspective; it achieved a 53% yield using H_2SO_4 instead of TFA. The use of homogeneous catalysts is not optimal for the environmental impact of the reaction, but the water-based approach can be economically appealing if the ruthenium catalyst is efficiently recovered.

Work by Triemer *et al.*, which was publicised as being "literally" green, since chlorophylls are used as a photocatalyst, is a further addition to this field.[93] In their paper, crude extracts from *Artemisia annua* underwent photoreaction to give artemisinin from the dihydroartemisinic acid naturally present in the leaves. The extraction was performed using toluene at 50 °C for 10 minutes to obtain a mixture of reagents and chlorophyll derivatives. This crude mixture was then fed to a flow photoreactor equipped with LEDs giving yields of between 52 and 67% at 420 nm (depending on operating temperature) or 44 to 64% at 660 nm. This approach is interesting because it can enrich the plant extracts with artemisinin, without the addition of an external photocatalyst. However, toluene should be substituted as a solvent for the extraction and reaction.

Figure 20.11 Reaction tubes for the photo-acylation of 1,4-naphthoquinone. Reproduced from ref. 99, doi: 10.1007/s41061-018-0223-2, under the terms of a CC BY 4.0 license (http://creativecommons.org/licenses/by/4.0/).

Photochemical reactors exist on a variety of scales, from laboratory to industrial plants, and are already applied to different compounds of pharmaceutical interest.[94–97] The use of sunlight is even more appealing than LEDs for this technology, as it is basically free energy. However, its broad emission band and highly variable power output (which alternates from day to night and from sunny to cloudy days) are far from optimal characteristics. Smart ways to circumvent these problems have been found; reactions have been run in dyed solutions to create a monochromatic environment for a reaction,[98] and surprisingly there are examples of chemical reactors that are powered by sunlight on a pilot-plant scale (an example is shown in Figure 20.11).[99]

One of the major drawbacks for photochemistry as a green methodology is that it needs to work at low concentrations to guarantee that light can sufficiently penetrate into a solution. This means that large quantities of solvent are required, and the use of green, safe and easily recovered solvents becomes even more pressing.

20.4.2 Microwave Reactors

Professional MW reactors are now common tools on lab- and pilot scales. The significant majority of this equipment operates in batch mode. However, successful scale-up requires a flow-mode setup. A study by Kappe's team has shown how batch MW reactors on a litre scale lose competitivity against conventional heating microreactors for organic synthesis.[100] The first thing to consider is the scarce penetration depth of MW radiation, which is inversely proportional to the dielectric constant of the absorbing material. MWs will penetrate deep into a non-polar matrix, but will not heat it up, whereas

strongly polar solvents and solutions, such as brine, will heat up quickly, but the MWs will only penetrate a few centimetres. Furthermore, scaling-up the reaction often changes the distribution of the electric field and both these phenomena contribute to inhomogeneities in heating; it is possible that the portion of liquid next to the waveguide is overheated, while the bulk of the reactor is cold. Temperature behaviour becomes even harder to predict when we consider that the dielectric properties of the materials change with temperature itself. This can also cause safety issues as overheated materials tend to absorb MWs more efficiently leading to thermal runaway. Goyal *et al.* have worked on the scale up of a single mode MW reactor that overcomes these problems with the help of computer simulations.[101] With this tool, the team were able to predict and measure the absorbed power and heating distribution in a reactor using water, ethanol and hexane as the solvents in the MW chamber (Figure 20.12). This is a useful tool for moving from the laboratory to production.

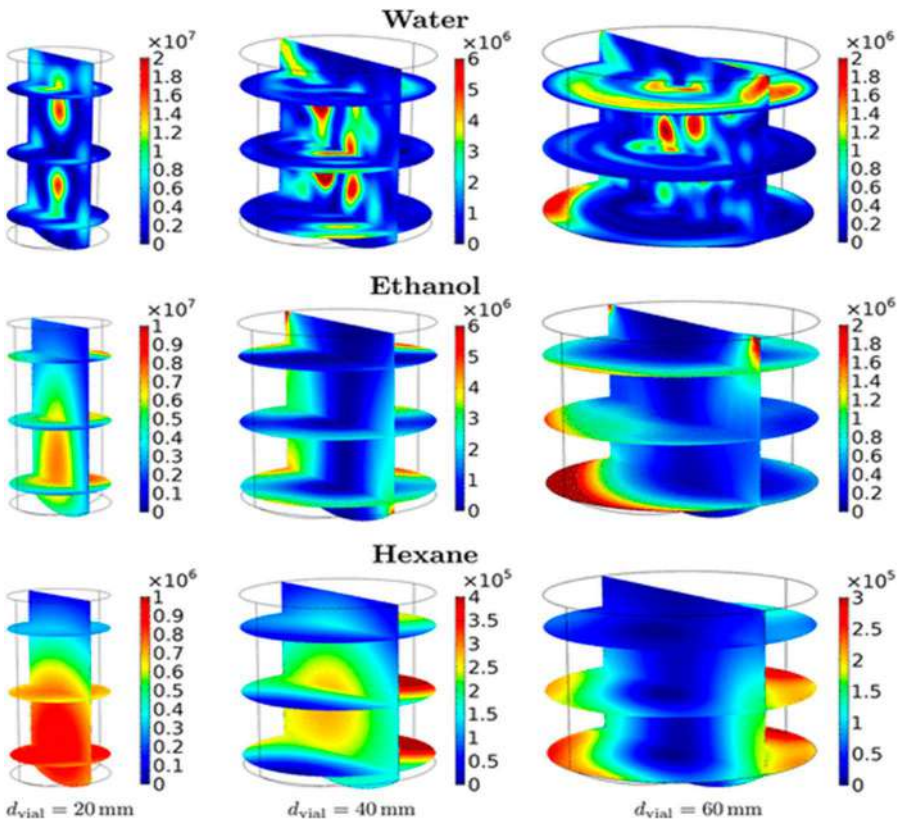

Figure 20.12 Heat distribution as predicted by computational simulations. Reproduced from ref. 101 with permission from American Chemical Society, Copyright 2020.

Maintaining the scale at semi-production, or even miniaturising reactors may be more efficient ways to achieve process intensification with MWs. This approach removes the technical limitations of dielectric heating and, in particular, temperature control. Temperature is a key parameter for successful syntheses and safe processes, and can be determined using thermocouples, infrared (IR) sensors or optical fibres. Thermocouples are resilient sensors that are widely used in laboratories and industries. However, being composed of metal strips, they function as antennae for MWs and are heated as well. If this is not accounted for, temperature readings can be overestimated, leading to poor results. IR sensors are inexpensive and do not need to be in direct contact with the reaction vessel. However, they only read temperature from the surface, which can be different to that of the bulk. This characteristic impedes their use in large scale reactors, but in reactors that are made up of thin tubes, the "bulk" becomes less relevant. Finally, optical fibres are inert to MWs and can be placed directly inside reactors. They only require chemical protection from corroding elements, making them ideal candidates for measuring temperature in MW processes. However, the problem of sampling remains; we know that heating can be non-homogeneous in large bulks, meaning that the position of the optical fibre sensors has a substantial influence on the readings. Once again, in a flow reactor, the thickness of the reaction chamber is reduced so that more homogeneous heat distribution and dispersion are expected. We must not forget that the adsorption of MWs also depends on the scale of the reaction. Working with small reagent quantities, or in extremely small tubes, would not be an efficient use of the radiating power of the magnetron. A scrupulous tailor-made screening should be performed for the desired reaction. Comer *et al.* have successfully applied this methodology for a series of organic syntheses in a microfluidic reactor under MW radiation.[102]

Today, MWs are often used in food and in inorganic fields primary as a fast drying technology, while their application in the chemical and pharmaceutical sectors is still limited. However, works such as those of Nagahata *et al.* and Morschhäuser *et al.* show that the scale-up of MW reactors to production scales is possible with reproducible results.[12,103] Perhaps, what is really needed is a change of perspective; the next-generation green chemical industries may not need huge reactors, but perhaps many miniaturised ones or reactions that run in parallel lines. This could provide the opportunity to implement enabling technologies, such as MWs, and for the successful application of flow photochemistry.

20.5 Conclusions

Green chemistry is a formidable subject and one that can enhance the chemical and economic efficiency of organic synthesis at industrial scales, but it sometimes requires counterintuitive measures and the cooperation of many scientific fields to be implemented. Last but not least, the firepower of public institutions should be aimed towards its swift implementation in order to create competitive and innovative green chemical industries.

References

1. Strategic Intelligence, https://intelligence.weforum.org/topics/a1Gb0000001RIhBEAW?tab=publications, accessed April 2020.
2. What is the European Green Deal?, https://ec.europa.eu/commission/presscorner/detail/en/fs_19_6714, accessed October 2020.
3. T. Sakakura and K. Kohno, *Chem. Commun.*, 2009, 1312.
4. J. W. Comerford, I. D. V. Ingram, M. North and X. Wu, *Green Chem.*, 2015, **17**, 1966.
5. H. Jing, in *Chemistry beyond Chlorine*, ed. Tundo P., He L., Lokteva E. and Mota C., Springer International Publishing, Switzerland, 1st edn, 2016, ch. 17, pp. 457–482.
6. P. Tundo, L. N. He, E. Lokteva and E. Mota, *Chemistry beyond Chlorine*, Springer International Publishing, Switzerland, 1st edn, 2016.
7. S. Grego, F. Aricò and P. Tundo, *Pure Appl. Chem.*, 2012, **84**, 695.
8. F. Aricò, A. S. Aldoshin and P. Tundo, *ChemSusChem*, 2017, **10**, 53.
9. G. Cravotto and D. Carnaroglio, *Microwave Chemistry*, De Gruyter, Berlin, Germany, 1st edn, 2017.
10. J. E. Muir, *Manuf. Chem.*, 2010, **81**, 22.
11. T. Nakamura, R. Nagahata, K. Kunii, H. Soga, S. Sugimoto and S. Takeuchi, *Org. Process Res. Dev.*, 2010, **14**, 781.
12. R. Morschhäuser, M. Krull, C. Kayser, C. Boberski, R. Bierbaum, P. A. Pushner, T. N. Glasnov and C. O. Kappe, *Green Process. Synth.*, 2012, **1**, 281.
13. Merk Sharp & Dohme Corp, *WO Pat.*, 213944A1, 2017.
14. Greener Reaction Conditions Award, Presidential Green Chemistry Challenge, 2019, http://www.epa.gov/greenchemistry/pubs/pgcc/winners/grca07.html%5Cnhttp://www.epa.gov/greenchemistry/pubs/docs/award_entries_and_recipients2007.pdf, accessed April 2020.
15. K. B. Hansen, Y. Hsiao, F. Xu, N. Rivera, A. Clausen, M. Kubryk, S. Krska, T. Rosner, B. Simmons, J. Balsnells, N. Ikemoto, Y. Sun, F. Spindler, C. Malan, E. J. J. Gabowski and J. D. Armstrong, *J. Am. Chem. Soc.*, 2009, **131**, 8798.
16. A. A. Desai, *Angew. Chem., Int. Ed.*, 2011, **50**, 1974.
17. J. Liang, J. Lalonde, B. Borup, V. Mitchell, E. Mundorff, N. Trinh, D. A. Kochrekar, R. N. Cherat and G. G. Pai, *Org. Process Res. Dev.*, 2010, **14**, 193.
18. P. Anastas and N. Eghbali, *Chem. Soc. Rev.*, 2010, **39**, 301.
19. F. J. Keil, *Rev. Chem. Eng.*, 2018, **34**, 135.
20. A. Dicks and A. Hent, *Green Chemistry Metrics: A Guide to Determining and Evaluating Process Greenness*, Springer, Switzerland, 1st edn, 2015.
21. F. G. Calvo-Flores, *ChemSusChem*, 2009, **2**, 905.
22. R. A. Sheldon, *ACS Sustainable Chem. Eng.*, 2018, **6**, 32.
23. Insights into the European Market for Bio-based Chemicals, https://ec.europa.eu/jrc/en/publication/insights-european-market-bio-based-chemicals, accessed April 2020.

24. A sustainable Bioeconomy for Europe: Strengthening the Connection Between Economy, Society and the Environment, https://ec.europa.eu/research/bioeconomy/pdf/ec_bioeconomy_strategy_2018.pdf, accessed February 2020.
25. The European Chemical Industry Facts and Figures 2020, https://cefic.org/app/uploads/2019/01/The-European-Chemical-Industry-Facts-And-Figures-2020.pdf, accessed April 2020.
26. Plastics – the Facts 2018 An Analysis of European Plastics Production, Demand and Waste Data, https://www.plasticseurope.org/application/files/6315/4510/9658/Plastics_the_facts_2018_AF_web.pdf, accessed April 2020.
27. Global Production Capacities of Bioplastics 2017–2022, https://docs.european-bioplastics.org/publications/market_data/2017/Report_Bioplastics_Market_Data_2017.pdf, accessed April 2020.
28. C. Boyère, C. Jérôme and A. Debuigne, *Eur. Polym. J.*, 2014, **61**, 45.
29. S. M. Gross, G. W. Roberts, D. J. Kiserow and J. M. DeSimone, *Macromolecules*, 2001, **34**, 3916.
30. P. O'Connor, R. Yang, W. M. Carroll, Y. Rochev and F. Aldabbagh, *Eur. Polym. J.*, 2012, **48**, 1279.
31. B. Grignard, C. Jérôme, C. Calberg, R. Jerome and C. Detrembleur, *Eur. Polym. J.*, 2008, **44**, 861.
32. D. Wu, F. Xu, B. Sun, R. Fu, H. He and K. Matyjaszewski, *Chem. Rev.*, 2012, **112**, 3959.
33. D. Yuan, J. Bao, Y. Ren, W. Li, L. Huang and X. Cai, *CrystEngComm*, 2018, **20**, 4676.
34. M. Watanabe, Y. Hashimoto, T. Kimura and A. Kishida, *Polymers*, 2020, **12**, 134.
35. R. Zhang, J. Chen, Y. Zhu, J. Zhang, G. Luo, P. Cao, Q. Shen and L. Zhang, *Polymers*, 2020, **12**, 315.
36. Dow Chemical Company, *US Pat.*, 5250577A, 1989.
37. J. H. Clark, T. J. Farmer, A. J. Hunt and J. Sherwood, *Int. J. Mol. Sci.*, 2015, **16**, 17101.
38. Q. Zhang, K. De Oliveira Vigier, S. Royer and F. Jerome, *Chem. Soc. Rev.*, 2012, **41**, 7108.
39. S. Sowmiah, V. Srinivasadesikan, M. C. Tseng and Y. H. Chu, *Molecules*, 2009, **14**, 3780.
40. H. Wang, G. Gurau and R. D. Rogers, *Chem. Soc. Rev.*, 2012, **41**, 1519.
41. K. E. Gutowski, *Phys. Sci. Rev.*, 2018, **3**, 1.
42. A. Paiva, R. Craveiro, I. Aroso, M. Martins, R. L. Reis and A. R. C. Duarte, *ACS Sustainable Chem. Eng.*, 2014, **5**, 1063.
43. S. K. Singh and A. W. Savoy, *J. Mol. Liq.*, 2020, **297**, 1.
44. P. Kubisa, *Prog. Polym. Sci.*, 2004, **29**, 3.
45. E. Kowsari and M. Mallakmohammadi, *Ultrason. Sonochem.*, 2011, **18**, 447.
46. A. Hasaninejad, A. Zare, M. Shekouhy and J. A. Rad, *J. Comb. Chem.*, 2010, **12**, 844.

47. V. V. Namboodiri and R. S. Varma, *Tetrahedron Lett.*, 2002, **43**, 5381.
48. R. S. Varma and V. V. Namboodiri, *Chem. Commun.*, 2001, **12**, 643.
49. B. M. Khadilkar and G. L. Rebeiro, *Org. Process Res. Dev.*, 2002, **6**, 826.
50. M. Volland, V. Seitz, M. Maase, M. Flores, R. Papp, K. Massonne, V. Stegmann, K. Halbritter, R. Noe, M. Bartsch, W. Siegel, M. Becker and O. Huttenloch, Method for the separation of acids from chemical reaction mixtures by means of ionic fluids, *WO Pat.*, WO2003062251A1, 2003.
51. S. Tabasso, G. Grillo, D. Carnaroglio, E. C. Gaudino and G. Cravotto, *Molecules*, 2016, **21**, 1.
52. F. Bucciol, S. Tabasso, G. Grillo, F. Menegazzo, M. Signoretto, M. Manzoli and G. Cravotto, *J. Catal.*, 2019, **380**, 267.
53. I. Obregón, I. Gandarias, M. G. Al-Shaal, C. Mevissen, P. L. Arias and R. Palkovits, *ChemSusChem*, 2016, **9**, 2488.
54. Y. Shen, S. Zhang, H. Li, Y. Ren and H. Liu, *Chem. - Eur. J.*, 2010, **16**, 7368.
55. M. A. Abdel-Rahman, Y. Tashiro and K. Sonomoto, *Biotechnol. Adv.*, 2013, **31**, 877.
56. A. Komesu, J. A. R. de Oliveira, L. H. Martins, M. R. Wolf Maciel and R. Maciel Filho, *BioResources*, 2017, **12**, 4364.
57. S. M. Nikles, M. Piao, A. M. Lane and D. E. Nilles, *Green Chem.*, 2001, **3**, 109.
58. J. S. Bennett, K. L. Charles, M. R. Miner, C. F. Heueberger, E. J. Spina, M. F. Bartels and T. Foreman, *Green Chem.*, 2009, **11**, 166.
59. S. Planer, A. Jana and K. Grela, *ChemSusChem*, 2019, **12**, 4655.
60. S. G. Babu, M. Ashokkumar and B. Neppolian, *Top. Curr. Chem.*, 2016, **374**, 375.
61. L. S. Castillo-Peinado and M. D. Luque de Castro, *J. Pharm. Pharmacol.*, 2016, **68**, 1249.
62. H. U. Rodríguez Vera, F. Baillon, F. Espitalier, P. Accart and O. Louisnard, *Ultrason. Sonochem.*, 2019, **58**, 104671.
63. Y. I. Sánchez-García, K. S. García-Vega, M. Y. Leal-Ramos, I. Salmeron and N. Gutiérrez-Méndez, *Ultrason. Sonochem.*, 2018, **42**, 714.
64. R. K. Bund and A. B. Pandit, *Ultrason. Sonochem.*, 2007, **14**, 143.
65. S. Kaur Bhangu, M. Ashokkumar and J. Lee, *Cryst. Growth Des.*, 2016, **16**, 1934.
66. T. Nguyen, A. Khan, L. Bruce, C. Forbes, R. L. O'Leary and C. J. Price, *Crystals*, 2017, **7**, 294.
67. Y. Ike and I. Hirasawa, *Chem. Eng. Technol.*, 2017, **40**, 1318.
68. Y. Ike and I. Hirasawa, *Chem. Eng. Technol.*, 2018, **41**, 1093.
69. Thomas J Limpton Co, *US pat.*, 6630185B2, 2001.
70. Glaxo Group Ltd, *Eu pat.*, 1438023B1, 2002.
71. Merk Sharp & Dohme Corp, *WO Pat.*, 035558, 2009.
72. Boehringer Ingelheim Pharma GmbH & Co.KG, *WO Pat.*, 034943, 2004.
73. Bristol Meyers Squibb Company, *WO Pat.*, 044468A1, 2000.
74. S. Bechtel, M. Rauls, R. Van Gelder and S. Simpson, *US Pat.*, 0122421A1, 2006.

75. Arkema France, Katholieke Universiteit Leuven, *WO pat.*, 138069A1, 2019.
76. G. Ruecroft, C. Jones and D. Hipkiss, in *Rdd 2010*. Edinburgh, June, 2010.
77. Industrial Waste Water Treatment Pressures on Environment, https://www.eea.europa.eu/publications/industrial-waste-water-treatment-pressures, accessed October 2020.
78. V. Homem and L. Santos, *J. Environ. Manage.*, 2011, **92**, 2304.
79. T. A. Ternes, M. Meisenheimer, D. McDowell, F. Sacher, H. J. Brauch, B. Haist-Gulde, G. Preuss, U. Wilme and N. Zulei-Seibert, *Environ. Sci. Technol.*, 2002, **36**, 3855.
80. A. Mehrdad and R. Hashemzadeh, *Ultrason. Sonochem.*, 2010, **17**, 168.
81. H. Ghodbane and O. Hamdaoui, *Ultrason. Sonochem.*, 2009, **16**, 593.
82. R. H. Jawale, A. Tandale and P. R. Gogate, *Ultrason. Sonochem.*, 2017, **38**, 402.
83. L. Jing, B. Chen, D. Wen, J. Zheng and B. Zhang, *J. Environ. Manage.*, 2017, **203**, 182.
84. N. N. Mahamuni and Y. G. Adewuyi, *Ultrason. Sonochem.*, 2010, **17**, 990.
85. H. Kim, A. Nagaki and J. I. Yoshida, *Nat. Commun.*, 2011, **2**, 1.
86. L. D. Proctor and A. J. Warr, *Org. Process Res. Dev.*, 2002, **6**, 884.
87. D. Cambié, C. Bottecchia, N. J. W. Straathof, V. Hessel and T. Noel, *Chem. Rev.*, 2016, **116**, 10276.
88. R. Porta, M. Benaglia and A. Puglisi, *Org. Process Res. Dev.*, 2016, **20**, 2.
89. K. Loubière, M. Oelgemöller, T. Aillet, O. Dechy-Cabaret and L. E. Prat, *Chem. Eng. Process.*, 2016, **104**, 120.
90. L. D. Elliott, J. P. Knowles, P. J. Koovits, K. G. Maskill, M. J. Ralph, G. Lejeune, L. J. Edwards, R. I. Robinson, I. R. Clemens, B. Cox, D. D. Pascoe, G. Koch, M. Eberle, M. B. Berry and K. Booker-Milburn, *Chem. - Eur. J.*, 2014, **20**, 15226.
91. F. Lévesque and P. H. Seeberger, *Angew. Chem., Int. Ed.*, 2012, **51**, 1706.
92. Z. Amara, J. F. B. Bellamy, R. Horvath, S. J. Miller, A. Beeby, A. Burgard, K. Rossen, M. Poliakoff and M. W. George, *Nat. Chem.*, 2015, **6**, 489.
93. S. Triemer, K. Gilmore, G. T. Vu, P. H. Seeberger and A. Siedel-Morgenstern, *Angew. Chem., Int. Ed.*, 2018, **57**, 5525.
94. S. Fuse, Y. Mifune, N. Tanabe and T. Takahashi, *Org. Biomol. Chem.*, 2012, **10**, 5205.
95. M. Escribà-Gelonch, T. Noël and V. Hessel, *Org. Process Res. Dev.*, 2018, **22**, 147.
96. K. Gilmore, D. Kopetzki, J. Weon Lee, Z. Horvath, D. T. McQuade, A. Seidel-Morgenstern and P. H. Seeberger, *Chem. Commun.*, 2014, **50**, 12652.
97. R. G. Gérardy, M. Winter, C. R. Horn, A. Vizza, K. Van Hecks and J. C. M. Monbaliu, *Org. Process Res. Dev.*, 2017, **21**, 117.
98. F. Zhao, D. Cambié, J. Janse, E. W. Wieland, K. P. L. Kuijpers, V. Hessel, M. G. Debjie and T. Noel, *ACS Sustainable Chem. Eng.*, 2018, **6**, 422.

99. D. Cambié and T. Noël, *Top. Curr. Chem.*, 2018, **376**, 1.
100. M. Damm, T. N. Glasnov and C. O. Kappe, *Org. Process Res. Dev.*, 2010, **14**, 215.
101. H. Goyal, A. Mehdad, R. F. Lobo, G. D. Stefanidis and D. G. Vlachos, *Ind. Eng. Chem. Res.*, 2020, **59**, 2516.
102. E. Comer and M. G. Organ, *J. Am. Chem. Soc.*, 2005, **127**, 8160.
103. R. Nagahata and K. Takeuchi, *Chem. Rec.*, 2019, **19**, 51.

Subject Index